EMERGING INFECTIOUS DISEASES®

CDC
Centers for Disease Control and Prevention

Respiratory Infections

November 2022

Neil Welliver (1929–2005), *Flotsam Allagash*, 1988. Oil on canvas. 48 in x 48 in/122 cm x 122 cm. © Neil Welliver, Courtesy Alexandre Gallery, New York.

EMERGING INFECTIOUS DISEASES®

Emerging Infectious Diseases is published monthly by the Centers for Disease Control and Prevention, 1600 Clifton Rd NE, Mailstop H16-2, Atlanta, GA 30329-4027, USA. Telephone 404-639-1960; email, eideditor@cdc.gov

EMERGING INFECTIOUS DISEASES®

Respiratory Infections **November 2022**

On the Cover

Neil Welliver (1929–2005), *Flotsam Allagash*, 1988. Oil on canvas. 48 in x 48 in/122 cm x 122 cm. ©Neil Welliver, Courtesy Alexandre Gallery, New York.

About the Cover p. 2369

Synopses

Medscape EDUCATION ACTIVITY

Severe Pneumonia Caused by *Corynebacterium striatum* in Adults, Seoul, South Korea, 2014–2019

Most (70.4%) cases were hospital-acquired, and 51.9% of patients were immunocompromised

Medscape EDUCATION ACTIVITY

Multispecies Outbreak of *Nocardia* Infections in Heart Transplant Recipients and Association with Climate Conditions, Australia

Extreme weather conditions, coupled with greater susceptibility to opportunistic infection, could explain this outbreak.

Research

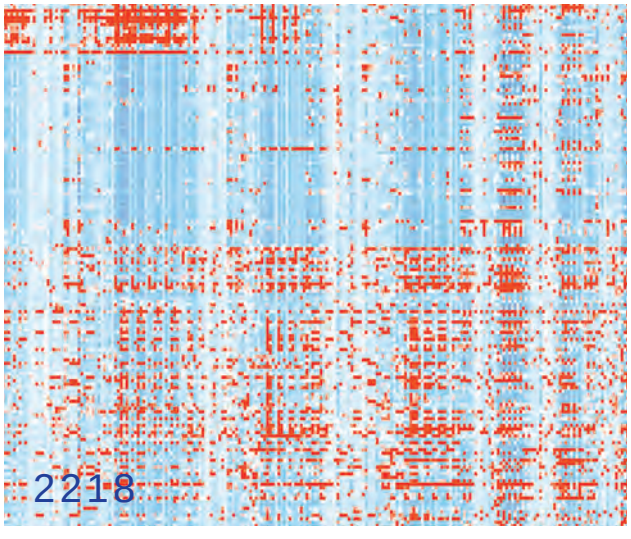

EMERGING INFECTIOUS DISEASES®
November 2022

Dispatches

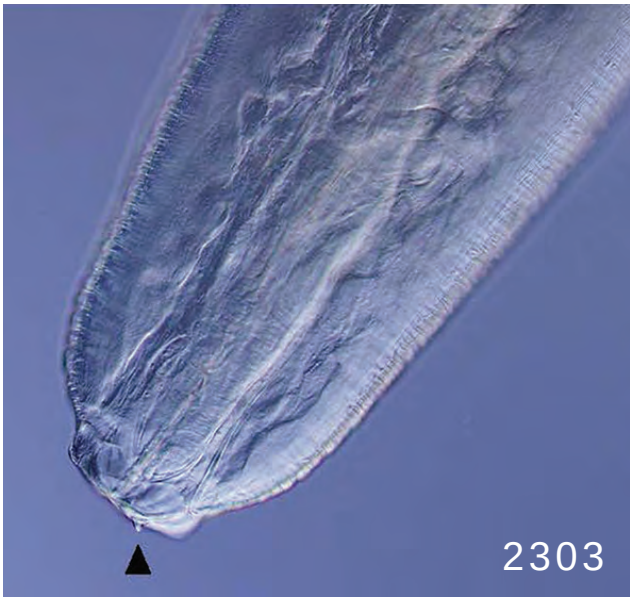

Research Letters

EMERGING INFECTIOUS DISEASES®
November 2022

About the Cover

Etymologia

Online Report

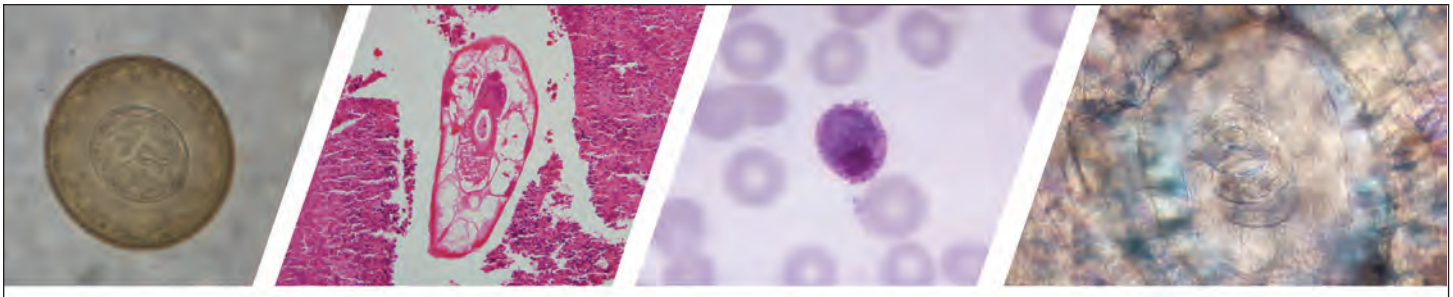

DPDx

Diagnostic Assistance and Training in Laboratory Identification of Parasites

A free service of CDC available to laboratorians, pathologists, and other health professionals in the United States and abroad

- Diagnosis from photographs of worms, histological sections, fecal, blood, and other specimen types
- Expert diagnostic review
- Formal diagnostic laboratory report
- Submission of samples via secure file share

Visit the DPDx website for information on laboratory diagnosis, geographic distribution, clinical features, parasite life cycles, and training via Monthly Case Studies of parasitic diseases.

www.cdc.gov/dpdx
dpdx@cdc.gov

U.S. Department of Health and Human Services
Centers for Disease Control and Prevention

CS272346-DE

Severe Pneumonia Caused by *Corynebacterium striatum* in Adults, Seoul, South Korea, 2014–2019

Yun Woo Lee[1], Jin Won Huh[1], Sang-Bum Hong, Jiwon Jung, Min Jae Kim, Yong Pil Chong, Sung-Han Kim, Heungsup Sung, Kyung-Hyun Do, Sang-Oh Lee, Chae-Man Lim, Yang Soo Kim, Younsuck Koh, Sang-Ho Choi

In support of improving patient care, this activity has been planned and implemented by Medscape, LLC and Emerging Infectious Diseases. Medscape, LLC is jointly accredited with commendation by the Accreditation Council for Continuing Medical Education (ACCME), the Accreditation Council for Pharmacy Education (ACPE), and the American Nurses Credentialing Center (ANCC), to provide continuing education for the healthcare team.

Medscape, LLC designates this Journal-based CME activity for a maximum of 1.00 ***AMA PRA Category 1 Credit(s)™***. Physicians should claim only the credit commensurate with the extent of their participation in the activity.

Successful completion of this CME activity, which includes participation in the evaluation component, enables the participant to earn up to 1.0 MOC points in the American Board of Internal Medicine's (ABIM) Maintenance of Certification (MOC) program. Participants will earn MOC points equivalent to the amount of CME credits claimed for the activity. It is the CME activity provider's responsibility to submit participant completion information to ACCME for the purpose of granting ABIM MOC credit.

All other clinicians completing this activity will be issued a certificate of participation. To participate in this journal CME activity: (1) review the learning objectives and author disclosures; (2) study the education content; (3) take the post-test with a 75% minimum passing score and complete the evaluation at http://www.medscape.org/journal/eid; and (4) view/print certificate. For CME questions, see page 2372.

Release date: October 19, 2022; Expiration date: October 19, 2023

Learning Objectives

Upon completion of this activity, participants will be able to:

- Assess the proportion, demographics, underlying diseases, and pathogens of severe *Corynebacterium striatum* hospital-acquired pneumonia in adults compared with those of severe methicillin-resistant *Staphylococcus aureus* hospital-acquired pneumonia, based on a retrospective study
- Evaluate the clinical characteristics, laboratory findings, and outcomes of severe *Corynebacterium striatum* hospital-acquired pneumonia in adults compared with those of severe methicillin-resistant *Staphylococcus aureus* hospital-acquired pneumonia, based on a retrospective study
- Determine the clinical implications of the proportion, clinical characteristics, and outcomes of severe *Corynebacterium striatum* hospital-acquired pneumonia in adults compared with those of severe methicillin-resistant *Staphylococcus aureus* hospital-acquired pneumonia, based on a retrospective study

CME Editor

Amy J. Guinn, BA, MA, Technical Writer/Editor, Emerging Infectious Diseases. *Disclosure: Amy J. Guinn, BA, MA, has disclosed no relevant financial relationships.*

CME Author

Laurie Barclay, MD, freelance writer and reviewer, Medscape, LLC. *Disclosure: Laurie Barclay, MD, has the following relevant financial relationships: formerly owned stocks in AbbVie Inc.*

Authors

Yun Woo Lee, MD, MS; Jin Won Huh, MD, PhD; Sang-Bum Hong, MD, PhD; Jiwon Jung, MD, PhD; Min Jae Kim, MD, PhD; Yong Pil Chong, MD, PhD; Sung-Han Kim, MD, PhD; Heungsup Sung, MD, PhD; Kyung-Hyun Do, MD, PhD; Sang-Oh Lee, MD, PhD; Chae-Man Lim, MD, PhD; Yang Soo Kim, MD, PhD; Younsuck Koh, MD, PhD; and ***Sang-Ho Choi, MD, PhD.***

Authors affiliation: University of Ulsan College of Medicine, Seoul, South Korea

[1]These authors contributed equally to this article.

DOI: https://doi.org/10.3201/eid2811.220273

We investigated the proportion and characteristics of severe *Corynebacterium striatum* pneumonia in South Korea during 2014–2019. As part of an ongoing observational study of severe pneumonia among adult patients, we identified 27 severe *C. striatum* pneumonia cases. Most (70.4%) cases were hospital-acquired, and 51.9% of patients were immunocompromised. *C. striatum* cases among patients with severe hospital-acquired pneumonia (HAP) increased from 1.0% (2/200) during 2014–2015 to 5.4% (10/185) during 2018–2019, but methicillin-resistant *Staphylococcus aureus* (MRSA) infections among severe HAP cases decreased from 12.0% to 2.7% during the same timeframe. During 2018–2019, *C. striatum* was responsible for 13.3% of severe HAP cases from which bacterial pathogens were identified. The 90-day mortality rates were similarly high in the *C. striatum* and MRSA groups. *C. striatum* was a major cause of severe HAP and had high mortality rates. This pathogen is emerging as a possible cause for severe pneumonia, especially among immunocompromised patients.

Corynebacterium striatum is a nonlipophilic, fermentative coryneform bacterium that commonly occupies the normal flora of the skin and oropharynx (*1*). Although *C. striatum* isolated from clinical specimens has frequently been considered a contaminant, it is increasingly recognized as a pathogen of various infections, including central line-associated bacteremia (*2*), endocarditis (*3*), and pleuropulmonary infection (*4*–*6*). In 1980, *C. striatum* was reported as a cause of pleuropulmonary infection in a patient with chronic lymphocytic leukemia (*4*). In 2018, a group of researchers in the United States reported 3 cases of community-acquired pneumonia (CAP) in which *Corynebacterium* species were the predominant isolate and suggested that *Corynebacterium* species are a noteworthy clinical cause of pneumonia (*6*). However, scarce information is available on the incidence, clinical characteristics, and outcomes of severe *C. striatum* pneumonia in critically ill adult patients, because previous studies included ≤5 patients with severe *C. striatum* pneumonia, except those reporting hospital outbreak events.

Methicillin-resistant *Staphylococcus aureus* (MRSA) is a major cause of severe hospital-acquired pneumonia (HAP), and the clinical characteristics and outcomes of severe MRSA pneumonia are well-documented. Therefore, comparing *C. striatum* and MRSA pneumonia could clarify the clinical characteristics of *C. striatum* pneumonia for clinicians. We investigated the proportion, clinical characteristics, and outcomes of severe *C. striatum* pneumonia in adults and compared those aspects with those for severe MRSA pneumonia.

Methods

Study Design, Setting, Data Collection, and Patient Selection

This study is part of an ongoing prospective observational study on severe pneumonia in critically ill adult (≥16 years of age) patients at Asan Medical Center, a 2,700-bed tertiary referral center in Seoul, South Korea. Since March 2010, we have prospectively identified all adult patients admitted to the 28-bed medical intensive care unit (ICU) who were clinically suspected of having severe pneumonia and monitored them until hospital discharge (*7*–*10*). We collected data on patient demographics; underlying diseases or conditions; category of pneumonia; initial clinical manifestations; laboratory, microbiologic, and radiologic findings; treatment; complications; and mortality rates. For this study, we investigated patients with severe *C. striatum* pneumonia who were admitted to the medical ICU during January 2014–December 2019. This study was approved by the institutional review board of Asan Medical Center (IRB no. 2010–0079), which waived the need for informed consent due to the observational nature of the study.

Definitions

We defined and categorized pneumonia as previously stated (*11*–*13*). We defined severe pneumonia as the necessity for mechanical ventilation or having septic shock at ICU admission (*12*). We defined sepsis and septic shock according to Sepsis-3 criteria (*14*). We defined immunocompromised state as described previously (*15*).

C. striatum Identification and Antimicrobial Susceptibility Testing

We cultured sputum specimens on a 5% sheep blood plate and MacConkey agar (Synergy Innovation, http://www.synergyinno.com). When coryneform gram-positive bacilli were isolated, we identified and performed antimicrobial susceptibility testing for specimens that were urea positive or from the ICU (*16*). We quantitatively cultured bronchoalveolar lavage specimens on chocolate agar and identified and performed susceptibility testing when coryneform gram-positive bacilli exclusively grew at $\geq 10^4$ CFU/mL (*16*). Until August 2015, our facility used the triple sugar iron, motility, API Coryne (bioMérieux-Vitek, https://www.biomerieux.com) system to identify coryneform gram-positive rods. In September 2015, our facility began using matrix-assisted laser desorption/ionization time-of-flight mass spectrometry (Bruker Daltonik, https://www.bruker.

com). We determined antimicrobial susceptibility profiles by ETEST (bioMérieux-Vitek) with MHF medium (Mueller-Hinton agar with 5% horse blood + 20 mg/L β-NAD; bioMérieux-Vitek). We used the Clinical and Laboratory Standards Institute M45 guideline for interpreting susceptibility test results (*17*) and defined multidrug resistance as resistance to ≥3 antimicrobial drug families.

Statistical Analysis

We compared patient demographics, underlying diseases and conditions, and clinical and laboratory parameters between the *C. striatum* group and the MRSA group. We used χ^2 or Fisher exact test to compare categorical variables and Student *t*-test or Mann-Whitney U test to compare continuous variables. We analyzed changes in the proportions of pneumonic pathogens over time by using a χ^2 test for trend. We performed all analyses in SPSS Statistics 24.0 (IBM Corp., https://www.ibm.com) and considered $p<0.05$ statistically significant.

Results

Demographics, Underlying Diseases and Conditions, and Pneumonia Categories

During the study period, we identified a total of 1,740 patients with severe pneumonia. Among them, 27 had severe *C. striatum* pneumonia and 103 had severe MRSA pneumonia (Table 1). The median patient age in the *C. striatum* group was 72.0 years and in the MRSA group was 71.0 years. Solid cancer, diabetes mellitus, and structural lung diseases were the most common underlying conditions in both groups. More patients in the *C. striatum* group were immunocompromised (51.9% vs. 26.2%; p = 0.01). Most (70.4%) patients in the *C. striatum* group had HAP, 14.8% had healthcare-associated pneumonia (HCAP), 11.1% had ventilator-associated pneumonia, and 3.7% had CAP. HAP was significantly more common in the *C. striatum* group than the MRSA group (70.4% vs. 42.7%; p = 0.01); HCAP was more common in the MRSA group (32.0% vs. 14.8%; p = 0.08), albeit without statistical significance.

Table 1. Characteristics of adult patients with severe pneumonia caused by *Corynebacterium striatum*, Seoul, South Korea, 2014–2019*

Characteristics	Total, n = 130	*C. striatum*, n = 27	MRSA, n = 103	p value
Sex				
M	92 (70.8)	18 (66.7)	74 (71.8)	0.60
F	38 (29.2)	9 (33.3)	33 (32.0)	
Median age (interquartile range)	71.0 (63.8–77.0)	72.0 (66.0–80.0)	71.0 (63.0–76.0)	0.17
Underlying disease or condition†				
Solid cancer	32 (24.6)	4 (14.8)	28 (27.2)	0.18
Diabetes mellitus	30 (23.1)	6 (22.2)	24 (23.3)	0.91
Structural lung disease	24 (18.5)	4 (14.8)	20 (19.4)	0.78
Chronic obstructive lung disease	12 (9.2)	3 (11.1)	9 (8.7)	0.71
Interstitial lung disease	5 (3.8)	0	5 (4.9)	0.58
Bronchiectasis	4 (3.1)	0	4 (3.9)	0.58
Destroyed lung due to tuberculosis	1 (0.8)	0	1 (1.0)	1.00
Pneumoconiosis	1 (0.8)	0	1 (1.0)	1.00
Bronchiolitis obliterans	1 (0.8)	1 (3.7)	0	0.21
Hematologic malignancy	13 (10.0)	5 (18.5)	8 (7.8)	0.14
Liver cirrhosis	11 (8.5)	2 (7.4)	9 (8.7)	1.00
End-stage renal disease	7 (5.4)	2 (7.4)	5 (4.9)	0.64
Chronic renal failure	6 (4.6)	3 (11.1)	3 (2.9)	0.10
Congestive heart failure	3 (2.3)	1 (3.7)	2 (1.9)	0.51
Alcoholism	2 (1.5)	0	2 (1.9)	1.00
Cerebrovascular attack	12 (9.2)	5 (18.5)	7 (6.8)	0.13
Solid organ transplantation	2 (1.5)	0	2 (1.9)	0.63
Hematopoietic stem cell transplantation	3 (2.3)	2 (7.4)	1 (1.0)	0.11
Immunocompromised state‡	41 (31.5)	14 (51.9)	27 (26.2)	0.01
Recent chemotherapy	23 (17.7)	7 (25.9)	16 (15.5)	0.26
Recent surgery, ≤1 mo	19 (14.6)	2 (7.4)	17 (16.5)	0.36
Active smoker	10 (7.7)	1 (3.7)	9 (8.7)	0.69
Neutropenia, <500 cells/mL	8 (6.2)	4 (14.8)	4 (3.9)	0.06
Category of pneumonia				
Community-acquired	6 (4.6)	1 (3.7)	5 (4.9)	1.00
Healthcare-associated	37 (28.5)	4 (14.8)	33 (32.0)	0.08
Hospital-acquired	63 (48.5)	19 (70.4)	44 (42.7)	0.01
Ventilator-associated	24 (18.5)	3 (11.1)	21 (20.4)	0.40

*Values are no. (%) except as indicated. MRSA, methicillin-resistant *Staphylococcus aureus*.
†Patients could have ≥1 underlying disease or condition.
‡Defined as ≥1 of the following conditions: daily receipt of immunosuppressants, including corticosteroids; HIV infection; solid organ or hematopoietic stem cell transplant recipient; receipt of chemotherapy for underlying malignancy during the previous 6 months; or underlying immune deficiency disorder.

Bacterial Pathogens Identified in Severe HAP Patients

We identified bacterial pathogens in 565 patients who had severe HAP during 2014–2019 (Table 2). The proportion of severe MRSA HAP decreased significantly, from 12.0% (24/200) in 2014–2015 to 2.7% (5/185) in 2018–2019 (p<0.01), whereas the proportion of severe *C. striatum* HAP increased significantly, from 1.0% (2/200) in 2014–2015 to 5.4% (10/185) in 2018–2019 (p<0.001). Among 75 HAP cases from which bacterial pathogens were identified in 2018–2019, *C. striatum* was responsible for 13.3% (10/75) of cases, which was the fourth most common pathogen, after *Acinetobacter baumannii* (30.7%), *Klebsiella pneumoniae* (21.3%), and *Pseudomonas aeruginosa* (14.7%).

Co-infections

We identified co-infection pathogens in 13 (48.1%) patients in the *C. striatum* group and 37 (35.9%) patients in the MRSA group (p = 0.25) (Table 3). Co-infection with other bacteria was more common in the MRSA group (25.2% vs. 7.4%; p = 0.045), whereas viral co-infection was more common in the *C. striatum* group (33.3% vs. 14.6%; p = 0.047). Fungal co-infection, which included 4 *Aspergillus* species and 1 *Pneumocystis jirovecii*, was only found in the *C. striatum* group (14.8% vs. 0%; p<0.01).

Clinical Manifestations and Laboratory Findings

Dyspnea, fever, sputum, and cough were the most common signs and symptoms in both groups (Table 4). Fever tended to be less common in the *C. striatum* group (66.7% vs. 82.5%; p = 0.07). The proportion of patients with septic shock at the time of ICU admission was significantly higher in the MRSA group (67.0% vs. 44.4%; p = 0.03). However, the proportion of mechanical ventilation, acute physiology and chronic health evaluation (APACHE II) score, and sequential organ failure assessment (SOFA) score at the time of ICU admission were similar between the 2 groups. Peripheral leukocyte counts, platelet counts, and serum C-reactive protein levels also were similar between the 2 groups, but serum procalcitonin level was significantly higher in the MRSA group than the *C. striatum* group (median 0.3 ng/mL vs. 1.8 ng/mL; p<0.01).

C. striatum Gram Stain, Culture, and Antimicrobial Susceptibility Testing

On microscopic examination of Gram stain specimens, gram-positive rods were identified in 69.2% (18/26) of specimens. Among 27 cases, 10 were quantitative cultures and 17 were semiquantitative cultures. Bacterial counts were >10^5 CFU/mL in 8/10 quantitative cultures. Of the 17 semiquantitative culture specimens, 12 specimens were grade many (4+), 1 was

Table 2. Bacterial pathogens detected among 565 adult patients with severe hospital-acquired pneumonia, Seoul, South Korea, 2014–2019

Pathogens identified	No. (%) patients				p value*
	2014–2015, n = 200	2016–2017, n = 180	2018–2019, n = 185	Total, n = 565	
Total	88 (44.0)	66 (36.7)	75 (40.5)	229 (40.5)	0.35
Staphylococcus aureus	27 (13.5)	15 (8.3)	8 (4.3)	50 (8.8)	<0.01
Methicillin-susceptible	3 (1.5)	0	3 (1.6)	6 (1.1)	0.24
Methicillin-resistant	24 (12.0)	15 (8.3)	5 (2.7)	44 (7.8)	<0.01
Corynebacterium striatum	2 (1.0)	7 (3.9)	10 (5.4)	19 (3.4)	0.05
Streptococcus pneumoniae	4 (2.0)	2 (1.1)	1 (0.5)	7 (1.2)	0.43
Legionella pneumophila	1 (0.5)	1 (0.6)	0	2 (0.4)	0.61
Moraxella catarrhalis	0	0	1 (0.5)	1 (0.2)	0.36
Streptococcus pyogenes	0	1 (0.6)	0	1 (0.2)	0.34
Nocardia species	0	0	1 (0.5)	1 (0.2)	0.36
Enteric gram-negative bacilli	18 (9.0)	22 (12.2)	20 (10.8)	60 (10.6)	0.59
Klebsiella pneumoniae	13 (6.5)	14 (7.8)	16 (8.6)	43 (7.6)	0.73
Escherichia coli	4 (2.0)	4 (2.2)	3 (1.6)	11 (1.9)	0.92
Enterobacter cloacae	1 (0.5)	3 (1.7)	2 (1.1)	6 (1.1)	0.54
Citrobacter freundii	1 (0.5)	2 (1.1)	0	3 (0.5)	0.34
Klebsiella oxytoca	0	0	2 (1.1)	2 (0.4)	0.13
Hafnia alvei	0	0	1 (0.5)	1 (0.2)	0.36
Nonenteric gram-negative bacilli	47 (23.5)	22 (12.2)	37 (20.0)	106 (18.8)	0.02
Acinetobacter baumannii	24 (12.0)	13 (7.2)	23 (12.4)	60 (10.6)	0.20
Pseudomonas aeruginosa	19 (9.5)	6 (3.3)	11 (5.9)	36 (6.4)	0.047
Stenotrophomonas maltophilia	4 (2.0)	2 (1.1)	7 (3.8)	13 (2.3)	0.22
Burkholderia cepacia	0	0	1 (0.5)	1 (0.2)	0.36
Acinetobacter lwoffii	0	1 (0.6)	0	1 (0.2)	0.34
Chryseobacterium indologenes	0	1 (0.6)	0	1 (0.2)	0.34
Chryseobacterium meningosepticum	1 (0.5)	0	0	1 (0.2)	0.40
Chlamydia pneumoniae	1 (0.5)	0	0	1 (0.2)	0.40

*p value based on χ^2 test for trend.

Table 3. Additional pathogens detected among adult patients with severe *Corynebacterium striatum* pneumonia and methicillin-resistant *Staphylococcus aureus* pneumonia, Seoul, South Korea, 2014–2019*

Pathogens	No. (%) co-infecting pathogens			p value
	Total, n = 130	*C. striatum*, n = 27	MRSA, n = 103	
Any	50 (38.5)	13 (48.1)	37 (35.9)	0.25
Other bacteria	28 (21.5)	2 (7.4)	26 (25.2)†	0.045
Pseudomonas aeruginosa	7	0	7	
Acinetobacter baumannii	6	0	6	
Klebsiella pneumoniae	5	0	5	
Escherichia coli	4	1	3	
Haemophilus influenzae	2	0	2	
Streptococcus pneumoniae	2	0	2	
Citrobacter freundii	1	0	1	
Enterobacter cloacae	1	1	0	
Elizabethkingia meningosepticum	1	0	1	
Klebsiella aerogenes	1	0	1	
Stenotrophomonas maltophilia	1	0	1	
Virus	24 (18.5)	9 (33.3)‡	15 (14.6)§	0.047
Influenza virus	8	4	4	
Influenza virus A	3	3	0	
Influenza virus B	1	1	1	
Parainfluenza virus type 3	4	1	3	
Rhinovirus	3	1	2	
Adenovirus	3	1	2	
Respiratory syncytial virus	2	1	1	
Respiratory syncytial virus A	1	1	0	
Respiratory syncytial virus B	1	0	1	
Human coronavirus	2	1	1	
229E	1	1	0	
OC43/HKU1	1	0	1	
Human metapneumovirus	2	1	1	
Bocavirus	1	0	1	
Enterovirus	1	0	1	
Fungus	4 (3.1)	4 (14.8)¶	0	<0.01
Aspergillus species	4 (3.1)	4 (14.8)	0	
Pneumocystis jirovecii	1 (0.8)	1 (3.7)	0	

*Categories of co-infection were not mutually exclusive; some cases were associated with ≥2 categories of pathogens.
†Three patients were co-infected with 2 bacteria: *H. influenzae* and *S. pneumoniae*; *E. coli* and *K. pneumoniae*; and *A. baumannii* and *K. pneumoniae*.
‡One patient was co-infected with influenza A virus and human metapneumovirus.
§One patient was co-infected with bocavirus and rhinovirus.
¶One patient was co-infected with *Aspergillus* species and *P. jirovecii*.

grade moderate (3+), 1 grade few (2+), and 3 were grade rare (1+) (Appendix Table, https://wwwnc.cdc.gov/EID/article/28/11/22-0273-App1.pdf). All 27 *C. striatum* isolates underwent antimicrobial susceptibility testing. All isolates were resistant to penicillin, ceftriaxone, erythromycin, and ciprofloxacin, and susceptible to vancomycin, and all isolates were multidrug resistant.

Outcomes

The mortality rates between the *C. striatum* and MRSA group showed no statistically significant differences: 30-day mortality (40.7% vs. 29.1%; p = 0.25), 60-day (48.1% vs. 42.7%; p = 0.61), and 90-day (59.3% vs. 50.5%; p = 0.42) (Table 5). In-hospital mortality rates were higher (70.4%) in the *C. striatum* group than in the MRSA group (52.4%), albeit without statistical significance (p = 0.09). Mortality rates were similar for *C. striatum* and MRSA in subgroups regardless of the patient's immune status. We noted no statistically significant differences in the median length of ICU stay between the *C. striatum* and MRSA group, both 14 days (p = 0.33), nor in the length of hospital stay after ICU admission, 30 days for the *C. striatum* versus 29 days for the MRSA group (p = 0.48).

Discussion

We investigated the proportion and characteristics of severe *C. striatum* pneumonia compared with severe MRSA pneumonia. Although the proportion of severe MRSA HAP greatly decreased during 2014–2019, the proportion of severe *C. striatum* pneumonia sharply increased and surpassed that of severe MRSA pneumonia. *C. striatum* pneumonia was more commonly associated with immunocompromise, viral co-infection, and fungal co-infection. Mortality rates between the *C. striatum* and MRSA groups were comparable.

We found that the proportion of severe MRSA pneumonia decreased while severe *C. striatum* pneumonia greatly increased and that *C. striatum* emerged as one of the most common pathogens in patients with severe HAP. Strengthened infection control measures

Table 4. Clinical and laboratory characteristics of patients with severe *Corynebacterium striatum* pneumonia and methicillin-resistant *Staphylococcus aureus* pneumonia, Seoul, South Korea, 2014–2019*

Characteristics	Total, n = 130	*C. striatum*, n = 27	MRSA, n = 103	p value
Clinical manifestation				
Dyspnea	106 (81.5)	25 (92.6)	81 (78.6)	0.16
Fever, temperature >38°C	103 (79.2)	18 (66.7)	85 (82.5)	0.07
Sputum	92 (70.8)	16 (59.3)	76 (73.8)	0.14
Cough	57 (43.8)	11 (40.7)	46 (44.7)	0.72
Altered mental status	46 (35.4)	10 (37.0)	36 (35.0)	0.84
Diarrhea	4 (3.1)	2 (7.4)	2 (1.9)	0.19
Septic shock at ICU admission	81 (62.3)	12 (44.4)	69 (67.0)	0.03
Mechanical ventilation	127 (97.7)	27 (100)	100 (97.1)	1.00
APACHE II score, mean (SD)	25.6 (8.1)	26.4 (11.9)	26.0 (7.0)	0.72
SOFA score, mean (SD)	9.5 (3.7)	9.5 (3.4)	9.5 (3.7)	0.99
Bacteremia	19 (14.6)	1 (3.7)	18 (17.5)	0.12
Laboratory findings, median (IQR)				
Leukocyte count, cells/mL	10,950 (7,800–15,625)	11,600 (4,800–15,900)	10,700 (8,400–15,600)	0.26
Platelets, $\times 10^3$/mL	159 (81–242)	123 (55–230)	171 (102–245)	0.14
C-reactive protein, mg/dL	11.3 (5.5–19.3)	13.6 (8.0–19.8)	10.8 (5.4–18.6)	0.61
Procalcitonin, ng/mL	1.1 (0.3–3.9)	0.3 (0.1–1.3)	1.8 (0.4–4.2)	<0.01

*Values are no. (%) except as indicated APACHE, acute physiology and chronic health evaluation; BAL, bronchoalveolar lavage; ICU, intensive care unit; IQR, interquartile range; MRSA, methicillin-resistant *Staphylococcus aureus*; SOFA, sequential organ failure assessment.

during the study period might have contributed to the decline of severe MRSA pneumonia (*18*); however, severe *C. striatum* pneumonia demonstrated the opposite trend. Several possible explanations for this discrepancy exist. First, detection of *C. striatum* from respiratory specimens in clinical laboratories increased, possibly because experience among laboratory staff accumulated over time. Also, new reliable identification techniques, such as matrix-assisted laser desorption/ionization time-of-flight mass spectrometry, were introduced and enabled precise and rapid detection and identification of bacteria in clinical samples, which might have contributed to the increased reports of severe *C. striatum* pneumonia (*19*,*20*). Second, *C. striatum* can be resistant to infection control measures and can adhere to abiotic surfaces and form biofilms on various medical devices, such as feeding tubes, endotracheal tubes, and ventilators (*21*,*22*). Some reports documented *C. striatum* strains with resistance to high-level disinfectants, such as 2% glutaraldehyde and other biocides (*23*,*24*). These findings suggest that appropriate environmental infection control measures for *C. striatum* should be further investigated and implemented. Finally, hospital outbreaks also might have contributed to the seeming discrepancy. Colonized patients and contaminated inanimate objects could be reservoirs for prolonged outbreaks. However, when we chronologically analyzed the occurrence patterns according to time and place, we could not find any suggestions of notable outbreaks. Clinical observation alone creates difficulties and limitations in distinguishing outbreaks; therefore, future studies should include more detailed

Table 5. Outcomes of adult patients with severe *Corynebacterium striatum* and methicillin-resistant *Staphylococcus aureus* pneumonia, Seoul, South Korea, 2014–2019*

Outcome	Total, n = 130	*C. striatum*, n = 27	MRSA, n = 103	p value
Death				
Total	n = 103	n = 27	n = 103	NA
30 days	41 (31.5)	11 (40.7)	30 (29.1)	0.25
60 days	57 (43.8)	14 (48.1)	44 (42.7)	0.61
90 days	68 (52.3)	16 (59.3)	52 (50.5)	0.42
In-hospital	73 (56.2)	19 (70.4)	54 (52.4)	0.09
Death among patient categories				
Nonimmunocompromised patients	n = 89	n = 13	n = 76	NA
30 days	21 (23.6)	5 (38.5)	16 (21.1)	0.18
60 days	31 (34.8)	5 (38.5)	26 (34.2)	0.76
90 days	40 (44.9)	7 (53.8)	33 (43.4)	0.49
In-hospital	40 (44.9)	7 (53.8)	33 (43.4)	0.49
Immunocompromised patients	n = 41	n = 14	n = 27	NA
30 days	20 (48.8)	6 (42.9)	14 (51.9)	0.59
60 days	26 (63.4)	8 (57.1)	18 (66.7)	0.55
90 days	28 (68.3)	9 (64.3)	19 (70.4)	0.73
In-hospital	33 (80.5)	12 (85.7)	21 (77.8)	0.69
Median ICU stay, d (IQR)	14.0 (8.0–26.3)	14.0 (9.0–27.0)	14.0 (8.0–26.0)	0.33
Median hospital stay after ICU admission, d (IQR)	29.5 (14.0–57.0)	30.0 (16.0–81.0)	29.0 (14.0–55.0)	0.48

*Values are no. (%) except as indicated. ICU, intensive care unit; MRSA, methicillin-resistant *Staphylococcus aureus*; NA, not applicable.

typing analysis of *C. striatum* isolates to identify and curb possible healthcare-associated outbreaks.

In this study, viral or fungal co-infection was more common in the *C. striatum* group, whereas other bacterial co-infection was more common in the MRSA group. This finding could represent the host factor because a greater proportion of *C. striatum* patients were in an immunocompromised state, which would make them vulnerable to opportunistic infections. Of note, fewer cases of bacterial coinfection were diagnosed in the *C. striatum* group, but the cause for this difference is uncertain. One possible explanation is that *C. striatum* might influence the behavior and fitness of other bacteria. A recent study reported that *Corynebacterium* species can reduce the toxicity of *Staphylococcus aureus* by exhibiting decreased hemolysin activity and displaying diminished fitness of in vivo coinfection (*25*). Further targeted studies on this issue are needed.

We found that serum procalcitonin level was higher in the MRSA group than in the *C. striatum* group (median 1.8 ng/mL vs. 0.3 ng/mL). Some studies suggest that serum procalcitonin can be used as a marker for bacterial infection and to differentiate bacterial from viral infection or noninfectious causes of inflammation (*26*,*27*). In 2017, a group of researchers in China reported that the median serum procalcitonin level of an *S. aureus* bacteremia group of patients was higher (1.18 ng/mL) than that of a coagulase-negative staphylococci bacteremia group (0.21–0.31 ng/mL) (*28*). We speculate that infections caused by low-virulence bacteria, such as *C. striatum* in our study, might have low levels of procalcitonin and this warrants further investigation.

Mortality rates were similarly high in both groups, but septic shock at the time of initial clinical manifestation was less common in the *C. striatum* group. Immunocompromised conditions were more common in the *C. striatum* group, which could suggest that *C. striatum* is less virulent than MRSA. Host factor might contribute to the development of severe *C. striatum*–associated pneumonia and the subsequent outcomes; however, we noted no statistically significant differences in mortality rates between the 2 groups after stratification by immunocompromised conditions. The existence of co-infection and pathogen types (e.g., other bacteria, viruses, fungi) involved might have affected mortality rates, but we were unable to effectively evaluate each effect because of the small number of patients in each subgroup.

The first limitation of our study is that we used a single-center design and our results might not be replicable in other centers or hospital systems. In addition, as we mentioned previously, we were not able to effectively evaluate the sole contribution of *C. striatum* because co-infection with other pathogens was common among the patient cohort. Finally, we included all *C. striatum* isolates from sputum, endotracheal aspirate, and bronchoalveolar lavage, but the cultures were mostly semiquantitative, and some of the *C. striatum* isolates might have been nonpathogenic colonizers. A 2020 study from the United States reported that normal respiratory flora appears to have caused one quarter of CAP cases (*29*), which supports our finding that bacteria previously considered as colonizers or normal flora can be a cause of pneumonia.

In conclusion, we found *C. striatum* was associated with severe HAP. Patients with severe *C. striatum* pneumonia showed similar clinical and laboratory features as patients with severe MRSA pneumonia, and both infections were associated with high mortality rates. Further investigations could clarify incidence, clinical characteristics, and outcomes of severe *C. striatum* pneumonia in critically ill adults and determine whether infections are due to colonization, or community- or healthcare-acquired infections. Clinicians should be aware of this emerging pathogen as a possible cause for severe pneumonia, especially among immunocompromised patients.

This work was supported by the Asan Institute of Life Sciences (grant no. 2010-0079) and generous gifts from Sam Won Song.

About the Author

Dr. Lee is a physician at Asan Medical Center, University of Ulsan College of Medicine in Seoul, South Korea. Her research interests include infectious diseases and clinical microbiology. Dr. Huh is an intensivist and professor at Asan Medical Center, University of Ulsan College of Medicine in Seoul, South Korea. Her main research interest is the pathogenesis and management of acute respiratory distress syndrome.

References

1. Funke G, von Graevenitz A, Clarridge JE III, Bernard KA. Clinical microbiology of coryneform bacteria. Clin Microbiol Rev. 1997;10:125–59. https://doi.org/10.1128/CMR.10.1.125
2. Chen FL, Hsueh PR, Teng SO, Ou TY, Lee WS. *Corynebacterium striatum* bacteremia associated with central venous catheter infection. J Microbiol Immunol Infect. 2012;45:255–8. https://doi.org/10.1016/j.jmii.2011.09.016
3. Hong HL, Koh HI, Lee AJ. Native valve endocarditis due to *Corynebacterium striatum* confirmed by 16S ribosomal RNA sequencing: a case report and literature review. Infect Chemother. 2016;48:239–45. https://doi.org/10.3947/ic.2016.48.3.239
4. Bowstead TT, Santiago SM Jr. Pleuropulmonary infection due to *Corynebacterium striatum*. Br J Dis Chest. 1980;74:198–200. https://doi.org/10.1016/0007-0971(80)90035-2

5. Díez-Aguilar M, Ruiz-Garbajosa P, Fernández-Olmos A, Guisado P, Del Campo R, Quereda C, et al. Non-diphtheriae *Corynebacterium* species: an emerging respiratory pathogen. Eur J Clin Microbiol Infect Dis. 2013;32:769–72. https://doi.org/10.1007/s10096-012-1805-5
6. Yang K, Kruse RL, Lin WV, Musher DM. Corynebacteria as a cause of pulmonary infection: a case series and literature review. Pneumonia (Nathan). 2018;10:10. https://doi.org/10.1186/s41479-018-0054-5
7. Choi SH, Hong SB, Ko GB, Lee Y, Park HJ, Park SY, et al. Viral infection in patients with severe pneumonia requiring intensive care unit admission. Am J Respir Crit Care Med. 2012; 186:325–32. https://doi.org/10.1164/rccm.201112-2240OC
8. Hong HL, Hong SB, Ko GB, Huh JW, Sung H, Do KH, et al. Viral infection is not uncommon in adult patients with severe hospital-acquired pneumonia. PLoS One. 2014;9:e95865. https://doi.org/10.1371/journal.pone.0095865
9. Choi SH, Hong SB, Hong HL, Kim SH, Huh JW, Sung H, et al. Usefulness of cellular analysis of bronchoalveolar lavage fluid for predicting the etiology of pneumonia in critically ill patients. PLoS One. 2014;9:e97346. https://doi.org/10.1371/journal.pone.0097346
10. Choi SH, Huh JW, Hong SB, Lee JY, Kim SH, Sung H, et al. Clinical characteristics and outcomes of severe rhinovirus-associated pneumonia identified by bronchoscopic bronchoalveolar lavage in adults: comparison with severe influenza virus-associated pneumonia. J Clin Virol. 2015;62:41–7. https://doi.org/10.1016/j.jcv.2014.11.010
11. American Thoracic SocietyInfectious Diseases Society of America. Guidelines for the management of adults with hospital-acquired, ventilator-associated, and healthcare-associated pneumonia. Am J Respir Crit Care Med. 2005; 171:388–416. https://doi.org/10.1164/rccm.200405-644ST
12. Mandell LA, Wunderink RG, Anzueto A, Bartlett JG, Campbell GD, Dean NC, et al.; Infectious Diseases Society of America; American Thoracic Society. Infectious Diseases Society of America/American Thoracic Society consensus guidelines on the management of community-acquired pneumonia in adults. Clin Infect Dis. 2007;44:S27–72. https://doi.org/10.1086/511159
13. Carratalà J, Mykietiuk A, Fernández-Sabé N, Suárez C, Dorca J, Verdaguer R, et al. Health care-associated pneumonia requiring hospital admission: epidemiology, antibiotic therapy, and clinical outcomes. Arch Intern Med. 2007;167:1393–9. https://doi.org/10.1001/archinte.167.13.1393
14. Singer M, Deutschman CS, Seymour CW, Shankar-Hari M, Annane D, Bauer M, et al. The third international consensus definitions for sepsis and septic shock (Sepsis-3). JAMA. 2016;315:801–10. https://doi.org/10.1001/jama.2016.0287
15. Micek ST, Kollef KE, Reichley RM, Roubinian N, Kollef MH. Health care-associated pneumonia and community-acquired pneumonia: a single-center experience. Antimicrob Agents Chemother. 2007;51:3568–73. https://doi.org/10.1128/AAC.00851-07
16. Gilligan PH, Alby K, York MK. Respiratory tract cultures. In: Leber AL, editor. Clinical microbiology procedures handbook, 4th edition, volume 1. Washington: ASM Press; 2016. pp. 3.11.1.1–9.4.
17. Clinical and Laboratory Standards Institute. Methods for antimicrobial dilution and disk susceptibility testing of infrequently isolated or fastidious bacteria, third edition (M45). Wayne (PA): The Institute; 2016.
18. Kim H, Kim ES, Lee SC, Yang E, Kim HS, Sung H, et al. Decreased Incidence of methicillin-resistant *Staphylococcus aureus* bacteremia in intensive care units: a 10-year clinical, microbiological, and genotypic analysis in a tertiary hospital. Antimicrob Agents Chemother. 2020;64:e01082-20. https://doi.org/10.1128/AAC.01082-20
19. Khamis A, Raoult D, La Scola B. Comparison between *rpoB* and 16S rRNA gene sequencing for molecular identification of 168 clinical isolates of *Corynebacterium*. J Clin Microbiol. 2005; 43:1934–6. https://doi.org/10.1128/JCM.43.4.1934-1936.2005
20. Vila J, Juiz P, Salas C, Almela M, de la Fuente CG, Zboromyrska Y, et al. Identification of clinically relevant *Corynebacterium* spp., *Arcanobacterium haemolyticum*, and *Rhodococcus equi* by matrix-assisted laser desorption ionization-time of flight mass spectrometry. J Clin Microbiol. 2012;50:1745–7. https://doi.org/10.1128/JCM.05821-11
21. Souza C, Faria YV, Sant'Anna LO, Viana VG, Seabra SH, Souza MC, et al. Biofilm production by multiresistant *Corynebacterium striatum* associated with nosocomial outbreak. Mem Inst Oswaldo Cruz. 2015;110:242–8. https://doi.org/10.1590/0074-02760140373
22. Ramos JN, Souza C, Faria YV, da Silva EC, Veras JFC, Baio PVP, et al. Bloodstream and catheter-related infections due to different clones of multidrug-resistant and biofilm producer *Corynebacterium striatum*. BMC Infect Dis. 2019;19:672. https://doi.org/10.1186/s12879-019-4294-7
23. Souza C, Mota HF, Faria YV, Cabral FO, Oliveira DR, Sant'Anna LO, et al. Resistance to antiseptics and disinfectants of planktonic and biofilm-associated forms of *Corynebacterium striatum*. Microb Drug Resist. 2020;26:1546–58. https://doi.org/10.1089/mdr.2019.0124
24 Silva-Santana G, Silva CMF, Olivella JGB, Silva IF, Fernandes LMO, Sued-Karam BR, et al. Worldwide survey of *Corynebacterium striatum* increasingly associated with human invasive infections, nosocomial outbreak, and antimicrobial multidrug-resistance, 1976–2020. Arch Microbiol. 2021;203:1863–80. https://doi.org/10.1007/s00203-021-02246-1
25. Ramsey MM, Freire MO, Gabrilska RA, Rumbaugh KP, Lemon KP. *Staphylococcus aureus* shifts toward commensalism in response to *Corynebacterium* species. Front Microbiol. 2016;7:1230. https://doi.org/10.3389/fmicb.2016.01230
26. Simon L, Gauvin F, Amre DK, Saint-Louis P, Lacroix J. Serum procalcitonin and C-reactive protein levels as markers of bacterial infection: a systematic review and meta-analysis. Clin Infect Dis. 2004;39:206–17. https://doi.org/10.1086/421997
27. Limper M, de Kruif MD, Duits AJ, Brandjes DP, van Gorp EC. The diagnostic role of procalcitonin and other biomarkers in discriminating infectious from non-infectious fever. J Infect. 2010;60:409–16. https://doi.org/10.1016/j.jinf.2010.03.016
28. Yan ST, Sun LC, Jia HB, Gao W, Yang JP, Zhang GQ. Procalcitonin levels in bloodstream infections caused by different sources and species of bacteria. Am J Emerg Med. 2017;35:579–83. https://doi.org/10.1016/j.ajem.2016.12.017
29. Musher DM, Jesudasen SS, Barwatt JW, Cohen DN, Moss BJ, Rodriguez-Barradas MC. Normal respiratory flora as a cause of community-acquired pneumonia. Open Forum Infect Dis. 2020;7:ofaa307. https://doi.org/10.1093/ofid/ofaa307

Address for correspondence: Sang-Ho Choi, Department of Infectious Diseases, Asan Medical Center, 88 Olympic-Ro 43-Gil Pungnap-dong, Songpa-gu, Seoul 05505, South Korea; email: sangho@amc.seoul.kr

Multispecies Outbreak of *Nocardia* Infections in Heart Transplant Recipients and Association with Climate Conditions, Australia

Jonathan Li, Cindy Lau, Naomi Anderson, Fay Burrows, Feras Mirdad, Lilibeth Carlos, Andrew J. Pitman, Kavitha Muthiah, David R. Darley, David Andresen, Peter Macdonald, Deborah Marriott,[1] Nila J. Dharan[1]

In support of improving patient care, this activity has been planned and implemented by Medscape, LLC and Emerging Infectious Diseases. Medscape, LLC is jointly accredited with commendation by the Accreditation Council for Continuing Medical Education (ACCME), the Accreditation Council for Pharmacy Education (ACPE), and the American Nurses Credentialing Center (ANCC), to provide continuing education for the healthcare team.

Medscape, LLC designates this Journal-based CME activity for a maximum of 1.00 ***AMA PRA Category 1 Credit(s)™***. Physicians should claim only the credit commensurate with the extent of their participation in the activity.

Successful completion of this CME activity, which includes participation in the evaluation component, enables the participant to earn up to 1.0 MOC points in the American Board of Internal Medicine's (ABIM) Maintenance of Certification (MOC) program. Participants will earn MOC points equivalent to the amount of CME credits claimed for the activity. It is the CME activity provider's responsibility to submit participant completion information to ACCME for the purpose of granting ABIM MOC credit.

All other clinicians completing this activity will be issued a certificate of participation. To participate in this journal CME activity: (1) review the learning objectives and author disclosures; (2) study the education content; (3) take the post-test with a 75% minimum passing score and complete the evaluation at http://www.medscape.org/journal/eid; and (4) view/print certificate. For CME questions, see page 2373.

Release date: October 21, 2022; Expiration date: October 21, 2023

Learning Objectives

Upon completion of this activity, participants will be able to:

- Compare patient demographic characteristics, host risk factors (underlying medical conditions, rejection rates, immunosuppressive regimens), and antimicrobial prophylaxis regimens in heart transplant recipients and lung transplant recipients with *Nocardia* infections, based on a retrospective review of an outbreak of *Nocardia* infections in heart transplant recipients at St Vincent's Hospital, Australia, between 2018 and 2019
- Assess climate characteristics during the time of the outbreak of *Nocardia* infections in heart transplant recipients at St Vincent's Hospital, Australia between 2018 and 2019, based on a retrospective review
- Evaluate clinical and public health implications of clinical factors and climate conditions in an outbreak of *Nocardia* infections in heart transplant recipients at St Vincent's Hospital, Australia between 2018 and 2019, based on a retrospective review

CME Editor

Dana C. Dolan, BS, Technical Writer/Editor, Emerging Infectious Diseases. *Disclosure: Dana C. Dolan, BS, has disclosed no relevant financial relationships.*

CME Author

Laurie Barclay, MD, freelance writer and reviewer, Medscape, LLC. *Disclosure: Laurie Barclay, MD, has the following relevant financial relationships: formerly owned stocks in AbbVie Inc.*

Authors

Jonathan Li, MD; Cindy Lau, BPharm; Naomi Anderson, RN; Fay Burrows, GradDipPharmPrac; Feras Mirdad, MBBS; Lilibeth Carlos, BPharm; Andrew Pitman, PhD; Kavitha Muthiah, MBChB, PhD; David R. Darley, MBBS; David Andresen, MBBS; Peter Macdonald, MBBS, PhD; Deborah Marriott, MBBS, PhD; and ***Nila J. Dharan, MD, PhD.***

Author affiliations: St Vincent's Hospital Sydney, Darlinghurst, New South Wales, Australia (J. Li, C. Lau, N. Anderson, F. Burrows, F. Mirdad, L. Carlos, K. Muthiah, D.R. Darley, D. Andresen, P. Macdonald, D. Marriott, N.J. Dharan); Australian Research Council Centre of Excellence for Climate Extremes and Climate Change Research Centre, at UNSW Sydney, Sydney, New South Wales(A.J. Pitman); Victor Chang Cardiac Research Institute, Darlinghurst (K. Muthiah, P. Macdonald); UNSW Sydney, Sydney (D.R. Darley, N.J. Dharan); University of Notre Dame, Sydney (D. Andresen)

DOI: https://doi.org/10.3201/eid2811.220262

[1]These authors contributed equally to this article.

A multispecies outbreak of *Nocardia* occurred among heart transplant recipients (HTR), but not lung transplant recipients (LTR), in Sydney, New South Wales, Australia, during 2018–2019. We performed a retrospective review of 23 HTR and LTR who had *Nocardia* spp. infections during June 2015–March 2021, compared risk factors for *Nocardia* infection, and evaluated climate conditions before, during, and after the period of the 2018–2019 outbreak. Compared with LTR, HTR had a shorter median time from transplant to *Nocardia* diagnosis, higher prevalence of diabetes, greater use of induction immunosuppression with basiliximab, and increased rates of cellular rejection before *Nocardia* diagnosis. During the outbreak, Sydney experienced the lowest monthly precipitation and driest surface levels compared with time periods directly before and after the outbreak. Increased immunosuppression of HTR compared with LTR, coupled with extreme weather conditions during 2018–2019, may explain this outbreak of *Nocardia* infections in HTR.

Nocardia is an environmental aerobic actinobacterium (*Actinomycete*) that stains positive on Gram stain and forms commonly in soil and water. Infection is primarily acquired through inhalation; however, it may also occur through direct inoculation into the skin or via ingestion of the microorganism (*1*,*2*). Depending on the route of infection, clinical manifestations may include pulmonary, cutaneous, intravenous line infections, and disseminated disease, which frequently involves the nervous system and skeletal or soft-tissue structures (*1*,*2*). Noncutaneous disease is most commonly reported in immunocompromised persons such as solid organ transplant recipients; recent studies showed the greatest risk is among lung transplant recipients (LTR, 3.5%) followed by heart transplant recipients (HTR, 2.5%) (*3*). Treatment in immunocompromised patients is generally for a minimum period of 6 months. Nocardiosis in solid organ transplant recipients is associated with a 10-fold increase in 1-year mortality rate (16.2%, compared with 1.3% in recipients without nocardiosis) (*4*).

In January 2018, an increased rate of *Nocardia* infections was noted among HTR at St Vincent's Hospital in Sydney, New South Wales (NSW), Australia, but not among LTR who underwent transplants during the same timeframe. The rise in *Nocardia* infections coincided with a period of extreme weather conditions in NSW; 2018 was the second warmest and seventh driest year, and 2019 was the warmest and driest year on record in NSW (*5*,*6*). Similar extreme weather patterns were experienced across the rest of Australia (*7*,*8*). Previous studies have observed that *Nocardia* infections occur more frequently in dry and windy climates, such as that of the Southwest region of the United States (*1*,*9*). Such climate conditions are thought to increase aerosolization of *Nocardia* organisms from soil, increasing the possibility of inhalation and therefore subsequent infection (*1*,*9*,*10*).

We report an outbreak of *Nocardia* infections in HTR at St Vincent's Hospital during January 2018–August 2019. Because *Nocardia* infections in LTR did not increase during that period, we sought to compare patient demographic characteristics, host risk factors (underlying medical conditions, rejection rates, immunosuppressive regimens), and antimicrobial prophylaxis regimens for HTR and LTR. In addition, because *Nocardia* is an environmental organism and the outbreak occurred during some of the driest years recorded in Australia, we sought to characterize climate characteristics during the time of the outbreak (*7*,*8*). St Vincent's Hospital Human Research Ethics Committee reviewed and approved the study.

Methods

Study Population and Clinical Data

We conducted a retrospective review of *Nocardia* infections among HTR and LTR at St Vincent's Hospital, Sydney. We defined a *Nocardia* case as a microbiological diagnosis of *Nocardia* in an HTR or LTR during June 2015–March 2021. Data before June 2015 were unavailable for extraction. We used the center point of a case-patient's residential suburb as a proxy for case location to define a geographic cluster of cases as those located ≤5 km from the center of each cluster. We extracted clinical data from the patients' medical records for the date of transplantation, date of *Nocardia* diagnosis, *Nocardia* species identified, site of infection, antimicrobial prophylaxis, diagnosis of other respiratory infections or cytomegalovirus (CMV) in the previous 6 months, intravenous immunoglobulin therapy, induction and maintenance immunosuppression regimens, donor and recipient CMV status, and organ rejection rates.

We defined CMV mismatch as a heart or lung transplant from a CMV-positive donor to a CMV-negative recipient. We defined CMV viremia as detectable CMV DNA (≥34.5 IU/mL by Roche cobas 6800 [https://www.roche.com] CMV DNA quantitative PCR) in the 6 months preceding the *Nocardia* diagnosis. We defined significant CMV viremia as having a highest CMV DNA PCR value in the 6 months preceding *Nocardia* diagnosis >1,000 IU/mL. We defined respiratory infections by microbiological detection of pathogen using a multiplex PCR EasyScreen respiratory assay (Genetic Signatures, https://geneticsignatures.com) targeting 12 pathogens: influenza

A and B, respiratory syncytial virus, parainfluenza, adenovirus, rhinovirus, metapneumovirus, seasonal coronaviruses, enterovirus, *Pneumocystis jirovecii*, *Mycoplasma pneumoniae*, and *Bordetella pertussis*.

We defined organ rejection as grade 1R or greater on endomyocardial biopsy for HTR and grade A1 or greater on transbronchial biopsy for LTR, in accordance with the International Society of Heart and Lung Transplantation 2004 and 2007 grading guidelines (*11*,*12*). At St Vincent's Hospital, routine surveillance biopsies are performed for HTR at weeks 1, 2, 3, 4, 6, 8, and 10 and months 4, 5, 6, 8, and 10 posttransplant, and at any other time for clinically suspected rejection. In LTR, routine surveillance biopsies are performed at weeks 3, 6, and 12 posttransplant (and at week 9 if there is evidence of rejection at week 6 for early follow-up), and at any other time for substantial declines in forced expiratory volume in 1 second or for any clinically suspected rejection. In general, HTR and LTR are managed for life at our institution for any serious posttransplant complications such as opportunistic infections.

Microbiology

We isolated *Nocardia* from induced sputum, bronchoalveolar lavage, and tissue biopsies by routine culture-based methods, including inoculation onto nonselective and enriched agar media such as horse blood, chocolate blood, and buffered charcoal yeast extract agar and incubated at 35°C. Preliminary identification was based on colony morphology, Gram stain appearance and a positive modified acid-fast stain. Mass spectrometry confirmed the identification of *Nocardia* to the genus level. Species-level identification was performed by the Institute for Clinical Pathology and Medical Research at Westmead Hospital (Sydney, NSW, Australia) and was determined by PCR and DNA sequencing of partial 5′ 16s rRNA and *Nocardia secA1* gene.

We determined in vitro antibiotic susceptibility testing by broth microdilution using a Thermo Scientific sensititer RAPMYCO AST panel (TREK Diagnostic Systems Ltd., https://www.trekds.co), performed at the reference laboratory according to manufacturer's instructions. The antimicrobial agents tested were amoxicillin/clavulanic acid, amikacin, cefepime, cefoxitin, ceftriaxone, ciprofloxacin, clarithromycin, sulphamethoxazole, doxycycline, imipenem, linezolid, minocycline, tigecycline, and tobramycin.

Climate Data Sources

We obtained meteorological data of monthly precipitation (mm/mo), temperature (°C), windspeed (m/sec), and evaporation (mm/mo) over the period June 2015–March 2021 from the European Centre for Medium-Range Weather Forecasts reanalysis (ERA5) (*13*) for each suburb in which *Nocardia* patients resided. ERA5 is based on the Integrated Forecasting System Cy41r2, a global numerical weather prediction system. The ERA5 reanalyses provide a gridded set of consistent daily meteorological data from 1950 through the present at 31 km spatial resolution (*13*).

We defined dryness as the ratio of actual evaporation to potential evaporation, reflecting the moisture content of the surface, such that values near 0 indicate a very dry surface, whereas values near 1.0 indicate a saturated surface. We derived erodibility as (1 – dryness) × windspeed and calculated normalized erodibility by dividing each suburb's erodibility by the highest erodibility value experienced across all suburbs. We normalized erodibility and windspeed to transfer the spatial patterns to a 0.0–1.0 scale, which enabled us to differentiate relatively erodible locations (dry and windy) from those where erosion is likely to be low (wet and still). We chose a central location in Greater Sydney, the suburb of Greystanes, as the reference site to compare meteorological reanalysis data for all *Nocardia* infections in Greater Sydney. The benchmark for Australia and NSW comparisons was averaged values during 1961–1990 because this period includes the satellite record that is important for the reanalyses and is used as the global standard period for comparison globally (*13*).

Statistical Analyses

We performed Mann-Whitney U test to compare the median age at *Nocardia* diagnosis and the median time from transplant to diagnosis in HTR and LTR. We performed a z-score test for 2 population proportions to compare demographic, clinical, and microbiologic characteristics between HTR and LTR. We used a 1-way analysis of variance test to compare differences in the meteorological reanalysis data in Greater Sydney in the periods of June 2015–December 2017 (before the outbreak), January 2018–December 2019 (during the outbreak) and January 2020–March 2021 (after the outbreak). We considered a p value <0.05 statistically significant. We analyzed all data using Microsoft Excel version 16.53 with Analysis ToolPak (Microsoft, https://www.microsoft.com).

Results

We identified a total of 23 cases of *Nocardia* in heart and lung transplant recipients at St Vincent's Hospital during June 2015–March 2021; of those, 16 were HTR and 7 were LTR (Figure 1, panel A). Compared with

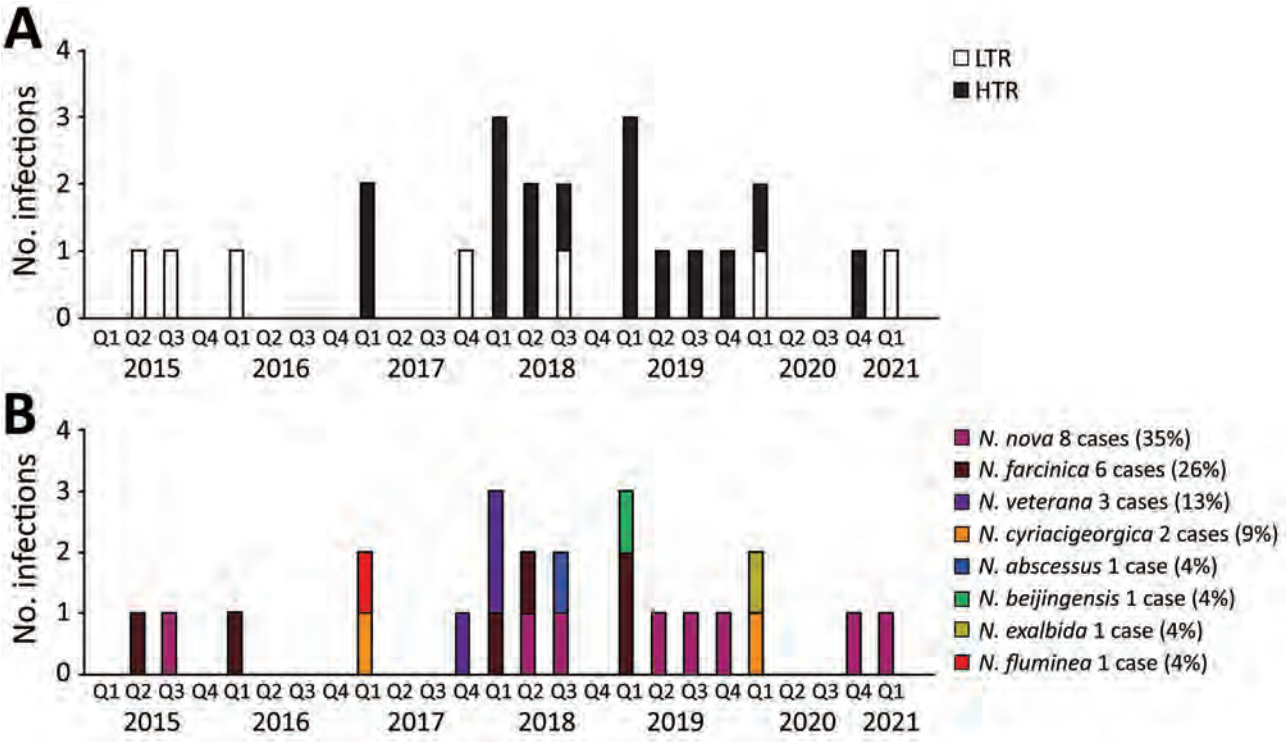

Figure 1. *Nocardia* infections among HTR and LTR, by date of first positive specimen, Greater Sydney, New South Wales, Australia, June 2015–March 2021. During June 2015–December 2017, there were 6 *Nocardia* cases (0.19/mo), of which 2 (33%) were in HTR. During January 2018–December 2019, there were 13 *Nocardia* case-patients (0.54/mo), of which 12 (92%) were in HTR. During January 2020–March 2021, there were 4 *Nocardia* cases (0.26 per month) of which 2 (50%) were HTR. A) *Nocardia* cases over time by type of transplant. B) *Nocardia* cases over time by *Nocardia* species. HTR, heart transplant recipient; LTR, lung transplant recipient.

the years before and after the outbreak period (2018–2019), we saw no significant change in the annual total of heart and lung transplants performed (40–50/year). Over the entire study period, the total number of transplants performed was similar across the 2 services: 289 lung transplants and 275 heart transplants. There was no increase in the number of cases of *Nocardia* across other hospital departments during the study period: 2 cases during the preoutbreak period (June 2015–December 2017), 3 during the outbreak period (January 2018–December 2019), and 2 during the postoutbreak period (January 2020–March 2021).

Overall, the median age at *Nocardia* diagnosis was 59 (range 38–71) years; 15 (65.2%) patients were male (Table 1). Sites of *Nocardia* infection were lung (11 HTR, 4 LTR); bloodstream (1 HTR); skin (1 HTR); lung and bloodstream (1 LTR); lung and brain (2 HTR); skin and brain (1 LTR); lung, skin, and brain (1 LTR); and lung, brain, and kidney (1 HTR).

When comparing heart and lung transplant recipients, we saw no substantial differences in age at *Nocardia* diagnosis, sex, CMV mismatch status, use of intravenous immunoglobulin, CMV viremia, significant CMV viremia, diagnosis of other respiratory infections within 6 months preceding the *Nocardia* diagnosis, or use of sulfamethoxazole/trimethoprim for *Pneumocystis jirovecii* prophylaxis. In addition, all heart and lung transplant recipients received a similar combination of maintenance immunosuppression therapy with tacrolimus, mycophenolate mofetil, and prednisone.

We identified significant differences between LTR and HTR that suggested greater immunosuppression in HTR before and at the time of *Nocardia* diagnosis (Table 1). These differences included a shorter median time from transplant to *Nocardia* diagnosis (4.8 months, vs. 22.8 months in LTR; $p<0.05$), higher prevalence of diabetes at the time of *Nocardia* diagnosis (81.3%, vs. 28.6% in LTR; $p<0.05$), greater use of basiliximab for induction immunosuppression (100%, vs. 40.0% in LTR; $p<0.05$), increased rates of any grade of cellular rejection at any time before *Nocardia* diagnosis (100%, vs. 42.9% in LTR; $p<0.05$), and increased rates of moderate to severe rejection at any time before *Nocardia* diagnosis (62.5%, vs. 0 in LTR; $p<0.05$). In addition, azithromycin prophylaxis rates were lower in HTR (6.25%) than in LTR (100%) ($p<0.05$).

We found no significant difference in the types of *Nocardia* species between HTR and LTR (Table 2)

Table 1. Clinical characteristics of heart and lung transplant recipients with confirmed *Nocardia* infection, Greater Sydney, New South Wales, Australia, June 2015–March 2021*

Characteristic	Heart transplant, n = 16	Lung transplant, n = 7	p value	All patients, n = 23
Median age at *Nocardia* diagnosis, y (range)	61 (38–71)	59 (50–70)	0.98	61 (38–71)
Sex				
M	10 (62.5)	5 (71.4)	0.68	15 (65.2)
F	6 (37.5)	2 (28.6)	0.68	8 (34.8)
Median no. months from transplant to *Nocardia* diagnosis (range)	4.8 (3–19)	22.8 (5–263)	<0.01	6.3 (3–263)
CMV, donor positive/recipient negative	4 (25.0)	0	0.17	4 (17.4)
Episodes of organ rejection from date of transplant to diagnosis of *Nocardia*				
Any grade†	16 (100)	3 (42.9)	<0.01	19 (82.6)
<2R/A3	6 (37.5)	3 (42.9)	0.81	9 (39.1)
≥2R/A3	10 (62.5)	0	<0.01	10 (43.4)
Diabetic at time of diagnosis	13 (81.3)	2 (28.6)	<0.01	15 (65.2)
Received intravenous immunoglobulin therapy	7 (43.8)	6 (85.7)	0.06	13 (56.5)
Respiratory virus ≤6 mo before *Nocardia*	9 (56.3)	6 (85.7)	0.17	15 (65.2)
CMV DNA detected by PCR ≤6 mo before *Nocardia*	6 (37.5)‡	1 (14.3)§	0.27	7 (30.4)
Significant CMV viremia ≤6 mo before *Nocardia*¶	4 (25.0)	1 (14.3)	0.57	5 (21.7)
Medications received				
Sulfamethoxazole/trimethoprim prophylaxis	13 (81.3)	7 (100)	0.22	20 (87.0)
Azithromycin prophylaxis	1 (6.3)	7 (100)	<0.01	8 (34.8)
Induction with basiliximab	16 (100)	2/5 (40.0)	<0.01	18/21 (85.7)
Tacrolimus immunosuppression	16 (100)	7 (100)	1	23 (100)
Mycophenolic acid immunosuppression	16 (100)	5/5 (100)	1	21/21 (100)
Prednisone immunosuppression	16 (100)	5/5 (100)	1	21/21 (100)

*Values are no. (%) patients except as indicated. Denominators are indicated for categories in which only some patients had data available. CMV, cytomegalovirus.
†Defined as ≥1R on endomyocardial biopsy for heart transplant rejections and ≥A1 on bronchial biopsy for lung transplant rejections in accordance with International Society of Heart and Lung Transplantation 2004 and 2007 grading guidelines.
‡Among heart transplant recipients, the highest CMV PCR values (IU/mL) included: 1,169 copies 3 mo before *Nocardia* diagnosis; 16,271 4 mo before *Nocardia* diagnosis; 4,446 3 mo before *Nocardia* diagnosis; 27,1942 within a month before *Nocardia* diagnosis; 324 within a month before *Nocardia* diagnosis; and 103 within 1 month before *Nocardia* diagnosis.
§The highest CMV PCR value (IU/mL) was 1,240 within a month before *Nocardia* diagnosis.
¶Defined as CMV PCR copies >1,000 IU/mL.

and no apparent clustering of *Nocardia* species over time to suggest a single source of the outbreak (Figure 1, panel B). We also found no differences between HTR and LTR in *Nocardia* susceptibilities to amikacin, amoxicillin/clavulanic acid, ceftriaxone, ciprofloxacin, clarithromycin, doxycycline, imipenem, linezolid, minocycline, moxifloxacin, and tobramycin (Table 3). *Nocardia* in LTR were more likely to be susceptible to cefepime than in HTR (50% vs. 6.7%; p<0.05), however, this difference may have been related to differences in *Nocardia* species across type of transplant.

Six *Nocardia* cases were located outside Greater Sydney, and 17 were within the Greater Sydney region (Figure 2). During June 2015–March 2021, no *Nocardia* patients changed their residential address within 3 months before *Nocardia* diagnosis. The 6 *Nocardia* cases outside Greater Sydney were situated in northern coastal NSW (n = 4), central NSW (n = 1), and Tasmania (n = 1). In western Sydney, 2 clusters of *Nocardia* were in geographic proximity (Figure 2, panel B). However, those clusters did not represent an outbreak because different species were identified within each cluster and cases diagnosed in the clusters were separated in time by ≥6 months.

Because 74% of cases were from Greater Sydney, our climate data analysis focused on that region. We chose the suburb of Greystanes as the reference location for all climate data comparisons because of its central geographic location. Five *Nocardia* cases were reported from Greater Sydney

Table 2. Comparison of *Nocardia* species infecting heart and lung transplant recipients, Greater Sydney, New South Wales, Australia, June 2015–March 2021*

Nocardia species	Heart transplant, n = 16	Lung transplant, n = 7	p value	All patients, n = 23
N. abscessus	0	1 (14)	0.12	1 (4)
N. beijingensis	1 (6)	0	0.50	1 (4)
N. cyriacigeorgica	2 (13)	0	0.33	2 (9)
N. exalbida	0	1 (14)	0.12	1 (4)
N. farcinica	4 (25)	2 (29)	0.85	6 (26)
N. fluminea	1 (6)	0	0.50	1 (4)
N. nova	6 (38)	2 (29)	0.68	8 (35)
N. veterana	2 (13)	1 (14)	0.91	3 (13)

*Values are no. (%) patients except as indicated.

Table 3. Comparison of the number and proportion of *Nocardia* isolates susceptible to select antimicrobial drugs between heart and lung transplant recipients, Greater Sydney, New South Wales, Australia, June 2015–March 2021*

Drug	Heart transplant, n = 16	Lung transplant, n = 7	p value	All patients, n = 23
Amikacin	16 (100)	7 (100)	Referent	23 (100)
Augmentin	0	0/6	Referent	0/22 (0)
Cefepime	1/15 (6.7)	3/6 (50.0)	0.02	4/21 (19.0)
Ceftriaxone	3 (18.8)	4 (57.1)	0.07	7 (30.4)
Ciprofloxacin	4 (25.0)	1 (14.3)	0.57	5 (21.7)
Clarithromycin	10 (62.5)	4 (57.1)	0.81	14 (60.9)
Doxycycline	1/15 (6.7)	2 (28.6)	0.16	3/22 (13.6)
Imipenem	7 (43.8)	3 (42.9)	0.97	10 (43.5)
Linezolid	16 (100)	7 (100)	Referent	23 (100)
Minocycline	1 (6.3)	2 (28.6)	0.14	3 (13.0)
Moxifloxacin	4 (25.0)	1/6 (16.7)	0.68	5/22 (22.7)
Tobramycin	4 (25.0)	2/6 (33.3)	0.70	6/22 (27.3)]
Sulfamethoxazole/trimethoprim	15 (93.8)	7 (100)	0.50	22 (95.7)

*Values are no. (%) patients except as indicated. Denominators are indicated for categories in which only some patients had data available.

during June 2015–December 2017 (0.16/month), of which 1 (20%) was an HTR. During January 2018–December 2019, a total of 11 *Nocardia* cases (0.46/month) were diagnosed, of which 10 (91%) were HTR; during January 2020–March 2021, there was 1 *Nocardia* case (0.07/month) in an HTR (Figure 3). The increased incidence of *Nocardia* from January 2018 to December 2019 occurred during times of lower rainfall and a drier surface (Figure 3).

When comparing averaged values of climate parameters in Greater Sydney between the time of the outbreak (January 2018–December 2019), and the periods before (June 2015–December 2017) and after (January 2020–March 2021), we found the outbreak coincided with average monthly precipitation of 40.0 mm/month, significantly lower than that for the time periods before and after ($p<0.01$) (Table 4). During the same period, average monthly dryness reached its lowest (driest) value of 0.3 compared with the time periods before and after ($p<0.01$). We observed no significant differences in the average monthly temperature, windspeed, or erodibility during the outbreak period (January 2018–December 2019) (Table 4), compared with the time periods before and after. However, when we compared months with a *Nocardia* diagnosis with months without a *Nocardia* diagnosis, windspeed was higher (0.4 vs. 0.2 m/s; $p<0.01$) and surface levels were drier (0.3 vs. 0.4; $p<0.01$); because erodibility is derived from dryness and windspeed, erodibility was also higher

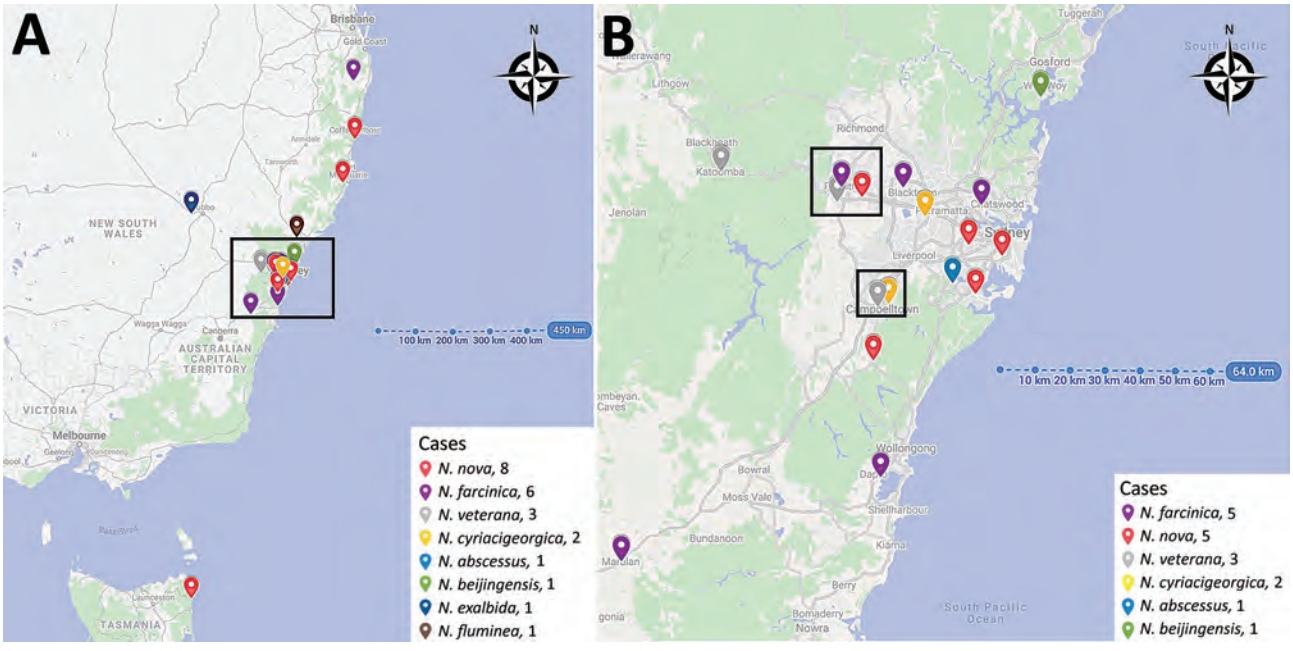

Figure 2. Location of *Nocardia* infections among heart and lung transplant recipients identified at St Vincent's Hospital, Sydney, New South Wales, Australia, June 2015–March 2021. A) All *Nocardia* cases. Box indicates Greater Sydney region. B) All *Nocardia* cases within the Greater Sydney region.

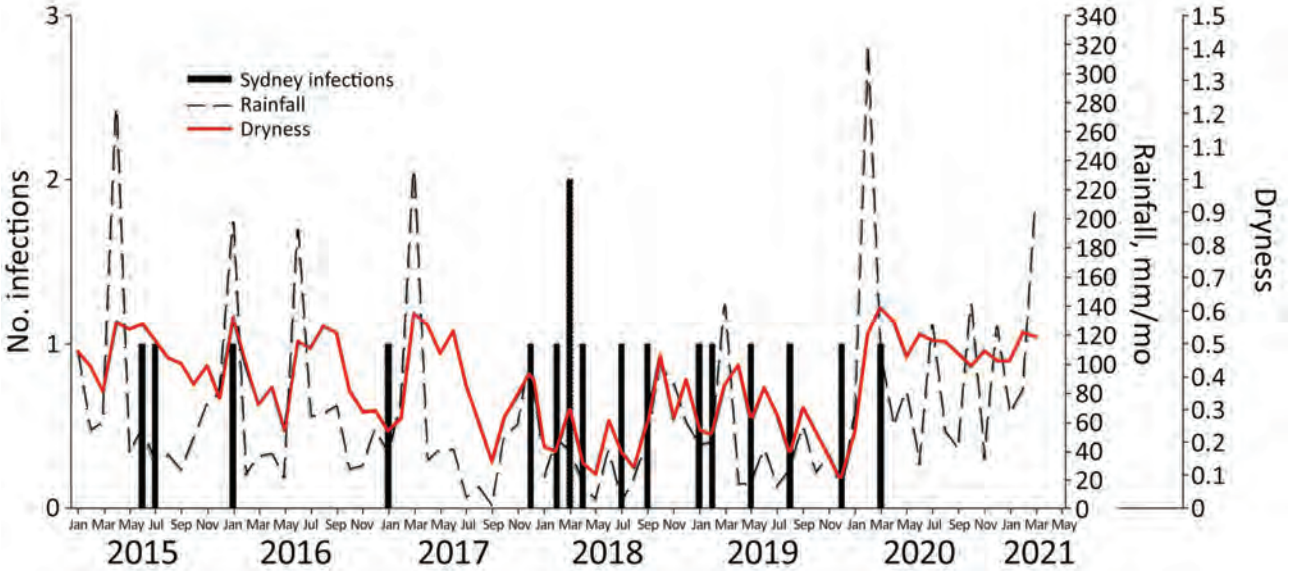

Figure 3. *Nocardia* cases among heart and lung transplant recipients compared with precipitation and dryness in Greystanes, the central location for cases in Greater Sydney, New South Wales, Australia, June 2015–March 2021. We defined dryness as the ratio of evaporation to potential evaporation, such that 0.0 is perfectly dry and 1.0 is perfectly wet.

(0.4 vs. 0.1 m/s for months without a *Nocardia* diagnosis; p<0.01). The average temperature was also higher in months with a *Nocardia* diagnosis (18.9°C vs. 17.4°C in months without a *Nocardia* diagnosis), although this difference was not statistically significant (p<0.24) (Table 5).

Discussion

In this study, we observed no differences in *Nocardia* species isolated from HTR compared with LTR and no clustering of *Nocardia* species in space or time to suggest a single source for the outbreak. We found that HTR had evidence of greater immunosuppression before their *Nocardia* diagnosis than LTR, including higher use of basiliximab for induction immunosuppression, higher rates of cellular rejection, and a shorter median time from transplant to *Nocardia* diagnosis. Our analysis of climate data revealed that low local precipitation and drier surface levels correlated with increased incidence of *Nocardia* diagnosis.

Previous studies have shown that high-dose steroids, calcineurin inhibitor usage, CMV disease in the 6 months before diagnosis, and increased age are risk factors for nocardiosis (*3*,*14*). In our cohort, HTR and LTR did not have demonstrable differences in age, CMV disease status, or use of tacrolimus, mycophenolate mofetil, or prednisone. However, our data indicate that HTR had more characteristics indicating immunosuppression than LTR, including higher rates of basiliximab induction, diabetes, and cellular rejection (including treated moderate-to-severe rejection). Because basiliximab is an immunosuppressant with interleukin-2R α antagonist properties, increased use of basiliximab among HTR compared with LTR may have increased the risk for *Nocardia* infection through a diminished T-cell response in HTR. Similarly, additional immunosuppression in the setting of treating moderate to severe acute organ rejection may have further increased the risk for *Nocardia* infection among HTR.

We found no difference in the proportion of macrolide susceptible *Nocardia* isolates in HTR versus

Table 4. Climate conditions and *Nocardia* incidence before, during, and after a *Nocardia* outbreak among heart and lung transplant recipients, Greater Sydney, New South Wales, Australia, January 2018–December 2019*

Characteristic	Preoutbreak, Jun 2015–Dec 2017	Outbreak, Jan 2018–Dec 2019	Postoutbreak Jan 2020–Mar 2021	p value
Nocardia cases/mo	0.16	0.46	0.07	
Average monthly precipitation, mm/mo	60.4	40.0	103.2	<0.01
Average monthly temperature °C	17.0	17.8	17.8	0.79
Average monthly dryness*	0.4	0.3	0.5	<0.01
Average monthly windspeed, m/s	1.0	0.9	1.0	0.62
Average monthly erodibility†	0.1	0.2	0.1	0.26

*Ratio of evaporation to potential evaporation, such that 0.0 is perfectly dry and 1.0 is perfectly wet.
†Calculated by the formula (1 – dryness) × windspeed.

Table 5. Comparison of climate conditions during months with and without *Nocardia* infections, Greater Sydney, New South Wales, Australia, June 2015–March 2021

Climate conditions	Monthly average with no *Nocardia* cases, n = 73	Monthly average with confirmed *Nocardia* cases, n = 17	p value	All months, n = 90
Precipitation, mm/mo	66.3	63.3	0.42	65.7
Dryness	0.4	0.3	<0.01	0.4
Temperature, °C	17.4	18.9	0.24	17.7
Windspeed, m/s	1.0	1.1	0.37	1.0
Normalized windspeed, m/s	0.2	0.4	<0.01	0.2
Normalized erodibility, m/s	0.1	0.4	<0.01	0.2

LTR despite increased use of azithromycin for prophylaxis in LTR compared with HTR. The possibility that azithromycin use lowered the risk for *Nocardia* infections in LTR compared with HTR warrants further investigation.

Seasonality and changes in climate conditions are known to affect the incidence and distribution of various infectious pathogens, particularly those acquired by inhalation or exposure to the respiratory tract (*15*). Respiratory viruses and environmental fungi, such as *Coccidioides immitis*, *Aspergillus* spp., and *Cryptococcus gattii*, are highly influenced by climate patterns, having enhanced infection risk in the setting of increased aerosolised dust particulate matter (*9*,*10*,*16*,*17*). In a study of *Aspergillus* infections among stem cell transplant recipients in the United States, Panackal et al. identified an increased incidence of invasive *Aspergillosis* in drier and warmer conditions by comparing incidence rates across different seasons (*16*). Tong et al. identified a correlation between increased frequencies of dust storms, precipitated by low moisture level soils, and higher rates of inhaled soil-dwelling fungi such as *Coccidioides immitis* and *C. posadasii* (*17*). Similarly, Majeed et al. (*9*) and Saubolle et al. (*10*) observed that the greatest number of *Nocardia* infections occur in dry, warm climates, such as in the Southwest United States.

In Greater Sydney, the increase in *Nocardia* cases occurred during a time of decreased rainfall and a very dry surface (evaporation/potential evaporation), supporting our hypothesis that the increase in *Nocardia* infections may have been driven by extreme climate conditions. In NSW, 2019 was the warmest and driest year, with the annual mean temperature 1.95 degrees above average and average rainfall 55% below average (*6*); 2018 was NSW's second warmest and seventh driest year, with an annual mean temperature 1.68 degrees above average and average rainfall 40% below average (*5*).

The Australian Therapeutic Guidelines for treating moderate nocardiosis recommend dual therapy with sulfamethoxazole/trimethoprim and either ceftriaxone or linezolid; for severe nocardiosis, a third agent (amikacin, imipenem or meropenem), is added to this regimen (*18*). Most *Nocardia* isolates identified in this cohort were reassuringly susceptible to sulfamethoxazole/trimethoprim (95.7%); however, only 30.4% of isolates were susceptible to ceftriaxone and 43.5% to imipenem, corresponding well with previous data (*19*). All isolates were susceptible to linezolid and amikacin, supporting the usage of empiric linezolid or amikacin in addition to sulfamethoxazole/trimethoprim over ceftriaxone or imipenem for moderate and severe disease in our cohort.

Our study's first limitation is that our small study population size limited our analyses to primarily descriptive statistics and correlations with climate data. Most of our patients were from the Greater Sydney region and underwent heart or lung transplantation at a single medical center, further limiting the generalizability of our findings. The retrospective study design and reliance on data from the medical record limited our ability to comment on patient practices, including use of personal protective equipment such as masks when gardening and participating in other activities that may increase the risk for infection. However, postoperative patient education on use of personal protective equipment did not change during the study period; we would therefore not expect to see changes in patient practices that would affect the incidence of *Nocardia* infections. The retrospective study design meant that data on intraoperative care, such as changes in procedures, personnel, and infection control practices, were not available. However, because the surgical teams and theater conditions remained consistent throughout the study period, differences in intraoperative care that may have affected risk for *Nocardia* infection would be unlikely. Data on environmental sources within and around the hospital, such as construction projects and water sources, were also not available. However, given the broad range in times from transplant to diagnosis and the multispecies nature of the outbreak, it is unlikely that environmental contamination was a potential source of the outbreak. Although more surveillance biopsies are routinely performed among HTR than LTR at our institution, which may have contributed to the higher rates of any grade of rejection detected in HTR, treated rejection episodes (i.e., moderate to severe rejection) are likely to

be symptomatic and therefore unlikely to be biased by differences in routine surveillance biopsy schedules. *Nocardia* infections can be indolent and subclinical for some time, which limited our analyses comparing climate conditions in months with and without *Nocardia* diagnoses. Larger studies and studies in other regions are needed to confirm the correlations we identified between climate conditions and *Nocardia* infections.

In conclusion, this study examined the association between climate conditions and *Nocardia* infection in HTR and LTR. Periods of low precipitation and dryer surface levels were associated with an increased incidence of *Nocardia* diagnoses, suggesting that environmental conditions affected the risk for *Nocardia* infection. In addition, HTR had a shorter time to *Nocardia* diagnosis and increased rates of markers of immunosuppression, suggesting that HTR had greater susceptibility to infection at the time of diagnosis than LTR. We hypothesize that the increased environmental risk from climate conditions during 2018–2019, coupled with increased host susceptibility related to immunosuppression in HTR, may explain the increased incidence of *Nocardia* infections during 2018–2019. Further studies should evaluate the influence of climate characteristics on *Nocardia* infections in immunocompromised hosts, as well as potential screening or other preventive measures that might decrease disease burden in these vulnerable patients. Because *Nocardia* is an environmental organism, these results highlight the importance of wearing personal protective equipment around soil exposures, particularly for immunocompromised patients during periods of increased soil dryness.

Acknowledgments

We thank Nomvuyo Mothobi and Helen Gray for their assistance with identifying *Nocardia* cases. We acknowledge and thank the Microbiology, Molecular and Genomics Departments at Institute for Clinical Pathology and Medical Research at Westmead Hospital (Sydney, NSW, Australia) for assisting with final identification via genome sequencing of the *Nocardia* isolates, in addition to completing antibiotic susceptibility testing. We thank Claire Carouge for retrieval of the data used in this study from the ERA5 reanalysis.

A.J.P. was supported by the ARC Centre of Excellence for Climate Extremes (grant no. CE170100023). N.J.D. has received research support through an Australian Government Research Training Program Scholarship.

About the Author

Dr. Li is a doctor at St Vincent's Hospital Sydney. His primary research interests are infections in solid organ transplant recipients.

References

1. Restrepo A, Clark NM; Infectious Diseases Community of Practice of the American Society of Transplantation. *Nocardia* infections in solid organ transplantation: guidelines from the Infectious Diseases Community of Practice of the American Society of Transplantation. Clin Transplant. 2019;33:e13509. https://doi.org/10.1111/ctr.13509
2. Lerner PI. Nocardiosis. Clin Infect Dis. 1996;22:891–903, quiz 904–5. https://doi.org/10.1093/clinids/22.6.891
3. Peleg AY, Husain S, Qureshi ZA, Silveira FP, Sarumi M, Shutt KA, et al. Risk factors, clinical characteristics, and outcome of *Nocardia* infection in organ transplant recipients: a matched case-control study. Clin Infect Dis. 2007;44:1307–14. https://doi.org/10.1086/514340
4. Lebeaux D, Freund R, van Delden C, Guillot H, Marbus SD, Matignon M, et al.; European Study Group for Nocardia in Solid Organ Transplantation; European Study Group for Nocardia in Solid Organ Transplantation. Outcome and treatment of nocardiosis after solid organ transplantation: new insights from a European study. Clin Infect Dis. 2017;64:1396–405. 10.1093/cid/cix124 https://doi.org/10.1093/cid/cix124
5. Bureau of Meteorology. New South Wales in 2018: warmest year on record, very dry. 2019 [cited 2021 Jul 30]. https://www.bom.gov.au/climate/current/annual/nsw/archive/2018.summary.shtml
6. Bureau of Meteorology. New South Wales in 2019: record warm and record dry. 2020 [cited 2021 Jul 30]. https://www.bom.gov.au/climate/current/annual/nsw/archive/2019.summary.shtml
7. Bureau of Meteorology. Annual climate statement 2018. 2019 [cited 2021 Jul 30]. https://www.bom.gov.au/climate/current/annual/aus/2018/
8. Bureau of Meteorology. Annual climate statement 2019. 2020 [cited 2021 Jul 30]. https://www.bom.gov.au/climate/current/annual/aus/2019/
9. Majeed A, Beatty N, Iftikhar A, Mushtaq A, Fisher J, Gaynor P, et al. A 20-year experience with nocardiosis in solid organ transplant (SOT) recipients in the southwestern United States: a single-center study. Transpl Infect Dis. 2018;20:e12904. https://doi.org/10.1111/tid.12904
10. Saubolle MA, Sussland D. Nocardiosis: review of clinical and laboratory experience. J Clin Microbiol. 2003;41:4497–501. https://doi.org/10.1128/JCM.41.10.4497-4501.2003
11. Stewart S, Winters GL, Fishbein MC, Tazelaar HD, Kobashigawa J, Abrams J, et al. Revision of the 1990 working formulation for the standardization of nomenclature in the diagnosis of heart rejection. J Heart Lung Transplant. 2005;24:1710–20. https://doi.org/10.1016/j.healun.2005.03.019
12. Stewart S, Fishbein MC, Snell GI, Berry GJ, Boehler A, Burke MM, et al. Revision of the 1996 working formulation for the standardization of nomenclature in the diagnosis of lung rejection. J Heart Lung Transplant. 2007;26:1229–42. https://doi.org/10.1016/j.healun.2007.10.017
13. Hersbach H, Bell B, Berrisford P, Hirahara S, Horányi A, Muñoz-Sabater J, et al. The ERA5 global reanalysis. Q J R Meteorol Soc. 2020;146:1999–2049. https://doi.org/10.1002/qj.3803
14. Coussement J, Lebeaux D, van Delden C, Guillot H, Freund R, Marbus S, et al.; European Study Group for Nocardia in Solid Organ Transplantation. *Nocardia* infection in solid organ transplant recipients: a multicenter European case-control study. Clin Infect Dis. 2016;63:338–45. https://doi.org/10.1093/cid/ciw241

15. Dowell SF. Seasonal variation in host susceptibility and cycles of certain infectious diseases. Emerg Infect Dis. 2001;7:369–74. https://doi.org/10.3201/eid0703.017301
16. Panackal AA, Li H, Kontoyiannis DP, Mori M, Perego CA, Boeckh M, et al. Geoclimatic influences on invasive aspergillosis after hematopoietic stem cell transplantation. Clin Infect Dis. 2010;50:1588–97. https://doi.org/10.1086/652761
17. Tong DQ, Wang JXL, Gill TE, Lei H, Wang B. Intensified dust storm activity and Valley fever infection in the southwestern United States. Geophys Res Lett. 2017;44:4304–12. https://doi.org/10.1002/2017GL073524
18. Guidelines T. Nocardiosis. 2019 [cited 2021 Nov 20]. https://www.tg.org.au
19. Tan YE, Chen SCA, Halliday CL. Antimicrobial susceptibility profiles and species distribution of medically relevant *Nocardi*a species: results from a large tertiary laboratory in Australia. J Glob Antimicrob Resist. 2020;20:110–7.8 https://doi.org/10.1016/j.jgar.2019.06.018

Address for correspondence: Nila J. Dharan, Kirby Institute, UNSW Sydney, Wallace Wurth Bldg, Sydney, NSW 2052, Australia; email: ndharan@kirby.unsw.edu.au

Effectiveness of Second mRNA COVID-19 Booster Vaccine in Immunocompromised Persons and Long-Term Care Facility Residents

Yoo-Yeon Kim,[1] Young June Choe,[1] Jia Kim, Ryu Kyung Kim, Eun Jung Jang, Seon Kyeong Park, Do-Sang Lim, Seonju Yi, Sangwon Lee, Geun-Yong Kwon, Jee Yeon Shin, Sang-Yoon Choi, Mi Jin Jeong, Young-Joon Park

We used a nationwide population registry in South Korea to estimate the effect of a second booster dose of mRNA COVID-19 vaccine on the risk for laboratory-confirmed SARS-CoV-2 infection, critical infection, and death in immunocompromised persons and long-term care facility (LTCF) residents. During February 16–May 7, 2022, among 972,449 eligible persons, 736,439 (75.7%) received a first booster and 236,010 (24.3%) persons received a second booster. Compared with the first booster group, at 30–53 days, the second booster recipients had vaccine effectiveness (VE) against all infections of 22.28% (95% CI 19.35%–25.11%), VE against critical infection of 56.95% (95% CI 29.99%–73.53%), and VE against death of 62.96% (95% CI 34.18%–79.15%). Our findings provide real-world evidence that a second booster dose of mRNA vaccine substantially increases protection against critical infection and death in these high-risk population groups.

Booster doses of mRNA vaccines have been shown to reduce the risk for severe SARS-CoV-2 infection (*1*,*2*); however, protection wanes a few months after vaccination, particularly in high-risk populations (*3*,*4*). A second booster dose at least 4 months after the first booster dose of mRNA vaccine was found to increase immunity against COVID-19; thus, the second booster has been introduced in some countries (*5*).

Other studies have postulated that additional doses of the COVID-19 vaccine can enhance cellular and humoral immunity against the Omicron variant (*6*,*7*), and some studies have already shown the effectiveness of second boosters in preventing COVID-19 infections (*5*,*8*,*9*). However, population-based studies are needed to assess the effect of the second booster vaccine on COVID-19 in high-risk groups.

During February–April 2022, a second booster of mRNA vaccine was recommended for immunocompromised persons and long-term care facility (LTCF) residents in South Korea. We used a nationwide population registry to estimate the effect of a second booster dose of mRNA vaccine on risk for laboratory-confirmed SARS-CoV-2 infection, critical infection, and death in immunocompromised persons and LTCF residents.

Methods

In South Korea, COVID-19 is a notifiable disease; all laboratory-confirmed cases are reported to the Korea Disease Control and Prevention Agency (KDCA). COVID-19 vaccination records, including the date of vaccination and type of vaccine, are also collected and maintained by the KDCA. All suspected COVID-19 case-patients (anyone with a history of close contact with a COVID-19 patient) or SARS-CoV-2–infected persons, regardless of symptoms, were mandated to be tested by PCR or rapid antigen test during the observation period. By linking the vaccination registry and the surveillance database, we created a large-linked database through unique resident registration number. The observation period was February–May 2022, when 100% of SARS-CoV-2 detected in South Korea was identified as an Omicron variant (BA1.1, BA2, and BA2.3 subvariants) (*10*).

Author affiliations: Korea Disease Control and Prevention Agency, Cheongju, South Korea (Y.-Y. Kim, J. Kim, R.K. Kim, E.J. Jang, S.K. Park, D.-S. Lim, S. Yi, S. Lee, G.-Y. Kwon, J.Y. Shin, S.-Y. Choi, M.J. Jeong, Y.-J. Park); Korea University Anam Hospital, Seoul, South Korea (Y.J. Choe)

DOI: https://doi.org/10.3201/eid2811.220918

[1]These authors contributed equally to this article.

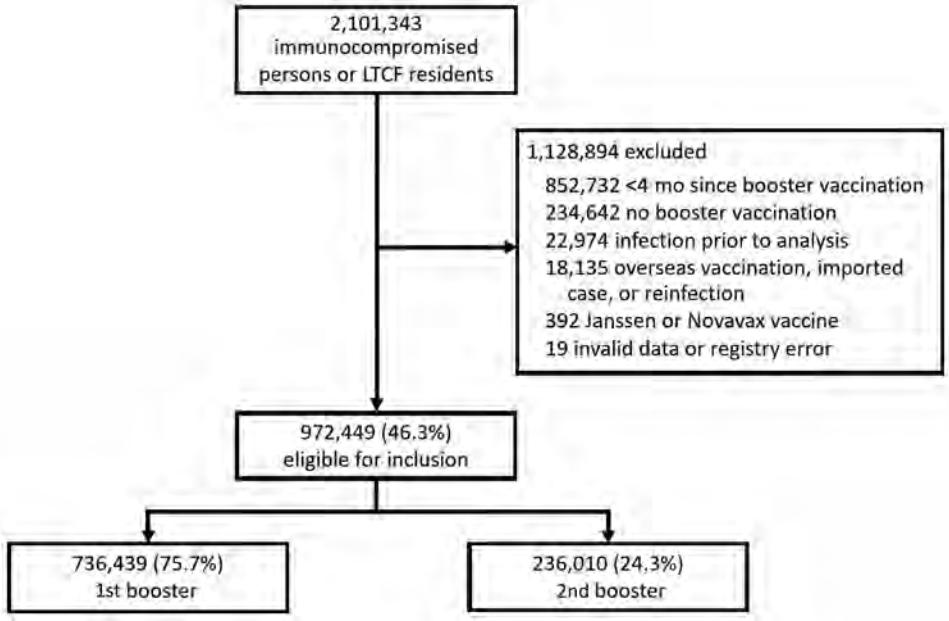

Figure 1. Flowchart of COVID-19 vaccine effectiveness study among immunocompromised persons and LTCF residents, South Korea, February–May 2022. Johnson & Johnson/Janssen, https://www.jng.com; Novavax, https://www.novavax.com. LTCF, long-term care facility.

In South Korea, 2 adenoviral vector-based vaccines, ChAdOx1 nCov-19 (AstraZeneca, https://www.astrazeneca.com) and Ad26.COV2.S (Johnson & Johnson/Janssen, https://www.jng.com); 2 mRNA-based vaccines, BNT162b2 (Pfizer-BioNTech, https://www.pfizer.com) and mRNA-1273 (Moderna, https://www.moderna.com); and 1 protein subunit vaccine (Novavax, https://www.novavax.com) were introduced. Since February 2021, all immunocompromised persons and LTCF residents have been prioritized to receive COVID-19 vaccines (*11*). The first booster dose of Pfizer-BioNTech or Moderna vaccine has been offered since October 2021, and the second booster dose of Pfizer-BioNTech or Moderna vaccine has been offered since February 2022. We included all immunocompromised persons and LTCF residents who received the first booster vaccine >120 days before the study.

We defined immunocompromised persons as cancer patients, transplant patients, patients with primary immune deficiencies, patients with human immunodeficiency virus infections, and patients receiving high-dose corticosteroids or immunosuppressants. We defined having the first booster vaccine as the third dose of vaccination after receiving 2 doses of the primary series of AstraZeneca vaccine, Pfizer-BioNTech vaccine, or Moderna vaccine and second booster dose as reaching day 14 after receiving the fourth dose of vaccine.

We examined the 3 health outcomes of infection, critical infection, and death during the period of day 0–53. We defined day 0 as the 14th day after receiving the second booster dose. We defined infection as a SARS-CoV-2–positive PCR or rapid antigen test conducted by a healthcare

Table 1. Characteristics among immunocompromised persons and LTCF residents in COVID-19 vaccine effectiveness study, South Korea, February–May 2022

	1st booster		2nd booster	
Characteristics	No. (%) participants	Person-days	No. (%) participants	Person-days
Total	736,439	39,175,439	236,010	5,197,160
Sex				
F	294,572 (40.0)	16,096,170	94,864 (40.2)	2,129,509
M	441,867 (60.0)	23,079,269	141,146 (59.8)	3,067,651
Age group, y				
18–39	33,010 (4.5)	1,609,745	8,811 (3.7)	196,656
40–59	171,954 (23.3)	8,916,315	57,425 (24.3)	1,233,939
60–74	332,987 (45.2)	17,958,470	96,829 (41.0)	2,165,276
>75	198,488 (27.0)	10,690,910	72,945 (30.9)	1,601,290
Location				
Metropolitan area	344,722 (46.8)	18,053,072	95,738 (40.6)	2,084,863
Nonmetropolitan area	391,717 (53.2)	21,122,367	140,272 (59.4)	3,112,297
Risk factors				
Immunocompromised	477,215 (64.8)	25,564,786	97,478 (41.3)	2,132,538
Long-term care facility residents	259,224 (35.2)	13,610,653	138,532 (58.7)	3,064,622

Table 2. Result of booster vaccination among immunocompromised persons and LTCF residents in COVID-19 vaccine effectiveness study, South Korea, February–May 2022*

Characteristics	Population		All infection, no. (%)	Critical infection, no. (%)	Death, no. (%)
	No. (%)	Person-days			
Total	972,449	44,372,598	313,388	2,951	2,441
1st booster	736,439 (75.7)	39,175,439	268,278 (85.6)	2,609 (88.4)	2,148 (88.0)
2nd booster	236,010 (24.3)	5,197,160	45,110 (14.4)	342 (11.6)	293 (12.0)
Sex					
F	583,013 (60.0)	26,146,920	206,478 (65.9)	1,236 (41.9)	1,474 (60.4)
M	389,436 (40.0)	18,225,678	106,910 (34.1)	1,715 (58.1)	967 (39.6)
Age group, y					
18–39	41,821 (4.3)	1,806,401	17,391 (5.5)	4 (0.1)	1 (0.0)
40–59	229,379 (23.6)	10,150,253	86,230 (27.5)	97 (3.3)	62 (2.5)
60–74	429,816 (44.2)	20,123,745	117,935 (37.6)	511 (17.3)	335 (13.7)
≥75	271,433 (27.9)	12,292,199	91,832 (29.3)	2,339 (79.3)	2,043 (83.7)
Location					
Metropolitan area	440,460 (45.3)	20,137,934	137,973 (44.0)	1,328 (45.0)	1,012 (41.5)
Nonmetropolitan area	531,989 (54.7)	24,234,664	175,415 (56.0)	1,623 (55.0)	1,429 (58.5)
Risk factors					
Immunocompromised	574,693 (59.1)	27,697,324	124,950 (39.9)	531 (18.0)	339 (13.9)
LTCF residents	397,756 (40.9)	16,675,274	188,438 (60.1)	2,420 (82.0)	2,102 (86.1)

*LTCF, long-term care facility.

professional in any symptomatic or asymptomatic patient and critical infection as illness in hospitalized SARS-CoV-2–positive patients that necessitated high-flow oxygen therapy, mechanical ventilation, extracorporeal membrane oxygenation, or continuous renal replacement therapy or that resulted in death within 28 days after laboratory confirmation of SARS-CoV-2. Death was death attributable to COVID-19 as diagnosed by physicians.

We compared the rates of all infections, critical infections, and deaths by sex, age, geographic region, and number of vaccinations in immunocompromised persons and LTCF residents. We computed the cumulative incidence curves of all infections, critical infections, and deaths in the first booster group versus second booster group using the Kaplan–Meier estimator. We used a time-dependent Cox proportional hazard model and estimated hazard ratios (HRs) with 95% CIs from an adjusted Cox model with covariates (sex, age, days elapsed since vaccination, census regions, residence in a facility, and immunocompromised status) to compare the rates. We calculated vaccine effectiveness (VE) for the second booster compared with the first booster in preventing infection, critical infection, and death by using the HR from this model: vaccine effectiveness (against all infections, critical infections, and death) = (1 – HR) × 100. We calculated time-varying

Table 3. Incidence of SARS-CoV-2 infection, critical infection, and death among immunocompromised persons and LTCF residents after first and second mRNA booster vaccine, South Korea, February–May 2022

Category	Follow-up time, d					
	0	10.6	21.2	31.8	42.4	53.0
All infections						
First booster						
No. at risk	972,449	937,931	822,346	653,579	540,367	470,791
No. events	0	24,129	76,592	158,059	227,409	268,278
Second booster						
No. at risk	850	10,365	72,142	150,436	175,606	192,093
No. events	0	24	1,369	10,375	29,070	45,110
Critical infections						
First booster						
No. at risk	972,449	937,931	822,346	653,579	540,367	470,791
No. events	0	377	998	1,762	2,298	2,609
Second booster						
No. at risk	850	10,365	72,142	150,436	175,606	192,093
No. events	0	0	8	68	218	342
Deaths						
First booster						
No. at risk	972,449	937,931	822,346	653,579	540,367	470,791
No. events	0	283	782	1,445	1,901	2,148
Second booster						
No. at risk	850	10,365	72,142	150,436	175,606	192,093
No. events	0	0	5	58	193	293

VE 0–14 days, 15–30 days, and >30 days after the second booster vaccine. We used R software (The R Project for Statistical Computing, https://www.r-project.org) to prepare the data and perform statistical analyses.

This study was conducted as a legally mandated public health investigation under the authority of the Korean Infectious Diseases Control and Prevention Act (Nos. 12,444 and 13,392) and was not subject to institutional review board approval; therefore, written informed consent was not required. The investigators shared anonymized clustered data.

Results

During February 16–May 7, 2022, a total of 2,101,343 persons were assessed for inclusion, of whom 972,449 (46.3%) were eligible (Figure 1). A total of 736,439 (75.7%) of these persons had received the first booster dose, and 236,010 (24.3%) received the second booster dose.

The observed periods were 39,175,439 person-days for the first booster group and 5,197,160 person-days for the second booster group (Table 1). Immunocompromised patients accounted for 64.8% (n = 477,215) of the first booster group and 41.3% (n = 97,478) of the second booster group.

During the 44,372,598 person-days of follow-up, 313,388 infections, 2,951 critical infections, and 2,441 deaths occurred (Table 2). Of all infections, 85.6% (n = 268,278) occurred in the first booster group, and 88.5% (n = 2,148) of deaths occurred in the first booster group. Of all infections, 37.6% (n = 117,935) were in persons 60–74 years of age, whereas 79.3% (n = 2,339) of critical infections and 83.7% (n = 2,043) of deaths were in persons ≥75 years of age.

We calculated time-varying VE against all infections, critical infections, and deaths in persons who received the second booster vaccination (Table 3; Figures 2, 3). At ≥30 days after the second booster vaccination, VE against all infections was low at 22.28% (95% CI 19.35%–25.11%), whereas VE was higher against both critical infection at 56.95% (95% CI 29.99%–73.53%) and against death at 62.96% (95% CI 34.18%–79.15%) (Figure 3).

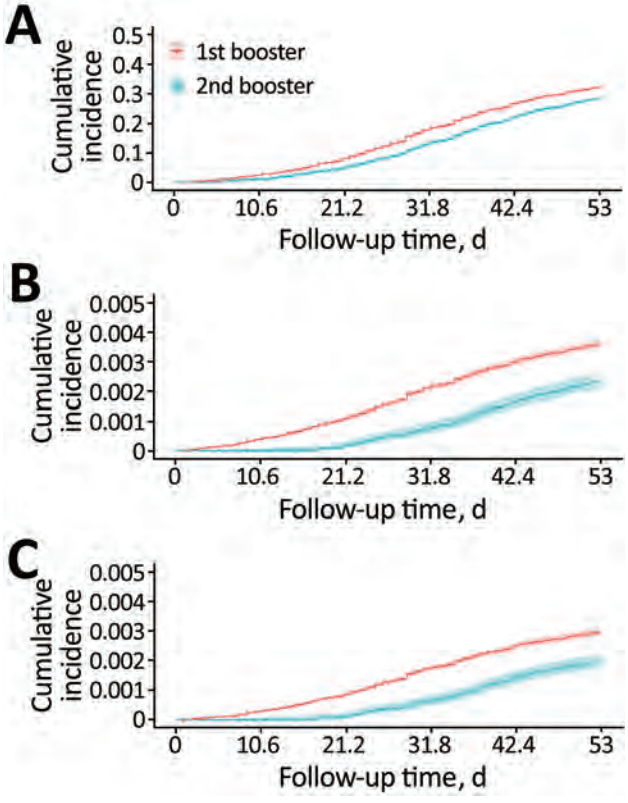

Figure 2. Cumulative incidence of all infections (A), critical infections (B), and death (C) in persons who received a second COVID-19 booster vaccination compared with those who received only the first booster dose in study of vaccine effectiveness among immunocompromised persons and long-term care facility residents, South Korea, February–May 2022.

Discussion

In this study that included ≈970,000 persons at high risk, we found that the second booster of mRNA vaccines provided greater protection against critical infection and death in patients with the Omicron variant than the first booster vaccination alone. Our finding is consistent with previous results, including a study among LTCF residents in Sweden during a period of Omicron variant predominance in which the effectiveness of the second booster dose compared with the first booster dose alone was reported to range from 31% to 42% against all-cause death (*12*). Our relative VE estimates were slightly lower than those in a study from Israel (HR 0.22–0.36), which might reflect declines in VE because the population in our study was a high-risk group consisting of immunocompromised persons and LTCF residents (*8*). In the general population ≥60 years of age in Israel, the estimated VE after the second booster dose was 45% against laboratory-confirmed infection, 55% against symptomatic infection, and 75% against death (*9*). A systematic review found that the seroconversion rates after COVID-19 vaccination were lower in immunocompromised patients, which might explain the difference in VE between populations (*13*). Despite this factor, our findings indicate that a second booster dose lowered the risk for severe infection in LTCF residents and immunocompromised persons, the most vulnerable population in the community. On

the basis of these results, we recommend a second booster dose in at-risk populations to maximize the public benefit of protection against COVID-19 related illness and death.

Our findings also suggest that the second booster dose offers higher levels of protection against critical infection and death in immunocompromised persons and LTCF residents, who are at highest risk for severe COVID-19. A systematic review of 11 studies showed that a third dose of the mRNA vaccine was associated with seroconversion among vaccine nonresponders with malignancies and immune-mediated disorders, which is consistent with our findings (*13*). The immunogenicity in immunocompromised persons might be lower than that in immunocompetent persons; however, the second booster dose clearly provides additional protection in this population (*14*). The relatively low VE against all infections seems to be consistent with previous studies that examined VE in LTCFs; however, its effectiveness against severe infection or death was relatively sustained, as observed elsewhere (*15*,*16*). During the observation period, we saw no clear evidence of waning against critical infection or death >30 days after the second booster (Appendix, https://wwwnc.cdc.gov/EID/article/28/11/22-0918-App1.pdf). Given the recent introduction of the second booster program in all adults in South Korea, further follow-up is needed to understand how protection changes in both persons at high risk and the general population.

The first limitation of our study is that our results might be affected by confounding bias if the first booster and second booster groups had different diagnostic intensity between groups. However, this difference in behavior that could have caused confounding would be smaller than in the general population, given that the study population included LTCF residents and immunocompromised persons, who receive the highest level of medical attention compared with other populations. Second, we were only able to estimate VE through days 30–53 of follow-up. Thus, the duration of protection against all infections will need to be monitored over a longer duration. Finally, during the peak surge of the Omicron outbreak in South Korea in February, persons who tested SARS-CoV-2–positive by self-administered rapid antigen tests might not have been included in the report. Despite these limitations, the second booster VE estimates against critical infection and death in persons at high risk were >50% compared with those in the first booster group, which suggests that additional doses continue to be an effective strategy to protect health in persons at higher risk.

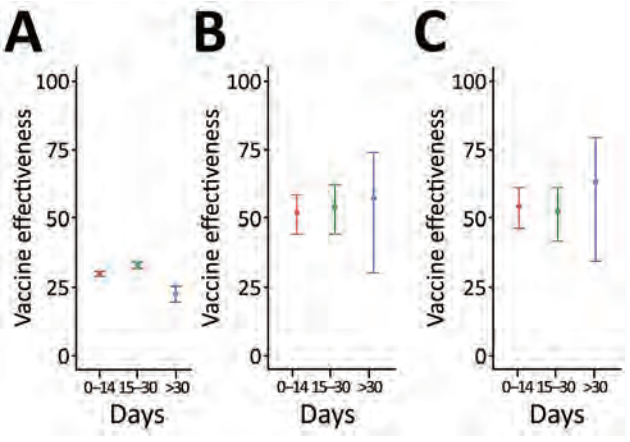

Figure 3. Time-varying COVID-19 vaccine effectiveness against all infections (A), critical infections (B), and death (C) in persons who received a second booster vaccination compared with those who received only the first booster dose in study of vaccine effectiveness among immunocompromised persons and long-term care facility residents, South Korea, February–May 2022. Error bars indicate 95% CIs.

In conclusion, our study provides real-world evidence that a second booster dose of mRNA COVID-19 vaccine provides substantially increased protection against critical infection and death in LTCF residents and immunocompromised persons receiving the booster dose. This protection will be key in the next wave of SARS-CoV-2 infection, when COVID-19 is again likely to pose a substantial burden to persons at high risk for serious health effects.

Acknowledgments

We thank the COVID-19 Vaccination Task Force and Division of National Immunization, Korea Disease Control and Prevention Agency; relevant ministries, including the Ministry of Interior and Safety, Si/Do and Si/Gun/Gu; medical staff in health centers; and medical facilities for their efforts in responding to the COVID-19 outbreak. This study was part of the Korea COvid-19 Vaccine Effectiveness (K-COVE) Initiative.

About the Author

Dr. Kim is a public health officer at the Korea Disease Control and Prevention Agency. Her main research interests are epidemiologic investigations and surveillance measures of infectious diseases.
Dr. Choe is a clinical associate professor of pediatrics at the Korea University Anam Hospital. His main research addresses quantifying and understanding the mechanisms of the immunization program's impact on public health.

References

1. Monge S, Rojas-Benedicto A, Olmedo C, Mazagatos C, José Sierra M, Limia A, et al.; IBERCovid. Effectiveness of mRNA vaccine boosters against infection with the SARS-CoV-2 omicron (B.1.1.529) variant in Spain: a nationwide cohort study. Lancet Infect Dis. 2022;22:1313–20. https://doi.org/10.1016/S1473-3099(22)00292-4
2. Sheikh A, Kerr S, Woolhouse M, McMenamin J, Robertson C, Simpson CR, et al.; EAVE II Collaborators. Severity of omicron variant of concern and effectiveness of vaccine boosters against symptomatic disease in Scotland (EAVE II): a national cohort study with nested test-negative design. Lancet Infect Dis. 2022;22:959–66. https://doi.org/10.1016/S1473-3099(22)00141-4
3. Abu-Raddad LJ, Chemaitelly H, Bertollini R; National Study Group for COVID-19 Vaccination. Waning mRNA-1273 vaccine effectiveness against SARS-CoV-2 infection in Qatar. N Engl J Med. 2022;386:1091–3. https://doi.org/10.1056/NEJMc2119432
4. Andrews N, Tessier E, Stowe J, Gower C, Kirsebom F, Simmons R, et al. Duration of protection against mild and severe disease by COVID-19 vaccines. N Engl J Med. 2022;386:340–50. https://doi.org/10.1056/NEJMoa2115481
5. Munro APS, Feng S, Janani L, Cornelius V, Aley PK, Babbage G, et al.; COV-BOOST study group. Safety, immunogenicity, and reactogenicity of BNT162b2 and mRNA-1273 COVID-19 vaccines given as fourth-dose boosters following two doses of ChAdOx1 nCoV-19 or BNT162b2 and a third dose of BNT162b2 (COV-BOOST): a multicentre, blinded, phase 2, randomised trial. Lancet Infect Dis. 2022;22:1131–41. https://doi.org/10.1016/S1473-3099(22)00271-7
6. Garcia-Beltran WF, St Denis KJ, Hoelzemer A, Lam EC, Nitido AD, Sheehan ML, et al. mRNA-based COVID-19 vaccine boosters induce neutralizing immunity against SARS-CoV-2 Omicron variant. Cell. 2022;185:457–466.e4. https://doi.org/10.1016/j.cell.2021.12.033
7. Minka SO, Minka FH. A tabulated summary of the evidence on humoral and cellular responses to the SARS-CoV-2 Omicron VOC, as well as vaccine efficacy against this variant. Immunol Lett. 2022;243:38–43. https://doi.org/10.1016/j.imlet.2022.02.002
8. Bar-On YM, Goldberg Y, Mandel M, Bodenheimer O, Amir O, Freedman L, et al. Protection by a fourth dose of BNT162b2 against Omicron in Israel. N Engl J Med. 2022;386:1712–20. https://doi.org/10.1056/NEJMoa2201570
9. Magen O, Waxman JG, Makov-Assif M, Vered R, Dicker D, Hernán MA, et al. Fourth dose of BNT162b2 mRNA Covid-19 vaccine in a nationwide setting. N Engl J Med. 2022;386:1603–14. https://doi.org/10.1056/NEJMoa2201688
10. Kim EY, Choe YJ, Park H, Jeong H, Chung JH, Yu J, et al. Community transmission of SARS-CoV-2 Omicron variant, South Korea, 2021. Emerg Infect Dis. 2022;28:898–900. https://doi.org/10.3201/eid2804.220006
11. Yi S, Choe YJ, Lim DS, Lee HR, Kim J, Kim YY, et al. Impact of national Covid-19 vaccination Campaign, South Korea. Vaccine. 2022;40:3670–5. https://doi.org/10.1016/j.vaccine.2022.05.002
12. Nordström P, Ballin M, Nordström A. Effectiveness of a second COVID-19 vaccine booster on all-cause mortality in long-term care facility residents and in the oldest old: a nationwide, retrospective cohort study in Sweden. Lancet Reg Health Eur. 2022 Jul 13 [Epub ahead of print].
13. Lee ARYB, Wong SY, Chai LYA, Lee SC, Lee MX, Muthiah MD, et al. Efficacy of covid-19 vaccines in immunocompromised patients: systematic review and meta-analysis. BMJ. 2022;376:e068632. https://doi.org/10.1136/bmj-2021-068632
14. Tenforde MW, Patel MM, Gaglani M, Ginde AA, Douin DJ, Talbot HK, et al.; IVY Network. IVY Network. Effectiveness of a third dose of Pfizer-BioNTech and Moderna vaccines in preventing COVID-19 hospitalization among immunocompetent and immunocompromised adults—United States, August–December 2021. MMWR Morb Mortal Wkly Rep. 2022;71:118–24. https://doi.org/10.15585/mmwr.mm7104a2
15. Paranthaman K, Subbarao S, Andrews N, Kirsebom F, Gower C, Lopez-Bernal J, et al. Effectiveness of BNT162b2 and ChAdOx-1 vaccines in residents of long-term care facilities in England using a time-varying proportional hazards model. Age Ageing. 2022;51:afac115.
16. Sánchez Ruiz MA, Adonias G, Robaglia-Schlupp A, Rapilly F, Chabert M, Ramalli L, et al. Effectiveness of mRNA BNT162b2 COVID-19 vaccine against SARS-CoV-2 Delta variant among elderly residents from a long-term care facility, South of France, May 2021. Eur Rev Med Pharmacol Sci. 2022;26:2586–91.

Address for correspondence: Young-Joon Park, Director of Epidemiologic Investigation, Korea Disease Control and Prevention Agency, (28159) Korea Disease Control and Prevention Agency, Osong Health Technology Administration Complex, 187, Osongsaengmyeong 2-ro, Osong-eup, Heungdeok-gu, Cheongju-si, Chungcheongbuk-do, South Korea; email: pahmun@korea.kr

Racial/Ethnic Disparities in Exposure, Disease Susceptibility, and Clinical Outcomes during COVID-19 Pandemic in National Cohort of Adults, United States

McKaylee M. Robertson, Meghana G. Shamsunder, Ellen Brazier, Mekhala Mantravadi, Rebecca Zimba, Madhura S. Rane, Drew A. Westmoreland, Angela M. Parcesepe, Andrew R. Maroko, Sarah G. Kulkarni, Christian Grov, Denis Nash

We examined racial/ethnic disparities for COVID-19 seroconversion and hospitalization within a prospective cohort (n = 6,740) in the United States enrolled in March 2020 and followed-up through October 2021. Potential SARS-CoV-2 exposure, susceptibility to COVID-19 complications, and access to healthcare varied by race/ethnicity. Hispanic and Black non-Hispanic participants had more exposure risk and difficulty with healthcare access than white participants. Participants with more exposure had greater odds of seroconversion. Participants with more susceptibility and more barriers to healthcare had greater odds of hospitalization. Race/ethnicity positively modified the association between susceptibility and hospitalization. Findings might help to explain the disproportionate burden of SARS-CoV-2 infections and complications among Hispanic/Latino/a and Black non-Hispanic persons. Primary and secondary prevention efforts should address disparities in exposure, vaccination, and treatment for COVID-19.

Researchers have identified underlying medical conditions, comorbidities, older age, and male sex as biologic vulnerabilities for more severe COVID-19 outcomes (*1*,*2*). Evidence also suggests a disproportionate burden of COVID-19 infection, hospitalization, and death among Hispanic/Latino/a, Black non-Hispanic, and American Indian and Alaskan Native populations in the United States. (*3*–*6*). Early in the pandemic (March 2020), the Centers for Disease Control and Prevention (CDC) reported that twice as many Black persons were hospitalized because of COVID-19 than are proportionally represented in the United States. (*3*). Long-standing health and social inequities probably contribute to disparities in COVID-19 illness and death (*7*–*9*).

Public health interventions and policies with the potential to improve health might inadvertently amplify existing health disparities (*7*). Prevention efforts, such as social distancing or work from home policies, might have inequitable benefits across racial and ethnic groups because of differential employment in essential work settings or likelihood of living in multigenerational households (*7*,*8*,*10*). Less access to or use of healthcare also result in differential COVID-19 outcomes among racial and ethnic minority groups because later care presentation might limit treatment options (*6*,*8*). Blumenshine et al. proposed a pandemic disease model in which differences in exposure to the pathogen, susceptibility to severe illness if infected, and poor/delayed access to treatment might lead to disproportionate infection, illness, and death during a pandemic (*11*). To avoid exacerbating existing disparities, effective public health interventions and pandemic guidelines need to anticipate and mitigate the contribution of social determinants to disparities in exposure, susceptibility if exposed and access to treatment (*9*,*11*,*12*).

Author affiliations: Institute for Implementation Science in Population Health, New York, New York, USA (M.M. Robertson, M.G. Shamsunder, E. Brazier, M. Mantravadi, R. Zimba, M.S. Rane, D.A. Westmoreland, A.M. Parcesepe, A.R. Maroko, S.G. Kulkarni, C. Grov, D. Nash); Graduate School of Public Health and Health Policy, New York (M.G. Shamsunder, R. Zimba, A.R. Maroko, C. Grov, D. Nash); University of North Carolina at Chapel Hill Gillings School of Public Health and Carolina Population Center, Chapel Hill, North Carolina, USA (A.M. Parcesepe)

DOI: https://doi.org/10.3201/eid2811.220072

Our objective was to examine the influence of racial and ethnic differences in social determinants on COVID-19 outcomes within a large US national cohort of adults that was enrolled during the spring of 2020, the early phase of the COVID-19 pandemic. Using the Blumenshine model as a framework, we created 3 indices to assess social determinants: the ability to social distance as a measure of potential SARS-CoV-2 exposure, susceptibility to COVID-19 complications, and access to healthcare. We examined the relationship between each index with COVID-19 outcomes (COVID-19 hospitalization or seroconversion). Considering race/ethnicity as a social, rather than biologic construct (*13*), we assessed it as a potential effect measure modifier (EMM) of the relationship between each index and COVID-19 outcome.

Methods

Data Source and Population

The Communities, Households, and SARS-CoV-2 Epidemiology COVID Cohort Study is a geographically and sociodemographically diverse sample of adults (≥18 years of age) residing in the United States or US territories who enrolled into a prospective cohort study during emergence of the COVID-19 pandemic in the United States (*14*). We used internet-based strategies to recruit a fully online cohort. We recruited study participants during March 28, 2020–April 20, 2020, by advertisements on various social media platforms (e.g., Facebook) or by referral (anyone with knowledge of the study was allowed to invite others to participate). Internet-based strategies are effective for recruiting and following large and geographically diverse online cohorts and collecting at-home biological specimens (*15*–*17*). Details of cohort recruitment and follow-up been described by Robertson et al. (*14*). The study protocol was approved by the Institutional Review Board at the City University of New York (CUNY) Graduate School for Public Health and Health Policy.

Variable Definitions

Race/Ethnicity

Respondents were asked: "Are you Hispanic, Latino/a, or Spanish origin?" and "Which of these groups would you say best represents your race?" Participants were then categorized as Hispanic/Latino/a, Black non-Hispanic, Asian/Pacific Islander non-Hispanic, White non-Hispanic, or other (which included participants identifying >1 race, along with those identifying as American Indian or Alaskan Native and other) (*18*). To reduce the number of participants in the other category, we used a hierarchical approach to assign participants to 1 of the predominant race/ethnicity groups in the United States, first categorizing all Black non-Hispanic and all multiracial participants who identified as Black (n = 103), and then categorizing the remaining multiracial participants as Asian/Pacific Islander non-Hispanic (n = 80) or White non-Hispanic (n = 1). The remaining 222 participants in the other category were participants who did not identify as Black, Asian, or White.

Potential SARS-CoV-2 Exposure, COVID-19 Susceptibility, and Healthcare Access

We created 3 summative indices as proxies for potential SARS-CoV-2 exposure, susceptibility to COVID-19 complications, and difficulty with access to healthcare (*9*). We drew the indices and assessment items from a national survey that explored the experience of adults during the 2009–2010 influenza A(H1N1) pandemic (*9*,*19*). Specifically, the survey assessed disparities in H1N1 virus exposure, susceptibility to influenza complications, and access to healthcare during this influenza pandemic. We used the same exposure and access to care indices as the H1N1 survey and modified the susceptibility index to align with the conditions or exposures that CDC had identified in March 2020 as increasing the risk for COVID-19 complications. Each index was a summative score, in which a higher risk response was given a value of 1, and a lower or no risk response was given a value of 0. Therefore, a higher value would indicate a greater exposure risk, greater susceptibility, and greater difficulty with access to care and treatment.

First, as the measure of potential SARS-CoV-2 exposure, we included built-environment and work-related items that contributed to the ability to social distance. The built-environment items included living in an urban area, living in a multiunit dwelling (e.g., apartment building), and the ability to avoid public transportation. The work-related items included essential worker status and whether respondents were able to stay home from work or work from home, if needed. Specifically, respondents were asked to indicate yes, no or not applicable to the following statements: I am able to work at home; if I do not go to work because I am ill, I will not get paid for the time I am at home; I have sick leave at my job if I need to use it; I could lose my job or business if I am not able to go into work; my job can only be done in my workplace. Respondents who did not work were considered not at risk for the work-related items (i.e., a score of 0). Essential worker status was defined as having been

involved in healthcare or other essential work (e.g., first responders) in the 2 weeks before the survey (*14*).

Second, as the measure of COVID-19 susceptibility, we used conditions or exposures that CDC had identified as increasing the risk for COVID-19 complications given SARS-CoV-2 infection in March 2020: age ≥60 years, daily smoking, and underlying chronic conditions (chronic lung disease including chronic obstructive pulmonary disease, emphysema, and chronic bronchitis; serious heart conditions including angina/coronary heart disease, high blood pressure, history of myocardial infarction; current asthma; type 2 diabetes; kidney disease; immunocompromised condition; or HIV positive). Finally, as the measure of healthcare access, we used factors that affect medical care access: no primary care doctor, concerns about the costs of healthcare, concerns about seeing a doctor because of immigration status, or no healthcare coverage/insurance.

We dichotomized each index as less than or equal to the median value for statistical models: more versus less potential exposure risk, more versus less susceptible to COVID-19 complications, and more versus less difficulty with access to care. The indices (exposure, susceptibility, and access) came from baseline recruitment surveys.

COVID-19 Outcomes by Hospitalization and Seroconversion

We examined the association of potential exposure, susceptibility, or access to care with 2 COVID-19 outcomes: COVID-19 hospitalization and observed seroconversion. We defined COVID-19 hospitalization as a self-report of hospitalization for any COVID-19–like symptoms from baseline through the eighth follow-up assessment (V0–V8, March 2020–October 2021). We asked the following question: "Since you completed your last survey on DD/MM/YYYY, were you hospitalized for any of these symptoms?" We dichotomized outcome as yes or no and classified persons who reported do not know/not sure as no.

The procedure for at-home specimen collection for serologic testing has been reported (*20*). In brief, all participants were invited to participate in serologic testing by using an at-home self-collected dried blood spot specimen collection kit during May–August 2020 (period 1) and November 2020–January 2021 (period 2). All dried blood spot specimens were tested by the study laboratory for total antibodies by using the Platelia Test (Bio-Rad Laboratories, https://www.bio-rad.com) for IgA, IgM, and IgG, which targets the SARS-CoV-2 nucleocapsid protein (*21*). A total of 4,233 (63%) participants underwent serologic testing in period 1 and 3,884 (58%) in period 2. Of the 4,510 participants who tested at least once, 3,605 (80%) tested at both time points (*20*). Among those persons who had 2 total antibody tests, an observed seroconversion was defined as a negative total antibody test result in period 1, followed by a positive total antibody test result in period 2 (n = 3,422).

Confounders

We treated age, sex, presence of children in the household, income, education, or employment as possible confounders of the hypothesized exposure-outcome relationships. We identified confounders a priori based on directed acyclic graph framework (Appendix Figures 1–3, https://wwwnc.cdc.gov/EID/article/28/11/22-0072-App1.pdf) (*22*) and identified the minimum sufficient adjustment set for estimating the total effect of a given exposure on outcomes.

Statistical Analysis

We used descriptive statistics to examine participant demographics and indices reflecting potential SARS-CoV-2 exposure, susceptibility, and access to healthcare stratified by race/ethnicity. We assessed differences between groups by using the χ^2 or Kruskal-Wallis test as appropriate.

We used a logistic regression model to assess the association between each index and outcomes of interest: COVID-19-hospitalization or seroconversion. We separately modeled each exposure-outcome relationship. When potential SARS-CoV-2 exposure was the explanatory index of interest, we adjusted for age, presence of children in the household, employment, income, race/ethnicity. When susceptibility was the explanatory index of interest, we adjusted for employment, income, race/ethnicity, and we did not adjust for age because age was used to create the susceptibility summative score. When access was the explanatory index of interest, we adjusted for age, employment, sex, income, race/ethnicity.

We assessed whether the effect of each index on COVID-19 outcomes was modified by race/ethnicity. We assessed EMM on the additive scale and present the relative excess risk caused by interaction (RERI) (*23*,*24*). Because EMM on the additive scale indicates whether the effect of an exposure is different in 1 subpopulation relative to another, assessing the additive interaction is useful for identifying the specific population for whom public health interventions will have the greatest effect (*23*,*24*). We collapsed the race variable to White non-Hispanic versus Hispanic/Latino/a and Black non-Hispanic for assessment of EMM.

We conducted logistic regression models with SAS version 9.4 (https://www.sas.com). We generated

95% CIs for RERI by using the spreadsheet tool reported by Knol and VanderWeele. (*23*).

Results

This analysis used data for 6,740 persons enrolled into prospective follow-up for analyses assessing the hospitalization outcome reported through October 20, 2021. Among the full cohort, 19% (n = 1,308) identified as Hispanic/Latino/a ethnicity, 13% (n = 899) as Black non-Hispanic, 7% (n = 465) as Asian/Pacific Islander non-Hispanic, 57% (n = 3,846) as White non-Hispanic, and 3% (n = 222) as other non-Hispanic race (Table 1). Hispanic/Latino/a (mean ±SD age 35 ±13 years), Black non-Hispanic (mean ±SD age 35 ±13 years), or Asian/Pacific Islander non-Hispanic participants (mean ±SD age 33 ±12 years) were younger on average than White non-Hispanic participants (mean ±SD age 45 ±16). More than half (52%) of the cohort were women. More than half (57%) of the cohort had a college-level education, and the proportion with a college-education was highest among Asian/Pacific Islander non-Hispanic (69%) and lowest among Black non-Hispanic participants (33%).

For seroconversion analyses, we used a subset of 3,422 participants seronegative in May–September 2020 who tested again during November 2020–January 2021. Compared with the full cohort, the subset of testers had more White non-Hispanic participants (57% vs. 67%), was older (mean age 44 years vs. 41 years), and had higher educational attainment (57% vs. 67% with at least a college education) (Appendix Table 1).

Potential SARS-CoV-2 Exposure Risk by Built-Environment and Work-Related Ability to Social Distance

For built-environment measures of exposure (Table 2), greater percentages of Hispanic/Latino/a, Black non-Hispanic, and Asian/Pacific Islander non-Hispanic participants lived in urban areas and in multiunit dwellings compared with White non-Hispanic participants. A greater percentage of Hispanic/Latino/a and Black non-Hispanic participants were unable to avoid public transportation compared with Asian/Pacific Islander non-Hispanic and White non-Hispanic participants. For work-related measures, the percentage of participants with less ability to social distance was generally highest among Black non-Hispanic participants and lowest among White non-Hispanic participants. A greater percentage of Black non-Hispanic participants than White non-Hispanic participants who were employed reported that they were unable

Table 1. Demographic and socioeconomic characteristics of communities, households, and SARS-CoV-2 epidemiology for Chasing COVID study participants, stratified by race and ethnicity, United States, March 28–April 20, 2020*

Variable	Total	Hispanic or Latino/a	Black non-Hispanic	Asian/Pacific Islander non-Hispanic	White non-Hispanic	Other non-Hispanic	p value
Total	6,740 (100.00)	1,308 (19.41)	899 (13.33)	465 (6.90)	3,846 (57.06)	222 (3.30)	
Age, y							<0.001
Mean (SD)	40.61 (15.28)	35.19 (13.33)	35.31 (12.80)	32.73 (11.95)	44.64 (15.54)	40.74 (14.06)	
Median (IQR)	37 (29–51)	33 (25–42)	32 (26–42)	30 (24–39)	42 (32–57)	39 (29–49)	
Sex							<0.001
M	3,043 (45.15)	568 (43.43)	411 (45.72)	195 (41.94)	1,762 (45.81)	107 (48.2)	
F	3,526 (52.31)	718 (54.89)	468 (52.06)	260 (55.91)	1,983 (51.56)	97 (43.69)	
Nonbinary	171 (2.54)	22 (1.68)	20 (2.22)	10 (2.15)	101 (2.63)	18 (8.11)	
Education							<0.001
<12th grade	123 (1.82)	34 (2.6)	25 (2.78)	9 (1.94)	54 (1.4)	1 (0.45)	
12th grade/GED	875 (12.98)	282 (21.56)	191 (21.25)	36 (7.74)	330 (8.58)	36 (16.22)	
College, 1–3 y	1,889 (28.03)	436 (33.33)	385 (42.83)	100 (21.51)	894 (23.24)	74 (33.33)	
College, ≥4 y	3,853 (57.17)	556 (42.51)	298 (33.15)	320 (68.82)	2,568 (66.77)	111 (50.00)	
Employment status							<0.001
Employed	4,247 (63.01)	811 (62)	587 (65.29)	267 (57.42)	2,443 (63.52)	139 (62.61)	
Out of work	830 (12.31)	206 (15.75)	131 (14.57)	55 (11.83)	402 (10.45)	36 (16.22)	
Other	1,663 (24.67)	291 (22.25)	181 (20.13)	143 (30.75)	1,001 (26.03)	47 (21.17)	
Income							<0.001
<$35,000	1,969 (29.21)	468 (35.78)	415 (46.16)	111 (23.87)	878 (22.83)	97 (43.69)	
$35,000–$49,999	753 (11.17)	180 (13.76)	111 (12.35)	39 (8.39)	394 (10.24)	29 (13.06)	
$50,000–$69,999	959 (14.23)	210 (16.06)	148 (16.46)	58 (12.47)	520 (13.52)	23 (10.36)	
$70,000–$99,999	1,058 (15.70)	179 (13.69)	82 (9.12)	88 (18.92)	683 (17.76)	26 (11.71)	
≥$100,000	1,793 (26.60)	228 (17.43)	115 (12.79)	142 (30.54)	1,266 (32.92)	42 (18.92)	
Do not know	208 (3.09)	43 (3.29)	28 (3.11)	27 (5.81)	105 (2.73)	5 (2.25)	
Children <18 y of age							<0.001
No	4,564 (67.72)	692 (52.91)	534 (59.40)	314 (67.53)	2,879 (74.86)	145 (65.32)	
Yes	2,176 (32.28)	616 (47.09)	365 (40.60)	151 (32.47)	967 (25.14)	77 (34.68)	

*Values are no. (%) unless otherwise indicated. Chasing COVID, Communities, Households, and SARS-CoV-2 Epidemiology COVID Cohort Study; GED, general educational development; IQR, interquartile range.

Table 2. Measures of potential SARS-CoV-2 exposure, susceptibility to COVID-19 complications, and access to care for Chasing COVID study participants, stratified by race/ethnicity, United States, March 28–April 20, 2020*

Variable	Overall, n = 6,740	Hispanic, n = 1,308	Black non-Hispanic, n = 899	Asian/Pacific Islander, n = 465	White non-Hispanic, n = 3,846	Other, n = 222	p value†
Measures of potential exposure: inability to impose social distance							
Built environment measures							
Living in urban area	2,820 (41.84)	563 (43.04)	414 (46.05)	225 (48.39)	1,528 (39.73)	90 (40.54)	0.001
Living in multidwelling building	2,636 (39.11)	505 (38.61)	416 (46.27)	202 (43.44)	1,420 (36.92)	93 (41.89)	<0.001
Ability to avoid public transportation	629 (9.33)	155 (11.85)	153 (17.02)	27 (5.81)	266 (6.92)	28 (12.61)	<0.001
Median no. measures (IQR)	1 (0–2)	1 (0–2)	1 (0–2)	1 (0–2)	1 (0–1)	1 (0–2)	<0.001
Work-related measures							
Unable to work from home	1,825 (27.08)	398 (30.43)	299 (33.26)	102 (21.94)	952 (24.75)	74 (33.33)	<0.001
Will not get paid if at home	1,585 (23.52)	364 (27.83)	263 (29.25)	110 (23.66)	781 (20.31)	67 (30.18)	<0.001
Does not have sick leave	1,754 (26.02)	375 (28.67)	300 (33.37)	115 (24.73)	888 (23.09)	76 (34.23)	<0.001
Could lose job or business if unable to go to work	1,542 (22.88)	372 (28.44)	285 (31.70)	95 (20.43)	723 (18.80)	67 (30.18)	<0.001
Job can only be done in workplace	2,023 (30.01)	456 (34.86)	331 (36.82)	121 (26.02)	1,049 (27.28)	66 (29.73)	<0.001
Essential worker	588 (8.72)	116 (8.87)	84 (9.34)	38 (8.17)	329 (8.55)	21 (9.46)	0.92
Median no. measures (IQR)	1 (02)	1 (0–3)	2 (0–3)	1 (0–2)	0 (0–2)	1 (0–3)	<0.001
Median no. built-environment and work-related measures (IQR)	2 (1–3)	2 (1–4)	3 (1–4)	2 (1–3)	2 (1–3)	2 (1–4)	<0.001
More potential exposure risk: index >2	2,596 (38.52)	601 (45.95)	462 (51.39)	166 (35.70)	1,272 (33.07)	95 (42.79)	<0.001
Measures of susceptibility							
Age ≥60 y	1,027 (15.24)	76 (5.81)	54 (6.01)	22 (4.73)	847 (22.02)	28 (12.61)	<0.001
Chronic lung disease	194 (2.88)	35 (2.68)	18 (2.00)	8 (1.72)	120 (3.12)	13 (5.86)	0.01
Asthma (current)	752 (11.16)	143 (10.93)	108 (12.01)	34 (7.31)	429 (11.15)	38 (17.12)	<0.01
T2 diabetes	490 (7.27)	129 (9.86)	66 (7.34)	15 (3.23)	259 (6.73)	21 (9.46)	<0.001
Serious heart condition	1,542 (22.88)	271 (20.72)	240 (26.7)	42 (9.03)	938 (24.39)	51 (22.97)	<0.001
Kidney disease	105 (1.56)	23 (1.76)	8 (0.89)	1 (0.22)	69 (1.79)	4 (1.8)	0.04
Immunocompromised	180 (2.67)	27 (2.06)	13 (1.45)	6 (1.29)	126 (3.28)	8 (3.60)	<0.01
HIV	268 (3.98)	49 (3.75)	63 (7.01)	5 (1.08)	143 (3.72)	8 (3.60)	<0.001
Daily smoker	997 (14.79)	228 (17.43)	208 (23.14)	30 (6.45)	470 (12.22)	61 (27.48)	<0.001
Median no. measures (IQR)	1 (0–1)	0 (0–1)	1 (0–1)	0 (0–1)	1 (0–1)	1 (0–2)	<0.001
More susceptible index >1	1,453 (21.56)	238 (18.20)	202 (22.47)	30 (6.45)	924 (24.02)	59 (26.58)	<0.001
Measures of healthcare access							
Does not have 1 person as doctor	1,960 (29.08)	464 (35.47)	330 (36.71)	156 (33.55)	921 (23.95)	89 (40.09)	<0.001
Did not see doctor due to cost	1,277 (18.95)	327 (25.00)	221 (24.58)	84 (18.06)	591 (15.37)	54 (24.32)	<0.001
Did not see doctor due to immigration	288 (4.27)	124 (9.48)	66 (7.34)	16 (3.44)	71 (1.85)	11 (4.95)	<0.001
No insurance	1,172 (17.39)	347 (26.53)	242 (26.92)	87 (18.71)	450 (11.7)	46 (20.72)	<0.001
Median no. measures (IQR)	0 (0–1)	1 (0–2)	1 (0–2)	0 (0–1)	0 (0–1)	1 (0–1)	<0.001
More barriers to access: index >0	3,050 (45.25)	749 (57.26)	510 (56.73)	231 (49.68)	1,430 (37.18)	231 (49.68)	<0.001

*Values are no. (%) responding yes unless otherwise indicated. Chasing COVID, Communities, Households, and SARS-CoV-2 Epidemiology COVID Cohort Study; IQR, interquartile range.
†Based on the χ^2 test for categorical data or the Kruskal-Wallis test for summative indices.

to work from home and could lose their job if unable to go to work. The percentage with more exposure risk was highest among Black non-Hispanic participants (51%) and Hispanic/Latino/a participants (46%) and lowest among Asian/Pacific Islander non-Hispanic participants (36%) and White non-Hispanic participants (33%). All reported differences were statistically significant.

Susceptibility

Asian/Pacific Islander non-Hispanic participants generally had the lowest frequency of individual metrics of COVID-19 susceptibility. Hispanic/Latino/a, Black, and White non-Hispanic participants were more likely to report a serious heart condition and current asthma than were Asian/Pacific Islander non-Hispanic participants (p<0.01). Hispanic/Latino/a and Black non-Hispanic participants were more likely to report daily smoking than were Asian/Pacific Islander non-Hispanic or White non-Hispanic participants (p<0.001). The percentage more susceptible was higher for White non-Hispanic (24%), Black non-Hispanic (23%), and Hispanic/Latino/a (18%) participants than for Asian/Pacific Islander non-Hispanic participants (7%) (p<0.001).

Healthcare Access

Hispanic/Latino/a, Black non-Hispanic, and Asian/Pacific Islander non-Hispanic participants were more likely than White non-Hispanic participants to report having no primary care doctor, not seeing a doctor because of cost, not seeing a doctor because of immigration status, and not having insurance (p<0.001). The percentage reporting more difficulty with access to healthcare was higher among Hispanic/Latino/a (57%), Black non-Hispanic (57%), and Asian/Pacific Islander non-Hispanic participants (50%) than among White non-Hispanic participants (37%) (p<0.001). Trends in potential exposure, susceptibility, and healthcare access in the subset of testers mirrored trends in the full cohort (Appendix Table 2).

Association of Potential Exposure, Susceptibility, and Access to Care with COVID-19 Outcomes

Approximately 5% (n = 161/3,422) of participants seroconverted, and 6% (n = 401/6,070) were hospitalized (Table 3). In models adjusted for sociodemographics including age, participants who had more (versus less) exposure risk had greater odds of seroconversion (adjusted odds ratio [aOR] 1.64, 95% CI 1.17–2.30) and hospitalization (aOR 1.70, 95% CI 1.37–2.12) (Table 3). Neither susceptibility nor access to care was associated with seroconversion. However, participants who had more (versus less) susceptibility and those who had more (versus less) difficulty with healthcare access had greater odds of hospitalization ($aOR_{susceptibility}$ 2.35, 95% CI 1.88–2.92 and aOR_{access} 2.28, 95% CI 1.81–2.87).

EMM by Race/Ethnicity

Hispanic/Latino/a and Black non-Hispanic participants were more likely to seroconvert or to be hospitalized for COVID-19 than Asian/Pacific Islander non-Hispanic or White non-Hispanic participants (seroconversion 7% and 6% vs. 4% and 3%, respectively [p<0.01]; hospitalization 8%, and 9% vs. 5% and 3%, respectively [p<0.001]) (Appendix Table 3). For the seroconversion outcome, we saw no evidence of EMM by race/ethnicity (Appendix Table 4). For the hospitalization outcome, we saw evidence of EMM by race/ethnicity for the susceptibility index (RERI 1.75; p<0.01), meaning that Hispanic/Latino/a or Black non-Hispanic participants who had a high score on the susceptibility index were at disproportionately higher odds of COVID hospitalization compared with White non-Hispanic participants. The odds of COVID hospitalization were 2.70 (95% CI 1.95–3.72) for Hispanic/Latino/a or Black non-Hispanic participants and 2.14 (95% CI 1.55–2.14) for White non-Hispanic participants. In contrast, there was no evidence of EMM by race/ethnicity for potential SARS-CoV-2 exposure or healthcare access indices with hospitalization (Table 4).

Discussion

Our study confirms the existence of major racial and ethnic differences in potential SARS-CoV-2 exposure risk, susceptibility to COVID-19 complications, and access to healthcare within a large US national cohort. The percentage of those with more potential exposure risk and more difficulty with healthcare access was higher among Black non-Hispanic, Hispanic/Latino/a, and Asian/Pacific Islander non-Hispanic participants than among White non-Hispanic participants. Greater potential exposure, as measured by reduced ability to social distance, increased the odds of seroconversion by 64% and hospitalization by 70%. Greater underlying susceptibility and difficulty with access to care increased the odds of hospitalization by 128% to 135%.

Table 3. Effects of potential SARS-CoV-2 exposure, susceptibility to COVID-19 complications, and access to healthcare on odds of seroconversion (n = 3,422) and hospitalization (n = 6,740) for Chasing COVID study participants, United States, March 28–April 20, 2020*

	Seroconversion			Hospitalization		
Variable	No. (%)	OR (95% CI)	aOR (95% CI)	No. (%)	OR (95% CI)	aOR (95% CI)
Overall	161 (4.70)			401 (5.95)		
Potential exposure†						
Less exposure risk	86 (3.73)	Referent	Referent	178 (4.30)	Referent	Referent
More exposure risk	75 (6.73)	1.86 (1.35–2.56)	1.64 (1.17–2.30)	223 (8.59)	2.09 (1.71– 2.57)	1.70 (1.37–2.12)
Susceptibility‡						
Less susceptible	130 (4.95)	Referent	Referent	258 (4.88)	Referent	Referent
More susceptible	31 (3.90)	0.78 (0.52–1.16)	0.82 (0.54–1.24)	143 (9.84)	2.13 (1.72– 2.63)	2.35 (1.88–2.92)
Access to healthcare§						
Less barriers	93 (4.21)	Referent	Referent	130 (3.52)	Referent	Referent
More barriers	68 (5.61)	1.35 (0.98–1.86)	1.22 (0.87–1.71)	271 (8.89)	2.67 (2.15–3.31)	2.28 (1.81–2.87)

*aOR, adjusted OR; Chasing COVID, Communities, Households, and SARS-CoV-2 Epidemiology COVID Cohort Study; OR, odds ratio.
†Model adjusted for age, presence of children in the household, employment, income, race/ethnicity.
‡Model adjusted for employment, income, race/ethnicity.
§Model adjusted for age, employment, sex, income, race/ethnicity.

Table 4. Modification of the association between race/ethnicity and hospitalization by potential SARS-CoV-2 exposure, susceptibility, and healthcare access for Chasing COVID study participants (n = 6,053), United States, March 28–April 20, 2020*

Variable	White non-Hispanic		Hispanic/Latino/a or Black non-Hispanic		aOR (95% CI) within exposed strata, Hispanic/Latino/a or Black non-Hispanic versus White
	No. hospitalized/ denominator (%)	aOR (95% CI)	No. hospitalized/ denominator (%)	aOR (95% CI)	
Measure of potential exposure†					
Less exposure risk	99/2,574 (3.85)	Referent	63/1,144 (5.51)	1.10 (0.78–1.55)	1.10 (0.78–1.55)
More exposure risk	86/1272 (6.76)	1.57 (1.16–2.15)	123/1,063 (11.57)	2.30 (1.69–3.13)	1.46 (1.08–1.97)
Less versus more within strata		1.57 (1.16–2.15)		2.09 (1.51–2.89)	
p value		p<0.01		p<0.001	
RERI (95% CI): measure of interaction on the additive scale				0.63 (−0.01 to 1.26)	
p value				p = 0.05	
Susceptibility‡					
Less susceptible	119/2,922 (4.07)	Referent	118/1,767 (6.68)	1.71 (1.30–2.23)	1.71 (1.30–2.23)
More susceptible	66/924 (7.14)	2.14 (1.55–2.94)	68/440 (15.45)	4.60 (3.33–6.36)	2.15 (1.49–3.10)
More versus less within strata		2.14 (1.55–2.94)		2.70 (1.95–3.72)	
p value		p<0.001		p<0.001	
RERI (95% CI): measure of interaction on the additive scale				1.75 (0.39–3.11)	
p value				p = 0.001	
Healthcare access§					
Less barriers to access	78/2,416 (3.23)	Referent	44/948 (4.64)	1.37 (0.93–2.03)	1.37 (0.93–2.03)
More barriers to access	107/1,430 (7.48)	2.23 (1.63–3.04)	142/1,259 (11.28)	3.41 (2.47–4.71)	1.53 (1.17–2.01)
Less versus more within strata of race/ethnicity		2.23 (1.63–3.04)		2.48 (1.74–3.54)	
p value		p<0.001		p<0.001	
RERI (95% CI): measure of interaction on the additive scale				0.81 (−0.06 to 1.69)	
p value				p = 0.07	

*aOR, adjusted OR; Chasing COVID, Communities, Households, and SARS-CoV-2 Epidemiology COVID Cohort Study; OR, odds ratio: RERI, relative excess risk caused by interaction.
†Model adjusted for age, presence of children in the household, employment, income, race/ethnicity.
‡Model adjusted for employment, income, race/ethnicity.
§Model adjusted for age, employment, sex, income, race/ethnicity.

Many researchers have hypothesized that social determinants have driven disparities in the effect of the COVID-19 pandemic, either directly or indirectly, because of occupation, living and working conditions, health-related behaviors, comorbidities, and immune functioning (*6*,*8*,*11*). However, the influence of social determinants on COVID-19 outcomes is understudied, and existing research has largely characterized social determinants by using geography and race/ethnicity as proxies (*25*–*30*). For example, US counties that have a higher proportion of Black or Hispanic population or of adults with less than a high school diploma had disproportionately higher numbers of COVID-19 cases (*29*). Using data from the American Community Survey to characterize socioeconomic vulnerability at the neighborhood level, ecologic analyses have demonstrated that increasing levels of socioeconomic vulnerability were associated with gaps in COVID-19 testing coverage in Massachusetts and COVID-19 deaths in Chicago, Illinois (*25*,*30*). Although useful, such approaches might mask the extent of COVID-19 disparities and the influence of social determinants at the individual level. We are aware of 1 study that included individual-level social indicators to assess COVID-19 outcomes (*31*).

Hispanic ethnicity, inability to shelter in place and maintain income, frontline service work, unemployment, and household income <$50,000 increased the risk for COVID-19 infection among residents and workers located in small community within San Francisco, California (*31*). We provide empirical evidence to support the conceptual model of Blumenshine et al. (*11*) in the context of the COVID-19 pandemic. Differences in social factors contribute to disparities in SARS-CoV-2 exposure, susceptibility to illness given infection, and access to care. Furthermore, reduced ability to social distance was positively associated with seroconversion and hospitalization, and increased susceptibility to COVID-19 complications and poor access to healthcare were positively associated with hospitalization.

We did not observe an association between seroconversion and susceptibility or access to care. The null finding is unsurprising given susceptibility to complications and access to care would be expected to influence illness after infection. Primary and secondary prevention efforts should address potential social disparities in exposure, COVID-19 vaccination, and access to care/treatment.

Our finding that Hispanic or Latino/a and Black non-Hispanic participants had more potential exposure risk and more difficulty with healthcare access than White non-Hispanic participants is consistent with other research showing a disproportionate burden of COVID-19 infections, complications, and deaths among racial and ethnic minorities (*3*,*5*,*8*,*27*,*32*–*37*). The positive additive interaction observed between racial and ethnic minority group status and susceptibility to more severe COVID-19 outcomes with hospitalization is especially concerning. We did not observe evidence of EMM by race/ethnicity in terms of the COVID exposure index or the healthcare access index. Recommendations for and discussions about social distancing fail to account for the reality of differential ability to adopt and benefit from these approaches, creating inequities in health outcomes. Longstanding social and health inequities contribute to susceptibility among Hispanic/Latino/a and Black non-Hispanic persons, and susceptibility is also influenced by lower healthcare access. Mitigation strategies and messaging should intensify focus on Hispanic/Latino/a and Black non-Hispanic persons who have conditions that increase risk for COVID-19 illness and death and incorporate tailored, culturally appropriate communication.

The first limitation of our study is that unmeasured confounding might effect exposure-outcome effect measures. We did not control for the time-varying nature of vaccination status or mask use because we considered these variables to lie on the causal pathway (Appendix Figures 1–3). We also did not address the possibility of joint effects of the indices.

Second, participants might not have completed every survey or serologic test, which would affect outcome measurement. Enrollment into the prospective cohort required 2 study interactions (i.e., completing the baseline survey and a second survey or the first serologic test). There was no missing data for the exposure measures or confounder measures because these measures were derived from the enrollment assessment, and participants had ≥1 opportunity to contribute data to the hospitalization outcome. Furthermore, cohort participation was high. A total of 58% (n = 3,913) of participants completed all 8 surveys included in this analysis, whereas 16% (n = 1,073) completed only 1 survey. Analyses of seroconversion were restricted to the population of persons who were seronegative at survey 1 and had 2 serologic tests (n = 3,422) (Appendix Table 1).

Third, measurement error and reporting bias might be a concern for measures of the exposure indices and hospitalizations. Although the indices have been previously used in national surveys conducted during the influenza A(H1N1) pandemic, those indices were proxies for exposure, seroconversion, and access to care and did not fully capture all aspects of these constructs (e.g., health literacy). This survey was launched in March 2020, when access to SARS-CoV-2 tests was severely limited and persons were hospitalized on the basis of symptoms. Therefore, we asked participants about hospitalization caused by COVID-19–like symptoms, rather than COVID-19 specifically. Accordingly, we might have inadvertently included some non–COVID-19 hospitalizations, particularly later in the pandemic.

Fourth, small numbers prevented us from assessing effect modification for each race/ethnicity group. We ran models comparing all race/ethnicities (Hispanic/Latino/a, Black non-Hispanic, Asian/Pacific Islander non-Hispanic, or other non-Hispanic) versus White non-Hispanic, and the results were similar to the models comparing Hispanic/Latino/a and Black non-Hispanic versus White non-Hispanic. Last, because our study is not a probability or population-based sample, findings might not be generalizable to all of the US population.

There have been increasing calls for research to better capture and report on socioeconomic determinants of COVID-19 outcomes alongside race/ethnicity to identify populations that might experience a disproportionate burden of risk or ability to benefit from pandemic mitigation strategies (*10*,*12*). We observed major racial/ethnic inequities in ability to social distance as a measure of potential SARS-CoV-2 exposure, susceptibility to COVID-19 complications, and access to healthcare in our national cohort. Future pandemic mitigation strategies should account for the contribution of social factors to racial and ethnic disparities in pathogen exposure, susceptibility to disease, and healthcare access.

Acknowledgments

We thank the participants of the Communities, Households, and SARS-CoV-2 Epidemiology COVID Cohort Study for providing contributions to the advancement of science around the SARS-CoV-2 pandemic.

This study was supported by the National Institutes of Health, National Institute of Allergy and Infectious Diseases (grant 3UH3AI133675-04S1 to D.N. and C.G), the CUNY Institute for Implementation Science in Population Health (cunyisph.org), the COVID-19 Grant Program of the CUNY Graduate School of Public Health and Health Policy, and National Institute of Child Health and Human Development (grant P2C HD050924) (Carolina Population Center).

About the Author

Dr. Robertson is an investigator at the CUNY Institute for Implementation Science in Population Health, New York, NY. Her primary research interests focus on the epidemiology of infectious diseases.

References

1. Centers for Disease Control and Prevention. Assessing risk factors for severe COVID-19 illness, November 26, 2021 [cited 2022 May 26]. https://www.cdc.gov/coronavirus/2019-ncov/covid-data/investigations-discovery/assessing-risk-factors.html
2. Ko JY, Danielson ML, Town M, Derado G, Greenlund KJ, Daily Kirley P, et al. Risk factors for COVID-19–associated hospitalization: COVID-19–associated hospitalization surveillance network and behavioral risk factor surveillance system. Clin Infect Dis. 2021;72:e695–e703. https://doi.org/10.1093/cid/ciaa1419
3. Garg S, Kim L, Whitaker M, O'Halloran A, Cummings C, Holstein R, et al. Hospitalization rates and characteristics of patients hospitalized with laboratory-confirmed coronavirus disease 2019—COVID-NET, 14 states, March 1–30, 2020. MMWR Morb Mortal Wkly Rep. 2020;69:458–64. https://doi.org/10.15585/mmwr.mm6915e3
4. Pareek M, Bangash MN, Pareek N, Pan D, Sze S, Minhas JS, et al. Ethnicity and COVID-19: an urgent public health research priority. Lancet. 2020;395:1421–2. https://doi.org/10.1016/S0140-6736(20)30922-3
5. Golestaneh L, Neugarten J, Fisher M, Billett HH, Gil MR, Johns T, et al. The association of race and COVID-19 mortality. EClinicalMedicine. 2020;25:100455. https://doi.org/10.1016/j.eclinm.2020.100455
6. Centers for Disease Control and Prevention. Health equity considerations and racial and ethnic minority groups, October 6, 2020 [cited 2020 Oct 21]. https://www.cdc.gov/coronavirus/2019-ncov/community/health-equity/race-ethnicity.html
7. Webb Hooper M, Nápoles AM, Pérez-Stable EJ. COVID-19 and racial/ethnic disparities. JAMA. 2020;323:2466–7. https://doi.org/10.1001/jama.2020.8598
8. McClure ES, Vasudevan P, Bailey Z, Patel S, Robinson WR. Racial capitalism within public health: how occupational settings drive COVID-19 disparities. Am J Epidemiol. 2020;189:1244–53. https://doi.org/10.1093/aje/kwaa126
9. Quinn SC, Kumar S, Freimuth VS, Musa D, Casteneda-Angarita N, Kidwell K. Racial disparities in exposure, susceptibility, and access to health care in the US H1N1 influenza pandemic. Am J Public Health. 2011;101:285–93. https://doi.org/10.2105/AJPH.2009.188029
10. Chowkwanyun M, Reed AL Jr. Racial health disparities and covid-19 - caution and context. N Engl J Med. 2020;383:201–3. https://doi.org/10.1056/NEJMp2012910
11. Blumenshine P, Reingold A, Egerter S, Mockenhaupt R, Braveman P, Marks J. Pandemic influenza planning in the United States from a health disparities perspective. Emerg Infect Dis. 2008;14:709–15. https://doi.org/10.3201/eid1405.071301
12. Khalatbari-Soltani S, Cumming RC, Delpierre C, Kelly-Irving M. Importance of collecting data on socioeconomic determinants from the early stage of the COVID-19 outbreak onwards. J Epidemiol Community Health. 2020;74:620–3. https://doi.org/10.1136/jech-2020-214297
13. Adkins-Jackson PB, Chantarat T, Bailey ZD, Ponce NA. Measuring structural racism: a guide for epidemiologists and other health researchers. Am J Epidemiol. 2022;191:539–47. https://doi.org/10.1093/aje/kwab239
14. Robertson MM, Kulkarni SG, Rane M, Kochhar S, Berry A, Chang M, et al.; CHASING COVID Cohort Study Team. Cohort profile: a national, community-based prospective cohort study of SARS-CoV-2 pandemic outcomes in the USA-the CHASING COVID cohort study. BMJ Open. 2021;11:e048778. https://doi.org/10.1136/bmjopen-2021-048778
15. Grov C, Westmoreland DA, Carneiro PB, Stief M, MacCrate C, Mirzayi C, et al. Recruiting vulnerable populations to participate in HIV prevention research: findings from the Together 5000 cohort study. Ann Epidemiol.2019;35:4–11. https://doi.org/10.1016/j.annepidem.2019.05.003
16. Nash D, Stief M, MacCrate C, Mirzayi C, Patel VV, Hoover D, et al. A web-based study of HIV prevention in the era of pre-exposure prophylaxis among vulnerable HIV-negative gay and bisexual men, transmen, and transwomen who have sex with men: protocol for an observational cohort study. JMIR Res Protoc. 2019;8:e13715. https://doi.org/10.2196/13715
17. Grov C, Westmoreland D, Rendina HJ, Nash D. Seeing is believing? Unique capabilities of internet-only studies as a tool for implementation research on HIV prevention for men who have sex with men: a review of studies and methodological considerations. J Acquir Immune Defic Syndr. 2019;82(Suppl 3):S253–60. https://doi.org/10.1097/QAI.0000000000002217
18. Office of Management and Budget. Office of management and budget (OMB) standards [cited 2022 May 26]. https://orwh.od.nih.gov/toolkit/other-relevant-federal-policies/OMB-standards
19. Kumar S, Quinn SC, Kim KH, Daniel LH, Freimuth VS. The impact of workplace policies and other social factors on self-reported influenza-like illness incidence during the 2009 H1N1 pandemic. Am J Public Health. 2012;102:134–40. https://doi.org/10.2105/AJPH.2011.300307
20. Nash D, Rane M, Robertson MM, Chang M, Kulkarni SG, Zimba R, You W, et al. SARS-CoV-2 incidence and risk factors in a national, community-based prospective cohort of U.S. adults. Clin Infect Dis.2022;May 27:ciac423. https://doi.org/10.1093/cid/ciac423
21. Food and Drug Administration. Center for Devices. Radiological health. EUA authorized serology test performance [cited 2022 May 26]. https://www.fda.gov/medical-devices/coronavirus-disease-2019-covid-19-emergency-use-authorizations-medical-devices/eua-authorized-serology-test-performance
22. Hernán MA, Robins JM. Causal inference: what if. Boca Raton (FL): Chapman & Hall/CRC; 2020 [cited 2022 May 26]. https://www.hsph.harvard.edu/miguel-hernan/causal-inference-book
23. Knol MJ, VanderWeele TJ. Recommendations for presenting analyses of effect modification and interaction. Int J Epidemiol. 2012;41:514–20. https://doi.org/10.1093/ije/dyr218
24. VanderWeele TJ, Knol MJ. A tutorial on interaction. Epidemiol Methods. 2014;3:33–72. https://doi.org/10.1515/em-2013-0005
25. Kim SJ, Bostwick W. Social vulnerability and racial inequality in COVID-19 deaths in Chicago. Health Educ Behav. 2020;47:509–13. https://doi.org/10.1177/1090198120929677
26. Figueroa JF, Wadhera RK, Lee D, Yeh RW, Sommers BD. Community-level factors associated with racial and ethnic disparities in COVID-19 rates in Massachusetts. Health Aff (Millwood). 2020;39:1984–92. https://doi.org/10.1377/hlthaff.2020.01040

27. Escobar GJ, Adams AS, Liu VX, Soltesz L, Chen YI, Parodi SM, et al. Racial disparities in COVID-19 testing and outcomes: retrospective cohort study in an integrated health system. Ann Intern Med. 2021;174:786–93. https://doi.org/10.7326/M20-6979
28. Millett GA, Jones AT, Benkeser D, Baral S, Mercer L, Beyrer C, et al. Assessing differential impacts of COVID-19 on black communities. Ann Epidemiol. 2020;47:37–44. https://doi.org/10.1016/j.annepidem.2020.05.003
29. Khanijahani A. Racial, ethnic, and socioeconomic disparities in confirmed COVID-19 cases and deaths in the United States: a county-level analysis as of November 2020. Ethn Health. 2021;26:22–35. https://doi.org/10.1080/13557858.2020.1853067
30. Dryden-Peterson S, Velásquez GE, Stopka TJ, Davey S, Lockman S, Ojikutu BO. Disparities in SARS-CoV-2 testing in Massachusetts during the COVID-19 pandemic. JAMA Netw Open. 2021;4:e2037067. https://doi.org/10.1001/jamanetworkopen.2020.37067
31. Chamie G, Marquez C, Crawford E, Peng J, Petersen M, Schwab D, et al.; CLIAhub Consortium. Community transmission of severe acute respiratory syndrome coronavirus 2 disproportionately affects the Latinx populationduring shelter-in-place in San Francisco. Clin Infect Dis. 2021;73(Suppl 2):S127–35. https://doi.org/10.1093/cid/ciaa1234
32. Van Dyke ME, Mendoza MC, Li W, Parker EM, Belay B, Davis EM, et al. Racial and ethnic disparities in COVID-19 incidence by age, sex, and period among persons aged <25 years—16 US jurisdictions, January 1–December 31, 2020. MMWR Morb Mortal Wkly Rep. 2021;70:382–8. https://doi.org/10.15585/mmwr.mm7011e1
33. Mackey K, Ayers CK, Kondo KK, Saha S, Advani SM, Young S, et al. Racial and ethnic disparities in COVID-19-related infections, hospitalizations, and deaths: a systematic review. Ann Intern Med. 2021;174:362–73. https://doi.org/10.7326/M20-6306
34. Wadhera RK, Wadhera P, Gaba P, Figueroa JF, Joynt Maddox KE, Yeh RW, et al. Variation in COVID-19 hospitalizations and deaths across New York City Boroughs. JAMA. 2020;323:2192–5. https://doi.org/10.1001/jama.2020.7197
35. Kaiser Family Foundation. Racial disparities in COVID-19: key findings from available data and analysis—issue brief, August 17, 2020 [cited 2022 May 26]. https://www.kff.org/report-section/racial-disparities-in-covid-19-key-findings-from-available-data-and-analysis-issue-brief
36. Gross CP, Essien UR, Pasha S, Gross JR, Wang S-Y, Nunez-Smith M. Racial and ethnic disparities in population level COVID-19 mortality. J Gen Intern Med. 2020;35:3097–9. https://doi.org/10.1007/s11606-020-06081-w
37. Adegunsoye A, Ventura IB, Liarski VM. Association of Black race with outcomes in COVID-19 disease: a retrospective cohort study. Ann Am Thorac Soc. 2020;17:1336–9. https://doi.org/10.1513/AnnalsATS.202006-583RL

Address for correspondence: McKaylee Robertson, Institute for Implementation Science in Population Health, City University of New York, 55 W 125th St, New York, NY 10027, USA; email: mckaylee.robertson@sph.cuny.edu

etymologia revisited

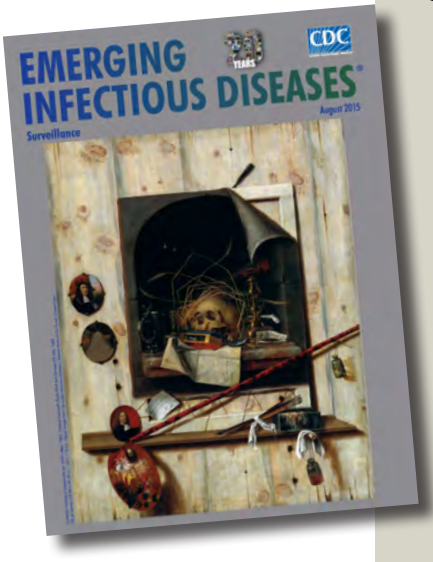

Originally published in August 2015

Escherichia coli

[esh"ə-rik'e-ə co'lī]

A gram-negative, facultatively anaerobic rod, *Escherichia coli* was named for Theodor Escherich, a German-Austrian pediatrician. Escherich isolated a variety of bacteria from infant fecal samples by using his own anaerobic culture methods and Hans Christian Gram's new staining technique. Escherich originally named the common colon bacillus *Bacterium coli commune*. Castellani and Chalmers proposed the name *E. coli* in 1919, but it was not officially recognized until 1958.

Sources:

1. Oberbauer BA. Theodor Escherich—Leben und Werk. Munich: Futuramed-Verlag; 1992.
2. Shulman ST, Friedmann HC, Sims RH. Theodor Escherich: the first pediatric infectious diseases physician? Clin Infect Dis. 2007;45:1025–9 .

https://wwwnc.cdc.gov/eid/article/21/8/et-2108_article

Effects of the COVID-19 Pandemic on Incidence and Epidemiology of Catheter-Related Bacteremia, Spain

Oriol Gasch, Laia Badia-Cebada, Joao Carmezim, Montserrat Vaqué, Virginia Pomar, Encarna Moreno, Anna Marrón, Emili Jiménez-Martínez, Maria José García-Quesada, Xavier Garcia-Alarcón, Dolors Domènech, Jordi Càmara, Marta Andrés, Judith Peñafiel, Rosario Porrón, Enric Limón, Esther Calbo, Miquel Pujol

We compared hospital-acquired catheter-related bacteremia (CRB) episodes diagnosed at acute care hospitals in Catalonia, Spain, during the COVID-19 pandemic in 2020 with those detected during 2007–2019. We compared the annual observed and predicted CRB rates by using the negative binomial regression model and calculated stratified annual root mean squared errors. A total of 10,030 episodes were diagnosed during 2007–2020. During 2020, the observed CRB incidence rate was $0.29/10^3$ patient-days, whereas the predicted CRB rate was $0.14/10^3$ patient-days. The root mean squared error was 0.153. Thus, a substantial increase in hospital-acquired CRB cases was observed during the COVID-19 pandemic in 2020 compared with the rate predicted from 2007–2019. The incidence rate was expected to increase by 1.07 (95% CI 1–1.15) for every 1,000 COVID-19–related hospital admissions. We recommend maintaining all CRB prevention efforts regardless of the coexistence of other challenges, such as the COVID-19 pandemic.

In December 2019, the first cases of COVID-19 were reported in Wuhan, China (*1*). On March 11, 2020, the World Health Organization declared COVID-19 a global pandemic because of the spread of SARS-CoV-2 infections worldwide (*2*). Subsequent waves related to the spread of different SARS-CoV-2 serotypes forced healthcare systems and, specifically, acute care hospitals to modify their structural and human resource organization (*3*); scheduled elective surgeries were cancelled, and healthcare workers had to change their specific clinical roles to address the abrupt increase in admissions of SARS-CoV-2–infected patients. To reduce SARS-CoV-2 nosocomial transmission, airborne and contact precaution measures were reinforced, personal protective equipment was worn by healthcare providers, and strict hand hygiene measures were observed at most centers (*4*).

Hand hygiene is a cornerstone of healthcare-associated infection (HAI) prevention, and reductions in *Clostridioides difficile* colitis incidence (*5*,*6*) and surgical-site infections (*7*,*8*) have been observed in different settings during the COVID-19 pandemic. However, reductions in other HAIs, such as catheter-associated urinary tract infections, ventilator-associated pneumonia, or catheter-related bacteremia (CRB) (*9*,*10*), were not observed. In addition, multidrug-resistant microorganisms were increasingly involved in these other HAIs (*10*–*12*).

CRB is one of the most frequent HAIs (*13*,*14*) and represents a major health challenge because of its high association with illness and death (*15*,*16*). CRB is currently considered a leading safety concern in healthcare settings and is a clinical practice quality

Author affiliations: Universitat Autònoma de Barcelona, Barcelona, Spain (O. Gasch); Hospital Universitari Parc Taulí I3PT, Sabadell, Spain (O. Gasch, L. Badia-Cebada, A. Marrón); Institut d'Investigació Biomèdica de Bellvitge-IDIBELL, L'Hospitalet de Llobregat, Spain (J. Carmezim, J. Càmara, J. Peñafiel, M. Pujol); Hospital de Barcelona, Barcelona (M. Vaqué); Hospital de la Santa Creu i Sant Pau, Barcelona (V. Pomar); Parc Sanitari Sant Joan de Déu, Sant Boi de Llobregat, Spain (E. Moreno); Hospital Universitari de Bellvitge, L'Hospitalet de Llobregat (E. Jiménez-Martínez, J. Càmara, M. Pujol); Hospital Germans Trias i Pujol, Badalona, Spain (M.J. García-Quesada); Hospital Josep Trueta, Girona, Spain (X. Garcia-Alarcón, D. Domènech); Hospital Consorci de Terrassa, Terrassa, Spain (M. Andrés); VINCat, Barcelona (R. Porrón, E. Limón); Universitat de Barcelona, Barcelona (E. Limón); Hospital Universitari Mútua Terrassa, Terrassa (E. Calbo)

DOI: https://doi.org/10.3201/eid2811.220547

indicator (*17*). For these reasons, CRB surveillance is mandatory in most countries (*18*–*20*).

In Catalonia, Spain, CRB surveillance is guided by the VINCat program of the Catalan Health Service (*21*), which provides a surveillance system for healthcare-associated nosocomial infections. The VINCat program was launched in 2006; the main objective of this program is to reduce the incidence of HAIs through continuous active monitoring and implementation of preventive programs (*21*). During recent decades, the incidence of healthcare-acquired CRB has decreased in most hospitals, especially in intensive care units (ICUs), because of the application of preventive measures (*22*,*23*). Some of the most critical evidence-based preventive interventions have been using appropriate barrier precautions and hand hygiene before handling catheters, disinfecting skin with chlorhexidine solutions, using appropriate catheter materials, carefully selecting insertion sites that avoid the femoral site, and withdrawing catheters whenever possible (*24*). During the COVID-19 pandemic, adherence to some of these preventive measures has notably affected HAI incidence rates (*11*); however, the effect of COVID-19 on CRB incidence is not definitively known. The aim of this study was to assess the effects of the COVID-19 pandemic on the incidence of hospital-acquired CRB.

Materials and Methods

Clinical Setting

Bacteremia associated with the use of venous catheters was continuously monitored under the VINCat program. All nosocomial episodes of CRB diagnosed in adult patients at each participating hospital were prospectively followed and reported to the VINCat program by infection control teams. CRB cases were identified by daily evaluation of all patients with bacteria-positive blood cultures.

Hospitals participating in the VINCat program are classified into 3 categories according to the number of beds available for hospitalization: ≥500 beds (group I), 200–499 beds (group II), and <200 beds (group III). Data from each hospital are continuously monitored and presented in general clinical sessions. A public annual report is published on the VINCat website (*21*).

Definitions

We defined catheter-related bacteremia as the detection of bacterial growth in patient blood using a venous catheter; ≥1 set of blood cultures were obtained from a peripheral vein and 2 sets were obtained to identify habitual skin-colonizing microorganisms, such as coagulase-negative staphylococci, *Micrococcus* spp., *Propionibacterium acnes*, *Bacillus* spp., and *Corynebacterium* spp. Positive bacterial cultures had to be associated with clinical manifestations of infection, such as fever, chills, or hypotension, and absence of any apparent alternative source of bloodstream infection (BSI). The conditions had to be accompanied by ≥1 of the following criteria: >15 CFU per catheter segment in semiquantitative cultures or $>10^3$ CFU per catheter segment in quantitative cultures that detected the same microorganism found in peripheral blood cultures; quantitative blood cultures that detected the same microorganism and showed a difference of ≥5:1 between the blood obtained from the lumen of a venous catheter and that obtained from a peripheral vein by puncture; difference of >2 hours between positive bacterial cultures obtained from a peripheral vein and the lumen of a venous catheter; presence of inflammatory signs or purulent secretions in the insertion point or the subcutaneous tunnel of a venous catheter (a culture of the secretion showing growth of the same microorganism detected in the blood cultures was also useful); and resolution of clinical signs and symptoms after catheter withdrawal with or without appropriate antibiotic treatment. For the clinical diagnosis of peripheral venous CRB, we required signs of phlebitis (induration, pain, or signs of inflammation at the insertion point or the catheter route).

Exclusion Criteria

We excluded patients if they were under 18 years of age, were outpatients, and had a hospital stay <48 hours at the time of BSI detection. We also excluded those who had CRB detected at an outpatient service or had CRB associated with arterial catheters.

Microbiology

Two sets of 2 blood samples from a peripheral vein were obtained from all patients with a suspected BSI. An additional blood sample was also obtained through the catheter. When possible, the catheter tip was cultured after removal. Blood samples were processed at the microbiology laboratories of each center in accordance with standard operating procedures. All microorganisms were identified by using standard microbiological techniques at each center.

Statistical Analysis

We reported categorical variables as the number of cases and percentages and continuous variables as means ±SD or medians with interquartile ranges,

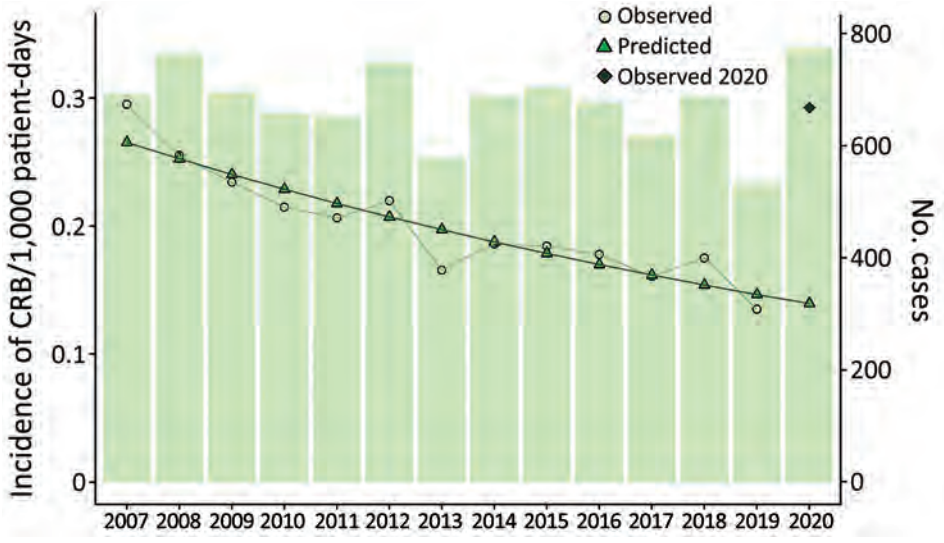

Figure 1. Observed and predicted incidence rates of CRB during 2007–2020 in study of effects of the COVID-19 pandemic on incidence and epidemiology of CRB, Spain. We calculated the CRB incidence rate by dividing the total number of episodes of catheter-related bloodstream infections by the total number of hospital stays (patient-days) for each year from 2007 to 2020. We predicted incidence rates by using the negative binomial regression model and compared the predicted rates with observed rates for each year. CRB, catheter-related bacteremia.

depending on whether the distribution was normal or nonnormal. We assessed normality of variables graphically by using quantile-quantile and density plots. We calculated the CRB incidence rate by dividing the total number of episodes of CRB by the total number of hospital stays (patient-days) in 1 year.

We used a negative binomial regression model to assess the rate trend of CRBs diagnosed at VINCat hospitals each year during 2007–2019. We used the number of admissions per year as the offset variable, number of events as the dependent variable, and year as the main independent variable. We performed stratified analyses according to hospital ward, catheter type, catheter insertion site, catheter use, and type of identified microorganism. We reported the annual rate of CRBs diagnosed per 1,000 patient-days and the incidence rate ratio (IRR) and 95% CI for each model. We focused the interpretation of the IRR on the annual rate of increase or decrease.

We plotted and compared the annual CRB rates observed during 2007–2020 and annual CRB rates predicted by our model. We calculated the average root mean squared error (RMSE) of the model predictions for CRB rates during 2007–2019 and

Table 1. Incidence rates of CRB per 1,000 patient-days in 2020 stratified by catheter characteristics and microorganisms in study of effects of the COVID-19 pandemic on incidence and epidemiology of catheter-related bacteremia, Spain*

Category	Observed rate	Predicted rate	Observed/predicted (95% CI)	RMSE
Location acquired				
ICU	1.62	0.48	3.42 (3.04–3.79)	1.147
Non-ICU	0.19	0.12	1.51 (1.37–1.65)	0.062
Catheter type				
CVC	0.16	0.06	2.54 (2.29–2.78)	0.094
PICVC	0.06	0.04	1.73 (1.46–2.00)	0.025
PVC	0.06	0.05	1.24 (1.06–1.43)	0.012
Catheter insertion site				
Arm/forearm	0.12	0.08	1.45 (1.29–1.60)	0.038
Jugular	0.09	0.03	2.64 (2.30–2.97)	0.056
Subclavian	0.04	0.02	1.88 (1.53–2.22)	0.020
Femoral	0.02	0.01	3.12 (2.27–3.96)	0.013
Catheter use				
Serum/medication	0.22	0.10	2.14 (1.97–2.31)	0.117
Hemodialysis	0.00	0.00	1.25 (0.51–1.99)	0.001
Parenteral nutrition	0.06	0.03	1.62 (1.36–1.89)	0.021
Microorganism				
Staphylococcus aureus	0.06	0.04	1.26 (1.06–1.46)	0.012
Coagulase-negative staphylococci	0.11	0.05	2.41 (2.14–2.68)	0.066
Gram-negative bacteria	0.04	0.03	1.69 (1.38–2.01)	0.017
Enterococcus sp.	0.03	0.01	5.41 (4.16–6.65)	0.022
Pseudomonas aeruginosa	0.01	0.01	2.20 (1.46–2.94)	0.007
Candida sp.	0.02	0.01	2.24 (1.59–2.90)	0.009

*We predicted expected rates of CRB by using negative binomial regression models and compared predicted rates with observed CRB rates in 2020. CRB, catheter-related bacteremia; RMSE, root mean squared error; ICU, intensive care unit; CVC, central vascular catheter; PICVC, peripherally inserted central vascular catheter; PVC, peripheral vascular catheter.

compared the RMSEs between the expected rate according to the model and observed rate in 2020. We replicated these analyses after stratifying by hospital ward, catheter type, catheter insertion site, catheter use, and type of microorganism.

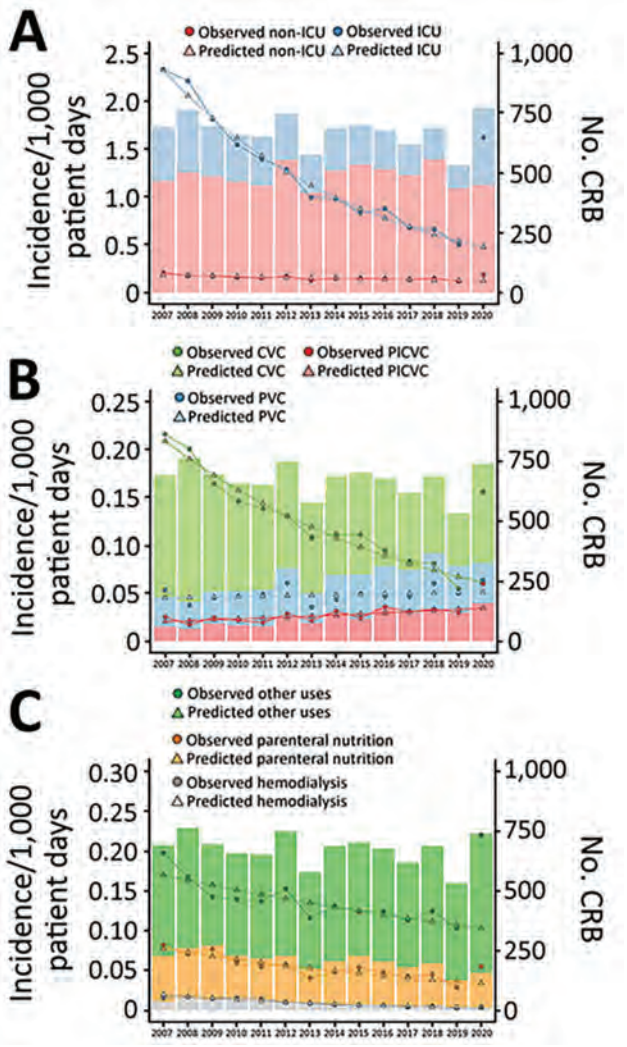

Figure 2. Observed and predicted incidence rates of CRB and number of CRB cases stratified by hospital ward, catheter type, and catheter use during 2007–2020 in study of effects of the COVID-19 pandemic on incidence and epidemiology of CRB, Spain. We calculated the CRB incidence rate by dividing the total number of episodes of catheter-related bloodstream infections by the total number of patient-days for each year from 2007 to 2020. We predicted incidence rates by using the negative binomial regression model and compared the predicted rates with observed rates for each year. A) CRB incidence per 1,000 patient-days, stratified by the type of hospital ward. B) CRB incidence per 1,000 patient-days, stratified by the type of catheter used. C) CRB incidence per 1,000 patient-days was stratified according to the reason for catheter use. CRB, catheter-related bacteremia; ICU, intensive care unit; CVC, central vascular catheter; PICVC, peripherally-inserted central vascular catheter; PVC, peripheral vascular catheter; PN, parenteral nutrition; HD, hemodialysis.

We evaluated the conditions of application in all models and calculated the 95% CI for each estimator. We arbitrarily set the level of statistical significance at 5%. We performed the analyses using the statistical package R version 4.0.3 (The R Project for Statistical Computing, https://www.r-project.org) for Windows.

Ethical Considerations

Participation in the VINCat program was voluntary, and data confidentiality was guaranteed. This study was evaluated and approved by the Parc Taulí Hospital Research Ethics Committee, Sabadell, Spain.

Results

Study Periods

During 2007–2020, a total of 10,030 nosocomial episodes of CRB were diagnosed. Data from the 2007–2019 period have been analyzed and described previously (*25*). In summary, during 2007–2019, a total of 9,290 episodes of CRB were diagnosed. The mean annual incidence was 0.2 episodes/10^3 patient-days, 73.7% of episodes occurred in non-ICU wards, 62.7% of episodes were related to central vascular catheters, 24.1% of episodes were related to peripheral venous catheters, and 13.3% of episodes were related to peripherally inserted central venous catheters (*25*). The incidence rate of CRB decreased substantially over the 2007–2019 study period (IRR 0.94, 95% CI 0.93–0.96), especially in ICU wards. CRB episodes caused by central vascular catheters fell markedly (IRR 0.90, 95% CI 0.89–0.92), whereas those associated with peripherally inserted catheters increased.

In 2020, a total of 774 CRB episodes were diagnosed at the participating hospitals. We determined that the incidence rate was 0.29 episodes/10^3 patient-days (Figure 1). Of 774 episodes, 297 (40.1%) were acquired in conventional medical wards, 127 (17.2%) in surgical wards, and 316 (42.7%) in ICUs. We found that the catheters most frequently implicated in CRB were central venous catheters (412 cases, 55.7%), peripheral catheters (169 cases, 22.8%), and peripherally inserted central venous catheters (159 cases, 21.5%). Catheters causing CRB were located in the arm/forearm (323 cases, 43.6%), jugular (237 cases, 32.0%), subclavian (116 cases, 15.7%), or femoral (52 cases, 7.03%) sites. The catheters were used for medication and serum infusion (583 cases, 78.8%), parenteral nutrition (146 cases, 19.7%), or hemodialysis (11 cases, 1.5%). The most frequent causes of CRB were coagulase-negative staphylococci (299 cases, 41.3%), *Staphylococcus aureus* (155 cases, 21.4%), gram-negative

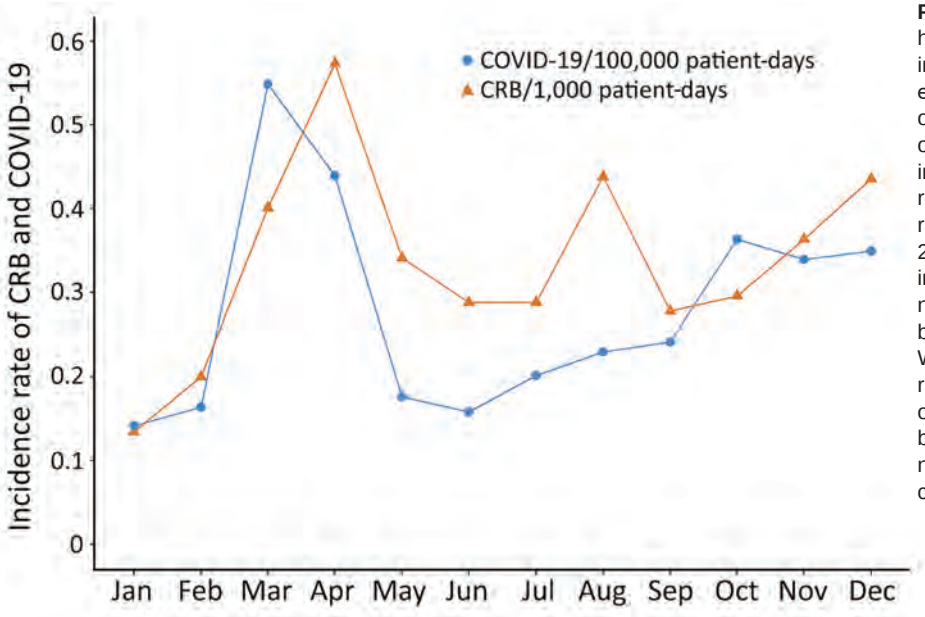

Figure 3. COVID-19–related hospital admissions and CRB incidence rates in 2020 in study of effects of the COVID-19 pandemic on incidence and epidemiology of CRB, Spain. We compared the incidence rates for COVID-19-related hospital admissions with rates for CRB each month during 2020. We calculated the COVID-19 incidence rates by dividing the total number of COVID-19 admissions by the total number of patient-days. We calculated CRB incidence rates by dividing the total number of episodes of catheter-related bloodstream infections by the total number of patient-days. CRB, catheter-related bacteremia.

enterobacteria (112 cases, 15.5%), enterococci (72 cases, 9.9%), *Candida* sp. (45 cases, 6.2%), and *Pseudomonas aeruginosa* (34 cases, 4.7%).

Comparison of Observed and Expected Incidence Rates

According to the case mix index observed during 2007–2019, we predicted that the incidence rate for CRB in 2020 was 0.14 episodes/10^3 patient-days. However, we observed 0.29 episodes/10^3 patient-days (observed/predicted [O/P] ratio 2.10, 95% CI 1.95–2.25) in 2020. The RMSE was 0.015 during 2007–2019 and 0.153 in 2020 (Figure 1). Disparities between predicted and observed rates were consistent among the different participating hospitals (Appendix Figure 1, https://wwwnc.cdc.gov/EID/article/28/11/22-0547-App1.pdf).

In conventional surgical and medical wards, we found that the predicted incidence rate for CRB was 0.12 episodes/10^3 patient-days, and the observed rate was 0.19/10^3 patient-days in 2020 (O/P 1.51, 95% CI 1.37–1.65). However, in ICUs, we predicted the incidence rate was 0.48 episodes/10^3 patient-days, but the observed rate was 1.62/10^3 patient-days in 2020 (O/P 3.42, 95% CI 3.04–3.79). The average RMSE was 0.013 for conventional wards and 0.069 for ICUs during 2007–2019, whereas, in 2020, the RMSE was 0.062 for conventional wards and 1.147 for ICUs (Table 1; Figure 2).

We observed an incidence rate of 0.064 for CRB caused by peripheral catheters in 2020; the predicted rate according to the negative binomial regression model was 0.05 (O/P 1.24, 95% CI 1.06–1.43). When

Table 2. Temporal evolution of COVID-19–related hospital admissions and catheter-related bacteremia incidence rates in study of effects of the COVID-19 pandemic on incidence and epidemiology of catheter-related bacteremia, Spain, 2020

	Conventional ward		ICU		Total*	
Month	Rate of COVID-19 admissions†	CRB incidence rate‡	Rate of COVID-19 admissions†	CRB incidence rate‡	Rate of COVID-19 admissions†	CRB incidence rate‡
January	14.11	0.12	15.15	1.39	14.15	0.13
February	16.12	0.15	21.78	2.86	16.36	0.20
March	52.81	0.13	76.14	3.29	54.87	0.40
April	41.30	0.20	83.44	5.55	43.95	0.57
May	17.02	0.22	31.33	4.49	17.6	0.34
June	15.56	0.21	21.37	2.81	15.8	0.29
July	19.50	0.17	32.94	2.83	20.15	0.29
August	22.10	0.24	38.41	5.73	22.96	0.44
September	23.06	0.18	46.00	3.43	24.15	0.28
October	34.20	0.14	70.45	3.20	36.33	0.30
November	31.87	0.20	68.22	4.09	33.93	0.36
December	33.73	0.29	68.43	7.11	34.94	0.44

*Total rates for conventional plus ICU wards. ICU, intensive care unit; CRB, catheter-related bacteremia.
†Values are COVID-19 admission rates per 100,000 patient-days.
‡Values are episodes of CRB per 1,000 patient-days.

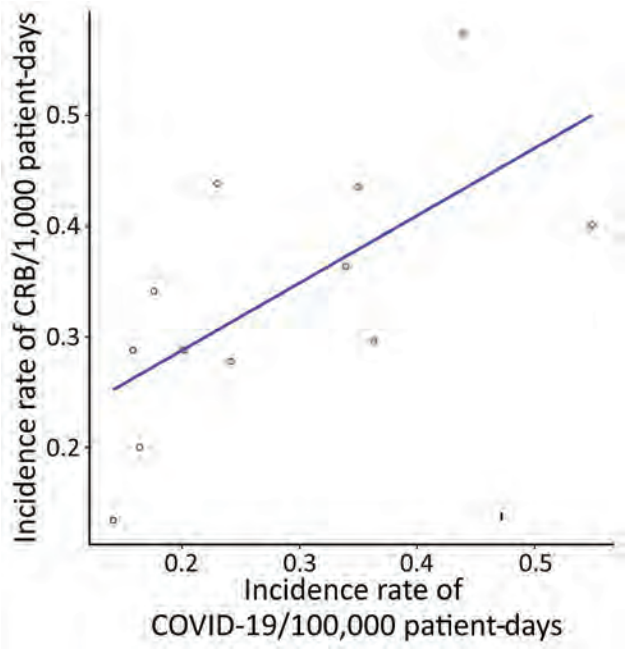

Figure 4. Association between COVID-19–related hospital admissions and CRB incidence rate in 2020 in study of effects of the COVID-19 pandemic on incidence and epidemiology of CRB, Spain. We calculated COVID-19 incidence rates by dividing the total number of COVID-19 admissions by the total number of patient-days and CRB incidence rates by dividing the total number of episodes of catheter-related bloodstream infections by the total number of patient-days. We used linear regression analysis to determine the relationship between COVID-19–related hospital admissions and the incidence of CRB. We found a positive association between the incidence of COVID-19–related hospital admissions and incidence rate of CRB ($R^2 = 0.45$). CRB, catheter-related bacteremia.

central catheters were used, the observed rate for CRB was 0.16, and the predicted rate was 0.06 (O/P 2.54, 95% CI 2.29–2.78). When peripherally inserted central catheters were used, the observed rate for CRB was 0.06, and the predicted rate was 0.04 (O/P 1.73, 95% CI 1.46–2.00). We observed increases in RMSEs in 2020 compared with the 2007–2019 period for peripheral catheters (0.012 vs. 0.007), central catheters (0.094 vs. 0.008), and peripherally inserted central catheters (0.025 vs. 0.004) (Table 1; Figure 2). In addition, we determined that the number of observed CRB episodes in 2020 were higher than predicted episodes depending on the location of the catheter; increased incidence was more pronounced in catheters located in femoral (O/P 3.11, 95% CI 2.27–3.96), jugular (O/P 2.64, 95% CI 2.30–2.97), and subclavian (O/P 1.88, 95% CI 1.53–2.22) sites (Table 1; Appendix Figure 2).

In 2020, we found increases in observed CRB incidence rates compared with rates predicted by the binomial regression model according to catheter use and causative microorganisms. For hemodialysis, the observed CRB rate was 0.004, and the predicted rate was 0.003 (O/P 1.25, 95% CI 0.51–1.99). For parenteral nutrition, the observed CRB rate was 0.06, and the predicted rate was 0.03 (O/P 1.62, 95% CI 1.36–1.89). For other uses, the observed CRB rate was 0.22, and the predicted rate was 0.10 (O/P 2.14, 95% CI 1.97–2.31); the last category increased most notably (Table 1; Figure 2). Observed CRB rates were increased compared with predicted rates for all causative microorganisms, especially enterococci (O/P 5.41, 95% CI 4.16–6.65).

Relationship between Monthly CRB Incidence Rates and SARS-CoV-2 Admissions

The total number of hospital admissions and the proportion of patients affected by COVID-19 changed substantially during 2020 (Figure 3). We recorded more COVID-19–related admissions during February–June in both conventional wards and ICUs (Table 2; Figure 3). The peak rate of COVID-19 hospital admissions was 54.87 in March, and the lowest rate was 14.15 in January.

Concomitantly, CRB incidence rates also varied during 2020, reaching a peak in April (0.57 episodes of CRB/10^3 admissions), followed by August and December (0.44 episodes of CRB/10^3 admissions for each month) (Table 2). We observed the lowest CRB rate at the beginning of the year (0.13 episodes of CRB/10^3 admissions).

We observed an association between CRB and COVID-19 incidence rate. The CRB incidence rate was expected to increase by 1.07 (IRR 1.07, 95% CI 1–1.15) for every 1,000 COVID-19 admissions if all factors remained constant (Figure 4).

Discussion

We demonstrated that the COVID-19 pandemic increased CRB incidence in 2020 in our hospitals in Catalonia, Spain. We found that months with the highest proportion of COVID-19 admissions were strongly associated with increased CRB incidence. We also described the most critical CRB characteristics that changed during the pandemic in 2020. Compared with previous years, we observed increased CRB incidence in both ICUs and conventional wards in 2020.

Other studies conducted around the same time observed increased HAI incidence rates during 2020, especially in ICUs. Catheter-associated urinary tract infections, ventilator-associated pneumonia, and CRB were the HAIs with the greatest increases (*9*–*11*). In contrast, other HAIs, such as nosocomial-acquired *C. difficile* colitis (*5*,*6*) or surgical-site infections (*7*,*8*,

decreased during the same period. Of note, HAIs may be more frequently associated with patients receiving steroids or tocilizumab (*26*), although a specific association with BSI was not observed (*27*).

In most cases, the increased rates of CRB were likely associated with a lower adherence to specific preventive measures during the months when the pandemic caused the most hospital admissions, despite the generalized reinforcement of contact precautions and hand hygiene to reduce SARS-CoV-2 nosocomial transmission. Of note, in our hospital settings, alcohol-based product consumption for hand hygiene during 2020 increased 2.4-fold overall and 1.9-fold in ICUs compared with the previous year, and a similar trend was observed in a hospital in Taiwan (*28*). Therefore, although proper hand hygiene is necessary to prevent CRB and other HAIs, it is not sufficient to avoid HAIs if other measures are not performed during the insertion and care of vascular catheters. Specifically, since 2006, various evidence-based bundles for CRB interventions have been shown to reduce CRB, especially in the ICU setting. These bundles include handwashing, using full-barrier precautions, cleaning the skin with chlorhexidine, avoiding the femoral site if possible, and removing unnecessary catheters (*22*,*23*). Among the different preventive measures, both hand hygiene and catheter insertion measures were associated with reduced incidence of CRB, and they were most effective when both measures were applied simultaneously (*24*).

The first limitation of our study is that heterogeneity of COVID-19 pandemic responses existed between hospitals, resulting in lack of data on adherence to CRB preventive measures at each center. Second, there was a lack of clinical information regarding the presence of chronic diseases or clinical conditions that might influence CRB incidence rates. However, the availability of a large number of CRB episodes diagnosed by standardized definitions is a strength that enables generalization of our observations. In addition, CRB incidence rates were adjusted by patient-days rather than catheter-days, which enabled surveillance of all types of catheters inserted in all hospital wards.

In 2020, substantial resources were allocated for infection prevention to manage the SARS-CoV-2 outbreak, which also affected HAI prevention programs. Because CRB is a key healthcare quality indicator (*29*), our observations stress the importance of maintaining all prevention efforts, regardless of the coexistence of other challenges, such as the worldwide COVID-19 pandemic.

Additional members of the Catalan Infection Control and Antimicrobial Stewardship Program: Alfredo Jover, Dolors Castellana (Hospital Universitari Arnau de Vilanova, Lleida, Spain); Montserrat Olona, Antonia García Pino (Hospital Universitari Joan XXIII, Tarragona, Spain); Josep Rebull Fatsini, M France Domènech (Hospital Verge de la Cinta, Tortosa, Spain); Miquel Pujol, Ana Hornero (Hospital Universitari de Bellvitge, L'Hospitalet de Llobregat, Spain); Joaquín López-Contreras, Engracia Fernández (Hospital de la Santa Creu i Sant Pau. Barcelona, Spain); Xavier Salgado, Dolors Domènech (Hospital Universitari Doctor Josep Trueta. Girona. Spain); Ana Lérida, Lydia Martin (Hospital deViladecans, Viladecans, Spain); Nieves Sopena, Irma Casas Garcia (Hospital Universitari Germans Tries i Pujol. Badalona. Spain); Rafel Pérez, Encarna Maraver (Althaia Xarxa Asistencia, Manresa, Spain); Eva Palau, Pepi Serrats (Clinica de Girona, Girona, Spain); José Antonio Martínez, Gemina Santana (Hospital Clínic i Provincial, Barcelona, Spain); Ana Martínez, Anna Martínez (Hospital de Campdevànol, Campdevànol, Spain); Lourdes Ferrer, M. José Moreno (Hospital Dos de Maig, Barcelona, Spain); Esther Calbo, Carolina Porta (Hospital Mútua de Terrassa, Terrassa, Spain); Alex Smithson (Hospital de l'Esperit Sant, Barcelona, Spain); Maria de la Roca Toda, Teresa Aliu (Hospital de Palamos, Palamós, Spain); Susanna Camps, Montserrat Ortega (Corporació Sanitària Parc Taulí, Sabadell, Spain); Vicens Diaz-Brito, Encarna Moreno (Hospital Sant Joan de Déu, Sant Boi, Spain); Carme Agustí, Miquel Perea Garcia (Hospital de Sant Celoni, Sant Celoni, Spain); Marta Andrés, Laura Grau Palafox (Hospital de Terrassa, Terrassa, Spain); Raquel Carrera, Anna Besolí (Consorci Hospitalari, Vic, Spain); Juan Pablo Horcajada, Cristina Gonzalez (Hospital del Mar/ Esperança, Barcelona, Spain); Jordi Cuquet, Demelsa Maria Maldonado López (Hospital General, Granollers, Spain); Rosa Benítez, Mirella Duch (Serveis Assistencials, Badalona, Spain); David Blancas, Esther Moreno (Consorci Sanitari del Garraf, Vilanova, Spain); Naiara Villalba, Sara Martínez (Hospital Sant Bernabé, Berga, Spain); Àngels García Flores, Roser Ferrer (Hospital Sant Jaume, Calella, Spain); Josep Bisbe, Montse Blascó (Hospital Sant Jaume, Olot, Spain); Antoni Castro Salom, Ana Felisa López (Hospital Universitari Sant Joan, Reus, Spain); Joan Espinach Alvarós, Àngels Perez (Hospital Sant Joan de Deu, Martorell, Spain); David Castander, Elisabet Calaf (Hospital Sant Pau i Santa Tecla, Tarragona, Spain); Mercè Clarós (Hospital Sant Rafael, Barcelona, Spain); Núria Bosch Ros (Hospital Sta. Caterina, Girona, Spain); Irene Montardit (Hospital Sta. Maria, Lleida, Spain); Roser Porta, Pilar De la Cruz Sol (Hospital Universitari Quirón Dexeus, Barcelona, Spain); Mª Rosa Coll Colell, Rosa García Penche Sanches (Hospital

Universitari Sagrat Cor, Barcelona, Spain); Josep Maria Tricas, Eva Redon (Fundació Privada Hopstital de Mollet, Mollet, Spain); Montse Brugués (Consorci Sanitari de l'Anoia, Igualada, Spain); Laura Linares, Maria Cusco (Hospital Comarcal de l'Alt Penedés, Vilafranca, Spain); Mª Pilar Barrufet, Elena Vidal (Consorci Hospitalari del Maresme, Mataró, Spain); Sandra Barbadillo, Mariló Marimón (Hospital Universitari General de Catalunya, Sant Cugat, Spain); Yolanda Meije, Montserrat Vaqué (Hospital de Barcelona, Barcelona, Spain); M. Rosa Laplace Enguinados, Blanca Vila (Hospital del Vendrell, El Vendrell, Spain); Ana Guadalupe Coloma, Lucrecia López (Hospital Moisés Broggi, Sant Joan Despí, Spain); Magda Campins, Carme Ferrer, Benito Almirante (Hospital Universitari. Vall d'Hebrón, Barcelona, Spain); Natalia Juan Serra, Josep Farguell Carrera (Hospital Quiron Salud Barcelona, Spain); Àngels Garcia Flores, Roser Ferrer (Hospital Comarcal de Blanes, Blanes, Spain); Marta Milian Sanz, Alexandra Moise (Pius Hospital de Valls, Valls, Spain); Ana Mª Jiménez Zarate, M. Carmen Eito Navasal (Institut Català d'Oncologia, L'Hospitalet, Spain); Maria Gracia Garcia Ramirez (Centre mèdicoquirúrgic, Reus, Spain); Ana Mª Jiménez Zarate (Institut Català d'Oncologia, Girona, Spain); Ana Mª Jiménez Zarate, Mar Armario Fernández (Institut Català d'Oncologia, Badalona, Spain).

Acknowledgments

We thank Johanna-Milena Caro and Garazi Carrillo-Aguirre for their help obtaining data for this project.

The study is part of the doctoral thesis of L.B.C. in the medicine department at Autonomous University of Barcelona. O.G. received a personal research grant from Pla estratègic de recerca i innovació en salut (PERIS) 2019–2021 (Departament de Salut, Generalitat de Catalunya). This work was supported by the Ministry of Economy and Competitiveness, Spain, Carlos II Institute Expedient: PI20/01563, Red Española de Investigación en Patología Infecciosa (REIPI), Centro de Investigación Biomédica en Red (CIBER) de Enfermedades Respiratorias (CIBERES CB06/06/0037), and CIBER of Infectious Diseases (INFEC, CB21/13/00009, IDIBELL), an initiative of the Instituto de Salud Carlos III, Madrid, Spain.

About the Author

Dr. Gasch is a clinician, associate of the Infectious Diseases Service at the Corporació Sanitària Parc Taulí (Sabadell), and a member of the infection control team of the institution. He is an associate professor in the Faculty of Medicine at Autonomous University of Barcelona, Spain, and his research interests are focused on the study of bloodstream infections and infective endocarditis.

References

1. Huang C, Wang Y, Li X, Ren L, Zhao J, Hu Y, et al. Clinical features of patients infected with 2019 novel coronavirus in Wuhan, China. Lancet. 2020;395:497–506. https://doi.org/10.1016/S0140-6736(20)30183-5
2. World Health Organization. Coronavirus disease 2019 (COVID-19) situation report—52 [cited 2022 Sep 21]. https://www.who.int/docs/default-source/coronaviruse/situation-reports/20200312-sitrep-52-covid-19.pdf
3. Weiner-Lastinger LM, Dudeck MA, Allen-Bridson K, Dantes R, Gross C, Nkwata A, et al. Changes in the number of intensive care unit beds in US hospitals during the early months of the coronavirus disease 2019 (COVID-19) pandemic. Infect Control Hosp Epidemiol. 2021;Jun 3;1–5. https://doi.org/10.1017/ice.2021.266
4. Centers for Disease Control and Prevention. Infection control guidance for healthcare professionals about coronavirus (COVID-19) [cited 2022 Sep 21]. https://www.cdc.gov/coronavirus/2019-ncov/hcp/infection-control.html
5. Bentivegna E, Alessio G, Spuntarelli V, Luciani M, Santino I, Simmaco M, et al. Impact of COVID-19 prevention measures on risk of health care-associated *Clostridium difficile* infection. Am J Infect Control. 2021;49:640–2. https://doi.org/10.1016/j.ajic.2020.09.010
6. Ponce-Alonso M, Sáez de la Fuente J, Rincón-Carlavilla A, Moreno-Nunez P, Martínez-García L, Escudero-Sánchez R, et al. Impact of the coronavirus disease 2019 (COVID-19) pandemic on nosocomial *Clostridioides difficile* infection. Infect Control Hosp Epidemiol. 2021;42:406–10. https://doi.org/10.1017/ice.2020.454
7. Chacón-Quesada T, Rohde V, von der Brelie C. Less surgical site infections in neurosurgery during COVID-19 times—one potential benefit of the pandemic? Neurosurg Rev. 2021;44:3421–5. https://doi.org/10.1007/s10143-021-01513-5
8. Losurdo P, Paiano L, Samardzic N, Germani P, Bernardi L, Borelli M, et al. Impact of lockdown for SARS-CoV-2 (COVID-19) on surgical site infection rates: a monocentric observational cohort study. Updates Surg. 2020;72:1263–71. https://doi.org/10.1007/s13304-020-00884-6
9. Baccolini V, Migliara G, Isonne C, Dorelli B, Barone LC, Giannini D, et al. The impact of the COVID-19 pandemic on healthcare-associated infections in intensive care unit patients: a retrospective cohort study. Antimicrob Resist Infect Control. 2021;10:87. https://doi.org/10.1186/s13756-021-00959-y
10. Baker MA, Sands KE, Huang SS, Kleinman K, Septimus EJ, Varma N, et al. The impact of coronavirus disease 2019 (COVID-19) on healthcare-associated infections. Clin Infect Dis. 2022;74:1748–54. https://doi.org/10.1093/cid/ciab688
11. Weiner-Lastinger LM, Pattabiraman V, Konnor RY, Patel PR, Wong E, Xu SY, et al. The impact of coronavirus disease 2019 (COVID-19) on healthcare-associated infections in 2020: a summary of data reported to the National Healthcare Safety Network. Infect Control Hosp Epidemiol. 2022;43:12–25. https://doi.org/10.1017/ice.2021.362
12. Bhargava A, Riederer K, Sharma M, Fukushima EA, Johnson L, Saravolatz L. High rate of multidrug-resistant organisms (MDROs) among COVID-19 patients presenting with bacteremia upon hospital admission. Am J Infect Control. 2021;49:1441–2. https://doi.org/10.1016/j.ajic. 2021.08.010
13. Zarb P, Coignard B, Griskeviciene J, Muller A, Vankerckhoven V, Weist K, et al.; National Contact Points for the ECDC pilot point prevalence survey; Hospital Contact Points for the ECDC pilot point prevalence survey. The European Centre for Disease Prevention and Control (ECDC) pilot point prevalence survey of healthcare-associated

infections and antimicrobial use. Euro Surveill. 2012;17:20316. https://doi.org/10.2807/ese.17.46.20316-en
14. Zingg W, Metsini A, Balmelli C, Neofytos D, Behnke M, Gardiol C, et al. National point prevalence survey on healthcare-associated infections in acute care hospitals, Switzerland, 2017. Euro Surveill. 2019;24:1800603. https://doi.org/10.2807/1560-7917.ES.2019.24.32.1800603
15. Zhong Y, Zhou L, Liu X, Deng L, Wu R, Xia Z, et al. Incidence, risk factors, and attributable mortality of catheter-related bloodstream infections in the intensive care unit after suspected catheters infection: a retrospective 10-year cohort study. Infect Dis Ther. 2021;10:985–99. https://doi.org/10.1007/s40121-021-00429-3
16. Chou EH, Mann S, Hsu TC, Hsu WT, Liu CCY, Bhakta T, et al. Incidence, trends, and outcomes of infection sites among hospitalizations of sepsis: a nationwide study. PLoS One. 2020;15:e0227752. https://doi.org/10.1371/journal.pone.0227752
17. O'Grady NP, Alexander M, Burns LA, Dellinger EP, Garland J, Heard SO, et al.; Healthcare Infection Control Practices Advisory Committee. Guidelines for the prevention of intravascular catheter-related infections. Am J Infect Control. 2011;39:S1–34. https://doi.org/10.1016/j.ajic.2011.01.003
18. European Union. Council recommendation of 9 June 2009 on patient safety, including the prevention and control of healthcare associated infections [cited 2022 Sep 21]. https://op.europa.eu/en/publication-detail/-/publication/8ae80abf-31cd-4577-b0be-4f2fe108f6f9
19. Centers for Disease Control and Prevention. National Healthcare Safety Network (NHSN) patient safety component manual. 2022 January [cited 2022 Sep 21]. https://www.cdc.gov/nhsn/pdfs/pscmanual/pcsmanual_current.pdf
20. Centers for Disease Control and Prevention. Current HAI progress report. 2020 National and state healthcare-associated infections progress report [cited 2022 Sep 21]. https://www.cdc.gov/hai/data/portal/progress-report.html
21. Catalan Health Service. VINCat program [cited 2022 Sep 21]. https://catsalut.gencat.cat/ca/proveidors-professionals/vincat
22. Pronovost P, Needham D, Berenholtz S, Sinopoli D, Chu H, Cosgrove S, et al. An intervention to decrease catheter-related bloodstream infections in the ICU. N Engl J Med. 2006;355:2725–32. https://doi.org/10.1056/NEJMoa061115
23. Palomar M, Álvarez-Lerma F, Riera A, Díaz MT, Torres F, Agra Y, et al.; Bacteremia Zero Working Group. Impact of a national multimodal intervention to prevent catheter-related bloodstream infection in the ICU: the Spanish experience. Crit Care Med. 2013;41:2364–72. https://doi.org/10.1097/CCM.0b013e3182923622
24. van der Kooi T, Sax H, Pittet D, van Dissel J, van Benthem B, Walder B, et al.; PROHIBIT consortium. Prevention of hospital infections by intervention and training (PROHIBIT): results of a pan-European cluster-randomized multicentre study to reduce central venous catheter-related bloodstream infections. Intensive Care Med. 2018;44:48–60. https://doi.org/10.1007/s00134-017-5007-6
25. Badia-Cebada L, Peñafiel J, Saliba P, Andrés M, Càmara J, Domenech D, et al.; VINCat programme (Infection Control Catalan Programme). Trends in the epidemiology of catheter-related bloodstream infections; towards a paradigm shift, Spain, 2007 to 2019. Euro Surveill. 2022;27:2100610. https://doi.org/10.2807/1560-7917.ES.2022.27.19.2100610
26. Kumar G, Adams A, Hererra M, Rojas ER, Singh V, Sakhuja A, et al. Predictors and outcomes of healthcare-associated infections in COVID-19 patients. Int J Infect Dis. 2021;104:287–92. https://doi.org/10.1016/j.ijid.2020.11.135
27. Abelenda-Alonso G, Rombauts A, Gudiol C, Oriol I, Simonetti A, Coloma A, et al. Immunomodulatory therapy, risk factors and outcomes of hospital-acquired bloodstream infection in patients with severe COVID-19 pneumonia: a Spanish case-control matched multicentre study (BACTCOVID). Clin Microbiol Infect. 2021;27:1685–92. https://doi.org/10.1016/j.cmi.2021.06.041
28. Lo SH, Lin CY, Hung CT, He JJ, Lu PL. The impact of universal face masking and enhanced hand hygiene for COVID-19 disease prevention on the incidence of hospital-acquired infections in a Taiwanese hospital. Int J Infect Dis. 2021;104:15–8. https://doi.org/10.1016/j.ijid.2020.12.072
29. World Health Organization. Global patient safety action plan 2021–2030 [cited 2022 Sep 21]. https://www.who.int/teams/integrated-health-services/patient-safety/policy/global-patient-safety-action-plan

Address for correspondence: Oriol Gasch, Hospital Parc Taulí de Sabadell, Institut d'Investigació i Innovació Parc Taulí (IL3PT), Universitat Autònoma de Barcelona, 08208 Sabadell, Spain; email: ogasch@tauli.cat

Invasive Infections Caused by Lancefield Groups C/G and A *Streptococcus*, Western Australia, Australia, 2000–2018

Cameron M. Wright, Rachael Moorin, Glenn Pearson, John Dyer, Jonathan Carapetis, Laurens Manning

Epidemiologic data on invasive group C/G *Streptococcus* (iGCGS) infections are sparse internationally. Linked population-level hospital, pathology, and death data were used to describe the disease burden in Western Australia, Australia, during 2000–2018 compared with that of invasive group A *Streptococcus* (GAS, *Streptococcus pyogenes*) infections. Of 1,270 cases, 866 (68%) occurred in men. Patients with iGCGS infection were older (median age 62 years) than those with invasive GAS (median age 44 years; p<0.0001). The age and sex-adjusted incidence rate ratio by year was 1.08 (95% CI 1.07–1.09). The incidence rate ratio for Indigenous compared with non-Indigenous Australians was 3.6 (95% CI 3.0–4.3). The all-cause 90-day death rate was 9% for iGCGS infection compared with 7% for invasive GAS (p = 0.03). iGCGS infection was more common in men and older persons and had a higher death rate, perhaps reflecting the effect of age and comorbidities on incidence and death.

Invasive, β-hemolytic *Streptococcus* disease is associated with high rates of illness and death and substantial financial cost (*1*–*3*). Human pathogenic β-hemolytic *Streptococcus* include Lancefield groups A (GAS, *Streptococcus pyogenes*), B (GBS, *S. agalactiae*), and C and G (GCGS, multiple species) (*4*). An understanding of the population-level disease burden is essential for planning preventive and management strategies (*2*). For GCGS, the major subspecies causing human infection is *S. dysgalactiae* subspecies *equisimilis*, which shares virulence factors with GAS, including the M protein (*2*). Evidence from epidemiologic studies and animal models also link GCGS infection to postinfectious immunologic complications such as rheumatic heart disease (*5*,*6*). For these reasons, GCGS and GAS have overlapping clinical manifestations and, from a prevention perspective, development efforts toward a vaccine for GAS may have off-target effects in preventing GCGS infection (*7*).

Compared with knowledge about invasive GAS infections, much less is known about the epidemiology of invasive GCGS (iGCGS) disease or how clinical features and outcomes differ between them. Unlike GAS, which is notifiable in many jurisdictions, such as the United Kingdom (*8*) and Canada (*9*), iGCGS is not considered a notifiable disease in any jurisdiction. For the few settings where comparative epidemiologic data are available, the incidence of iGCGS infection is similar or higher than for invasive GAS (*10*,*11*). Also shared in common with invasive GAS infections, iGCGS has a death rate of 5%–10%, and its incidence appears to be increasing in recent years in some countries (*10*,*12*–*14*).

In a recent study, we demonstrated an increasing incidence of invasive GAS infection that disproportionately affects Indigenous Australians (*15*). By using this same methodology, we sought to describe the epidemiology of iGCGS infection in terms of incidence, median length of hospital stay, and all-cause deaths and to compare these metrics with those in patients with invasive GAS infections.

Author affiliations: Curtin University, Perth, Western Australia, Australia (C.M. Wright); University of Tasmania, Hobart, Tasmania, Australia (C.M. Wright, R. Moorin); The University of Western Australia, Crawley, Western Australia, Australia (C.M. Wright, R. Moorin, J. Carapetis, L. Manning); Fiona Stanley Fremantle Hospitals Group, Murdoch, Western Australia, Australia (C.M. Wright, J. Dyer, L. Manning); Telethon Kids Institute, University of Western Australia, Perth (G. Pearson, J. Carapetis, L. Manning); Perth Children's Hospital, Perth (J. Carapetis)

DOI: https://doi.org/10.3201/eid2811.220029

Methods

Reporting was based on the RECORD (REporting of studies Conducted using Observational Routinely collected health Data) statement (*16*). Ethics approval was provided by the Western Australia (WA) Department of Health Human Research Ethics Committee (HREC) (#2019/03) and the WA Aboriginal Health Ethics Committee (#899). The University of WA HREC acknowledged external approval by the WA Department of Health HREC (RA/4/20/5695). A consent waiver was granted, meaning individual consent was not required. This study was designed as a population-based data linkage study.

Setting

WA is the largest state in Australia, covering about one third of the continent (2.6 million km^2). In 2018, the population was 2.6 million persons (10% of the population of Australia), including ≈2 million persons living in the capital city, Perth (*17*); 4% of the population were Indigenous persons (*18*). The climate ranges from tropical in the north to desert in the central regions and temperate in the south. The climate of the Kimberley and Pilbara regions is tropical, and the proportion of Indigenous persons is higher there than in other regions of WA (in 2016, accounting for 42% of the population in Kimberley and 14% in Pilbara) (*19*). Regional, climate-based, and demographic variation in health-related variables can accordingly be explored in WA, as we did in our previous investigation of lower leg cellulitis, by using linked hospital and emergency department data (*20*,*21*).

Data Sources and Measurement

The WA Data Linkage System used best-practice methods (*22*) to link the Hospital Morbidity Data Collection (HMDC), consisting of all WA public and private hospital records; PathWest, the government-owned pathology services provider for metropolitan and regional public hospitals; and death registrations, which are used in state-level and national-level death statistics. Linked data had a scrambled unique identifier for each person.

Case Definition

We analyzed data for cases of iGCGS and invasive GAS infection occurring during January 1, 2000–December 31, 2018, among WA residents. Methods relating to invasive GAS infections are described elsewhere (*15*). In brief, microbiologically confirmed cases were defined as GCGS isolated from a normally sterile site (blood, cerebrospinal fluid, or other normally sterile fluid or sterile tissue) identified in PathWest laboratory data. Group C and G *Streptococcus* were grouped together as GCGS as characterized in the PathWest data. Diagnoses of iGCGS infection were identified in the HMDC by principal diagnostic codes from the International Classification of Diseases, 10th Revision, Australian Modification (ICD-10-a.m.) for GCGS-specific invasive disease (Appendix Table 1, https://wwwnc.cdc.gov/EID/article/28/11/22-0029-App1.pdf), referred to hereafter as the HMDC cohort definition. To be included, a case had to be accompanied by the ICD-10-a.m. code for GCGS infection (B95.41, Streptococcus, group C, as the cause of diseases classified to other chapters; or B95.42, Streptococcus, group G, as the cause of diseases classified to other chapters) as the first additional diagnosis, without any ICD-10-a.m. codes for other bacterial infection diagnoses. We included all cases of iGCGS infection according to PathWest or HMDC cohort definitions (or both) in our analysis.

Pathology data were grouped within a hospitalization (regardless of whether the hospitalization fulfilled the HMDC cohort definition) if collection was within 2 days of an admission date, thus enabling previous outpatient clinic or emergency department specimen collection. The record date for a case was the first collection date for each episode or the admission date if there was no confirmatory isolate. Because iGCGS infection is an acute condition, persons could have incident disease more than once, but all records for a person occurring within 30 days were considered a single event (*23*). We also conducted a sensitivity analysis restricting to 1 case per person only.

Case Characteristics

Age, sex, hospital admission and separation (discharge) dates, diagnostic codes, region of residence, census-specific remoteness of residence area (major cities, inner regional, outer regional, remote, or very remote) (*24*), census-specific postcode-based values according to socioeconomic index for relative social disadvantage (separated into quintiles) (*25*), and admission to an intensive care unit were extracted from the HMDC. Indigenous status was provided as part of the linkage process. Date of death was extracted from death registrations. Region of residence was divided into tropical (Kimberley and Pilbara regions) and nontropical and into metropolitan and regional. PathWest data included the unique patient identifier code, sample collection date, and isolation site. For cases identified through PathWest only, we sourced relevant demographic data (e.g., age, sex) from the HMDC, because all hospital records for the cohort

were available. Case-patients were designated as a WA resident, Indigenous, or living in a tropical area (not mutually exclusive) if assigned one of these designations for any part of a case.

Statistical Analyses

Descriptive Statistics

We included cases with missing demographic data but did not include them in analyses stratified by the missing variable. For statistical comparisons of categorical variables, we used a χ^2 test and a nonparametric equality of medians test for continuous variables. We explored seasonality as wet (November–April) and dry (May–October) seasons for tropical and 4 seasons for nontropical regions.

Table. Descriptive statistics of invasive group C/G *Streptococcus* disease, Western Australia, Australia, 2000–2018*

Characteristic	No. (%)
Total	1,270
Sex	
F	400 (31)
M	866 (68)
Missing/unknown	<5
Age group, y	
<1	5 (0)
1–4	<5
5–14	6 (0)
15–24	52 (4)
25–34	80 (6)
35–44	133 (10)
45–54	181 (14)
55–64	222 (17)
65–74	244 (19)
75–84	215 (17)
≥85	126 (10)
Missing/unknown	<5
Indigenous status	
Non-Indigenous	1,067 (84)
Indigenous	148 (12)
Missing/unknown	55 (4)
Region of occurrence	
Nontropical	1,175 (93)
Tropical	91 (7)
Missing/unknown	<5
Remoteness	
Major cities	855 (67)
Inner regional	92 (7)
Outer regional	128 (10)
Remote	81 (6)
Very remote	59 (5)
Missing/unknown	55 (4)
Socioeconomic status	
Most disadvantaged	384 (30)
More disadvantaged	280 (22)
Moderately disadvantaged	220 (17)
Less disadvantaged	184 (14)
Least disadvantaged	198 (16)
Missing/unknown	<5
30-d all-cause deaths	85 (7)
90-d all-cause deaths	114 (9)

*Categories with <5 patients are shown without accompanying percentage values to comply with confidentiality data requirements. Some rows do not sum to 100 because of this or because of rounding. Analogous data for invasive group A *Streptococcus* disease has been published separately (*15*).

Crude and Age-Standardized Incidence

We included only WA residents in incidence calculations and sourced midyear population denominators from the Australian Bureau of Statistics census estimates and projections (*17*). We calculated crude incidence stratified by sex, age group, Indigenous status (from 2001, owing to readily publicly available denominators) and region (from 2001, for the same reason). We calculated direct age-standardized annual incidence standardizing to the age-based population structure of cases in 2000. We also conducted subanalyses for cases in which GCGS was isolated only from blood or tissue culture. We performed negative binomial regression, selected because of overdispersed data, for incidence adjusting for year, age group, and sex. We also used negative binomial regression to model incidence adjusting for Indigenous status and year and separately by Indigenous status adjusting for year.

Median Length of Stay and All-Cause Deaths

For median length of stay, we treated interhospital transfers as a single admission. We calculated all-cause death at 30 days and 90 days after record date. We assessed differences in 30-day deaths by Indigenous status by using age group–adjusted and sex-adjusted logistic regression. We performed all analyses by using Stata SE version 14.0 (StataCorp LLC, https://www.stata.com).

Results

Demographic and Clinical Characteristics of Patients with iGCGS Infection

A total of 1,270 cases occurred during the study period. Of those, 1,195 (94%) were confirmed with PathWest microbiological data. Only 112 (9%) had an iGCGS-specific HMDC discharge diagnosis; of those, 37 (33%) had both HMDC-confirmed cases and microbiologic confirmation. This percentage was higher for public hospital cases (41%, 33/80) than for private hospital cases (13%, 4/32; p = 0.003). Of microbiologically confirmed cases, GCGS was isolated from blood in 713/1,195 (60%) cases, from tissue in 388 (32%) cases, and from other sterile fluids in 208 (17%) cases, although these types were not mutually exclusive. The most frequent principal diagnoses for hospitalizations with a corresponding GCGS isolate (i.e., samples within 2 days of admission) were other streptococcal sepsis (151 [12%]), cellulitis of other

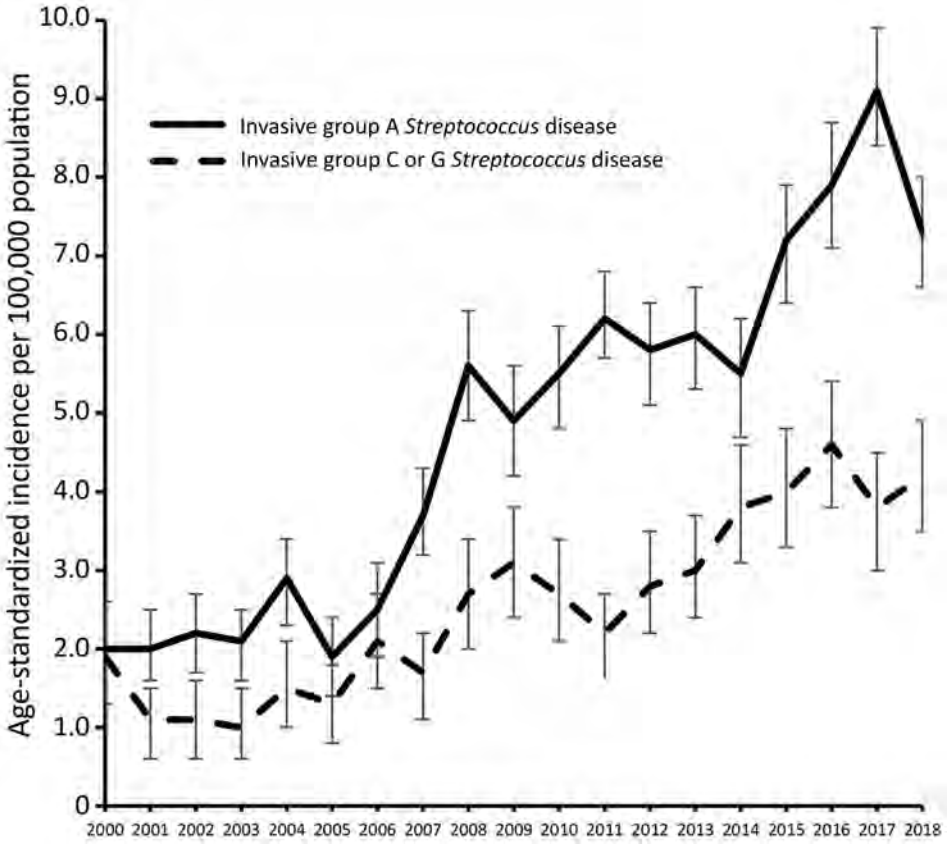

Figure 1. Age-standardized incidence of invasive group A and C/G *Streptococcus* disease, Western Australia, Australia, 2000–2018. The baseline age distribution is the year 2000. Error bars indicate 95% CI.

parts of limb (118 [9%]), and type 2 diabetes with foot ulcer with multiple causes (71 [6%]).

More than two thirds of cases were in men (866/1,270 [68%]; p<0.001) (Table), and the median age was 62 years (interquartile range [IQR] 47–75 years). Only 13 (1%) of 1,270 cases occurred in persons who were ≤14 years of age (Table). A total of 148 cases (12%) occurred in Indigenous Australians and 91 case-patients (7%) were from a tropical region of the state. Just over two thirds of cases were among persons from a major city (855/1,270 [67%]), and nearly one third of cases (384/1,270 [30%]) were in the most disadvantaged quintile in the index for relative social disadvantage. Seasonality was not evident among nontropical cases: 306/1,175 cases occurred during summer (26%), 298 occurred in autumn (25%), 268 occurred in winter (23%), and 303 occurred in spring (26%). In the tropics, more cases occurred in the wet season (59%) than in the dry season (41%; p = 0.07).

Crude and Age-Standardized Incidence

The age-standardized incidence of iGCGS disease increased from a low of 1.0 (95% CI 0.5–1.4) cases/100,000 population in 2003 to a peak of 4.6 (95% CI 3.8–5.4 cases) cases/100,000 population in 2017 (Figure 1). The adjusted incidence rate ratio (IRR) for year of diagnosis since 2000 was 1.08 (95% CI 1.07–1.09). A sensitivity analysis restricted to 1 case per person (76 [6%] had >1 iGCGS infection) did not show any difference in incidence, compared with analysis allowing repeat infection separated by ≥30 days (Appendix Figure 1). The numbers of incident cases with blood or tissue isolates each increased over time (Appendix Figure 2). The age-group based crude incidence of iGCGS disease increased with age (Figure 2).

Crude incidence increased over time for Indigenous persons (per year: IRR 1.11, 95% CI 1.07–1.15) and non-Indigenous persons (IRR 1.09, 95% CI 1.07–1.10). Crude incidence was higher for Indigenous persons than for non-Indigenous persons from 2004 on, peaking in 2018 at 17.2 (95% CI 9.2–25.1) cases/100,000 population in Indigenous persons and 4.1 (95% CI 3.3–4.9) cases/100,000 population in non-Indigenous persons (Figure 3). The year-adjusted IRR comparing Indigenous and non-Indigenous Australians was 3.6 (95% CI 3.0–4.3). Crude incidence was higher for Indigenous persons in both metropolitan and regional areas (data not shown). Incidence was consistently higher among men than women (adjusted IRR 2.3, 95% CI 2.1–2.6) (Appendix Figure 3).

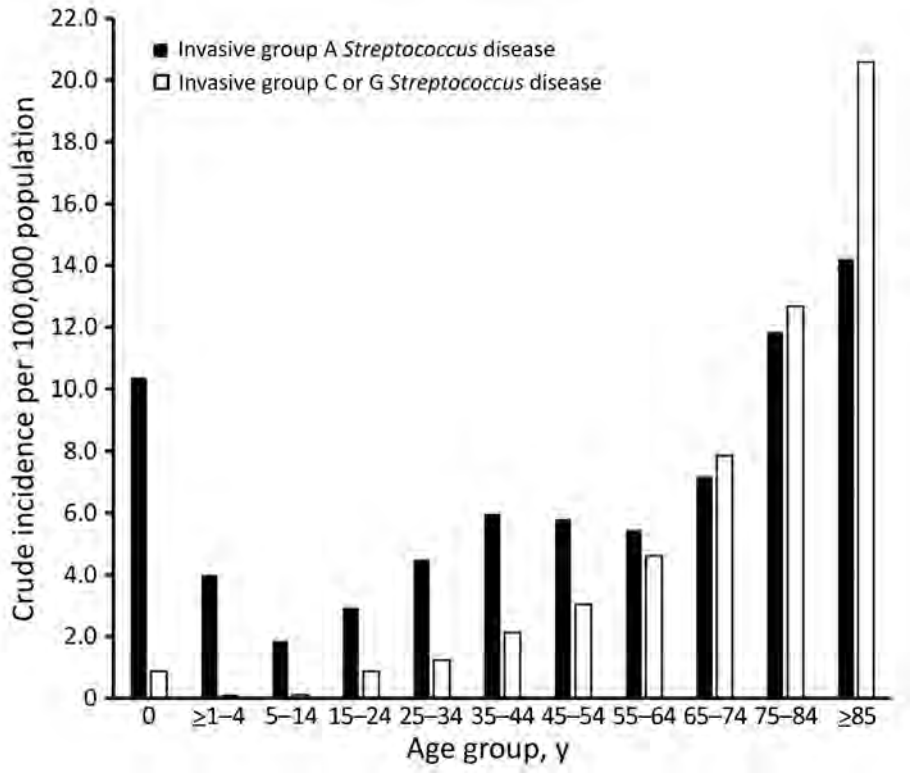

Figure 2. Age group distribution of invasive group A and C/G *Streptococcus* disease, Western Australia, Australia, 2000–2018.

Median Length of Stay and All-Cause Death

Median length of stay was 10 days (IQR 2–24 days). In 85 (7%) cases, the patient had died of any cause by 30 days, and 114 (9%) patients had died by 90 days (Table). All-cause death was lower at 30 days for Indigenous patients (4/148 cases [3%]) than non-Indigenous patients (81/1,067 [8%]), but the difference was not statistically significant after adjustment for age group and sex (adjusted odds ratio 0.7, 95% CI 0.3–1.4). At 30 days, the all-cause death rate was higher in cases in which GCGS was isolated from blood (92/713 [13%]) than in cases with no blood isolate (22/557 [4%]; p<0.001) and higher if the patient was admitted to intensive care (9/55 [16%]) than if not (76/1,215 [6%]; p<0.001). In cases involving patients ≥85 years of age, the 90-day all-cause death rate was 32%.

Comparison with Invasive GAS Infection

The incidence of invasive GAS infection was higher than for iGCGS disease over the study period but increased at a similar annual rate; the yearly IRR was 1.09 (Figure 1). Visual assessment of the age distribution (Figure 2) indicates a higher concentration of iGCGS disease in older age groups compared with invasive GAS disease. Compared with patients with invasive GAS infections, patients with iGCGS were older (median 62 [IQR 47–75] vs. 44 [IQR 29 – 62] years; p<0.0001). The percentage of men with invasive GAS disease was lower than the percentage of men with iGCGS disease (57% vs. 68%; p<0.001). Conversely, the proportion of cases among Indigenous persons was higher for invasive GAS than for iGCGS (34% vs. 12%; p<0.001).

The median length of stay was also higher for iGCGS patients than for invasive GAS patients (10 [IQR 2–24] vs. 7 [IQR 3–16] days; p<0.0001). The 30-day all-cause death rate was higher for patients with invasive GAS disease than for those with iGCGS disease (Appendix Table 2), but this difference was not significant (p = 0.06). The 90-day death rate for iGCGS was higher than that for invasive GAS disease (9% [114/1,270] vs. 7% [156/2,237]; p = 0.03). However, the age-adjusted odds of 90-day death were higher for invasive GAS disease than for iGCGS disease (adjusted odds ratio 1.33, 95% CI 1.02–1.73).

Discussion

These data show an increasing incidence of iGCGS infections over time in WA. Cases occurred predominately among older persons and men, and the all-cause 90-day death rate among infected persons was high. As with invasive GAS, the incidence of iGCGS among Indigenous Australians was higher than among non-Indigenous Australians, although the

respective IRRs over the study period were similar (1.11 and 1.09). The increase in iGCGS disease in WA is a critical finding, because development of a GAS vaccine could benefit the older population affected more commonly by iGCGS infection, if there are off-target protective effects across Lancefield groups (*7*).

In a 2017 study using similar methodology and dataset, we demonstrated that the combined incidence of iGCGS was approximately half that of invasive GAS disease (*15*). Similarly, although both diseases were more common among Indigenous than among non-Indigenous Australians, the relative risk was higher for invasive GAS (IRR 13.1) (*15*) than for iGCGS (IRR 3.6). Compared with findings for other settings, the reported incidence in this study (4.6 cases/100,000 population) was lower than that in a study from southern Hungary (11 cases/100,000 population) (*12*) but higher than that reported in the United States (2.8 cases/100,000 population) (*26*).

In the context of Australia, these data extend previous work from North Queensland (*27*). Harris et al. (*27*) reported on GCCS bacteremia in North Queensland during 1996–2009, finding two thirds of group G cases occurred in men. Our data are in accordance with this finding; 68% of cases occurred in men. Harris et al. (*27*) found a 28-day all-cause death rate of 5.5% (5/91) for GCCS bacteremia, lower than the 9% rate in our study, although with a much smaller denominator. The mean age of patients with GCCS bacteremia reported by Harris et al. (*27*) was 43 years, younger than those in this study.

The age distribution of iGCGS infection differs from invasive GAS disease (*15*). Unlike GAS, which occurs most frequently in older and younger age groups but also occurs in the middle age groups, iGCGS is characteristically an infection of middle-aged and older persons. Age is likely a surrogate marker for comorbidities such as diabetes (*28*), alcohol use, and liver diseases, which have been reported elsewhere as risk factors for iGCGS infection (*10*).

Factors predisposing persons to iGCGS disease might also contribute to the high observed all-cause death rate and prolonged length of hospital stay reported in this study. To place all-cause deaths in context, the 30-day death rate among those ≥85 years of age at diagnosis was much higher (25%) than the rate of ≈10% for this age group after neck of femur fracture (*29*). When compared with invasive GAS disease, the 30-day death rate in older age groups (>65 years of age) was similar to or marginally lower than that

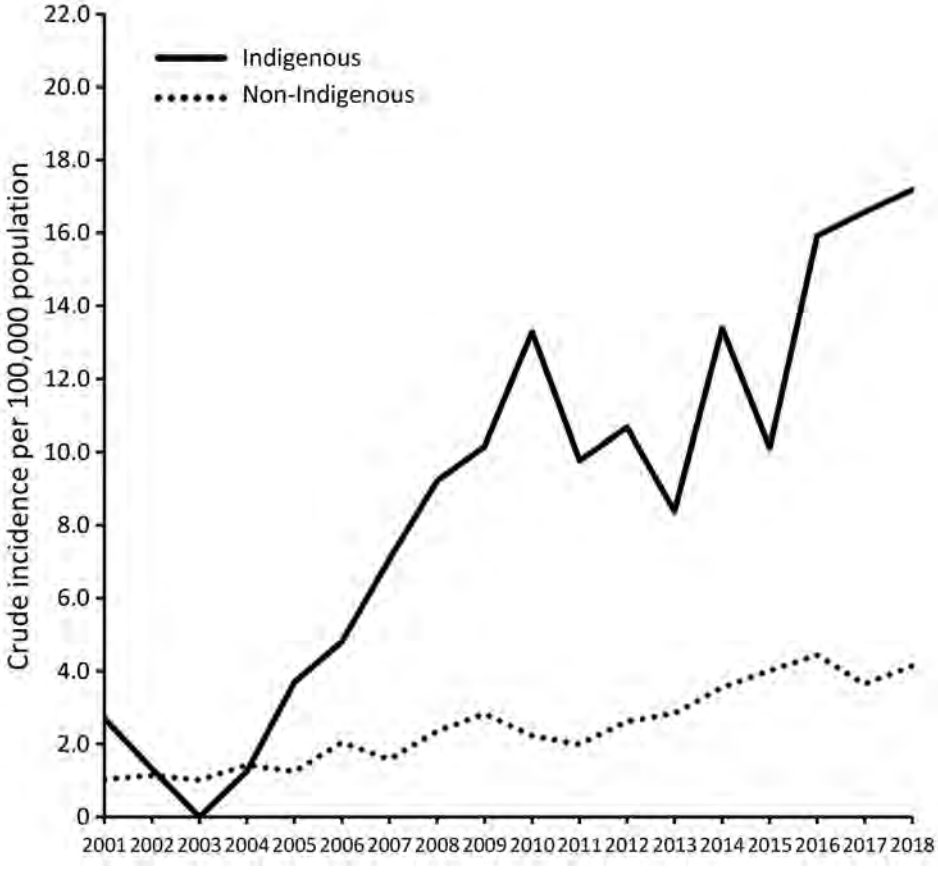

Figure 3. Indigenous versus non-Indigenous distribution of invasive group C/G *Streptococcus* disease, Western Australia, Australia, 2000–2018.

for patients with iGCGS disease (Appendix Table 2), indicating that the differences in overall death proportions for each is driven primarily by age.

Although it serves most public hospitals, PathWest is not the sole pathology provider in WA. For this reason, we augmented laboratory data with hospital records, including 75 cases (6%) without laboratory confirmation. The percentage of microbiologically confirmed HMDC cases was larger for public hospitals than private hospitals, which suggests that HMDC cases without PathWest confirmations were probably confirmed by private microbiology providers. The conservative diagnostic definition for HMDC cases minimized the effect of any HMDC coding errors. However, because of the requirement for a GCGS-specific descriptor as an additional diagnostic code (B95.41 or B95.42), some underreporting of cases confirmed by an alternative microbiology service provider could have occurred. Multiple potential drivers for the increase in iGCGS disease exist, such as changing risk factor prevalence (e.g., immunocompromise or immune senescence) (*30*,*31*) and changing demographics (e.g., an aging population). However, the similar increases in iGCGS infection and invasive GAS disease make system-level factors a probable contributor. These factors could include increased blood culture and other usually sterile specimen collection, enabling detection of previously undetected infections; increased referral of specimens from private laboratories to PathWest; or improved capture in routinely collected data. Repeat surveillance will be useful for monitoring contemporary trends in disease burden. We did not perform adjustment of all-cause deaths for chronic medical conditions because the comorbidity information was limited to that coded as relevant for individual hospital stays. The administrative data we analyzed were not collected for research purposes, but the use of these data in clinical practice (PathWest), clinical activity reporting (HMDC), and for informing national mortality data (death registrations) meant that the linked data analysis was appropriate for our study.

The incidence of iGCGS disease in WA increased during 2000–2018; cases occurred predominately among older persons and men, and Indigenous persons were at increased risk. This infection was marked by high all-cause death within 30 and 90 days, especially among the elderly, and a prolonged length of hospital stay. Although further research should assess the contribution of such comorbidities as diabetes to inform preventive efforts, these data highlight that iGCGS infection has been a neglected pathogen of older persons and that Indigenous persons face a higher risk for infection.

Acknowledgments

We thank the Linkage, Data Outputs, and Research Data Services Teams at the Western Australian Data Linkage Branch, in particular Mikhalina Dombrovskaya, as well as the data custodians for the following datasets: PathWest, death registrations, and the hospital morbidity data collection. We also thank Ryan Shave for assistance with research governance approvals, Brett Cawley for assisting with defining the PathWest cohort, Susan Benson for assistance on blood culture results interpretation, and the people whose data have been analyzed for this study.

This work was supported by the Telethon Kids Institute and the Department of Infectious Diseases, Fiona Stanley Fremantle Hospitals Group, for data acquisition costs.

About the Author

Dr. Wright is a resident medical officer at Fiona Stanley Hospital with qualifications in medicine, pharmacy, and public health. His primary research interests are infectious diseases epidemiology and applied health economics.

References

1. Hughes GJ, VAN Hoek AJ, Sriskandan S, Lamagni TL. The cost of hospital care for management of invasive group A streptococcal infections in England. Epidemiol Infect. 2015;143:1719–30. https://doi.org/10.1017/S0950268814002489
2. Parks T, Barrett L, Jones N. Invasive streptococcal disease: a review for clinicians. Br Med Bull. 2015;115:77–89. https://doi.org/10.1093/bmb/ldv027
3. Centers for Disease Control and Prevention. Case definitions for infectious conditions under public health surveillance. MMWR Recomm Rep. 1997;46(RR-10):1–55.
4. Facklam R. What happened to the streptococci: overview of taxonomic and nomenclature changes. Clin Microbiol Rev. 2002;15:613–30. https://doi.org/10.1128/CMR.15.4.613-630.2002
5. Sikder S, Williams NL, Sorenson AE, Alim MA, Vidgen ME, Moreland NJ, et al. Group G Streptococcus induces an autoimmune carditis mediated by interleukin 17A and interferon γ in the Lewis rat model of rheumatic heart disease. J Infect Dis. 2018;218:324–35. https://doi.org/10.1093/infdis/jix637
6. Haidan A, Talay SR, Rohde M, Sriprakash KS, Currie BJ, Chhatwal GS. Pharyngeal carriage of group C and group G streptococci and acute rheumatic fever in an Aboriginal population. Lancet. 2000;356:1167–9. https://doi.org/10.1016/S0140-6736(00)02765-3
7. Brandt ER, Sriprakash KS, Hobb RI, Hayman WA, Zeng W, Batzloff MR, et al. New multi-determinant strategy for a group A streptococcal vaccine designed for the Australian Aboriginal population. Nat Med. 2000;6:455–9. https://doi.org/10.1038/74719
8. Public Health England. Notifiable diseases: annual report. Manchester: Public Health England; 2020 [cited 2020 Oct 6]. https://www.gov.uk/government/publications/notifiable-diseases-annual-report
9. Government of Canada. National case definition: Invasive group A streptococcal disease. Ottawa: Government of

Canada; 2019 [cited 2019 Mar 30]. https://www.canada.ca/en/public-health/services/diseases/group-a-streptococcal-diseases/health-professionals/national-case-definition.html
10. Fujiya Y, Hayakawa K, Gu Y, Yamamoto K, Mawatari M, Kutsuna S, et al. Age-related differences in clinical characteristics of invasive group G streptococcal infection: comparison with group A and group B streptococcal infections. PLoS One. 2019;14:e0211786. https://doi.org/10.1371/journal.pone.0211786
11. Babiker A, Li X, Lai YL, Strich JR, Warner S, Sarzynski S, et al. Effectiveness of adjunctive clindamycin in β-lactam antibiotic-treated patients with invasive β-haemolytic streptococcal infections in US hospitals: a retrospective multicentre cohort study. Lancet Infect Dis. 2021;21:697–710. https://doi.org/10.1016/S1473-3099(20)30523-5
12. Gajdács M, Ábrók M, Lázár A, Burián K. Beta-haemolytic group A, C and G streptococcal infections in southern Hungary: a 10-year population-based retrospective survey (2008–2017) and a review of the literature. Infect Drug Resist. 2020;13:4739–49. https://doi.org/10.2147/IDR.S279157
13. Kittang BR, Bruun T, Langeland N, Mylvaganam H, Glambek M, Skrede S. Invasive group A, C and G streptococcal disease in western Norway: virulence gene profiles, clinical features and outcomes. Clin Microbiol Infect. 2011;17:358–64. https://doi.org/10.1111/j.1469-0691.2010.03253.x
14. Oppegaard O, Mylvaganam H, Kittang BR. Beta-haemolytic group A, C and G streptococcal infections in western Norway: a 15-year retrospective survey. Clin Microbiol Infect. 2015;21:171–8. https://doi.org/10.1016/j.cmi.2014.08.019
15. Wright CM, Moorin R, Pearson G, Dyer JR, Carapetis JR, Manning L. Increasing incidence of invasive group A streptococcal disease in Western Australia, particularly among Indigenous people. Med J Aust. 2021;215:36–41. https://doi.org/10.5694/mja2.51117
16. Benchimol EI, Smeeth L, Guttmann A, Harron K, Moher D, Petersen I, et al.; RECORD Working Committee. The REporting of studies Conducted using Observational Routinely-collected health Data (RECORD) statement. PLoS Med. 2015;12:e1001885. https://doi.org/10.1371/journal.pmed.1001885
17. Australian Bureau of Statistics. Table 4. Estimated resident population, states and territories (Number). 2020 [cited 2020 Jan 8]. http://www.abs.gov.au/AUSSTATS/abs@.nsf/DetailsPage/3101.0Mar%202018?OpenDocument
18. Australian Bureau of Statistics. Estimates and Projections, Aboriginal and Torres Strait Islander Australians [cited 2020 Jun 2]. https://www.abs.gov.au/AUSSTATS/abs@.nsf/mf/3238.0
19. Government of Western Australia. Regional Population Data [cited 2020 Sep 17]. https://catalogue.data.wa.gov.au/dataset/western-australia-regional-population/resource/eeecaf08-55e3-4026-99fc-f98a383e2812
20. Cannon J, Dyer J, Carapetis J, Manning L. Epidemiology and risk factors for recurrent severe lower limb cellulitis: a longitudinal cohort study. Clin Microbiol Infect. 2018;24:1084–8. https://doi.org/10.1016/j.cmi.2018.01.023
21. Cannon J, Rajakaruna G, Dyer J, Carapetis J, Manning L. Severe lower limb cellulitis: defining the epidemiology and risk factors for primary episodes in a population-based case-control study. Clin Microbiol Infect. 2018;24:1089–94. https://doi.org/10.1016/j.cmi.2018.01.024
22. Kelman CW, Bass AJ, Holman CD. Research use of linked health data—a best practice protocol. Aust N Z J Public Health. 2002;26:251–5. https://doi.org/10.1111/j.1467-842X.2002.tb00682.x
23. Boyd R, Patel M, Currie BJ, Holt DC, Harris T, Krause V. High burden of invasive group A streptococcal disease in the Northern Territory of Australia. Epidemiol Infect. 2016;144:1018–27. https://doi.org/10.1017/S0950268815002010
24. Australian Bureau of Statistics. The Australian Statistical Geography Standard (ASGS) remoteness structure [cited 2018 Oct 5]. http://www.abs.gov.au/websitedbs/d3310114.nsf/home/remoteness+structure
25. Australian Bureau of Statistics. Socioeconomic indices for areas [cited 2018 Oct 15]. http://www.abs.gov.au/websitedbs/censushome.nsf/home/seifa
26. Broyles LN, Van Beneden C, Beall B, Facklam R, Shewmaker PL, Malpiedi P, et al. Population-based study of invasive disease due to beta-hemolytic streptococci of groups other than A and B. Clin Infect Dis. 2009;48:706–12. https://doi.org/10.1086/597035
27. Harris P, Siew DA, Proud M, Buettner P, Norton R. Bacteraemia caused by beta-haemolytic streptococci in North Queensland: changing trends over a 14-year period. Clin Microbiol Infect. 2011;17:1216–22. https://doi.org/10.1111/j.1469-0691.2010.03427.x
28. Thomsen RW, Riis AH, Kjeldsen S, Schønheyder HC. Impact of diabetes and poor glycaemic control on risk of bacteraemia with haemolytic streptococci groups A, B, and G. J Infect. 2011;63:8–16. https://doi.org/10.1016/j.jinf.2011.05.013
29. Moon A, Gray A, Deehan D. Neck of femur fractures in patient's aged more than 85 years—are they a unique subset? Geriatr Orthop Surg Rehabil. 2011;2:123–7. https://doi.org/10.1177/2151458511414562
30. Shahin A, Saba M, Greene J. A retrospective chart review on the clinical characteristics and outcomes of cancer patients with group C, F, or G β-hemolytic streptococcal infections. Infect Dis Clin Pract. 2019;27:205–10. https://doi.org/10.1097/IPC.0000000000000723
31. Lewthwaite P, Parsons HK, Bates CJ, McKendrick MW, Dockrell DH. Group G streptococcal bacteraemia: an opportunistic infection associated with immune senescence. Scand J Infect Dis. 2002;34:83–7. https://doi.org/10.1080/00365540110077209

Address for correspondence: Cameron M. Wright, Fiona Stanley Fremantle Hospitals Group, Murdoch, Western Australia, 6150, Australia; email: cameron.wright@curtin.edu.au

Age-Stratified Seroprevalence of SARS-CoV-2 Antibodies before and during the Vaccination Era, Japan, February 2020–March 2022

Seiya Yamayoshi, Kiyoko Iwatsuki-Horimoto, Moe Okuda, Michiko Ujie, Atsuhiro Yasuhara, Jurika Murakami, Calvin Duong, Taiki Hamabata, Mutsumi Ito, Shiho Chiba, Ryo Kobayashi, Satoshi Takahashi, Keiko Mitamura, Masao Hagihara, Akimichi Shibata, Yoshifumi Uwamino, Naoki Hasegawa, Toshiaki Ebina, Akihiko Izumi, Hideaki Kato, Hideaki Nakajima, Norio Sugaya, Yuki Seki, Asef Iqbal, Isamu Kamimaki, Masahiko Yamazaki, Yoshihiro Kawaoka, Yuki Furuse

Japan has reported a relatively small number of COVID-19 cases. Because not all infected persons receive diagnostic tests for COVID-19, the reported number must be lower than the actual number of infections. We assessed SARS-CoV-2 seroprevalence by analyzing >60,000 samples collected in Japan (Tokyo Metropolitan Area and Hokkaido Prefecture) during February 2020–March 2022. The results showed that ≈3.8% of the population had become seropositive by January 2021. The seroprevalence increased with the administration of vaccinations; however, among the elderly, seroprevalence was not as high as the vaccination rate. Among children, who were not eligible for vaccination, infection was spread during the epidemic waves caused by the SARS-CoV-2 Delta and Omicron variants. Nevertheless, seroprevalence for unvaccinated children <5 years of age was as low as 10% as of March 2022. Our study underscores the low incidence of SARS-CoV-2 infection in Japan and the effects of vaccination on immunity at the population level.

SARS-CoV-2, the etiologic agent of COVID-19, emerged at the end of 2019 and caused a pandemic. As of April 2022, despite the development of effective vaccines and therapeutics, >500 million persons had been infected with the virus and ≈6 million had died (*1*). In Japan, with a population of ≈125 million, the reported numbers are ≈7 million infections and ≈30,000 deaths by that time (*2*); however, the actual number of infected persons must be higher than the reported figure because not all infected persons undergo diagnostic testing.

A serologic survey can retrospectively find persons who have been infected with the virus (*3*). Antibodies against the SARS-CoV-2 spike protein are generated by vaccination and natural infection. In contrast, antibodies against other components of the virus, such as the nucleoprotein, represent a history of SARS-CoV-2 natural infection but not vaccination with the COVID-19 vaccines currently available in Japan. Analyses of seroprevalence in several countries have revealed that the actual incidence of SARS-CoV-2 infection is much higher than the reported COVID-19 cases (*3*). For example, in the United States, the seroprevalence of antibodies against the SARS-CoV-2 nucleoprotein ranged from 3% to 10% in 2020 (*4*–*7*), and this number reached roughly 20%–60% in 2021 (*8*,*9*). However, diagnostic tests confirmed only a

Author affiliations: University of Tokyo, Tokyo, Japan (S. Yamayosh, K. Iwatsuki-Horimoto, M. Okuda, M. Ujie, A. Yasuhara, J. Murakami, C. Duong, T. Hamabata, M. Ito, Y. Kawaoka); National Center for Global Health and Medicine, Tokyo (S. Yamayoshi, Y. Kawaoka); University of Wisconsin–Madison, Madison, Wisconsin, USA (S. Chiba, Y. Kawaoka); Sapporo Medical University Hospital, Sapporo, Japan (R. Kobayashi); Sapporo Medical University School of Medicine, Sapporo (S. Takahashi); Eiju General Hospital, Tokyo (K. Mitamura, M. Hagihara); Japanese Red Cross Ashikaga Hospital, Ashikaga, Japan (A. Shibata); Keio University School of Medicine, Tokyo (A. Shibata, Y. Uwamino, N. Hasegawa, N. Sugaya); Yokohama City University Medical Center, Yokohama, Japan (T. Ebina, A. Izumi); Yokohama City University Hospital, Yokohama (H. Kato); Yokohama City University Graduate School of Medicine, Yokohama (H. Kato, H. Nakajima); Keiyu Hospital, Yokohama (Y. Seki); National Hospital Organization Saitama Hospital, Wako, Japan (A. Iqbal, I. Kamimaki); Zama Children's Clinic, Zama, Japan (M. Yamazaki); Nagasaki University Graduate School of Biomedical Sciences, Nagasaki, Japan (Y. Furuse); Nagasaki University Hospital, Nagasaki, Japan (Y. Furuse)

DOI: https://doi.org/10.3201/eid2811.221127

fraction of the infections, especially at the beginning of the pandemic. The ascertainment rate was <10%–30% in 2020 (*4*–*7*) and increased to ≈50% in 2021 (*10*).

Vaccines for SARS-CoV-2 can prevent severe illness and death from COVID-19 for persons at high risk, such as the elderly (*11*). In addition, they can prevent viral infection and therefore have the potential to contribute to herd immunity and the containment of the disease (*12*). However, the continuous emergence of novel variants of SARS-CoV-2 and waning immunity have enabled the pandemic to linger (*13*,*14*).

We measured the seroprevalence of antibodies against the spike protein of SARS-CoV-2 in Japan by analyzing >60,000 samples obtained during February 2020–March 2022. We compared the results with the number of reported COVID-19 cases to discuss the actual incidence and the ascertainment rate. Furthermore, our findings reveal how vaccination influenced COVID-19 immunity in Japan at the population level.

Methods

Study Participants and Samples

The study participants were patients who visited Sapporo Medical University Hospital, Japanese Red Cross Ashikaga Hospital, Keio University Hospital, National Hospital Organization Saitama Hospital, Eiju General Hospital, Yokohama City University Medical Center, Yokohama City University Hospital, Keiyu Hospital, or Zama Children's Clinic, Japan, during February 2020–March 2022. Sapporo Medical University Hospital is located in Hokkaido Prefecture, whereas all of the other healthcare facilities are located in the Tokyo Metropolitan Area and its suburbs.

We analyzed residual serum or plasma samples collected for medical examination. The reason for the healthcare facility visit was not considered for inclusion in this study, except that patients positive by SARS-CoV-2 nucleic acid test or antigen test were excluded. Because the samples were collected anonymously, some of them might have been from multiple visits by the same patients, but we could not identify or exclude them.

Measurement of Antibodies

We performed ELISA to detect antibodies against SARS-CoV-2 as described previously (*15*). We incubated 96-well MaxiSorp microplates (ThermoFisher, https://www.thermofisher.com) with 2 μg/mL of the recombinant receptor-binding domain (RBD) of the spike protein, the whole length of the nucleoprotein, or phosphate-buffered saline (PBS) at 4°C overnight. We then incubated the microplates with 5% skim milk in PBS containing 0.05% tween-20. We incubated the antigen-coated microplates with the serum or plasma samples 40-fold diluted in 5% skim milk in PBS containing 0.05% tween-20, followed by the peroxidase-conjugated goat antihuman IgG, Fcγ fragment–specific antibody (Jackson ImmunoResearch Laboratories, https://www.jacksonimmuno.com). We added One-Step Ultra TMB-Blotting Solution (ThermoFisher) to each well and incubated for 3 min at room temperature. We stopped the reaction by adding 2 M H_2SO_4 and immediately measured the optical density at 450 nm (OD_{450}). We subtracted the OD_{450} value of the PBS wells from the OD_{450} value of the spike protein or nucleoprotein wells as background.

Validation Samples for ELISA

We used convalescent serum samples from patients with laboratory-confirmed COVID-19 as positive controls to validate the ELISA tests. We used residual serum samples collected in 2012 as negative controls.

Other Data Sources

We obtained the daily number of reported COVID-19 cases from the website and press releases of each prefecture in the study area. Confirmation and reports of COVID-19 were based on PCR testing at the beginning of the pandemic, and antigen testing, which was approved and used after May 2020. Vaccine administration data were available in the Vaccination Record System (https://cio.go.jp/vrs). This system was launched in April 2021, and the number of vaccines administered before that timepoint was included on the first day of the record. All vaccines available in Japan require 2 doses for immunization; a third dose was administered as a booster after December 2021. We downloaded and used census data of Japan to obtain demographic information in the study area (https://www.stat.go.jp/data/jinsui/2021np/index.html).

Statistical Analysis

We drew a receiver operating characteristic curve for the ELISA OD_{450} values to set a threshold. We used this threshold to determine whether samples were negative or positive for SARS-CoV-2 spike protein and nucleoprotein by using Youden's index (*16*).

We investigated the proportion of seropositive samples by month and age group. We computed the Wilson 95% CI for the seroprevalence data (*17*). Using the census data, we calculated an age-structure adjusted estimation of seroprevalence in the total population and the rates of reported COVID-19 cases and vaccine administrations.

Ethics Considerations

The study protocol was reviewed and approved by the institutional review board of the Institute of Medical Science, University of Tokyo (protocol no. 2019-75). The protocol was also checked and approved by each research institute and healthcare facility involved. The study participants gave informed consent during their healthcare facility visits for their data and residual samples to be used anonymously for clinical research.

Results

During the study period, Japan had 6 COVID-19 epidemic waves (Figure 1). The cumulative number of confirmed COVID-19 cases by the end of March 2022 was ≈6.7 million in a population of ≈125 million. Vaccinations started in February 2021 for healthcare workers; then, in April 2021, they were expanded to the general population, prioritizing persons at high risk, such as the elderly and those with certain underlying conditions, including respiratory disorders and immunocompromised diseases. Approximately 256.9 million doses of vaccine were administered during the study period. The 2 mRNA vaccines, BNT162b2 (Pfizer-BioNTech, https://www.pfizer.com) and mRNA-1273 (Moderna, https://www.modernatx.com), were the main vaccines administered in Japan.

We first assessed SARS-CoV-2 antibody titers in prepandemic samples from 2012 (n = 200) and in COVID-19 convalescent serum samples (n = 113). The median time from PCR-positive result to sample collection for the serologic assay for the convalescent serum samples was 40 days (interquartile range 32–64 days). We determined the thresholds for discriminating infected convalescent samples from uninfected prepandemic samples by using receiver operating characteristic curves (Appendix Figure 1, https://wwwnc.cdc.gov/EID/article/28/11/22-1127-App1.pdf). The ELISA test for antinucleoprotein antibodies had 98.0% specificity and 95.6% sensitivity.

The antibody titer for the RBD of the spike protein, which has a specificity of 99.5% and a sensitivity of 100%, can be used to clearly differentiate convalescent samples from naive samples. Hence, we measured the antibody titers for the spike protein in further analyses. Our seroprevalence data cannot determine whether immunity was generated by natural infection or vaccination.

We also checked whether our assay could detect the history of infection with SARS-CoV-2 variants, such as Delta and Omicron. We ensured that the sensitivity of the assay for the anti–spike protein antibodies did not decrease because of

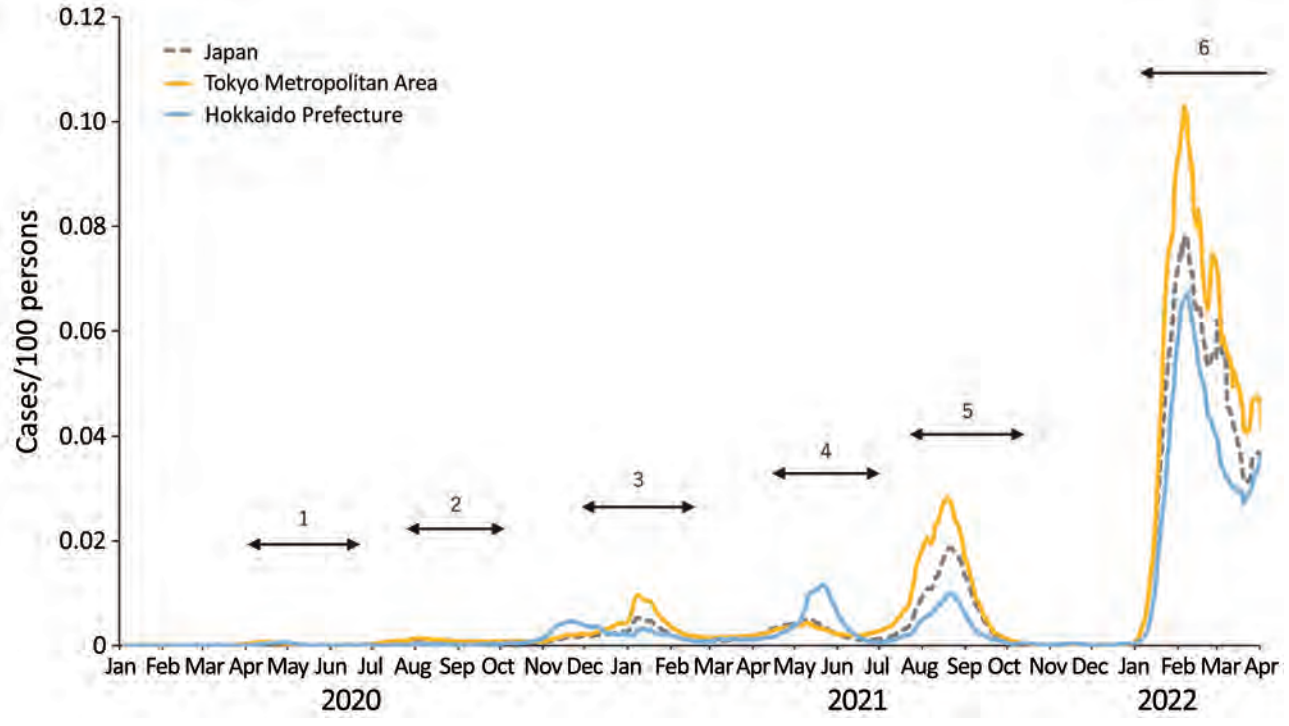

Figure 1. Epidemic curve of COVID-19 in Japan, January 2020–March 2022. The daily numbers of reported COVID-19 cases per100 persons in all of Japan, the Tokyo Metropolitan Area, and Hokkaido Prefecture are shown. The numbers indicate the 6 epidemic waves. The fourth, fifth, and sixth waves were driven by the Alpha, Delta, and Omicron variants of SARS-CoV-2, respectively.

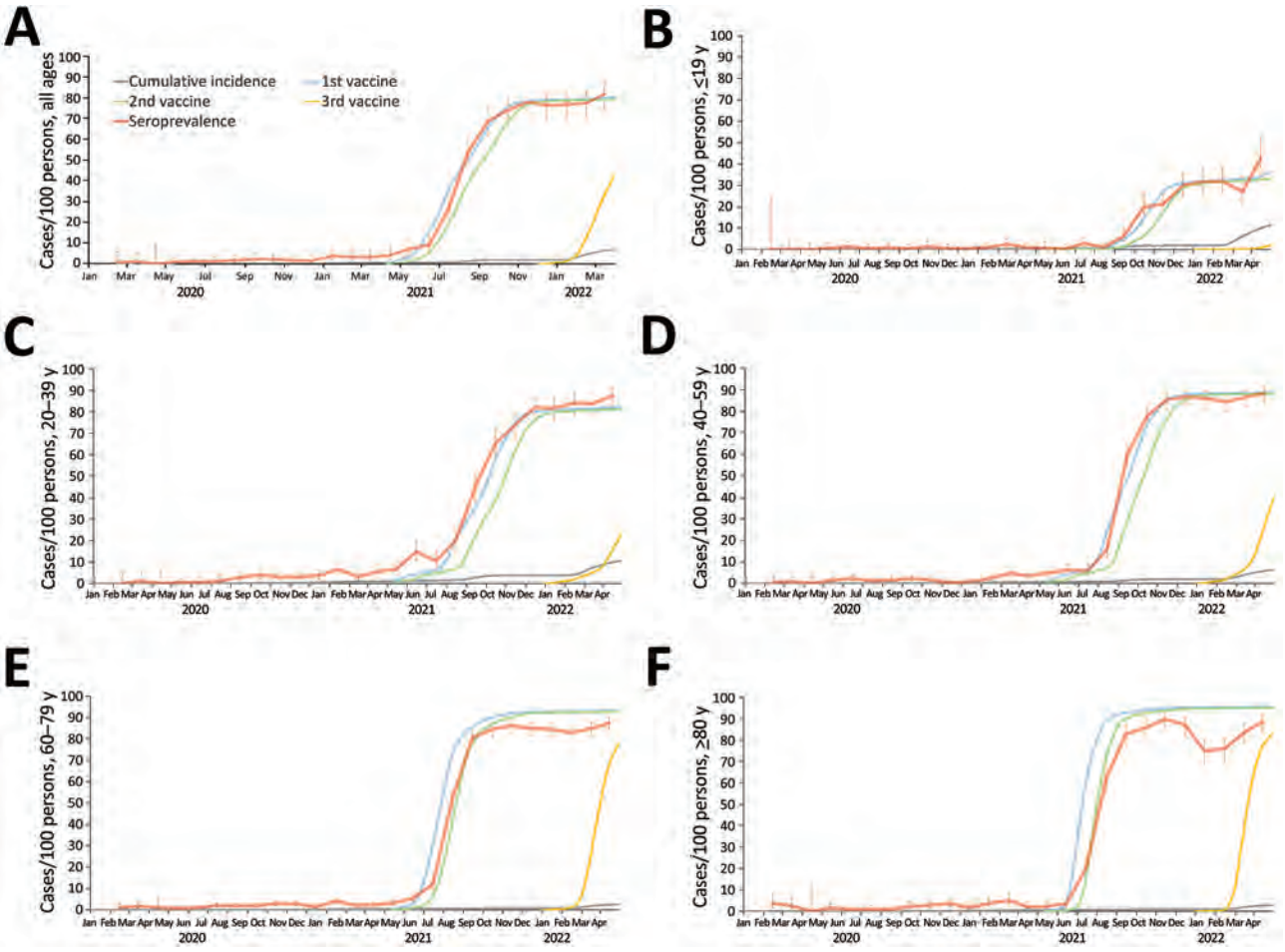

Figure 2. Seroprevalence of SARS-CoV-2 in the Tokyo Metropolitan Area, Japan, February 2020–March 2022. A) Rates for the total population of the Tokyo Metropolitan Area; B–F) rates by 20-year age groups. The cumulative number of reported COVID-19 cases and the cumulative number for the first, second, and third vaccine administrations per population are also shown. Error bars indicate 95% CIs. Detailed age-stratified data are shown in Appendix Figure 2 (https://wwwnc.cdc.gov/EID/article/28/11/22-1127-App1.pdf).

antigenic changes in such variants, confirming 100% positivity in samples from unvaccinated persons infected with those variants (24/24 for Delta and 5/5 for Omicron).

We collected a total of 44,681 samples in the Tokyo Metropolitan Area during February 2020–March 2022. Of these samples, 44,672 (99.9%) were analyzed for the study, and 9 were excluded because the metadata were incomplete. We collected the samples from persons 0 to 105 years of age and summarized the numbers of analyzed samples by age group and month (Appendix Table 1).

SARS-CoV-2 seroprevalence was low in 2020 in the Tokyo Metropolitan Area (Figure 2; Appendix Figure 2). In January 2021, just before the vaccine rollout, the estimated seropositivity was 3.8% in the total population when we adjusted our data to age structure in the area. The proportions of serum samples positive for SARS-CoV-2 in each age group at the time were 0% among persons 0–9 years of age, 2.5% among persons 10–19 years of age, 8.2% among persons 20–29 years of age, 5.7% among persons 30–39 years of age, 2.8% among persons 40–49 years of age, 2.0% among persons 50–59 years of age, 4.2% among persons 60–69 years of age, 4.0% among persons 70–79 years of age, and 3.7% among persons ≥80 years of age (Appendix Figure 2).

We then calculated the ratio of the seroprevalence to the cumulative incidence by the time of vaccination for the general public (Figure 3). This rate can correspond to the number of actual infected persons per detected case. However, a low antibody titer in some infected persons because of a weak immune response and waning immunity could affect the accuracy of the estimation.

In the early phase of the pandemic, diagnostic tests detected as few as 1 case in >10 infections (an

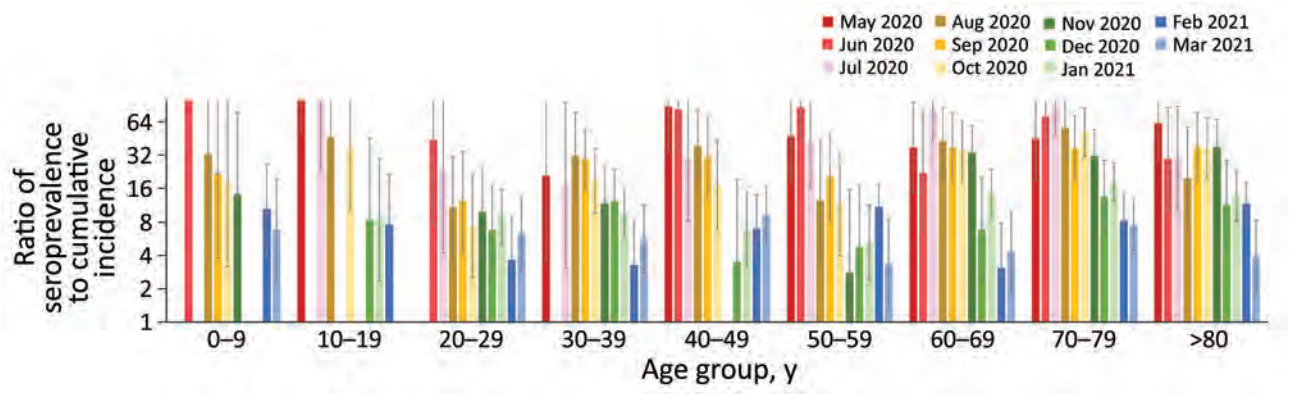

Figure 3. Ratios of SARS-CoV-2 seroprevalence to cumulative incidence by month in the Tokyo Metropolitan Area, Japan, May 2020–March 2021. Ratios for each month were calculated in comparison to the cumulative incidence of reported COVID-19 from January 2020 to that month. The ratio corresponds to the actual number of infected persons per reported case-patient. Error bars indicate 95% CIs. Data are blank for months when no samples were positive for SARS-CoV-2.

ascertainment rate of <10%). The rate increased over time, such that by March 2021, one case in ≈3–10 infections was detected (an ascertainment rate of ≈10%–33%). This change is probably attributable to an increase in the proportion of infected persons who underwent diagnostic testing rather than an improvement in testing accuracy.

The proportion of samples positive for antibodies against the SARS-CoV-2 spike protein dramatically increased with the rollout of vaccination (i.e., after April 2021) (Figure 2). However, the seropositive proportions were slightly lower than the vaccination rates in persons 70–79 and ≥80 years of age (Appendix Figure 2). Furthermore, seropositive rates peaked and then declined for persons ≥50 years of age. The administration of the third vaccination after January 2022 restored the drop in seroprevalence.

The SARS-CoV-2 seroprevalence among persons 0–9 years of age increased during the Delta-dominant fifth epidemic wave, which started in July 2021, and the Omicron-dominant sixth epidemic wave, which started in January 2022. Vaccination of children ≥5 years of age was approved and administered after February 2022 in Japan. Therefore, we subdivided the data for the 0–9 years age group into 0–5 months, 6 months–4 years, and 5–9 years of age (Appendix Figure 2, panel C, D). The first subset age group (0–5 months of age) showed a very high seroprevalence compared to the other 2 subset age groups. The seroprevalence for the 2 older groups was low but increased after August 2021, reaching 8.0% for the 6 months–4 years age group and 9.3% for the 5–9 years age group in December 2021. In March 2022, a further increase of seroprevalence was observed in children 5–9 and 10–19 years of age.

We also tested samples from Hokkaido Prefecture, which is situated ≈800 km north of Tokyo. We collected and analyzed a total of 17,079 serum samples from Hokkaido Prefecture (Appendix Table 2). The results were comparable to those obtained from the Tokyo Metropolitan Area (Appendix Figure 3). The seroprevalence was <5% for all age groups until the vaccination program began. The seroprevalence increased as the vaccines were administered, although the older age groups showed lower seropositivity rates compared with their vaccination rates.

Discussion

We examined the time course of seroprevalence of antibodies against SARS-CoV-2 by age group by analyzing >60,000 samples from Japan over a 25-month period. In addition to previous studies (*18*,*19*), our study expands knowledge about SARS-CoV-2 seroprevalence in the country. Diagnostic testing to identify persons infected with SARS-CoV-2 is important for gaining a better understanding of the epidemiologic situation of COVID-19. The incidence and mortality rates of COVID-19 are considerably low in Japan (*20*). However, the low number of tests per population may have caused many cases of infection to go undetected and the reported statistics may not have reflected the actual situation (*21*).

Our data show that ≈5% of the population of Japan had become seropositive for SARS-CoV-2 by January 2021. That figure is much higher than the reported number of COVID-19 cases. Still, the low rate was in stark contrast to other countries, many of which had seroprevalences >30% at that time (*3*). Nonpharmaceutical interventions, such as physical distancing and wearing a face mask, played a critical role in

controlling the COVID-19 pandemic, especially in the prevaccination era. Although Japan did not impose a lockdown, the country issued a state of emergency, asking persons to stay at home and limit mass gatherings and asking businesses, including restaurants and bars, to reduce their hours or close when COVID-19 cases surged (*22*). The country also implemented a unique strategy focusing on case-clusters (*23*,*24*).

Because we measured antibodies for the viral spike protein, we could not differentiate immunity by natural infection from immunity by vaccination after February 2021. The seroprevalence among children who were not yet eligible for vaccination in December 2021 was still as low as 10% in Japan. Thereafter, the infection was spread among children during the Omicron-dominant sixth epidemic wave (*25*), and their seropositive rates gradually increased at the beginning of 2022. The especially high seroprevalence among children 0–5 months of age after August 2021 must be the result of antibodies transferred from vaccinated mothers (Appendix Figure 2, panel C, D).

Japan has achieved a high rate of SARS-CoV-2 seroprevalence among adults because of vaccinations since April 2021. A low seroconversion rate by vaccination and rapid immunity waning in the elderly have been reported at the person level (*26*,*27*). In our study, we observed this effect at the population level. In addition to vaccinating the elderly, who are at a high risk for experiencing severe illness, reducing their exposure to the virus should be key to protecting this vulnerable population. Booster shots also helped provide a high degree of population immunity.

In this study, we measured the antibody titers for the RBD of SARS-CoV-2 spike protein. Therefore, samples from both infected persons and from vaccinated persons showed positive results. Although the measurement of the antibody titers for the nucleoprotein can reflect only a history of natural infection with SARS-CoV-2, in our study, the sensitivity and specificity were not as high as the test for the spike protein (Appendix Figure 1). The low sensitivity might have been attributable to the weak immunogenicity of the nucleoprotein, and the low specificity may be attributable to cross-reactivity between the seasonal coronavirus and SARS-CoV-2. Still, we must pursue analyzing the actual infection rate, especially after vaccination rollout, by investigating the prevalence of antinucleoprotein antibodies. We should establish an assay that detects antibodies for the SARS-CoV-2 nucleoprotein without any cross-reactivity with other antigens in the future.

By testing antibodies for the spike protein, we gauged the actual incidence of COVID-19 in a prevaccine era. We validated the considerably high sensitivity and specificity of the test. Still, the estimate cannot be 100% accurate. Because of the effect of waning immunity, investigation of seropositivity could lead to an underestimation of the infection rate. In addition, our test participants may not represent the general public in Japan. Our samples were from patients who visited healthcare facilities for various reasons other than COVID-19. Persons with underlying diseases could be more cautious about healthcare issues and avoid high-risk behavior, or patients with some symptoms could have had a high pretest probability of past infection with SARS-CoV-2.

Our study highlights the very low SARS-CoV-2 infection rate in Japan. It also unveils a hurdle to maintaining a high degree of population immunity among the elderly. In future studies, we should investigate how population immunity has affected and will affect the course of the pandemic. We must explore the levels of immunity required to prevent infection, hospitalization, and death from different SARS-CoV-2 variants. Because our findings suggests that most populations in Japan have not yet been infected with the virus, the country's current and future paths regarding the COVID-19 pandemic may continue to hold the world's attention.

Acknowledgments

We thank Tomoka Nagashima, Chiaki Kawana, Naoko Mizutani, Kyoko Yokota, Mikuru Sato, Shihomi Kuwano, Noriaki Harada, Izuru Iwase, Junya Shigenaga, Kazumi Yanagi, Taro Kaneda, Ryoko Karakama, Yuka Suzuki, Shoma Ookaji, Ayano Aketa, Sayaka Sato, Misako Sugaya, Misa Hayasaka, Yoko Kira, Yuki Fujiwara, Akimi Kaku, Masako Moteki, Masami Isizaki, and other clinical laboratory staff for their efforts with the organization and collection of blood samples. We thank Kozue Amemiya, Kayako Chishima, Aya Fujiwara, Yoko Hamasaki, Naomi Ikeda, Tadatsugu Imamura, Takeaki Imamura, Keiya Inoue, Sachi Ishida, Mariko Kanamori, Tsuyoki Kawashima, Yura K Ko, Tomoe Mashiko, Rie Masuda, Reiko Miyahara, Konosuke Morimoto, Shohei Nagata, Yoshifumi Nin, Kota Ninomiya, Yukiyo Nitta, Hitoshi Oshitani, Mayuko Saito, Akiko Sakai, Eiichiro Sando, Kazuaki Sano, Asako Sato, Akiko Sayama, Yugo Shobugawa, Motoi Suzuki, Ayaka Takeuchi, Hiroto Tanaka, Fumie Tokuda, Naho Tsuchiya, Shogo Yaegashi, Yoko Yamagiwa, Lisa Yamasaki, Ikkoh Yasuda, and Fumi Yoshimatsu for the collection and management of COVID-19-related epidemiologic data from public databases and press releases. We also thank Susan Watson for editing the manuscript.

This work was supported by Research Program on Emerging and Re-emerging Infectious Diseases (grant nos. JP19fk0108166 and JP20fk0108451s0301) and Japan Program for Infectious Diseases Research and Infrastructure (grant no. JP22wm0125002) from the Japan Agency for Medical Research and Development. The funder of the study had no role in study design, data collection, data analysis, data interpretation, or writing of the report.

About the Author

Dr. Yamayoshi is a director at Department of Viral Dynamics, Research Center for Global Viral Diseases, National Center for Global Health and Medicine Research Institute. His research interests are virus–host interactions at the community, individual, cellular, and molecular levels.

References

1. World Health Organization. Weekly epidemiological update on COVID-19—4 May 2022. 2022 [cited 2022 Jun 12]. https://www.who.int/publications/m/item/weekly-epidemiological-update-on-covid-19—4-may-2022
2. Ministry of Health. Labour and Welfare. Situation report on COVID-19. 2022 [cited 2022 Jun 12]. https://www.mhlw.go.jp/stf/covid-19/kokunainohasseijoukyou_00006.html
3. Barber RM, Sorensen RJD, Pigott DM, Bisignano C, Carter A, Amlag JO, et al.; COVID-19 Cumulative Infection Collaborators. Estimating global, regional, and national daily and cumulative infections with SARS-CoV-2 through Nov 14, 2021: a statistical analysis. Lancet. 2022;399:2351–80. https://doi.org/10.1016/S0140-6736(22)00484-6
4. Pei S, Yamana TK, Kandula S, Galanti M, Shaman J. Burden and characteristics of COVID-19 in the United States during 2020. Nature. 2021;598:338–41. https://doi.org/10.1038/s41586-021-03914-4
5. Lim T, Delorey M, Bestul N, Johannson MA, Reed C, Hall AJ, et al. Changes in severe acute respiratory syndrome coronavirus 2 seroprevalence over time in 10 sites in the United States, March–August, 2020. Clin Infect Dis. 2021;73:1831–9. https://doi.org/10.1093/cid/ciab185
6. Havers FP, Reed C, Lim T, Montgomery JM, Klena JD, Hall AJ, et al. Seroprevalence of antibodies to SARS-CoV-2 in 10 sites in the United States, March 23–May 12, 2020. JAMA Intern Med. 2020;180:1576–86. https://doi.org/10.1001/jamainternmed.2020.4130
7. Anand S, Montez-Rath M, Han J, Bozeman J, Kerschmann R, Beyer P, et al. Prevalence of SARS-CoV-2 antibodies in a large nationwide sample of patients on dialysis in the USA: a cross-sectional study. Lancet. 2020;396:1335–44. https://doi.org/10.1016/S0140-6736(20)32009-2
8. Clarke KEN, Jones JM, Deng Y, Nycz E, Lee A, Iachan R, et al. Seroprevalence of infection-induced SARS-CoV-2 antibodies—United States, September 2021–February 2022. MMWR Morb Mortal Wkly Rep. 2022;71:606–8. https://doi.org/10.15585/mmwr.mm7117e3
9. Jones JM, Opsomer JD, Stone M, Benoit T, Ferg RA, Stramer SL, et al. Updated US infection- and vaccine-induced SARS-CoV-2 seroprevalence estimates based on blood donations, July 2020–December 2021. JAMA. 2022;328:298–301. https://doi.org/10.1001/jama.2022.9745
10. Jones JM, Stone M, Sulaeman H, Fink RV, Dave H, Levy ME, et al. Estimated US infection- and vaccine-induced SARS-CoV-2 seroprevalence based on blood donations, July 2020–May 2021. JAMA. 2021;326:1400–9. https://doi.org/10.1001/jama.2021.15161
11. Tregoning JS, Flight KE, Higham SL, Wang Z, Pierce BF. Progress of the COVID-19 vaccine effort: viruses, vaccines and variants versus efficacy, effectiveness and escape. Nat Rev Immunol. 2021;21:626–36. https://doi.org/10.1038/s41577-021-00592-1
12. Anderson RM, Vegvari C, Truscott J, Collyer BS. Challenges in creating herd immunity to SARS-CoV-2 infection by mass vaccination. Lancet. 2020;396:1614–6. https://doi.org/10.1016/S0140-6736(20)32318-7
13. Feikin DR, Higdon MM, Abu-Raddad LJ, Andrews N, Araos R, Goldberg Y, et al. Duration of effectiveness of vaccines against SARS-CoV-2 infection and COVID-19 disease: results of a systematic review and meta-regression. Lancet. 2022;399:924–44. https://doi.org/10.1016/S0140-6736(22)00152-0
14. Goldblatt D. SARS-CoV-2: from herd immunity to hybrid immunity. Nat Rev Immunol. 2022;22:333–4. https://doi.org/10.1038/s41577-022-00725-0
15. Yamayoshi S, Yasuhara A, Ito M, Akasaka O, Nakamura M, Nakachi I, et al. Antibody titers against SARS-CoV-2 decline, but do not disappear for several months. EClinicalMedicine. 2021;32:100734. https://doi.org/10.1016/j.eclinm.2021.100734
16. Youden WJ. Index for rating diagnostic tests. Cancer. 1950;3:32–5. https://doi.org/10.1002/1097-0142(1950)3:1<32::AID-CNCR2820030106>3.0.CO;2-3
17. Wilson EB. Probable inference, the law of succession, and statistical inference. J Am Stat Assoc. 1927;22:209–12. https://doi.org/10.1080/01621459.1927.10502953
18. Doi A, Iwata K, Kuroda H, Hasuike T, Nasu S, Nishioka H, et al. A cross-sectional follow up study to estimate seroprevalence of coronavirus disease 2019 in Kobe, Japan. Medicine (Baltimore). 2021;100:e28066. https://doi.org/10.1097/MD.0000000000028066
19. Suemori K, Taniguchi Y, Okamoto A, Murakami A, Ochi F, Aono H, et al. Two-year seroprevalence surveys of SARS-CoV-2 antibodies among outpatients and healthcare workers in Japan. Jpn J Infect Dis. 2022 May 31 [Epub ahead of print]. https://doi.org/10.7883/yoken.JJID.2022.155
20. Furuse Y, Ko YK, Ninomiya K, Suzuki M, Oshitani H. Relationship of test positivity rates with COVID-19 epidemic dynamics. Int J Environ Res Public Health. 2021;18:4655. https://doi.org/10.3390/ijerph18094655
21. Shimizu K, Tokuda Y, Shibuya K. Japan should aim to eliminate covid-19 [editorial]. BMJ. 2021;372:n294. https://doi.org/10.1136/bmj.n294
22. Furuse Y. Simulation of future COVID-19 epidemic by vaccination coverage scenarios in Japan. J Glob Health. 2021;11:05025. https://doi.org/10.7189/jogh.11.05025
23. Furuse Y, Sando E, Tsuchiya N, Miyahara R, Yasuda I, Ko YK, et al. Clusters of coronavirus disease in communities, Japan, January–April 2020. Emerg Infect Dis. 2020;26:2176–9. https://doi.org/10.3201/eid2609.202272
24. Oshitani H; Expert Members of The National COVID-19 Cluster Taskforce at The Ministry of Health, Labour and Welfare, Japan. Cluster-based approach to coronavirus disease 2019 (COVID-19) response in Japan—February–April 2020. Jpn J Infect Dis. 2020;73:491–3. https://doi.org/10.7883/yoken.JJID.2020.363
25. Furuse Y. Properties of the Omicron variant of SARS-CoV-2 affect public health measure effectiveness in the COVID-19

epidemic. Int J Environ Res Public Health. 2022;19:4930. https://doi.org/10.3390/ijerph19094930
26. Müller L, Andrée M, Moskorz W, Drexler I, Walotka L, Grothmann R, et al. Age-dependent immune response to the Biontech/Pfizer BNT162b2 coronavirus disease 2019 vaccination. Clin Infect Dis. 2021;73:2065–72. https://doi.org/10.1093/cid/ciab381
27. Levin EG, Lustig Y, Cohen C, Fluss R, Indenbaum V, Amit S, et al. Waning immune humoral response to BNT162b2 Covid-19 vaccine over 6 months. N Engl J Med. 2021;385:e84. https://doi.org/10.1056/NEJMoa2114583

Address for correspondence: Seiya Yamayoshi, Institute of Medical Science, University of Tokyo, 4-6-1 Shirokanedai, Minato-ku, Tokyo 108-8639, Japan; email: yamayo@ims.u-tokyo.ac.jp; Yoshihiro Kawaoka, Research Institute National Center for Global Health and Medicine, 1-21-1 Toyama, Shinjuku-ku, Tokyo 162-8655, Japan; email: yoshihiro.kawaoka@wisc.edu; Yuki Furuse, Nagasaki University Graduate School of Biomedical Sciences, 1-12-4 Sakamoto, Nagasaki 852-8523, Japan; email: furusey.nagasaki@gmail.com

Spatiotemporal Patterns of Anthrax, Vietnam, 1990–2015

Morgan A. Walker,[1] Luong Minh Tan,[1] Le Hai Dang, Pham Van Khang, Hoang Thi Thu Ha, Tran Thi Mai Hung, Ho Hoang Dung, Dang Duc Anh, Tran Nhu Duong, Ted Hadfield, Pham Quang Thai, Jason K. Blackburn[1]

Anthrax is a priority zoonosis for control in Vietnam. The geographic distribution of anthrax remains to be defined, challenging our ability to target areas for control. We analyzed human anthrax cases in Vietnam to obtain anthrax incidence at the national and provincial level. Nationally, the trendline for cases remained at ≈61 cases/year throughout the 26 years of available data, indicating control efforts are not effectively reducing disease burden over time. Most anthrax cases occurred in the Northern Midlands and Mountainous regions, and the provinces of Lai Chau, Dien Bien, Lao Cai, Ha Giang, Cao Bang, and Son La experienced some of the highest incidence rates. Based on spatial Bayes smoothed maps, every region of Vietnam experienced human anthrax cases during the study period. Clarifying the distribution of anthrax in Vietnam will enable us to better identify risk areas for improved surveillance, rapid clinical care, and livestock vaccination campaigns.

Pathogens that persist in environmental reservoirs represent a major and underappreciated risk for humans and animals (*1*). *Bacillus anthracis*, the causative agent of anthrax, is an extreme example of environmental pathogen persistence because its spores persist for long periods (*2*), and indirect transmission from environment-to-host is obligate (*3*). Outbreaks are documented nearly worldwide, and the distribution of disease is constrained by specific environmental conditions (e.g., soil pH, organic matter, calcium) (*2*,*4*,*5*). Outbreaks generally arise in steppe/grassland habitats in wildlife populations (*6*) and livestock; this pattern was modeled globally (*7*), nationally (*8*–*13*) and locally (*14*–*16*) for several regions. The primary hypothesized infection route for livestock/wildlife is ingestion of *B. anthracis* spores during feeding at sites in which spores are concentrated (*17*). Human cases are primarily results of spillover from animal cases, particularly by handling carcasses or meat of livestock (*18*) or wildlife (*19*,*20*). Anthrax remains a major disease in developing countries in Africa and Asia (*21*,*22*). Where present, anthrax is major factor in public health (*23*), food web dynamics (*24*), and wildlife conservation (*25*).

An estimated 20,000–100,000 human cases of anthrax occur annually worldwide, mostly in poor rural areas (*26*). Cutaneous exposure to *B. anthracis* accounts for most human cases worldwide, typically with low mortality rates; gastrointestinal exposure shows intermediate-to-high case-fatality rates. Cutaneous and gastrointestinal cases of anthrax are most commonly caused by handling and slaughtering infected livestock or butchering and eating contaminated meat; untreated gastrointestinal cases account for most human deaths (*4*,*21*).

In Vietnam, anthrax has been identified as a priority zoonotic disease for control in a joint Ministry of Health and Ministry of Agriculture and Rural Development Circular (#16, 2013) (http://vbpl.yte.gov.vn/van-ban-phap-luat/TTLT-162013ttlt-byt-bnnptnt-.12.1706.html#pdf). Disease reports of anthrax in Vietnam in the literature date to the 1940s, with reports of agricultural risk for terrace-working farmers (*27*) (a dominant farming practice across much of current-day, mountainous rural Vietnam). Historically, anthrax foci were defined in southern Vietnam and along the northern border with China. Today, anthrax appears concentrated in 6 northern provinces, 5 of which border China (the Northern Midlands and Mountainous region) (Figure 1), with few reports from southern Vietnam (*28*). Several recent studies in China have reported sustained, as well as increasing areas of moderate human and livestock anthrax in provinces bordering northern Vietnam (*29*,*30*), an area with known transborder trade and livestock

Author affiliations University of Florida, Gainesville, Florida, USA (M.A. Walker, L.M. Tan, T. Hadfield, J.K. Blackburn); National Institute of Hygiene and Epidemiology, Hanoi, Vietnam (LH. Dang, P.V. Khang, H.T.T. Ha, T.T.M. Hung, H.H. Dung, D. Duc Anh, T.N. Duong, P.Q. Thai)

DOI: https://doi.org/10.3201/eid2811.212584

[1]These authors contributed equally to this article.

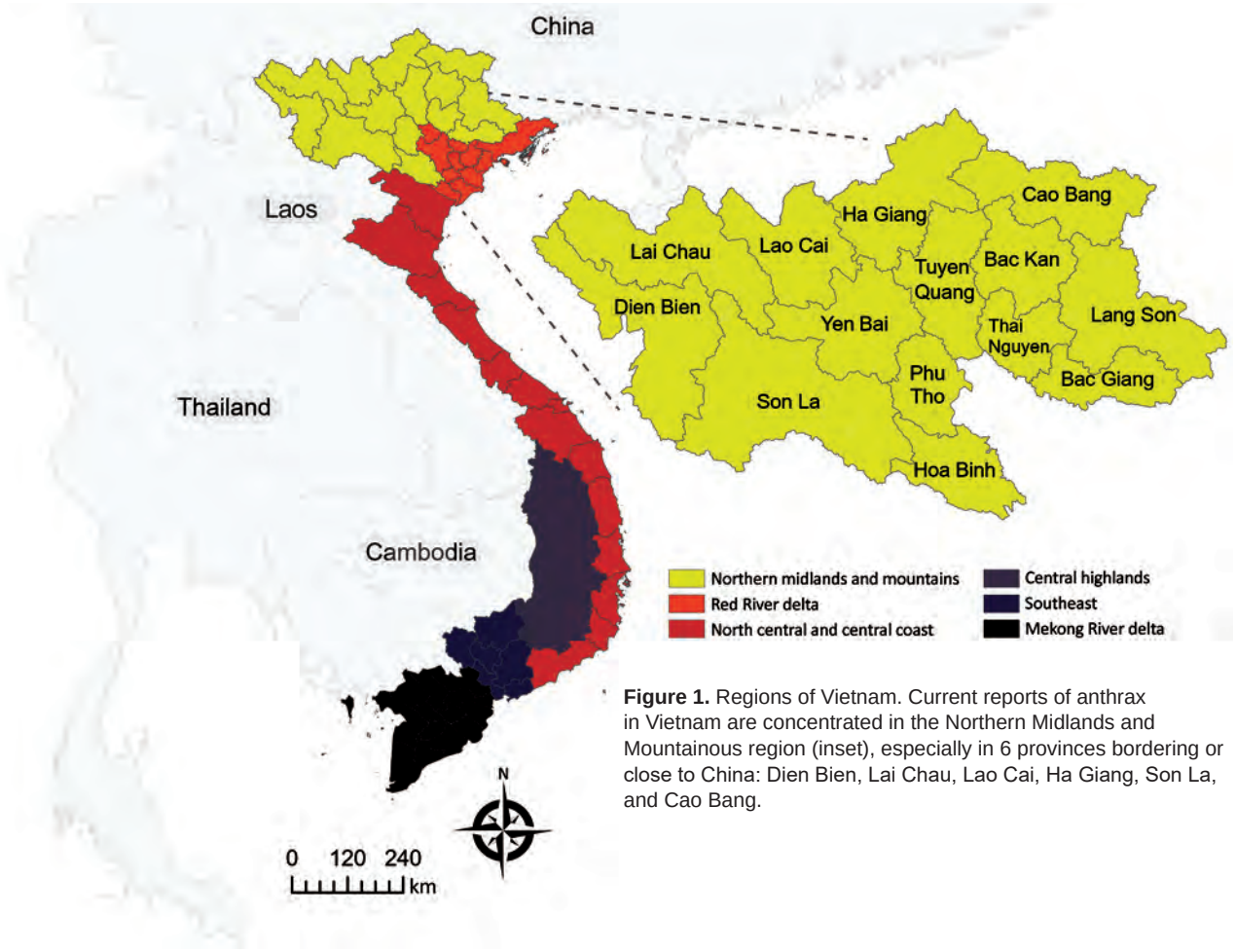

Figure 1. Regions of Vietnam. Current reports of anthrax in Vietnam are concentrated in the Northern Midlands and Mountainous region (inset), especially in 6 provinces bordering or close to China: Dien Bien, Lai Chau, Lao Cai, Ha Giang, Son La, and Cao Bang.

markets (temporarily restricted because of the COVID-19 pandemic). Generally, surveillance is anthropocentric with limited livestock reporting; comparable records are not currently available for livestock. Therefore, anthrax burden is unknown/underestimated, and the geographic distribution of anthrax in Vietnam remains to be defined, challenging our ability to identify target areas for control.

Because most human infections with anthrax are caused by contact with infected animals or their byproducts (e.g., meat or hides), targeting livestock with annual vaccination is the most effective method to control anthrax in animals and, consequently, in humans (*31*–*33*). Despite the effectiveness of vaccination, anthrax persists in areas with weakened health infrastructures; as a result, long-term vaccination strategies are often needed in disease-endemic areas (*31*). To prioritize areas for vaccination campaigns and disease surveillance and control, an understanding of risk areas is a necessity. To clarify anthrax risk areas in Vietnam, we retrospectively analyzed human anthrax case data for 1990–2015. We calculated nationwide and province-level anthrax incidence rates for this period, with the goal of assessing disease burden, a first step to prioritizing risk areas for management.

Methods

Epidemiologic Data

We extracted province-level data on human anthrax cases for 1990–2015 from the Vietnam Health Statistics Yearbooks published for 1991–2016 by epidemiologists of the National Institute of Hygiene and Epidemiology, Ministry of Health, Vietnam. Before 2015, anthrax was reported on weekly, monthly, and annual bases from commune health centers and district hospitals to District Medical Centers. From there, weekly, monthly, and annual reports were provided to the Provincial Preventative Medicine Centers, which reorganized into the Provincial Centers for Disease Control as of 2015. Reports of Provincial

Preventative Medicine Centers/Provincial Centers for Disease Control were submitted monthly and annually to National Institute of Hygiene and Epidemiology and 3 other regional institutes corresponding to each region of Vietnam. The institutes reviewed, compiled, and submitted the annual data to the Ministry of Health for further compilation and publication together with other health data. Anthrax was made reportable within 24 hours in 2015 as a class B infectious disease by circular number 54/2015/TT-BYT issued by the Ministry of Health (*34*).

Population Data

We obtained population data for the provinces of Vietnam for 2000–2015 from the WorldPop population counts database (*35*). This database incorporates census and open access ancillary data in a random forest estimation technique. The random forest model generates a gridded prediction of population density at 100-meter spatial resolution, which is used as a weighting surface to perform dasymetric redistribution, resulting in pixel-level census counts available for the whole country (*35*).

We aggregated these gridded population data to the provincial level by using the zonal statistic routine in QGIS 3.8 (https://www.qgis.org). In this instance, the provinces of Vietnam acted as the polygon layer, and the pixels of population data in each province were summed by using the zonal statistic to achieve a final calculation of the population of each province. The population was calculated by using this method for each province during 2000–2015. However, because WorldPop data are not available for years before 2000, we used a different approach for 1990–1999. For these years, we back calculated the population by using the United Nations average annual rate of change (*36*) for 2000–2001 and applying it to the provinces (Appendix Equation, https://wwwnc.cdc.gov/EID/article/28/11/21-2584-App1.pdf).

To verify the accuracy of this approach, we compared census population data collected by the country of Vietnam with the WorldPop population dataset. Census data from the 2019, 2009, and 1999 censuses were publicly available. We provide a comparison of population data from the 2 datasets, as well as the national incidence of anthrax cases (Appendix Figure 1). The WorldPop estimate is slightly higher than the census population data, especially for 1995–2005. However, our national incidence rate calculations were nearly identical regardless of the population estimate used (Appendix Figure 1).

The administrative boundaries of the provinces of Vietnam have changed several times since 1980 (*37*,*38*). During our study period, splits or merges occurred in 1990, 1991, 1992, 1997, 2004, and 2008 (Appendix Figure 2). During 1990–2015, the number of provinces in Vietnam increased from 44 to 63 (*39*). These administrative boundary changes were considered when calculating the populations of each province as outlined; thus, the zonal statistic was used on different polygon layers that corresponded to the provincial boundaries of that year. Administrative boundaries of the choropleth maps in the results are also displayed accurately to the corresponding year.

Once population data were available as denominators, we plotted total cases and incidence per 10,000 persons annually for all of Vietnam. We also fitted a linear trend for each case and incidence in Excel 365 (Microsoft, https://www.microsoft.com).

Spatial Incidence Mapping

For mapping, we calculated provincial level human anthrax incidence rates annually for 1990–2015. We obtained incidence rates by dividing raw cases numbers in each province by the population of each province and multiplying by 10,000 for each year. Accordingly, all incidence rates reported are per 10,000 persons. We spatially smoothed raw incidence rates to improve estimates of anthrax cases that might have gone unreported.

Smoothing is a method of statistically adjusting the estimate for the underlying risk in each spatial unit by using information provided by the other spatial units (*39*,*40*). When subdividing national estimates into individual provinces, variance estimates can be unstable (*41*), and instability is increased in rural areas. The goal of smoothing is to adjust rate estimates toward a global or local mean, with a larger effect on spatial units (here, provinces) that have smaller populations (*39*). We applied spatial Bayes in GeoDa 1.20 (*39*). In brief, spatial Bayes smoothing uses the raw rate for each areal unit averaged with a localized reference estimate, the extent of which is based on a weights matrix. We used a first-order queen contiguity weights matrix, which defines the neighbors of a location as those that have either a shared border or vertex with the polygon of interest (*39*).

We compared empirical Bayes smoothing, which adjusts values to the global mean (all of Vietnam) to spatial Bayes, which adjusts to the local mean defined by the weights matrix, reducing the adjustment to the mean incidence of immediate neighbors. For incidence rate smoothing comparisons, we chose the years with the lowest (1990) and highest (2011) incidence rates, as well as 4 additional, randomly chosen years (Appendix Figure 3). Box plots showed that

spatial Bayes and empirical Bayes smoothing were similar, but spatial Bayes outperformed empirical Bayes in collapsing lower percentile outliers, the SD, and the mean (Appendix Figure 3). Accordingly, spatial Bayes smoothing was chosen for use in this study.

After smoothing, we constructed choropleth maps of the province-level incidence rates by using ArcGIS Pro 2.4.0 (https://support.esri.com). To evaluate results, we mapped each year separately (Appendix Figure 4) and developed an animated GIF enabling us to view interannual variability (Appendix Figure 5). We mapped a selection of years to illustrate areas of sustained anthrax and the wider geography of reported human anthrax over the 26 years.

Results

National Incidence of Human Anthrax

During 1990–2015, Vietnam reported 1,600 human anthrax cases with an annual average of 61.5 cases (Figure 2). During the study period, human deaths were reported in 1992, 1995, 2001, 2003, and 2011. Some years had >200 cases, and deaths were not necessarily in severe years (Figure 2). The trendline for cases remained at ≈61 cases per year throughout the 26 years of the study period. The trendline for incidence showed a slight decrease over time, probably a reflection of the increasing population in Vietnam (Figure 3). Years with the highest number of human cases were 1992 (166 cases) and 2011 (201 cases), reflecting large outbreaks early and late in the study period. In 1992 and 2011, the incidence rate reached 2.3 cases/10,000 persons. Between these 2 large outbreak years, incidence fluctuated with peaks every 3–to 4 years.

Provincial Incidence of Human Anthrax

Of the 63 total provinces in Vietnam, 20 provinces reported ≥1 human anthrax case during 1990–2015. Four provinces reported ≥1 death. Most cases were reported in the Northern Midlands and Mountainous region (Figure 1), but smoothed maps identified case incidence in several years in the Red River Delta, North Central and Central Coast, Central Highlands, South East, and Mekong River Delta regions (Figure 4). The provinces of Lai Chau, Dien Bien, Lao Cai, Ha Giang, and Cao Bang had some of the highest incidence rates. Dien Bien had the highest incidence rate of all provinces in 2011 (2.62 cases/10,000 persons). Of the North Central and Central Coast region of Vietnam, Ha Tinh was the province with the highest incidence rate (0.33 cases/10,000 persons in 1992). In the Central Highlands region, Dak Lak had the highest incidence and in the South East region Dong Nai was the province that had the highest incidence. Anthrax incidence was highest in, but not exclusive to, the northern provinces (Figure 4). Anthrax incidence was widespread throughout the country during our study (Appendix Figure 4).

Discussion

We examined the interannual patterns of human anthrax in Vietnam at the national and provincial level for 1990–2015. There was no annual decrease in reported human anthrax cases nationally over the 26 years for which data were available. Although the national incidence rate decreased slightly during 1990–2015, this decrease was probably caused by an increase in the population of Vietnam, rather than a decrease in raw case numbers (Figure 3). For example, the median percentage change of the population in the communes of Vietnam during 1990–2015 was 11%. Furthermore, 56% of communes had a population increase, and 1,200 communes had a population increase of >500%. The increasing population and steady case numbers indicate that over our study period, control efforts did not effectively reduce disease

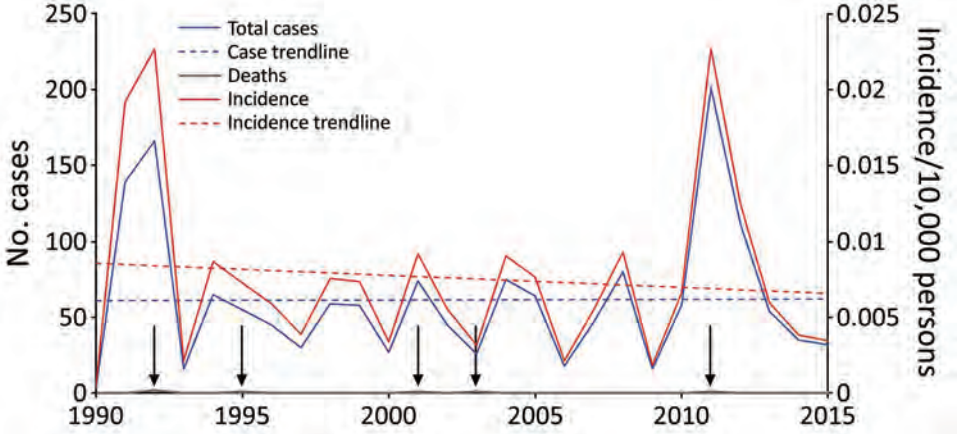

Figure 2. National human anthrax cases and incidence per 10,000 persons per year in Vietnam, 1990–2015. Gray arrows indicate deaths.

burden nationally. In addition, the years in which deaths occurred (Figure 2) did not necessarily correspond to the years with the highest incidence rates, suggesting that deaths are driven by access to healthcare or knowledge of disease, rather disease intensity.

Historically, anthrax foci have appeared concentrated at the northern border with China, in the Northern Midlands and Mountainous region of Vietnam. Our study supports this finding because some of the highest incidence rates were found in the provinces of Lai Chau, Dien Bien, Ha Giang, Cao Bang, Lao Cai, and Son La. Of these provinces, only Son La does not have a border with China. However, Son La and Dien Bien both have a border with Laos. Borders that serve as areas of international transit and trade might play a major role when addressing disease control. Because *B. anthracis* is most commonly transmitted to humans through infected livestock, trading animals or meat across borders could be a cause for concern. Although this practice has been limited by COVID-19 restrictions since 2020, transnational livestock trade is a major industry in Vietnam (*42*). For example, Turner (*42*) reported how regular trade in buffalo, which are vital farming tools for ploughing terraced fields, spans the China–Vietnam border and takes place through legal and illegal routes. On legal paths, buffalo are inspected at border checkpoints for disease, but other traders use secret routes to smuggle buffalo without permits (*42*). Livestock trade also occurs at the Laos–Vietnam border because Laos is an importer and exporter of cattle and buffalo and a transit country for livestock destined for Vietnam and China (*43*).

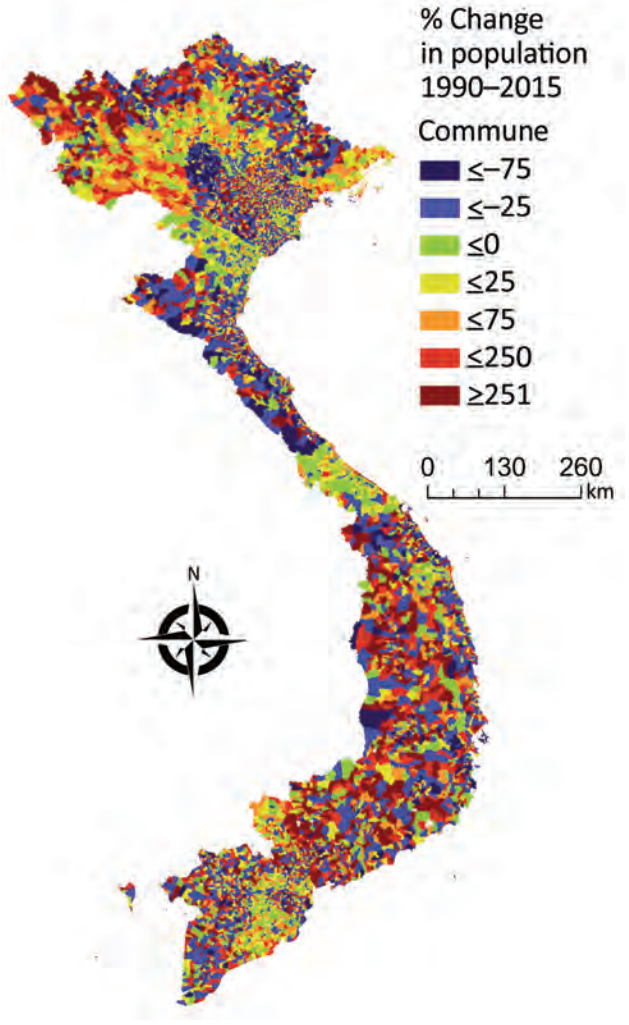

Figure 3. Percentage population change in the communes of Vietnam during 1990–2015. Light blue, dark blue, and green values indicate communes that had population decreases, and yellow, orange, and red values indicate communes that had population growth.

Recent disease reporting from China has shown high incidence of human cutaneous anthrax in southwestern China, including Yunnan and Guangxi Provinces, which border northern Vietnam (*29,30*). In contrast, although anthrax is a reportable disease in Laos, publicly available data on human anthrax cases are limited (*44,45*). Of the provinces in Laos that reported outbreaks during 1984–2010, none of them border the northern provinces of Vietnam where high incidence rates were reported from our study (*45*). However, this finding could be a case of underreporting and data inaccessibility, rather than an indication that anthrax outbreaks have not occurred in northeastern Laos.

Although most reported anthrax cases and the highest anthrax incidence were found in the Northern Midlands and Mountainous regions of Vietnam, our study shows that human anthrax incidence is much more widespread throughout the country; smoothed rate maps showed that all regions of Vietnam have probably had anthrax cases during the study period (Figure 4). This major finding helps identify risk areas and target regions for public health intervention. Furthermore, because of the ability of *B. anthracis* to form long-lasting spores resistant to multiple environmental conditions (*46*), cases occurring in these other regions of Vietnam are a good indication of the presence of *B. anthracis* in the environment. Therefore, cases could reoccur in these areas, even if outbreaks have not been reported in recent years. In addition, because of limited data available on the domestic livestock trade within Vietnam, it is unknown how movement of livestock within the country contributes to anthrax incidence. Domestic trade and transportation of draft and livestock animals from regions with a high burden of disease could contribute to the sporadic occurrence of anthrax cases in other regions.

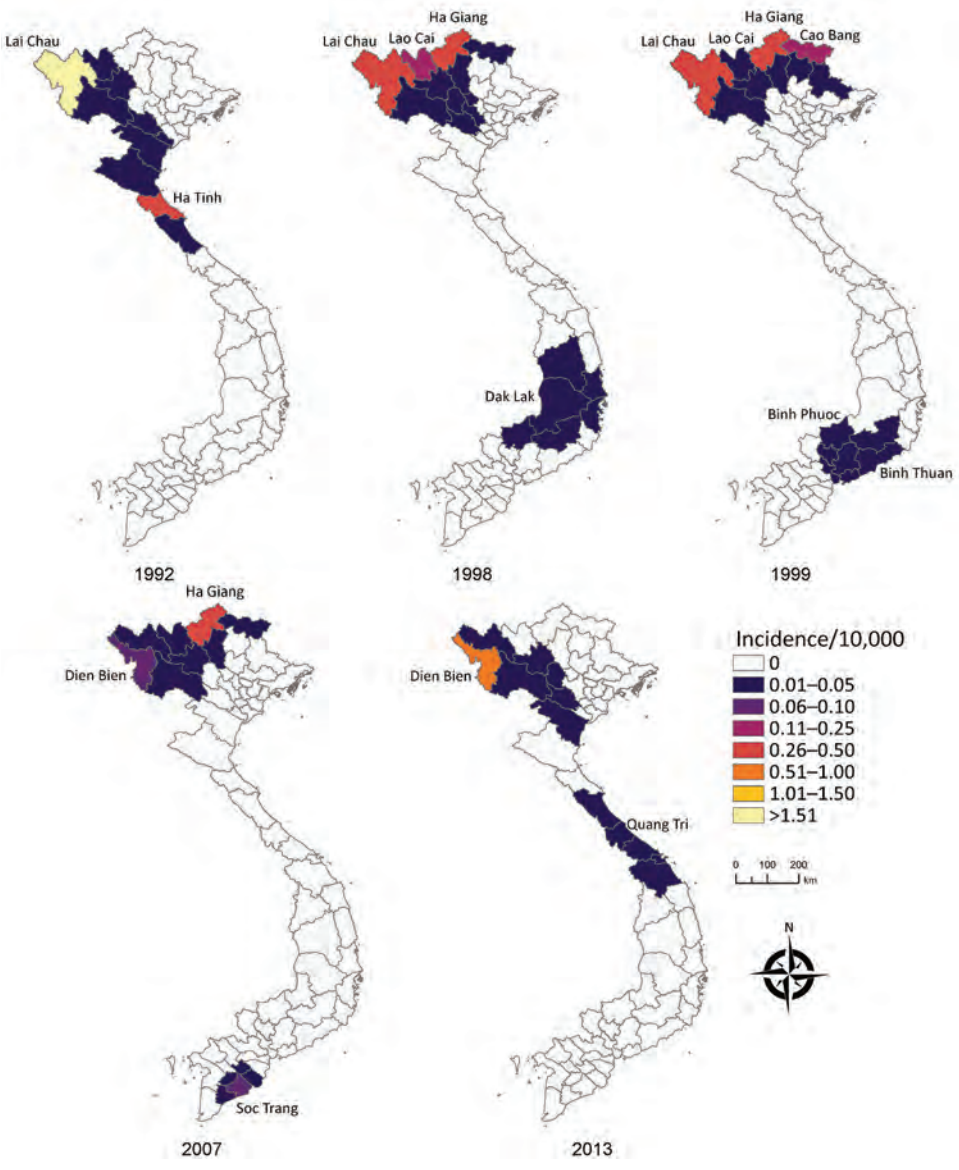

Figure 4. Choropleth maps of spatial Bayes smoothed human anthrax incidence rates in provinces of Vietnam. The years are not necessarily those with the highest anthrax incidence rates but those with the most widespread range of anthrax. Although anthrax incidence rates were highest in the northern provinces, they were not limited to those provinces.

As for all neglected zoonoses, our data probably represent an underestimation of true disease burden, which is a limitation of our study. Although anthrax is a reportable disease in Vietnam (*34*), it might go unreported because of a multitude of reasons, including lack of public awareness, stigma, or travel distance to a health provider. Case identification is also dependent on the diagnostic capacity existing in the clinical and laboratory chain down to the local level. A breakdown in any of these steps might result in underreporting of anthrax cases.

Previous research has shown that human anthrax rates increase with limited vaccination of livestock (*47*) and a decrease in sustained livestock vaccination (*48*). Although there is national policy on livestock vaccination for Vietnam, it is not clear how vaccination rules and distribution of livestock vaccines differ between provinces. Goletti et al. (*49*) found that although the supply of vaccines is not a constraint within the country, their price and quality might impede their effective use. Furthermore, limited animal health knowledge at the farm and field service levels is a key factor in the low adoption of proven disease control measures. More data on the distribution and use of anthrax vaccines is needed in Vietnam and worldwide (*7*).

In conclusion, the current anthrax situation in Vietnam remains a public and veterinary health threat because of challenges with reporting, surveillance, and control. Our findings suggest anthrax has

occurred throughout Vietnam, and the highest incidence are in provinces of the Northern Midlands and Mountainous region. Future control efforts need to focus on improving (and reporting) livestock vaccination rates, as well as advancing public awareness and knowledge of the disease, especially in these risk areas. The interconnectedness of humans, livestock, and wildlife is evident when examining anthrax outbreaks and emphasizes the need for a true One Health approach to effectively prevent and control this neglected zoonosis.

This study was supported by the US Defense Threat Reduction Agency (grant DTRA12010003).

About the Author

Mx. Walker is a spatial epidemiologist at the Spatial Epidemiology and Ecology Research Laboratory, Department of Geography, University of Florida, Gainesville, FL. Their primary research interests include zoonoses and wildlife ecology.

References

1. Blackburn JK, Ganz HH, Ponciano JM, Turner WC, Ryan SJ, Kamath P, et al. Modeling R_0 for pathogens with environmental transmission: animal movements, pathogen populations, and local infectious zones. Int J Environ Res Public Health. 2019;16:954. https://doi.org/10.3390/ijerph16060954
2. Hugh-Jones M, Blackburn J. The ecology of *Bacillus anthracis*. Mol Aspects Med. 2009;30:356–67. https://doi.org/10.1016/j.mam.2009.08.003
3. Alexander KA, Lewis BL, Marathe M, Eubank S, Blackburn JK. Modeling of wildlife-associated zoonoses: applications and caveats. Vector Borne Zoonotic Dis. 2012;12:1005–18. https://doi.org/10.1089/vbz.2012.0987
4. Carlson CJ, Getz WM, Kausrud KL, Cizauskas CA, Blackburn JK, Bustos Carrillo FA, et al. Spores and soil from six sides: interdisciplinarity and the environmental biology of anthrax (*Bacillus anthracis*). Biol Rev Camb Philos Soc. 2018;93:1813–31. https://doi.org/10.1111/brv.12420
5. Keim P, Price LB, Klevytska AM, Smith KL, Schupp JM, Okinaka R, et al. Multiple-locus variable-number tandem repeat analysis reveals genetic relationships within Bacillus anthracis. J Bacteriol. 2000;182:2928–36. https://doi.org/10.1128/JB.182.10.2928-2936.2000
6. Blackburn J. Integrating geographic information systems and ecological niche modeling into disease ecology: a case study of *Bacillus anthracis* in the United States and Mexico. In: O'Connell KP, Sulakvelidze EW, Bakanidze L, editors. Emerging and endemic pathogens: advances in surveillance, detection, and identification. New York: Springer; 2010. p. 59–88.
7. Carlson CJ, Kracalik IT, Ross N, Alexander KA, Hugh-Jones ME, Fegan M, et al. The global distribution of *Bacillus anthracis* and associated anthrax risk to humans, livestock and wildlife. Nat Microbiol. 2019;4:1337–43. https://doi.org/10.1038/s41564-019-0435-4
8. Blackburn JK, McNyset KM, Curtis A, Hugh-Jones ME. Modeling the geographic distribution of *Bacillus anthracis*, the causative agent of anthrax disease, for the contiguous United States using predictive ecological [corrected] niche modeling. Am J Trop Med Hyg. 2007;77:1103–10. https://doi.org/10.4269/ajtmh.2007.77.1103
9. Mullins J, Lukhnova L, Aikimbayev A, Pazilov Y, Van Ert M, Blackburn JK. Ecological niche modelling of the *Bacillus anthracis* A1.a sub-lineage in Kazakhstan. BMC Ecol. 2011;11:32. https://doi.org/10.1186/1472-6785-11-32
10. Blackburn JK, Odugbo MO, Van Ert M, O'Shea B, Mullins J, Perreten V, et al. *Bacillus anthracis* diversity and geographic potential across Nigeria, Cameroon and Chad: further support of a novel West African lineage. PLoS Negl Trop Dis. 2015;9:e0003931. https://doi.org/10.1371/journal.pntd.0003931
11. Blackburn JK, Matakarimov S, Kozhokeeva S, Tagaeva Z, Bell LK, Kracalik IT, et al. Modeling the ecological niche of *Bacillus anthracis* to map anthrax risk in Kyrgyzstan. Am J Trop Med Hyg. 2017;96:550–6. https://doi.org/10.4269/ajtmh.16-0758
12. Kracalik IT, Kenu E, Ayamdooh EN, Allegye-Cudjoe E, Polkuu PN, Frimpong JA, et al. Modeling the environmental suitability of anthrax in Ghana and estimating populations at risk: implications for vaccination and control. PLoS Negl Trop Dis. 2017;11:e0005885. https://doi.org/10.1371/journal.pntd.0005885
13. Barro AS, Fegan M, Moloney B, Porter K, Muller J, Warner S, et al. Redefining the Australian anthrax belt: modeling the ecological niche and predicting the geographic distribution of *Bacillus anthracis*. PLoS Negl Trop Dis. 2016;10:e0004689. https://doi.org/10.1371/journal.pntd.0004689
14. Morris LR, Blackburn JK. Predicting disease risk, identifying stakeholders, and informing control strategies: a case study of anthrax in Montana. EcoHealth. 2016;13:262–73. https://doi.org/10.1007/s10393-016-1119-7
15. Morris LR, Proffitt KM, Asher V, Blackburn JK. Elk resource selection and implications for anthrax management in Montana. J Wildl Manage. 2016;80:235–44. https://doi.org/10.1002/jwmg.1016
16. Steenkamp PJ. Ecological suitability modelling for anthrax in the Kruger National Park. Pretoria (South Africa): University of Pretoria; 2013.
17. Turner WC, Kausrud KL, Krishnappa YS, Cromsigt JP, Ganz HH, Mapaure I, et al. Fatal attraction: vegetation responses to nutrient inputs attract herbivores to infectious anthrax carcass sites. Proc Biol Sci. 2014;281:20141785. https://doi.org/10.1098/rspb.2014.1785
18. Woods CW, Ospanov K, Myrzabekov A, Favorov M, Plikaytis B, Ashford DA. Risk factors for human anthrax among contacts of anthrax-infected livestock in Kazakhstan. Am J Trop Med Hyg. 2004;71:48–52. https://doi.org/10.4269/ajtmh.2004.71.48
19. Katani R, Schilling MA, Lyimo B, Eblate E, Martin A, Tonui T, et al. Identification of *Bacillus anthracis, Brucella* spp., and *Coxiella burnetii* DNA signatures from bushmeat. Sci Rep. 2021;11:14876. https://doi.org/10.1038/s41598-021-94112-9
20. Sidwa T, Salzer JS, Traxler R, Swaney E, Sims ML, Bradshaw P, et al. Control and prevention of anthrax, Texas, USA, 2019. Emerg Infect Dis. 2020;26:2815–24. https://doi.org/10.3201/eid2612.200470
21. World Health Organization. Anthrax in humans and animals. International Office of Epizootics; 2008 [cited 2022 Sep 1]. https://apps.who.int/iris/handle/10665/97503
22. Hugh-Jones M. 97 global anthrax report. J Appl Microbiol. 1999;87:189–91. https://doi.org/10.1046/j.1365-2672.1999.00867.x

23. Kracalik IT, Malania L, Tsertsvadze N, Manvelyan J, Bakanidze L, Imnadze P, et al. Evidence of local persistence of human anthrax in the country of Georgia associated with environmental and anthropogenic factors. PLoS Negl Trop Dis. 2013;7:e2388. https://doi.org/10.1371/journal.pntd.0002388
24. Getz WM. Disease and the dynamics of food webs. PLoS Biol. 2009;7:e1000209. https://doi.org/10.1371/journal.pbio.1000209
25. Clegg SB, Turnbull PC, Foggin CM, Lindeque PM. Massive outbreak of anthrax in wildlife in the Malilangwe Wildlife Reserve, Zimbabwe. Vet Rec. 2007;160:113–8. https://doi.org/10.1136/vr.160.4.113
26. Swartz MN. Recognition and management of anthrax: an update. N Engl J Med. 2001;345:1621–6. https://doi.org/10.1056/NEJMra012892
27. Chambon L, Dutrenit J. Note on a human epidemic of anthrax with two cases of anthrax meningitis [in French]. Bull Soc Pathol Exot Filiales. 1955;48:544–52.
28. Hoang TT, Dang DA, Pham TH, Luong MH, Tran ND, Nguyen TH, et al. Epidemiological and comparative genomic analysis of *Bacillus anthracis* isolated from northern Vietnam. PLoS One. 2020;15:e0228116. https://doi.org/10.1371/journal.pone.0228116
29. Chen WJ, Lai SJ, Yang Y, Liu K, Li XL, Yao HW, et al. Mapping the distribution of anthrax in Mainland China, 2005–2013. PLoS Negl Trop Dis. 2016;10:e0004637. https://doi.org/10.1371/journal.pntd.0004637
30. Zhang WY, Wang LY, Zhang XS, Han ZH, Hu WB, Qian Q, et al. Spatiotemporal clustering analysis and risk assessments of human cutaneous anthrax in China, 2005–2012. PLoS One. 2015;10:e0133736. https://doi.org/10.1371/journal.pone.0133736
31. Turnbull PC. Anthrax vaccines: past, present and future. Vaccine. 1991;9:533–9. https://doi.org/10.1016/0264-410X(91)90237-Z
32. Turnbull PC. Guidelines for the surveillance and control of anthrax in humans and animals, 3rd ed. Office of Justice Programs [cited 2021 Dec 8]. https://www.ojp.gov/ncjrs/virtual-library/abstracts/guidelines-surveillance-and-control-anthrax-humans-and-animals
33. Beyer W, Turnbull PC. Anthrax in animals. Mol Aspects Med. 2009;30:481–9. https://doi.org/10.1016/j.mam.2009.08.004
34. Vietnam Ministry of Health. Circular 54/2015/TT-BYT guiding the infectious disease notification and report, Ministry of Health; 2015 [cited 2021 Nov 24]. http://vbpl.yte.gov.vn/van-ban-phap-luat/thong-tu-542015tt-byt.6.1508.html
35. Gaughan AE, Stevens FR, Linard C, Jia P, Tatem AJ. High resolution population distribution maps for Southeast Asia in 2010 and 2015. PLoS One. 2013;8:e55882. https://doi.org/10.1371/journal.pone.0055882
36. United Nations. World urbanization prospects. Population Division [cited 2021 Nov 22]. https://population.un.org/wup/General/GlossaryDemographicTerms.aspx
37. Pham QT. The epidemiology and control of human influenza in Vietnam. 2014 [cited 2021 Nov 30]. http://oro.open.ac.uk/id/eprint/39878
38. Nguyen G. Statistical yearbook 2000. et]. General Statistics Office of Vietnam [cited 2021 Dec 9]. https://www.gso.gov.vn/en/data-and-statistics/2020/02/statistical-yearbook-2000
39. Anselin L, Syabri I, Kho Y. GeoDa: an introduction to spatial data analysis. In: Fischer MM, Getis A, editors. Handbook of applied spatial analysis: software tools, methods and applications. Springer (Berlin, Heidelberg); 2010. p. 73–89 [cited 2021 Nov 30]. https://doi.org/10.1007/978-3-642-03647-7_5
40. Hu W, Clements A, Williams G, Tong S. Spatial analysis of notified dengue fever infections. Epidemiol Infect. 2011;139:391–9. https://doi.org/10.1017/S0950268810000713
41. Anselin L. Exploring spatial data with GeoDaTM: a workbook. Center for Spatially Integrated Social Science; 2005 [cited 2022 Sep 1]. https://www.geos.ed.ac.uk/~gisteac/fspat/geodaworkbook.pdf
42. Turner S. Under the state's gaze: upland trading-scapes on the Sino-Vietnamese border. Singap J Trop Geogr. 2013;34:34. https://doi.org/10.1111/sjtg.12010
43. Sieng S. Livestock trading and foot-and-mouth disease risk. Sep 20, 2020. Livestock trading and foot-and-mouth disease risk. Animal Biosecurity in the Mekong: Future Directions for Research and Development. Proceedings of an International Workshop, Siem Reap, Cambodia, August 10–13, 2010. Canberra: Australian Centre for International Agricultural Research Proceedings 137 [cited 2022 Sept 6]. https://www.aciar.gov.au/sites/default/files/legacy/node/14481/pr137_pdf_76587.pdf
44. Linthavong S, Ouandala V, Dusan F, Vongphrachanh P, Kounnavong B, Corwin A, et al. Anthrax knowledge, attitudes and practice survey—Lao PDR, 2010. Int J Infect Dis. 2012;16:e456. https://doi.org/10.1016/j.ijid.2012.05.654
45. Leuangvilay P, Chapman RS, Siriwong W. Associated environmental factor and past practices regarding to anthrax infection in human in the Salavan District, Salavan Province, Lao PDR: case–control study. J Health Res. 2012;26:5.
46. Dragon DC, Rennie RP. The ecology of anthrax spores: tough but not invincible. Can Vet J. 1995;36:295–301.
47. Kracalik I, Malania L, Broladze M, Navdarashvili A, Imnadze P, Ryan SJ, et al. Changing livestock vaccination policy alters the epidemiology of human anthrax, Georgia, 2000–2013. Vaccine. 2017;35:6283–9. https://doi.org/10.1016/j.vaccine.2017.09.081
48. Kracalik I, Abdullayev R, Asadov K, Ismayilova R, Baghirova M, Ustun N, et al. Changing patterns of human anthrax in Azerbaijan during the post-Soviet and preemptive livestock vaccination eras. PLoS Negl Trop Dis. 2014;8:e2985. https://doi.org/10.1371/journal.pntd.0002985
49. Goletti F, Smith D, Gruhn P. Policy option for using livestock to promote rural income diversification and growth in Viet Nam; 2015 [cited 2022 Sep 1]. https://agris.fao.org/agris-search/search.do?recordID=QB2015100771

Address for correspondence: Jason K. Blackburn, Emerging Pathogens Institute and Department of Geography, University of Florida, 3141 Turlington Hall, Gainesville, FL 32611, USA; email: jblack6@gmail.com

Coronavirus Antibody Responses before COVID-19 Pandemic, Africa and Thailand

Yifan Li, Mélanie Merbah, Suzanne Wollen-Roberts, Bradley Beckman, Thembi Mdluli, Isabella Swafford, Sandra V. Mayer, Jocelyn King, Courtney Corbitt, Jeffrey R. Currier, Heather Liu, Allahna Esber, Suteeraporn Pinyakorn, Ajay Parikh, Leilani V. Francisco, Nittaya Phanuphak, Jonah Maswai, John Owuoth, Hannah Kibuuka, Michael Iroezindu, Emmanuel Bahemana, Sandhya Vasan, Julie A. Ake, Kayvon Modjarrad, Gregory Gromowski, Dominic Paquin-Proulx, Morgane Rolland

Prior immune responses to coronaviruses might affect human SARS-CoV-2 response. We screened 2,565 serum and plasma samples collected from 2013 through early 2020, before the COVID-19 pandemic began, from 2,250 persons in 4 countries in Africa (Kenya, Nigeria, Tanzania, and Uganda) and in Thailand, including persons living with HIV-1. We detected IgG responses to SARS-CoV-2 spike (S) subunit 2 protein in 1.8% of participants. Profiling against 23 coronavirus antigens revealed that responses to S, subunit 2, or subunit 1 proteins were significantly more frequent than responses to the receptor-binding domain, S-Trimer, or nucleocapsid proteins ($p<0.0001$). We observed similar responses in persons with or without HIV-1. Among all coronavirus antigens tested, SARS-CoV-2, SARS-CoV-1, and Middle East respiratory syndrome coronavirus antibody responses were much higher in participants from Africa than in participants from Thailand ($p\leq0.01$). We noted less pronounced differences for endemic coronaviruses. Serosurveys could affect vaccine and monoclonal antibody distribution across global populations.

COVID-19 clinical manifestations range from asymptomatic infection to death. Whether prior immune responses to human coronaviruses affect responses to SARS-CoV-2 remains unclear. At the population level, disparities in COVID-19 outcomes have been observed across geographic regions. For instance, countries in Africa have reported lower mortality rates than high-income countries, which can be attributed to the small percentage of persons in the oldest age groups and to underreporting (*1*,*2*). Previous responses to endemic coronaviruses also could influence how different populations responded to SARS-CoV-2.

Findings conflict as to whether previous coronavirus antigen responses cross-react with SARS-CoV-2. Depending on the antigen and cohort tested, binding responses have been detected in prepandemic samples at varying frequencies, but neutralizing antibodies have been identified in fewer samples (*3*–*8*). Some studies of prepandemic samples indicated that neutralizing responses to endemic coronaviruses could protect against SARS-CoV-2 infection, but the effects of previous coronavirus responses on SARS-CoV-2 have not been clearly elucidated (*6*,*7*,*9*–*13*).

To investigate coronavirus-specific antibody responses in different settings, we analyzed 2,565 samples collected during 2013 through early 2020 from persons living with HIV-1 (PLHIV) and persons without HIV in Kenya, Nigeria, Tanzania, Uganda, and Thailand. We profiled antibody binding responses to coronavirus antigens, including spike (S) and nucleocapsid (N) proteins of SARS-CoV-2, SARS-CoV-1, MERS-CoV, and 4 endemic coronaviruses. We further evaluated a subset of samples with strong binding responses for neutralizing, antibody-dependent cellular

Author affiliations: Walter Reed Army Institute of Research, Silver Spring, Maryland, USA (Y. Li, M. Merbah, S. Wollen-Roberts, B. Beckman, T. Mdluli, I. Swafford, S.V. Mayer, J. King, C. Corbitt, H. Liu, A. Esber, S. Pinyakorn, A. Parikh, L.V. Francisco, S. Vasan, J.A. Ake, K. Modjarrad, G. Gromowski, D. Paquin-Proulx, M. Rolland); Henry M. Jackson Foundation for the Advancement of Military Medicine, Inc., Bethesda, Maryland, USA (Y. Li, M. Merbah, S. Wollen-Roberts, B. Beckman, T. Mdluli, I. Swafford, H. Liu, A. Esber, S. Pinyakorn, A. Parikh, L.V. Francisco, S. Vasan, D. Paquin-Proulx, M. Rolland); Institute of HIV Research and Innovation, Bangkok, Thailand (N. Phanuphak); HJF Medical Research International, Kericho, Kenya (J. Maswai, J. Owuoth, M. Iroezindu, E. Bahemana); Makerere University Walter Reed Project, Kampala, Uganda (H. Kibuuka)

DOI: https://doi.org/10.3201/eid2811.221041

phagocytosis (ADCP), and antibody-dependent cellular cytotoxicity (ADCC) responses. We compared responses across geographic locations and according to HIV-1 status.

Methods

Ethics Statement

We adhered to the policies for protection of human subjects, as prescribed in AR70-25 (*14*). All participants provided written informed consent. We used samples collected in 3 clinical cohort studies that investigated HIV-1 and other infectious diseases. Institutional review boards at local institutions and at Walter Reed Army Institute of Research approved the study (approval nos. WRAIR 1494, WRAIR 1897, and WRAIR 2383).

Samples and Antigens

We obtained serum and plasma specimens from 2 study cohorts in Africa and 1 in Thailand. Cohorts in Africa included the RV329 African Cohort Study (RV329/AFRICOS), which predominantly enrolled PLHIV with chronic infection, and study RV466 of the Joint West Africa Research Group (RV466/JWARG), which was designed to diagnose acute febrile illnesses in Nigeria. The cohort in Thailand was from the RV254 South East Asia Research Collaboration in HIV (RV254/SEARCH 010) study, which enrolls persons with acute HIV-1 infection. For negative controls, we used prepandemic plasma samples, including Zika Negative Plasma (SeraCare, https://www.seracare.com), Pooled Normal Human Plasma (Innovative Research, https://www.innov-research.com), and 2 human serum coronavirus panels, MSRM-CR1 and HMSRM-CR22 (BioIVT, https://bioivt.com). For positive controls, we used 2 SARS-CoV-2–positive plasma samples with high neutralization titers and 2 serum panels, HMSRM-COVIDPOS and HMSRM-COVIDREC (BioIVT). We also used 12 matched SARS-CoV-2 patient convalescent serum and plasma samples (Innovative Research). We divided 51 antigens into custom panels, including panels for coronaviruses (SARS-CoV-2, SARS-CoV-1, MERS-CoV, OC43, NL63, HKU1, 229E), flaviviruses, and HIV-1 (Appendix Table 1, https://wwwnc.cdc.gov/EID/article/28/11/22-1041-App1.pdf). We included an alphavirus, chikungunya Envelope 1 antigen (E1), in the flavivirus panel.

Bead-Based Multiplex Assay

We adapted assays from a previous study (*15*). Per 1 million beads, we coupled 10 μg of antigen for flavivirus proteins (*15*); 2.5 μg for coronavirus nucleocapsid (N) proteins; 5 μg for HIV-1 proteins; and 5 μg for coronavirus spike (S) proteins, including subunit 1 (S1), subunit 2 (S2), receptor-binding domain (RBD), and S-Trimer. We used 1,200 conjugated beads of each antigen per well and ran samples in triplicate at 2 dilutions, 1:100 and 1:400. We tagged biotinylated Fc gamma receptors (FcγR) FcγRIIa-H131, FcγRIIb, FcγRIIIa-F158, and FcγRIIIb-NA2 (Duke Human Vaccine Institute, https://dhvi.duke.edu) with a 1:4 molar ratio of Streptavidin-R-Phycoetherin (ProZyme-Agilent, https://www.agilent.com). We stored the tagged FcγR conjugated beads at 4°C and used within 24 hours of conjugation. We detected FcγR binding by using 20 μL of Streptavidin-R-Phycoethrerin–bound FcγR (3μg/mL). We acquired ≥100 beads/antigen/well on a FlexMap-3D (Luminex Corporation, https://www.luminexcorp.com) by using the xPONENT software (Luminex Corporation, https://www.luminexcorp.com) to measure the median fluorescence intensity (MFI). We assayed 3 plates per detection and used 4 negative and 4 positive controls per plate, 2 each of plasma and serum. We used a conservative cutoff by setting the positive threshold at 6 times the response for the highest negative control (*16*).

Pseudovirus Neutralization Assay

We ran assays as previously described (*17*). We reported neutralization values as fold changes corresponding to the ratio of the 50% inhibitory dilution (ID_{50}) for SARS-CoV-1 or SARS-CoV-2 over the ID_{50} for S glycoprotein of vesicular stomatitis virus.

ADCP

We measured ADCP as previously described (*18*). We incubated biotinylated SARS-CoV-2, SARS-CoV-1, or MERS-CoV S protein with yellow-green neutravidin-fluorescent beads (Molecular Probes-Thermo Fisher Scientific, https://www.thermofisher.com) for 2 h (37°C). We incubated a 100-fold dilution of beads to protein (10 μL) for 2 h at 37°C along with 100 μL of 100-fold diluted plasma before adding THP-1 cells (MilliporeSigma, https://www.sigmaaldrich.com) at 25,000 cells per well. After a 19-h incubation, we fixed cells with 4% formaldehyde solution (Tousimis, https://www.tousimis.com) and evaluated fluorescence on an LSRII (BD Biosciences, https://www.bdbiosciences.com). We calculated the phagocytic score by multiplying the percentage of bead-positive cells by the geometric MFI and dividing by 10^4.

ADCC

We generated SARS-CoV-2 S-expressing CEM cells by transfection with linearized plasmid (pcDNA3.1) encoding codon-optimized SARS-CoV-2 S that matched wild-type SARS-CoV-2 (GenBank accession no. MN988713). We plated 100,000 wild-type S-CEM cells per well with 100 μL of 1:100 diluted plasma in round bottom 96-well plates and incubated for 30 min at 4°C. We washed cells and added 200,000 Jurkat-Lucia NFAT-CD16 cells (Invivogen, https://www.invivogen.com) to each well in 100 μL of Iscove's Modified Dulbecco Medium (Gibco-Thermo Fisher Scientific, https://www.thermofisher.com) and 10% fetal bovine serum (MilliporeSigma). We then centrifuged cells for 1 min at low speed and cocultured for 24 h at 37°C. Then, we added 50 μL of QUANTI-Luc (Invivogen) to 20 μL of coculture supernatant and immediately measured luminescence on an EnVision 2104 Multilabel Plate Reader (PerkinElmer, https://www.perkinelmer.com).

Statistical Analysis

We used R (R Foundation for Statistical Computing, https://www.r-project.org) to visualize data and perform statistical analyses by using the ggplot2, ComplexHeatmap, and ggpubr packages. We performed Wilcoxon rank-sum tests to compare responses across antigens and participant groups and Wilcoxon signed-rank tests to compare antigen responses between samples collected in 2019 and 2020 from Thailand. We used Spearman ρ to estimate correlations between variables, a false discovery rate to adjust p values for multiple testing, and McNemar test to compare the proportion of reactivity to different antigens.

Results

SARS-CoV-2 S2 IgG Reactivity

We analyzed coronavirus-specific antibody responses by using 2,565 samples collected from 2,250 participants in 5 countries (Appendix Table 2). Among participants, 1,868 (83%) were PLHIV, most of whom received antiretroviral treatment; participants from Africa initiated treatment during chronic infection, and participants from Thailand initiated treatment during acute infection. Most (1,652/2,565; 64%) samples were from participants in Africa: 653 from Kenya, 366 from Nigeria, 234 from Tanzania, and 399 from Uganda. Samples were collected in Africa during August 2013–February 2020; samples from Thailand were collected during August 2019–April 2020. Among 913 samples from Thailand, 598 were from PLHIV, including 315 participants who had 2 samples.

We screened all samples for IgG reactivity against the conserved S2 subunit of SARS-CoV-2 S protein (Figure 1). We selected for further analysis 173 samples that had a signal above the maximum seen with known negative samples: 108 from RV329/AFRICOS, 9 from RV466/JWARG, and 56 from RV254/SEARCH 010. Among samples from Africa, 33 (2% of all samples) had a signal-to-noise ratio (S/N) >6. Among the cohort from Thailand, 11 (1% of all samples) samples from 7 participants had S/N >6. Among 315 participants from Thailand, we detected no evidence of increased SARS-CoV-2 S2 IgG responses between samples collected in 2019 and those collected in 2020 (Appendix Figure 1). Overall, 1.78% of participants showed SARS-CoV-2–like S2 IgG responses before the pandemic, 5.38% when we considered S/N >3 as the cutoff. We noted no major differences across country of origin, sex, HIV-1 status, or year of sample collection; thus, we saw no evidence these samples corresponded to a specific subset of participants.

Responses to Coronavirus Antigens

We tested the 173 selected samples by using a multiplex bead-based immunoassay to measure antibody responses against 23 human coronavirus antigens corresponding to S and N for all 7 human coronaviruses and for S1, S2, and RBD antigens for outbreak coronaviruses. We obtained 312,048 measurement that mapped isotypes, subclasses, and responses for FcγR-IIa, FcγR-IIb, FcγR-IIIa, and FcγR-IIIb (Figure 2). For SARS-CoV-2 antigens, 16 samples had IgG responses for N with S/N >6; for S antigens, 72 samples had S/N >6 for S1, 86 for S2, 21 for RBD, and 11 for S-Trimer (Figure 3, panels A, B). For all 2,250 cohort participants, these findings translate to SARS-CoV-2 reactivity ranging from 0.44% for S-Trimer to 3.69% for S2.

Compared with samples from 12 SARS-CoV-2 convalescent patients, 30 prepandemic samples showed higher SARS-CoV-2 responses for N and 28 were higher for S than the median observed across convalescent patients, but only 1 sample was above the median for RBD (Figure 3, panel A). No prepandemic samples showed RBD, S-Trimer, or N responses above the maximum signal seen for samples from convalescent patients; however, 5 to 9 prepandemic samples had S/N for S, subunit S2, and subunit S1 above the maximum seen in convalescent samples. We noted this pattern of lower recognition for N, RBD, or S-Trimer across all 3

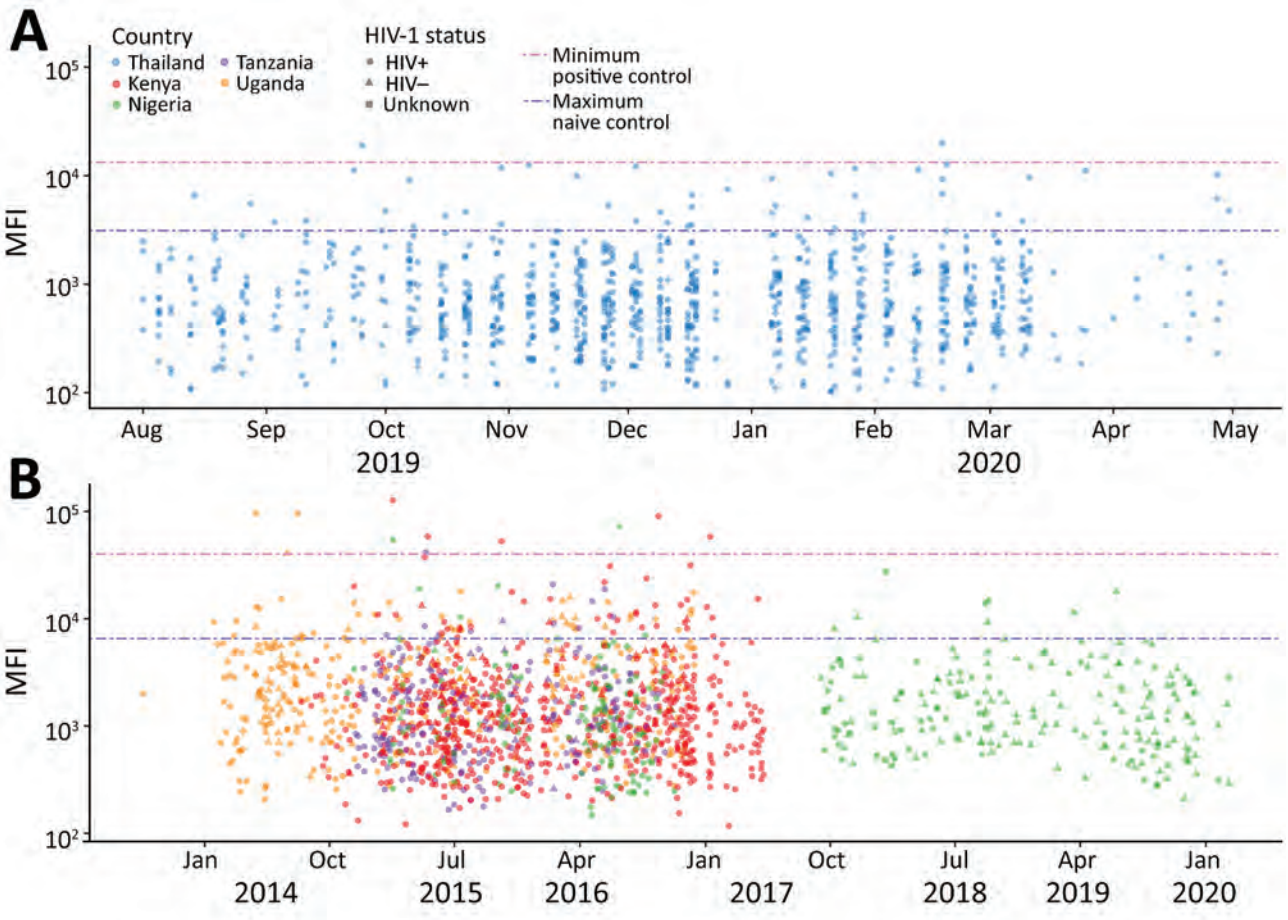

Figure 1. IgG responses to S2 protein among HIV-positive and HIV-negative participants in a study of coronavirus antibody responses before COVID-19 pandemic, Thailand (2019–2020) and Africa (2013–2020). A) Thailand; B) Kenya, Nigeria, Tanzania, and Uganda. We measured MFI for SARS-CoV-2 S2 IgG binding responses in 2,565 serum and plasma samples. Blue dashed line indicates maximum observed signal in 2 negative control samples; pink dashed line indicates minimum observed signal in positive control samples collected from SARS-CoV-2 convalescent patients. Symbols indicate the country of origin, collection date, and HIV-1 status of each participant. Dates indicate sample collection date. MFI, mean fluorescent intensity; S2, subunit 2 protein.

outbreak coronaviruses; significantly fewer samples responded to N, RBD, or S-Trimer than to S, S1, or S2 ($p<0.0001$) (Figure 3, panel B). Using S/N >6, 76 samples showed IgG responses to S of SARS-CoV-2, 41 to S of SARS-CoV-1, and 64 to S of MERS-CoV; however, 16 samples showed IgG responses to N of SARS-CoV-2, 19 to N of SARS-CoV-1, and 11 to N of MERS-CoV. Few (15/76) samples with S responses also responded to RBD. Responses were more frequently detected against SARS-CoV-2 than SARS-CoV-1 (for S, $p<0.0001$) or MERS-CoV (for S and RBD, $p\leq0.025$). Across endemic coronaviruses, S and N of OC43 were recognized most frequently, albeit S was recognized less frequently (Figure 3, panel C). We noted strong positive relationships between IgG responses for SARS-CoV-2 and other coronaviruses. For S, Spearman correlations ranged from 0.58 for SARS-CoV-1 to 0.87 for MERS-CoV; for N, Spearman correlations ranged from 0.43 for 229E to 0.91 for SARS-CoV-1 (Appendix Figure 2). FcγR binding response rates were generally higher than those for Ig rates, but recognition patterns were similar, and far fewer persons' samples recognized N (5–22 samples), RBD (26–53 samples), or S-Trimer (4–14 samples) than S (90–121 samples), S1 (80–97 samples), or S2 (10–123 samples) ($p<0.0001$) (Figure 3, panel B).

Samples from the Thailand cohort were collected during August 2019–April 2020, before documented SARS-CoV-2 infections in the cohort; 18 of 38 participants provided samples at 2 time points. For SARS-CoV-2 S2 IgG screening (Appendix Figure 1), we saw no evidence of increased SARS-CoV-2–specific reactivity in early 2020 compared with 2019 (Appendix Figure 3).

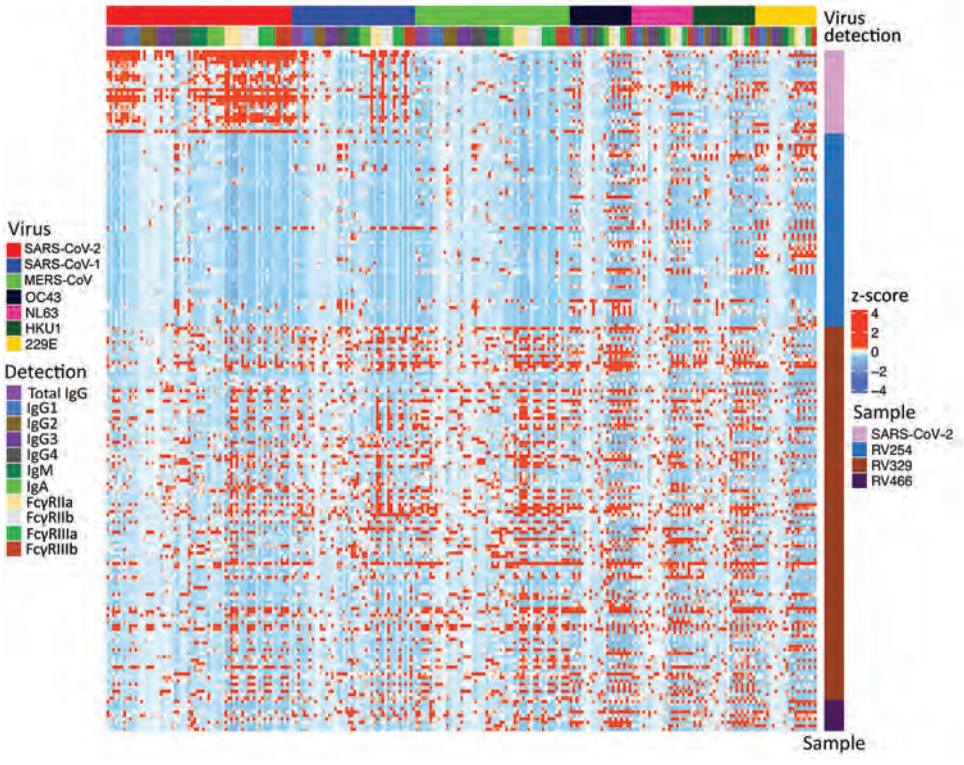

Figure 2. Heat map of coronavirus-specific antibody responses in a study of coronavirus antibody responses before COVID-19 pandemic, Thailand and Africa. We measured antibody responses for in 173 prepandemic serum and plasma samples and 12 samples collected from SARS-CoV-2 convalescent patients. Samples were tested for human coronaviruses SARS-CoV-2, SARS-CoV-1, MERS-CoV, OC43, NL63, HKU1, and 229E. Binding responses are given as z-scores. Each column corresponds to a specific antigen and detection combination. Each row represents a sample; the top 24 rows correspond to positive controls from SARS-CoV-2 convalescent patients. FcγR, Fc gamma receptor (FcγRIIa, FcγRIIb, FcγRIIIa, and FcγRIIIb).

Coronavirus-Specific Responses

We found a strikingly different pattern of reactivity in Kenya, Nigeria, Tanzania, and Uganda than in Thailand. Samples from participants in Africa had much higher SARS-CoV-2–like, SARS-CoV-1–like, and MERS-CoV–like responses (Figures 4–6). Although samples from Africa had more reactivity across all 7 coronaviruses than samples from Thailand, the difference was most striking for outbreak coronaviruses (Figure 4). Participants from Africa also had much higher SARS-CoV-2 IgG responses compared with participants from Thailand across all antigens except for S-Trimer (median S/N for S 7.95 vs. 3.4; $p<0.01$). We saw similar patterns for SARS-CoV-1 (median S/N for S 3.63 vs. 1.0; $p<0.0001$) and MERS-CoV (median S/N for S 7.0 vs. 1.64; $p<0.0001$). For endemic coronaviruses, responses tended to be higher in samples from Africa than in samples from Thailand but the difference was less pronounced: S responses for HKU1 and NL63 were significantly higher in participants from Africa ($p\leq0.0037$) but not for 229E or OC43 ($p\geq0.097$); however, N responses for HKU1 were significantly higher ($p = 0.012$) but not for OC43, NL63, and 229E ($p\geq0.093$) (Figure 5). We saw similar patterns for IgM and IgA responses (Appendix Figure 4). We noted more variability across samples from Africa than across those from Thailand. We tested whether this was because of the larger number of samples pooled from Africa by analyzing data from each country separately (Figure 6), or by downsampling data from each of the 4 countries (Appendix Figure 5). These comparisons showed lower coronavirus-specific responses in samples from Thailand than in samples from countries in Africa (Figure 6; Appendix Figure 5). Comparisons across the 4 countries in Africa showed different distributions, but we noted no consistent country-specific patterns across antigens or detection reagents (Appendix Figure 6).

Correlation between Coronavirus and Other Pathogen Responses

Because most (83%) participants were PLHIV, we compared responses against coronavirus antigens to HIV-1–specific IgG responses in 173 samples (Figure 7, panels A, B). Participants from Thailand showed no IgG reactivity to HIV-1 antigens, reflecting the initiation of antiretroviral therapy in acute infection, typically before seroconversion; 34/38 participants received diagnoses by Fiebig stage III and initiated treatment immediately (Appendix Table 3). In contrast, most participants from Africa showed HIV-1 responses (median S/N 277), consistent with the initiation of antiretroviral therapy during chronic infection. However, higher HIV-1 responses for participants from Africa did not correlate with SARS-CoV-2 reactivity. Although S, S1, or S2 responses were

higher in PLHIV than in persons without HIV-1, we noted little difference for RBD or N responses (Appendix Figure 7, panel A). In addition, we saw no correlation between coronavirus binding responses and HIV-1 markers of disease progression, either CD4+ T-cell counts or HIV-1 viral loads (Appendix Figure 7, panel B).

We also profiled responses against 23 flaviviruses and 1 alphavirus (Figure 7, panel C; Appendix Figure 8). Antibody responses did not show the dichotomous pattern seen between Thailand and Africa for coronavirus responses. Rather, flavivirus responses were seen in a subset of participants. Participant samples from Thailand often recognized most flavivirus antigens, typically with S/N >6. Among participants from Africa, samples from Nigeria and Uganda recognized several flavivirus antigens, but samples from Kenya and Tanzania seldom did. Some responses likely derived from yellow fever vaccination because we saw no comparable nonstructural 1 (NS1) protein responses. Responses might have been cross-reactive to common flavivirus epitopes because we often saw more responses to E than to NS1 antigens. We did not test binding responses to malaria antigens, but

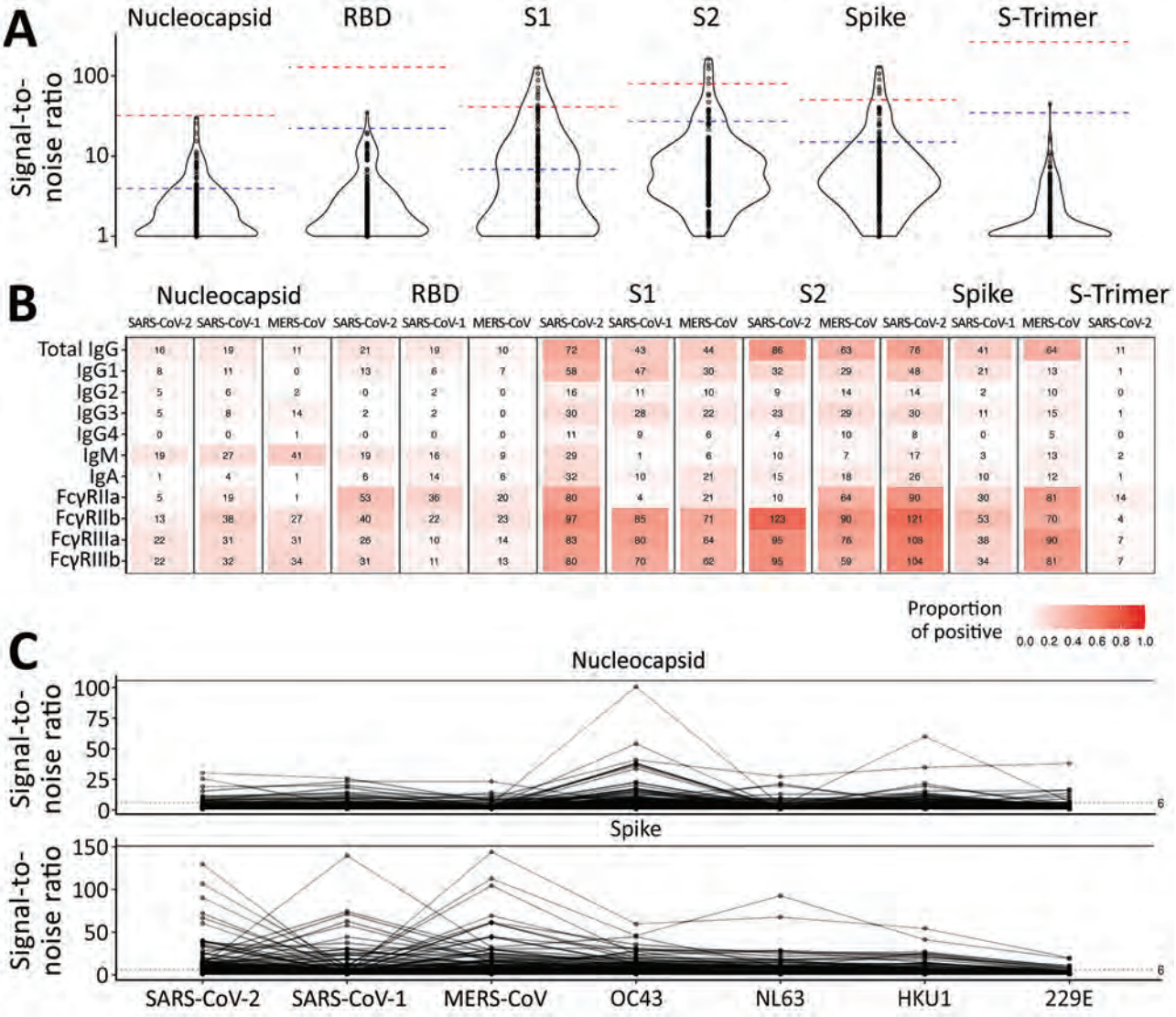

Figure 3. Comparison of antibody responses to human coronaviruses in serum and plasma samples collected before COVID-19 pandemic and from convalescent SARS-CoV-2 patients, Thailand and Africa. A) Violin plot comparing SARS-CoV-2 IgG binding responses against positive control samples. Blue dashed lines indicate median observed signal in positive control samples; pink dashed lines indicate maximum observed signal in positive control samples collected from SARS-CoV-2 convalescent patients. B) Number of coronavirus-positive samples detected by using a signal-to-noise ratio >6 across 3 outbreak coronaviruses and all antigens. C) IgG binding responses in nucleocapsid (top) and spike (bottom) proteins against all 7 human coronaviruses investigated. MERS-CoV, Middle East respiratory syndrome coronavirus; RBD, receptor-binding domain; S1, subunit 1; S2, subunit 2.

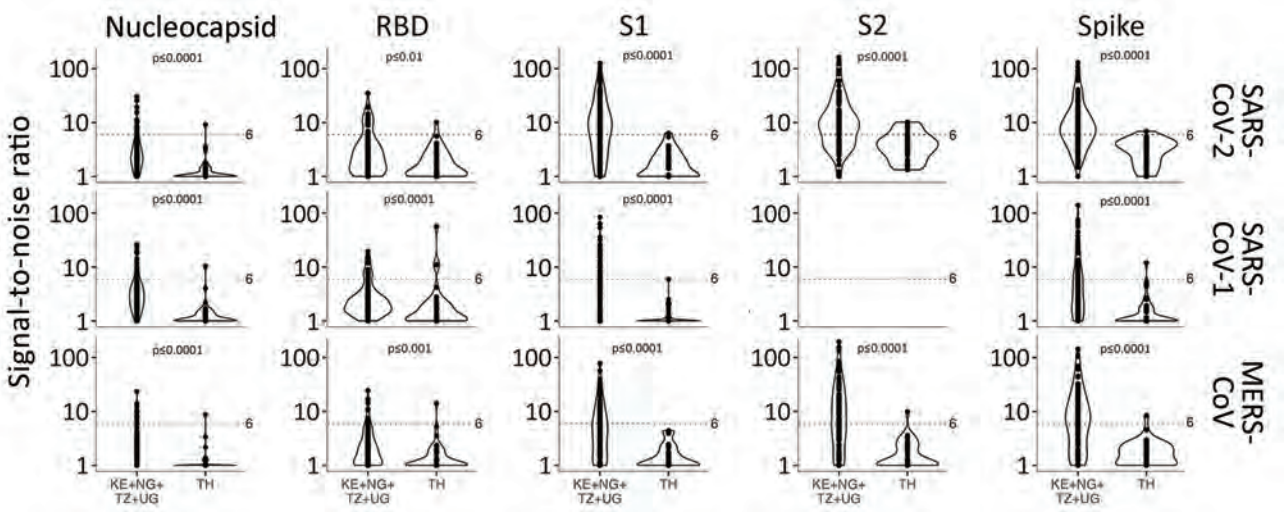

Figure 4. Violin plots of IgG signal-to-noise ratio comparing coronavirus antibody responses before COVID-19 pandemic, Thailand and Africa. We investigated IgG responses across 14 antigens from 3 coronaviruses, SARS-CoV-2, SARS-CoV-1, and Middle East respiratory syndrome coronavirus. Dotted line indicates signal-to-noise ratio cutoff. Significance was determined by Wilcoxon rank-sum test. KE, Kenya; NG, Nigeria; RBD, receptor-binding domain; S1, subunit 1; S2, subunit 2; TH, Thailand; TZ, Tanzania; UG, Uganda.

we had results of malaria smear tests for a subset of participants. Samples from 206 participants from Nigeria showed no difference in SARS-CoV-2 S2 IgG responses when comparing participants who had either a negative or positive malaria smear test (p = 0.15) (Appendix Figure 9). Together, these data demonstrate that higher reactivity among samples from Africa was not uniform across pathogens, emphasizing some genuinely higher coronavirus-like responses.

SARS-CoV-2 Neutralization and Fc Effector Function

We tested for neutralization, ADCP, and ADCC in 60 samples (4 from Thailand, 21 from Kenya, 4 from Nigeria, 5 from Tanzania, and 26 from Uganda) with the highest outbreak coronavirus binding responses of the 173 samples with multiplex binding data. These samples represented the top 18 responders for IgG against N, RBD, and S against SARS-CoV-1 and SARS-CoV-2. Samples from 9 participants neutralized SARS-CoV-2; samples from 13 participants neutralized SARS-CoV-1 (Figure 8, panel A; Appendix Table 4). Most (8/9) samples that neutralized SARS-CoV-2 also neutralized SARS-CoV-1, and vice versa (8/13). Similarly, a subset of 30 participants showed strong ADCP against SARS-CoV-2, 15 against SARS-CoV-1, and 14 against MERS-CoV, and some samples had responses above the positive controls (Figure 8, panel B; Appendix Table 4). Most ADCP-positive samples showed responses against the 3 outbreak coronaviruses. For ADCC against SARS-CoV-2, most (48/60) participants showed responses above S/N >3 (Figure 8, panel C).

We found no strong relationship between binding and functional responses, even among samples with the most functionally relevant RBD responses or those recognizing multiple antigens, including antigens for RBD and N (Appendix Figure 10, panels A–C). We saw no correlation between neutralizing, ADCP, and ADCC responses (Appendix Figure 11). Functional responses were potent in a subset of participants, but these responses corresponded to a small fraction of the cohort: 0.4% for SARS-CoV-2 neutralization, 0.6% for SARS-CoV-1 neutralization, 1.3% for ADCP against SARS-CoV-2, 0.7% for ADCP against SARS-CoV-1, and 2.1% for ADCC against SARS-CoV-2.

Discussion

We profiled antibody responses against 7 coronaviruses in a large multinational cohort of 2,250 persons from Thailand, Kenya, Nigeria, Tanzania, and Uganda, including PLHIV and persons without HIV-1. Among prepandemic samples, >5% had SARS-CoV-2–like responses to S or S2 antigens. We detected SARS-CoV-1 and MERS-CoV responses in a similar proportion of samples. We conducted our serosurvey in 2 steps: first, we screened for SARS-CoV-2 S2 reactivity; then, we selected reactive samples for further testing against 23 coronavirus antigens. We chose S2 because it is the most conserved segment of S across coronaviruses and sequence similarity for S2 between SARS-CoV-2 and the 6 other human coronaviruses ranges from 40% for 229E and NL63 to 91% for SARS-CoV-1; similarity for S1 ranges from 12% for 229E to 75% for SARS-CoV-1.

We observed less frequent responses to S-Trimer, RBD, or N compared with S, S1, or S2 responses, as previously reported (*4*,*7*,*8*,*10*,*19*). The limited S-Trimer, RBD, and N responses likely mark crucial gene functions like neutralization, whereas S or S2 responses could reflect the prevalence of cross-reactive responses, possibly linked to antibody-mediated Fc effector functions. We saw various antigen response combinations across participants, and we rarely saw persons with responses targeting all antigens from a given coronavirus. Furthermore, responses among outbreak coronaviruses correlated strongly and correlated with endemic coronavirus antigens; thus, we could not ascertain which pathogen or pathogens initiated the distinct recognition patterns across participants or whether specific responses are more functionally relevant.

We also characterized the neutralization, ADCP, and ADCC capacity of samples against outbreak coronaviruses. Some samples neutralized SARS-CoV-2, SARS-CoV-1, or both, but we saw no strong association between binding and neutralizing responses. Among 60 participants with the strongest binding responses to outbreak coronaviruses, ≈1/4 showed notable neutralization, ADCP, or ADCC responses. In the overall cohort, this number translates to <1% of participants, indicating that prior responses that could counteract SARS-CoV-2 infection were exceptionally rare in prepandemic samples. Nonetheless, some of these responses were high compared with responses induced after SARS-CoV-2 infection. What these functional responses signify and their clinical implications merit further clarification.

We showed that PLHIV had similar responses as HIV-negative persons, and PLHIV had even higher responses for some antigens. Rather than reflecting a true biologic difference, this finding likely is a statistical consequence of the higher percentage (83%) of PLHIV in the study. As such, we identified no association between coronavirus responses and typical markers of HIV-1 disease progression, such as viral loads and CD4+ T-cell counts. COVID-19 vaccine–induced immunity is less robust in PLHIV, especially for persons with low CD4+ T-cell counts or unsuppressed viremia (*20*–*25*), but our results indicate that this deficit is likely not linked to cross-reactive prepandemic responses.

Our most unexpected finding was that antibody responses against coronaviruses were much higher among participants from Africa than those from Thailand, especially for outbreak coronaviruses. No specific features distinguished participants from Africa and Thailand in our cohorts and we identified few differences across samples from the 4 countries in Africa. Previous studies showed differences across geographic settings, and higher SARS-CoV-2 antibody responses were detected in samples from sub-Saharan Africa than in samples from the United States (*19*). Because our knowledge of wild-type coronaviruses comes predominantly from Asia and SARS-CoV-1 spillover, we hypothesized that responses would be higher in Thailand. Although the mechanistic basis and functional consequences of more frequent responses in participants from Africa needs further study, our report underlines that our knowledge of the interplay between humans and coronavirus animal reservoirs remains vastly unexplored in Africa. Recent studies revealed that

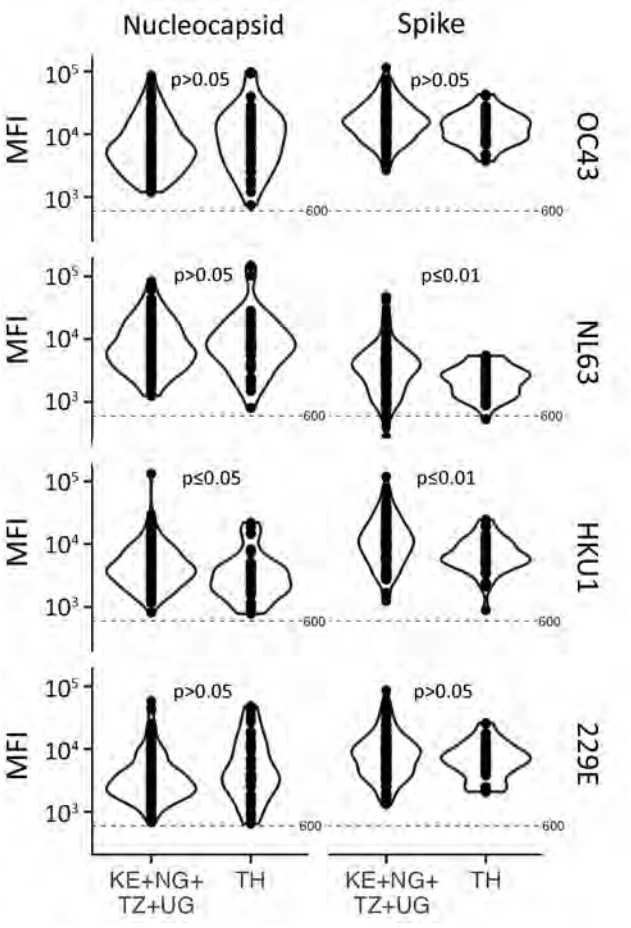

Figure 5. Violin plots of IgG mean fluorescent intensity for nucleocapsid and spike proteins of 4 endemic human coronaviruses in serum and plasma samples collected before the COVID-19 pandemic, Thailand and Africa. Samples comprised 117 participants from Kenya, Nigeria, Tanzania, and Uganda and 38 participants from Thailand. Significance was determined by Wilcoxon rank-sum test. Dotted line indicates MFI cutoff. KE, Kenya; MFI, mean fluorescent intensity; N, nucleocapsid; NG, Nigeria; RBD, receptor-binding domain; S1, subunit 1; S2, subunit 2; TH, Thailand; TZ, Tanzania; UG, Uganda.

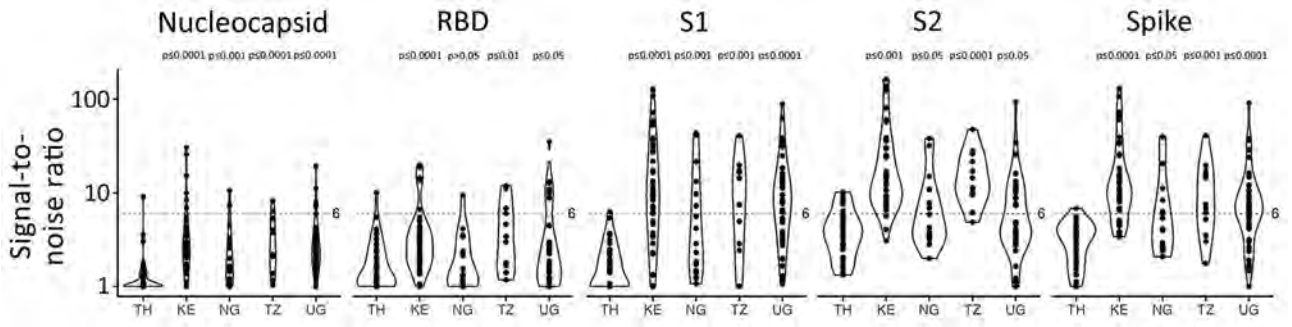

Figure 6. Violin plots of signal-to-noise ratio comparing SARS-CoV-2 IgG responses in serum and plasma samples before COVID-19 pandemic, Thailand and Africa. Dotted line indicates signal-to-noise ratio cutoff. Results show higher SARS-CoV-2 responses in participants from Africa than in participants from Thailand. Significance was determined by Wilcoxon rank-sum test. KE, Kenya; N, nucleocapsid; NG, Nigeria; RBD, receptor-binding domain; S1, subunit 1; S2, subunit 2; TH, Thailand; TZ, Tanzania; UG, Uganda.

angiotensin-converting enzyme 2 (ACE2) use among bat coronavirus strains was not restricted to strains in Asia but was more broadly distributed; bat coronavirus RBD sequences from Bulgaria, Russia, and Kenya also used ACE2 (*26*–*30*). Further testing of animal reservoirs in Africa could elucidate whether additional bat coronavirus strains that readily use ACE2 are circulating.

To verify that high coronavirus responses seen in samples from Africa were specific, we tested 2 other antigen panels. The different reactivity profiles seen for coronavirus, HIV-1, or flavivirus antigens indicated that the SARS-CoV-2, SARS-CoV-1, and MERS-CoV responses observed among samples from Africa were not caused by high overall reactivity levels in the samples irrespective of the antigen and suggested that the responses could be coronavirus-specific. A previous report showed cross-reactivity between SARS-CoV-2 and Zika virus (*31*), but we saw no evidence of cross-reactivity against 8 Zika virus antigens tested, which aligns with another study (*32*). Multiple studies showed associations between SARS-CoV-2 antibody responses and malaria antigens (*11*,*33*–*36*). We did

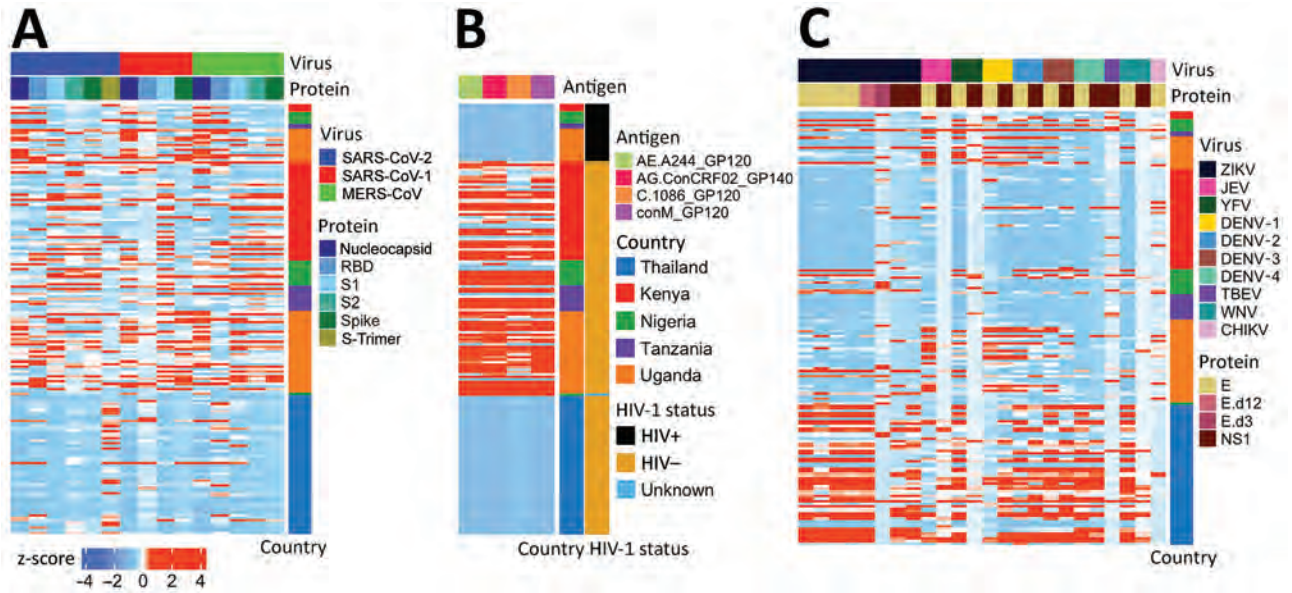

Figure 7. Heatmaps for outbreak coronaviruses, HIV-1, and flavivirus responses compared in a study of coronavirus antibody responses before COVID-19 pandemic, Thailand and Africa. A) IgG binding responses against SARS-CoV-2, SARS-CoV-1, and MERS-CoV. B) IgG binding responses against HIV-1 envelope antigens corresponding to CRF01_AE, CRF02_AG, subtype C, and group M. C) IgG binding responses against flaviviruses. Binding responses are presented as Z scores. Each column corresponds to a specific antigen. Each row represents a sample; the country of origin and HIV-1 status are marked in different colors. CHIKV, chikungunya virus; DENV, dengue virus; E, envelope; JEV, Japanese encephalitis virus; MERS-CoV, Middle East respiratory syndrome coronavirus; N, nucleocapsid; NS1, nonstructural 1; PLWH, persons living with HIV; PWOH, persons without HIV; RBD, receptor-binding domain; S1, subunit 1; S2, subunit 2; TBEV, tickborne encephalitis virus; YFV, yellow fever virus; WNV, West Nile virus; ZIKV, Zika virus.

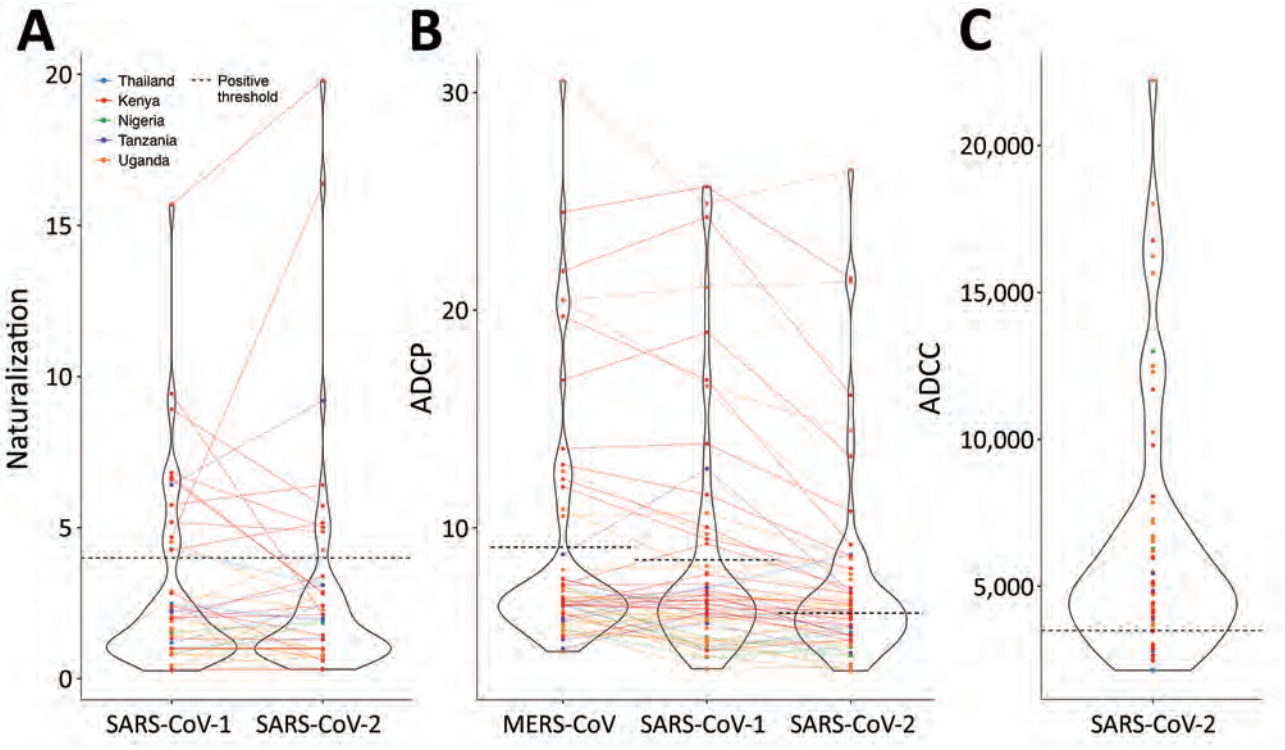

Figure 8. Violin plots of neutralizing, ADCP, and ADCC responses in prepandemic serums and plasma samples used to study coronavirus antibody responses before COVID-19 pandemic, Thailand and Africa. A) Pseudovirus neutralization against SARS-CoV-1 and SARS-CoV-2. The plot shows fold change of the ID_{50} for SARS-CoV-1 or SARS-CoV-2 over the ID_{50} for spike glycoprotein of the vesicular stomatitis virus control pseudoviruses. B) ADCP against MERS-CoV, SARS-CoV-1, and SARS-CoV-2. C) ADCC against SARS-CoV-2. Positive threshold is defined as mean of the negative control samples ±3 SD. Solid lines link each sample between plots. Dotted lines indicate positive thresholds for each assay. Samples are color-coded for the participant's country of origin. ADCC, antibody-dependent cellular cytotoxicity; ADCP, antibody-dependent cellular phagocytosis; ID_{50}, 50% inhibitory dilution; MERS-CoV, Middle East respiratory syndrome coronavirus.

not test binding to malaria antigens but saw no difference in SARS-CoV-2 IgG responses between persons with positive or negative malaria smear tests. We investigated the possibility of SARS-CoV-2 cross-reactivity with flavivirus and HIV-1 antibody responses, but other pathogens could be the cause of the higher responses in participants from Africa than participants from Thailand. Nonetheless, the higher coronavirus-specific reactivity observed in samples from Africa warrants further analysis. Since the beginning of the pandemic, SARS-CoV-2 mortality rates have been lower in Africa than in other parts of the world. The younger population and underreporting of COVID-19 deaths likely contribute to this observation; nonetheless, hypothesizing that some preexisting coronavirus-specific responses affect COVID-19 disease severity is tempting. Further studies evaluating longitudinal samples obtained before and after the SARS-CoV-2 pandemic are needed to compare COVID-19 outcomes as a function of prepandemic cross-reactive coronavirus responses in Africa.

In conclusion, our study illustrates high coronavirus-specific reactivity in samples from Africa compared with samples from Thailand before the SARS-CoV-2 pandemic. Although we identified genuine antibody binding and neutralizing responses, such responses were rare, and their functional significance remains unclear. Findings from large coronavirus serosurveys can have implications for vaccine and monoclonal antibody distribution across global populations. Expanding such serosurveys to include diverse pathogens could help pandemic preparedness.

Acknowledgments

We thank the study participants and staff of the RV254/SEARCH 010, RV329/AFRICOS, and RV466/JWARG studies.

This work was supported by a cooperative agreement (no. WW81XWH-18-2-0040) between the Henry M. Jackson Foundation for the Advancement of Military Medicine,

Inc., and the US Department of Defense. The RV254/SEARCH 010 study was also supported by an intramural grant from the Thai Red Cross AIDS Research Centre and, in part, by the Division of AIDS, National Institute of Allergy and Infectious Diseases, National Institute of Health (grant no. AAI20052001). Antiretroviral therapy for RV254/SEARCH 010 participants was supported by the Thai Government Pharmaceutical Organization, Gilead Sciences, Merck, and ViiV Healthcare. RV329/AFRICOS study was supported by the US President's Emergency Plan for AIDS Relief through DoD. The RV466/JWARG protocol is a multisite study under the Joint West Africa Research Group, which is supported, as a program of record, by the US Defense Health Agency in partnership with the Nigeria Ministry of Defence, Ghana Armed Forces, and the Armed Forces of Liberia. The AFRICOS study would not be possible without support from the hospital leadership at Kayunga District Hospital, Kericho District Hospital, AC Litein Mission Hospital, Kapkatet District Hospital, Tenwek Mission Hospital, Kapsabet District Hospital, Nandi Hills District Hospital, Kisumu West District Hospital, Mbeya Zonal Referral Hospital, Mbeya Regional Referral Hospital, Defence Headquarters Medical Center, and 68 Nigerian Army Reference Hospital.

Some antigens were produced under the direction of James Peacock of Duke Human Vaccine Institute Research Protein Production Facility, which received funding support from the Collaboration for AIDS Vaccine Research Bill and Melinda Gates Foundation (grant no. OPP1066832).

The views expressed are those of the authors and should not be construed to represent the positions of the US Army, Department of Defense, or Department of Health and Human Services. The authors declare no competing interests. The funders of this study had no role in the study design, data collection, data analysis, data interpretation, or writing of the report.

M.R conceived study design; M.M., S.W.-R., B.B., C.C., J.R.C., G.G., and D.P.P. conducted experiments; Y.L., M.M., T.M., S.W.-R., M.R. conducted data analysis; Y.L., H.L., A.E., S.P. performed data curation; N.P., J.M., J.O., H.K., M.I., E.B., S.V., J.A.A., K.M. designed and conducted clinical cohorts; S.V., J.A.A., K.M. acquired funding; M.R. wrote the original draft and all authors reviewed and edited final draft.

About the Author

Ms. Li is a biostatistician in the Viral Genomics Section and Systems Serology Core of the US Military HIV Research Program. Her research interests focus on infectious disease genetics and systems immunology.

References

1. Lawal Y. Africa's low COVID-19 mortality rate: a paradox? Int J Infect Dis. 2021;102:118–22. https://doi.org/10.1016/j.ijid.2020.10.038
2. Gill CJ, Mwananyanda L, MacLeod W, Kwenda G, Pieciak R, Etter L, et al. Sustained high prevalence of COVID-19 deaths from a systematic post-mortem study in Lusaka, Zambia: one year later. medRxiv. 2022. https://doi.org/10.1101/2022.03.08.22272087
3. Shrock E, Fujimura E, Kula T, Timms RT, Lee I-H, Leng Y, et al.; MGH COVID-19 Collection & Processing Team. Viral epitope profiling of COVID-19 patients reveals cross-reactivity and correlates of severity. Science. 2020;370:eabd4250. https://doi.org/10.1126/science.abd4250
4. Nguyen-Contant P, Embong AK, Kanagaiah P, Chaves FA, Yang H, Branche AR, et al. S protein-reactive IgG and memory B cell production after human SARS-CoV-2 infection includes broad reactivity to the S2 subunit. MBio. 2020;11:e01991-20. https://doi.org/10.1128/mBio.01991-20
5. Huey L, Andersen G, Merkel PA, Morrison TE, McCarthy M, DomBourian MG, et al. Evaluation of a multiplexed coronavirus antigen array for detection of SARS-CoV-2 specific IgG in COVID-19 convalescent plasma. J Immunol Methods. 2021;497:113104. https://doi.org/10.1016/j.jim.2021.113104
6. Song G, He WT, Callaghan S, Anzanello F, Huang D, Ricketts J, et al. Cross-reactive serum and memory B-cell responses to spike protein in SARS-CoV-2 and endemic coronavirus infection. Nat Commun. 2021;12:2938. https://doi.org/10.1038/s41467-021-23074-3
7. Anderson EM, Goodwin EC, Verma A, Arevalo CP, Bolton MJ, Weirick ME, et al.; UPenn COVID Processing Unit. Seasonal human coronavirus antibodies are boosted upon SARS-CoV-2 infection but not associated with protection. Cell. 2021;184:1858–1864.e10. https://doi.org/10.1016/j.cell.2021.02.010
8. Galipeau Y, Siragam V, Laroche G, Marion E, Greig M, McGuinty M, et al. Relative ratios of human seasonal coronavirus antibodies predict the efficiency of cross-neutralization of SARS-CoV-2 spike binding to ACE2. EBioMedicine. 2021;74:103700. https://doi.org/10.1016/j.ebiom.2021.103700
9. Abela IA, Pasin C, Schwarzmüller M, Epp S, Sickmann ME, Schanz MM, et al. Multifactorial seroprofiling dissects the contribution of pre-existing human coronaviruses responses to SARS-CoV-2 immunity. Nat Commun. 2021;12:6703. https://doi.org/10.1038/s41467-021-27040-x
10. Tamminen K, Salminen M, Blazevic V. Seroprevalence and SARS-CoV-2 cross-reactivity of endemic coronavirus OC43 and 229E antibodies in Finnish children and adults. Clin Immunol. 2021;229:108782. https://doi.org/10.1016/j.clim.2021.108782
11. Manning J, Zaidi I, Lon C, Rosas LA, Park JK, Ponce A, et al. SARS-CoV-2 cross-reactivity in prepandemic serum from rural malaria-infected persons, Cambodia. Emerg Infect Dis. 2022;28:440–4. https://doi.org/10.3201/eid2802.211725
12. Yu ED, Narowski TM, Wang E, Garrigan E, Mateus J, Frazier A, et al. Immunological memory to common cold coronaviruses assessed longitudinally over a three-year period pre-COVID19 pandemic. Cell Host Microbe. 2022;30:1269–78e.4. https://doi.org/10.1016/j.chom.2022.07.012
13. Kaplonek P, Wang C, Bartsch Y, Fischinger S, Gorman MJ, Bowman K, et al. Early cross-coronavirus reactive signatures of humoral immunity against COVID-19. Sci Immunol. 2021;6:eabj2901. https://doi.org/10.1126/sciimmunol.abj2901

14. US Army. Army regulation AR70-25: use of volunteers as subjects of research. Silver Spring (MD): The Army; 1990 [cited 2022 Mar 23]. https://armypubs.army.mil/ProductMaps/PubForm/Details.aspx
15. Merbah M, Wollen-Roberts S, Shubin Z, Li Y, Bai H, Dussupt V, et al. A high-throughput multiplex assay to characterize flavivirus-specific immunoglobulins. J Immunol Methods. 2020;487:112874. https://doi.org/10.1016/j.jim.2020.112874
16. Styer LM, Hoen R, Rock J, Yauney E, Nemeth K, Bievenue R, et al. High-throughput multiplex SARS-CoV-2 IgG microsphere immunoassay for dried blood spots: a public health strategy for enhanced serosurvey capacity. Microbiol Spectr. 2021;9:e0013421. https://doi.org/10.1128/Spectrum.00134-21
17. King HAD, Joyce MG, Lakhal-Naouar I, Ahmed A, Cincotta CM, Subra C, et al. Efficacy and breadth of adjuvanted SARS-CoV-2 receptor-binding domain nanoparticle vaccine in macaques. Proc Natl Acad Sci U S A. 2021;118:e2106433118. https://doi.org/10.1073/pnas.2106433118
18. Ackerman ME, Moldt B, Wyatt RT, Dugast AS, McAndrew E, Tsoukas S, et al. A robust, high-throughput assay to determine the phagocytic activity of clinical antibody samples. J Immunol Methods. 2011;366:8–19. https://doi.org/10.1016/j.jim.2010.12.016
19. Tso FY, Lidenge SJ, Peña PB, Clegg AA, Ngowi JR, Mwaiselage J, et al. High prevalence of pre-existing serological cross-reactivity against severe acute respiratory syndrome coronavirus-2 (SARS-CoV-2) in sub-Saharan Africa. Int J Infect Dis. 2021;102:577–83. https://doi.org/10.1016/j.ijid.2020.10.104
20. Corey L, Beyrer C, Cohen MS, Michael NL, Bedford T, Rolland M. SARS-CoV-2 variants in patients with immunosuppression. N Engl J Med. 2021;385:562–6. https://doi.org/10.1056/NEJMsb2104756
21. Levy I, Wieder-Finesod A, Litchevsky V, Biber A, Indenbaum V, Olmer L, et al. Immunogenicity and safety of the BNT162b2 mRNA COVID-19 vaccine in people living with HIV-1. Clin Microbiol Infect. 2021;27:1851–5. https://doi.org/10.1016/j.cmi.2021.07.031
22. Ruddy JA, Boyarsky BJ, Werbel WA, Bailey JR, Karaba AH, Garonzik-Wang JM, et al. Safety and antibody response to the first dose of severe acute respiratory syndrome coronavirus 2 messenger RNA vaccine in persons with HIV. AIDS. 2021;35:1872–4. https://doi.org/10.1097/QAD.0000000000002945
23. Feng Y, Zhang Y, He Z, Huang H, Tian X, Wang G, et al. Immunogenicity of an inactivated SARS-CoV-2 vaccine in people living with HIV-1: a non-randomized cohort study. EClinicalMedicine. 2022;43:101226. https://doi.org/10.1016/j.eclinm.2021.101226
24. Netto LC, Ibrahim KY, Picone CM, Alves APPS, Aniceto EV, Santiago MR, et al. Safety and immunogenicity of CoronaVac in people living with HIV: a prospective cohort study. Lancet HIV. 2022;9:e323–31. https://doi.org/10.1016/S2352-3018(22)00033-9
25. Brumme ZL, Mwimanzi F, Lapointe HR, Cheung PK, Sang Y, Duncan MC, et al. Humoral immune responses to COVID-19 vaccination in people living with HIV receiving suppressive antiretroviral therapy. NPJ Vaccines. 2022;7:28. https://doi.org/10.1038/s41541-022-00452-6
26. Wells HL, Letko M, Lasso G, Ssebide B, Nziza J, Byarugaba DK, et al. The evolutionary history of ACE2 usage within the coronavirus subgenus *Sarbecovirus*. Virus Evol. 2021;7:veab007. https://doi.org/10.1093/ve/veab007
27. Tao Y, Tong S. Complete genome sequence of a severe acute respiratory syndrome-related coronavirus from Kenyan bats. Microbiol Resour Announc. 2019;8:e00548-19. https://doi.org/10.1128/MRA.00548-19
28. Alkhovsky S, Lenshin S, Romashin A, Vishnevskaya T, Vyshemirsky O, Bulycheva Y, et al. SARS-like coronaviruses in horseshoe bats (*Rhinolophus* spp.) in Russia, 2020. Viruses. 2022;14:113. https://doi.org/10.3390/v14010113
29. Starr TN, Zepeda SK, Walls AC, Greaney AJ, Alkhovsky S, Veesler D, et al. ACE2 binding is an ancestral and evolvable trait of sarbecoviruses. Nature. 2022;603:913–8. https://doi.org/10.1038/s41586-022-04464-z
30. Seifert SN, Bai S, Fawcett S, Norton EB, Zwezdaryk KJ, Robinson J, et al. An ACE2-dependent Sarbecovirus in Russian bats is resistant to SARS-CoV-2 vaccines. PLoS Pathog. 2022;18:e1010828. https://doi.org/10.1371/journal.ppat.1010828
31. Faccini-Martínez AA, Rivero R, Garay E, García A, Mattar S, Botero Y, et al. Serological cross-reactivity using a SARS-CoV-2 ELISA test in acute Zika virus infection, Colombia. Int J Infect Dis. 2020;101:191–3. https://doi.org/10.1016/j.ijid.2020.09.1451
32. Munoz-Jordan J, Cardona J, Beltrán M, Colón C, Schiffer J, Stewart-Clark E, et al. Evaluation of serologic cross-reactivity between dengue virus and SARS-CoV-2 in patients with acute febrile illness—United States and Puerto Rico, April 2020–March 2021. MMWR Morb Mortal Wkly Rep. 2022;71:375–7. https://doi.org/10.15585/mmwr.mm7110a3
33. Yadouleton A, Sander AL, Moreira-Soto A, Tchibozo C, Hounkanrin G, Badou Y, et al. Limited specificity of serologic tests for SARS-CoV-2 antibody detection, Benin. Emerg Infect Dis. 2021;27:233–7. https://doi.org/10.3201/eid2701.203281
34. Steinhardt LC, Ige F, Iriemenam NC, Greby SM, Hamada Y, Uwandu M, et al. Cross-reactivity of two SARS-CoV-2 serological assays in a setting where malaria is endemic. J Clin Microbiol. 2021;59:e0051421. https://doi.org/10.1128/JCM.00514-21
35. Emmerich P, Murawski C, Ehmen C, von Possel R, Pekarek N, Oestereich L, et al. Limited specificity of commercially available SARS-CoV-2 IgG ELISAs in serum samples of African origin. Trop Med Int Health. 2021;26:621–31. https://doi.org/10.1111/tmi.13569
36. Traoré A, Guindo MA, Konaté D, Traoré B, Diakité SA, Kanté S, et al. Seroreactivity of the severe acute respiratory syndrome coronavirus 2 recombinant S protein, receptor-binding domain, and its receptor-binding motif in COVID-19 patients and their cross-reactivity with pre-COVID-19 samples from malaria-endemic areas. Front Immunol. 2022;13:856033. https://doi.org/10.3389/fimmu.2022.856033

Address for correspondence: Morgane Rolland, Walter Reed Army Institute of Research, 503 Robert Grant Ave, Silver Spring, MD 20910-7500, USA; email: mrolland@hivresearch.org

Fungal Endophthalmitis Outbreak after Cataract Surgery, South Korea, 2020

Soo Jeong Yoon,[1] Soo Hyun Kim,[1] Hyun Jung Bahk, Yeong Seo Ahn, Ji Joo Lee, Hye Jin Kim, Ha Jin Lim, Min Ji Choi, Jong Hee Shin, Yeon-Kyeng Lee

In November 2020, an unusual increase in fungal endophthalmitis cases after cataract surgery was reported to the Korea Disease Control and Prevention Agency, South Korea. We initiated an outbreak investigation to identify the cause. We identified 156 cases nationwide, 62 confirmed and 94 probable. Most case-patients were exposed during surgery to ocular viscoelastic devices (OVDs) from the same manufacturer (company A). We isolated *Fusarium* spp. from 50 confirmed cases. Molecular identification of 39 fungal isolates from clinical samples and 13 isolates from OVDs confirmed *F. oxysporum* caused the infections. The risk ratio for fungal endophthalmitis from company A's OVDs was 86.0 (95% CI 27.4–256.9), much higher than risk from other manufacturers' products. We determined this fungal endophthalmitis outbreak was caused by a contaminated lot of OVDs and recommended discontinued use of this product. Early recognition of outbreaks and joint responses from related government agencies can reduce risk for fungal endophthalmitis.

Although the number of cataract surgery procedures is increasing globally because of an aging population, the incidence of postoperative endophthalmitis is declining because hygiene and surgical environments have improved (*1*,*2*). Postsurgical fungal endophthalmitis is difficult to diagnose because symptoms, such as decreased vision and eye pain, are nonspecific (*3*). Most cases of postoperative endophthalmitis are caused by bacteria, and ≈75% occur within 1 week after surgery (*4*). Because the symptoms of bacterial and fungal endophthalmitis are similar, intraocular fluid culture is crucial for an accurate diagnosis (*5*). Preventing serious complications such as vision loss requires immediate diagnosis, vitrectomy, and long-term antifungal therapy (*6*,*7*).

Postoperative endophthalmitis rarely occurs in South Korea; only ≈63 cases are reported per 100,000 cataract surgeries (*8*). However, the Korean Ophthalmological Society (KOS) recognized a sudden increase in endophthalmitis cases after cataract surgeries during September–November 2020, when ≈100 cases were reported nationwide. Cases included clinical findings of fungal endophthalmitis, including isolation of *Fusarium* species. Thus, in November 2020, KOS informed the Korea Disease Control Agency (KDCA), which promptly collaborated with the Korea Ministry of Food and Drug Safety (KMFDS) to investigate the unusual increase in fungal endophthalmitis, identify the cause, and recommend control measures.

During the epidemiologic investigation, KMFDS collected commercially available samples of ocular viscoelastic devices (OVDs) from 6 manufacturers to conduct quality testing. OVDs are substances injected under the cornea to maintain the shape of the eye during cataract surgery and remain in the eyeball until the last step of surgery, when the OVD is removed. Thus, contaminated OVDs can cause intraocular infection. We describe an outbreak of fungal endophthalmitis after cataract surgery and confirmation of the cause through epidemiologic and microbiologic investigations.

Materials and Methods

Outbreak Determination

To determine whether the cases reported by KOS could be classified as an outbreak, KDCA analyzed data from Health Insurance Review and Assessment

Author affiliations: Korea Disease Control and Prevention Agency, Cheongju, South Korea (S.J. Yoon, H.J. Bahk, Y.S. Ahn, J.J. Lee, H.J. Kim, Y.-K. Lee); Chonnam National University Medical School, Hwasun, South Korea (S.H. Kim, H.J. Lim, M.J. Choi, J.H. Shin)

DOI: https://doi.org/10.3201/eid2811.220361

[1]These first authors contributed equally to this work.

(HIRA) service records from the previous 3 years. Among 1,614,961 cataract surgeries performed during January 2018–September 2020, we estimated 702 (0.04%) cases of endophthalmitis, among which only 25 (0.002%) cases were presumed to be fungal infections. Thus, KDCA judged infections that occurred after September 2020 comprised an outbreak and suspected the cause was a contaminated batch of OVDs used in case-occurrence ophthalmology hospitals nationwide.

Endophthalmitis Case Investigation

KDCA documented reported endophthalmitis cases after cataract surgeries during September 1, 2020–January 11, 2021, in 101 referral centers nationwide. During that time, 182 cases were reported from certified tertiary hospitals, general hospitals (including ophthalmology departments), and specialized ophthalmology hospitals and in 45 referral centers. KDCA developed 2 epidemiologic investigation forms: 1 for hospitals that performed cataract surgery and 1 for referral centers that treated endophthalmitis. Ophthalmologists from hospitals and referral centers completed the epidemiologic investigation forms. Data collected from 69 hospitals where cataract surgeries were performed comprised patients' demographic information, date of cataract surgery, date of endophthalmitis diagnosis, and the OVD brand and batch used in each surgery. Data collected from 45 referral centers comprised patient sample culture results and endophthalmitis treatment methods. In addition, the KDCA epidemiologic investigation team collected and reviewed medical records for all 182 cases from 45 referral centers.

Case Definition

For this outbreak, we defined a case as endophthalmitis in a patient who had cataract surgery during between September 1–November 30, 2020; had >1 of hypopyon, vitreous opacity, artificial lens infiltration, or retinal infiltration; had been transferred to an advanced ophthalmological hospital (retinal surgery hospital) nationwide; and had received antifungal drugs and surgical treatment under the advice of KOS. We defined a confirmed case as endophthalmitis in a patient in a referral center who had ≥1 positive fungal culture test results from surgical specimens, anterior chamber fluid, lens, or vitreous body. We defined a probable case as endophthalmitis in a patient who had negative fungal culture but who received antifungal treatment after a diagnosis of fungal endophthalmitis. We excluded patients whose samples tested positive for bacteria and those who had negative cultures and did not receive antifungal drugs. In all, the study encompassed 156 case-patients, 62 with confirmed cases and 94 with probable cases, from 43 referral centers nationwide (Figure 1).

OVD Data Collection

We investigated the brands of OVD and other materials used in the 69 hospitals that performed cataract surgeries for the 156 identified case-patients. We used the 2020 HIRA Drug Supplier data records to identify the quantity of 6 brandstypes of OVDs supplied and when OVDs were sold to the hospitals.

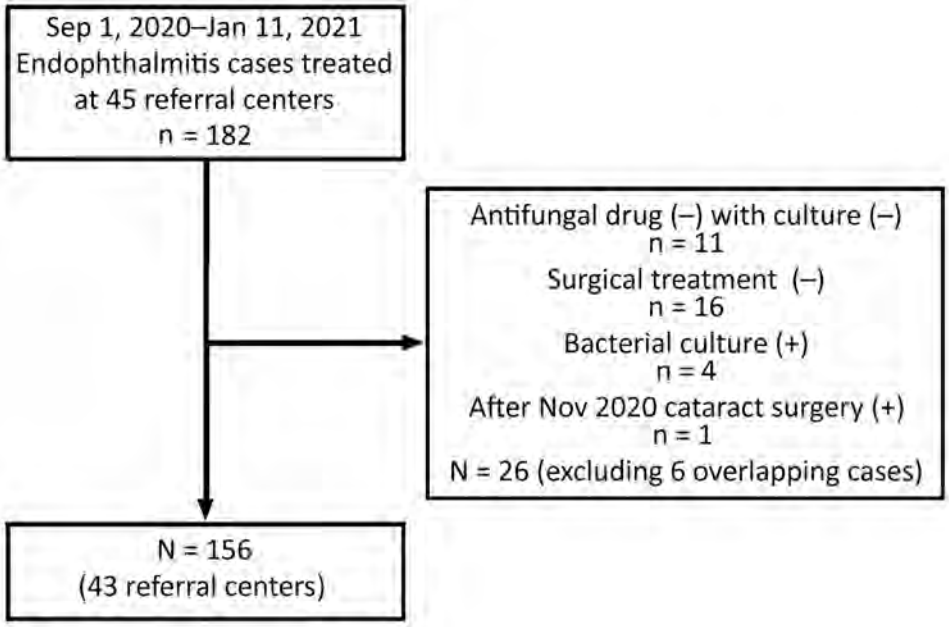

Figure 1. Flowchart for case-patient selection during fungal endophthalmitis outbreaks after cataract surgery, South Korea, 2020. Surgeries took place at 69 cataract surgery hospitals during September 1–November 30, 2020, and cases of *Fusarium oxysporum* endophthalmitis were identified during September 1, 2020–January 11, 2021.

Laboratory Testing

KDCA designated a pathogen laboratory to conduct species identification and genotyping tests, including sequencing, to confirm whether isolates obtained from OVDs and patient samples were identical strains. KDCA sent 39 *Fusarium* spp. isolates collected from patients at 16 hospitals and 13 fungal isolates from OVDs that were collected by KMFDS and 2 university hospitals for sequencing. All 52 isolates were submitted for matrix-assisted laser desorption/ionization time-of-flight mass spectrometry analysis on VITEK MS (bioMérieux, https://www.biomerieux.com) or ASTA MicroIDSys (ASTA Inc, https://www.astams.co.kr). Sequencing identified the internal transcribed spacer and D1/D2 domain of 26S ribosomal DNA and *Fusarium*-specific translation elongation factor 1-alpha (*TEF1α*) gene. Sequencing analysis was performed by Macrogen (https://www.macrogen.com), and we used the BLAST (https://blast.ncbi.nlm.nih.gov/Blast.cgi) database to identify species.

We chose 12 clinical isolates for multilocus sequencing typing (MLST) analysis to confirm the genotype by using *TEF1α*, *RPB1*, and *RPB2* as target genes (*9*,*10*). We selected these isolates because they were collected from patients whose surgeries occurred during September–November 2020 in 6 certified tertiary hospitals evenly distributed throughout the nation. We also used isolates from OVDs collected by KMFDS and a university hospital. We analyzed genotypes of control strains for comparison with the outbreak strain. The control strains included 2 clinical isolates (1 from an eye specimen and the other from sputum) obtained before the outbreak period and 1 environmental isolate from the Korean Collection for Type Cultures (KCTC; https://kctc.kribb.re.kr), KCTC strain no. KCTC16654. We performed phylogenetic analysis by maximum-likelihood method using Kimura 2-parameter model and bootstrap analysis of 1,000 replications in MEGA version 11.0.11 (*11*). To elucidate the clustering of outbreak strains, we collected further outgroup data from GenBank.

Table 1. Characteristics of patients with fungal endophthalmitis after cataract surgery, South Korea, 2020

Characteristics	No. (%), n = 156	Mean (±SD)
Sex		
M	59 (37.8)	
F	97 (62.2)	
Age range, y		66.3 (10.9)
≤59	44 (28.2)	
60–69	55 (35.2)	
70–79	41 (26.3)	
≥80	16 (10.3)	
Underlying conditions*		
None	70 (44.9)	
≥1	86 (55.1)	
Involved eye		
Left	65 (41.7)	
Right	91 (58.3)	
Date of symptom onset		
October 2020	35 (22.4)	
November 2020	92 (59.0)	
December 2020	27 (17.3)	
January 1–11, 2021	2 (1.3)	
Latent period, d†		24.3 (14.8)
0–14	42 (26.9)	
15–28	60 (38.5)	
29–42	38 (24.4)	
43–56	11 (7.1)	
57–70	4 (2.6)	
70–84	1 (0.6)	

*Includes hypertension, diabetes mellitus, heart disease, cerebrovascular disease, hyperlipidemia, and other conditions.
†Time from surgery to clinical manifestations.

Data Analysis

We found that the monthly number of cataract surgeries performed in hospitals and the HIRA records for the monthly supply of OVDs were almost identical. Thus, we used the number of OVDs supplied to estimate the total number of cataract surgeries. We calculated the risk ratio and 95% CI by comparing the number of surgeries involving contaminated OVDs from 1 manufacturer, company A, and the occurrence of endophthalmitis with surgeries involving the other 5 OVD brands. We used EpiInfo (Centers for Diseases Control and Prevention, https://www.cdc.gov/epiinfo) for the statistical analysis.

Results

Epidemiologic Investigations

The mean age of the 156 case-patients was 66 years; 55 (35.3%) patients were in their 60s. Most (55%) patients had ≥1 underlying condition, including diabetes and high blood pressure. The left eye was affected in 65 (42%) cases; the right eye was affected in the remaining 91 cases (58%). More women (62%) than men were affected. The mean time from cataract surgery to the onset of symptoms was 24.3 days (range 1–84 days) (Table 1).

A batch of fungal-contaminated OVDs was supplied to medical institutions nationwide by 1 manufacturer, company A, in September 2020. Ophthalmology departments stopped using this product after KOS recognized the outbreak and contacted KDCA in November 2020. Correspondingly, the number of cases of fungal endophthalmitis occurring within 3 months of cataract surgery increased after September and then decreased again after November; 35 cases were reported in October, 92 in November, 27 in December, and 2 in January, the last on January 11, 2021 (Figure 2).

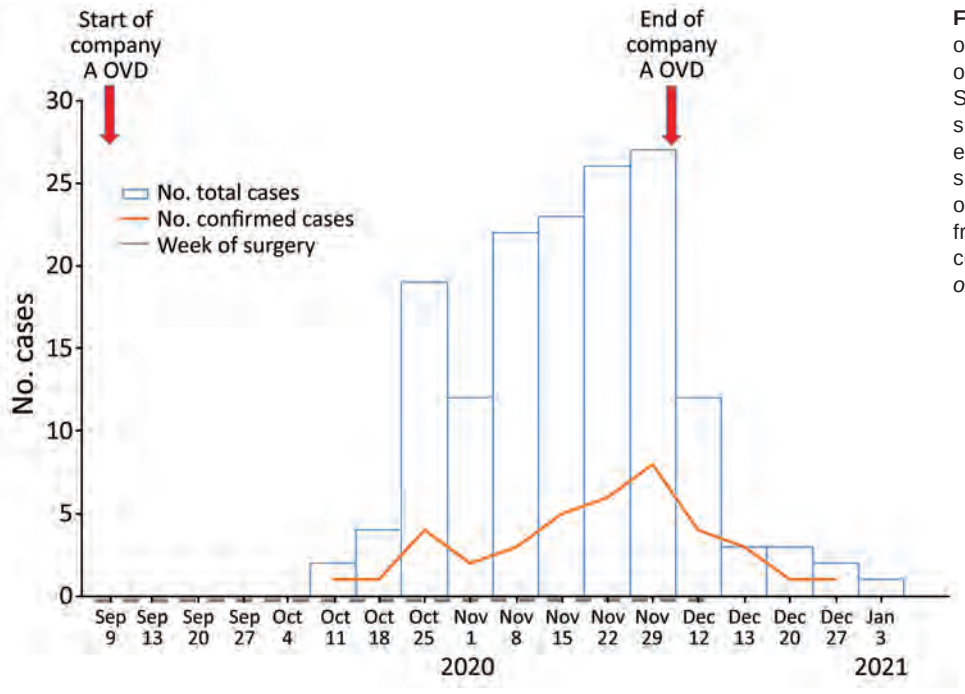

Figure 2. Epidemic curve of fungal endophthalmitis outbreaks after cataract surgery, South Korea, 2020. The curve shows 156 cases of fungal endophthalmitis after cataract surgery. Cases were linked to ophthalmic viscoelastic devices from company A (A-OVD) contaminated with *Fusarium oxysporum*.

Fungal endophthalmitis was reported from 14 cities and provinces nationwide; no cases were reported for Sejong, Ulsan, or Jeju (Figure 3). In 152 (98%) cases, OVDs from company A were used in cataract surgery. Cases were reported from 65 of the 69 medical institutions in the study, which comprised 60 clinics, 8 specialized ophthalmology hospitals, and 1 general hospital (Table 2).

Microbiologic Results

We isolated *Fusarium* species from 50 (33%) patient samples, and identified other fungal species in 12 cases, including *Aspergillus* in 6 cases, *Acremonium* in 4 cases, *Exophiala* in 1 case, and an undetermined type in 1 case. In addition, 93 cases had negative cultures and 1 case had an unclear microbial test result (Table 2).

KMFDS determined 2 strains of fungus contaminated a batch of OVDs from company A. We collected 39 *Fusarium* isolates from case-patients and all isolates were confirmed as *F. oxysporum* by visual and microscopic fungal identification tests and matrix-assisted laser desorption/ionization time-of-flight mass spectrometry in the pathogen laboratory.

Sequencing typing of *TEF1a*, a *Fusarium*-specific target gene, confirmed that the *TEF1a* sequence of the *F. oxysporum* strain registered in the database matched 100% with the submitted query of 630 bp (Figure 4, panel A). MLST revealed that 12 *F. oxysporum* isolates from patients and 2 isolates from the contaminated OVDs were same type, which we classified as clade A. Of 3 control strains, 2 strains (1 clinical strain from an eye specimen obtained before the outbreak period and environmental strain no. KCTC16654 from KCTC) disclosed different MLST types, but the clinical strain from sputum showed the same clade A type (Figure 4, panel B).

We conducted an onsite epidemiologic investigation on December 21, 2020, at an ophthalmologic clinic where cases of postsurgery endophthalmitis had occurred in October 2020. We collected 13 types of environmental samples from materials and devices used for surgeries, from water tap, and from a refrigerator in the operating room. We cultured the environmental samples and found no discernable microbes, including fungi.

Risk Assessment

We used ophthalmic surgery supply records from HIRA for the 6 brands of OVDs to estimate the number of cataract surgeries that occurred during September–November 2020. We assumed that most OVDs were used for cataract surgery and that 1 OVD was used per surgery. Then, using patients' medical records and case-study reports, we determined 62 confirmed cases and 94 probable cases of fungal endophthalmitis after cataract surgery occurred during the study period. We excluded 1 case from our statistical analysis because it had insufficient information regarding the OVD supplied. We calculated the rate of

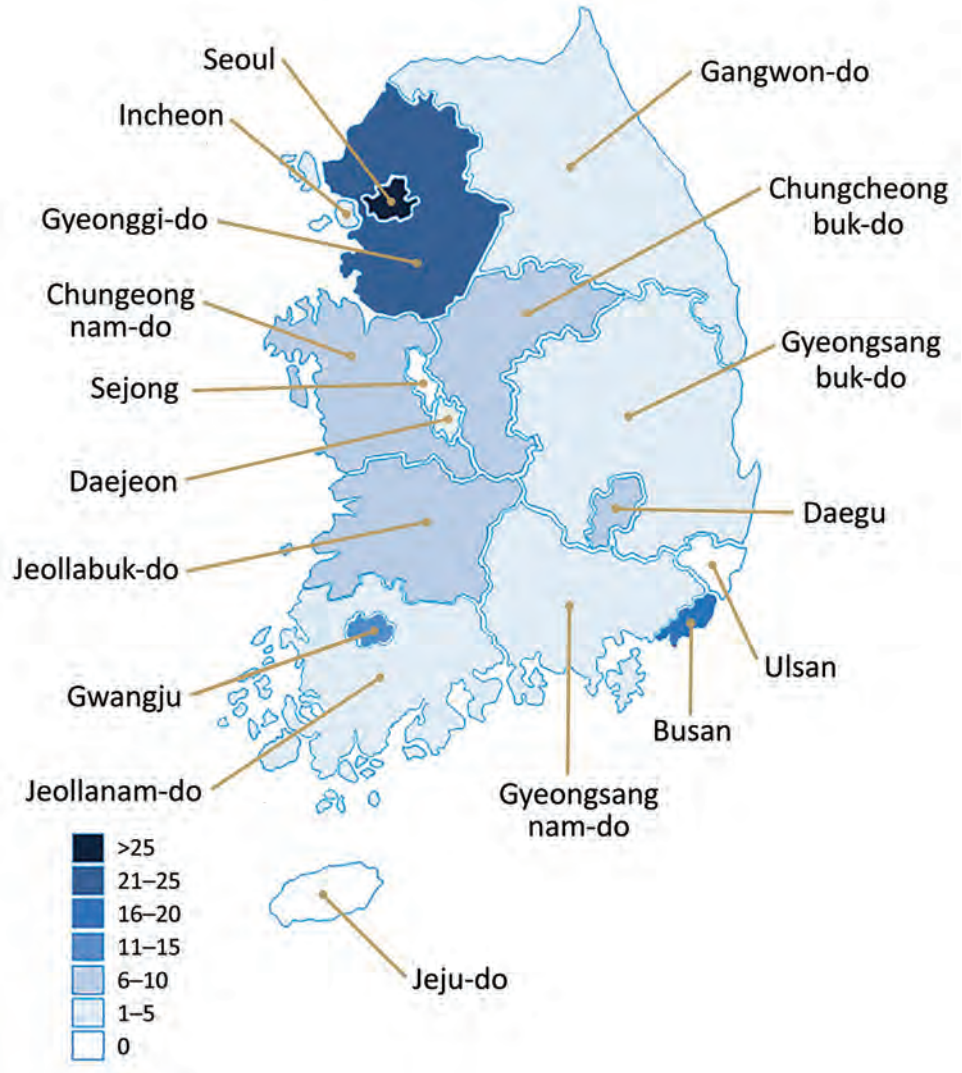

Figure 3. Geographic distribution of cases in fungal endophthalmitis outbreak after cataract surgery, South Korea, 2020. Surgeries took place during September 1–November 30, 2020, and cases of *Fusarium oxysporum* endophthalmitis were identified during September 1, 2020–January 11, 2021.

infection for company A OVDs compared with the 5 other OVD brands. We found the incidence risk for infection for manufacturer A OVDs was 0.3% and risk for infection from the other 5 OVDs was 0.004%, indicating an 86-fold higher risk for fungal endophthalmitis when manufacturer A OVDs were used compared with the other brands (Table 3).

Public Health and Regulatory Actions

On November 23, 2020, as the epidemiologic investigation began, KDCA recommended that KOS immediately issue a warning to its surgeons to stop using the suspected devices. Once fungal contamination was confirmed in a batch of OVDs from company A, KMFDS implemented

Table 2. Ophthalmic viscoelastic device brands and microbiological spectrum of 156 cases of fungal endophthalmitis after cataract surgery, South Korea, 2020*

Brand of OVD	No. (%) cases	*Fusarium* spp.	Other fungus†	Culture-negative	Unknown
A	152 (97.4)	50	11	90	1
B	2 (1.4)	NA	1	1	NA
C	1 (0.6)	NA	NA	1	NA
D	1 (0.6)	NA	NA	1	NA
E	0	NA	NA	NA	NA
F	0	NA	NA	NA	NA
Total	156 (100)	50	12	93	1

*OVD, ophthalmic viscoelastic device; NA, not applicable.
†Includes *Aspergillus* (n = 6), *Acremonium* (n = 4), and *Exophiala spp.* (n = 1), and undetermined type (n = 1).

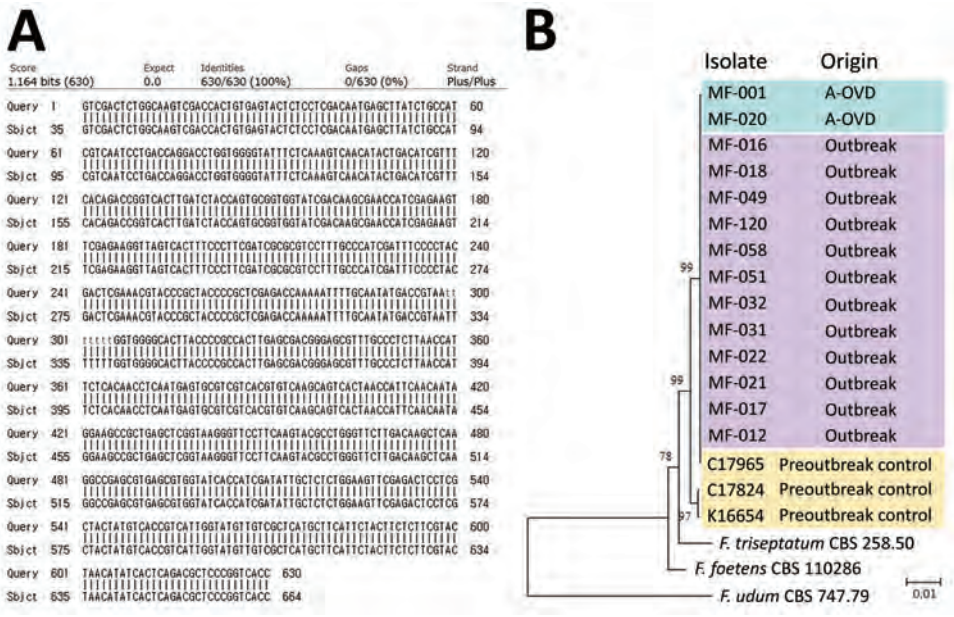

Figure 4. Sequence of outbreak strain matched to *Fusarium oxysporum* strain in a study of fungal endophthalmitis outbreaks after cataract surgery, South Korea, 2020. A) We matched 2020ASF-167 translation elongation factor 1-α (*TEF1α*) gene of the outbreak strain with a control strain (GenBank accession no. MN646762.1) B) Phylogenetic tree of the concatenated sequences from 3 genes (*TEF1α*, *RPB1*, and *RPB2*). Phylogenetic data include outbreak strain from 2 A-OVDs, 12 clinical isolates, 3 preoutbreak controls, and 3 outgroup sequences collected from GenBank database. Scale bar indicates the number of nucleotide substitutions per site. A-OVD, ocular viscoelastic devices from company A.

measures to stop production and recall the product on December 11, 2020.

Discussion

In this investigation of an outbreak of endophthalmitis after cataract surgeries, we identified OVDs as a common substance used in nearly all the surgical procedures that led to endophthalmitis and confirmed fungal contamination in a batch of product from 1 manufacturer. Using genetic sequencing, we identified *F. oxysporum* as the causative fungus in patient samples and isolates from contaminated OVDs.

In 2005, a total of 20 cases of postoperative fungal endophthalmitis infection caused by contaminated OVDs were reported in the Czech Republic (*12*). Similarly, 47 cases of infection caused by intraocular dye and contaminated medication from the same manufacturer were reported in the United States (*13*). In addition, retrospective studies analyzing the causes, treatments, and prognoses on the basis of hospital medical records over several years and a report on treatment results in 7 individual cases have been published (*5*,*14*,*15*). In 2 previous outbreaks involving contaminated medical products in the United States, epidemiologic investigations of the reported medical institutions identified intraocular dye used in retinal surgery that was contaminated with *F. incarmatum-equiseti* (*13*) and prefilled saline flush syringes contaminated with *Burkholderia cepacia* complex because of an inappropriate sterilization process (*16*). In both outbreaks, subsequent investigations expanded nationwide and documented additional cases (*13*,*16*). In this outbreak, we investigated postoperative infections reported across South Korea and used data to trace cases to specific cataract surgery hospitals because no information was available on the specific medical institutions where the cases occurred and South Korea does not have a reporting system for case data, as the United States does.

Most (70%–95%) post–cataract surgery endophthalmitis cases involve gram-positive bacteria (*17*); fungal causes are quite rare, accounting for <5%. Causative fungi are usually *Aspergillus*, *Candida*, *Acremonium*, and *Fusarium* spp. (*5*,*7*). *F. oxysporum*, the causative agent in the outbreak we report, occurs in plants and soil and secretes mycotoxins that can cause local and systemic infections in humans (*12*). Microbiologic testing identified *Fusarium* spp. in ≈30% of 156 patient samples obtained. Because of drugs administered during treatment

Table 3. Relative risk for fungal endophthalmitis after cataract surgery using ophthalmic viscoelastic device from company A, South Korea, 2020*

Brand of OVD	No. cases†	No. surgeries	Incidence risk per 100,000 population	Risk ratio (95% CI)
Company A OVD	152	49,193	309.0	86.0 (27.4–269.7)
Other OVDs, referent	3	83,554	3.6	

*OVD, ophthalmic viscoelastic device.
†Among 156 total cases; excludes 1 case that used an OVD without sufficient database information.

and technical problems during testing, microbiologic testing identifies the causative agent in only 30%–50% of endophthalmitis cases (*12*,*18*). Therefore, we did not rule out *Fusarium* spp. infection in patients whose samples tested positive for other fungi or tested negative altogether.

This outbreak occurred at various clinics, specialized ophthalmology hospitals, and general hospitals across the country over a short period; thus, we inferred that the possibility of infection from the environment was small. The incubation period for bacterial endophthalmitis is relatively short, just 7 days (*17*). For cases in our outbreak, patient symptoms were delayed until ≈24 days after surgery, which is a clinical manifestation of fungal endophthalmitis (*5*); moreover, fungi were cultured in samples obtained from the eye fluid of some patients. Therefore, we hypothesized that the most likely cause of the outbreak was contamination of the eyeball during surgery with a fungus emanating from a common source. After the batch of contaminated OVDs from company A were supplied for to institutions for use, the number of reported fungal endophthalmitis infections rapidly increased, but after the cause of the outbreak was eliminated, infections decreased. Because the data collection period was prolonged, we examined the suspected causative agent by confirming that the same fungus was in the suspect OVDs and patient samples before we conducted the final data analysis. The purpose of the epidemiologic investigation was to identify the causative agent for the outbreak; therefore, we did not conduct a case–control study to determine any other potential causes. We did not have epidemiologic bias when calculating the risk ratio because we equally applied the conditions, estimated number of cataract surgeries, and parameters for case inclusion to contaminated OVDs and other OVDs.

The first limitation of this study is that we excluded patients who were not sent to a higher-level hospital and had not undergone surgical treatment; thus, we might not have identified the actual number of infected persons. Second, we did not investigate possible causes of fungal endophthalmitis other than the OVDs. Third, we did not investigate other patients whose surgery involved the contaminated product but who did not seek care for fungal infection. However, this study reports a large-scale fungal endophthalmitis outbreak related to the use of OVDs. In this case, fungal-contaminated devices were supplied nationwide beginning in September 2020 and used for surgical procedures in many facilities. The outbreak was recognized at the end of November 2020, by which time >100 cases had occurred. We surmise delayed outbreak recognition was mainly due to the ambiguous symptoms and slow progression of fungal endophthalmitis, in addition to difficulties in performing fungal culture. A further follow-up study of infected patients is needed to determine their prognosis and to investigate possible factors other than contaminated OVDs that could cause fungal endophthalmitis. Such a study also could collect samples from cataract surgery patients for whom similarly contaminated OVDs were used but who did not develop infection.

In summary, we identified *F. oxysporum* as the cause of an outbreak of fungal endophthalmitis after cataract surgery in South Korea and confirmed the association between the causative agent and the outbreak through an epidemiologic investigation. We concluded that a batch of OVDs, devices commonly used at ophthalmic hospitals nationwide, was contaminated with *F. oxysporum*, causing post–cataract surgery fungal endophthalmitis throughout the country. We identified the same *F. oxysporum* strain in contaminated OVDs and in patient samples, and most cases occurred among patients whose OVDs came from 1 manufacturer. The data we provide can help estimate infection factors, provide early recognition of simultaneous outbreaks, and aid rapid quarantine of suspected causative agents in similar cases in the future.

About the Authors

Dr. Yoon is a medical doctor and public health officer at the Korea Disease Control and Prevention Agency, Chengju, South Korea. Her main interest is epidemiologic investigation of infectious diseases. Dr. Kim is a professor at Chonnam National University Hwasun Hospital, Hwasun, South Korea. His main research interest is healthcare-associated infection, including fungal infections.

References

1. Keay L, Gower EW, Cassard SD, Tielsch JM, Schein OD. Postcataract surgery endophthalmitis in the United States: analysis of the complete 2003 to 2004 Medicare database of cataract surgeries. Ophthalmology. 2012;119:914–22. https://doi.org/10.1016/j.ophtha.2011.11.023
2. Nowak MS, Grzybowski A, Michalska-Małecka K, Szaflik JP, Kozioł M, Niemczyk W, et al. Incidence and characteristics of endophthalmitis after cataract surgery in Poland, during 2010–2015. Int J Environ Res Public Health. 2019;16:2188. https://doi.org/10.3390/ijerph16122188
3. Rahmani S, Eliott D. Postoperative endophthalmitis: a review of risk factors, prophylaxis, incidence, microbiology, treatment, and outcomes. Semin Ophthalmol. 2018;33:95–101. https://doi.org/10.1080/08820538.2017.1353826

4. Endophthalmitis Vitrectomy Study Group. Results of the Endophthalmitis Vitrectomy Study. A randomized trial of immediate vitrectomy and of intravenous antibiotics for the treatment of postoperative bacterial endophthalmitis. Arch Ophthalmol. 1995;113:1479–96. https://doi.org/10.1001/archopht.1995.01100120009001
5. Narang S, Gupta A, Gupta V, Dogra MR, Ram J, Pandav SS, et al. Fungal endophthalmitis following cataract surgery: clinical presentation, microbiological spectrum, and outcome. Am J Ophthalmol. 2001;132:609–17. https://doi.org/10.1016/S0002-9394(01)01180-1
6. Chen YH, Chen JT, Tai MC, Chou YC, Chen CL. Acute postcataract endophthalmitis at a referral center in northern Taiwan: causative organisms, clinical features, and visual acuity outcomes after treatment: a retrospective cohort study. Medicine (Baltimore). 2017;96:e8941. https://doi.org/10.1097/MD.0000000000008941
7. Jeong SH, Cho HJ, Kim HS, Han JI, Lee DW, Kim CG, et al. Acute endophthalmitis after cataract surgery: 164 consecutive cases treated at a referral center in South Korea. Eye (Lond). 2017;31:1456–62. https://doi.org/10.1038/eye.2017.85
8. Kim SH, Yu MH, Lee JH, Kim SW, Rah SH. Endophthalmitis after cataract surgery in Korea: a nationwide study evaluating incidence and risk factors in a Korean population. Yonsei Med J. 2019;60:467–73. https://doi.org/10.3349/ymj.2019.60.5.467
9. Moretti ML, Busso-Lopes AF, Tararam CA, Moraes R, Muraosa Y, Mikami Y, et al. Airborne transmission of invasive fusariosis in patients with hematologic malignancies. PLoS One. 2018;13:e0196426. https://doi.org/10.1371/journal.pone.0196426
10. O'Donnell K, Gueidan C, Sink S, Johnston PR, Crous PW, Glenn A, et al. A two-locus DNA sequence database for typing plant and human pathogens within the *Fusarium oxysporum* species complex. Fungal Genet Biol. 2009;46:936–48. https://doi.org/10.1016/j.fgb.2009.08.006
11. Kumar S, Tamura K, Nei M. MEGA: Molecular Evolutionary Genetics Analysis software for microcomputers. Comput Appl Biosci. 1994;10:189–91. https://doi.org/10.1093/bioinformatics/10.2.189
12. Buchta V, Feuermannová A, Váša M, Bašková L, Kutová R, Kubátová A, et al. Outbreak of fungal endophthalmitis due to *Fusarium oxysporum* following cataract surgery. Mycopathologia. 2014;177:115–21. https://doi.org/10.1007/s11046-013-9721-5
13. Mikosz CA, Smith RM, Kim M, Tyson C, Lee EH, Adams E, et al.; Fungal Endophthalmitis Outbreak Response Team. Fungal endophthalmitis associated with compounded products. Emerg Infect Dis. 2014;20:248–56. https://doi.org/10.3201/eid2002.131257
14. Alagöz N. Ten years after an outbreak of *Fusarium* endophthalmitis following cataract surgery. Arq Bras Oftalmol. 2020;83:454–6.
15. Yang YS. Results of extensive surgical treatment of seven consecutive cases of postoperative fungal endophthalmitis. Korean J Ophthalmol. 2009;23:159–63. https://doi.org/10.3341/kjo.2009.23.3.159
16. Brooks RB, Mitchell PK, Miller JR, Vasquez AM, Havlicek J, Lee H, et al.; Burkholderia cepacia Workgroup. Multistate outbreak of *Burkholderia cepacia* complex bloodstream infections after exposure to contaminated saline flush syringes: United States, 2016–2017. Clin Infect Dis. 2019;69:445–9. https://doi.org/10.1093/cid/ciy910
17. Durand ML. Bacterial and fungal endophthalmitis. Clin Microbiol Rev. 2017;30:597–613. https://doi.org/10.1128/CMR.00113-16
18. Choi SC, Cho HJ, Kim HS, Han JI, Lee DW, Cho SW, et al. Analysis of referred 113 patients with endophthalmitis after cataract surgery and associated prognostic factors. J Korean Ophthalmol Soc. 2016;57:420–8. https://doi.org/10.3341/jkos.2016.57.3.420

Address for correspondence: Yeon-Kyeng Lee, Division of Healthcare Associated Infection Control and Prevention, Korea Disease Control and Prevention Agency, 187, Osongsaengmyeong 2-ro, Osong-eup, Heungdeok-gu, Cheongju-si, Chungcheongbuk-do,, South Korea; email: yeonkyenglee@cdc.go.kr

Incidence, Etiology, and Healthcare Utilization for Acute Gastroenteritis in the Community, United States

Mark A. Schmidt, Holly C. Groom, Andreea M. Rawlings, Claire P. Mattison, Suzanne B. Salas, Rachel M. Burke, Ben D. Hallowell, Laura E. Calderwood, Judy Donald, Neha Balachandran, Aron J. Hall

Knowledge of the epidemiology of sporadic acute gastroenteritis (AGE) in the United States is limited. During September 2016–September 2017, we surveyed Kaiser Permanente Northwest members in Oregon and Washington, USA, to collect data on the 30-day prevalence of dually defined AGE and diarrhea disease and related health-seeking behavior; from a subset of participants, we obtained a stool specimen. Using the iterative proportional fitting algorithm with raked weights, we generated AGE prevalence and annualized rate estimates. We detected norovirus, rotavirus, astrovirus, and sapovirus from submitted stool specimens through real-time quantitative reverse transcription PCR (qRT-PCR). We estimated a 30-day prevalence of 10.4% for AGE and 7.6% for diarrhea only; annual rates were 1.27 cases/person/year for AGE and 0.92 cases/person/year for diarrhea only. Of those with AGE, 19% sought medical care. Almost one quarter (22.4%) of stool specimens from those reporting AGE tested positive for ≥1 viral pathogen, compared with 8.2% from those without AGE.

In the United States, the incidence of acute gastroenteritis (AGE) is high. AGE is estimated to cause 179 million illnesses annually (*1*,*2*). Precise data are limited on the occurrence and characteristics of sporadic AGE, particularly because the illnesses are generally mild and usually do not require medical care; may not have had diagnostic testing even if care was sought; and, depending on the pathogen, may not be reportable through public health surveillance systems. Previous US publications, using data from the US Foodborne Diseases Active Surveillance Network (FoodNet), have reported AGE prevalence ranging from 7.7 to 11%, equivalent to roughly 0.7–1.4 illnesses/person/year, depending on the recall period (i.e., 7 or 28 days) and symptom profile (i.e., diarrheal illness alone or with the presence of additional symptoms) (*1*,*3*–*5*). These studies have been essential in establishing estimates of AGE incidence in the community and highlighting the substantial burden of disease. However, differences in AGE case definitions have complicated efforts to compare findings across studies and time periods, and robust estimates of occurrence across the age spectrum remain limited. Consequently, there is a need to obtain all-age, population-based estimates of AGE within the United States.

Even assuming the lowest reported AGE prevalence of 7.7%, there is potential for substantial disease burden on the local healthcare systems and on society, such as through lost productivity (*6*). Among persons with AGE, 12%–20% have reported visiting a healthcare provider to manage their symptoms, and AGE has been estimated to contribute to 2–3 million ambulatory visits and 900,000 hospitalizations per year in the United States (*1*,*3*,*4*,*7*–*10*). However, these data have relied on samples of persons within a geographic area who may differentially seek care depending on if they have medical insurance or access to an affordable care source. As a result, these studies may not accurately estimate the true potential burden on a healthcare system.

Clarifying the etiology of AGE illness within communities and healthcare systems can help to effectively target prevention efforts. Sporadic cases of AGE are largely attributable to viral pathogens; norovirus is the most common cause of AGE across the age spectrum. Evidence in the literature suggests that intensity of viral shedding among those with asymptomatic norovirus infections is similar to that of symptomatic infections (*2*,*8*,*11*); however, according to transmission modeling of a healthcare-

Author affiliations: Center for Health Research, Kaiser Permanente Northwest, Portland, Oregon, USA (M.A. Schmidt, H.C. Groom, A.M. Rawlings, S.B. Salas, J. Donald); Centers for Disease Control and Prevention, Atlanta, Georgia, USA (C.P. Mattison, R.M. Burke, B.D. Hallowell, L.E. Calderwood, N. Balachandran, A.J. Hall); Cherokee Nation Assurance, Arlington, Virginia, USA (C.P. Mattison, N. Balachandran); Oak Ridge Institute for Science and Education, Oak Ridge, Tennessee, USA (L.E. Calderwood)

DOI: http://doi.org/10.3201/eid2811.220247

associated outbreak, symptomatic shedders are more likely to transmit norovirus to others than those without symptoms (*12*).

To better characterize the incidence of AGE in the community, the associated healthcare utilization, and the prevalence of viral enteropathogens among both symptomatic and asymptomatic persons, we conducted the Community Acute Gastroenteritis (CAGE) Study among the membership population of a large, integrated healthcare system. The aims of the CAGE Study were to generate 30-day prevalence and annualized incidence estimates of AGE occurrence across the age spectrum, describe the proportion of symptomatic persons seeking healthcare, and calculate the prevalence of enteric viral pathogens among those who did and did not report AGE. To contextualize our results with previously reported literature, we report our findings here using 2 validated case definitions (*1*,*13*).

Methods

Study Population

We conducted the CAGE Study within Kaiser Permanente Northwest (KPNW), an integrated health care delivery system with >600,000 current members. This network comprises 24% of, and is demographically similar to, the underlying population of northwest Oregon and southwest Washington, USA (*14*).

Sampling and Recruitment

We targeted enrollment to ≈3,000 members of all ages over a 12-month period. To achieve this goal, we selected age-stratified, simple random weekly samples of KPNW members from September 26, 2016, through September 19, 2017. Sampling was conducted without replacement through automated abstraction of health plan enrollment records, updated monthly, and was unrelated to AGE illness status or healthcare utilization. We excluded members who were in hospice care, non-English speaking, decisionally or cognitively impaired, previously recruited for the study, or had opted out of all KPNW research activities. Within the randomly sampled population, we targeted enrollment of an age-stratified subset of 500 members to complete a survey and provide a stool sample for virologic testing (SS cohort); the remaining 2,500 targeted enrollees were asked to complete a survey only (SO cohort). Although we describe the prevalence of viral pathogens among both cohorts, we sampled 500 in the SS cohort to have adequate power to detect an estimated 5% prevalence of these pathogens among asymptomatic persons.

Every week, we first invited our selected sample to participate by mailing recruitment postcards containing information about the study and a link to an online survey. Three days later, we sent recruitment email invitations to sampled members with active email addresses on file; we sent a reminder email invitation 1 week later. For participants within the SO cohort, we made no further recruitment efforts. To sampled members within the SS cohort, study staff made recruitment phone calls beginning 1 week after email invitations were sent; staff made ≥3 phone call attempts over the course of 1 week.

To compensate for their time, we provided enrolled participants who completed only the survey (all SO participants and those SS participants who did not provide a stool specimen) a $10 gift card. We compensated SS participants who completed a stool specimen with a $20 gift card.

Survey

The 34-item survey administered to participants comprised questions on demographic characteristics and about AGE symptoms in the previous 30 days. For those reporting AGE symptoms, we collected the frequency of vomiting/diarrhea for the most recent illness and information on any related medical encounters. We assessed encounter types separately and included inpatient hospitalizations; urgent care, emergency department, and outpatient visits; and telephone and email encounters. We defined telephone and email encounters as remote and defined the remaining encounter types as in-person. We also asked survey respondents to self-report medical conditions associated with the occurrence of chronic diarrhea as a major symptom (i.e., Crohn's disease, ulcerative colitis, inflammatory bowel disease, or abdominal or colorectal cancer).

Case Definitions

Our primary AGE case definition included participants who reported any vomiting (≥1 episode within 24 hours) or diarrhea (≥3 loose stools in any 24-hour period) (*3*). Participants with <3 loose stools in a 24-hour period and no vomiting were not considered to have AGE. Persons with medical conditions associated with chronic diarrhea were considered to have AGE if they reported vomiting; otherwise, they were categorized as noncases, regardless of diarrhea episodes.

For incidence and healthcare utilization analyses, we separately considered a second case definition limited to all persons reporting acute diarrhea, which we defined as having ≥3 loose stools in any 24-hour

period (*15*). Participants with <3 loose stools in a 24-hour period, those reporting vomiting only, and those with medical conditions associated with chronic diarrhea were categorized as noncases.

Stool Collection and Laboratory Testing

For SS participants, we employed the same method for stool sample self-collection as previously described for our medically attended acute gastroenteritis (MAAGE) study; stool sample kits were sent to responders by overnight courier within 1 day of survey completion (*14*). Once returned, the Oregon State Public Health Laboratory (OSPHL) conducted laboratory testing of stool specimens submitted by study participants to detect norovirus, rotavirus, astrovirus, and sapovirus, using TaqMan real-time quantitative reverse transcription PCR (qRT-PCR) protocols developed by the Centers for Disease Control and Prevention (CDC), also as previously described (*14*). OSPHL forwarded stool specimens testing positive for rotavirus to the CDC for confirmatory testing by qRT-PCR and enzyme immunoassay (EIA).

Statistical Analyses

We conducted all analyses using weights to account for the age-stratified probability sampling. In brief, we calculated a base weight to account for the initial probabilities of selection within each age stratum and week of sample selection. For the SO sample, we calculated a nonresponse adjustment factor using 10 strata defined by age group (0–4, 5–17, 18–44, 45–64, and ≥65 years) and sex to reduce potential bias due to nonresponse; for the SS sample, we calculated the nonresponse adjustment factor using the 5 age strata. Last, we raked the weights using the iterative proportional fitting algorithm (*16*) so that the marginal totals by age and sex matched known KPNW population totals from September 2017, when the CAGE survey was completed. We obtained SEs using Taylor series linearization and calculated 95% CIs by using exact (Clopper-Pearson) formulas.

We report population characteristics using unweighted counts and weighted means or proportions. We estimated 30-day point prevalence with 95% CIs by using weighted proportions. We calculated prevalence estimates overall, by age group, and by month. For monthly estimates, we included responses to the survey occurring before the 15th of the previous month; we included responses that occurred on or after the 15th in the calculation of prevalence for the current month. Using the prevalence estimate, we then calculated an annualized rate by multiplying the prevalence by 365/30, which yields and estimate of the average number of AGE cases per person per year.

For prevalence and reported healthcare encounter estimates, we report calculations using the AGE

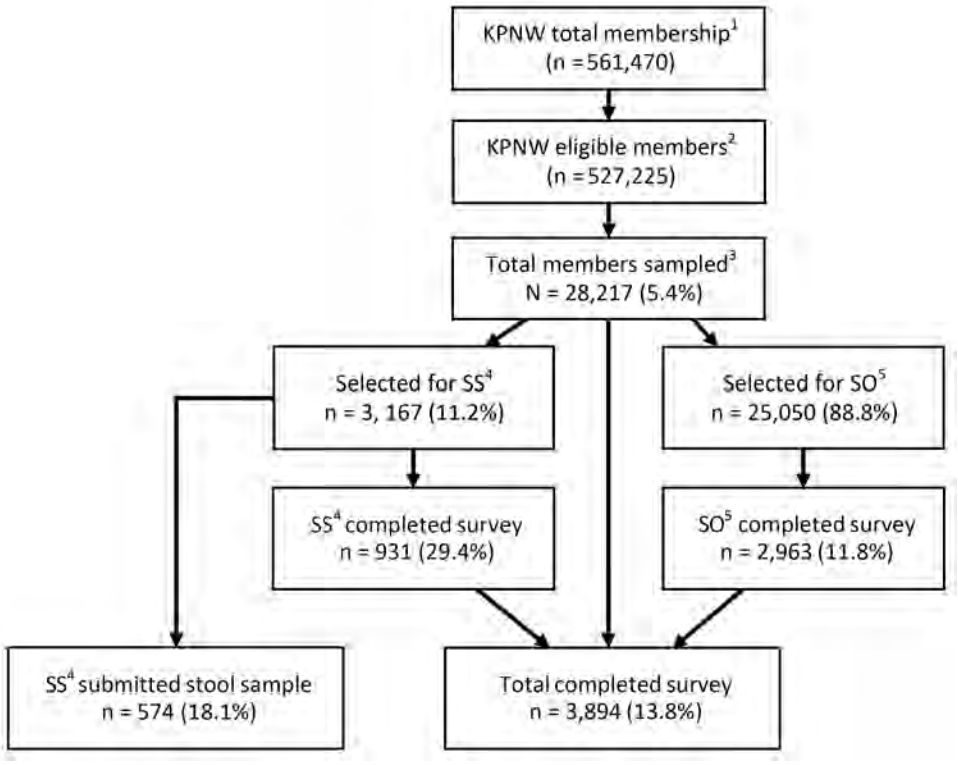

Figure 1. Sampling and inclusion of participants in Community Acute Gastroenteritis Study, Oregon and Washington, USA, September 2016–September 2017. KPNW membership as September 19, 2017; eligible members excluded those who were deceased, in hospice care, non-English speakers, decisionally/cognitively impaired, or opted out of all KPNW research activities. Sampling strategy was revised on April 10, 2017, to account for differences in response rates by age. AGE, acute gastroenteritis; KPNW, Kaiser Permanente Northwest; SO, survey only cohort, recruited to complete survey only; SS, stool sample cohort, recruited to complete survey and submit a stool sample.

and acute diarrhea case definitions. Because of the small sample of persons meeting the acute diarrhea case definition from among those submitting a stool specimen for virologic testing, we report results using only the AGE case definition. We conducted all analyses in Stata version 15.1 (https://www.stata.com).

Ethics Statement

This project was reviewed and approved by the KPNW Institutional Review Board (FWA00002344). Participants provided informed consent to participate in this study.

Results

In our 52-week study period, our sex- and age-stratified random sample comprised 28,217 KPNW members; 3,167 were selected for the SS cohort and 25,050 for the SO cohort. From this sample, we received a total of 3,894 surveys and 574 stool specimens. (Figure 1). On an unweighted basis, we observed a higher proportion of responses for those <5 years of age, >45 years of age, female, and of non-Hispanic ethnicity; we observed a lower proportion of responses among those 18–44 years of age (Table 1). After weighting, we observed a similar distribution across demographic characteristics between survey responders and the KPNW membership. The weighted mean age of participants was 40.1 years; weighted percentage by sex was 52% female and by race was 81% White (Table 1).

Overall, 395 participants met our primary AGE case definition, resulting in a 30-day AGE age-weighted prevalence of 10.4%, equivalent to a rate of 1.27 cases/person/year. Among those participants, 23% reported both diarrhea and vomiting, 50% reported only diarrhea, and 27% reported only vomiting. A total of 289 participants reported having acute diarrhea, resulting in a 30-day diarrheal prevalence of 7.6%, equivalent to a rate of 0.92 cases/person/year (Table 2). A total of 124 participants (3.2%) reported having had 1–2 loose stools but did not meet criteria for either case definition.

We observed no significant difference in prevalence estimates between male and female participants ($p = 0.264$). When examined by age, the prevalence of AGE illness was highest among the youngest age group (0–4 years, 13.5%) and lowest among the oldest (>65 years, 6.4%). For acute diarrhea, the highest prevalence occurred among those 18–44 years of age (10.2%) and those 5–17 years of age (3.3%). Those 0–4 years and 5–17 years of age had comparatively low prevalence (7.8% and 3.3%, respectively) when using the diarrhea-based definition, compared with a prevalence of 13.5% and 10.6%, respectively, when using the primary case definition (Table 2). We observed monthly variability in the occurrence of AGE, but we observed no statistically significant seasonal patterns (Figure 2).

Table 1. Demographic characteristics of participants in Community Acute Gastroenteritis Study, Oregon and Washington, USA, September 2016–September 2017

Characteristic	Unweighted no.	Weighted %*
All participants	3,894	
Age group, y		
<5	473	4.8
5–17	334	14.6
18–44	951	38.0
45–64	1,283	27.3
≥65	853	15.3
Sex		
M	1,542	
F	2,352	51.8
Race		
White	3,276	81.5
Other/unknown		
Ethnicity		
Hispanic	224	7.4
Non-Hispanic	3,261	87.6
Unknown/not specified	215	5.0
Education		
Less than high school	33	1.1
High school diploma/GED	320	10.7
Some college	942	30.8
College graduate	982	33.4
Postgraduate	752	24.0
Residence		
Urban	1548	40.7
Suburban	1555	41.8
Other	711	17.5
Insurance status		
Commercial only	2763	77.0
Medicaid	221	6.0
Medicare	871	15.9
Both Medicare and Medicaid	2	0.1
None	37	1.0
Income		
<$50,000	428	10.4
$50,000–$75,000	664	16.2
>$75,000	520	12.9
Missing/declined to state	2282	60.5

*Weighted to account for age-stratified probability sampling.

Healthcare Encounters

Overall, 80 (19%) persons with AGE had ≥1 AGE-related healthcare encounters within KPNW. Most of those (63 [79%]) had an in-person encounter, 37 (46%) of whom also had a remote encounter; 17 (19%) had only a remote encounter (Table 3). The percentage of participants seeking AGE-related medical care was slightly lower among persons reporting only acute diarrhea; 17% had ≥1 encounter overall, of which 77% had an in-person visit and 23% had a remote encounter only.

Pathogen Testing

In total, 574 SS study participants (with and without AGE) returned stool samples. On average, stool

Table 2. Estimated 30-day prevalence and number of persons with AGE, by age group, in Community Acute Gastroenteritis Study, Oregon and Washington, USA, September 2016–September 2017*

	Case definition: diarrhea or vomiting		Case definition: acute diarrhea	
Category	AGE illness, unweighted no.	Prevalence (95% CI)	AGE illness, unweighted no.	Prevalence (95% CI)
By age group†				
<5	65	13.5 (10.6–16.9)	37	7.8 (5.5–10.6)
5–17	36	10.6 (7.5–14.5)	12	3.3 (1.7–5.8)
18–44	120	12.5 (10.3–15.0)	96	10.2 (8.2–12.6)
45–65	119	9.2 (7.6–11.0)	104	8.0 (6.5–9.7)
>65	55	6.4 (4.9–8.3)	40	4.7 (3.4. 6.3)
By sex‡				
M	153	10.1 (8.4–12.1)	106	7.5 (5.9–9.3)
F	242	10.7 (9.4–12.2)	183	7.8 (6.7–9.0)
Overall	395	10.4 (9.3–11.6)	289	7.6 (6.7–8.7)

*AGE episodes were defined based on self-report as any illness in the previous 30 day with diarrhea or vomiting that included ≥3 loose stools in any 24-hour period. Data from participants who completed the survey on or before the 15th of the month were included in estimates for the preceding month, whereas information from surveys completed after the 15th contribute to the current month. Prevalence estimates are weighted to account for the sampling scheme; 95% CIs are estimated using exact (Clopper-Pearson) formulas. AGE, acute gastroenteritis.
†Survey design-based F-tests comparing differences in proportion of AGE across age groups are significant for both the diarrhea or vomiting definition ($p = 0.0014$) and the diarrhea definition ($p<0.001$).
‡Survey design-based F-tests comparing differences in proportion of AGE across sex are not significant for either the diarrhea or vomiting definition ($p = 0.264$) nor the diarrhea definition ($p = 0.112$).

samples were collected within 10 days of survey completion; 83% of samples were collected within 2 weeks of survey completion. Of the samples, 570 (99%) were usable and tested at OSPHL, 70 collected from persons who met our primary definition for AGE and 500 collected from those who did not. As a weighted percentage, those totals yield an estimated 30-day AGE prevalence of 12.3% (95% CI 8.8%–16.5%) in this group. Overall, norovirus and rotavirus were the most commonly detected viral pathogens (Figure 3). Using this sample, we estimated that 22.4% (95% CI 9.6%–40.8%) of our total KPNW population with AGE would test positive for ≥1 viral pathogen. An estimated 7.2% (95% CI 2.0%–17.5%) would test positive for norovirus alone, 11.5% (95% CI 2.4%–30.1%) for rotavirus alone, 3.5% (95% CI 0.1%–19.0%) for sapovirus alone, and <1% for both norovirus and rotavirus. Using the sample of 500 specimens from persons without AGE, we estimate that 8.2% (95% CI 5.5%–11.7%) would test positive for ≥1 viral pathogen: 1.4% (95% CI 0.4%–3.4%) for norovirus alone, 5.8% (95% CI 3.5%–9.0%) for rotavirus alone, 0.98% (95% CI 0.32%-2.32%) for sapovirus alone, and 0.59% (95% CI 0.12%-1.74%) for astrovirus alone.

Of the 23 total stool specimens that tested positive for norovirus, 5 were determined to be genogroup I and 18 to be genogroup II. Forty of the 41 stool specimens (98%) testing positive for rotavirus by qRT-PCR at OSPHL were available for confirmatory testing at

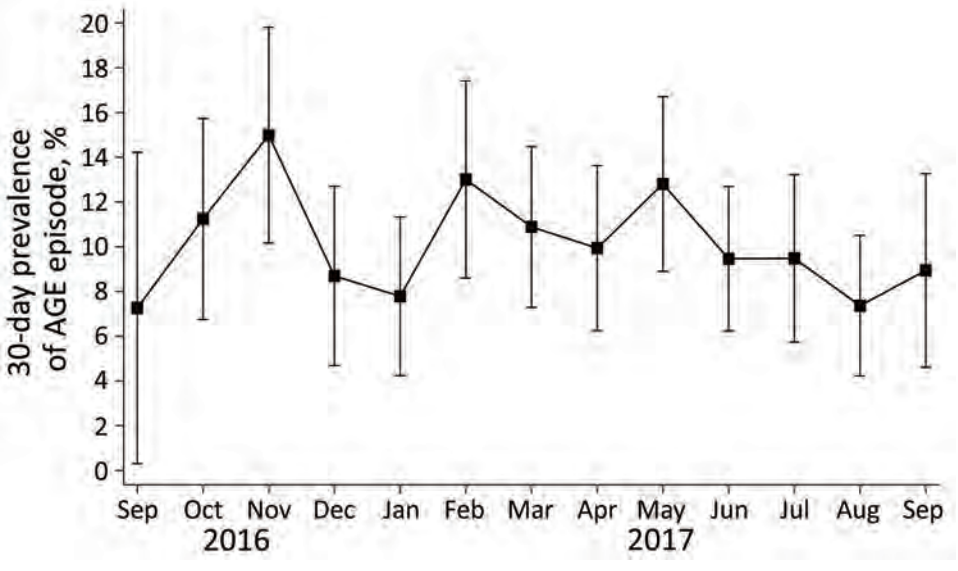

Figure 2. Estimated 30-day prevalence of AGE episodes by month, primary case definition, in Community Acute Gastroenteritis Study, Oregon and Washington, USA, September 2016–September 2017. AGE episode was defined based on self-report as any illness in the previous 30 days with diarrhea or vomiting that included ≥3 loose stools in any 24-hour period. Data from participants who completed the survey on or before the 15th of the month were included in estimates for the preceding month, whereas information from surveys completed after the 15th contributed to the current month. Prevalence estimates are unadjusted and weighted to account for the sampling scheme; 95% CIs are estimated using the delta method and normal approximations. AGE, acute gastroenteritis.

Table 3. Distribution of encounters and encounter types among persons with AGE in Community Acute Gastroenteritis Study, Oregon and Washington, USA, September 2016–September 2017*

Category	Case definition: diarrhea or vomiting		Case definition: diarrhea	
	Unweighted no. encounters	% Encounters (95% CI)	Unweighted no. encounters	% Encounters (95% CI)
No encounter	313	80.9 (76.0–85.1)	288	83.3 (77.7–87.9)
Any encounter, by type	80	19.1 (14.9–24.0)	51	16.7 (12.1–22.3)
Inpatient	10	12.2 (5.5–22.3)	5	9.2 (2.6–21.7)
Urgent care or emergency department	37	49.5 (35.8–63.1)	24	52.0 (34.1–69.6)
Outpatient	55	69.8 (56.4–81.2)	33	63.8 (44.9–80.0)
Remote	54	64.4 (50.4–76.9)	35	67.3 (48.3–82.9)
Any encounter, by delivery method	80	19.1 (14.9–24.0)	51	16.7 (12.1–22.3)
Remote only†	17	18.8 (10.8–29.4)	13	23.5 (11.5–39.7)
In-person only‡	26	35.5 (23.1–49.6)	16	32.7 (17.1–51.7)
Both in-person and remote	37	45.6 (32.1–59.6)	22	43.8 (26.2–62.3)

*Percentage estimates are unadjusted and weighted to account for the sampling scheme. AGE, acute gastroenteritis.
†Email, video call, or call nurse contact without an in-person visit.
‡Inpatient, urgent care, emergency department, or outpatient visit without any remote contact.

CDC. Of those, 1 (3%) was determined to be rotavirus vaccine shedding, and 3 (8%) asymptomatic persons tested positive by rotavirus EIA (however, all 3 had high Ct values, indicating lower viral load, and could not be genotyped).

Discussion

Our study results confirm that use of an expanded case definition that includes persons reporting only vomiting increases prevalence estimates by ≈50% compared with a definition that includes only diarrhea (*13*). Our 30-day AGE prevalence estimates are broadly consistent with the range observed in previous literature, although the use of differing case definitions make direct comparisons more complex. Reporting our results in 2 ways improves our ability to compare our findings to those of others; however, doing so reduces the consistency observed between our prevalence estimates. For our AGE case definition, we observed a prevalence estimate of 10.4%, compared with Canada's Foodbook estimate of 5.7% in 2014–2015 (*15*). For our diarrhea-only case definition, our estimate of 7.6% was lower than FoodNet's estimate of 10%–11% from 1996–1999 (*1*,*3*,*4*). Those differences highlight the inherent variability in estimates of AGE, which may reflect variations in occurrence due to geography, time, or other factors.

Previous work has argued for use of the expanded AGE case definition (*7*). Excluding symptoms of vomiting has been associated with decreased sensitivity for identifying norovirus infections (*1*,*13*,*17*). Further, research has shown age-related differences in AGE symptom profiles, particularly with vomiting

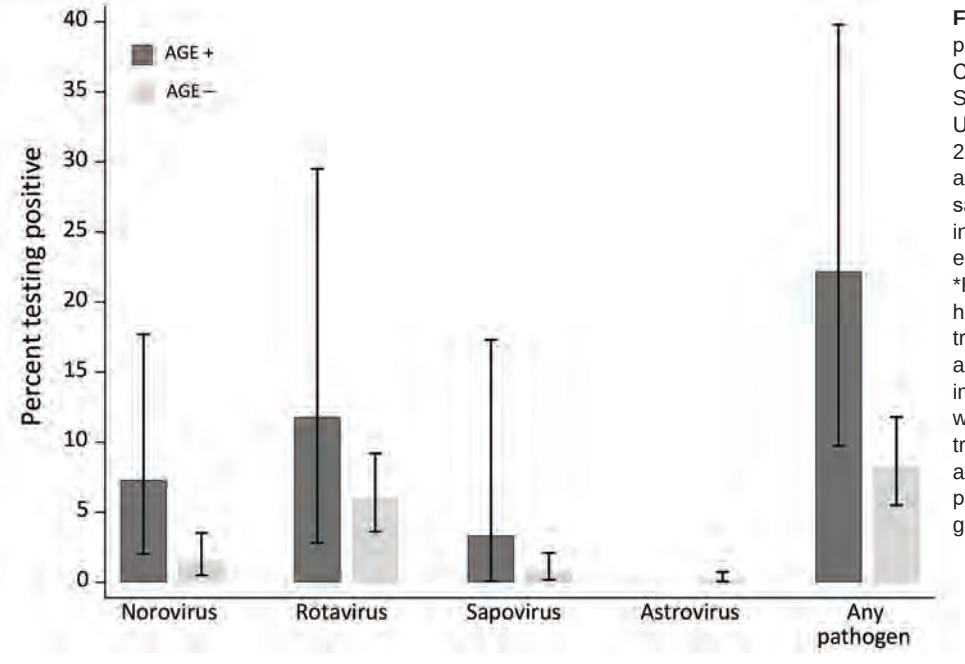

Figure 3. Viral prevalence by primary AGE case definition in Community Acute Gastroenteritis Study, Oregon and Washington, USA, September 2016–September 2017. Estimates are unadjusted and weighted to account for the sampling scheme; confidence intervals are estimated using exact (Clopper-Pearson) formulas. *Rotavirus results reported here reflect quantitative reverse transcription PCR testing results and not subsequent enzyme immunoassay test results (for which only 4 quantitative reverse transcription PCR positives were also enzyme immunoassay–positive). AGE, acute gastroenteritis.

(*18*,*19*). For instance, 1 study found that vomiting was reported for 37% of AGE patients <5 years of age, compared with only 17% of those 65–74 years of age (*20*). This finding is further supported by our data, where we saw a lower prevalence of AGE among participants 0–4 years of age when we used the case definition that did not include vomiting (7.8%) compared with the definition that did (13.5%). Considering that norovirus is the most common cause of AGE among children younger than 5 years (*2*), use of an expanded AGE surveillance case definition will yield more complete estimates of norovirus burden.

Nearly 1 in 5 (19%) of our respondents sought medical care for their AGE symptoms, consistent with behaviors reported in other US studies, even where 8%–9% did not have insurance coverage (*1*). Our study is unique in describing AGE-related healthcare seeking behavior that includes not only telephone consultations with a clinician for illness management but also other remote encounters, such as email exchange via patient portal and video appointments. One previous FoodNet publication asked whether respondents made a call to a medical provider, but it is unclear whether the calls were used to discuss management of clinical symptoms (in place of in-person visits) (*3*). KPNW encourages members to use those remote technologies for initial access to medical providers to make healthcare more accessible; to reduce the burden of in-person visits to medical offices; and to reduce the risk for transmission of communicable diseases to other members, staff, and clinicians. Whereas most clinical care was in-person, 19% of our population exclusively used remote encounters. As healthcare delivery systems increasingly expand access to virtual care, more research is needed to determine how this shift affects the burden of AGE on the healthcare system. If our population were generalizable to the US population, there would be an estimated 415 million AGE illness episodes per year, with an associated 5.4 million in-person AGE-related encounters. Our novel findings of an extrapolated 1.2 million remote AGE-related healthcare encounters indicate a potential higher burden on the healthcare system due to AGE that has not been well-captured in previous studies.

We observed an overall pathogen positivity of roughly 10% from among all submitted stool specimens; differences observed in pathogen positivity between those who did and did not have AGE were not statistically significant. This finding is likely because of the small numbers within our SS cohort and the potential time lag between occurrence of symptoms and collection of stool sample, as well as the high rate of rotavirus detection by qRT-PCR. Further work in this area is needed, but our study was powered to calculate the prevalence of viral pathogens among asymptomatic persons, rather than to detect significant differences between those with and without symptoms of AGE. Among those not meeting the AGE case definition, we observed a norovirus prevalence of 1.4% and a rotavirus prevalence of 5.8% by qRT-PCR; both values are slightly lower than previously published estimates of 4% and 11%, respectively (*21*,*22*). The prevalence of rotavirus detection is higher when using qRT-PCR versus EIA testing, because of the increased sensitivity of PCR tests for detecting viral pathogens at a lower viral load (*23*), which is supported by our findings. Because lower levels of shedding may be less clinically relevant, EIA continues to be preferred for routine surveillance rotavirus testing (*24*). However, the detection of both norovirus and rotavirus from persons without recognized AGE highlights a potential reservoir for sporadic AGE within the community, although asymptomatic infections are believed to be less contagious. Even so, interventions designed to reduce the transmission of AGE-related pathogens are important to follow for both symptomatic and asymptomatic persons.

A key strength of our study is that participants were selected via an age-stratified, representative sample of KPNW enrollees, which is reflective of the underlying population base. Consequently, we have been able to more accurately calculate the estimated number of AGE episodes per person per year when compared with other studies, and our findings are generalizable to the target population of this area. Further, conducting this study within our population reduces the likelihood that access to care is a barrier to seeking treatment in the healthcare system. Conversely, our study may have been limited by a low overall participation rate of 13.8%. This percentage is higher than reported in a comparable study from the United Kingdom (*25*), and we exceeded our sample size goal by obtaining 3,874 completed surveys and 574 stool specimens; however, the percentage is lower than those for other published studies of comparable design, such as FoodNet (*1*). We attempted to minimize the effects of this bias by using weighting that incorporated a nonresponse correction factor to improve the generalizability of our findings. Although we recognize the potential for recall bias, because our findings are based on reports of AGE within the previous 30-days, previous work examining the effects of a

7-day versus 1-month recall period found no difference in monthly prevalence estimates (*5*). Therefore, we believe any effect on our findings will be minimal. Our study may also have been limited by a delay between survey completion and stool sample collection, resulting in an underestimate of the prevalence of viral pathogens among those meeting our AGE case definition during the 30-days before survey completion. Because our study was powered to detect the prevalence of viral pathogens among those asymptomatic for AGE, we believe the effects on our findings would have been minimal.

In conclusion, AGE continues to exert a substantial burden of disease within the population, as well as upon healthcare delivery systems. This effect is particularly notable when vomiting is considered as part of the AGE case definition; prevalence estimates were nearly 50% higher when including this symptom. Our findings also provide key estimates of the prevalence of asymptomatic shedding of AGE-related viral pathogens, which can help contextualize viral prevalence data from AGE cases to assess disease burden. General interventions designed to reduce the transmission of AGE-related viral pathogens (e.g., hand hygiene) continue to be crucial as a means to reduce the extent of AGE in the population, even among persons without symptomatic disease. However, the high number of AGE cases in the community, particularly when including vomiting-only symptoms, leads to a heavy burden on the healthcare system. Additional targeted interventions, such as vaccines, could help reduce AGE in the community and, thus, reduce strain on healthcare systems.

Acknowledgments

We thank Peggy Cook, Camille Friason, Valerie Grim, Ann Macfarlane, Sergey Nazarov, Joanne Price, Sperry Robinson, Samantha Sahnow, and Sarah Vertrees for their participant recruitment efforts. We are also grateful for the contributions of Eric Katz, Michael Bowen, Christianne Biggs, and Laura Tsaknaridis. Finally, we thank the CAGE study participants for their essential contributions to this research study.

This work was supported by investigator-initiated research grants from Takeda Vaccines, Inc. (IISR-2015-101015 and ISSR-2017-101938). Takeda had no role in study design, data collection and analysis, decision to publish, or preparation of the manuscript. CDC received no funding from Takeda.

M.A.S., H.G., A.M.R., S.B.S., and J.D. received institutional research grant support for this project. C.P.M., R.M.B., B.D.H., L.E.C., N.B., and A.J.H. report no conflict of interest.

About the Author

Dr. Schmidt is an infectious disease epidemiologist and investigator at the Kaiser Permanente Center for Health Research. His primary research interests include diarrheal diseases (norovirus and *Clostridioides difficile*), SARS-CoV-2 epidemiology and vaccine efficacy, extraintestinal *Escherichia coli* infection, and chronic hepatitis B and C.

References:

1. Jones TF, McMillian MB, Scallan E, Frenzen PD, Cronquist AB, Thomas S, et al. A population-based estimate of the substantial burden of diarrhoeal disease in the United States; FoodNet, 1996–2003. Epidemiol Infect. 2007;135:293–301. https://doi.org/10.1017/S0950268806006765
2. Grytdal SP, DeBess E, Lee LE, Blythe D, Ryan P, Biggs C, et al. Incidence of norovirus and other viral pathogens that cause acute gastroenteritis (AGE) among Kaiser Permanente member populations in the United States, 2012–2013. PLoS One. 2016;11:e0148395. https://doi.org/10.1371/journal.pone.0148395
3. Herikstad H, Yang S, Van Gilder TJ, Vugia D, Hadler J, Blake P, et al.; THE FOODNET WORKING GROUP. A population-based estimate of the burden of diarrhoeal illness in the United States: FoodNet, 1996–7. Epidemiol Infect. 2002;129:9–17. https://doi.org/10.1017/S0950268801006628
4. Imhoff B, Morse D, Shiferaw B, Hawkins M, Vugia D, Lance-Parker S, et al.; Emerging Infections Program FoodNet Working Group. Burden of self-reported acute diarrheal illness in FoodNet surveillance areas, 1998–1999. Clin Infect Dis. 2004;38(Suppl 3):S219–26. https://doi.org/10.1086/381590
5. Cantwell LB, Henao OL, Hoekstra RM, Scallan E. The effect of different recall periods on estimates of acute gastroenteritis in the United States, FoodNet Population Survey 2006–2007. Foodborne Pathog Dis. 2010;7:1225–8. https://doi.org/10.1089/fpd.2010.0567
6. Bartsch SM, Lopman BA, Ozawa S, Hall AJ, Lee BY. Global economic burden of norovirus gastroenteritis. PLoS One. 2016;11:e0151219. https://doi.org/10.1371/journal.pone.0151219
7. Everhart J, editor. The burden of digestive diseases in the United States. Washington, DC: US Department of Health and Human Services, Public Health Service, National Institutes of Health, National Institute of Diabetes and Digestive and Kidney Diseases; 2008.
8. Hall AJ, Rosenthal M, Gregoricus N, Greene SA, Ferguson J, Henao OL, et al. Incidence of acute gastroenteritis and role of norovirus, Georgia, USA, 2004–2005. Emerg Infect Dis. 2011;17:1381–8. https://doi.org/10.3201/eid1708.101533
9. Lopman BA, Hall AJ, Curns AT, Parashar UD. Increasing rates of gastroenteritis hospital discharges in US adults and the contribution of norovirus, 1996–2007. Clin Infect Dis. 2011;52:466–74. https://doi.org/10.1093/cid/ciq163
10. Gastañaduy PA, Hall AJ, Curns AT, Parashar UD, Lopman BA. Burden of norovirus gastroenteritis in the ambulatory setting—United States, 2001–2009. J Infect Dis. 2013;207:1058–65. https://doi.org/10.1093/infdis/jis942
11. Atmar RL, Opekun AR, Gilger MA, Estes MK, Crawford SE, Neill FH, et al. Norwalk virus shedding after experimental human infection. Emerg Infect Dis. 2008;14:1553–7. https://doi.org/10.3201/eid1410.080117
12. Teunis PF, Sukhrie FH, Vennema H, Bogerman J, Beersma MF, Koopmans MP. Shedding of norovirus in symptomatic and asymptomatic infections. Epidemiol

Infect. 2015;143:1710–7. https://doi.org/10.1017/S095026881400274X
13. Majowicz SE, Hall G, Scallan E, Adak GK, Gauci C, Jones TF, et al. A common, symptom-based case definition for gastroenteritis. Epidemiol Infect. 2008;136:886–94. https://doi.org/10.1017/S0950268807009375
14. Schmidt MA, Groom HC, Naleway AL, Biggs C, Salas SB, Shioda K, et al. A model for rapid, active surveillance for medically-attended acute gastroenteritis within an integrated health care delivery system. PLoS One. 2018;13:e0201805. https://doi.org/10.1371/journal.pone.0201805
15. Thomas MK, Murray R, Nesbitt A, Pollari F. The incidence of acute gastrointestinal Illness in Canada, foodbook survey 2014–2015. Can J Infect Dis Med Microbiol. 2017;2017:5956148. https://doi.org/10.1155/2017/5956148
16. Kolenikov S. Calibrating survey data using iterative proportional fitting (raking). Stata J. 2014;14:22–59. https://doi.org/10.1177/1536867X1401400104
17. Pindyck T, Hall AJ, Tate JE, Cardemil CV, Kambhampati AK, Wikswo ME, et al. Validation of acute gastroenteritis-related International Classification of Diseases, Clinical Modification codes in pediatric and adult US populations. Clin Infect Dis. 2020;70:2423–7. https://doi.org/10.1093/cid/ciz846
18. Scallan E, Crim SM, Runkle A, Henao OL, Mahon BE, Hoekstra RM, et al. Bacterial enteric infections among older adults in the United States: foodborne diseases active surveillance network, 1996–2012. Foodborne Pathog Dis. 2015;12:492–9. https://doi.org/10.1089/fpd.2014.1915
19. Chen Y, Liu BC, Glass K, Kirk MD. High incidence of hospitalisation due to infectious gastroenteritis in older people associated with poor self-rated health. BMJ Open. 2015;5:e010161. https://doi.org/10.1136/bmjopen-2015-010161
20. White AE, Ciampa N, Chen Y, Kirk M, Nesbitt A, Bruce BB, et al. Characteristics of *Campylobacter* and *Salmonella* infections and acute gastroenteritis in older adults in Australia, Canada, and the United States. Clin Infect Dis. 2019;69:1545–52. https://doi.org/10.1093/cid/ciy1142
21. Qi R, Huang YT, Liu JW, Sun Y, Sun XF, Han HJ, et al. Global prevalence of asymptomatic norovirus infection: a meta-analysis. EClinicalMedicine. 2018;2-3:50–8. https://doi.org/10.1016/j.eclinm.2018.09.001
22. Phillips G, Lopman B, Rodrigues LC, Tam CC. Asymptomatic rotavirus infections in England: prevalence, characteristics, and risk factors. Am J Epidemiol. 2010;171:1023–30. https://doi.org/10.1093/aje/kwq050
23. Tate JE, Mijatovic-Rustempasic S, Tam KI, Lyde FC, Payne DC, Szilagyi P, et al. Comparison of 2 assays for diagnosing rotavirus and evaluating vaccine effectiveness in children with gastroenteritis. Emerg Infect Dis. 2013;19:1245–52. https://doi.org/10.3201/eid1908.130461
24. Stockman LJ, Staat MA, Holloway M, Bernstein DI, Kerin T, Hull J, et al. Optimum diagnostic assay and clinical specimen for routine rotavirus surveillance. J Clin Microbiol. 2008;46:1842–3. https://doi.org/10.1128/JCM.02329-07
25. Tam CC, Rodrigues LC, Viviani L, Dodds JP, Evans MR, Hunter PR, et al.; IID2 Study Executive Committee. Longitudinal study of infectious intestinal disease in the UK (IID2 study): incidence in the community and presenting to general practice. Gut. 2012;61:69–77. https://doi.org/10.1136/gut.2011.238386

Address for correspondence: Mark A. Schmidt, Kaiser Permanente, 3800 N Interstate Ave, Portland, OR 97232, USA; email: mark.a.schmidt@kpchr.org

Socioeconomic Inequalities in COVID-19 Vaccination and Infection in Adults, Catalonia, Spain

Elena Roel, Berta Raventós, Edward Burn, Andrea Pistillo, Daniel Prieto-Alhambra, Talita Duarte-Salles

Evidence on the impact of the COVID-19 vaccine rollout on socioeconomic COVID-19–related inequalities is scarce. We analyzed associations between socioeconomic deprivation index (SDI) and COVID-19 vaccination, infection, and hospitalization before and after vaccine rollout in Catalonia, Spain. We conducted a population-based cohort study during September 2020–June 2021 that comprised 2,297,146 adults ≥40 years of age. We estimated odds ratio of nonvaccination and hazard ratios (HRs) of infection and hospitalization by SDI quintile relative to the least deprived quintile, Q1. Six months after rollout, vaccination coverage differed by SDI quintile in working-age (40–64 years) persons: 81% for Q1, 71% for Q5. Before rollout, we found a pattern of increased HR of infection and hospitalization with deprivation among working-age and retirement-age (≥65 years) persons. After rollout, infection inequalities decreased in both age groups, whereas hospitalization inequalities decreased among retirement-age persons. Our findings suggest that mass vaccination reduced socioeconomic COVID-19–related inequalities.

The COVID-19 pandemic has caused an unprecedented global health crisis, resulting in >540 million cases worldwide as of July 2022 (*1*). However, the impact of the pandemic has not been uniform across or within countries (*2*). Disadvantaged populations, such as individuals with low socioeconomic status, display higher incidence rates of COVID-19 infection and hospitalization (*3*,*4*). To date, vaccines against SARS-CoV-2, the virus that causes COVID-19, are the cornerstone of the COVID-19 response. Yet, emerging evidence shows socioeconomic inequalities in COVID-19 vaccination coverage within countries with high access to vaccines, such as the United Kingdom or the United States (*5*–*8*). For instance, a report from May 2021 from the United Kingdom showed that vaccination coverage was 94% in the least areas and 84% in the most deprived areas (deprivation was measured using an index based on income, employment, education, health, crime, barriers to housing and services, and living environment) (*8*,*9*). Similarly, in the United States, vaccination coverage was lower (49%) among adults living in counties with the highest overall social vulnerability index (SVI) scores (based on socioeconomic status, household composition and disability, racial/ethnic minority status and language, and housing type and transportation) when compared to the coverage (59%) among adults living in counties with the lowest overall SVI scores in May 2021 (*10*). However, evidence is scarce regarding socioeconomic inequalities in COVID-19 vaccine uptake from other countries and the effect of the COVID-19 vaccine rollout on socioeconomic COVID-19–related outcomes inequalities.

In Spain, the COVID-19 vaccine rollout started on December 27, 2020. The first population groups eligible for vaccination were persons living in nursing homes and healthcare workers (*11*). Subsequently, other groups became eligible, taking into account age, starting with the eldest; underlying conditions, prioritizing persons with risk factors for COVID-19; and occupation, prioritizing essential workers. In Catalonia, a region located in northeast Spain, 52% of the population had received ≥1 dose of a COVID-19 vaccine as of June 30, 2021 (*12*). Determining patterns of socioeconomic inequalities in relation to COVID-19 vaccination and COVID-19 outcomes in Catalonia could provide valuable information to public health

Author affiliations: Universitat Autònoma de Barcelona, Barcelona, Spain (E. Roel, B. Raventós); Fundació Institut Universitari per a la recerca a l'Atenció Primària de Salut Jordi Gol i Gurina, Barcelona, Spain (E. Roel, B. Raventós, E. Burn, A. Pistillo, T. Duarte-Salles); Centre for Statistics in Medicine, Nuffield Department of Orthopaedics, Rheumatology, and Musculoskeletal Sciences, University of Oxford, Oxfordshire, United Kingdom (E. Burn, D. Prieto-Alhambra); Erasmus University Medical Center Department of Medical Informatics, Rotterdam, Netherlands (D. Prieto-Alhambra)

DOI: https://doi.org/10.3201/eid2811.220614

authorities to guide immunization efforts among vulnerable populations in Spain and in other countries with widespread access to vaccines.

We analyzed the association between a socioeconomic deprivation index (SDI) score based on place of residence (a proxy measure of socioeconomic status) and COVID-19 vaccination coverage 6 months after the start of vaccine rollout among adults ≥40 years of age living in urban areas of Catalonia. Subsequently, we analyzed the associations between SDI score and COVID-19 infection, hospitalization, and death, before and after the start of vaccine rollout. The Clinical Research Ethics committee of Fundació Institut Universitari per a la recerca a l'Atenció Primària de Salut Jordi Gol i Gurina (IDIAPJGol) approved this study (project code 21/052-PCV), with no required written consent from participants.

Methods

Study Design and Data Source

We conducted a population-based cohort study during September 1, 2020–June 30, 2021, using primary care data from the Information System for Research in Primary Care (SIDIAP; https://www.sidiap.org) database, standardized to the Observational Medical Outcomes Partnership Common Data Model (*13*,*14*). SIDIAP contains pseudoanonymized electronic health records from ≈75% of the population in Catalonia, which has ≈7.5 million inhabitants, and is representative in terms of age, sex, and geographic distribution (*15*). SIDIAP includes data on sociodemographics, diagnoses, laboratory tests, medication use, and deaths. In addition, SIDIAP has been linked to the Catalan public health vaccine registry and to a population-based register of hospital discharge records from public and private hospitals of Catalonia (Conjunt Mínim Bàsic de Dades d'Alta Hospitalària, CMBD-AH) (E. Burn, et al., unpub. data, https://doi.org/10.1101/2021.11.23.21266734).

Study Participants

We included 2,297,146 adults 40–110 years of age registered in SIDIAP as of September 1, 2020, after excluding those with <1 year of medical history available (n = 23,705), those with a previous COVID-19 infection (n = 125,111), those living in nursing homes (n = 31,091) and in rural areas (n = 513,386), and those with missing data on SDI (n = 307,038) (Figure 1). We included adults ≥40 years of age because those younger were not generally eligible for vaccination before mid-June 2021. We excluded persons living in rural areas, which included municipalities with <10,000 inhabitants and a population density <150 habitants/km^2 (*16*), because information on SDI was unavailable for these areas. We identified persons with a previous COVID-19 infection using SARS-CoV-2 positive tests or clinical COVID-19 diagnoses because SARS-CoV-2 tests were restricted to severe cases during the first months of the pandemic in Spain (*17*). We used Systematized Nomenclature of Medicine codes to identify COVID-19 diagnoses (Appendix Table 1, https://wwwnc.cdc.gov/EID/article/28/11/22-0614-App1.pdf).

To assess inequalities in COVID-19 vaccination coverage 6 months after the start of vaccine rollout (i.e., June 30, 2021), we restricted our analyses to persons with complete follow-up (vaccine coverage dataset, n = 2,258,866). We analyzed inequalities on COVID-19 outcomes for 2 time periods: 3 months before and 1–6 months after the start of vaccine rollout. For each period, we followed participants until the occurrence of the outcome of interest, end of study period, exit from database, or death, whichever occurred first. The period 3 months before vaccine rollout was September 1–December 26, 2020. The period 1–6 months after vaccine rollout was January 27–June 30, 2021; we excluded patients with a COVID-19 infection or lost before January 27, 2021 (n = 106,945), from analysis.

Outcomes

We identified persons vaccinated against COVID-19 as those who had received a dose of any COVID-19 vaccine: BNT162b2 mRNA (Pfizer-BioNTech, https://www.pfizer.com), mRNA-1273 (Moderna, https://www.modernatx.com), ChAdOx1 nCoV-19 (Oxford-AstraZeneca, https://www.astrazeneca.com), or Ad.26.COV2.S (Janssen/J&J, https://www.janssen.com). The date of vaccination was the date of the first dose administration. We identified COVID-19 infections based on a positive SARS-CoV-2 antigen or reverse transcription PCR test, using the test date as the date of infection; we considered the first infection per person. We defined COVID-19 hospitalizations as hospitalizations with a positive SARS-CoV-2 test result between 21 days before and 3 days after the date of admission. We defined COVID-19–related deaths as deaths occurring ≤28 days after the date of infection.

Variables

We measured SDI score using the Mortalidad en áreas pequeñas españolas y desigualdades socioeconómicas y ambientales (MEDEA) deprivation index (*16*). The MEDEA index was calculated for census tract urban

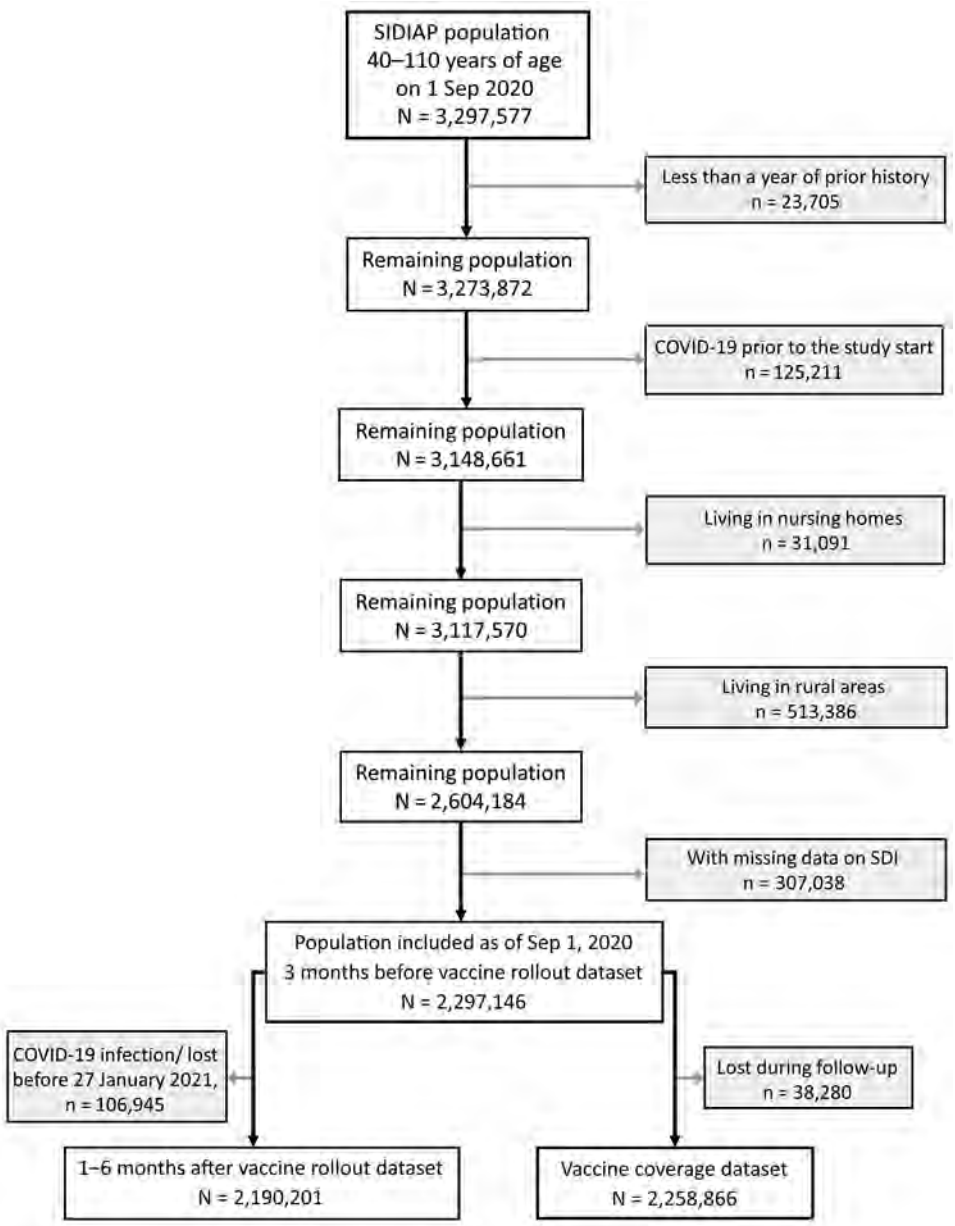

Figure 1. Flowchart showing the inclusion and exclusion criteria for study population in analysis of socioeconomic inequalities in COVID-19 vaccination and infection in adults, Catalonia, Spain. SDI, Socioeconomic Deprivation Index; SIDIAP, Information System for Research in Primary Care.

areas using information related to 5 indicators (related to work and education) from the 2001 national census in Spain. We linked the MEDEA deprivation index to each participant's most recent site of residence and categorized it into quintiles of socioeconomic deprivation, with the first quintile (Q1) representing the least deprived and the fifth (Q5) the most deprived area. We extracted age in years, sex, nationality by the country's geographic region, and comorbidities recorded before study start that were identified using Systematized Nomenclature of Medicine codes (Appendix Table 1). We categorized age into 2 groups: ≥65 (retirement age) and 40–64 years (working age).

Statistical Analysis

We described participants' characteristics at baseline and by vaccination status, COVID-19 infection, hospitalization, and death over study follow-up period; we used counts and percentages for categorical variables and median and interquartile ranges (IQRs) for continuous variables. In accordance with information-governance requirements intended to protect confidentiality, we reported results with <5 persons as <5 rather than specific numbers. We also compared baseline characteristics of persons with and without missing data on SDI, and those with and without complete follow-up, using standardized mean differences (SMD). We

considered an absolute SMD ≥0.1 to be a meaningful difference in the distribution of a given characteristic between the groups compared (*18*). We generated charts of weekly cumulative vaccination coverages and incidence rates (IRs; cases/100,000 person-years) of COVID-19 infection, hospitalization, and death during September 1, 2020–June 30, 2021, by SDI quintile and age group. We used R version 4.1 (The R Project for Statistical Computing, https://www.r-project.org) for data curation, analysis, and visualization.

To assess the association between SDI quintile and nonvaccination, we performed crude and adjusted logistic regression models and calculated odds ratios (ORs) with 95% CIs by age group. We included persons with complete follow-up for these analyses (vaccine coverage dataset). To assess the association between SDI quintile and COVID-19 infection, hospitalization and death, we performed crude and adjusted Cox proportional-hazards models and calculated hazard ratios (HRs) with 95% CIs by age group and period using the 3 months before and 1–6 months after vaccine rollout datasets. We visually inspected log-log survival curves to check the proportional hazard assumptions for the variables included in the models. We did not estimate models in which the number of events per SDI quintile was <5. Models were relative to the least deprived quintile (Q1) and adjusted by age, sex, and nationality; we developed a directed acyclic graph to guide our modeling strategy (Appendix Figure 1) (*19*). Of note, rates of hospitalization and death were estimated among the total population rather than among those infected with COVID-19 to prevent collider bias (*20*).

In addition, we performed 3 sensitivity analyses. First, we reestimated our models for vaccination coverage after excluding persons with a COVID-19 infection during follow-up, because they were not eligible for vaccination until 6 months after the infection. Second, we reestimated our models for COVID-19 outcomes restricting our analyses to citizens of Spain because the proportionality assumption was violated for nationality and all the COVID-19 outcomes. Third, we estimated socioeconomic inequalities on COVID-19 outcomes for the time period 3–6 months after the start of vaccine rollout, March 27– June 30, 2021, after excluding those with a COVID-19 infection, deceased, or lost before March 27, 2021 (n = 137,663).

Results

Among the 2,297,146 participants included, most (n = 1,518,851; 66.1%) were 40–64 years of age (median 57 years of age), were citizens of Spain (88.8%), and had few comorbidities (Table). Persons living in more deprived areas were younger, less frequently citizens of Spain, and had more comorbidities than those living in the least deprived ones (Appendix Table 2). Persons excluded because of missing data on SDI were slightly younger (median age 55 years), more frequently from Europe and North America, and less frequently from Asia and Oceania than those without missing data on SDI (Appendix Table 3). Compared with those in the vaccine coverage dataset (i.e., with complete follow-up), persons with incomplete follow-up (lost to follow-up) (n = 38,280; 1.7%) were older (median age 69 years), were less frequently citizens of Spain (80.3%), and had more comorbidities (Appendix Table 4). For 51.5% of that population, death was the reason patients were lost to follow-up.

Vaccination Coverage and COVID-19 Infections, Hospitalizations, and Deaths at Study End

Six months after vaccine rollout, among those with complete follow-up (n = 2,258,866), 82.0% had been vaccinated. Vaccination coverage was highest among older persons (≥80 years; 92.6%), women (83.5%), those living in the least deprived areas (84.6% for Q1 vs. 76.7% for Q5), and those with comorbidities (e.g., 92.7% among persons with dementia) (Table). Vaccination coverage was particularly low among persons of other nationality: ≈60% for those from western Europe and America and <50% for those from Africa, Asia, and Oceania and from eastern Europe.

During September 1, 2020–June 30, 2021, a total of 134,966 (5.9%) persons were infected with COVID-19; of those, 16,921 (0.7%) were hospitalized for COVID-19, and 1,881 (0.1%) died (Table). Cases of COVID-19 were highest among younger persons, 40–49 years of age (6.8%), followed by those ≥80 years of age (4.9%); COVID-19 was also more common among migrants from Central and South America (9.1%) and Africa (7.5%) than for citizens of Spain (5.8%) and in the most deprived areas (6.8% for Q5) than the least deprived (5.3% for Q1). Conversely, hospitalizations were highest among the eldest (≥80 years; 1.5%), men (0.9%), those from Central and South America (1.1%), those with comorbidities (e.g., 1.8% among those with renal impairment), and those from the most deprived areas (0.9% for Q5 vs. 0.6% for Q1). Death rates were overall similar by sex, nationality, and SDI quintile but were higher among the eldest (0.6%) and those with comorbidities.

Trends in Vaccination Coverage and COVID-19 Infection, Hospitalization, and Death over Time

Among participants ≥65 years of age, vaccination coverage over time was similar across all SDI quintiles, whereas in those 40–64 years of age we observed a pattern of lower vaccination coverage in areas with increased socioeconomic deprivation (Figure 2). Regarding COVID-19 outcomes, IR of infection peaked in mid-October 2020 and mid-January 2021 and plateaued after March 2021. We observed a similar pattern for COVID-19 hospitalizations and deaths. Infection rates were higher among those 40–64 years of age, whereas hospitalization and death rates were higher among those ≥65 years of age. Overall, we observed a pattern of higher IR of infection and hospitalization in areas with increased socioeconomic deprivation among both age groups for the IR peaks. As for COVID-19 deaths, we found those living in the most deprived areas had the the higher IR for those peaks, without a clear pattern of increased IR with increased socioeconomic deprivation. After March 2021, differences by SDI quintile for all COVID-19 outcomes were less obvious, because IR of infection, hospitalization, and death were much lower.

Associations between SDI Quintile and Nonvaccination

Compared with persons ≥65 years of age living in the least deprived areas (Q1), those living in Q2, Q3, and Q4 areas had a lower probability of nonvaccination. In Q2 areas, OR was 0.97 (95% CI 0.95–1.00); in Q3 areas, 0.93 (95% CI 0.90–0.95); in Q4 areas, 0.90 (95% CI 0.88–0.93); and in Q5 areas, 1.01 (95% CI 0.99–1.04) (Figure 3; Appendix Figure 2). Conversely, among those 40–64 years of age, we found increased odds of nonvaccination for persons living in more deprived areas. For instance, when compared with those living

Table. Population characteristics in study of socioeconomic inequalities in COVID-19 vaccination and infection, Catalonia, Spain, 2020–2021*

Characteristic	Population	Vaccinated†	Infected with COVID-19	Hospitalized with COVID-19	COVID-19–related death
Total	2,297,146 (100.0)	1,852,361 (82.0)	134,966 (5.9)	16,921 (0.7)	1,881 (0.1)
Loss to follow-up	38,280 (1.7)	0	3,580 (9.4)	1,779 (4.6)	1,881 (4.9)
Median age, y (IQR)	57 (48–69)	59 (49–71)	54 (47–66)	66 (55–77)	84 (76–89)
Age category, y					
40–49	694,924 (30.3)	481,716 (70.2)	47,121 (6.8)	2,330 (0.3)	10 (0.0)
50–59	582,558 (25.4)	473,371 (82.1)	38,092 (6.5)	3,530 (0.6)	64 (0.0)
60–69	450,173 (19.6)	385,155 (86.6)	23,525 (5.2)	3,815 (0.8)	162 (0.0)
70–79	345,152 (15.0)	316,244 (93.2)	15,221 (4.4)	3,793 (1.1)	402 (0.1)
≥80	224,339 (9.8)	195,875 (92.6)	11,007 (4.9)	3,453 (1.5)	1,243 (0.6)
Sex					
F	1,200,296 (52.3)	987,415 (83.5)	71,185 (5.9)	7,262 (0.6)	802 (0.1)
M	1,096,850 (47.7)	864,946 (80.4)	63,781 (5.8)	9,659 (0.9)	1,079 (0.1)
Nationality					
Spain	2,040,130 (88.8)	1,726,192 (85.9)	117,423 (5.8)	14,864 (0.7)	1,833 (0.1)
Africa	69,086 (3.0)	30,053 (44.8)	5,161 (7.5)	580 (0.8)	13 (0.0)
Central & South America	70,312 (3.1)	40,287 (59.2)	6,368 (9.1)	740 (1.1)	10 (0.0)
Asia & Oceania	47,906 (2.1)	21,888 (46.9)	3,063 (6.4)	443 (0.9)	10 (0.0)
Eastern Europe	34,803 (1.5)	13,015 (38.4)	1,674 (4.8)	177 (0.5)	<5
Western Europe & North America	34,909 (1.5)	20,926 (61.9)	1,277 (3.7)	117 (0.3)	12 (0.0)
SDI quintile					
Q1	478,380 (20.8)	397,672 (84.6)	25,441 (5.3)	2,748 (0.6)	345 (0.1)
Q2	469,833 (20.5)	387,994 (83.8)	26,302 (5.6)	3,123 (0.7)	370 (0.1)
Q3	465,245 (20.3)	378,990 (82.7)	26,955 (5.8)	3,393 (0.7)	389 (0.1)
Q4	453,924 (19.8)	364,672 (81.7)	27,154 (6.0)	3,604 (0.8)	382 (0.1)
Q5	429,764 (18.7)	323,033 (76.7)	29,114 (6.8)	4,053 (0.9)	395 (0.1)
Comorbidities					
Asthma	141,725 (6.2)	118,256 (84.7)	9,344 (6.6)	1,373 (1.0)	134 (0.1)
Autoimmune disease	58,146 (2.5)	50,527 (88.6)	3,470 (6.0)	607 (1.0)	101 (0.2)
COPD	119,845 (5.2)	105,236 (91.4)	6,497 (5.4)	1,999 (1.7)	403 (0.3)
Dementia	30,223 (1.3)	24,747 (92.7)	2,082 (6.9)	597 (2.0)	314 (1.0)
Heart disease	402,389 (17.5)	353,597 (90.8)	22,829 (5.7)	5,696 (1.4)	1,172 (0.3)
Hypertension	775,420 (33.8)	681,602 (90.0)	43,425 (5.6)	9,319 (1.2)	1,498 (0.2)
Obesity	515,509 (22.4)	435,893 (85.9)	34,914 (6.8)	6,619 (1.3)	626 (0.1)
Malignant neoplastic disease	264,658 (11.5)	233,327 (91.4)	14,285 (5.4)	3,165 (1.2)	677 (0.3)
Renal impairment	169,947 (7.4)	149,516 (92.5)	9,690 (5.7)	3,131 (1.8)	840 (0.5)
Type 2 diabetes	288,188 (12.5)	251,117 (89.7)	17,689 (6.1)	4,637 (1.6)	758 (0.3)

*Values are no. (%) except as indicated. Study population as of September 1, 2020, We noted characteristics overall and by vaccination, COVID-19 infection, hospitalization, and death status over follow-up period. Quintiles listed from least deprived (Q1) to most deprived (Q5). COPD, chronic obstructive pulmonary disease; IQR, interquartile range; SDI, Socioeconomic Deprivation Index.
†Among those with complete follow-up, n = 2,258,866.

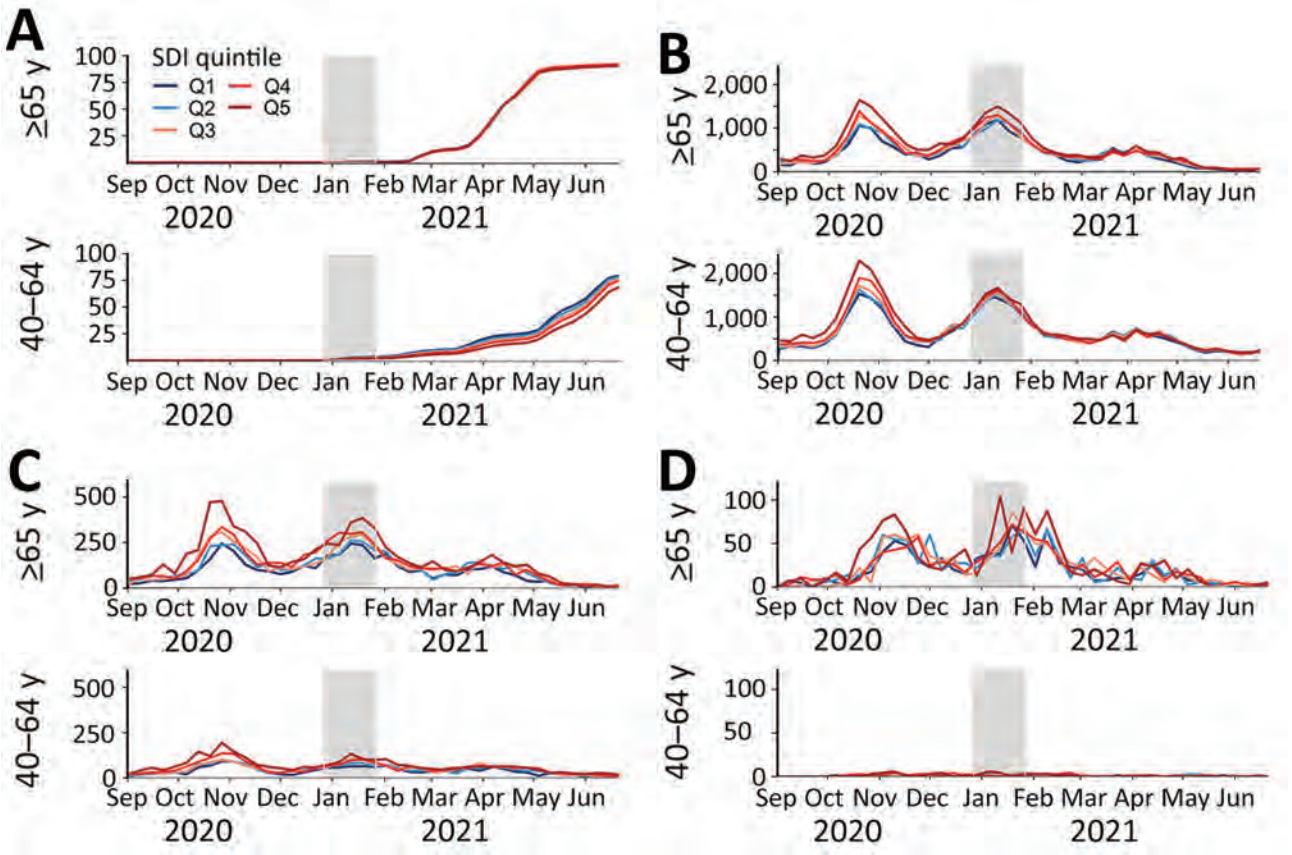

Figure 2. Vaccination coverage and incidence rates of COVID-19 infection, hospitalization, and death over time by SDI quintile and age group in study of socioeconomic inequalities in COVID-19 vaccination and infection, Catalonia, Spain, 2020–2021. Only persons with complete follow-up were included to estimate vaccination coverages. Gray area shows the first month after the start of vaccine rollout (December 27, 2020). Q1 represents the least deprived quintile, Q5 the most deprived. A) Vaccination coverage by age group, shown as percentage of population. B) COVID-19 infections by age group, shown as incidence rate per 100,000 person-years. C) COVID-19 hospitalizations, shown as incidence rate per 100,000 person-years. COVID-19–related deaths, shown as incidence rate per 100,000 person-years. Q, quintile; SDI, Socioeconomic Deprivation Index.

in Q1 areas, OR of nonvaccination was 1.01 (95% CI 1.00–1.02) in Q2 areas, 1.08 (95% CI 1.07–1.10) in Q3 areas, 1.11 (95% CI 1.10–1.13) in Q4 areas, and 1.33 (95% CI 1.31–1.35) in Q5 areas. Sensitivity analyses excluding persons with a COVID-19 infection before vaccination (n = 124,522) were consistent with our main analyses (Appendix Figure 3).

Association between SDI Quintile and COVID-19 Outcomes

Three months before vaccine rollout, we observed a pattern of increased HR of COVID-19 infection in more deprived areas in both age groups (Figure 4; Appendix Table 5). For example, among those ≥65 years of age, HR was 1.12 (95% CI 1.07–1.18) for those living in Q2 areas, 1.19 (95% CI 1.13–1.25) in Q3 areas, 1.26 (95% CI 1.20–1.32) in Q4 areas, and 1.54 (95% CI 1.46–1.61) in Q5 areas. A similar pattern was seen for COVID-19 hospitalizations among both age groups, with larger inequalities. Among persons ≥65 years of age, HR was 1.25 (95% CI 1.12–1.39) for those living in Q2 areas, 1.37 (95% CI 1.23–1.52) in Q3 areas, 1.53 (95% CI 1.38–1.70) in Q4 areas, and 1.99 (95% CI 1.80–2.19) in Q5 areas. Conversely, this pattern was not apparent for COVID-19–related deaths among persons ≥65 years of age; rates were only higher for those living in Q5 areas (HR 1.71 [95% CI 1.36–2.17]). We did not estimate models for death among persons 40–64 years of age because we observed <5 events in some SDI quintiles.

In the period 1–6 months after vaccine rollout, inequalities decreased in both age groups compared with the period before vaccine rollout (Figure 4: Appendix Table 5). Inequalities were still noticeable among those ≥65 years of age; HR was 1.08 (95% CI 1.02–1.14] for those living in Q2 areas, 1.09 (95% CI 1.03–1.15) in Q3 areas, 1.10 (95% CI 1.03–1.16) in Q4 areas, and 1.23 (95% CI 1.16–1.31) in Q5 areas. Conversely, among those 40–64 years of age, only those living in the most deprived

areas had higher rates of infection (Q5 HR 1.04 [95% CI 1.00–1.08]). Regarding hospitalizations, inequalities by SDI quintile remained in both age groups, although they decreased among those ≥65 years of age: HR was 1.17 (95% CI 1.04–1.32) for those living in Q2 areas, 1.27 (95% CI 1.14–1.43) in Q3 areas, 1.29 (95% CI 1.15–1.45) in Q4 areas, and 1.52 (95% CI 1.36–1.71) in Q5 areas. Similarly, rates of COVID-19-related deaths among those ≥65 years of age in Q5 areas moderately decreased; HR was 1.36 (95% CI 1.02–1.82).

In sensitivity analyses restricting participants to citizens of Spain, results were also consistent with our main analyses (Appendix Figure 4). In the period 3–6 months after vaccine rollout, results were overall similar to our main analysis, although among those ≥65 years of age, inequalities in hospitalizations were more apparent than 1–6 months after vaccine rollout. HR for hospitalizations 3–6 months after vaccine rollout were 1.33 (95% CI 1.10–1.60) for those living in Q2 areas, 1.47 (95% CI 1.23–1.77 in Q3 areas, 1.42 (95% CI 1.18–1.71) in Q4 areas, and 1.71 (95% CI 1.42–2.06) in Q5 areas (Appendix Table 6).

Discussion

In this cohort study comprising >2 million adults living in urban areas of Catalonia, Spain, vaccination coverage was high (>80%) 6 months after the COVID-19 vaccine rollout. However, coverage differed by SDI quintile for place of residence; coverage was 85% in the least deprived areas and 77% in the most deprived areas. Among retirement-age persons (≥65 years), SDI quintile was not associated with vaccination, whereas among working-age persons (40–64 years), nonvaccination increased among those living in more deprived areas. Three months before vaccine rollout, we found a pattern of increased rates of COVID-19 infection and hospitalization among retirement-age and working-age persons living in more deprived areas. However, 6 months after rollout, socioeconomic inequalities in COVID-19 infection substantially decreased among both age groups, whereas inequalities in COVID-19 hospitalization moderately decreased only among retirement-age persons.

Surveys assessing inequalities in willingness to vaccinate (mostly conducted before vaccine rollout or shortly after) found conflicting results across countries (*21*–*23*). A study of 13,000 participants from 19 countries reported that younger age was associated with less willingness to vaccinate in the United Kingdom, Sweden, and Spain, whereas the opposite was observed in China (*22*). Conversely, higher education levels were associated with more willingness to vaccinate in the United States, France, and Germany, but not in Spain or the United Kingdom (*23*). Regarding COVID-19 vaccination coverage, studies are mostly limited to the United Kingdom (*7*,*24*,*25*) and the United States (*10*,*26*,*27*). However, these studies consistently found lower vaccination rates among persons with low socioeconomic status (*7*,*10*,*24*–*27*). This finding is also in line with prior evidence in relation to other vaccines (*28*,*29*). We found an association between higher socioeconomic deprivation and nonvaccination only among working-age persons. Differences

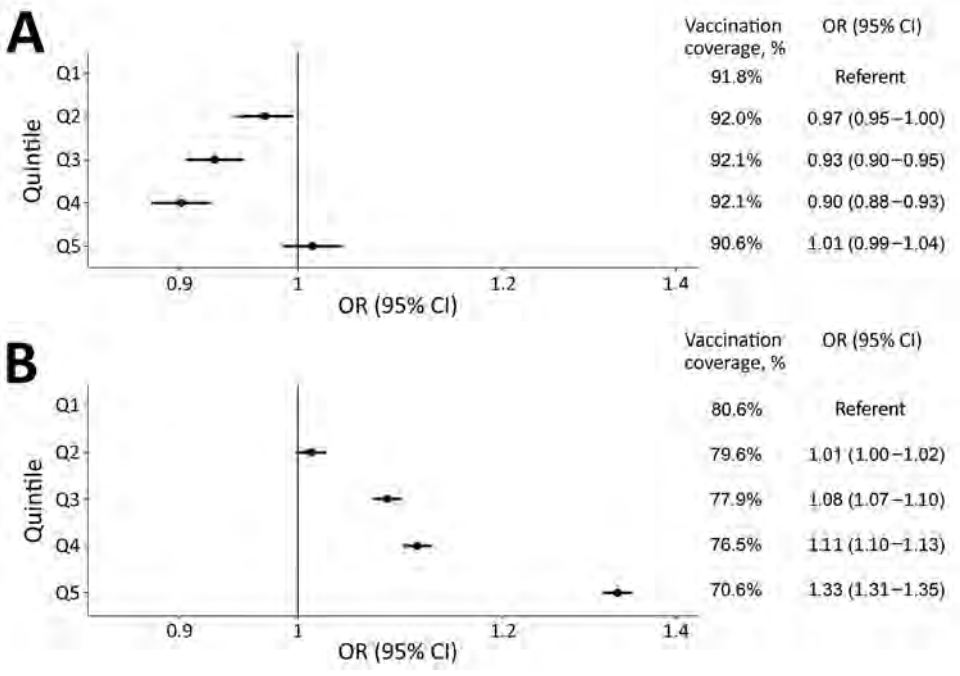

Figure 3. Odds ratios of nonvaccination 6 months after the start of COVID-19 vaccine rollout by Socioeconomic Deprivation Index quintile, stratified by age group, in study of socioeconomic inequalities in COVID-19 vaccination and infection, Catalonia, Spain, 2020–2021. A) OR for retirement-age persons ≥65 years of age. B) OR for working-age persons 40–64 years of age. Q1, the referent quintile, represents the least deprived areas; Q5, the most deprived. Persons with complete follow-up (n = 2,258,866) after vaccination were included. Models are adjusted for age, sex, and nationality. Dots indicate OR; bars, 95% CI. OR, odds ratio; Q, quintile.

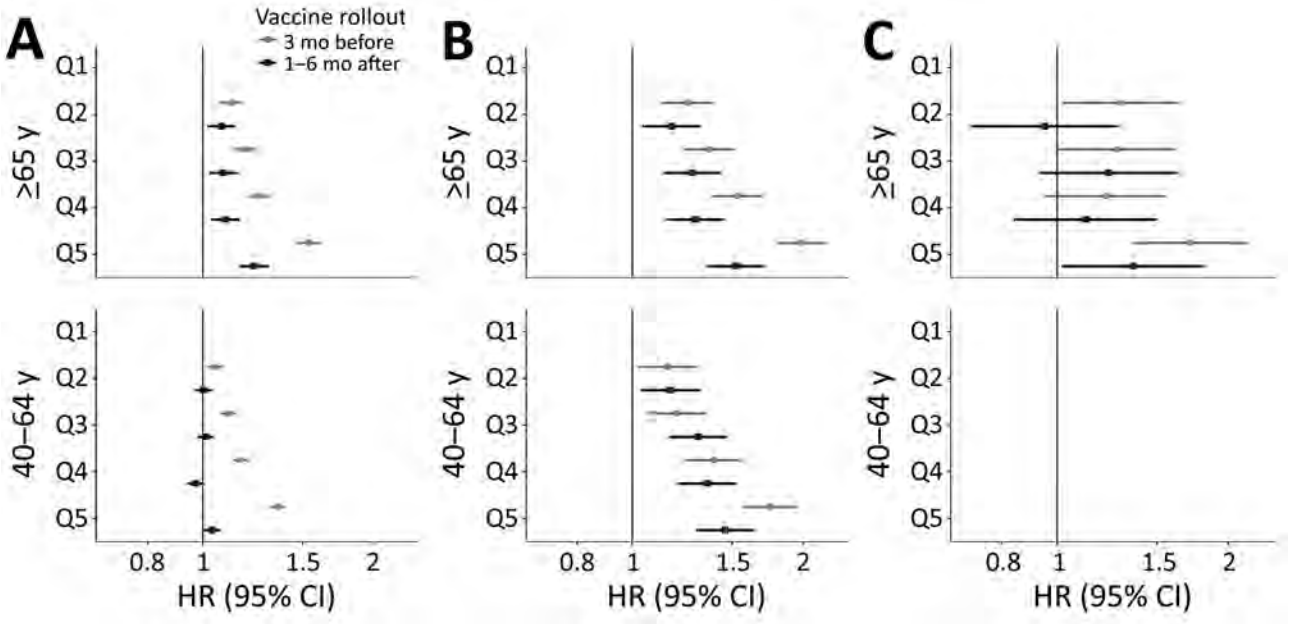

Figure 4. Fully adjusted hazard ratios of COVID-19 infection (A), hospitalization (B), and death (C) before and after vaccine rollout, by Socioeconomic Deprivation Index quintile and stratified by age group, in study of socioeconomic inequalities in COVID-19 vaccination and infection, Catalonia, Spain, 2020–2021. Q1, the referent quintile, represents the least deprived areas; Q5, the most deprived. Vaccine rollout started on December 27, 2020. Models before vaccine rollout are from September 1–December 26, 2020. Models after vaccine rollout are from January 27–June 30, 2021. All models are adjusted for age, sex, and nationality. Models in which the number of events for ≥1 deprivation area was <5 were not estimated. Dots indicate OR; bars, 95% CI. Q, quintile. HR, hazard ratio.

by age group could be related to working conditions (i.e., unavailability to miss work to vaccinate), as well as to an enhanced COVID-19 risk perception among older persons, who have a higher risk for severe disease (*22*,*30*). Unlike our study, UK studies also observed inequalities in coverage among the elderly (*7*,*25*). Differences in the development of the pandemic, the vaccination campaign, or cultural perspectives across countries might explain these discrepancies. Spain was severely hit by the first wave of the pandemic (*17*) and is one of the countries with the highest COVID-19 vaccination coverages (*31*). Furthermore, Spain is a country with traditionally high levels of vaccine confidence and with high vaccination coverages overall (*32*).

Inequalities among working-age persons are concerning, because those with low socioeconomic status are more likely to be exposed to infection because of poorer working and housing conditions and to develop severe disease because of poorer health status (*4*,*33*). Those findings are consistent with our findings before vaccine rollout, as well as with prior evidence from the United States and Europe, including Spain (*3*,*34*,*35*). In July–November 2020 the risk ratio of COVID-19 infection in residents of the poorest areas of Barcelona, the capital of Catalonia, was 1.67 (95% CI 1.41–196) in men and 1.71 (95% CI 1.44–1.99) in women, in line with our findings (*35*).

Despite inequalities in vaccination coverage, socioeconomic inequalities for COVID-19 infection decreased 6 months after vaccine rollout among both age groups, suggesting that vaccines reduced inequalities partly through mechanisms of herd immunity (*36*). Conversely, inequalities in hospitalizations decreased, although they still persisted, only among retirement-age persons. This finding highlights the importance of addressing vaccine inequalities among working-age persons. Persisting inequalities among the retirement-age persons might be related to differences in the risk for severe COVID-19 once infected because we found that those living in more deprived areas have more comorbidities and, thus, higher risk for complications (*33*). In addition to nationwide vaccination campaigns, strategies addressing structural inequalities are needed to reduce the burden of COVID-19–related outcomes among those most vulnerable (*6*).

The main strength of this study is the nature of our database, which encompasses ≈75% of the population of Catalonia. In addition, our data include a complete record of vaccines administered and of COVID-19 tests performed at public healthcare facilities. This study provides novel evidence regarding the associations between socioeconomic deprivation and COVID-19 infection, hospitalization, and death before and after the COVID-19 vaccine rollout in a country in southern Europe.

The first limitation of our study is that, although area-based indices of socioeconomic deprivation are widely used in epidemiologic studies, our results should be interpreted with caution considering the risks of ecologic bias. Second, we lacked information on occupation, which would have been of interest to have a better understanding of our results among working-age persons; a UK study reported lower vaccination coverage among persons working in manual occupations (*37*). Last, our results might not be generalizable to other contexts because of differences across countries, although they provide insights into the effects on socioeconomic COVID-19 inequalities of a mass vaccination campaign in a high-income country with high access to vaccination.

Despite socioeconomic inequalities in vaccination coverage, our results show that inequalities in COVID-19 infection and hospitalization in urban areas decreased but still persisted 6 months after the start of vaccine rollout in Catalonia. Our findings show that mass COVID-19 vaccination reduced COVID-19-related inequalities and emphasize the need to pursue efforts to vaccinate all population subgroups.

Acknowledgments

We thank all healthcare professionals in Catalonia who daily register information in the populations' electronic health records. We also want to thank the Institut Català de la Salut (ICS) and the Programa d'analítica de dades per a la recerca i la innovació en salut (PADRIS) for providing access to the different data sources accessible through SIDIAP.

This study was carried out as part of the doctoral program in methodology of biomedical research and public health at the Autonomous University of Barcelona. This work was supported by Instituto de Salud Carlos III (grant no. CM20/00174 to E.R. and CP21/00023 to T.D.S.) and by the National Institute for Health Research (grant no. SRF-2018-11-ST2-004 to D.P.A.). The funders of the study had no role in study design, data collection, analysis, and interpretation, or writing of the report.

D.P.A.'s research group has received grant support from Amgen, Chesi-Taylor, Novartis, and UCB Biopharma; D.P.A.'s department has received advisory or consultancy fees from Amgen, Astellas, AstraZeneca, Johnson and Johnson, and UCB Biopharma; as well as fees for speaker services from Amgen and UCB; Janssen, on behalf of IMI-funded EHDEN and EMIF consortiums, and Synapse Management Partners have supported training programs organized by D.P.A.'s department and open for external participants. No other relationships or activities that could do so appear to have influenced the submitted work accuracy of the data analysis.

About the Author

Dr. Roel is a medical doctor specialized in preventive medicine and public health. She is currently a predoctoral researcher at Fundació Institut Universitari per a la recerca a l'Atenció Primària de Salut Jordi Gol i Gurina (IDIAPJGol), Barcelona, Spain. Her thesis focuses on the use of real-world data to fill evidence gaps in the field of COVID-19.

References

1. World Health Organization. COVID-19 weekly epidemiological update. 2022 [cited 2022 Sep 22]. https://www.who.int/publications/m/item/weekly-epidemiological-update-on-covid-19---29-june-2022
2. Paremoer L, Nandi S, Serag H, Baum F. COVID-19 pandemic and the social determinants of health. BMJ. 2021;372:n129. https://doi.org/10.1136/bmj.n129
3. Mathur R, Rentsch CT, Morton CE, Hulme WJ, Schultze A, MacKenna B, et al.; OpenSAFELY Collaborative. Ethnic differences in SARS-CoV-2 infection and COVID-19-related hospitalisation, intensive care unit admission, and death in 17 million adults in England: an observational cohort study using the OpenSAFELY platform. Lancet. 2021;397:1711–24. https://doi.org/10.1016/S0140-6736(21)00634-6
4. Marmot M, Allen J, Goldblatt P, Herd E, Morrison J. Build back fairer: the COVID-19 Marmot review. London: Institute of Health Equity; 2020 [cited 2022 Sep 22]. https://www.health.org.uk/publications/build-back-fairer-the-covid-19-marmot-review
5. Hughes MM, Wang A, Grossman MK, Pun E, Whiteman A, Deng L, et al. County-level COVID-19 vaccination coverage and social vulnerability—United States, December 14, 2020–March 1, 2021. MMWR Morb Mortal Wkly Rep. 2021;70:431–6. https://doi.org/10.15585/mmwr.mm7012e1
6. Haque Z. Vaccine inequality may undermine the booster programme. BMJ. 2021;375:n3118. https://doi.org/10.1136/bmj.n3118
7. Curtis HJ, Inglesby P, Morton CE, MacKenna B, Green A, Hulme W, et al.; The OpenSAFELY Collaborative. Trends and clinical characteristics of COVID-19 vaccine recipients: a federated analysis of 57.9 million patients' primary care records in situ using OpenSAFELY. Br J Gen Pract. 2021;72:e51–62. https://doi.org/10.3399/BJGP.2021.0376
8. Mutebi N. COVID-19 vaccine coverage and targeted interventions to improve vaccination uptake. 2021 [cited 2022 Feb 8]. https://post.parliament.uk/covid-19-vaccine-coverage-and-targeted-interventions-to-improve-vaccination-uptake
9. Ministry of Housing Communities and Local Government. National statistics: English indices of deprivation 2019. Vol. 2019, Ministry of Housing, Communities & Local Government. 2019 [cited 2022 Feb 8]. https://www.gov.uk/government/statistics/english-indices-of-deprivation-2019
10. Barry V, Dasgupta S, Weller DL, Kriss JL, Cadwell BL, Rose C, et al. Patterns in COVID-19 vaccination coverage, by social vulnerability and urbanicity—United States, December 14, 2020–May 1, 2021. MMWR Morb Mortal Wkly Rep. 2021;70:818–24. https://doi.org/10.15585/mmwr.mm7022e1
11. Inter-territorial Council of the National Health System. COVID-19 vaccination strategy in Spain. Vol. 1. 2021 [cited 2022 Feb 8]. https://www.sanidad.gob.es/profesionales/saludPublica/prevPromocion/vacunaciones/covid19/Actualizaciones_Estrategia_Vacunacion/docs/COVID-19_Actualizacion7_EstrategiaVacunacion.pdf

12. Institute of Statistics of Catalonia. COVID-19 vaccination. 2022 [cited 2022 Feb 8]. https://www.idescat.cat/indicadors/?lang=es&id=conj&n=14357
13. Recalde M, Rodrıguez C, Burn E, Far M, García D, Carrere-Molina J, et al. Data resource profile: the Information System for Research in Primary Care (SIDIAP). Int J Epidemiol. 2022 Apr 13 [Epub ahead of print]. https://doi.org/10.1093/ije/dyac068 https://doi.org/10.1093/ije/dyac068
14. Observational Health Data Sciences and Informatics. The book of OHDSI. 2019 [cited 2022 Feb 8]. https://ohdsi.github.io/TheBookOfOhdsi/TheBookOfOhdsi.pdf
15. Bolíbar B, Fina Avilés F, Morros R, Garcia-Gil MM, Hermosilla E, Ramos R, et al.; Grupo SIDIAP. SIDIAP database: electronic clinical records in primary care as a source of information for epidemiologic research [in Spanish]. Med Clin (Barc). 2012;138:617–21.
16. Domínguez-Berjón MF, Borrell C, Cano-Serral G, Esnaola S, Nolasco A, Pasarín MI, et al. Constructing a deprivation index based on census data in large Spanish cities (the MEDEA project) [in Spanish]. Gac Sanit. 2008;22:179–87.
17. Henríquez J, Gonzalo-Almorox E, García-Goñi M, Paolucci F. The first months of the COVID-19 pandemic in Spain. Health Policy Technol. 2020;9:560–74. https://doi.org/10.1016/j.hlpt.2020.08.013
18. Austin PC. Using the standardized difference to compare the prevalence of a binary variable between two groups in observational research. Commun Stat Simul Comput. 2009;38:1228–34. https://doi.org/10.1080/03610910902859574
19. Greenland S, Pearl J, Robins JM. Causal diagrams for epidemiologic research. Epidemiology. 1999;10:37–48. https://doi.org/10.1097/00001648-199901000-00008
20. Griffith GJ, Morris TT, Tudball MJ, Herbert A, Mancano G, Pike L, et al. Collider bias undermines our understanding of COVID-19 disease risk and severity. Nat Commun. 2020;11:5749. https://doi.org/10.1038/s41467-020-19478-2
21. Sherman SM, Smith LE, Sim J, Amlôt R, Cutts M, Dasch H, et al. COVID-19 vaccination intention in the UK: results from the COVID-19 vaccination acceptability study (CoVAccS), a nationally representative cross-sectional survey. Hum Vaccin Immunother. 2021;17:1612–21. https://doi.org/10.1080/21645515.2020.1846397
22. Brailovskaia J, Schneider S, Margraf J. To vaccinate or not to vaccinate!? Predictors of willingness to receive COVID-19 vaccination in Europe, the U.S., and China. PLoS One. 2021;16:e0260230. https://doi.org/10.1371/journal.pone.0260230
23. Lazarus JV, Wyka K, Rauh L, Rabin K, Ratzan S, Gostin LO, et al. Hesitant or not? The association of age, gender, and education with potential acceptance of a COVID-19 vaccine: a country-level analysis. J Health Commun. 2020;25:799–807. https://doi.org/10.1080/10810730.2020.1868630
24. Perry M, Akbari A, Cottrell S, Gravenor MB, Roberts R, Lyons RA, et al. Inequalities in coverage of COVID-19 vaccination: a population register based cross-sectional study in Wales, UK. Vaccine. 2021;39:6256–61. https://doi.org/10.1016/j.vaccine.2021.09.019
25. Nafilyan V, Dolby T, Razieh C, Gaughan CH, Morgan J, Ayoubkhani D, et al. Sociodemographic inequality in COVID-19 vaccination coverage among elderly adults in England: a national linked data study. BMJ Open. 2021;11:e053402. https://doi.org/10.1136/bmjopen-2021-053402
26. Green-McKenzie J, Shofer FS, Momplaisir F, Kuter BJ, Kruse G, Bialal U, et al. Factors associated with COVID-19 vaccine receipt by health care personnel at a major academic hospital during the first months of vaccine availability. JAMA Netw Open. 2021;4:e2136582–2136582. https://doi.org/10.1001/jamanetworkopen.2021.36582
27. Cole MB, Raifman JR, Assoumou SA, Kim JH. Assessment of administration and receipt of COVID-19 vaccines by race and ethnicity in US federally qualified health centers. JAMA Netw Open. 2022;5:e2142698–e2142698. https://doi.org/10.1001/jamanetworkopen.2021.42698 PMID: 35006248 https://doi.org/10.1001/jamanetworkopen.2021.42698
28. Public Health England. National Immunisation Programme: health equity audit. 2021 [cited 2022 Feb 8]. https://assets.publishing.service.gov.uk/government/uploads/system/uploads/attachment_data/file/957670/immnstn-equity_AUDIT_v11.pdf
29. Arat A, Burström B, Östberg V, Hjern A. Social inequities in vaccination coverage among infants and pre-school children in Europe and Australia—a systematic review. BMC Public Health. 2019;19:290. https://doi.org/10.1186/s12889-019-6597-4
30. Burn E, Tebé C, Fernandez-Bertolin S, Aragon M, Recalde M, Roel E, et al. The natural history of symptomatic COVID-19 during the first wave in Catalonia. Nat Commun. 2021;12:777. https://doi.org/10.1038/s41467-021-21100-y
31. Mathieu E, Ritchie H, Ortiz-Ospina E, Roser M, Hasell J, Appel C, et al. A global database of coronavirus (COVID-19) vaccinations. Nat Hum Behav. 2020;5:947–53 [cited 2022 Feb 8]. https://ourworldindata.org/covid-vaccinations
32. Antonini M, Eid MA, Falkenbach M, Rosenbluth ST, Prieto PA, Brammli-Greenberg S, et al. An analysis of the COVID-19 vaccination campaigns in France, Israel, Italy, and Spain and their impact on health and economic outcomes. Heal Policy Technol. 2022;11:100594. https://doi.org/10.1016/j.hlpt.2021.100594 https://doi.org/10.1016/j.hlpt.2021.100594
33. Campos-Matos I, Mandal S, Yates J, Ramsay M, Wilson J, Lim WS. Maximising benefit, reducing inequalities and ensuring deliverability: prioritisation of COVID-19 vaccination in the UK. Lancet Reg Heal Eur. 2021;2:100021. https://doi.org/10.1016/j.lanepe.2020.100021
34. Politi J, Martín-Sánchez M, Mercuriali L, Borras-Bermejo B, Lopez-Contreras J, Vilella A, et al.; COVID-19 Surveillance Working Group of Barcelona. Epidemiological characteristics and outcomes of COVID-19 cases: mortality inequalities by socio-economic status, Barcelona, Spain, 24 February to 4 May 2020. Euro Surveill. 2021;26:2001138. https://doi.org/10.2807/1560-7917.ES.2021.26.20.2001138
35. Marí-Dell'Olmo M, Gotsens M, Pasarín MI, Rodríguez-Sanz M, Artazcoz L, Garcia de Olalla P, et al. Socioeconomic inequalities in COVID-19 in a European urban area: Two waves, two patterns. Int J Environ Res Public Health. 2021;18:1–12. https://doi.org/10.3390/ijerph18031256
36. Randolph HE, Barreiro LB. Herd immunity: understanding COVID-19. Immunity. 2020;52:737–41. https://doi.org/10.1016/j.immuni.2020.04.012
37. Nafilyan V, Dolby T, Finning K, Morgan J, Edge R, Glickman M, et al. Differences in COVID-19 vaccination coverage by occupation in England: a national linked data study. Occup Environ Med. 2022 Sept 22 [Epub ahead of print]. https://doi.org/10.1136/oemed-2021-108140

Address for correspondence: Talita Duarte-Salles, Fundació Institut Universitari per a la recerca a l'Atenció Primària de Salut Jordi Gol i Gurina (IDIAPJGol), Gran Via Corts Catalanes, 587 àtic, 08007 Barcelona, Spain; email: tduarte@idiapjgol.org

Genomic Epidemiology of *Vibrio cholerae* O139, Zhejiang Province, China, 1994–2018

Yun Luo, Julian Ye, Michael Payne, Dalong Hu, Jianmin Jiang,[1] Ruiting Lan[1]

Cholera caused by *Vibrio cholerae* O139 was first reported in Bangladesh and India in 1992. To determine the genomic epidemiology and origins of O139 in China, we sequenced 104 O139 isolates collected from Zhejiang Province, China, during 1994–2018 and compared them with 57 O139 genomes from other countries in Asia. Most Zhejiang isolates fell into 3 clusters (C1–C3), which probably originated in India (C1) and Thailand (C2 and C3) during the early 1990s. Different clusters harbored different antimicrobial resistance genes and IncA/C plasmids. The integrative and conjugative elements carried by Zhejiang isolates were of a new type, differing from ICEVchInd4 and SXT^{MO10} by single-nucleotide polymorphisms and presence of genes. Quinolone resistance–conferring mutations S85L in *parC* and S83I in *gyrA* occurred in 71.2% of the Zhejiang isolates. The *ctxB* copy number differed among the 3 clusters. Our findings provided new insights for prevention and control of O139 cholera .

Cholera is an acute watery diarrheal disease that has caused 7 global pandemics since 1817. The current, ongoing seventh pandemic started in 1961 and continues today (*1*). The causative agent of cholera is *Vibrio cholerae*; serogroups O1 and O139 cause epidemic- and pandemic-level disease. Serogroup O139 first caused an outbreak in Bangladesh and India in 1992 (*2*,*3*). However, the epidemic O139 clone was later found to be a derivative of a seventh pandemic O1 strain, having had its O1 gene cluster replaced with an O139 O antigen gene cluster (*4*) and therefore genetically belonging to the seventh pandemic clone and sharing the same sequence type (*5*).

Author affiliations: Zhejiang Provincial Center for Disease Control and Prevention, Hangzhou, China (Y. Luo, J. Ye, J. Jiang); University of New South Wales, Sydney, New South Wales, Australia (Y. Luo, M. Payne, D. Hu, R. Lan); Key Laboratory of Vaccine, Hangzhou (J. Jiang)

DOI: https://doi.org/10.3201/eid2811.212066

V. cholerae O139 spread to China and was reported in Xinjiang Uygur Autonomous Region (*6*) and Guangdong Province (*7*) in 1993 and in Jiangxi Province and the cities of Beijing and Shanghai in 1994 (*8*). Most studies on O139 in China have focused on virulence and resistance-gene profiles, cholera toxin (CTX) types (*7*,*8*), and plasmid carriage (*9*). The genomic epidemiology of O139 in China and the phylogenetic relationship of isolates from China to isolates from other countries in Asia are still unknown. A study of 9 O139 isolates suggested that O139 reached China soon after outbreaks in India in early 1990s and became dominant a few years later (*10*).

Antimicrobial therapy (in addition to rehydration therapy) plays a vital role in the management of cholera patients (*11*). In a previous study of 340 O139 isolates collect in China during 1993–2009, resistances to streptomycin, trimethoprim/sulfamethoxazole, and polymyxin B were found in isolates from early years (*12*). IncA/C conjugative plasmids can effectively mobilize genes associated with resistance to different classes of antibiotics, including β-lactams, aminoglycosides, chloramphenicol, folate-pathway inhibitors, quinolones, and tetracycline (*13*). IncA/C plasmids are widely present in Enterobacterales but not common in *V. cholerae* populations (*14*), although they have been found in the seventh pandemic *V. cholerae* lineage (*11*).

In this study, we sequenced the genomes of 104 *V. cholerae* O139 isolates collected from Zhejiang Province, China, during 1994–2018. Comparative genomic and phylogenetic analyses revealed the genetic characteristics of *V. cholerae* O139 isolates in Zhejiang and their evolutionary relationships to isolates from countries in Asia. We also analyzed the virulence and antimicrobial resistance (AMR) gene profiles and the distribution of IncA/C plasmids to elucidate the evolution of virulence and AMR.

[1]These authors contributed equally to this article.

Methods

Isolates

We recovered 104 *V. cholerae* O139 isolates collected during 1994–2018 from the Zhejiang Provincial Center for Disease Control and Prevention (Zhejiang CDC). We downloaded 57 public *V. cholerae* genomes from countries in Asia (Appendix 1 Table 1, https://wwwnc.cdc.gov/EID/article/28/11/21-2066-App1.xlsx) and 133 publicly available *V. cholerae* genomes from China from the European Nucleotide Archive database (https://www.ebi.ac.uk/ena) and identified them by searching for the O139 O-antigen–specific *wbf* gene using BLASTN version 2.9.0 (*15*).

Genome Sequencing

We performed whole-genome sequencing by using the Illumina Hiseq X-ten sequencing platform with TruePrepTM DNA Library Prep Kit version 2 and 150-bp paired-end sequencing (Illumina, https://www.illumina.com). We checked all input read sets for contamination by using kraken2 with a threshold of 10% for non–*V. cholerae* reads (*16*). We submitted genome sequences obtained in this study as raw reads under the National Center for Biotechnology Information's Sequence Read Archive database (Bioproject no. PRJNA643344).

Single-Nucleotide polymorphism Calling and Phylogenetic Analyses

We identified single-nucleotide polymorphisms (SNPs) by using a section of the SaRTree (*17*) pipeline. We removed Superintegron sequences on the small chromosome and all recombinant SNPs. The reference genome sequence (GenBank accession no. GCF_900324445.1) was from Bangladesh strain 4295STDY6534216, isolated in 2014 (*18*). We allocated SNPs to each branch of the tree by using the SaRTree pipeline (*17*). We performed phylogenetic analysis by constructing a maximum-likelihood tree using IQ-Tree version 2.0.4 (*19*) under default parameters (transversion model with AG = CT and empirical base frequencies) with 1,000 bootstrap replicates.

Antimicrobial-Resistance and Virulence Genes

For all genomes, we predicted AMR genes by using ABRicate (https://github.com/tseemann/abricate) with the AMRFinderPlus gene database (*20*), plasmids by using PlasmidFinder (*21*), and virulence genes by using a customized database of 67 virulence genes (Appendix 1 Table 2). We applied a cutoff of percentage nucleotide identity at 80% for virulence genes and plasmids and at 60% for resistance genes. We used k-mer alignment (*22*) to map raw reads against all these genes. As criteria for gene presence, we used a combination of minimum identity and coverage thresholds from ABRicate or the ratio of the gene depth to the average depth of housekeeping genes >20% from KMA. We used CNVnator version 0.4.1 (*23*) with default settings and a bin size of 100 bp to calculate copy numbers of *ctxB* genes.

Results

Whole-Genome Sequencing of *V. cholerae* O139 Isolates from Zhejiang Province

We recovered and sequenced 104 *V. cholerae* O139 isolates collected during 1994 to 2018 by Zhejiang CDC (Figure 1; Appendix 1 Table 1). For comparison with other isolates from China, we included 9 published isolates from Shanghai (*10*). We used another 133 publicly available O139 genomes from China without metadata only to infer phylogenetic relationships with Zhejiang isolates. For international comparison, we included 48 publicly available O139 genomes from India (*19*), Bangladesh (*19*), and Thailand (*10*). The earliest isolates were collected in 1983 in Bangladesh; other isolates were collected during 1992–2014 (Appendix 2 Figure 1, https://wwwnc.cdc.gov/EID/article/28/11/21-2066-App2.pdf).

Phylogenetic Analysis of O139 Isolates from China and Worldwide

We identified 629 SNPs from our 104 Zhejiang O139 isolates, 9 Shanghai isolates, and 48 isolates from other countries; 501 SNPs were on chromosome I and 128 SNPs were on chromosome II. We constructed a phylogenetic tree of the 161 isolates, using N16961 as the outgroup (Figure 2; Appendix 2 Figure 2). We further identified branch-supporting SNPs (Appendix 1 Table 3; Appendix 2 Figure 3). The tree can be divided into 2 distinctive lineages, defined as lineages 1 (L1) and 2 (L2). L1 contained 11 isolates from this study and 15 isolates from Bangladesh and India. L2 contained 92 isolates from this study and 8 Shanghai isolates.

The isolates from China grouped together as 3 clusters, which were each supported by unique SNPs (Appendix 2 Figures 2, 3). Cluster 1 (C1) consisted of 11 Zhejiang isolates collected during 1996–2000 supported by 3 SNPs on branch 233. Cluster 2 (C2) consisted of 59 isolates from this study and 4 Shanghai isolates collected during 1998–2008. C2 was supported by 1 SNP on branch 49. Cluster 3 (C3) consisted of 28 isolates from this study and 4 isolates from Shanghai collected during 1998–2018. C3 was supported by

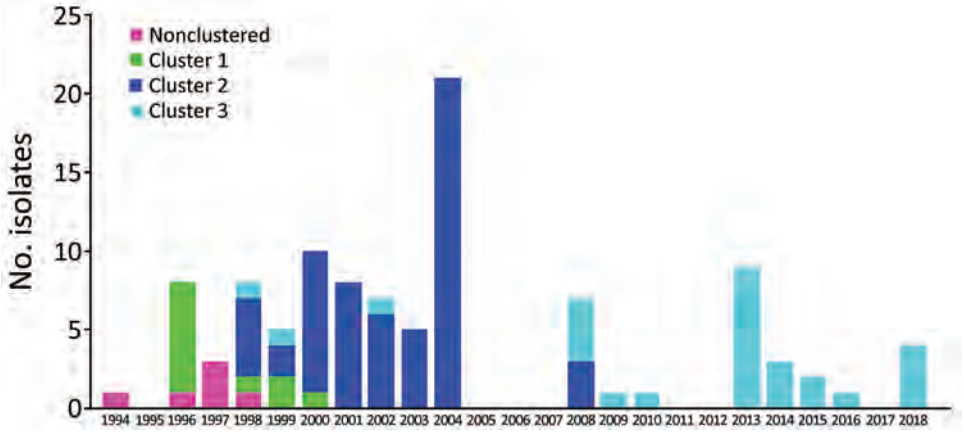

Figure 1. Distribution of *Vibrio cholerae* O139 isolates, by clusters and year of isolation, Zhejiang Province, China, 1994–2018. Bar sections represent isolate numbers in different clusters in each year (Appendix 1 Table 4, https://wwwnc.cdc.gov/EID/article/28/11/21-2066-App1.xlsx; Appendix 2 Figure 2, https://wwwnc.cdc.gov/EID/article/28/11/21-2066-App2.pdf).

1 SNP (branch 45). C1 was located within L1, whereas C2 and C3 were located within L2. The closest ancestral isolate of C1 was an isolate from India. C2 and C3 grouped together as L2, and all isolates in L2 originated in China. The L2 node was supported by 3 SNPs (branch 177), and the closest ancestral isolate of L2 was from Thailand.

Six isolates from Zhejiang fell outside of C2 and C3 and were referred to as outliers. These 6 isolates were obtained from patients in the 1990s. One isolate (V01) was isolated in 1994 from the first clinical case-patient in Zhejiang but shared a common ancestor with 1 isolate from Shanghai (isolated in 1994) and was sibling to L2.

We also constructed a phylogenetic tree of 349 genomes that included the 133 isolates from China without metadata (Appendix 2 Figure 4). The 2 lineages (L1 and L2) and 3 clusters were preserved on this tree. Most isolates from China fell into C2 (92/133 [69.2%]), 9 isolates fell into C3, and only 2 isolates fell into C1.

Genetic Elements and Virulence Genes

We searched the 104 genomes from this study by using ABRicate with our custom database of 67 known *V. cholerae* virulence genes. We further confirmed by reads mapping any genomes with a negative result for any of these virulence genes. The presence of a gene was a combined result of ABRicate searches of assembled genomes and reads mapping. Four core CTX phage genes (*ace*, *zot*, *ctxA*, and *ctxB*) and the repeat sequences were all present in 94 genomes. Three genomes (V31, V32, and V33) were all negative for these genes. The repeat sequences were not well assembled and on different contigs, whereas *ctxAB*, *zot*, and *ace* of 89/104 isolates were on the same contig.

All 104 genomes contained 19 *Vibrio* pathogenicity island genes, 18 genes on 2 *Vibrio* seventh pandemic islands, and 19 type VI secretion system–related genes. All but 1 genome contained the intact repeats-in-toxin gene cluster. (Appendix 1 Table 2). We found *Vibrio* pathogenicity island genes on the same contigs in 99/104 genomes, *Vibrio* seventh pandemic island I genes on the same contigs in 103/104 genomes, and *Vibrio* seventh pandemic island II genes on the same contigs in 104/104 genomes.

Because a strain may contain multiple copies of the CTX phage (*24*), we used CNVnator to estimate the number of copies of the *ctxB* gene in the 104 isolates by mapping reads to *V. cholerae* seventh pandemic reference genome N16961. The *ctxB* gene copies differed in the 3 clusters; on average, C2 had 4.4 copies/isolate, C3 had 1.2 copies/isolate, and C1 had 1.3 copies/isolate. A total of 68 isolates carried multiple copies of *ctxB* (range 4–22 copies) (Appendix 1 Table 2), whereas 38 isolates carried only 1 copy of *ctxB*. Most C2 isolates (81.4% [48/59]) carried >2 copies (average 5 copies) of *ctxB*. In contrast, only 3 isolates (10.7% [3/28]) in C3 carried >1 copy (average 2.6 copies), and 6 isolates (54.5% [6/11]) in C1 carried 2 copies. Six outlier isolates carried multiple copies of *ctxB* (range 2–22 copies). All 101 *ctxB*–positive isolates contained *ctxB* genotype 3.

Antimicrobial-Resistance Genes and Resistance Mutations of the O139 Isolates

We found the chromosomally encoded resistance genes *varG* and *catB9* in all isolates. *floR*, *dfr18*, *sul2*, *aph(3'')-lb*, and *aph(6)-ld* were in most of the isolates, including international isolates, and 8 AMR genes detected only in cluster 3 were present at low frequencies (3.13%–15.63%) (Table). We found bla_{TEM-1}, *catA2*, *aac(3)-lld*, *aadA2*, *aph(3')-la*, *mph(E)*, *msr(E)*, *sul*, *dfrA12*, *tet(M)*, and *tet(Y)* only in isolates from China, including Shanghai isolates, whereas bla_{CMY-2}, bla_{OXA-1}, *catB3*, *aac(6')-lb-cr5*, *aadA3*, *ere(A)*, *mph(A)*, *mph(F)*, *qnrA1*, *qnrA7*, *aar-3*,

dfrA27, *dfrA32*, *tet(A)*, *and tet(D)* were in Zhejiang isolates only (Appendix 1 Table 4). C1 carried only AMR genes common to all isolates, *aph(3')-Ia and sul1* were common to C2 and C3, *aac(3)II*, *aadA2*, *tet(D)*, *mph(E)*, *msr(E)*, bla_{TEM-1}, and *catA2* were more common in C2, and *tet(M)*, *mph(A)*, and *dfrA12* were more common in C3.

We also searched these isolates for quinolone-resistance mutations. Seventy-four isolates (74/104 [71.2%]) harbored mutations Ser85Leu in *parC* and Ser83Ile in *gyrA*. Ten isolates had a mutation in Asp87 of *gyrA*, of which 6 had Asp87Tyr, 3 had Asp87Gly, and 1 had Asp87Asn.

Association of Plasmids and Integrative and Conjugative Elements with AMR Genes

We analyzed the integrative and conjugative elements (ICEs) carried by our isolates and compared them with the 2 known ICE variants in O139 (SXT^{MO10} and ICE*Vch*Ind4) (*25*). SNP and phylogenetic analyses found that all O139 ICEs were closely related (difference of 0–13 SNPs) (Appendix 2 Figure 5). Our ICEs differed from ICEVchInd4 by 0–7 SNPs and from SXT^{MO10} by 10–13 SNPs. However, most of our isolates carried the 4 SXT^{MO10} genes, including *dfr*A18 that are absent in ICE*Vch*Ind4. The AMR genes present in our isolates, *dfr*A18, *floR*, *aph(3'')-Ib*, *aph(6)-Id*, and *sul2*, were probably carried by the ICE.

Eighty-three isolates carried an IncA/C plasmid. We found 2 IncA/C subtypes (IncA/C2_1_JN157804 type, belonging to plasmid pNDM-KN-lineage, and IncA/C_1_FJ705807 type, belonging to pRA1-lineage) (Appendix 1 Table 4). None of the C1 isolates contained an IncA/C plasmid. All except 2 C2 isolates contained an IncA/C2 plasmid (Appendix

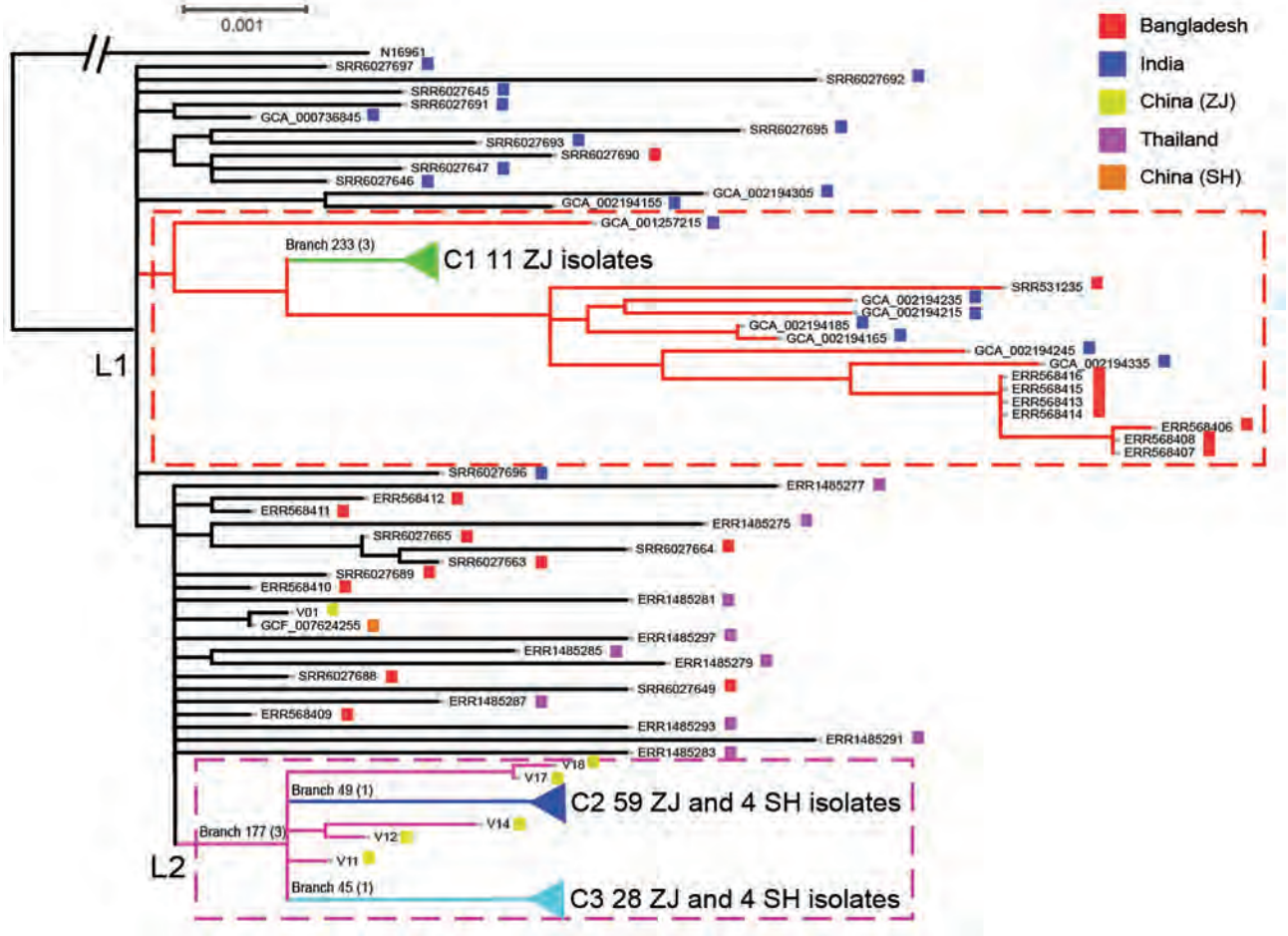

Figure 2. Maximum-likelihood phylogenetic tree of 161 *Vibrio cholerae* O139 (sequence type 69) isolates from Zhejiang Province, China, 1994–2018, and isolates from outside of China. The tree was rooted using the seventh pandemic O1 strain N16961 as an outgroup. Lineage 1 (L1) and lineage 2 (L2) are demarcated with red dashed lines and pink dashed-line boxes. The 3 clusters (C1, C2, and C3) are collapsed to reduce figure size (Appendix 2 Figure 2, https://wwwnc.cdc.gov/EID/article/28/11/21-2066-App2.pdf). Key branches are marked with a branch number followed in brackets by the number of single nucleotide polymorphisms that supported the branch. The colored solid squares at the end of isolate names indicate the location of isolation of the isolates. GenBank accession numbers were used as isolate names for O139 isolates not from Zhejiang Province. SH, Shanghai; ZJ, Zhejiang.

Table. Antimicrobial resistance gene profiles in 3 clusters of *Vibrio cholerae* O139 isolates from Zhejiang Province, China, 1994–2018, and in groups of isolates from outside of China

Gene	Cluster or group, no. (%)				
	Cluster 1, n = 11	Cluster 2, n = 63	Cluster 3, n = 32	Lineage 1 non-China, n = 15	Other* non-China, n = 33
aph (3")-Ib	11 (100)	59 (93.65)	31 (96.88)	6 (40)	33 (100)
aph (6)-Id	11 (100)	59 (93.65)	31 (96.88)	6 (40)	33 (100)
dfrA18	11 (100)	35 (55.56)	29 (90.63)	1 (6.67)	33 (100)
sul2	11 (100)	63 (100)	32 (100)	5 (33.33)	33 (100)
varG†	11 (100)	63 (100)	32 (100)	15 (100)	33 (100)
catB9†	11 (100)	63 (100)	32 (100)	15 (100)	33 (100)
floR	11 (100)	59 (93.65)	31 (96.88)	6 (40)	33 (100)
bla_{TEM-1}	0	61 (96.83)	0	0	0
aph(3')-Ia	0	57 (90.48)	23 (71.88)	0	0
aadA2	0	56 (88.89)	5 (15.63)	0	0
catA2	0	56 (88.89)	4 (12.50)	0	0
tet(D)	0	55 (87.30	9 (28.13)	0	0
sul1	0	54 (85.71)	26 (81.25)	0	0
aac(3)-IId	0	53 (84.13)	0	0	0
mph(E)	0	52 (82.54)	2 (6.25)	0	0
msr(E)	0	52 (82.54)	2 (6.25)	0	0
mph(A)	0	0	22 (68.75)	0	0
tet(M)	0	0	21 (65.63)	0	0
dfrA12	0	2 (3.17)	21 (65.63)	0	0
tet (Y)	0	5 (7.94)	2 (6.25)	0	0
aac(6')-Ib-cr5	0	0	1 (3.13)	0	0
aadA16	0	0	4 (12.50)	0	0
aadA3	0	0	4 (12.50)	0	0
arr-3	0	0	4 (12.50)	0	0
bla_{CMY-2}	0	0	1 (3.13)	0	0
bla_{OXA-1}	0	0	1 (3.13)	0	0
catB3	0	0	1 (3.13)	0	0
dfrA27	0	0	4 (12.50)	0	0
dfrA32	0	0	1 (3.13)	0	0
ere(A)	0	0	1 (3.13)	0	0
mph(F)	0	0	1 (3.13)	0	0
qnrA1	0	0	3 (9.38)	0	0
qnrA7	0	0	1 (3.13)	0	0
tet(A)	0	0	4 (12.50)	0	0

*Isolates not grouped in lineage 1 and clusters 1–3 and not isolated in China (Appendix 1 Table 4, https://wwwnc.cdc.gov/EID/article/28/11/21-2066-App1.xlsx).
†Genes that have not been associated with phenotypic resistance, determined on the basis of published data up to now.

1 Table 4). k-mer alignment analysis indicated that these C2 isolates carried a plasmid nearly identical to the known *V. cholerae* plasmid pVC1447 of 160 kb (*9*). pVC1447 is known to carry *aadA*, *sul1*, *tetD*, bla_{TEM}, *catA2*, *mph(E)*, *tet(R)*, *mel*, *qacEdelta1*, and *folP* genes (*9*). The last 4 AMR genes were not found in any of our C2 isolates. Most C2 isolates carried *aadA2*, *sul1*, *tetD*, *catA2*, *mph(E)*, *msr(E)*, and bla_{TEM}. Seven C2 isolates lost ≥1 of the AMR genes. Isolate V29 and V30 lost *sul1*, *tetD*, *mph(E)*, and *msr(E)* genes. The 2 C2 isolates without the pVC1447-like plasmid did not contain any of the pVC1447 AMR genes. All except 4 C3 isolates carried an IncA/C plasmid; 17 had the IncA/C_1_FJ705807 replicon type, and 5 had the IncA/C2_1_JN157804 replicon type. We further determined that the IncA/C_1_FJ705807 type plasmid is a novel plasmid that was most closely related to *Aeromonas veronii* plasmid p158496 (*26*), whereas the IncA/C2_1_JN157804 type plasmid was most similar to *V. cholerae* O139 pVC211 (GenBank accession no. KY399978.1). The p158496-like plasmid in the 17 C3 isolates shared an average nucleotide identity of 97.7% and length coverage of 82.89% with the 158 kb p158496 and probably carried *aadA2*, *tet(D)*, *tet(M)*, *mph(A)*, *dfrA12*, and *sul1* genes. However, more than half of these C3 isolates lost the *tet(D)* gene. Two outlier isolates (V17 and V18) also carried the p158496-like plasmid. The pVC211-like plasmid in the 5 C3 isolates shared an average nucleotide identity of 99.09% and length coverage of 92.46% with the 148 kb pVC211 plasmid and probably carried *aadA16*, *tet(A)*, *mph(A)*, *dfrA27*, *qnrA1*, and *arr-3* resistance genes. Some isolates had further loss and gain of AMR genes.

Discussion

The first *V. cholerae* O139 isolate in Zhejiang Province was reported in September 1994, which was 16 months after the first O139 case reported in China (*6*). Phylogenetic analysis grouped Zhejiang isolates into 2 independent lineages (L1 and L2) and 3 clusters (C1, C2, and C3). The origin of C1 was probably India and the origin of L2 (C2 and C3) was probably Thailand.

However, considerable uncertainty exists, as it does with L1, the sister clade of C1, which contained both India and Bangladesh isolates. Similarly, L2, which contained C2 and C3 of isolates from China only, shared a most recent common ancestor with isolates from India, Bangladesh, and Thailand. More isolates from the other countries in Asia would be required to resolve the origins of the clusters in China.

Other isolates in China also fell into the 3 Zhejiang clusters, suggesting that these clusters were circulating across China. However, because the publicly available O139 genomes from other parts of China contained no location metadata, we cannot infer whether O139 reached Zhejiang first and then spread to other parts of China or vice versa.

All isolates in this study were *ctxB* genotype 3. However, a study of isolates from south China found that a small proportion of *ctxB* genotypes 1 and 5 in isolates from the 1990s, although >90% of the isolates were *ctxB* genotype 3 (*7*). Most C2 isolates carried multiple copies of *ctxB*, suggesting that the cluster carried multiple copies of the CTX phage. The number of CTX carried by O139 may vary (*24*). In our study, we observed that the variation in the number of CTX carried occurred along lineages. The higher number of *ctx* copies might lead to greater toxin production, potentially affecting disease outcomes.

On the basis of the presence of AMR genes and resistant mutations, we determined that the evolution of resistance to antimicrobials changed substantially over time. Tetracycline resistance genes *tet*(M) and *tet*(Y) were present only in isolates in China, and *tet*(A) and *tet*(D) were only present in Zhejiang isolates. *tet*(M) was found in 65.6% of C3 isolates; some C3 isolates carried both *tet*(D) and *tet*(M). Previous studies found that O139 isolates from 1991–2013 in Thailand and from 1997 in India were susceptible to tetracycline (*27*,*28*), suggesting that the earlier O139 isolates in Asia did not carry the *tet* genes. Because tetracyclines were overused in China (*29*), it is not surprising that C2 and C3 isolates acquired tetracycline-resistance genes, and these events probably occurred in China.

mph(A) was present in 68.8% of C3 isolates only. *mph*(A) conferring azithromycin resistance is plasmid-borne and rarely found in *V. cholerae* (*30*). Azithromycin was first used in clinical treatment in 1988 (*31*). In our study, *mph*(A) was first identified in an isolate in 1998, only 10 years after azithromycin was first used for treatment. The high percentage of *mph*(A) in O139 C3 isolates in this study is concerning. However, because cholera was relatively infrequent in China, the acquisition of such resistance may not be attributable to selection pressure from clinical antimicrobial treatment.

C2 and C3 shared 2 nonsynonymous mutations, 1 each in the genes encoding for penicillin-binding protein 2 and a lytic murein transglycosylase with affinity to β-lactam antibiotic resistance (*32*). These genomic changes were previously reported in Shanghai O139 isolates and were attributed to the increasing usage of β-lactam antibiotics (*10*). These mutations were present only in isolates originating in China in L2 and may have evolved in China.

Plasmid analysis found that C2 and C3 isolates acquired different IncA/C plasmids. C2 carried a known plasmid (pVC1447), whereas C3 isolates acquired 2 different IncA/C plasmids, *A. veronii* plasmid p158496-like and *V. cholerae* pVC211-like. These plasmids were probably the carriers of the new AMR genes in different clusters and contributed to the differences of AMR gene profiles between clusters.

Although O139 spread to China in 1993 (*6*), our earliest isolates in Zhejiang were from 1994 and did not belong to any of the 3 clusters. Five more unclustered isolates were from 1996–1998, all of which belong to L2. Therefore, in early years of the O139 epidemic, multiple independent introductions of O139 cholera to Zhejiang directly from other countries or indirectly from other parts of China had probably occurred. However, the 3 clusters flourished at different times were successively replaced during 1994–2018. C1 was found in 1996 and persisted until 2000, C2 during 1998–2008, and C3 during 1998–2018. The earliest isolate from both C2 and C3 were 1998, suggesting that C2 and C3 were imported to China at similar times or a single importation of the most recent common ancestor of C2 and C3 had occurred from which the 2 clusters diverged in China. C2 became a dominant population in Zhejiang during 2000–2008 and then C3 took over from 2009, replacing the other clusters. Therefore, Zhejiang experienced O139 cholera in 3 waves caused by 3 clusters, each lasting up to a decade.

The epidemiologic pattern uncovered raises many interesting questions, most notably regarding what advantage did subsequent clusters have over their predecessor. C2 and C3 carried more resistance genes than C1. Although we have no AMR phenotypic data, difference in their AMR gene profiles suggests that AMR may have been the driver that caused C1 to be replaced by C2 and C3. C2 overall carried more copies of *ctxB*, suggesting that it may produce more CTX toxin than C3. Nearly 50% of the isolates from other parts of China from the unpublished genomes belonged to C2, suggesting that C2

was quite prevalent and more successful than C3. The increased number of copies of *ctxB* probably contributed to its success in replacing C1. However, this explanation does not account for why C2 was subsequently replaced by C3 in Zhejiang. Again, C3 acquired resistance to several additional AMR genes that may explain its fitness advantage over C2, given that *tet*(M) and *mph*(A) were only detected in C3 and *dfrA12* was mainly present in C3. In addition, the AMR genes present at low frequency in different C3 isolates may have also collectively contributed to C3's fitness. However, 63% of C2 isolates simultaneously carried *blaTEM1*, *catA2*, *aac(3)-lld*, *aadA2*, *aph(3')-la*, *sul1*, *mph(E)*, *and msr(E)* genes, a pattern not present in other clusters.

The persistence of each cluster for many years in Zhejiang is also intriguing. The clusters possibly were circulating in other parts of China and spread to Zhejiang. Most of the other isolates in China fell into C2, and Shanghai isolates were shown to be ancestral to some Zhejiang isolates within C2 and C3 (Appendix 2 Figure 2), supporting this hypothesis. Isolates may have also been continuously imported from other countries. However, we have no isolates from other countries of corresponding years to examine this hypothesis. Another possibility is that O139 has spread to the environment in Zhejiang, where it has established itself as a local reservoir. However, our extensive sampling of river waters over 2 years in 2 cities in Zhejiang only found non-O1/non-O139 isolates (*33*), although the sampling done in that study had only 2 years overlap with the isolation years of O139 isolates from those cities. Thus, it is less likely that these O139 cases were from local environmental reservoirs. A recent study of cholera in Africa also found repeated importation rather than local environmental reservoirs as the source of the seventh pandemic cholera during cholera resurgence over a 40-year period (*11*).

This study describes the possible origin, evolution, and spread of O139 cholera in a single province, Zhejiang. Further studies are required to expand this analysis to the national level. Most *V. cholerae* O139 isolates in Zhejiang grouped into 3 major clusters, which were probably derived from multiple independent importation events directly or indirectly from other countries in Asia and prevailed over the period 1994–2018, with one cluster replacing another sequentially. Variations in AMR gene content or resistance mutations suggest that acquisition of AMR probably has played a role in the succession of the *V. cholerae* O139 clusters in Zhejiang.

Acknowledgments

We thank the staff of Zhejiang CDC for their help with the isolation and conservation of the *V. cholerae* isolates used in this study. We also thank Shichang Xia for his conceptualization and support for this project. Y.L. is a PhD student supported by Australian Government Research Training Program Scholarship.

Author contributions: Y.L., J.J., and R.L. conceived of the study. J.Y. curated the data and resources. Y.L. did the data analysis and wrote the draft of the manuscript. M.P. and D.H. developed the methodology. M.P., D.L., and R.L. verified the underlying data. M.P. and R.L. reviewed and edited the manuscript. All authors reviewed and approved the final version of the manuscript. All authors had full access to all the data in this study. R.L. and J.J. had final responsibility for the decision to submit for publication.

About the Author

Ms. Luo is a PhD candidate in the School of Biotechnology and Biomolecular Sciences, University of New South Wales. Her primary research interests are the genomic epidemiology of enteric pathogens and control of infectious diseases.

References

1. Clemens JD, Nair GB, Ahmed T, Qadri F, Holmgren J. Cholera. Lancet. 2017;390:1539–49. https://doi.org/10.1016/S0140-6736(17)30559-7
2. Ramamurthy T, Garg S, Sharma R, Bhattacharya SK, Nair GB, Shimada T, et al. Emergence of novel strain of *Vibrio cholerae* with epidemic potential in southern and eastern India. Lancet. 1993;341:703–4. https://doi.org/10.1016/0140-6736(93)90480-5
3. Cholera Working Group, International Centre for Diarrhoeal Diseases Research, Bangladesh. Large epidemic of cholera-like disease in Bangladesh caused by *Vibrio cholerae* O139 synonym Bengal. Lancet. 1993;342:387–90. https://doi.org/10.1016/0140-6736(93)92811-7
4. Stroeher UH, Jedani KE, Dredge BK, Morona R, Brown MH, Karageorgos LE, et al. Genetic rearrangements in the *rfb* regions of *Vibrio cholerae* O1 and O139. Proc Natl Acad Sci U S A. 1995;92:10374–8. https://doi.org/10.1073/pnas.92.22.10374
5. Karaolis DK, Lan R, Reeves PR. The sixth and seventh cholera pandemics are due to independent clones separately derived from environmental, nontoxigenic, non-O1 *Vibrio cholerae*. J Bacteriol. 1995;177:3191–8. https://doi.org/10.1128/jb.177.11.3191-3198.1995
6. Liu J, Gao S, Gao T, Qi G, Cao X, Duan G, et al. Diarrhea outbreak by *Vibrio cholerae* O139 in Keping Xinjiang [in Chinese]. Dis Surveill. 1993;8:238–9.
7. Li BS, Xiao Y, Wang DC, Tan HL, Ke BX, He DM, et al. Genetic relatedness of selected clinical *Vibrio cholerae* O139 isolates from the southern coastal area of China over a 20-year period. Epidemiol Infect. 2016;144:2679–87. https://doi.org/10.1017/S0950268816001059
8. Zhang P, Zhou H, Diao B, Li F, Du P, Li J, et al. A molecular surveillance reveals the prevalence of *Vibrio cholerae* O139

isolates in China from 1993 to 2012. J Clin Microbiol. 2014;52:1146–52. https://doi.org/10.1128/JCM.03354-13
9. Wang R, Liu H, Zhao X, Li J, Wan K. IncA/C plasmids conferring high azithromycin resistance in *vibrio cholerae.* Int J Antimicrob Agents. 2018;51:140–4. https://doi.org/10.1016/j.ijantimicag.2017.09.009
10. Hu D, Yin Z, Yuan C, Yang P, Qian C, Wei Y, et al. Changing molecular epidemiology of *Vibrio cholerae* outbreaks in Shanghai, China. mSystems. 2019;4:e00561–19. https://doi.org/10.1128/mSystems.00561-19
11. Weill F-X, Domman D, Njamkepo E, Tarr C, Rauzier J, Fawal N, et al. Genomic history of the seventh pandemic of cholera in Africa. Science. 2017;358:785–9. https://doi.org/10.1126/science.aad5901
12. Yu L, Zhou Y, Wang R, Lou J, Zhang L, Li J, et al. Multiple antibiotic resistance of *Vibrio cholerae* serogroup O139 in China from 1993 to 2009. PLoS One. 2012;7:e38633. https://doi.org/10.1371/journal.pone.0038633
13. Carraro N, Matteau D, Burrus V, Rodrigue S. Unraveling the regulatory network of IncA/C plasmid mobilization: when genomic islands hijack conjugative elements. Mob Genet Elements. 2015;5:1–5. https://doi.org/10.1080/2159256X.2015.1045116
14. Carraro N, Rivard N, Ceccarelli D, Colwell RR, Burrus V. IncA/C conjugative plasmids mobilize a new family of multidrug resistance islands in clinical *Vibrio cholerae* non-O1/non-O139 isolates from Haiti. MBio. 2016;7:e00509–16. https://doi.org/10.1128/mBio.00509-16
15. Bhumiratana A, Siriphap A, Khamsuwan N, Borthong J, Chonsin K, Sutheinkul O. O serogroup-specific touchdown-multiplex polymerase chain reaction for detection and identification of *Vibrio cholerae* O1, O139, and non-O1/non-O139. Biochem Res Int. 2014;2014:295421. https://doi.org/10.1155/2014/295421
16. Wood DE, Salzberg SL. Kraken: ultrafast metagenomic sequence classification using exact alignments. Genome Biol. 2014;15:R46. https://doi.org/10.1186/gb-2014-15-3-r46
17. Hu D, Liu B, Wang L, Reeves PR. Living trees: high-quality reproducible and reusable construction of bacterial phylogenetic trees. Mol Biol Evol. 2020;37:563–75. https://doi.org/10.1093/molbev/msz241
18. Dorman MJ, Domman D, Uddin MI, Sharmin S, Afrad MH, Begum YA, et al. High quality reference genomes for toxigenic and non-toxigenic *Vibrio cholerae* serogroup O139. Sci Rep. 2019;9:5865. https://doi.org/10.1038/s41598-019-41883-x
19. Minh BQ, Schmidt HA, Chernomor O, Schrempf D, Woodhams MD, von Haeseler A, et al. IQ-TREE 2: new models and efficient methods for phylogenetic inference in the genomic era. Mol Biol Evol. 2020;37:1530–4. https://doi.org/10.1093/molbev/msaa015
20. Feldgarden M, Brover V, Haft DH, Prasad AB, Slotta DJ, Tolstoy I, et al. Validating the AMRFinder tool and resistance gene database by using antimicrobial resistance genotype-phenotype correlations in a collection of isolates. Antimicrob Agents Chemother. 2019;63:e00483–19. https://doi.org/10.1128/AAC.00483-19
21. Carattoli A, Zankari E, García-Fernández A, Voldby Larsen M, Lund O, Villa L, et al. In silico detection and typing of plasmids using PlasmidFinder and plasmid multilocus sequence typing. Antimicrob Agents Chemother. 2014;58:3895–903. https://doi.org/10.1128/AAC.02412-14
22. Clausen PTLC, Aarestrup FM, Lund O. Rapid and precise alignment of raw reads against redundant databases with KMA. BMC Bioinformatics. 2018;19:307. https://doi.org/10.1186/s12859-018-2336-6
23. Abyzov A, Urban AE, Snyder M, Gerstein M. CNVnator: an approach to discover, genotype, and characterize typical and atypical CNVs from family and population genome sequencing. Genome Res. 2011;21:974–84. https://doi.org/10.1101/gr.114876.110
24. Sharma C, Nair GB, Mukhopadhyay AK, Bhattacharya SK, Ghosh RK, Ghosh A. Molecular characterization of *Vibrio cholerae* O1 biotype El Tor strains isolated between 1992 and 1995 in Calcutta, India: evidence for the emergence of a new clone of the El Tor biotype. J Infect Dis. 1997;175:1134–41. https://doi.org/10.1086/516453
25. Wozniak RAF, Fouts DE, Spagnoletti M, Colombo MM, Ceccarelli D, Garriss G, et al. Comparative ICE genomics: insights into the evolution of the SXT/R391 family of ICEs. PLoS Genet. 2009;5:e1000786. https://doi.org/10.1371/journal.pgen.1000786
26. Lovero KG, Mota-Bravo L, Rasko D. Closed genome sequence of an environmental *Aeromonas veronii* strain from California, United States, with an IncA/C plasmid carrying an extended-spectrum β-lactamase gene, bla_{VEB-3}. Microbiol Resour Announc. 2022;11:e0103321. https://doi.org/10.1128/mra.01033-21
27. Siriphap A, Leekitcharoenphon P, Kaas RS, Theethakaew C, Aarestrup FM, Sutheinkul O, et al. Characterization and genetic variation of *Vibrio cholerae* isolated from clinical and environmental sources in Thailand. PLoS One. 2017;12:e0169324. https://doi.org/10.1371/journal.pone.0169324
28. Vijayalakshmi N, Rao RS, Badrinath S. Minimum inhibitory concentration (MIC) of some antibiotics against *Vibrio cholerae* O139 isolates from Pondicherry. Epidemiol Infect. 1997;119:25–8. https://doi.org/10.1017/S0950268897007553
29. Zhu Y-G, Johnson TA, Su J-Q, Qiao M, Guo G-X, Stedtfeld RD, et al. Diverse and abundant antibiotic resistance genes in Chinese swine farms. Proc Natl Acad Sci U S A. 2013;110:3435–40. https://doi.org/10.1073/pnas.1222743110
30. Mohanraj RS, Samanta P, Mukhopadhyay AK, Mandal J. Haitian-like genetic traits with creeping MIC of azithromycin in *Vibrio cholerae* O1 isolates from Puducherry, India. J Med Microbiol. 2020;69:372–8. https://doi.org/10.1099/jmm.0.001131
31. David G. Antimicrobial drugs: chronicle of a twentieth century medical triumph. First edition. Oxford: Oxford University Press; 2008.
32. Lamers RP, Nguyen UT, Nguyen Y, Buensuceso RN, Burrows LL. Loss of membrane-bound lytic transglycosylases increases outer membrane permeability and β-lactam sensitivity in *Pseudomonas aeruginosa.* MicrobiologyOpen. 2015;4:879–95. https://doi.org/10.1002/mbo3.286
33. Luo Y, Wang H, Liang J, Qian H, Ye J, Chen L, et al. Population structure and multidrug resistance of non-O1/non-O139 *Vibrio cholerae* in freshwater rivers in Zhejiang, China. Microb Ecol. 2021;82:319–33. https://doi.org/10.1007/s00248-020-01645-z

Address for correspondence: Ruiting Lan, School of Biotechnology and Biomolecular Sciences, University of New South Wales, Sydney, NSW 2052, Australia; email: r.lan@unsw.edu.au

Prevalence of Histoplasmosis among Persons with Advanced HIV Disease, Nigeria

Rita O. Oladele, Iriagbonse I. Osaigbovo, Alani S. Akanmu, Olukemi A. Adekanmbi, Bassey E. Ekeng, Yahaya Mohammed, Mary A. Alex-Wele, Mark O. Okolo, Stephen T. Ayanbeku, Uchechukwu S. Unigwe, Iorhen E. Akase, Alali Dan-Jumbo, Dennis Israelski, David W. Denning, Alessandro C. Pasqualotto, Tom Chiller

We sought to determine the prevalence of probable disseminated histoplasmosis among advanced HIV disease (AHD) patients in Nigeria. We conducted a cross-sectional study in 10 sites across 5 of 6 geopolitical zones in Nigeria. We identified patients with urinary samples containing CD4 cell counts <200 cells/mm^3 or World Health Organization stage 3 or 4 disease who also had ≥2 clinical features of disseminated histoplasmosis, and we tested them for *Histoplasma* antigen using a *Histoplasma* enzyme immune assay. Of 988 participants we recruited, 76 (7.7%) were antigen-positive. The 76 *Histoplasma* antigen–positive participants had significantly lower (p = 0.03) CD4 counts; 9 (11.8%) were also co-infected with tuberculosis. Most antigen-positive participants (50/76; 65.8%; p = 0.015) had previously received antiretroviral treatment; 26/76 (34.2%) had not. Because histoplasmosis is often a hidden disease among AHD patients in Nigeria, *Histoplasma* antigen testing should be required in the AHD package of care.

Histoplasmosis, an invasive fungal infection endemic in the Americas, Africa, and Asia, with a few cases reported among immigrants to Europe, was classified as an AIDS-defining disease in 1987 (*1*,*2*). Incidence of disseminated histoplasmosis is 5%–25% in persons with advanced HIV disease (AHD; World Health Organization [WHO]–preferred term for AIDS), and according to recent data from South America, mortality rates are similar to those for tuberculosis among this patient group (*3*,*4*). In Latin America, high prevalence rates have been reported for disseminated histoplasmosis in AHD populations in Brazil (22%; 123/570) and Mexico (30%; 85/288) (*5*,*6*). Histoplasmosis is the most common AIDS-defining infection in Guatemala, more common than tuberculosis (*7*). In a recent study from Cameroon, 26% (36/138) of HIV patients had *Histoplasma* antigen in their urine regardless of CD4 count; a 2015 report indicated a 13% (7/56) prevalence in the AHD population (*8*,*9*).

WHO in 2020 published its first guidelines for disseminated histoplasmosis among persons with AHD, including recommendations for diagnosis (*10*). WHO and the US President's Emergency Plan for AIDS Relief (PEPFAR) recommend providing differentiated care tailored to the unique needs of different HIV patient populations. Screening, treatment, and prophylaxis for major opportunistic infections is recommended for AHD (*10*). These key evidence-based interventions reduce illness and death among this clinically unstable population. Nigeria recently adopted a package of care for AHD that includes histoplasmosis screening, which has yet to be implemented. Nigeria has the 7th highest global tuberculosis

Author affiliations: Lagos University Teaching Hospital, Lagos, Nigeria (R.O. Oladele, I.E. Akase); University of Benin Teaching Hospital, Benin City, Nigeria (I.I. Osaigbovo); University of Lagos, Lagos, Nigeria (R.O. Oladele, A.S. Akanmu); University of Ibadan, Ibadan, Nigeria (O.A. Adekanmbi); University of Calabar Teaching Hospital, Calabar, Nigeria (B.E. Ekeng); Usmanu Danfodiyo University College of Health Sciences, Sokoto, Nigeria (Y. Mohammed); University of Port Harcourt Teaching Hospital, Port Harcourt, Nigeria (M.A. Alex-Wele); University of Jos, Jos, Nigeria (M.O. Okolo); Federal Medical Centre, Bida, Nigeria (S.T. Ayanbeku); University of Nigeria Teaching Hospital, Enugu, Nigeria (U.S. Unigwe); Rivers State University Teaching Hospital, Port Harcourt (A. Dan-Jumbo); Gilead Sciences International Medical Affairs, Global Patient Solution, San Francisco, California, USA (D. Israelski); University of Manchester, Manchester, UK (D.W. Denning); Universidade Federal de Ciencias da Saude de Porto Alegre, Porto Alegre, Brazil (A.C. Pasqualotto); Centers for Disease Control and Prevention, Atlanta, Georgia, USA (T. Chiller)

DOI: https://doi.org/10.3201/eid2811.220542

rate and, because histoplasmosis is commonly misdiagnosed as tuberculosis (*11*), the histoplasmosis rate in Nigeria is likely higher than currently estimated. A recent review also revealed that Nigeria had 124 documented historical cases of histoplasmosis, the highest number in Africa, but almost all were described before the HIV pandemic began (*12*). Therefore, the effect of histoplasmosis on AHD in Nigeria is largely unknown. Our primary objective was to determine the prevalence of histoplasmosis among AHD patients in Nigeria and to generate data that will help with designing and implementing guidelines for differentiated care.

Methods

We conducted a cross-sectional survey in 10 sites across large areas of Nigeria during November 2019–June 2021. The geopolitical zones we captured were South East (site: Enugu), South West (Lagos and Ibadan), South South (Benin, Port Harcourt, and Calabar), North Central (Bida, Jos, and Makurdi), and North West (Sokoto). Because of insurgent activities and security challenges, North East was excluded. We included antiretroviral treatment (ART) clinics and infectious disease units, in partnership with the AIDS Prevention Initiative in Nigeria program and other implementing partners in the zones; all sites included tertiary facilities (teaching hospitals). On the basis of data from the national database, selected sites all had >30% AHD prevalence among their overall populations. Five of the sites—Ibadan, Port Harcourt, Enugu, Jos, and Calabar—had histoplasmosis cases reported before the HIV epidemic (*12*); in 1 city, Benin, *Histoplasma* exposure had recently been determined by positive histoplasmin skin tests (*13*). The other 4 sites had no documented cases of histoplasmosis.

We obtained ethics clearance from national and institutional ethics committees before recruiting participants and received permission to contact patients from principal investigators or coordinators of the ART programs at each site. Managing clinicians assisted in recruiting participants. We obtained informed written consent from each study participant after adequately explaining the study and its objectives.

We recruited both ART-naive and ART-exposed outpatient or hospitalized HIV-infected patients who had a CD4 count <200 cells/mm^3 and met other inclusion criteria. Inclusion criteria were presence of AHD and ≥2 of 6 features commonly seen in patients with disseminated histoplasmosis: fever, chronic cough, weight loss, cutaneous lesions, oral ulcers, and diarrhea. Among participants in 1 study, 93.8% had fever, 87% weight loss, 76% cough; and 53.4% diarrhea (*14*). Whenever possible, we collected 2 urine samples from each participant with an interval of 1 week between collections. We collected other relevant biologic samples (sputum, bronchoalveolar lavage, skin lesion biopsy, and whole blood specimen) and stored them at −80°C for future research, including histologic and genomic studies.

Case Definitions

For our study we used the WHO AHD definition of CD4 cell count <200 cells/mm^3 or WHO stage 3 or 4 disease in adults and adolescents (*15*). We followed the European Organisation for Research and Treatment of Cancer Mycoses Study Group consensus definition for probable disseminated histoplasmosis as a *Histoplasma* antigenuria–positive test in the presence of compatible clinical findings (*16*).

Data Gathering and Response

We interviewed participants and reviewed their medical records and charts using a standardized checklist. This checklist encompassed sociodemographic characteristics, signs and symptoms, occupational history or exposure (e.g., gardening, civil construction, agriculture), recreational and travel history (e.g., visits to caves or farms, travel to South America), physical examination findings, working diagnoses (including the presence of other opportunistic infections), laboratory and imaging investigations, and current medications (including ARTs).

We collected participant urine samples in sterile universal screw cap containers and transported them with ice packs in refrigerator bags. Specimens were batched and stored for ≤2 months at −20°C before being shipped to a central laboratory for sample processing. We tested for urine *Histoplasma* antigen using the Clarus IMMY *Histoplasma* GM Enzyme immune assay from Immuno-Mycologics (https://www.immy.com) according to manufacturer instructions. We used the 9 standard positive control range and set an optical density cutoff value of 2.0 on the basis of a 4-parameter graph. We collected sputum samples from participants suspected of having tuberculosis because of signs or symptoms, such as cough, weight loss, fever, or other suggestive syndromes, and tested the samples for tuberculosis using the Cepheid Xpert MTB/RIF assay (https://www.cepheid.com).

We communicated positive *Histoplasma* antigenuria results to managing clinicians and advised them to manage those patients with a probable diagnosis of disseminated histoplasmosis according to current

standard-of-care guidelines. We contacted positive participants who had been hospitalized when recruited but released by the time testing results were received to schedule an outpatient clinic visit to propose a treatment plan. Duration of follow-up varied among sites; the longest recorded follow-up duration was 30 days for a study participant receiving antifungal therapy for treatment of histoplasmosis. Treatment, intravenous amphotericin B deoxycholate for 2 weeks followed by oral itraconazole until adequate immune reconstitution occurred, was rarely given because of logistic and financial constraints. Patients were provided ART according to national treatment guidelines.

Data Analysis

We entered all clinical and laboratory results into a spreadsheet and subsequently analyzed data by using SPSS Statistics 21 (https://www.ibm.com). We used descriptive statistics to summarize the data and determine mean, SD, median, interquartile range [IQR], and minimum and maximum for continuous variables. We determined absolute and relative frequencies to summarize categorical variables and used χ^2 testing to check for associations and either a 2-sample or paired-sample t-test to compare continuous variables. We stratified results by ART status (naive, experienced, failed treatment), demographics, and clinical features. We used $p<0.05$ as the cutoff for significant associations.

Results

Sociodemographic and Clinical Data

We recruited 988 participants, 377 (38.2%) male and 611 (61.8%) female, across 10 sites (Table 1); 685 (69.3%) were outpatients, 303 (30.7%) hospitalized. All participants had clinical symptoms suggestive of tuberculosis or histoplasmosis as stipulated in the inclusion criteria. Median age was 39 years (IQR 32–47 years). The most common age range for study participants was 25–40 years (n = 484; 48.9%); 80 (8.1%) were <25 years of age, 16 (1.6%) of those 13–19 years of age, and 43 (4.4%) were >60 years of age. Among participants, 259 (26.3%) had completed tertiary education and 216 (22%) had no formal education. We classified occupations into 6 groups (Table 1); the largest proportion (n = 437; 44.2%) were professionals, followed by unskilled laborers (n = 320; 32.4%), with pensioners (n = 13; 1.3%) the least common.

Histoplasmosis and Study Outcomes

We found 76 participants had *Histoplasma* antigenuria, a 7.7% prevalence of probable disseminated

Table 1. Sociodemographic data for study of prevalence of histoplasmosis among persons with AIDS, Nigeria

Variable	No. (%) participants	No. histoplasmosis urine Ag+/total no. (%)	p value
Geopolitical zones			0.097*
North Central	355 (35.9)	20/355 (5.6)	
North West	100 (10.1)	6/100 (6.0)	
South East	44 (4.5)	3/44 (6.8)	
South South	303 (30.7)	23/303 (7.6)	
South West	186 (18.8)	24/186 (12.9)	
Sex			0.461†
F	611 (61.8)	44/611 (7.2)	
M	377 (38.2)	32/377 (8.5)	
Age, y			0.891†
<25	80 (8.1)	5/80 (6.2)	
25–40	484 (48.9)	31/484 (6.4)	
41–60	381 (38.6)	39/381 (10.2)	
>60	43 (4.4)	1/43 (2.3)	
Educational qualification			0.920†
None	216 (22)	19/216 (8.8)	
Primary	126 (12.6)	11/126 (8.7)	
Quranic school	33 (3.3)	2/33 (6.1)	
Secondary	354 (35.8)	25/354 (7.1)	
Tertiary	259 (26.3)	19/259 (7.3)	
Occupation			<0.001†
Artisan	45 (4.6)	5/45 (11.1)	
Pensioner	13 (1.3)	1/13 (7.7)	
Professional	437 (44.2)	28/437 (6.4)	
Student	64 (6.5)	6/64 (9.4)	
Unemployed	109 (11.0)	3/109 (2.8)	
Unskilled labor	320 (32.4)	33/320 (10.3)	

*Fisher exact test.
†Pearson χ^2 test.

Table 2. Associated risk factors for histoplasmosis in study of prevalence of histoplasmosis among persons with AIDS, Nigeria

Risk factors	No. (%) participants	No. histoplasmosis urine Ag+/total no. (%)	p value
Thatched roof house			0.49*
N	917 (92.8)	72 (7.9)	
Y	71 (7.2)	4 (5.6)	
Corrugated roof house			0.379*
N	277 (28.0)	17 (6.1)	
Y	711 (72.0)	59 (8.3)	
Poultry within or around residence			0.423*
N	715 (72.4)	59 (8.3)	
Y	273 (27.6)	17 (6.2)	
Warehouse (home/place of work)			0.233†
N	915 (92.6)	73 (8.0)	
Y	73 (7.4)	3 (4.1)	
Home or place of work in forested regions			0.414†
N	825 (83.5)	66 (8)	
Y	163 (16.5)	10 (6.1)	
Home or work close to a sawmill			0.384*
N	926 (93.7)	73 (7.9)	
Y	62 (6.3)	3 (4.8)	
Contact with hunters			0.280*
N	919 (93.0)	73 (7.9)	
Y	69 (7.0)	3 (4.3)	
Recent travel to areas with caves			0.249†
N	964 (97.6)	76 (7.9)	
Y	24 (2.4)	0	
Heavy construction sites near workplace or home			0.548*
N	830 (84.0)	62 (7.5)	
Y	158 (16.0)	14 (8.9)	
Home near orchards			0.264†
N	913 (92.4)	73 (8.0)	
Y	75 (7.6)	3 (4.0)	
Smoking			0.037*
N	926 (93.7)	67 (7.2)	
Y	62 (6.3)	9 (14.5)	

*Pearson χ^2 test.
†Fisher exact test.

histoplasmosis; 44 (57.9%) were female and 32 (42.1%) were male. Among the 76 positive cases, both the first and second samples were positive in 45 (59.2%); 6 (7.9%) participants whose first samples were positive never returned to have a second test. Most (51.3%) participants with probable disseminated histoplasmosis were in the 41–60-year age range; 47.3% were ≤40 years of age (Table 1). The South West zone of Nigeria had the highest rate of probable histoplasmosis (12.9%), while the North Central had the lowest prevalence (5.6%). Across the various study sites, Ibadan in the South West zone had the highest rate, 20%; Benin in the South South had the lowest prevalence, 1.4% (Appendix Figure; https://wwwnc.cdc.gov/EID/article/28/11/22-0542-App1.pdf). Among possible risk factors, only occupation (p<0.001; Table 1) and smoking (p = 0.037; Table 2) were significantly associated with histoplasmosis.

Probable disseminated histoplasmosis participants had significantly lower CD4 counts (p = 0.03), and almost half, 36/76 (47.4%), had been hospitalized and had a median CD4 count of 96 cells/mm^3 (IQR 40.75–176.00 cells/mm^3) compared with nonhistoplasmosis participants, 128 cells/mm^3 (IQR 70–180 cells/mm^3) (Table 3). Prevalence of probable histoplasmosis was not significantly higher among hospitalized participants, 30/303 (9.9%), than outpatients, 46/685 (6.7%; p = 0.505) Conversely, the association

Table 3. Distribution of CD4 count cells among patients with histoplasmosis and tuberculosis in study of prevalence of histoplasmosis among persons with AIDS, Nigeria

CD4 count	No. (%) participants	No. histoplasmosis urine Ag+/total no. (%)*	No. with tuberculosi/total no. (%)†
0–50	129 (13.1)	15/129 (11.6)	11/129 (8.5)
51–100	136 (13.8)	8/136 (5.9)	36/136 (26.5)
101–200	420 (42.5)	23/420 (5.5)	11/420 (2.6)
WHO clinical stage 3/4	303 (30.7)	30/303 (9.9)	59/303 (19.5)

*p = 0.063 (Pearson χ^2 test).
†p<0.001 (Pearson χ^2 test).

Table 4. Clinical features of participants in study of prevalence of histoplasmosis among persons with AIDS, Nigeria

Clinical features	No. (%) participants	No. histoplasmosis urine Ag+/total no. (%)	p value
Fever			0.602*
N	290 (29.4)	20/290 (6.9)	
Y	698 (70.6)	56/698 (8)	
Cough			0.631*
N	437 (44.2)	36/437 (8.2)	
Y	551 (55.8)	40/551 (7.3)	
Weight loss			0.882*
N	200 (20.2)	16/200 (8.0)	
Y	788 (79.8)	60/788 (7.6)	
Diarrhea			0.055*
N	733 (74.2)	49/733 (6.7)	
Y	255 (25.8)	27/255 (10.6)	
Hepatomegaly			0.722†
N	944 (95.5)	72/944 (7.6)	
Y	44 (4.5)	3/44 (6.8)	
Central nervous system symptoms			0.166†
N	875 (88.6)	71/875 (8.1)	
Y	113 (11.4)	5/113 (4.4)	
Splenomegaly			0.307†
N	955 (96.7)	75/955 (7.9)	
Y	33 (3.3)	1/33 (3.0)	
Lymphadenopathy			0.163*
N	856 (86.6)	70/856 (8.2)	
Y	132 (13.4)	6/132 (4.5)	
Cutaneous lesions			0.329*
N	886 (89.7)	71/886 (8.0)	
Y	102 (10.3)	5/102 (4.9)	
Oral mucosal lesions/ulcers			0.562†
N	920 (93.1)	72/920 (7.8)	
Y	68 (6.9)	4/68 (5.9)	
GeneXpert			0.588†
Negative	871 (88.2)	67/871 (7.7)	
Positive	117 (11.8)	9/117 (7.7)	

*Fisher exact test.
†Pearson χ^2 test.

between tuberculosis and participant group was significant (p<0.001); hospitalized patients (59/303, 21.6%) tested positive for tuberculosis more frequently than did outpatients (58/685, 8.5%). Fifty (65.8%) participants with probable histoplasmosis were ART experienced (p = 0.015), whereas the other 26 (34.2%) were ART naive.

Most (788, 79.8%) study participants experienced weight loss, among whom 60 (7.6%) were positive for *Histoplasma* urinary antigen; 551 (55.8%) had a cough, 40 (7.3%) of whom were antigen positive. Among 102 (10.3%) participants with cutaneous lesions, only 5 (4.9%) tested positive for *Histoplasma* urinary antigen. No clinical signs or symptoms distinguished tuberculosis from disseminated histoplasmosis (Table 4). Using the Xpert MTB/RIF assay, we identified 117 (11.8%) participants who tested positive for tuberculosis.

Among participants, 420 (42.5%) had CD4 cell counts of 101–200 cells/mm^3 (IQR 126.00–181.25 cells/mm^3), but only 23/420 (5.5%) were *Histoplasma* urinary antigen positive; 303 (30.7%) were classified as having WHO clinical stage 3 or 4 disease, of whom 30/303 (9.9%) were antigen positive (Table 3). Despite comprising only 129/988 (13.1%), the lowest number of participants, those in the 0–50 cells/mm^3 CD4 cell count group, had the highest (15/129, 11.6%) frequency of *Histoplasma* urinary antigen positivity (Table 3).

Eleven (1.1%) participants died during the 30-day study period, 2 from Port Harcourt and 9 from Ibadan; 2/76 (2.6%) were positive for *Histoplasma* antigenuria, 1 co-infected with *Mycobacterium tuberculosis*. The other 9 who died had negative tests for histoplasmosis and tuberculosis; cause of death was not determined in these cases.

Histoplasmosis and Tuberculosis Coinfection

Nine (11.8%) participants, 8 female, had both histoplasmosis and tuberculosis. Co-infection occurred in all age groups. Seven of the participants were stage 3 or 4 HIV patients and 2 had 101–200/mm^3 CD4 counts (Table 3). One co-infected participant, a 32-year-old hospitalized patient with a working diagnosis of stage 4 HIV with pulmonary tuberculosis, died during the course of the study (Figure).

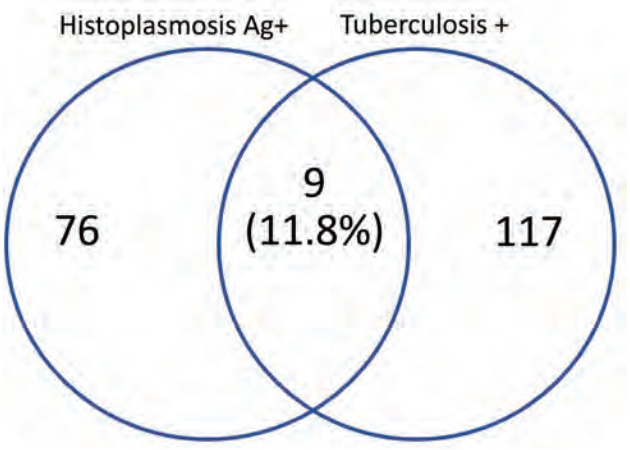

Figure. Case-patients with tuberculosis-histoplasmosis co-infection in study of prevalence of histoplasmosis among advanced HIV disease patients in Nigeria. Ag, antigen; +, positive.

Discussion

Although histoplasmosis is endemic in Nigeria, published data have been restricted to case reports that largely predate the HIV era. Disease incidence has not been well characterized, especially among persons living with AHD (*1*). We attempted to determine the frequency of disseminated histoplasmosis in the HIV population of Nigeria and found that >7% of persons with AHD have probable histoplasmosis on the basis of European Organisation for Research and Treatment of Cancer Mycoses Study Group consensus definitions.

The countrywide prevalence of *Histoplasma* antigenuria among AHD patients in this study was <26% in Cameroon and <14% in South Africa (*8*,*17*). Whereas we used a previously validated monoclonal *Histoplasma* galactomannan enzyme immunosorbent assays to detect *Histoplasma* antigen (*18*), the study from Cameroon used a different commercial assay. It has been acknowledged that using a higher cutoff would have been more realistic and would have changed prevalence to 8%, which is closer to our findings. The lower rate in our study may have been because of technical factors such as length and conditions of storage of urine samples because specimens had to be transferred to a central location for testing to optimize the use of the antigen detection kits. Furthermore, the studies (*8*,*17*) were both conducted in single locations in South Africa and Cameroon that might both have been hyperendemic for histoplasmosis. Our multicenter study showed regional variability with prevalence ranging from 5.6% in the North Central zone to 12.9% in the South West. Even within regions, prevalence varied widely from site to site. Such variability was similarly described among regions in a multicenter study conducted in Brazil (*5*) that demonstrated a pooled prevalence of 21.6% from 14 centers, far exceeding the pooled prevalence from Nigeria. However, in the study from Brazil, use of the antigen detection method was combined with classical mycology tests including culturing, whereas we used only antigen detection (*5*). Laboratory tests for histoplasmosis are seldom performed in Nigeria because of a combination of lack of awareness, facilities, biosafety cabinets, and staff with the expertise needed to perform isolator methods of blood culturing and other laboratory testing.

Histoplasmin skin sensitivity rates predict the level of exposure to *Histoplasma* spp. in a given geographic location (*13*,*19*,*20*). Surprisingly, antigenuria prevalence did not correlate well with histoplasmin reactivity rates observed in a previous multicenter survey (*13*) that included 4 of the sites in our study: Benin City, Calabar, Ibadan, and Lagos. Benin, which recorded the highest skin sensitivity in the previous study (*13*), ended up with the lowest antigenuria prevalence in our study. It is noteworthy that in the histoplasmin sensitivity survey (*13*), skin sensitivity was significantly associated with study site. A corresponding association between site and outcome of interest, *Histoplasma* antigenuria, was not demonstrated in this study, which suggests that other factors, such as the extent of immunosuppression, may have played a greater role in determining antigenuria prevalence. The histoplasmin employed in the skin sensitivity study is known to be cross-reactive for *H. capsulatum* var. *capsulatum* and *H. capsulatum* var. *duboisii* both of which cause disseminated histoplasmosis in persons with AHD and are present in Nigeria (*19*,*20*). On the other hand, there is no evidence that the EIA deployed in this study, or any other antigen detection method for that matter, reliably detects *H. capsulatum* var. *duboisii*. In a review of histoplasmosis caused by *H. capsulatum* var. *duboisii*, diagnosis relied mostly on direct examination of body fluids and skin scrapings or histopathologic examination of clinical specimens; few were confirmed by culture or PCR and none relied on *Histoplasma* antigen detection (*21*). Because of this methodologic variability among studies, the effect on observed antigenuria prevalence of *Histoplasma* spp. distribution in the various study sites deserves further investigation.

As observed in other studies, exposure to classic environmental risk factors such as caves, heavy construction, fruit trees, and poultry were not notable risk factors for antigenuria in this study (*8*,*22*). However, contrary to findings from Cameroon, occupation was linked to positivity, with some skilled laborers,

including painters, electricians, and plumbers, being more at risk than others (*8*). Another notable risk factor was smoking. Although not historically associated with progressive disseminated histoplasmosis, smoking has been recognized as a risk factor for the chronic pulmonary form of the disease (*22*).

Co-infection occurs commonly in AHD patients who have progressive disseminated histoplasmosis. Multiple studies from the Americas report tuberculosis as the most common coinfection (*23*–*27*). In the index cohort, 11.8% of participants with antigenuria had tuberculosis co-infection, which is close to the tuberculosis co-infection rate of 15.4% of participants with histoplasmosis in Brazil and 13.1% in Guatemala, both high-burden tuberculosis countries (*5*,*28*). The fact that histoplasmosis is often mistaken for and can coexist with tuberculosis is a substantial confounder in areas where the diseases are coendemic. Because tuberculosis awareness has grown and diagnostics have become more readily available, a diagnosis of tuberculosis alone might explain the signs and symptoms similar between the diseases, hiding diagnosis of the more obscure and neglected histoplasmosis in AHD patients. This shortfall suggests the need for active histoplasmosis screening in persons suspected to have tuberculosis, irrespective of confirmation with GeneXpert or other diagnostics. It is also critical to ensure that patients who screen positive for histoplasmosis can receive treatment. Several participants found to have probable histoplasmosis in this study were not treated because of financial constraints. Therefore, histoplasmosis treatment should also be included in the AHD package of care.

We found that 6.6% of participants with antigenuria had skin lesions, similar to what was found in Cameroon (6%) (*8*). However, among participants with lesions, histoplasma urinary antigen was no more common (p = 0.329). Skin lesions, which occur in 10%–25% of AIDS patients with disseminated histoplasmosis, have been linked with genetic variation among specific strains of the fungus that are dermatotropic or might be markers of histoplasmosis diagnosis when made at a very late stage (*29*). When present, biopsied lesions provide useful specimens for diagnostic confirmation of histoplasmosis. However, lesions were not very common among participants in our study, requiring us to use more available specimens. In addition, the skilled personnel needed to perform these biopsies might not be available in some settings.

One major strength of this study was that we included sites in virtually all the geopolitical zones in Nigeria that have had the most reported cases of histoplasmosis in the past. However, a study limitation was our lack of the mycology data from cultures or PCR needed to provide definitive proof of histoplasmosis and clarify the relative contributions of *H. capsulatum* var. *capsulatum* and *H. capsulatum* var. *duboisii* to its prevalence in Nigeria. Second, because it is unclear whether detecting *Histoplasma* antigen in urine provides reliable data for diagnosing *H. capsulatum* var. *duboisii*–caused histoplasmosis, we might have underestimated histoplasmosis prevalence. Third, the possibility of false positive antigenuria results cannot be entirely ruled out; however, although not tested on samples from the settings in our study, the assay we used has been validated in several studies to have good sensitivity and specificity. Fourth, our selection criteria increased the pretest probability for histoplasmosis among this cohort of participants. Fifth, we might have recorded some false-negative results as a consequence of the prolonged storage of samples. Another limitation was the lack of detailed ancillary tests, such as lactate dehydrogenase, aminotransferase, alkaline phosphatase, ferritin, and complete blood counts, which would have helped characterize patients.

Much remains to be elucidated about histoplasmosis in Nigeria, but this study confirms that it is certainly underreported among persons with HIV and AIDS, partly obscured by a diagnosis of tuberculosis, a disease with several manifestations in common with histoplasmosis. Further research using highly sensitive diagnostic approaches such as PCR and bone marrow examination is needed to gain insight into the precise epidemiology of the disease in Nigeria. To encourage proactive searching for histoplasmosis, use of specific diagnostic tools, including culturing, needs to be scaled up and management guidelines for AHD patients revised. After diagnosis, patients should be treated with appropriate antifungal agents, following the 2020 WHO guidelines. Patients suspected or confirmed to have tuberculosis should be investigated for histoplasmosis as well. Development of a molecular test in an easy-to-use format, such as the GeneXpert platform, that could be deployed in HIV treatment centers would be welcome.

In conclusion, histoplasmosis is not uncommon among AHD patients in Nigeria. Therefore, *Histoplasma* antigen screening should be included in the AHD package of care as a matter of urgent need to improve efficiency of diagnosis and reduce illness and death from histoplasmosis in an at-risk population.

Acknowledgment

We thank Tina Nwosu for processing the samples and collating laboratory data.

This study was funded by a grant from Gilead Sciences. IMMY supported this study with donations of test kits.

R.O.O. provided conceptualization, data curation, formal analysis, methodology, resources, validation, and writing of the original draft, review, and editing. I.I.O., A.S.A., O.A.A., B.E.E., Y.M., M.A.A.-W, M.O.O., U.S.U., and A.D.-J. provided data curation, resources, writing, review, and editing. S.T.A., I.E.A., and D.I. provided data curation and resources. D.W.D., A.C.P., and T.C. provided resources, writing, review, and editing

About the Author

Dr. Oladele is an associate professor of medical microbiology at the Department of Medical Microbiology and Parasitology, University of Lagos, and a consultant clinical microbiologist at the Lagos University Teaching Hospital, both in Lagos. Her research interests include epidemiology of fungal infections and health systems strengthening for diagnosis of serious fungal diseases.

References

1. Ekeng BE, Edem K, Amamilo I, Panos Z, Denning D, Oladele RO. Histoplasmosis in children; HIV/AIDS not a major driver. J Fungi (Basel). 2021;7:530. https://doi.org/10.3390/jof7070530
2. Sepúlveda VE, Márquez R, Turissini DA, Goldman WE, Matute DR. Genome sequences reveal cryptic speciation in the human pathogen *Histoplasma capsulatum*. MBio. 2017;8:e01339–17. https://doi.org/10.1128/mBio.01339-17
3. Silva TC, Treméa CM, Zara ALSA, Mendonça AF, Godoy CSM, Costa CR, et al. Prevalence and lethality among patients with histoplasmosis and AIDS in the Midwest Region of Brazil. Mycoses. 2017;60:59–65. https://doi.org/10.1111/myc.12551
4. Pasqualotto AC, Quieroz-Telles F. Histoplasmosis dethrones tuberculosis in Latin America. Lancet Infect Dis. 2018; 18:1058–60. https://doi.org/10.1016/S1473-3099(18)30373-6
5. Falci DR, Monteiro AA, Braz Caurio CF, Magalhães TCO, Xavier MO, Basso RP, et al. Histoplasmosis, an underdiagnosed disease affecting people living with HIV/AIDS in Brazil: results of a multicenter prospective cohort study using both classical mycology tests and *Histoplasma* urine antigen detection. Open Forum Infect Dis. 2019;6:ofz073. https://doi.org/10.1093/ofid/ofz073
6. Torres-González P, Niembro-Ortega MD, Martínez-Gamboa A, Ahumada-Topete VH, Andrade-Villanueva J, Araujo-Meléndez J, et al. Diagnostic accuracy cohort study and clinical value of the Histoplasma urine antigen (ALPHA Histoplasma EIA) for disseminated histoplasmosis among HIV infected patients: A multicenter study. PLoS Negl Trop Dis. 2018;12:e0006872. https://doi.org/10.1371/journal.pntd.0006872
7. Medina N, Rodriguez-Tudela JL, Aguirre L, Salazar LR, Gamboa O, Bonilla O, et al. Incidence of histoplasmosis in a cohort of people with HIV: from estimations to reality. Microorganisms. 2021;9:2596. https://doi.org/10.3390/microorganisms9122596
8. Kuate MPN, Nyasa R, Mandengue C, Tendongfor N, Bongomin F, Denning DW. Screening for acute disseminated histoplasmosis in HIV disease using urinary antigen detection enzyme immunoassay: a pilot study in Cameroon. J Microbiol Methods. 2021;185:106226. https://doi.org/10.1016/j.mimet.2021.106226
9. Mandengue CE, Ngandjio A, Atangana PJA. Histoplasmosis in HIV-infected persons, Yaoundé, Cameroon. Emerg Infect Dis. 2015;21:2094–6. https://doi.org/10.3201/eid2111.150278
10. Guidelines for diagnosing and managing disseminated histoplasmosis among people living with HIV. Washington, DC: Pan American Health Organization, and Geneva: World Health Organization; 2020.
11. Global tuberculosis report 2018. Geneva: World Health Organization; 2018.
12. Oladele RO, Ayanlowo OO, Richardson MD, Denning DW. Histoplasmosis in Africa: an emerging or a neglected disease? PLoS Negl Trop Dis. 2018;12:e0006046. https://doi.org/10.1371/journal.pntd.0006046
13. Oladele RO, Toriello C, Ogunsola FT, Ayanlowo OO, Foden P, Fayemiwo AS, et al. Prior subclinical histoplasmosis revealed in Nigeria using histoplasmin skin testing. PLoS One. 2018;13:e0196224. https://doi.org/10.1371/journal.pone.0196224
14. Brilhante RS, Fechine MA, Mesquita JR, Cordeiro RA, Rocha MF, Monteiro AJ, et al. Histoplasmosis in HIV-positive patients in Ceará, Brazil: clinical-laboratory aspects and in vitro antifungal susceptibility of *Histoplasma capsulatum* isolates. Trans R Soc Trop Med Hyg. 2012; 106:484–8. https://doi.org/10.1016/j.trstmh.2012.05.003
15. World Health Organisation. Interim WHO clinical staging of HIV/AIDS and HIV/AIDS case definitions for surveillance: African Region [cited 2022 Aug 3]. https://apps.who.int/iris/bitstream/handle/10665/69058/WHO_HIV_2005.02.pdf
16. Donnelly JP, Chen SC, Kauffman CA, Steinbach WJ, Baddley JW, Verweij PE, et al. Revision and update of the consensus definitions of invasive fungal disease from the European Organization for Research and Treatment of Cancer and the Mycoses Study Group Education and Research Consortium. Clin Infect Dis. 2020;71:1367–76. https://doi.org/10.1093/cid/ciz1008
17. van Schalkwyk E, Mhlanga M, Maphanga TG, Mpembe RS, Shillubane A, Iyaloo S, et al. Screening for invasive fungal disease using non-culture-based assays among inpatients with advanced HIV disease at a large academic hospital in South Africa. Mycoses. 2020;63:478–87. https://doi.org/10.1111/myc.13071
18. Cáceres DH, Samayoa BE, Medina NG, Tobón AM, Guzmán BJ, Mercado D, et al. Multicenter validation of commercial antigenuria reagents to diagnose progressive disseminated histoplasmosis in people living with HIV/AIDS in two Latin American countries. J Clin Microbiol. 2018;56:e01959–17. https://doi.org/10.1128/JCM.01959-17
19. Gugnani HC, Egere JU, Larsh H. Skin sensitivity to capsulatum and duboisii histoplasmins in Nigeria. J Trop Med Hyg. 1991;94:24–6.
20. Gugnani HC. Histoplasmosis in Africa: a review. Indian J Chest Dis Allied Sci. 2000;42:271–7.
21. Develoux M, Amona FM, Hennequin C. Histoplasmosis caused by *Histoplasma capsulatum* var. *duboisii*: a comprehensive review of cases from 1993 to 2019. Clin Infect Dis.2021;73:e543–9. https://doi.org/10.1093/cid/ciaa1304
22. Ekeng BE, Oladele RO, Emanghe UE, Ochang EA, Mirabeau TY. Prevalence of histoplasmosis and molecular characterization of histoplasma species in patients with presumptive pulmonary tuberculosis in Calabar, Nigeria. Open Forum Infect Dis. 2022;9:ofac368.

23. Caceres DH, Tobón ÁM, Restrepo Á, Chiller T, Gómez BL. The important role of co-infections in patients with AIDS and progressive disseminated histoplasmosis (PDH): a cohort from Colombia. Med Mycol Case Rep. 2018;19:41–4. https://doi.org/10.1016/j.mmcr.2017.07.004
24. Gutierrez ME, Canton A, Sosa N, Puga E, Talavera L. Disseminated histoplasmosis in patients with AIDS in Panama: a review of 104 cases. Clin Infect Dis. 2005;40:1199–202. https://doi.org/10.1086/428842
25. Mora DJ, dos Santos CT, Silva-Vergara ML. Disseminated histoplasmosis in acquired immunodeficiency syndrome patients in Uberaba, MG, Brazil. Mycoses. 2008;51:136–40. https://doi.org/10.1111/j.1439-0507.2007.01459.x
26. Huber F, Nacher M, Aznar C, Pierre-Demar M, El Guedj M, Vaz T, et al. AIDS-related *Histoplasma capsulatum* var. *capsulatum* infection: 25 years experience of French Guiana. AIDS. 2008;22:1047–53. https://doi.org/10.1097/QAD.0b013e3282ffde67
27. Adenis A, Nacher M, Hanf M, Basurko C, Dufour J, Huber F, et al. Tuberculosis and histoplasmosis among human immunodeficiency virus–infected patients: a comparative study. Am J Trop Med Hyg. 2014;90:216–23. https://doi.org/10.4269/ajtmh.13-0084
28. Samayoa B, Aguirre L, Bonilla O, Medina N, Lau-Bonilla D, Mercado D, et al.; "Fungired". The Diagnostic Laboratory Hub: a new health care system reveals the incidence and mortality of tuberculosis, histoplasmosis, and cryptococcosis of PWH in Guatemala. Open Forum Infect Dis. 2019;7:ofz534. https://doi.org/10.1093/ofid/ofz534
29. Morote S, Nacher M, Blaizot R, Ntab B, Blanchet D, Drak Alsibai K, et al. Temporal trends of cutaneo-mucous histoplasmosis in persons living with HIV in French Guiana: early diagnosis defuses South American strain dermotropism. PLoS Negl Trop Dis. 2020;14:e0008663. https://doi.org 10.1371/journal.pntd.0008663

Address for correspondence: Rita O. Oladele, Lagos University Teaching Hospital, Ishaga Rd, Idi-Araba 102215, Lagos, Nigeria; email: oladelerita@gmail.com

Differences in SARS-CoV-2 Clinical Manifestations and Disease Severity in Children and Adolescents by Infecting Variant

Ana Maria Quintero, Mariah Eisner, Rouba Sayegh, Tori Wright, Octavio Ramilo, Amy L. Leber, Huanyu Wang,[1] Asuncion Mejias [1]

Since the COVID-19 pandemic began, different SARS-CoV-2 variants have been identified and associated with higher transmissibility than the ancestral nonvariant strain. During January 1, 2021–January 15, 2022, we assessed differences in clinical and viral parameters in a convenience sample of COVID-19 outpatients and inpatients 0–21 years of age in Columbus, Ohio, USA, according to the infecting variant, identified using a mutation-specific reverse transcription PCR assay. Of the 676 patients in the study, 17.75% were infected with nonvariant strains, 18.49% with the Alpha variant, 41.72% with Delta, and 16.42% with Omicron. Rates of SARS-COV-2/viral co-infections were 15.66%–29.41% and were comparable across infecting variants. Inpatients with acute Delta and Omicron infections had lower SARS-CoV-2 cycle threshold values and more frequent fever and respiratory symptoms than those with nonvariant strain infections. In addition, SARS-COV-2/viral co-infections and the presence of underlying conditions were independently associated with worse clinical outcomes, irrespective of the infecting variant.

SARS-CoV-2, the etiologic agent of COVID-19, rapidly spread worldwide, causing a global pandemic with major social and economic disruption. Although the effects of COVID-19 have been greater in adults, children also are infected with SARS-CoV-2, and COVID-19 can lead to severe outcomes in pediatric patients (*1*–*3*). Nevertheless, the spectrum of clinical manifestations in children is broad and ranges from asymptomatic to mild upper respiratory infection to pneumonia or the more severe multisystem inflammatory syndrome in children (MIS-C), which typically occurs 2 to 6 weeks after acute SARS-CoV-2 infection (*4*–*7*).

Since the COVID-19 pandemic began, different SARS-CoV-2 variants have circulated worldwide. In the United States, the first variant that replaced the original strain was the Alpha variant (B 1.1.7) that circulated during April–June 2021. The Delta variant (B1.617.2) followed soon after and became predominant during July–mid-December 2021. Since then, different sublineages of Omicron quickly replaced other variants as the predominant variant as of September 2022. These newer variants have demonstrated higher transmissibility and have disproportionally affected unvaccinated persons and other vulnerable populations including children; rates of hospitalization have increased 5-fold to 10-fold in children, depending on the variant and age group (*8*–*13*). Epidemiologic studies that rely on SARS-CoV-2 circulation patterns have provided robust information; however, the role of specific SARS-CoV-2 variants on clinical disease severity in children and adolescents with COVID-19 is not fully known.

The objective of this study was to assess whether distinct SARS-CoV-2 variants were associated with differences in clinical and laboratory data and cycle threshold (Ct) values (as a surrogate of viral load) in children and adolescents with COVID-19. The Nationwide Children's Hospital (NCH; Columbus, OH, USA) Institutional Review Board approved the study (#STUDY00002002).

Author affiliations: Nationwide Children's Hospital, Columbus, Ohio, USA (A.M. Quintero, R. Sayegh, T. Wright, O. Ramilo, A.L. Leber, H. Wang, A. Mejias); Biostatistics Resource at Nationwide Children's Hospital, Columbus (M. Eisner); The Ohio State University, Columbus (M. Eisner, O. Ramilo, H. Wang, A. Mejias)

DOI: https://doi.org/10.3201/eid2811.220577

[1]These authors contributed equally to and co-directed this work.

Methods

Sample Collection and Testing Algorithm

During January 1, 2021–January 15, 2022, we identified nasopharyngeal (NP) samples from children and adolescents ≤21 years of age that tested positive by various nucleic acid amplification tests (NAATs) for SARS-CoV-2 at the Clinical Microbiology Laboratory at NCH, per standard of care (Appendix, https://wwwnc.cdc.gov/EID/article/28/11/22-0577-App1.pdf). Samples positive for SARS-CoV-2 by any of the NAATs assays were stored at −20°C.

From all available specimens, we selected a convenience sample for variant screening within 1 week of storage based on the clinical laboratory testing capability, sample volumes, and Ct values, considering a sample adequate when Ct values were <35. We used Ct values as a proxy for viral load quantification because they have an inverse relationship with quantitative viral loads (*14*).

SARS-CoV-2 Variant Testing

We screened SARS-CoV-2–positive samples by mutation-specific reverse transcription PCR assays for Alpha, Beta, Gamma, Omicron, and other variants of interest as described (*15*). We developed a T487K assay for screening of the Delta variant (Appendix).

We considered samples positive for P1 but not P2 to be negative for the T478K mutation, and samples positive for both P1 and P2 to be positive for the T478K mutation. We designated samples that carried both L452R and T478K mutations as the Delta variant. Because the Omicron variant appeared in the United States in December 2021 when the Alpha variant had effectively disappeared (*16*), we designated samples collected during December 1, 2021–January 15, 2022, that were positive for Δ69/70 and negative for the L452R mutation as Omicron (B.1.1.529).

Patient Selection and Data Collection

We linked identifiers from outpatients and inpatients whose samples underwent SARS-CoV-2 variant screening with their electronic healthcare records (EHRs), extracted pertinent data, and manually reviewed clinical data. We included in the inpatient cohort 1 patient who tested positive as outpatient but eventually required hospitalization within 4 weeks of diagnosis; for this patient, we considered for analyses the first sample obtained. For patients with multiple positive SARS-CoV-2 tests during the study, we included in the analyses the first sample collected and the data related to the first encounter. We considered subsequent samples collected for an individual patient or subsequent admissions to be duplicates and excluded them from analysis.

We described demographic characteristics including underlying conditions, the infecting variant type, and SARS-CoV-2 Ct values for the COVID-19 clinical cohort comprised of outpatients and inpatients; we analyzed clinical manifestations, laboratory parameters, and clinical outcomes exclusively in inpatients with acute COVID-19. We grouped underlying conditions into categories including respiratory, neurologic, genetic, immunocompromised conditions, renal/gastrointestinal, endocrine, and hematologic diseases. We also included obesity, defined as presence of age-sex-standardized body mass index z-scores ≥95th percentile, and overweight, defined as presence of age-sex-standardized body mass index z-scores ≥85th percentile; these values were based on weight (measured at the time of SARS-CoV-2 testing) and height registered in the EHR within 60 days of cohort entrance. For children <2 years of age, we determined the nutritional status by z-scores according to weight-for-age and weight-for-height, considering overweight as 1.0 to ≤2.0 SD and obesity as >2 SD. We grouped obesity and overweight as a single variable during data collection. To contrast the prevalence of underlying conditions between the COVID-19 clinical cohort and the patient population evaluated at NCH during the same period, we used the Pediatric Medical Complexity Algorithm (PMCA) version 2.0, which categorized patients as having no chronic conditions, noncomplex chronic conditions, or complex chronic condition comorbidities (*17*).

Statistical Analysis

We used descriptive analysis to summarize patients' characteristics. We analyzed categorical variables by χ^2 or Fisher exact tests and expressed them in frequencies and percentages. We analyzed continuous variables by Kruskal-Wallis rank-sum test and expressed them as median (interquartile range) because data were nonnormally distributed. We conducted multivariable analyses to identify risk factors associated with clinical outcomes in children and adolescents with acute COVID-19, including the need for hospitalization and, in inpatients, oxygen administration and pediatric intensive care unit (PICU) admission. We built statistical models using logistic regression; in all models, the primary exposure was the infecting variant. Other covariates included were age, underlying conditions, Ct values, and viral co-infections. We evaluated models for collinearity using the generalized variance inflation factor. We performed

statistical analyses in R version 4.0 (The R Project for Statistical Computing, https://www.r-project.org) and Prism version 9.0 (GraphPad Software, https://www.graphpad.com) and considered 2-sided $p<0.05$ statistically significant.

Results

Shifts in the Circulation of SARS-CoV-2 Strains

During January 1, 2021–January 15, 2022, of 169,908 samples tested for SARS-CoV-2 from children and adolescents of all ages, 15,320 (9.02%) were positive by an NAAT assay. (Figure 1). The monthly rate of SARS-CoV-2 NAAT positive tests fluctuated throughout the study, from ≈10.00% in January 2021, when the nonvariant strain predominated, to 3.78%–1.70% during March–June 2021, coinciding with the circulation of the Alpha variant ($p = 0.01$). After June there was a steady increase in SARS-COV-2 positivity rates when Delta predominated. The highest positivity rate of 33.05% was reached in January 2022 with the circulation of Omicron (Figure 1).

We performed variant screening on 1,058 (6.91%) positive samples for SARS-CoV-2, confirming the local circulation of 12 variants. Of those samples, 11.34% (120) corresponded to the nonvariant strain, 11.81% to Alpha, 62.77% to Delta, and 10.49% to Omicron. Thirty-eight patients (3.59%) were infected with other variants, including Beta, Gamma, Lota, Zeta, Eta, Epsilon, and Mu, as well as a single variant of uncertain importance.

Demographic Characteristics of the Clinical Cohort

We included in final analyses sample data from 676 (63.89%) unique patients, comprising the clinical cohort (Table 1; Figure 2). Of the 676 patients, those identified during January 1–September 19, 2021, corresponded to nonvariant (n = 120, 17.75%), Alpha (n = 125, 18.49%), and Delta infections (n = 282, 41.72%). Patients identified during December 15, 2021– January 15, 2022, corresponded to Omicron B.1.1.529 infections (n = 111, 16.42%). Patients identified during September 20–December 14, 2021, corresponded to Delta infections but were not included because sample size for Delta infections was deemed sufficient.

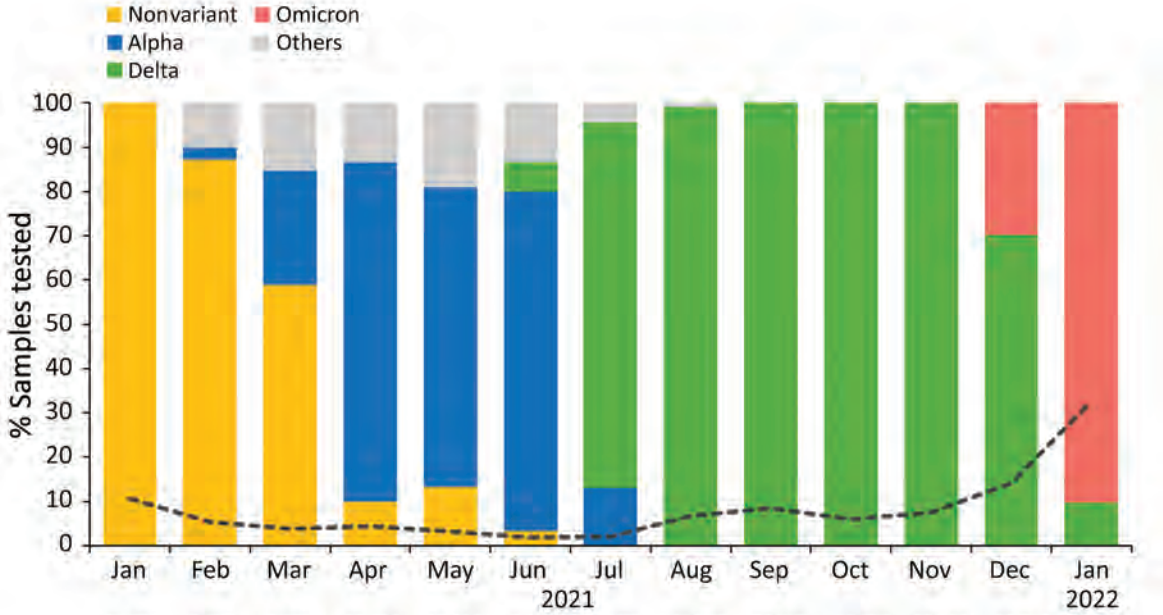

	Jan 2021	Feb	Mar	Apr	May	Jun	Jul	Aug	Sep	Oct	Nov	Dec	Jan 2022
No. tested	10,081	7,717	9,665	10,862	10,167	8,159	8,189	15,910	24,618	17,067	15,574	19,867	12,032
No. (%) tested positive	1,062 (10.53)	403 (5.22)	365 (3.78)	469 (4.32)	613 (6.03)	140 (1.72)	164 (2.0)	1,071 (6.73)	2,070 (8.41)	994 (5.82)	1,173 (7.53)	2,820 (14.19)	3,976 (33.05)
No. (%) screened for variants	50 (4.71)	30 (7.44)	48 (13.15)	85 (18.12)	59 (9.62)	21 (15.00)	23 (14.02)	118 (11.02)	153 (7.39)	117 (11.77)	115 (9.80)	168 (5.96)	78 (2.96)
No. (%) inpatient samples	39 (3.67)	16 (3.97)	31 (8.49)	39 (8.32)	17 (2.77)	14 (10.00)	9 (5.49)	36 (3.36)	80 (3.86)	52 (5.23)	48 (4.09)	131 (4.65)	97 (2.44)

Figure 1. Shifts in the circulating SARS-CoV-2 variants identified at Nationwide Children's Hospital, Columbus, Ohio, USA, by percentage of total cases irrespective of patient age, January 2021–January 2022. The others category comprises Beta (n = 12), Iota (n = 9), Zeta (n = 7), Eta (n = 2), Epsilon (n = 3), and Mu (n = 2) variants, as well as variants under investigation (n = 2). The black dotted line represents the rate of positive tests by month.

Table 1. Demographic characteristics of the clinical cohort in study of SARS-CoV-2 variants in children and adolescents, Columbus, Ohio, USA*

Clinical cohort characteristics	All patients, n = 676	Outpatients, n = 450	Inpatients, n = 226	p value
Median age, y (IQR)	8.98 (2.64–14.71)	9.40 (3.90–14.23)	6.55 (0.48–15.60)	
Age group, y				
<1	102 (15.09)	32 (7.11)	70 (30.97)	**<0.001**
1–4	129 (19.08)	96 (21.33)	33 (14.60)	
5–11	189 (27.96)	157 (34.89)	32 (14.16)	
12–21	256 (37.87)	165 (36.67)	91 (40.27)	
Sex				
M	356 (52.66)	230 (51.11)	126 (55.75)	0.25
F	320 (47.34)	220 (48.49)	100 (44.25)	
Race/ethnicity	n = 587	n = 365	n = 222	0.36
White	349 (59.45)	215 (58.90)	134 (60.36)	
Black	146 (24.87)	92 (25.21)	54 (24.32)	
Multiracial	38 (6.47)	26 (7.12)	12 (5.41)	
Hispanic	37 (6.30)	25 (6.85)	12 (5.41)	
Other	17 (2.90)	7 (1.92)	10 (4.51)	
Underlying conditions†	n = 538	n = 312	n = 226	**<0.001**
None	288 (53.53)	198 (63.46)	90 (39.82)	
Yes	250 (46.47)	114 (36.54)	136 (60.18)	
Obesity/overweight	141 (26.21)	68 (21.79)	73 (32.30)	
SARS-CoV-2 vaccination status	n = 565	n = 361	n = 204	0.62
Received ≥1 dose	17 (3.01)	12 (3.32)	5 (2.45)	
Not immunized	548 (96.99)	349 (96.68)	199 (97.55)	
SARS-COV-2 variant				
Nonvariant	120 (17.75)	88 (19.56)	32 (14.16)	**<0.001**
Alpha	125 (18.49)	98 (21.78)	27 (11.95)	
Delta	282 (41.72)	189 (42.00)	93 (41.15)	
Omicron	111 (16.42)	49 (10.89)	62 (27.43)	
Other‡	38 (5.62)	26 (5.78)	12 (5.31)	

*Values are no. (%) except as indicated. Continuous variables were analyzed by Mann-Whitney test. Categorical data were analyzed by Fisher exact test or χ^2 test. Bold indicates significance. IQR, interquartile range.
†Underlying conditions included respiratory (asthma, bronchopulmonary dysplasia, cystic fibrosis); cardiac (septal defects, valvopathies; dilated cardiomyopathy); endocrinologic (diabetes, dyslipidemia, panhypopituitarism, polyendocrinopathy); hematologic (sickle cell disease, spherocytosis, thalassemia, chronic idiopathy thrombocytopenia purpura); immunocompromised conditions (solid or hematopoietic organ transplantation, malignancies–leukemias, solid tumors, rheumatologic conditions receiving chronic immunosuppressive therapy, primary immunodeficiencies, HIV); neurologic and genetic conditions (cerebral palsy, autism, developmental delay); prematurity; renal/gastrointestinal conditions (Hirschsprung's, duodenal atresia, short bowel syndrome, chronic kidney disease, intestinal bowel disease, nephrotic syndrome), and obesity/overweight.
‡Other variants: Gamma (n = 12); Epsilon (n = 3); Eta (n = 2); Beta (n = 1); Iota (n = 9); Mu (n = 2); variants under investigation, (n = 2); Zeta (n = 7).

Of the 676 patients, we tested 450 (66.57%) as outpatients and 226 (33.43%) in the hospital. Median age for inpatients (6.6 [IQR 0.5–15.6] years) was lower than that for outpatients (9.4 [IQR 3.9–14.2] years; p<0.01). In both settings, infections were more common in adolescents 12–21 years of age, whereas in inpatients, infants were the second most common age group represented (30.97%). We observed no differences in sex and race/ethnicity between inpatients and outpatients. SARS-CoV-2 vaccination rates were low (3.01%) and did not differ between outpatients and inpatients either. Overall, Delta infections were the most common infections in inpatients (41.15%) and outpatients (42.00%). Alpha infections were more common in outpatients (21.78% vs. 11.95% in inpatients) and Omicron in inpatients (27.43% vs. 10.89% in outpatients). (Figure 3; Appendix Table 1).

Of the COVID-19 clinical cohort, 80.0% (538/676) had available data regarding underlying conditions. Underlying conditions were more prevalent in inpatients (60.18%) than in outpatients (36.54%; p<0.001); obesity/overweight was the most common. Compared with the overall population evaluated at NCH during the same period (NCH cohort; n = 444,425), the prevalence of complex chronic conditions identified by the PMCA algorithm was greater in the COVID-19 clinical cohort (31.56%) than in the overall NCH cohort (16.95%), whereas noncomplex chronic conditions were more common in the NCH cohort (20.76%) than in the clinical cohort (14.52%) (Appendix Table 2).

Clinical Cohort Viral Loads and Viral Co-infections

We assessed differences in SARS-CoV-2 Ct values in the clinical cohort according to the infecting variant and found comparable values (p = 0.35) (Figure 4, panel A). For 32.10% (217/676) of patients, we performed a multiplex respiratory viral panel; we identified SARS-CoV-2/viral coinfections in 43 patients (19.82%) (Figure 4, panel B). Rhinovirus/enterovirus (RV/EV) was the most common viral coinfection (n = 22) followed by respiratory syncytial virus (RSV; n = 7), human metapneumovirus (hMPV; n = 5), endemic coronavirus (n = 3), parainfluenza viruses (PIVs; n = 3), adenovirus

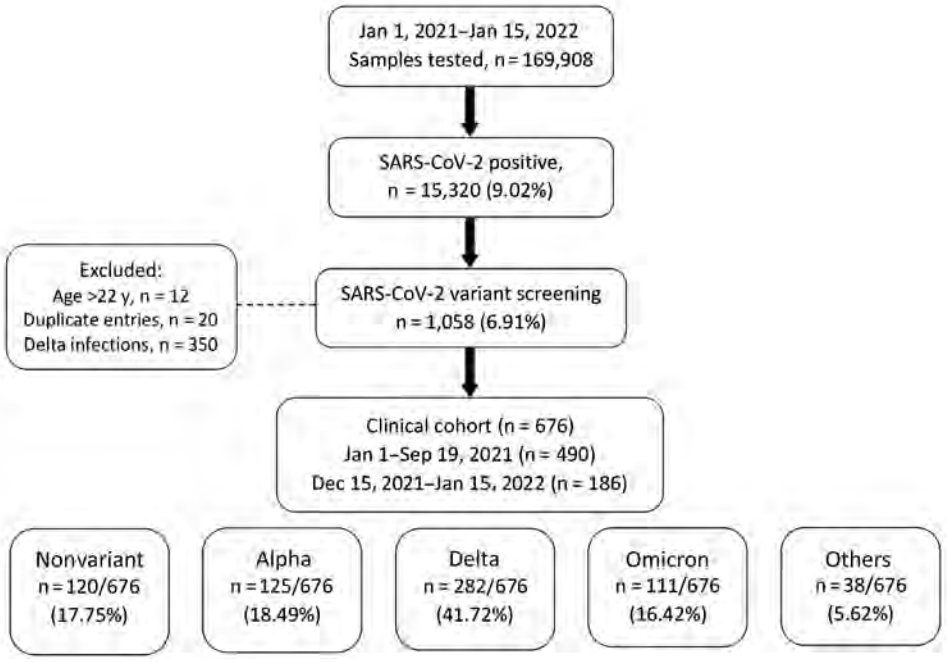

Figure 2. Flow diagram of sample and patient selection for SARS CoV-2 variant screening of nasopharyngeal samples at Nationwide Children's Hospital, Columbus, Ohio, USA, during January 1, 2021–January 15, 2022. After excluding patients ≥22 years of age and duplicate entries, 676 patients with positive SARS-CoV-2 tests during January 1–September 19, 2021, and December 15, 2021–January 15, 2022 were included in the clinical analyses. Other variants were Beta, Iota, Zeta, Eta, Epsilon, Gamma, Mu, and other variants under investigation.

(n = 3), and influenza viruses (n = 1). We observed no differences in the rates of co-infections according to the SARS-CoV-2 variant (p = 0.29). However, the type of viral coinfection varied throughout the study; RSV, hMPV, and influenza co-infections were identified only in children with Delta and Omicron infections.

Clinical Characteristics of the Inpatient Cohort

Because complete clinical and laboratory data were available for inpatients (n = 226), we further analyzed this cohort. We excluded 21 patients, 11 with MIS-C, because this condition represents a post-acute complication of COVID-19, and 10 who were diagnosed by screening upon admission, leaving a total of 205 inpatients with acute COVID-19. Of the 11 patients with MIS-C (median age 10.40 [IQR 2.10–15.70] years), 4 infections were related to the nonvariant strain, 2 to the Alpha variant, 3 to Delta, and 2 to Omicron. The 10 inpatients identified by SARS-CoV-2 screening were hospitalized with other infectious processes (i.e., rotavirus or *Clostridioides difficile* enteritis, intraabdominal abscesses, periorbital cellulitis) or trauma-related diagnoses.

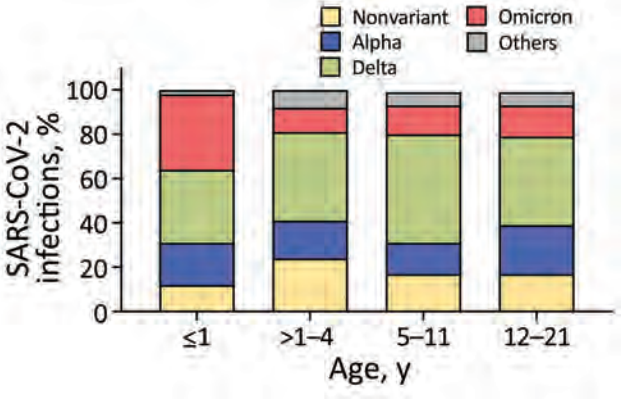

Figure 3. Distribution of SARS-CoV-2 variants in study of pediatric and adolescent patients included in a clinical cohort (n = 676) at Nationwide Children's Hospital, Columbus, Ohio, USA, by age group. Bars represent the percentage of each SARS-CoV-2–specific variant in the different age groups.

Of the 205 inpatients with acute COVID-19, a total of 26 (12.68%) were infected with the nonvariant strain, 21 (10.24%) with Alpha, 89 (43.41%) with Delta, and 59 (28.78%) with Omicron. Ten patients were infected with other SARS-CoV-2 variants (Epsilon, Eta, Gamma, and Iota); given their low representation, they were excluded from further analyses, leaving 195 inpatients for comparative clinical analyses.

Inpatients infected with Omicron were significantly younger (0.88 [IQR 0.13–11.72] years) than those infected with Delta (11.11 [IQR 0.69–16.05] years; p<0.001). Almost half (46.07%) of inpatients with Delta infections were adolescents, whereas infants represented 52.54% of Omicron infections (Table 2). Most inpatients in all variant groups were White, except inpatients with Alpha infections, who were mostly Black (57.14%). Underlying conditions were prevalent (61.03%); obesity/overweight was the most common chronic comorbidity irrespective of the infecting variant. Most (97.44%) inpatients were not immunized against SARS-CoV-2.

Duration of symptoms at the time of the SARS-CoV-2 testing was longer in inpatients with Delta infections than in those with nonvariant and Omicron infections (p<0.001), yet inpatients with Delta and Omicron infections had significantly lower Ct values than did those infected with the nonvariant strain (p = 0.04) (Figure 4, panel C). Compared with those with nonvariant infections, inpatients with Delta and Omicron infections were brought for care with fever and respiratory symptoms more frequently (p<0.05). Absolute lymphocyte counts (ALC) and lymphopenia, defined as an ALC of <4,500 cells/μL in children <12 months and <1,500 cells/μL in children >12 months of age (*18*), were more common in inpatients with Delta infections (p = 0.01) than those with nonvariant strain infections (p = 0.02).

COVID-19 therapy was provided to 42.70% of inpatients with Delta infections compared with 23.08% of those with nonvariant infections or 33.33% of inpatients infected with the Alpha variant, with no differences between groups (p = 0.26). Fifty-six percent of inpatients with Delta infections received oxygen, compared with ≈40.00% of those with other variants. Intensive care unit (ICU) admission was required for ≈25% of inpatients irrespective of the infecting variant; however, inpatients with Delta infections stayed in the ICU and in the hospital for a median of 1–2 days longer than those with other variants. These differences did not reach statistical significance.

One patient who had morbid obesity and acute COVID-19 associated with the Alpha variant died. In addition, 12 patients had more severe or unusual clinical manifestations: 6 were nonvaccinated patients 8–20 years of age with Delta infections whose illness manifested with severe myocarditis, pulmonary embolism, pneumothorax, or pneumomediastinum, and the other 6 were children <3 years of age with Omicron infections that manifested as croup.

Evaluation of Risk Factors for Severe COVID-19

We performed multivariable analyses to identify risk factors associated with disease severity defined as need for hospitalization, administration of supplemental oxygen, and PICU admission in patients with acute COVID-19. Fifteen children received mechanical ventilation, which precluded further multivariable analyses. Presence of underlying chronic conditions (odds ratio [OR] 4.53, 95% CI 1.48–15.10) and infants (OR 6.64, 1.34–36.00), but not the infecting SARS-CoV-2 variant or viral co-infections, were independently associated with increase odds of hospitalization (Appendix Table 3). In hospitalized patients, underlying conditions also increased the odds

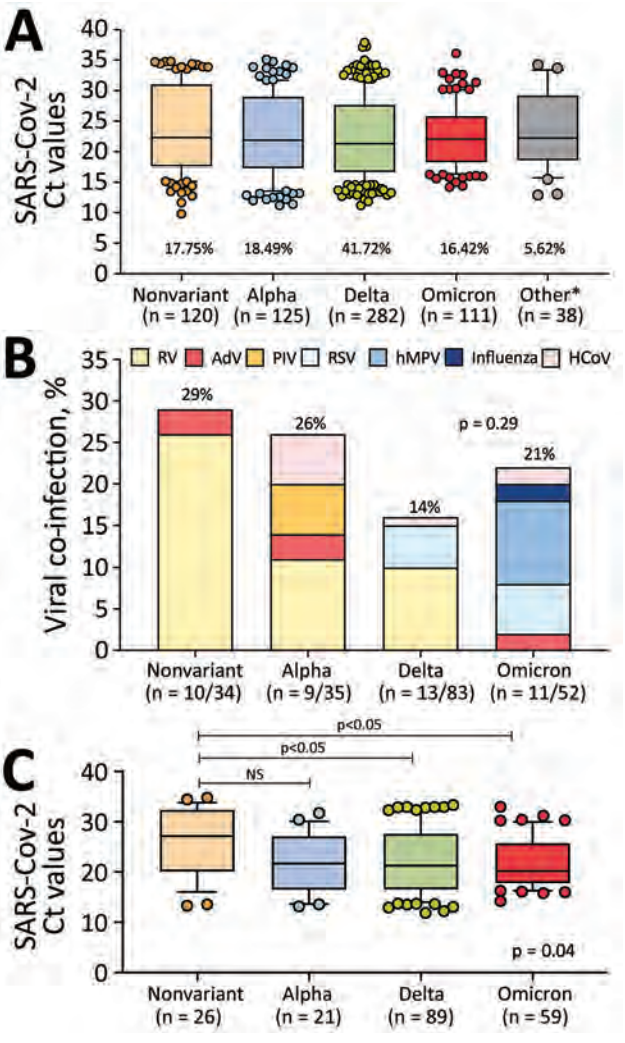

Figure 4. SARS-CoV-2 viral loads and viral co-infections among children and adolescents with COVID-19 at Nationwide Children's Hospital, Columbus, Ohio, USA, by the infecting SARS-CoV-2 variant, January 1, 2021–January 15, 2022. A) Nasopharyngeal SARS-CoV-2 viral loads expressed as Ct values according to the infecting SARS-CoV-2 variant in the clinical cohort (n = 676). Percentage of total infections for each variant is below each bar. B) Viral co-infections by SARS-CoV-2 variant during the study period in patients that underwent multiplex viral testing. Twelve patients with other variants tested negative for viral co-infections (not shown). Percentage of total co-infections is above each bar. p value was determined by χ^2 test. C) Nasopharyngeal SARS-CoV-2 Ct values by infecting SARS-CoV-2 variant among inpatients with acute COVID-19, excluding patients with MIS-C, SARS-CoV-2 detected by screening in inpatients, and those infected with uncommon SARS-CoV-2 strains. p value at bottom right represents the overall Kruskal-Wallis p value; values above bars indicate ad hoc pairwise comparisons by Dunn multiple test correction. For box plots in panels A and C, horizontal lines within boxes indicate medians; box tops and bottoms indicate interquartile ranges; error bars indicate 95% CIs. AdV, adenovirus; HCoV, human coronavirus; hPMV, human metapneumovirus; MIS-C, multisystem inflammatory syndrome in children; NS, not significant. PIV, parainfluenza virus; RSV, respiratory syncytial virus; RV, rhinovirus.

Table 2. Demographic, laboratory characteristics and clinical outcomes of children and adolescents hospitalized with acute COVID-19 by SARS-CoV-2 variant, Columbus, Ohio, USA*

Characteristic	Clinical inpatient cohort, n = 195†	Nonvariant, n = 26	Alpha, n = 21	Delta, n = 89	Omicron, n = 59	p value
Median age, y (IQR)	5.7 (0.36–15.41)	3.3 (1.25–15.46)	4.1 (0.48–14.84)	11.1 (0.69–16.05)	0.8 (0.13–11.72)	**0.01‡**
Age group, y						**<0.001‡**
<1 y	67 (34.36)	5 (19.23)	8 (38.10)	23 (25.84)	31 (52.54)	
1–4	27 (13.85)	10 (38.46)	3 (14.29)	8 (8.99)	6 (10.17)	
5–11	27 (13.85)	1 (3.85)	2 (9.52)	17 (19.10)	7 (11.87)	
12–21	74 (37.95)	10 (38.46)	8 (38.07)	41 (46.07)	15 (25.42)	
Sex						
M	106 (54.36)	15 (57.69)	10 (47.62)	50 (56.18)	31 (52.54)	0.89
F	89 (45.64)	11 (42.31)	11 (52.38)	39 (43.82)	28 (47.46)	
Race/ethnic group						**0.02‡**
White	113 (57.95)	18 (69.23)	8 (38.10)	59 (66.30)	28 (47.46)	
Black	46 (23.59)	4 (15.39)	12 (57.14)	16 (17.98)	14 (23.73)	
Multiracial	11 (5.64)	2 (7.69)	1 (4.77)	4 (4.49)	4 (6.78)	
Hispanic	11 (5.64)	1 (3.85)	0 (0.00)	5 (5.62)	5 (8.48)	
Other/unknown	14 (7.18)	1 (3.85)	0 (0.00)	5 (5.62)	8 (13.56)	
Underlying conditions§	119 (61.03)	17 (65.38)	14 (66.67)	58 (65.19)	30 (51.72)	0.3
Obesity/overweight	63 (32.30)	6 (23.08)	6 (28.57)	38 (42.70)	13 (22.03)	
Respiratory	21 (10.77)	3 (11.54)	6 (28.57)	10 (11.24)	2 (3.39)	
Genetic/neurologic	25 (12.82)	4 (15.38)	1 (4.76)	11 (12.36)	9 (15.25)	
Cardiac	5 (2.56)	3 (11.54)	0 (0.00)	1 (1.12)	1 (1.69)	
GI/renal	10 (5.13)	3 (11.54)	1 (4.76)	6 (6.74)	0 (0.00)	
Other	4 (24.10)	5 (19.23)	5 (23.81)	20 (22.47)	17 (28.81)	
SARS-CoV-2 vaccination	5 (2.82)	0 (0.00)	0 (0.00)	1 (1.13)	4 (6.78)	0.27
Duration of illness, d (IQR)	3 (1.00–7.00)	3 (1.00–6.00)	2 (1.00–5.00)	5 (2.00–8.00)	2 (1.00–4.00)	**<0.001‡**
Clinical manifestations						
Fever	147 (75.38)	14 (53.85)	16 (76.19)	71 (79.78)	46 (77.97)	**<0.05‡**
Respiratory	160 (82.05)	16 (61.54)	17 (80.95)	75 (84.27)	52 (88.14)	**0.03‡**
Upper respiratory	70 (43.75)	6 (23.08)	8 (38.10)	28 (31.46)	28 (47.46)	0.11
Lower respiratory	90 (56.25)	10 (38.46)	9 (42.86)	47 (52.81)	24 (40.68)	0.39
Cardiac	25 (12.82)	5 (19.23)	3 (14.29)	12 (13.48)	5 (8.48)	0.57
Gastrointestinal	83 (42.56)	11 (42.31)	9 (42.86)	36 (40.45)	27 (45.77)	0.94
Other¶	47 (24.10)	9 (34.62)	12 (57.14)	28 (31.46)	20 (33.90)	0.17
ALC, × 10^3/μL	1.6 (0.93–3.46)	2.2 (1.62–3.69)	1.90 (1.26–3.36)	1.20 (0.87–2.06)	2.7 (0.93–4.38)	**0.01‡**
Lymphopenia	105/170 (61.76)	9 (37.50)	13 (61.91)	57 (72.15)	26 (56.52)	**0.02‡**
CRP, mg/dL, median (IQR)	1.4 (0.50–4.10)	2.50 (0.65–5.75)	0.70 (0.50-.3.40)	1.70 (0.55–3.75)	1.30 (0.50–4.40)	0.62
Ct, median (IQR)	21.36 (17.28–27.69)	27.10 (20.16–31.98)	21.67 (16.64–26.35)	21.24 (16.54–27.35)	20.17 (17.80–25.26)	**0.04‡**
COVID-19 targeted therapy	70 (35.90)	6 (23.08)	7 (33.33)	38 (42.70)	19 (32.20)	0.26
Oxygen supplementation	91 (46.67)	10 (38.46)	9 (42.86)	50 (56.18)	22 (37.29)	0.1
PICU admission	53 (27.18)	7 (26.92)	5 (23.81)	26 (29.21)	15 (25.42)	0.94
Duration of PICU stay, d (IQR)	3.48 (1.00–7.46)	1.00 (1.00–2.50)	3.00 (2.00–34.00)	4.00 (1.63–7.65)	4.00 (2.03–5.44)	0.26
Duration of hospitalization, d (IQR)	2.86 (1.79–7.09)	2.10 (1.72–3.02)	2.89 (1.81–5.00)	3.91 (1.84–7.91)	2.20 (1.45–7.33)	0.17

*Values are no. (%) except as indicated. Continuous variables were analyzed by analyzed by Kruskal-Wallis test. Categorical data were analyzed by χ^2 test. Bold text indicates statistical significance. ALC, absolute lymphocyte count; CRP, C-reactive protein; GI, gastrointestinal; IQR, interquartile range; PICU, pediatric intensive care unit.

†Patients with multisystem inflammatory syndrome in children, SARS-CoV-2 detected by screening but hospitalized for other reasons, and those infected with uncommon SARS-CoV-2 strains were excluded from analyses.

‡p values represent statistical significance between groups based on Kruskal-Wallis or χ^2 test. Ad hoc adjusted p values from pairwise comparisons were as follows: age, p<0.01 between Omicron and Delta; duration of illness, Delta vs. nonvariant infections (p = 0.03), Delta vs. Alpha (p not significant); and Delta vs. Omicron (p<0.001); fever, nonvariant vs. Delta (p = 0.01), nonvariant vs. Omicron (p = 0.04); respiratory symptoms, nonvariant vs. Delta (p = 0.03), nonvariant vs Omicron (p < 0.01). Total ALC, Delta vs. nonvariant infections (p = 0.03); lymphopenia, Delta vs. nonvariant infections (p<0.01). Ct values: nonvariant vs. Delta (p = 0.03), nonvariant vs Omicron (p = 0.03).

§Underlying conditions: respiratory (asthma, bronchopulmonary dysplasia, cystic fibrosis); cardiac (septal defects, valvopathies; dilated cardiomyopathy); endocrinologic (diabetes, dyslipidemia, panhypopituitarism and polyendocrinopathy); hematologic (sickle cell disease, spherocytosis, thalassemia, chronic idiopathy thrombocytopenia purpura); immunocompromised conditions (solid or hematopoietic organ transplantation, malignancies–leukemias, solid tumors, rheumatologic conditions receiving chronic immunosuppressive therapy, primary immunodeficiencies, HIV); neurologic and genetic conditions (cerebral palsy, autism, developmental delay); prematurity; renal/gastrointestinal conditions (Hirschsprung's, duodenal atresia, short bowel syndrome, chronic kidney disease, intestinal bowel disease, nephrotic syndrome); and obesity/overweight.

¶Other symptoms: anosmia, fatigue, myalgias, headache, back pain, chills, polyarthralgia, hemoptysis, rash. Lymphopenia defined as ALC of <4,500 cells/μL in infants, and <1,500 cells/μL in children >12 mo of age (*18*).

for supplemental oxygen administration (OR 2.62 95% CI 1.01–6.95); viral co-infections increased the odds, but the difference was not significant (OR 2.75, 95% CI 0.98–8.17; p = 0.06) (Appendix Table 4). In addition, OR for PICU admission was higher in inpatients with SARS-CoV-2/viral co-infections (OR 2.89, 95% CI 1.03–8.99) (Appendix Table 5).

Discussion

The emergence of distinct SARS-CoV-2 variants since the beginning of the COVID-19 pandemic and the questionable differences in severity among variants in children remains poorly understood. To date, most of the studies describing the clinical effects of SARS-CoV-2 variants have been conducted in adults or derived from national or regional estimates, without a direct nexus between the specific SARS-CoV2 variant and the patient's clinical phenotype (*19*–*22*). In this study, we linked the PCR-identified SARS-CoV-2 variant and patient clinical characteristics. We found that children and adolescents hospitalized for acute Delta and Omicron infections had lower SARS-CoV-2 Ct values and experienced fever and respiratory symptoms more frequently than did inpatients infected with previous variants. In adjusted analyses, presence of underlying conditions and viral co-infections, but not the infecting variant, were associated with worse clinical outcomes. Overall, these data suggested that different SARS-CoV-2 variants are associated with distinct clinical manifestations; however, clinical risk factors remain important determinants of COVID-19 severity.

We documented the local circulation of 12 SARS-CoV-2 variants appearing temporally in waves that coincided with national reports (*19*). First, the Alpha variant circulated until June 2021, followed by Delta during July–December 2021, and more recently Omicron. In our study, the highest positivity rate for SARS-CoV-2 occurred in January 2022, when Omicron predominated, which mirrors findings of national reports (*23*,*24*) and supports the high transmissibility of this variant (*25*,*26*). The rates and pattern of viral co-infections with SARS-CoV-2 in our cohort are similar to those described previously (*27*–*29*). Whereas rhinovirus/enterovirus was the most common viral coinfection identified throughout the study, coinfections with enveloped viruses (coronavirus, RSV, PIV, hMPV, or influenza) increased as nonpharmacologic interventions to prevent SARS-COV-2 infections were discontinued (*30*). The atypical RSV season documented in summer 2021 (*31*,*32*) coinciding with the Delta wave was also evident in our cohort; most children with RSV/SARS-CoV-2 co-infections were identified during July–December 2021.

We observed a U-shaped age distribution of COVID-19 in children, which was previously reported (*33*,*34*). Within all age groups, patients 12–21 years of age were 37.87% of all patients and 40.27% of those who were hospitalized, especially with Delta, Alpha, and nonvariant infections. On the other hand, half of Omicron infections were documented in infants, compared with 20%–30% of infant infections with previous variants. These findings are consistent with other US and UK studies that reported an increased proportion of infants and young children hospitalized with COVID-19 during the Omicron wave (*23*,*24*). In our cohort, although the predominant race was White (59%), a significant number of Black and Hispanic children were affected irrespective of the infecting variant, confirming previous studies (*29*,*35*). Obesity has been consistently associated with severe COVID-19 in adults (*35*–*37*); we found that in children, obesity/overweight was the underlying condition most commonly associated with worse clinical outcomes irrespective of the infecting variant. Almost none of the children hospitalized with COVID-19 were vaccinated, reflecting national trends (*23*,*38*).

Studies conducted in adults suggested that infections with the Delta variant were associated with more severe disease and higher viral loads than infections with previous variants (*25*,*39*–*45*). On the other hand, subsequent reports using national US trends or EHR data not linked to specific variants showed that disease severity in children during the Delta wave was comparable to that described with the circulation of previous variants (*19*,*22*). In our study we found that PCR-typed Delta infections were associated with lower Ct values, more frequent fever and respiratory symptoms, and higher rates of lymphopenia than infections caused by the original strain. Moreover, a great proportion of children and adolescents with severe manifestations were infected with the Delta variant. On the other hand, children infected with Omicron were younger than in previous waves and had lower Ct values; nearly half (47.46%) experienced upper respiratory symptoms including croup, which was anecdotally reported earlier in the pandemic (*46*,*47*). Although information about preexisting antibodies or other host factors was not available in these children, the differences in clinical manifestations by variant might partially reflect the evolution and fitness of SARS-CoV-2 associated with differences in transmissibility or pathogenicity.

A recent retrospective study conducted in children <5 years of age with COVID-19 showed that those identified during the Omicron surge were younger and had a lower risk for severe disease than children

identified during the Delta wave (*48*). Similarly, another large retrospective study showed that rates of hospitalization in US children 0–4 years of age during the initial wave of Omicron (late December 2021–February 2022) were 5 times higher than with the circulation of Delta, yet clinical disease severity was worse during the Delta wave (*23*,*24*). Contrary to those studies, we found that rates of PICU admission were similar between children with Omicron and those infected with all other variants. We also found that a higher proportion of RSV and hMPV/SARS-CoV-2 co-infections were identified in children with Omicron and that SARS-CoV-2/viral co-infections were associated with increased odds of PICU admission. Our study is likely underpowered to determine whether it is plausible that RSV or hMPV co-infections could have played a role in the higher rates of PICU admission observed in children with Omicron infection.

One patient in our study who was infected with the Alpha variant and with multiple chronic conditions died. Although death associated with COVID-19 in children is low, >1,400 children and adolescents 0–18 years of age have died of COVID-19 in the United States as of September 2022 (*49*,*50*).

The first limitation of our study is that not all samples that tested positive for SARS-CoV-2 by NAAT underwent variant screening. The percentage of monthly samples screened varied based upon sample volumes and the availability of the personnel at the NCH clinical laboratory. Therefore, during months of high SARS-CoV-2 activity, a smaller percentage of samples underwent variant testing. In addition, clinical data from 350 patients with Delta infections identified during September–December 2021 were not collected because we had a sufficient sample size for Delta infections. Although the cohort we analyzed was a convenience sample, it is representative of the overall population evaluated in our center during the pandemic. Another limitation is related to the retrospective nature of data collection, which affected the outpatient cohort. We reviewed all patient records manually, but data regarding clinical manifestations or duration of symptoms were not available for all outpatients. Thus, to mitigate the impact of missing data, we analyzed clinical variables exclusively in inpatients.

In summary, our findings confirmed the local circulation of different SARS-CoV-2 variants over time infecting children and adolescents treated at a children's hospital in Ohio, USA. Infections caused by Delta and Omicron variants were associated with lower Ct values and with more frequent fever and respiratory symptoms than for infections with the original strain; at least one fourth of hospitalized children required ICU admission, irrespective of the infecting variant. These findings suggest that children are susceptible to SARS-CoV-2 infection by any of the circulating variants and that they can develop severe disease. The data also emphasize that active monitoring of the shift in SARS-CoV-2 variants is critical to understand their clinical effects and implications for managing COVID-19 in children.

Acknowledgments

We thank Swan Bee Liu for her help curating the EHR data.

This work was supported by intramural funds from the Department of Pathology at Nationwide Children's Hospital and the Center from Vaccines and Immunity. A.M. and O.R. are supported in part by the NIH grant UO1AI131386.

About the Author

Dr. Quintero is a pediatric infectious disease fellow at Nationwide Children's Hospital. Her primary research interests are related to the impact of SARS-CoV-2 infections in children and to identify biomarkers predictive of severe disease.

References

1. Brodin P. Immune determinants of COVID-19 disease presentation and severity. Nat Med. 2021;27:28–33. https://doi.org/10.1038/s41591-020-01202-8
2. Ludvigsson JF. Systematic review of COVID-19 in children shows milder cases and a better prognosis than adults. Acta Paediatr. 2020;109:1088–95. https://doi.org/10.1111/apa.15270
3. Arunachalam PS, Wimmers F, Mok CKP, Perera RAPM, Scott M, Hagan T, et al. Systems biological assessment of immunity to mild versus severe COVID-19 infection in humans. Science. 2020;369:1210–20. https://doi.org/10.1126/science.abc6261
4. Godfred-Cato S, Bryant B, Leung J, Oster ME, Conklin L, Abrams J, et al.; California MIS-C Response Team. COVID-19-associated multisystem inflammatory syndrome in children—United States, March–July 2020. MMWR Morb Mortal Wkly Rep. 2020;69:1074–80. https://doi.org/10.15585/mmwr.mm6932e2
5. Belay ED, Abrams J, Oster ME, Giovanni J, Pierce T, Meng L, et al. Trends in geographic and temporal distribution of US children with multisystem inflammatory syndrome during the COVID-19 pandemic. JAMA Pediatr. 2021;175:837–45. https://doi.org/10.1001/jamapediatrics.2021.0630
6. Dufort EM, Koumans EH, Chow EJ, Rosenthal EM, Muse A, Rowlands J, et al.; New York State and Centers for Disease Control and Prevention Multisystem Inflammatory Syndrome in Children Investigation Team. Multisystem inflammatory syndrome in children in New York State. N Engl J Med. 2020;383:347–58. https://doi.org/10.1056/NEJMoa2021756
7. Feldstein LR, Rose EB, Horwitz SM, Collins JP, Newhams MM, Son MBF, et al.; Overcoming COVID-19 Investigators; CDC

COVID-19 Response Team. Multisystem inflammatory syndrome in U.S. children and adolescents. N Engl J Med. 2020;383:334–46. https://doi.org/10.1056/NEJMoa2021680
8. Chen J, Wang R, Wang M, Wei GW. Mutations strengthened SARS-CoV-2 infectivity. J Mol Biol. 2020;432:5212–26. https://doi.org/10.1016/j.jmb.2020.07.009
9. Walensky RP, Walke HT, Fauci AS. SARS-CoV-2 variants of concern in the United States—challenges and opportunities. JAMA. 2021;325:1037–8. https://doi.org/10.1001/jama.2021.2294
10. Maslo C, Friedland R, Toubkin M, Laubscher A, Akaloo T, Kama B. Characteristics and outcomes of hospitalized patients in South Africa during the COVID-19 Omicron wave compared with previous waves. JAMA. 2022;327:583–4. https://doi.org/10.1001/jama.2021.24868
11. Jansen L, Tegomoh B, Lange K, Showalter K, Figliomeni J, Abdalhamid B, et al. Investigation of a SARS-CoV-2 B.1.1.529 (Omicron) variant cluster—Nebraska, November–December 2021. MMWR Morb Mortal Wkly Rep. 2021;70:1782–4. https://doi.org/10.15585/mmwr.mm705152e3
12. Delahoy MJ, Ujamaa D, Whitaker M, O'Halloran A, Anglin O, Burns E, et al.; COVID-NET Surveillance Team. Hospitalizations associated with COVID-19 among children and adolescents—COVID-NET, 14 States, March 1, 2020–August 14, 2021. MMWR Morb Mortal Wkly Rep. 2021;70:1255–60. https://doi.org/10.15585/mmwr.mm7036e2
13. Siegel DA, Reses HE, Cool AJ, Shapiro CN, Hsu J, Boehmer TK, et al.; MAPW1. Trends in COVID-19 cases, emergency department visits, and hospital admissions among children and adolescents aged 0–17 years—United States, August 2020–August 2021. MMWR Morb Mortal Wkly Rep. 2021;70:1249–54. https://doi.org/10.15585/mmwr.mm7036e1
14. Walker AS, Pritchard E, House T, Robotham JV, Birrell PJ, Bell I, et al.; COVID-19 Infection Survey team. Ct threshold values, a proxy for viral load in community SARS-CoV-2 cases, demonstrate wide variation across populations and over time. eLife. 2021;10: e64683. https://doi.org/10.7554/eLife.64683
15. Wang H, Jean S, Eltringham R, Madison J, Snyder P, Tu H, et al. Mutation-specific SARS-CoV-2 PCR screen: rapid and accurate detection of variants of concern and the identification of a newly emerging variant with spike L452R mutation. J Clin Microbiol. 2021;59:e0092621. https://doi.org/10.1128/JCM.00926-21
16. Nextstrain: real-time tracking of pathogen evolution. 2022 [cited 2022 Jan 28]. https://nextstrain.org
17. Simon TD, Cawthon ML, Popalisky J, Mangione-Smith R; Center of Excellence on Quality of Care Measures for Children with Complex Needs (COE4CCN). Development and validation of the Pediatric Medical Complexity Algorithm (PMCA) version 2.0. Hosp Pediatr. 2017;7:373–7. https://doi.org/10.1542/hpeds.2016-0173
18. Régent A, Kluger N, Bérezné A, Lassoued K, Mouthon L. Lymphocytopenia: aetiology and diagnosis, when to think about idiopathic CD4(+) lymphocytopenia? [in French]. Rev Med Interne. 2012;33:628–34.
19. Iuliano AD, Brunkard JM, Boehmer TK, Peterson E, Adjei S, Binder AM, et al. Trends in disease severity and health care utilization during the early omicron variant period compared with previous SARS-CoV-2 high transmission periods—United States, December 2020–January 2022. MMWR Morb Mortal Wkly Rep. 2022;71:146–52. https://doi.org/10.15585/mmwr.mm7104e4
20. Wolter N, Jassat W, Walaza S, Welch R, Moultrie H, Groome M, et al. Early assessment of the clinical severity of the SARS-CoV-2 omicron variant in South Africa: a data linkage study. Lancet. 2022;399:437–46. https://doi.org/10.1016/S0140-6736(22)00017-4
21. Meo SA, Meo AS, Al-Jassir FF, Klonoff DC. Omicron SARS-CoV-2 new variant: global prevalence and biological and clinical characteristics. Eur Rev Med Pharmacol Sci. 2021;25:8012–8.
22. Forrest CB, Burrows EK, Mejias A, Razzaghi H, Christakis D, Jhaveri R, et al. Severity of acute COVID-19 in children <18 years old March 2020 to December 2021. Pediatrics. 2022;149:e2021055765. https://doi.org/10.1542/peds.2021-055765
23. Marks KJ, Whitaker M, Anglin O, Milucky J, Patel K, Pham H, et al.; COVID-NET Surveillance Team. Hospitalizations of children and adolescents with laboratory-confirmed COVID-19—OVID-NET, 14 states, July 2021–January 2022. MMWR Morb Mortal Wkly Rep. 2022;71:271–8. https://doi.org/10.15585/mmwr.mm7107e4
24. Marks KJ, Whitaker M, Agathis NT, Anglin O, Milucky J, Patel K, et al.; COVID-NET Surveillance Team. Hospitalization of infants and children aged 0-4 years with laboratory-confirmed COVID-19—COVID-NET, 14 states, March 2020–February 2022. MMWR Morb Mortal Wkly Rep. 2022;71:429–36. https://doi.org/10.15585/mmwr.mm7111e2
25. Karim SSA, Karim QA. Omicron SARS-CoV-2 variant: a new chapter in the COVID-19 pandemic. Lancet. 2021;398:2126–8. https://doi.org/10.1016/S0140-6736(21)02758-6
26. Thakur V, Ratho RK. OMICRON (B.1.1.529): A new SARS-CoV-2 variant of concern mounting worldwide fear. J Med Virol. 2022;94:1821–4. https://doi.org/10.1002/jmv.27541
27. Si Y, Zhao Z, Chen R, Zhong H, Liu T, Wang M, et al. Epidemiological surveillance of common respiratory viruses in patients with suspected COVID-19 in southwest China. BMC Infect Dis. 2020;20:688. https://doi.org/10.1186/s12879-020-05392-x
28. Lai CC, Wang CY, Hsueh PR. Co-infections among patients with COVID-19: The need for combination therapy with non–anti-SARS-CoV-2 agents? J Microbiol Immunol Infect. 2020;53:505–12. https://doi.org/10.1016/j.jmii.2020.05.013
29. Richardson S, Hirsch JS, Narasimhan M, Crawford JM, McGinn T, Davidson KW, et al.; the Northwell COVID-19 Research Consortium. Presenting characteristics, comorbidities, and outcomes among 5,700 patients hospitalized with COVID-19 in the New York City area. JAMA. 2020;323:2052–9. https://doi.org/10.1001/jama.2020.6775
30. Park S, Michelow IC, Choe YJ. Shifting patterns of respiratory virus activity following social distancing measures for coronavirus disease 2019 in South Korea. J Infect Dis. 2021;224:1900–6. https://doi.org/10.1093/infdis/jiab231
31. Hernández-Rivas L, Pedraz T, Calvo C, San Juan I, Mellado MJ, Robustillo A. Respiratory syncytial virus outbreak during the COVID-19 pandemic. How has it changed? Enferm Infecc Microbiol Clin. 2021. 10.1016/j.eimc.2021.12.003 https://doi.org/10.1016/j.eimc.2021.12.003
32. Ohnishi T, Kawano Y. Resurgence of respiratory syncytial virus infection during an atypical season in Japan. J Pediatric Infect Dis Soc. 2021;10:982–3. https://doi.org/10.1093/jpids/piab065
33. DeBiasi RL, Song X, Delaney M, Bell M, Smith K, Pershad J, et al. Severe coronavirus disease-2019 in children and young adults in the Washington, DC, metropolitan region. J Pediatr. 2020;223:199–203.e1. https://doi.org/10.1016/j.jpeds.2020.05.007

34. Hobbs CV, Woodworth K, Young CC, Jackson AM, Newhams MM, Dapul H, et al.; Overcoming COVID-19 Investigators. Frequency, characteristics and complications of COVID-19 in hospitalized infants. Pediatr Infect Dis J. 2022; 41:e81–6. https://doi.org/10.1097/INF.0000000000003435
35. Yue H, Bai X, Wang J, Yu Q, Liu W, Pu J, et al.; Gansu Provincial Medical Treatment Expert Group of COVID-19. Clinical characteristics of coronavirus disease 2019 in Gansu province, China. Ann Palliat Med. 2020;9:1404–12. https://doi.org/10.21037/apm-20-887
36. Zhou Y, Chi J, Lv W, Wang Y. Obesity and diabetes as high-risk factors for severe coronavirus disease 2019 (COVID-19). Diabetes Metab Res Rev. 2021;37:e3377. https://doi.org/10.1002/dmrr.3377
37. Petrakis D, Margină D, Tsarouhas K, Tekos F, Stan M, Nikitovic D, et al. Obesity—a risk factor for increased COVID19 prevalence, severity and lethality. Mol Med Rep. 2020;22:9–19. https://doi.org/10.3892/mmr.2020.11127
38. León TM, Dorabawila V, Nelson L, Lutterloh E, Bauer UE, Backenson B, et al. COVID-19 cases and hospitalizations by COVID-19 vaccination status and previous COVID-19 diagnosis—California and New York, May–November 2021. MMWR Morb Mortal Wkly Rep. 2022;71:125–31. https://doi.org/10.15585/mmwr.mm7104e1
39. Wang Y, Chen R, Hu F, Lan Y, Yang Z, Zhan C, et al. Transmission, viral kinetics, and clinical characteristics of the emergent SARS-CoV-2 Delta VOC in Guangzhou, China. EClinicalMedicine. 2021;40:101129. https://doi.org/10.1016/j.eclinm.2021.101129
40. Despres HW, Mills MG, Shirley DJ, Schmidt MM, Huang ML, Jerome KR, et al. Measuring infectious SARS-CoV-2 in clinical samples reveals a higher viral titer:RNA ratio for Delta and Epsilon vs. Alpha variants. Proc Natl Acad Sci U S A. 2022;119:e2116518119. https://doi.org/10.1073/pnas.2116518119
41. Smith DR, Singh C, Green J, Lueder MR, Arnold CE, Voegtly LJ, et al. Genomic and virological characterization of SARS-CoV-2 variants in a subset of unvaccinated and vaccinated U.S. military personnel. Front Med (Lausanne). 2022;8:836658. https://doi.org/10.3389/fmed.2021.836658
42. Mlcochova P, Kemp SA, Dhar MS, Papa G, Meng B, Ferreira IATM, et al.; Indian SARS-CoV-2 Genomics Consortium (INSACOG); Genotype to Phenotype Japan (G2P-Japan) Consortium; CITIID-NIHR BioResource COVID-19 Collaboration. SARS-CoV-2 B.1.617.2 Delta variant replication and immune evasion. Nature. 2021;599: 114–9. https://doi.org/10.1038/s41586-021-03944-y
43. Luo CH, Morris CP, Sachithanandham J, Amadi A, Gaston D, Li M, et al. Infection with the SARS-CoV-2 Delta variant is associated with higher infectious virus loads compared to the Alpha variant in both unvaccinated and vaccinated individuals. Clin Infect Dis. 2022;75:e715–9 25. https://doi.org/10.1093/cid/ciab986
44. Harvey WT, Carabelli AM, Jackson B, Gupta RK, Thomson EC, Harrison EM, et al.; COVID-19 Genomics UK (COG-UK) Consortium. SARS-CoV-2 variants, spike mutations and immune escape. Nat Rev Microbiol. 2021;19:409–24. https://doi.org/10.1038/s41579-021-00573-0
45. Twohig KA, Nyberg T, Zaidi A, Thelwall S, Sinnathamby MA, Aliabadi S, et al.; COVID-19 Genomics UK (COG-UK) consortium. Hospital admission and emergency care attendance risk for SARS-CoV-2 delta (B.1.617.2) compared with alpha (B.1.1.7) variants of concern: a cohort study. Lancet Infect Dis. 2022;22:35–42. https://doi.org/10.1016/S1473-3099(21)00475-8
46. Murata Y, Tomari K, Matsuoka T. Children with croup and SARS-CoV-2 infection during the large outbreak of Omicron. Pediatr Infect Dis J. 2022;41:e249. https://doi.org/10.1097/INF.0000000000003484
47. Sharma S, Agha B, Delgado C, Walson K, Woods C, Gonzalez MD, et al. Croup associated with SARS-CoV-2: pediatric laryngotracheitis during the Omicron surge. J Pediatric Infect Dis Soc. 2022;11:371–4. https://doi.org/10.1093/jpids/piac032
48. Wang L, Berger NA, Kaelber DC, Davis PB, Volkow ND, Xu R. Incidence rates and clinical outcomes of SARS-CoV-2 infection with the Omicron and Delta variants in children younger than 5 years in the US. JAMA Pediatr. 2022;176:811–3. https://doi.org/10.1001/jamapediatrics.2022.0945
49. Haas EJ, Angulo FJ, McLaughlin JM, Anis E, Singer SR, Khan F, et al. Impact and effectiveness of mRNA BNT162b2 vaccine against SARS-CoV-2 infections and COVID-19 cases, hospitalisations, and deaths following a nationwide vaccination campaign in Israel: an observational study using national surveillance data. Lancet. 2021;397:1819–29. https://doi.org/10.1016/S0140-6736(21)00947-8
50. Danza P, Koo TH, Haddix M, Fisher R, Traub E, OYong K, et al. SARS-CoV-2 infection and hospitalization among adults aged ≥18 years, by vaccination status, before and during SARS-CoV-2 B.1.1.529 (Omicron) variant predominance—Los Angeles County, California, November 7, 2021–January 8, 2022. MMWR Morb Mortal Wkly Rep. 2022;71:177–81. https://doi.org/10.15585/mmwr.mm7105e1

Address for correspondence: Asuncion Mejias or Huanyu Wang, Nationwide Children's Hospital, 700 Children's Dr, Columbus, OH 43205, USA; email: Asuncion.Mejias@nationwidechildrens.org or Huanyu.Wang@Nationwidechildrens.org

Imported *Haycocknema perplexum* Infection, United States[1]

Bobbi S. Pritt, Blaine A. Mathison, Richard S. Bradbury, Teerin Liewluck, Stefan Nicolau, John C. O'Horo, David Grunst, Marcus V. Pinto, Amy A. Swanson, Abinash Virk

We report an imported case of myositis caused by a rare parasite, *Haycocknema perplexum*, in Australia in a 37-year-old man who had progressive facial, axial, and limb weakness, dysphagia, dysphonia, increased levels of creatine kinase and hepatic aminotransferases, and peripheral eosinophilia for 8 years. He was given extended, high-dose albendazole.

Haycocknema perplexum is an enigmatic nematode that is a rare cause of human parasitic myositis (*1*–*4*). Twelve cases have been reported since its initial description in 1998, all in humans (*1*–*10*). The mode of transmission is unclear, but 9 patients reported contact with native wildlife in Tasmania or tropical regions of Queensland, Australia. We report an imported case of myositis caused by infection with this rare parasite.

The Study

A 37-year-old man from New Zealand who had previous long-term residence in Australia came to the Mayo Clinic (Rochester, MN, USA) because of an 8-year history of progressive weakness, muscle atrophy, and 32-kg weight loss. Onset was gradual, first involving the pectoralis and biceps brachii, then neck, facial, and distal limb muscles. Additional symptoms included dysphagia, dysphonia, and dyspnea on exertion. Laboratory testing showed peripheral eosinophilia (5%, reference value ≤3%), and an increased level of creatine kinase (maximum ≈2,000 U/L, reference range 39–308 U/L). Toxoplasmosis had originally been suspected based on finding a possible *Toxoplasma gondii* cyst on muscle biopsy 1 year after symptom onset, but his weakness progressed despite trimethoprim/sulfamethoxazole therapy, and *T. gondii* serologic test results were negative. Prednisone therapy worsened his symptoms.

He became wheelchair-bound 7 years after onset of symptoms. He had lived in coastal northern Queensland (Mackay region), Australia from ages 8–20 years, where he had extensive bush exposure but denied bush meat consumption. Neurologic findings included profound asymmetric weakness predominantly affecting proximal upper and lower limbs, neck flexors, and sternocleidomastoids (Figure 1). He also had asymmetric scapular winging, severe weakness of the frontalis, and mild weakness of orbicularis oris.

A formalin-fixed, paraffin-embedded muscle tissue from a previous muscle biopsy specimen was obtained, and additional sections showed nonencapsulated male and gravid female nematodes within muscle fibers consistent with *H. perplexum* (Figure 2). The presence of adult worms enabled trichinellosis to be definitively excluded because only the larval stage of *Trichinella* sp. is detected in muscle. Attempts at molecular amplification of the cytochrome c oxidase subunit 1 and 18S rRNA genes as described (*2*,*8*) from archival formalin-fixed, paraffin-embedded tissue were unsuccessful.

The patient was prescribed a 3-month course of albendazole (400 mg 2×/d). Nineteen months after completing albendazole, the patient reported no further deterioration. However, his muscle power did not improve. Creatinine kinase levels decreased to within the reference range.

Conclusions

Haycocknema perplexum is an enigmatic and presumably zoonotic nematode. Clinical histories of

Author affiliations: Mayo Clinic, Rochester, Minnesota, USA (B.S. Pritt, T. Liewluck, J.C. O'Horo, D. Grunst, M.V. Pinto, A. Swanson, A. Virk); ARUP Laboratories, Salt Lake City, Utah, USA (B.A. Mathison); Federation University, Melbourne, Victoria, Australia (R.S. Bradbury); Nationwide Children's Hospital, Columbus, Ohio, USA (S. Nicolau)

DOI: https://doi.org/10.3201/eid2811.220286

[1]This study was presented as a late breaker abstract at the 68th Annual Meeting of the American Society of Tropical Medicine and Hygiene, November 20–24, 2019, National Harbor, Maryland, USA.

affected patients indicate that contact with wilderness or marsupial wildlife in Australia (n = 6) and consumption of bush meat (n = 4) might be associated with infection, but this possibility has not been confirmed (Table, https://wwwnc.cdc.gov/EID/article/28/11/22-0286-T1.htm). The phylogenetic position of *H. perplexum* is unresolved, but it appears to be intermediary between Oxyuridomorpha (e.g., *Enterobius vermicularis*) and Ascaridomorpha (e.g., *Ascaris lumbricoides*) (2). All cases of haycocknematosis to date have originated in Australia, specifically in the tropical north of Queensland and Tasmania (Table). Nonhuman animal hosts are unknown. The route of human infection is also unknown but is presumed to be linked to consumption of, or contact with, mammalian wildlife. Because females are ovoviviparous (eggs hatch in utero within the female worm), infection caused by the ingestion of embryonated eggs is unlikely. With an apparent single-host (monoxenous) life cycle, an arthropod vector is also unlikely. Ongoing release and maturation of larvae results in persistent infections.

Of the 13 known case-patients (Table), 12 had weakness and muscle wasting, 7 had dysphagia, and 2 had dysarthria or dysphonia. One case was discovered incidentally during evaluation of low back pain; the patient was otherwise asymptomatic. All case-patients had increased levels of creatinine kinase (270–6,218 U/L). Peripheral eosinophilia was observed in 12 (92%) of 13 patients. Myalgias, unintentional weight loss, increases in erythrocyte sedimentation rates, and mild-to-moderate increases in levels of liver aminotransferases were also common. Needle electromyography findings were available for 8 patients (patients 2, 4, 7, 8, 10, 11, 12, and 13). Except for patients 10 and 12, who had ambiguous or limited findings, the remaining patients had myopathic motor unit potentials. Results of nerve conduction studies were within reference ranges when described. The time from symptom onset to diagnosis ranged from 1.5 to 8 years, with the case-patient in this study having the longest known timeframe.

Seven patients had received corticosteroids at some point in their illness for a presumptive diagnosis of polymyositis, during which time most experienced progressive deterioration, including our patient. All patients were given extended, high-dose albendazole therapy, and 7 patients had a partial to near complete

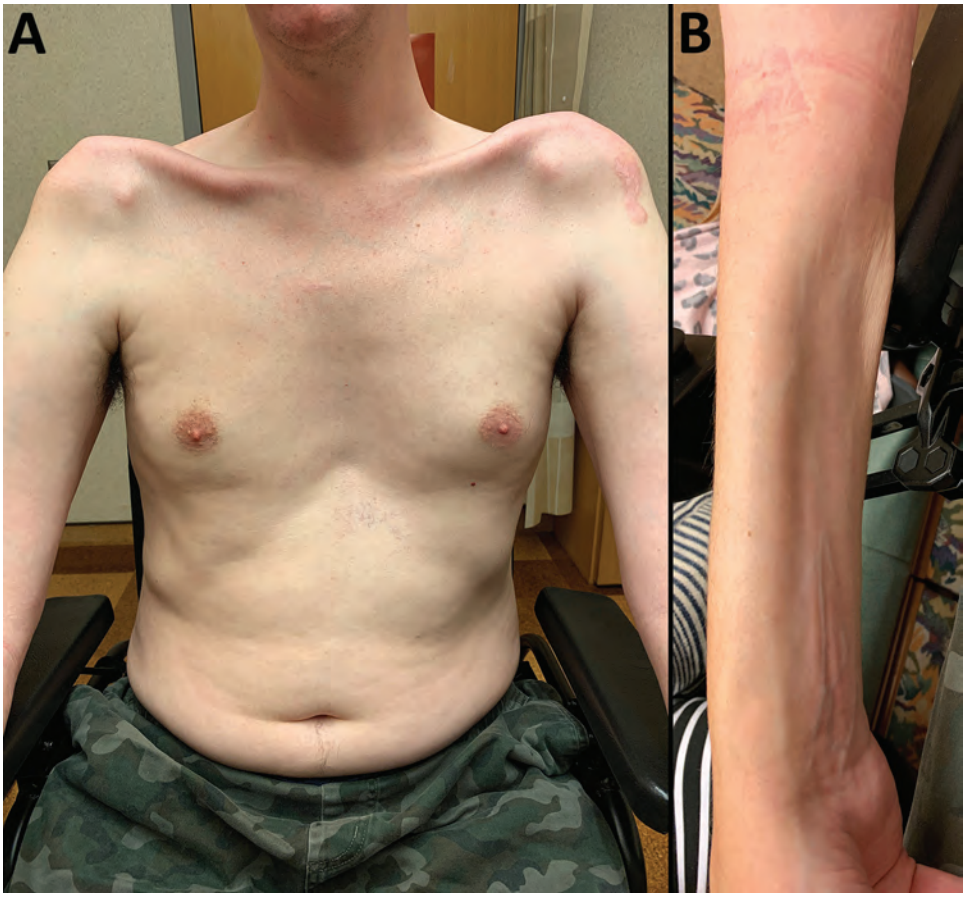

Figure 1. Physical manifestations of a patient who had imported *Haycocknema perplexum* infection, United States. Images show profound atrophy of the pectoralis and deltoid (A) and the forearm flexor musculature (B).

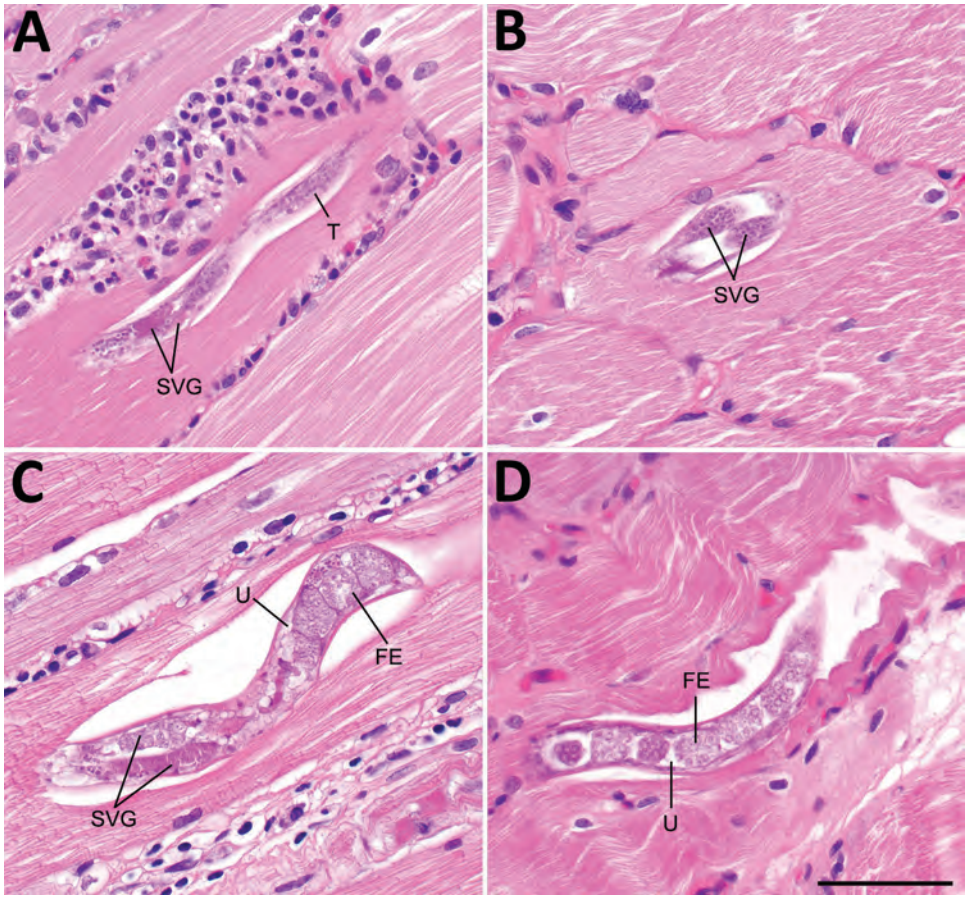

Figure 2. Histologic section of muscle tissue from the left deltoid of a patient who had imported *Haycocknema perplexum* infection, United States. A) Male *H. perplexum* in longitudinal section; B) anterior region of female *H. perplexum* in transverse section; C) anterior and midbody regions of gravid female; D) posterior region of gravid female. Scattered necrotic and regenerating fibers and dense inflammatory exudates were also observed. FE, fertilized eggs; SVG, subventral glands; T, testis; U, uterus. Scale bar indicates 50 μm.

recovery. One patient (*7*) died from complications resulting from corticosteroid administration, mechanical ventilation, and a prolonged stay in the intensive care unit.

Diagnosis of haycocknematosis is based primarily on histopathologic features. The morphologic characteristics of *H. perplexum* nematodes in histopathologic preparations include a thin cuticle, meromyarian/platymyarian musculature, amphidelphic uteri (females), lateral bacillary bands (especially conspicuous in immature females), and conspicuous subventral glands (*10*). There are no cephalic inflations or lateral alae. Adult males, adult females, and larvae might be observed in muscle specimens, but never in ex utero eggs. Adults often have an undulating, serpentine morphology, which is parallel with the muscle fibers. Male worms have a maximum width of 15 μm (range 14–15 μm), and female worms have a maximum width of 36 μm (range 15–36 μm) (*10*). Larvae are similar in size to adult males, have a maximum width of 15 μm (range 12–15 μm) (*10*), and complete their lifecycle in the host.

Although other parasites in biopsy specimens include *Trichinella* spp., *Strongyloides stercoralis*, and *Halicephalobus gingivalis*, these parasites can be differentiated by morphologic, clinical, and epidemiologic features. *H. perplexum* and other nematodes might also be potentially confused for tissue cysts of *Toxoplasma gondii* and *Sarcocystis* spp. when seen in cross-section (as in our case-patient), but this finding can usually be resolved by examining deeper sections from the tissue block to identify additional parasite forms.

A PCR was developed that enabled diagnosis of the 10th case of *H. perplexum* nematode infection from a muscle biopsy in the absence of visible nematodes (*2*,*8*). This PCR was unsuccessful when performed for our case-patient. However, this result is not unexpected, given the age of the block (7 years at time of testing) and the relatively large sizes of the PCR amplicons (400 bp for cytochrome c oxidase subunit 1 and 830 bp for 18S rRNA).

It is unknown why to date human cases appear to have been acquired only in Tasmania or the northern regions of Queensland. Molecular sequence data demonstrate that the strains from Queensland and Tasmania belong to the same species (*2*). Infections might occur in other areas of the East Coast of Australia, or

wider mainland Australia, but these infections have not been detected because of lack of awareness and difficulty in diagnosis.

The optimal antimicrobial drug management for treatment of haycocknematosis is unknown. Our patient was given albendazole based on experiences from previously reported cases. In 1 case, viable nematodes were still observed after 4 weeks of treatment, but not after 9 weeks (*7*). Additional studies are needed to determine the most efficacious antiparasitic treatment for haycocknematosis.

Patients who have *H. perplexum* parasitic myositis might be a diagnostic challenge to clinicians and pathologists, particularly when seen outside disease-endemic regions. The disease is progressive, potentially life-threatening, and might persist for ≥8 years with a delayed diagnosis, as shown by our case-patient. A high degree of suspicion is required to diagnose this treatable mimic of muscular dystrophy and inflammatory myopathy, and to avoid harm through corticosteroid treatment. Additional studies are needed to clarify the exposure risks, parasite life cycle, disease prevention, and treatment.

About the Author

Dr. Pritt is a professor of laboratory medicine and pathology at the Mayo Clinic, Rochester, MN. Her primary research interests are clinical parasitology, vector-borne diseases, and the pathology of infectious diseases.

References

1. Dennett X, Siejka SJ, Andrews JR, Beveridge I, Spratt DM. Polymyositis caused by a new genus of nematode. Med J Aust. 1998;168:226–7. https://doi.org/10.5694/j.1326-5377.1998.tb140136.x
2. Koehler AV, Spratt DM, Norton R, Warren S, McEwan B, Urkude R, et al. More parasitic myositis cases in humans in Australia, and the definition of genetic markers for the causative agents as a basis for molecular diagnosis. Infect Genet Evol. 2016;44:69–75. https://doi.org/10.1016/j.meegid.2016.06.026
3. Vos LJ, Robertson T, Binotto E. *Haycocknema perplexum*: an emerging cause of parasitic myositis in Australia. Commun Dis Intell Q Rep. 2016;40:E496–9.
4. *Haycocknema perplexum*: life threatening disease of humans, 2018 [cited 2022 Jan 2]. https://www.wildlifehealthaustralia.com.au/Portals/0/Documents/FactSheets/Public%20health/Haycocknema%20perplexum.pdf
5. Andrews JR, Ainsworth R, Abernethy D. *Trichinella pseudospiralis* in humans: description of a case and its treatment. Trans R Soc Trop Med Hyg. 1994;88:200–3. https://doi.org/10.1016/0035-9203(94)90295-X
6. Andrews JR, Ainsworth R, Pozio E. Nematodes in human muscle. Parasitol Today. 1997;13:488–9. https://doi.org/10.1016/S0169-4758(97)80002-6
7. Basuroy R, Pennisi R, Robertson T, Norton R, Stokes J, Reimers J, et al. Parasitic myositis in tropical Australia. Med J Aust. 2008;188:254–6. https://doi.org/10.5694/j.1326-5377.2008.tb01601.x
8. Koehler AV, Leung P, McEwan B, Gasser RB. Using PCR-based sequencing to diagnose *Haycocknema perplexum* infection in human myositis case, Australia. Emerg Infect Dis. 2018;24:2368–70. https://doi.org/10.3201/eid2412.181240
9. McKelvie P, Reardon K, Bond K, Spratt DM, Gangell A, Zochling J, et al. A further patient with parasitic myositis due to *Haycocknema perplexum*, a rare entity. J Clin Neurosci. 2013;20:1019–22. https://doi.org/10.1016/j.jocn.2012.08.009
10. Spratt DM, Beveridge I, Andrews JR, Dennett X. *Haycocknema perplexum* n. g., n. sp. (Nematoda: *Robertdollfusidae*): an intramyofibre parasite in man. Syst Parasitol. 1999;43:123–31. https://doi.org/10.1023/A:1006158218854
11. Ward K, Krishnan A, R Iyengar K, Robertson T, White R, Urkude R. *Haycocknema perplexum* myositis: the first description of subclinical disease and a proposed distinctive triad to evoke clinical suspicion. BMJ Neurol Open. 2022;4:e000290. https://doi.org/10.1136/bmjno-2022-000290

Address for correspondence: Bobbi S. Pritt, Division of Clinical Microbiology, Department of Laboratory Medicine and Pathology, Mayo Clinic, 200 1st St SW, Hilton Bldg 470-B, Rochester, MN 55905, USA; email: pritt.bobbi@mayo.edu

Deaths Related to Chagas Disease and COVID-19 Co-Infection, Brazil, March–December 2020

Francisco R. Martins-Melo, Marcia C. Castro, Antonio Luiz P. Ribeiro, Jorg Heukelbach, Guilherme L. Werneck

We analyzed epidemiologic characteristics and distribution of 492 deaths related to Chagas disease and coronavirus disease (COVID-19) co-infection in Brazil during March–December 2020. Cumulative co-infected death rates were highest among advanced age groups, persons of Afro-Brazilian ethnicity and with low education levels, and geographically distributed mainly in major Chagas disease–endemic areas.

Chagas disease, caused by the protozoan *Trypanosoma cruzi*, is a neglected public health problem in Latin America (*1*). It is the most common infectious cause of cardiomyopathy worldwide and for co-infections might play a role in clinical prognosis of COVID-19 patients (*2*,*3*). In Brazil, ≈1.4–3.4 million persons were estimated to be chronically infected with *T. cruzi* during 2015; 0.4–1.0 million of those persons had chronic Chagas heart disease (*4*).

On March 11, 2020, the World Health Organization declared COVID-19 a pandemic (*5*). In Brazil, a case of COVID-19 was detected on February 26, 2020, and a death from COVID-19 occurred on March 12, 2020 (*5*). COVID-19 vaccination campaigns started in late January 2021 (*6*). By September 18, 2022, there were >33.7 million confirmed cases and ≈685,000 deaths in Brazil (*7*).

Spread of COVID-19 in Chagas disease–endemic areas is a public health challenge because of advanced age of chronically infected patients and high occurrence of heart complications (*2*). This finding probably increases risk for severe forms and deaths from COVID-19 in co-infected patients (*5*,*8*). We assessed epidemiologic characteristics and distribution of deaths related to COVID-19 and Chagas disease co-infection in Brazil during March-December 2020.

Author affiliations: Federal Institute of Education, Science, and Technology of Ceará, Fortaleza, Brazil (F.R. Martins-Melo); Harvard T.H. Chan School of Public Health, Boston, Massachusetts, USA (M.C. Castro); Universidade Federal de Minas Gerais, Belo Horizonte, Brazil (A.L.P. Ribeiro); Federal University of Ceará, Fortaleza (J. Heukelbach); Federal University of Rio de Janeiro, Rio de Janeiro, Brazil (G.L. Werneck); State University of Rio de Janeiro, Rio de Janeiro (G.L. Werneck)

DOI: https://doi.org/10.3201/eid2811.212158

The Study

We conducted a nationwide analysis using mortality rate data for 2020 (preliminary records), obtained from the Brazilian Mortality Information System database (https://datasus.saude.gov.br/transferencia-de-arquivos) and extracted on September 4, 2021. We included all deaths reported from March 1–December 31, 2020, in which Chagas disease (International Classification of Diseases, 10th revision [ICD-10], codes B57–57.5, K23.1, and K93.1) and COVID-19 (ICD-10 codes B34.2, U0.71 or U0.72) were mentioned on the same death certificate as underlying or contributing to death.

Available sociodemographic and clinical data included sex (male, female), age (<1–19, 20–29, 30–39, 40–49, 50–59, 60–69, 70–79, ≥80 years), education (years of study: none, 1–3, 4–7, 8–11, ≥12), ethnicity (White, Black/Afro-Brazilian, mixed/Pardo Brazilian, Asian, indigenous), marital status (single, married, divorced/separated, widowed, other), place of residence (regions, states, municipalities), date of death (epidemiologic week, month), place of death (hospital, other health establishment, home, public thoroughfare, others), and underlying/contributing causes of death. We calculated cumulative mortality rates per 100,000 inhabitants and rate ratios with 95% CIs stratified by sex, age group, place of residence, ethnicity, and educational level using population estimates from the Brazilian Institute of Geography and Statistics as the denominator. We assessed significant differences by χ^2 test, performed analyses using Stata version 11.2 (StataCorp, https://www.stata.com), and created maps using ArcGIS version 9.3 (Esri, https://www.esri.com). Data were obtained anonymized, with no possibility of subject identification.

Table 1. Underlying causes on death certificates that listed Chagas disease and COVID-19 co-infection, Brazil, March–December 2020*

Underlying causes of death (ICD-10 codes)	No. (%)
Coronavirus disease 19 – COVID-19 (B34.2, U07.1, U07.2)†	434 (88.2)
Coronavirus infection, unspecified site + COVID-19, virus identified (laboratory confirmed) (B34.2 + U07.1)	335 (68.1)
Coronavirus infection, unspecified site + COVID-19, virus not identified (clinically or epidemiologically diagnosed (B34.2 + U07.2)	52 (10.6)
Coronavirus infection, unspecified site (B34.2)	47 (9.6)
Chagas disease (B57, K23.1, K93.1)	38 (7.7)
Chagas disease (chronic) with heart involvement (B57.2)	27 (5.5)
Chagas disease (chronic) with digestive system involvement (B57.3)	6 (1.2)
Acute Chagas disease with heart involvement (B57.0)	3 (0.6)
Chagas disease (chronic) with nervous system involvement (B57.4)	2 (0.4)
Pneumonia (J12-J18)	3 (0.6)
Chronic obstructive pulmonary disease (J40-J44)	3 (0.6)
Diabetes mellitus (E10-E14)	2 (0.4)
Hypertensive diseases (I10-I15)	2 (0.4)
Other respiratory disorders (J98)	1 (0.2)
Infection due to other mycobacteria (A31)	1 (0.2)
Sepsis (A40-A41)	1 (0.2)
Secondary and unspecified malignant neoplasm of lymph nodes (C77)	1 (0.2)
Dementia (F00-F04)	1 (0.2)
Other disorders of brain (G93)	1 (0.2)
Appendicitis (K35-K37)	1 (0.2)
Paralytic ileus and intestinal obstruction without hernia (K56)	1 (0.2)
Cholelithiasis (K80)	1 (0.2)
Maternal infectious and parasitic diseases classifiable elsewhere but complicating pregnancy, childbirth and puerperium (O98)	1 (0.2)
Total	492 (100.0)

*COVID-19, coronavirus disease; ICD-10, International Statistical Classification of Diseases and Related Health Problems, 10th revision.
†ICD-10 codes were based on the Brazilian Ministry of Health codification guidelines for COVID-19 (http://plataforma.saude.gov.br/cta-br-fic/codificacao-Covid-19.pdf), which recommends the standardized use of the ICD-10 code B34.2 (Coronavirus infection, unspecified site) for deaths of COVID-19 in Brazil, with the inclusion of pandemic marker codes U07.1 (COVID-19, identified virus) or U07.2 (COVID-19, unidentified virus, clinical or epidemiologic criteria), defined by the World Health Organization, next to code B34.2 in the same line of the death certificate.

Of 1,337,730 deaths recorded in Brazil during March–December 2020, we identified 492 deaths in which Chagas disease and COVID-19 were on the same death certificates (9.1% [492/5,395] of Chagas disease–related deaths and 0.2% [492/222,121] of COVID-19–related deaths for that period). The cumulative co-infected mortality rate was 0.23 (95% CI 0.21–0.25) deaths/100,000 inhabitants. COVID-19 was mentioned as the underlying cause in most co-infected deaths (88.2% [434/492]), of which 77.2% (335/492) were laboratory-confirmed COVID-19 deaths (B34.2 + U07.1). Chagas disease was the underlying cause in 7.7% (38/492) of co-infected deaths, with predominance of the chronic cardiac form (B57.2) (Table 1). The

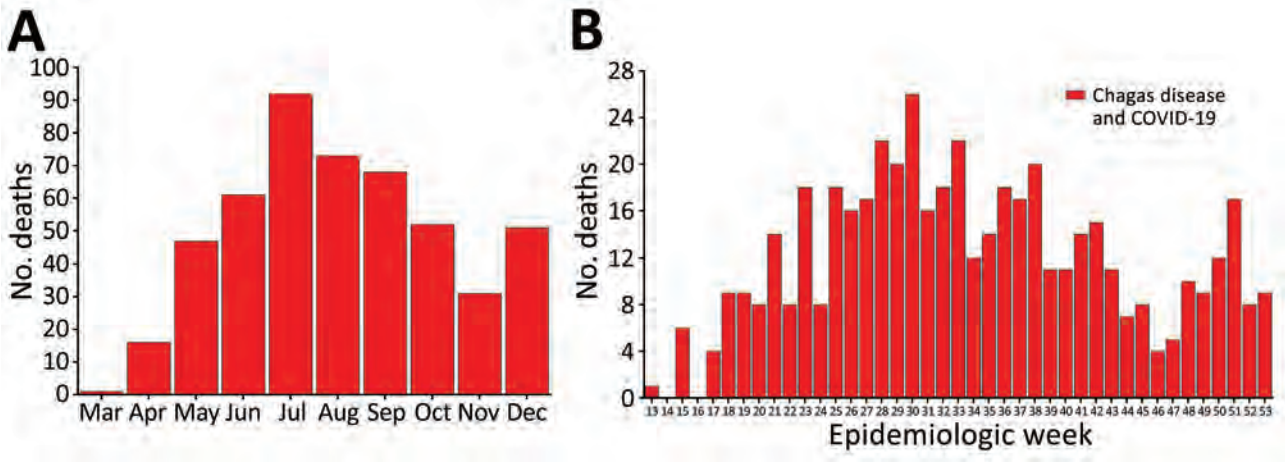

Figure 1. Number of deaths related to Chagas disease and COVID-19 co-infection, by month (A) and epidemiologic week (B) of death, Brazil, March–December 2020. Data shown are from the epidemiologic week of the first reported death related to Chagas disease and COVID-19 co-infection (March 26, 2020) to December 31, 2020 (epidemiologic weeks from 13 [March 22–28, 2020] to 53 [December 27, 2020–January 2, 2021; data available until December 31, 2020], according to the 2020 epidemiologic calendar (https://portalsinan.saude.gov.br/calendario-epidemiologico-2020). Red bars indicate the number of deaths related to Chagas and COVID-19 co-infection.

number of co-infected deaths peaked in July, in epidemiologic week 30 (July 19–25) (Figure 1), following the patterns of COVID-19 deaths during the 2020 pandemic time (Appendix Figures 1–3, https://wwwnc.cdc.gov/EID/article/28/11/21-2158-App1.pdf).

Overall, co-infected deaths were predominant among men (51%), persons 70–79 years of age (37%), persons of mixed ethnicity (44.9%), married persons (44.5%), persons who had schooling (1–3 years of study) (33.2%), and persons who resided in the Southeast region (43.7%) and São Paulo state (27%). The mean (±SD) age at death was 73.9 (±12.2) years, median (range) age at death was 75.5 (30.7–104.4) years, and 87% of deaths occurred in hospitals (Table 2).

Cumulative mortality rates were higher for men than for women, but not significantly. Highest age-specific mortality rates were found for older age groups, the maximum in persons ≥80 years of age (3.29/100,000 inhabitants). Persons of Afro-Brazilian ethnicity had higher mortality rates than did White persons.

Table 2. Epidemiologic characteristics and cumulative mortality rates per 100,000 inhabitants related to Chagas disease and COVID-19 co-infection by population subgroups, Brazil, March–December 2020*

Characteristic	Deaths, no. (%)†	Cumulative mortality rate (95% CI)‡	Mortality rate ratio (95% CI)	p value
All co-infected deaths	492 (100.0)	0.23 (0.21–0.25)		
Sex				
M	251 (51.0)	0.24 (0.21–0.27)	1.09 (0.91–1.30)	0.345
F	241 (49.0)	0.22 (0.20–0.25)	Referent	
Age group, y				
30–39	6 (1.2)	0.02 (0.01–0.04)	Referent	
40–49	14 (2.8)	0.05 (0.03–0.08)	2.73 (1.05–7.10)	0.032
50–59	40 (8.1)	0.17 (0.12–0.23)	9.56 (4.05–22.54)	<0.001
60–69	104 (21.1)	0.62 (0.51–0.75)	35.46 (15.57–80.75)	<0.001
70–79	182 (37.0)	2.02 (1.74–2.33)	115.08 (51.03–259.53)	<0.001
≥80	146 (29.7)	3.29 (2.80–3.87)	187.56 (82.90–424.34)	<0.001
Region of residence				
North	7 (1.4)	0.04 (0.02–0.08)	Referent	
Northeast	97 (19.7)	0.17 (0.14–0.21)	4.51 (2.09–9.71)	<0.001
Southeast	215 (43.7)	0.24 (0.21–0.28)	6.44 (3.04–13.68)	<0.001
South	18 (3.7)	0.06 (0.04–0.09)	1.59 (0.66–3.81)	0.293
Central-West	155 (31.5)	0.94 (0.80–1.10)	25.05 (11.75–53.43)	<0.001
Ethnicity§				
White (Caucasian)	204 (43.0)	0.22 (0.19–0.25)	Referent	
Mixed race (Pardo Brazilians)	213 (44.9)	0.22 (0.19–0.22)	0.98 (0.81–1.19)	0.838
Black (Afro-Brazilian)	55 (11.6)	0.30 (0.23–0.39)	1.36 (1.01–1.83)	0.042
Asian	2 (0.4)	NA	NA	NA
Schooling, y				
None (illiteracy)	93 (25.3)	0.62 (0.50–0.76)	24.90 (11.55–53.67)	<0.001
1–3	122 (33.2)	0.68 (0.57–0.81)	27.34 (12.76–58.55)	<0.001
4–7	99 (26.9)	0.23 (0.19–0.27)	9.09 (4.22–19.56)	<0.001
8–11	47 (12.8)	0.07 (0.05–0.09)	2.64 (1.19–5.83)	0.013
≥12	7 (1.9)	0.02 (0.01–0.05)	Referent	
Marital status				
Single	60 (13.8)	0.07 (0.05–0.09)	0.19 (0.15–0.26)	<0.001
Married	194 (44.5)	0.34 (0.30–0.40)	Referent	
Divorced/separated	33 (7.6)	0.42 (0.30–0.59)	1.23 (0.85–1.77)	0.278
Widowed	136 (31.2)	1.69 (1.43–1.99)	4.91 (3.94–6.11)	<0.001
Other	13 (3.0)	NA	NA	NA
Place of occurrence of death				
Hospital	428 (87.0)	NA	NA	NA
Other health establishment	40 (8.1)	NA	NA	NA
Home	23 (4.7)	NA	NA	NA
Other	1 (0.2)	NA	NA	NA

*IQR, interquartile range; NA, not available.
†Deaths with missing information are excluded: 18 for ethnicity, 124 for schooling, and 56 for marital status (not included in percentage calculations).
‡Deaths per 100,000 inhabitants. Population denominators used 2020 population estimates from the Brazilian Institute of Geography and Statistics (https://datasus.saude.gov.br/populacao-residente), except for ethnicity, schooling, and marital status. Population estimates for Brazil by ethnicity in 2020 were derived from the Continuous National Household Sample Survey (Continuous PNAD; https://sidra.ibge.gov.br/Tabela/6403), based on median estimates for each category (White, Black, and mixed [Pardo Brazilian]) in the continuous quarterly national surveys conducted in 2020. Population data on marital status in persons ≥10 years of age were obtained from the 2010 Brazilian Population Census (Brazilian Institute of Geography and Statistics, https://sidra.ibge.gov.br/tabela/1624). Population data on education for persons ≥10 years of age were extracted from the National Household Sample Survey (PNAD; https://sidra.ibge.gov.br/tabela/272) by using estimates for 2015 (most recent year with schooling estimates stratified by year of study >1 to 15 years).
§No measures were calculated for persons of Asian ethnicity because of lack of population denominator information from 2020 Continuous PNAD. There was no record of co-infected death in the indigenous ethnic group.

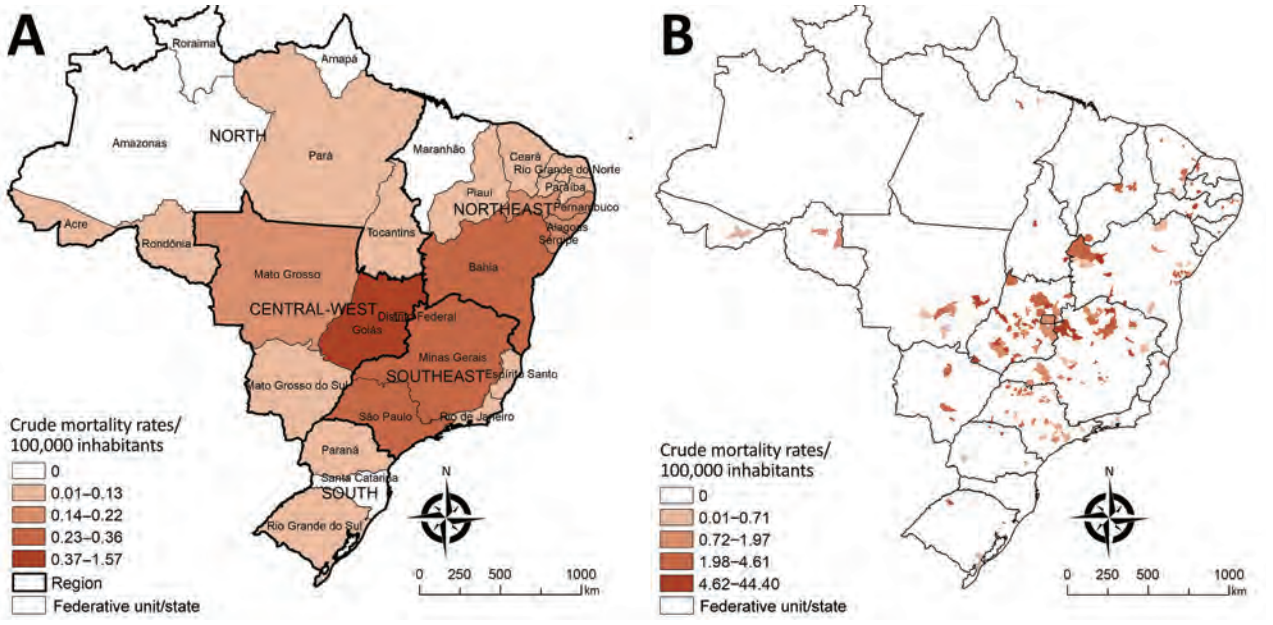

Figure 2. Spatial distribution of cumulative mortality rates per 100,000 inhabitants related to Chagas disease and COVID-19 co-infection by geographic units of residence, Brazil, March–December 2020. A) State-level crude rates. B) Municipality-level crude rates. Shading indicates levels of death. Data were mapped by using ArcGIS software version 9.3 (Esri, https://www.esri.com). In 2020, Brazil was divided into 5 regions (South, Southeast, Central-West, North, and Northeast), 27 Federative Units (26 states and 1 Federal District), and 5,570 municipalities.

Mortality rates were higher among persons who had low levels of education (none and 1–3 years of study) than persons who had advanced education. The Central-West region had the highest regional mortality rate, followed by Southeast and Northeast regions (Table 2). Federal District (1.57 deaths/100,000 inhabitants), Goiás (1.38 deaths/100,000 inhabitants), and Bahia (0.36 deaths/100,000 inhabitants) had the highest state-level mortality rates (Figure 2, panel A; Appendix Table).

A total of 4.1% (231/5,570) of municipalities in 22 of the 27 states of Brazil recorded ≥1 co-infected deaths during 2020. Cumulative mortality rates were 0.04–44.40 deaths/100,000 inhabitants among municipalities in Brazil that recorded ≥1 co-infected death. Municipalities that had high co-infected death rates were found mainly in the central region of Brazil (Goiás, Minas Gerais, São Paulo, Bahia, and the Federal District) (Figure 2, panel B).

Conclusions

We found higher death rates for Chagas disease and COVID-19 co-infection among older persons, persons who had Afro-Brazilian ethnicity, persons with low education levels, and persons lived in an area to which Chagas disease was previously endemic. The high co-infection mortality rate for older age groups is consistent with patterns of deaths for both infections in Brazil during 2020 because the highest age-specific death rates for the diseases were for these subgroup populations (*9*–*11*). Consistent with other reports for both infections, we found that the higher death rates found for persons of Black ethnicity and with low educational levels indicate social and structural inequities and health disparities in determination of severe illness and death related to Chagas disease and COVID-19 in Brazil (*9*,*11*,*12*).

The areas of Brazil that had the highest mortality rates were major disease-endemic areas for vector transmission in the past in the Central-West, Southeast, and Northeast regions (*4*,*9*,*13*). The extensive spread of COVID-19 in Brazil during 2020, including Chagas disease-endemic areas, caused substantial geographic overlap between the infections, increasing the risk of chronic Chagas disease patients, principally those with cardiac involvement, contracting SARS-CoV-2 infection (*2*,*5*). The high mortality rate for the Federal District when compared with other states, and the high number of co-infected deaths observed in state capitals of Brazil, such as Brasília, São Paulo, Goiânia, and Salvador, reflect urbanization of Chagas disease because of intense migratory movement from rural areas to urban areas in Brazil during the past 3 decades (*9*,*14*).

Our study's limitations were mainly related to coverage and quality of secondary mortality rate data (*9*,*13*). Brazilian Mortality Information System data for 2020 are preliminary and might not represent all deaths for 2020 because it is subject to corrections,

especially underlying causes of death. Even if minimal, frequencies might change after definitive consolidation (*15*). Other potential limitations are misclassification or underreporting and delays in reporting of COVID-19 deaths, especially in places where healthcare services were under stress because of the large COVID-19 caseload (*6*).

It is likely that a large number of patients who have chronic Chagas disease, especially the undetermined form, are not given a diagnosis in Brazil. Therefore, there might be more deaths of patients who have both infections than reported in this study. Schooling, ethnicity, and marital status included a considerable proportion of incomplete/unknown data, and these findings should be interpreted with caution.

Our findings show marked sociodemographic and geographic variations in deaths related to Chagas disease and COVID-19 co-infection in Brazil during 2020, occurring mainly in residents of Chagas disease–endemic areas and disproportionately affecting susceptible population groups. The real effect of death from co-infection might be underestimated in Brazil. Efforts must be made to ensure a high COVID-19 vaccination coverage, improve access to healthcare services, and provide adequate clinical management for co-infected patients especially in patients who have chronic Chagas disease.

A.L.P.R. is supported in part by Brazilian National Council for Scientific and Technological Development (CNPq; grants no. 310679/2016-8 and 465518/2014-1), by Fundação de Amparo à Pesquisa do Estado de Minas Gerais (FAPEMIG; grants no. PPM-00428-17 and RED-00081-16), and Coordination for the Improvement of Higher Education Personnel (CAPES; grant no. 88887.507149/2020-00). G.L.W receives a CNPq senior research scholarship and was supported in part by the Carlos Chagas Filho Foundation for Research Support of the State of Rio de Janeiro (FAPERJ; grant no. E-26/210.180/2020).

About the Author

Dr. Martins-Melo is a research scientist at the Federal Institute of Education, Science, and Technology of Ceará, Fortaleza, Brazil. His primary research interests include control and epidemiology of neglected and poverty-related diseases.

References

1. World Health Organization. Chagas disease (also known as American trypanosomiasis) – fact sheet. 2021 [cited 2021 Sep 15]. https://www.who.int/news-room/fact-sheets/detail/chagas-disease-(american-trypanosomiasis)
2. Zaidel EJ, Forsyth CJ, Novick G, Marcus R, Ribeiro AL, Pinazo MJ, et al. COVID-19: implications for people with Chagas disease. Glob Heart. 2020;15:69. https://doi.org/10.5334/gh.891
3. Molina I, Marcolino MS, Pires MC, Ramos LE, Silva RT, Guimarães-Júnior MH, et al. Chagas disease and SARS-CoV-2 coinfection does not lead to worse in-hospital outcomes. Sci Rep. 2021;11:20289. https://doi.org/10.1038/s41598-021-96825-3
4. Dias JC, Ramos AN Jr, Gontijo ED, Luquetti A, Shikanai-Yasuda MA, Coura JR, et al. Second Brazilian consensus on Chagas disease, 2015. Rev Soc Bras Med Trop. 2016;49(Suppl 1):3–60. https://doi.org/10.1590/0037-8682-0505-2016
5. Brazilian Ministry of Health, Health Surveillance Secretariat. Epidemiological Bulletin, COVID-19 - No. 20 [in Portuguese]. 2021 [cited 2021 Sep 21]. https://www.gov.br/saude/pt-br/coronavirus/boletins-epidemiologicos/boletim-epidemiologico-covid-19-no-20.pdf/view
6. Victora PC, Castro PM, Gurzenda S, Medeiros AC, França GV, Barros PA. Estimating the early impact of vaccination against COVID-19 on deaths among elderly people in Brazil: analyses of routinely-collected data on vaccine coverage and mortality. EClinicalMedicine. 2021;38:101036. https://doi.org/10.1016/j.eclinm.2021.101036
7. Brazilian Ministry of Health. COVID-19 dashboard: confirmed cases and deaths [in Portuguese]. 2022 [cited 2022 Sep 18]. https://covid.saude.gov.br/
8. Alberca RW, Yendo TM, Leuzzi Ramos YÁ, Fernandes IG, Oliveira LM, Teixeira FM, et al. Case report: COVID-19 and Chagas disease in two coinfected patients. Am J Trop Med Hyg. 2020;103:2353–6. https://doi.org/10.4269/ajtmh.20-1185
9. Martins-Melo FR, Castro MC, Werneck GL. Levels and trends in Chagas disease–related mortality in Brazil, 2000–2019. Acta Trop. 2021;220:105948. https://doi.org/10.1016/j.actatropica.2021.105948
10. Zimmermann IR, Sanchez MN, Frio GS, Alves LC, Pereira CC, Lima RT, et al. Trends in COVID-19 case-fatality rates in Brazilian public hospitals: a longitudinal cohort of 398,063 hospital admissions from 1st March to 3rd October 2020. PLoS One. 2021;16:e0254633. https://doi.org/10.1371/journal.pone.0254633
11. de Andrade CL, Pereira CC, Martins M, Lima SM, Portela MC. COVID-19 hospitalizations in Brazil's Unified Health System (SUS). PLoS One. 2020;15:e0243126. https://doi.org/10.1371/journal.pone.0243126
12. Ribeiro KB, Ribeiro AF, Veras MA, de Castro MC. Social inequalities and COVID-19 mortality in the city of São Paulo, Brazil. Int J Epidemiol. 2021;50:732–42. https://doi.org/10.1093/ije/dyab022
13. Martins-Melo FR, Ramos AN Jr, Alencar CH, Lange W, Heukelbach J. Mortality of Chagas' disease in Brazil: spatial patterns and definition of high-risk areas. Trop Med Int Health. 2012;17:1066–75. https://doi.org/10.1111/j.1365-3156.2012.03043.x
14. Pinto Dias JC. Human chagas disease and migration in the context of globalization: some particular aspects. J Trop Med. 2013;2013:789758. https://doi.org/10.1155/2013/789758
15. Santos AM, Souza BF, Carvalho CA, Campos MA, Oliveira BL, Diniz EM, et al. Excess deaths from all causes and by COVID-19 in Brazil in 2020. Rev Saude Publica. 2021;55:71. https://doi.org/10.11606/s1518-8787.2021055004137

Address for correspondence: Francisco R. Martins-Melo, Federal Institute of Education, Science and Technology of Ceará, Avenida Treze de Maio, 2081, Benfica, 60040-531 Fortaleza, Ceará, Brazil; email: rogerlandio@bol.com.br

Rift Valley Fever Outbreak during COVID-19 Surge, Uganda, 2021

Caitlin M. Cossaboom, Luke Nyakarahuka, Sophia Mulei, Jackson Kyondo, Alex Tumusiime, Jimmy Baluku, Gloria Grace Akurut, Dianah Namanya, Kilama Kamugisha, Hildah Tendo Nansikombi, Alex Nyabakira, Semei Mutesasira, Shannon Whitmer, Carson Telford, Julius Lutwama, Stephen Balinandi, Joel Montgomery, John D. Klena, Trevor Shoemaker

Rift Valley fever, endemic or emerging throughout most of Africa, causes considerable risk to human and animal health. We report 7 confirmed Rift Valley fever cases, 1 fatal, in Kiruhura District, Uganda, during 2021. Our findings highlight the importance of continued viral hemorrhagic fever surveillance, despite challenges associated with the COVID-19 pandemic.

Rift Valley fever (RVF), a zoonotic mosquito-borne disease of livestock caused by Rift Valley fever virus (RVFV), is endemic throughout most of Africa and the Arabian Peninsula (*1*,*2*). Humans can be infected with RVFV through contact with blood, body fluids, products from infected livestock, or bites from infected mosquitoes (*1*,*3*). No human-to-human transmission has been documented (*4*). In humans, infections are typically asymptomatic or result in mild influenza-like illness (*1*). Severe illness, including hemorrhagic manifestations, occurs in ≈1%–2% of cases; the case-fatality rate among severe cases is ≈10%–20% (*1*,*5*). No approved human vaccine or specific treatment is available, but early supportive care may prevent complications and decrease death (*1*). In livestock, RVFV infection can cause abortions and high mortality, leading to substantial economic losses (*1*,*6*). We describe a fatal human case of RVF and the subsequent investigation and identification of 6 additional cases in Kiruhura District, Uganda, in 2021. We also note the role a COVID-19 surge played in delayed testing and patient care.

Author affiliations: Centers for Disease Control and Prevention, Atlanta, Georgia, USA (C.M. Cossaboom, S. Whitmer, J. Montgomery, J.D. Klena, T. Shoemaker); Makerere University Department of Biosecurity, Ecosystems and Veterinary Public Health, Kampala, Uganda (L. Nyakarahuka); Uganda Virus Research Institute, Entebbe, Uganda (L. Nyakarahuka, S. Mulei, J. Kyondo, A. Tumusiime, J. Baluku, J. Lutwama, S. Balinandi); Uganda Wildlife Authority, Kampala (G.G. Akurut, D. Namanya, K. Kamugisha); Uganda Public Health Fellowship Program, Kampala (H.T. Nansikombi, A. Nyabakira); Case Hospital, Kampala (S. Mutesasira)

DOI: https://doi.org/10.3201/eid2811.220364

The Study

On May 7, 2021, fever, headache, fatigue, arthromyalgia, nausea, vomiting, and diarrhea developed in a previously healthy woman 19 years of age (P1), who sought treatment at a private clinic in Kinoni Subcounty, Kiruhura District, Uganda (Figure 1). She was treated empirically for malaria with no improvement. On May 9, after hematemesis developed, she sought treatment at and was admitted to another local private clinic. On May 11, the patient was transferred to the regional referral hospital in Mbarara District for further disease management (Figure 1). Anuric acute kidney injury, chest pain, and respiratory distress complicated her hospital course. She was transferred by ambulance the same day to the national referral hospital in Kampala (Figure 1) for critical care but was not admitted because the hospital had no available dialysis unit. She was subsequently referred to a nearby nonprofit private hospital but was not admitted because the intensive care unit was at capacity with patients with COVID-19. During transfer, P1's clinical status deteriorated, and her hemorrhagic signs worsened.

On May 12, she was admitted to a private tertiary hospital with fever (38.0°C), jaundice, epistaxis, ecchymoses, gingival hemorrhage, respiratory distress, hypotension, focal seizures, and altered mentation. At admission, she was thrombocytopenic and anemic with deranged liver and renal function and electrolyte abnormalities (Table). The clinical team suspected a viral hemorrhagic fever (VHF) and collected blood for testing at the Uganda Virus Research Institute (UVRI). The patient died on May 13.

UVRI testing confirmed RVFV infection by real-time reverse transcription PCR (rRT-PCR) (*7*) and

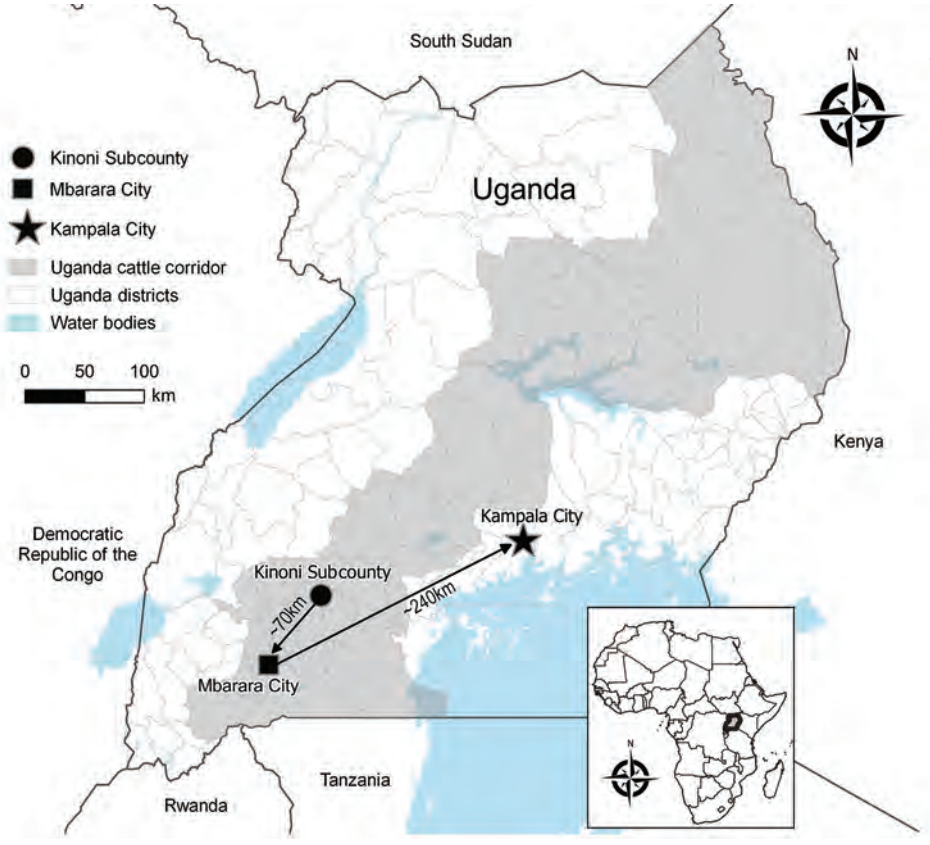

Figure 1. Locations where the index case-patient of a Rift Valley fever outbreak in Kinoni Subcounty sought care during the period of acute illness preceding her death, Uganda, 2021. Arrows indicate route patient followed during attempts to find diagnosis and care. Inset shows location of Uganda in Africa.

IgM and IgG ELISA (*3*,*5*). On May 14, UVRI reported the confirmed case to the Uganda Ministry of Health.

Until she became ill, P1 resided with 8 family members in a rural area of Kinoni Subcounty. The week after RVFV was confirmed, a team from the Uganda Public Health Fellowship Program conducted interviews with the deceased woman's family. The family owns large cattle herds that graze in pasture areas surrounding their homestead and reported that in the weeks before the woman's illness, their cattle had appeared unwell; 1 had died and several had experienced abortions. Several goats from a neighboring farm had also reportedly aborted recently. The family reported that P1 had regularly milked the family's cattle and that the family, including P1, had regularly consumed raw milk from the herd.

A male family member 20 years of age (P2), who lived ≈1 km away from P1, experienced signs and symptoms beginning May 28. On June 1, he sought treatment at a local health center with fever, headache, cough, nausea, abdominal pain, and hematemesis. A malaria rapid diagnostic test was negative. P2 was treated with paracetamol, promethazine, and ciprofloxacin and was discharged. RVF was immediately suspected because of increased awareness following P1's diagnosis, so the clinical team collected a blood sample the same day and sent it to UVRI for VHF testing using the National Laboratory sample transport system (*8*). On June 2, melena and gingival hemorrhage developed, and P2 sought care at a private clinic, where he was admitted for supportive care. His symptoms improved overnight, and he was discharged the next day.

Table. Selected results of hemogram and blood chemistry tests for specimen collected from case-patient 1 a day before she died of Rift Valley fever, Uganda, 2021

Selected tests	Absolute value	Reference range
Platelets, 10^3/μL	60.00	138–475
Hemoglobin, g/dL	6.7	≥12
Albumin, g/L	27.5	37–52
Total protein, g/L	50.7	68–90
Total bilirubin, μmol/L	109.32	5.13–32.49
Direct bilirubin, μmol/L	68.71	0.00–6.84
Alkaline phosphatase, U/L	313	47–160
Gamma-glutamyl transferase, U/L	173	8.0–41.3
Aspartate transferase, U/L	>913	11.4–28.8
Prothrombin time, s	15.8	10–13
Internal normalized ratio	1.1	≤1.1
Creatinine, μmol/L	1098.33	44.2–79.6
Urea, μmol/L	>44.60	2.7–7.1
Sodium, mmol/L	112	135–146
Potassium, mmol/L	8.4	3.5–5.5
Calcium, mmol/L	1.24	2.20–2.65

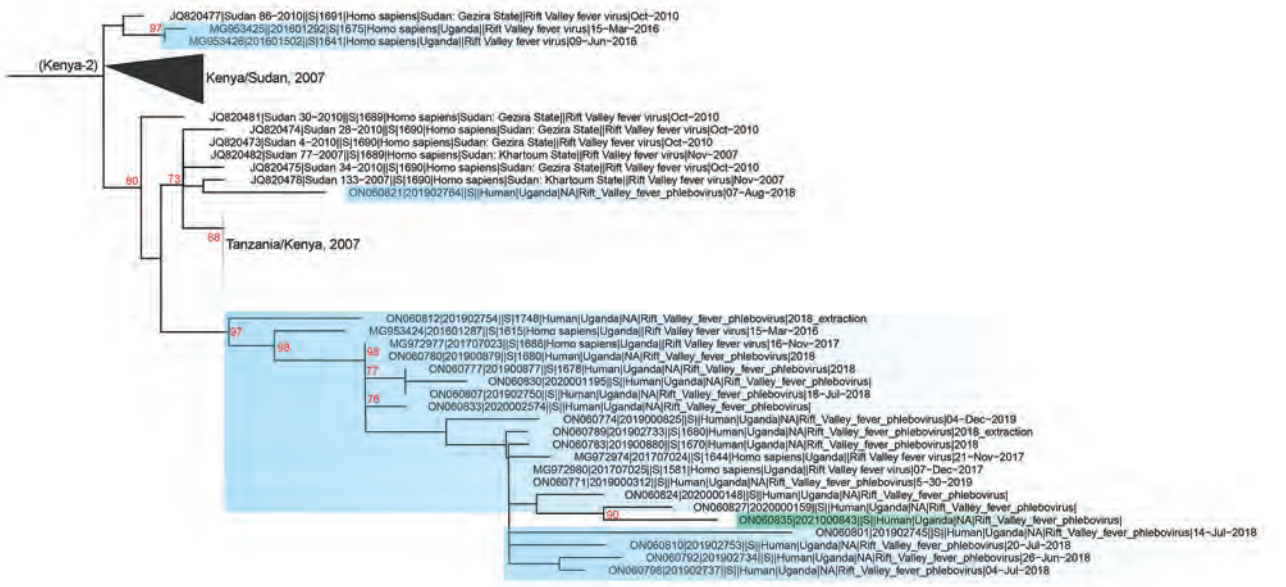

Figure 2. Phylogenetic analysis of Kenya-2 clade Rift Valley fever virus small segment from an outbreak in Uganda, 2021, compared with available full-length segments from GenBank (accession numbers shown). Green shading indicates sequence from Uganda outbreak; blue shading indicates historic RVFV sequences from Uganda. Red numbers indicate nodes with bootstrap support >70%. Complete phylogenies of small and large segments are shown in the Appendix (https://wwwnc.cdc.gov/EID/article/28/11/22-0364-App1.pdf).

On June 3, a field team from UVRI and the Centers for Disease Control and Prevention (CDC) interviewed and collected blood samples for RVFV testing from 20 persons living in or around P1's homestead that were willing to participate. The average age of participants was 28.6 years (range 9–67 years); 65% were male. Two participants, including P2, reported symptoms consistent with RVF at time of sampling and were tested using RVFV rRT-PCR and serology. The initial sample collected from P2 by the clinical team on June 1 was delayed in transit and not delivered to UVRI until June 8, but it eventually tested positive by rRT-PCR and IgM and IgG ELISA, as did the second sample collected from P2 by the field team on June 3. The other symptomatic participant tested negative. The remaining asymptomatic participants were tested by RVFV serology only; 2 were IgM and IgG positive, and 3 were IgM negative and IgG positive.

We conducted next-generation sequencing (NGS) and phylogenetic analysis on the rRT-PCR positive sample from P1 (Figure 2; Appendix, https://wwwnc.cdc.gov/EID/article/28/11/22-0364-App1.pdf). Sequencing generated complete large and small segments but only a partial medium segment. The large and small segments (deposited into GenBank under accession nos. ON060834–5) were members of the Kenya-2 clade and clustered with a Uganda-specific sublineage collected during 2016–2020. The most closely related sequences were collected from the Wakiso and Kyankwanzi districts, both 181 km from Kiruhura District, during February–March 2020. This finding suggests the strain represented by the sequence isolated from P1 had wide geographic and temporal circulation in Uganda and might be endemic. We did not attempt NGS on samples from P2 because the rRT-PCR cycle thresholds suggested it would be unsuccessful; the first sample from P2 was likely degraded from lack of cold chain continuity during delayed transportation, and the second sample was collected late in the course of illness.

Conclusion

We report 7 RVFV infections, 4 recent infections (positive by IgM testing, rRT-PCR, or both) and 3 past infections (IgG positive only), identified May–June 2021 in Kiruhura District, Uganda. The western region of Uganda, including Kiruhura District, is within the cattle corridor (Figure 1) and at high risk for RVF and Crimean-Congo hemorrhagic fever because of large livestock populations (*9*,*10*). The RVF case-patient who died was a young, previously healthy resident of a farming community with a history of contact with cattle and drinking raw milk from a herd with reported manifestations compatible with RVF.

In April–June 2021, Uganda experienced a second surge of COVID-19, leading to a nationwide lockdown in June 2021 (*11*), which likely delayed RVF

recognition and care provision to P1, contributing to her death. P1 traveled >300 km in 5 days seeking care at 6 healthcare facilities (Figure 1) before a VHF was suspected only hours before she died. In addition, the specimen transport system, slowed by COVID-19 demands, delayed RVF confirmation for P2.

Implications of delayed recognition and diagnosis could have been far worse with other VHFs endemic to western Uganda with higher case-fatality rates (e.g., Ebola, Marburg, and Crimean-Congo hemorrhagic fever viruses) (*9*,*12*,*13*), which unlike RVFV are capable of human-to-human transmission. Our findings highlight the critical need to improve access to diagnostics, renewed community and clinician education about VHFs in humans and animals, and improved surveillance and awareness of the continued threat of VHFs in Uganda and the region.

Acknowledgments

The authors thank the family and neighbors of the deceased woman and the healthcare workers at Kinoni Health Center III for their willingness to participate in and support this investigation. We also acknowledge B. Khainza, J. Mwesige, J. Kalungi, and the medical teams from Case Hospital and the other health facilities involved in the management of the cases. We also thank CDC Uganda, the Ministry of Health of Uganda, the Kiruhura District Health Team, and the Uganda Virus Research Institute for their support.

About the Author

Dr. Cossaboom is a veterinary epidemiologist in Viral Special Pathogens Branch, Division of High-Consequence Pathogens and Pathology, National Center for Emerging and Zoonotic Infectious Diseases, US Centers for Disease Control and Prevention, Atlanta. Her primary research interests include epidemiology of and outbreak response for zoonotic diseases of public health importance.

References

1. Bird BH, Ksiazek TG, Nichol ST, Maclachlan NJ. Rift Valley fever virus. J Am Vet Med Assoc. 2009;234:883–93. https://doi.org/10.2460/javma.234.7.883
2. Elliott RS. Bunyaviridae. In: Knipe DN, Howley PM, editors. Fields virology, 6th ed. Philadelphia: Lippincott Williams and Wilkins; 2013. p. 1245–78.
3. Nyakarahuka L, de St Maurice A, Purpura L, Ervin E, Balinandi S, Tumusiime A, et al. Prevalence and risk factors of Rift Valley fever in humans and animals from Kabale district in southwestern Uganda, 2016. PLoS Negl Trop Dis. 2018;12:e0006412. https://doi.org/10.1371/journal.pntd.0006412
4. Al-Hamdan NA, Panackal AA, Al Bassam TH, Alrabea A, Al Hazmi M, Al Mazroa Y, et al. The risk of nosocomial transmission of Rift Valley fever. PLoS Negl Trop Dis. 2015;9:e0004314. https://doi.org/10.1371/journal.pntd.0004314
5. Madani TA, Al-Mazrou YY, Al-Jeffri MH, Mishkhas AA, Al-Rabeah AM, Turkistani AM, et al. Rift Valley fever epidemic in Saudi Arabia: epidemiological, clinical, and laboratory characteristics. Clin Infect Dis. 2003;37:1084–92. https://doi.org/10.1086/378747
6. Rich KM, Wanyoike F. An assessment of the regional and national socio-economic impacts of the 2007 Rift Valley fever outbreak in Kenya. Am J Trop Med Hyg. 2010;83 (Suppl):52–7. https://doi.org/10.4269/ajtmh.2010.09-0291
7. Bird BH, Bawiec DA, Ksiazek TG, Shoemaker TR, Nichol ST. Highly sensitive and broadly reactive quantitative reverse transcription-PCR assay for high-throughput detection of Rift Valley fever virus. J Clin Microbiol. 2007;45:3506–13. https://doi.org/10.1128/JCM.00936-07
8. Kiyaga C, Sendagire H, Joseph E, McConnell I, Grosz J, Narayan V, et al. Uganda's new national laboratory sample transport system: a successful model for improving access to diagnostic services for Early Infant HIV Diagnosis and other programs. PLoS One. 2013;8:e78609. https://doi.org/10.1371/journal.pone.0078609
9. Mirembe BB, Musewa A, Kadobera D, Kisaakye E, Birungi D, Eurien D, et al. Sporadic outbreaks of Crimean-Congo haemorrhagic fever in Uganda, July 2018–January 2019. PLoS Negl Trop Dis. 2021;15:e0009213. https://doi.org/10.1371/journal.pntd.0009213
10. Birungi D, Aceng FL, Bulage L, Nkonwa IH, Mirembe BB, Biribawa C, et al. Sporadic Rift Valley fever outbreaks in humans and animals in Uganda, October 2017–January 2018. J Environ Public Health. 2021;2021:8881191. https://doi.org/10.1155/2021/8881191
11. Eyu P, Elyanu P, Ario AR, Ntono V, Birungi D, Rukundo G, et al. Investigation of possible preventable causes of COVID-19 deaths in the Kampala Metropolitan Area, Uganda, 2020–2021. Int J Infect Dis. 2022;122:10–4. https://doi.org/10.1016/j.ijid.2022.05.033
12. Nyakarahuka L, Schafer IJ, Balinandi S, Mulei S, Tumusiime A, Kyondo J, et al. A retrospective cohort investigation of seroprevalence of Marburg virus and ebolaviruses in two different ecological zones in Uganda. BMC Infect Dis. 2020;20:461. https://doi.org/10.1186/s12879-020-05187-0
13. Wamala JF, Lukwago L, Malimbo M, Nguku P, Yoti Z, Musenero M, et al. Ebola hemorrhagic fever associated with novel virus strain, Uganda, 2007–2008. Emerg Infect Dis. 2010;16:1087–92. https://doi.org/10.3201/eid1607.091525

Address for correspondence: Caitlin Cossaboom, Centers for Disease Control and Prevention, 1600 Clifton Rd NE, Mailstop H24-12, Atlanta, GA 30329-4027, USA; email: nrm9@cdc.gov

COVID-19 among Chronic Dialysis Patients after First Year of Pandemic, Argentina

Augusto Vallejos, Andrea E.M. Baldani, Micaela A. Gauto, Dalila V. Rueda, Federico M. Santoro, María Graciela Abriata

We performed a descriptive study to characterize effects from COVID-19 among chronic dialysis patients compared with the general population in Argentina during March 2020–February 2021. COVID-19 case-fatality rate of chronic dialysis patients was 10 times the national rate; the age-standardized mortality ratio was 6.8 (95% CI 6.3–7.3).

Patients requiring dialysis for chronic kidney disease comprise a high risk to public health (*1*), and need for this treatment precluded patients from being able to comply with COVID-19 isolation measures during the pandemic (*2*). Studies have reported high COVID-19 mortality rates among these patients, but such studies have been scarce in Latin America (*3*–*5*). We contrasted clinical and epidemiologic characteristics and outcomes between chronic dialysis (CD) patients and the general population to evaluate COVID-19 dynamics during the first year of the pandemic in Argentina.

The Study

We designed an observational, analytic, retrospective, nationwide study that included data from all COVID-19 cases reported to the National Health Surveillance System (SNVS$^{2.0}$) during epidemiologic weeks (EW) 10/2020 (March 1–7, 2020) through 08/2021 (February 21–27, 2021). COVID-19 cases in CD patients included all cases in persons on dialysis treatment at the time of COVID-19 diagnosis. On March 1, 2021, we downloaded data from an SNVS$^{2.0}$ database that included COVID-19 cases reported through EW 08/2021. Notifications provided demographic, clinical, and epidemiologic data; we validated cases involving CD patients with records from the network of local kidney health institutions of the National Program of Integral Approach to Renal Diseases (Programa Nacional de Abordaje Integral de Enfermedades Renales [PAIER]).

We used projections from the National Institute of Statistics and Census (Instituto Nacional de Estadística y Censos [INDEC]) for the population of Argentina (*6*) and the Argentine Registry of Chronic Dialysis (Registro Argentino de Diálisis Crónica [RADC]) for the population of CD patients (*2*). We performed a descriptive analysis of COVID-19 cases in CD patients and the general population during the first year of the pandemic. We included only data from complete records for each variable. For epidemiologic description in the temporal analysis, we determined EW dates on the basis of patient symptom onset or, if unavailable, sample collection. We classified cases as close-contact, community-acquired, or other according to epidemiologic history.

We described age-group distribution for total and deceased case-patients for both populations. We also calculated cumulative incidence and overall and age-group case-fatality rates (CFR) and age-standardized incidence and mortality ratios by indirect adjustment method. We counted as deceased those persons recorded as having died in their SNVS$^{2.0}$ notifications and the rest, including patients who had recovered or were active case-patients, as nondeceased. We did not include deaths that occurred after COVID-19 isolation and follow-up were completed.

We calculated qualitative variables with frequency distributions and quantitative variables using median and interquartile range (IQR). We performed quantitative data analysis using Student t-test and tested difference in proportions using Z-test or Fisher exact test according to assumptions. We defined 2-sided p values <0.05 as statistically significant. We performed statistical analyses using RStudio version 1.2 18 software (https://www.rstudio.com).

Author affiliations: Dirección Nacional de Abordaje Integral de Enfermedades no Transmisibles, Buenos Aires, Argentina (A. Vallejos, M.G. Abriata); Dirección Nacional de Epidemiología e Información Estratégica, Buenos Aires, Argentina (A.E.M. Baldani, M.A. Gauto, D.V. Rueda, F.M. Santoro).

DOI: https://doi.org/10.3201/eid2811.212597

Table. Characteristics of COVID-19 cases in the general population and in chronic dialysis patients, Argentina, 2020–2021

Characteristic	General population, n = 2,107,676	Chronic dialysis patients, n = 2,496
Sex, no. (%)		
F	1,045,989 (49.6)	1,076 (43.1)
M	1,036,211 (49.2)	1,419 (56.9)
Other	2,4631 (1.2)	1 (0.0)
Unknown	845 (0.0)	0 (0.0)
Median age, y (IQR)	37 (27–51)	60 (48–70)
Epidemiologic case classification, no. (%)		
Close-contact cases	310,041 (14.7)†	439 (17.6)
Community-acquired cases	1,546,887 (73.4)†	1,731 (69.3)
Other	249,712 (11.9)†	326 (13.1)
Deceased case-patients, no. (%)	52,075 (2.4)	617 (24.7)
Deceased case-patients median age, y (IQR)	73 (63–82)	67 (58–75)

*IQR, interquartile range.
†Relative frequencies were calculated according to the cases with information on the variable. A total of 2,106,640 COVID-19 cases were contemplated in the general population.

During the study period, 2,107,676 people from the general population and 2,496 persons requiring CD were diagnosed with COVID-19 (Table). Cumulative incidence was 46 cases per 1,000 among the general population and 83/1,000 among CD patients. The epidemic curve for COVID-19 cases in the general population started during EW 10/2020; the first COVID-19 case in a CD patient was registered during EW 13/2020. Epidemic curves for both populations followed the same trends over time (Figure 1).

Case distribution by age group showed higher proportions in older age groups among CD patients than the general population (Appendix, https://wwwnc.cdc.gov/EID/article/28/11/21-2597-App1.pdf) and a significantly higher median age among CD patients, 60.0 (IQR 48–70) years of age, than among the general population, 37.0 (IQR 27–51) years of age ($p<0.05$). When standardized by age, COVID-19 incidence in CD patients was 1.5 (95% CI 1.5–1.6) times the national rate. Case distribution by sex showed a slightly higher proportion of male case-patients among CD patients, although this difference was not significant (Table).

Deceased-case distribution was concentrated in older age groups among CD patients (Appendix). However, median age of death among CD patients was 67.0 (IQR 58–75) years of age, significantly lower than among the general population, 73.0 (IQR 63–82) years of age ($p<0.05$) (Table). There were 52,075 deaths among the general population (COVID-19 CFR 2.4%) and 617 among CD patients (COVID-19 CFR 24%) (Table); CFR among CD patients was significantly higher than for the general population among age groups 20–29 years and above (Figure 2). Age-standardized mortality ratio was 6.8 (95% CI 6.3–7.3).

Most close-contact cases were recorded during the first weeks of the pandemic, after which community-acquired cases trended upward. After EW 15/2020, the percentage of close-contact cases was always higher among CD patients than national rates, and a statistically significant difference ($p<0.05$) was seen during EWs 15–20/2020 and

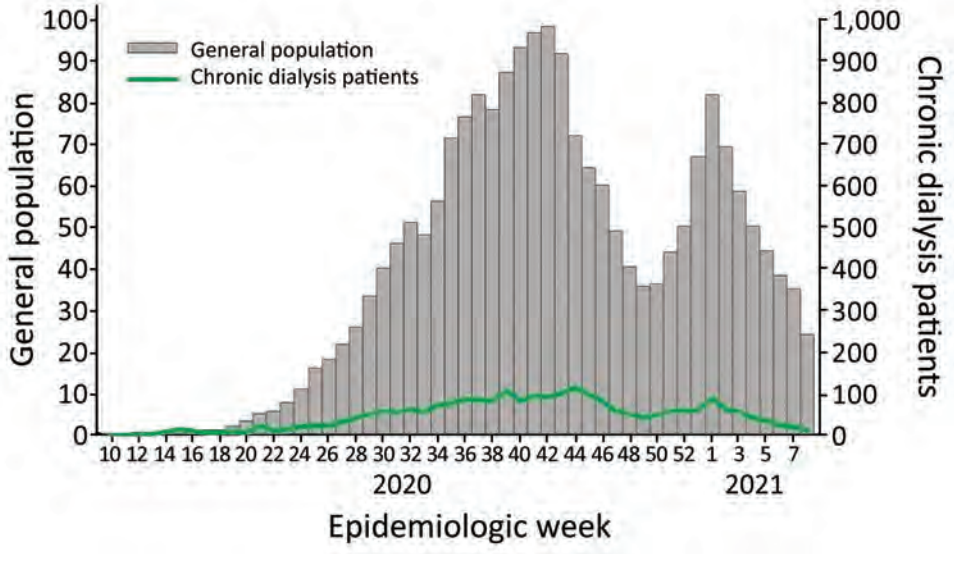

Figure 1. COVID-19 cases in the general population (per 1,000 persons) and chronic dialysis patients, by date of symptom onset, Argentina, epidemiological weeks 10/2020 (March 1–7, 2020) through 08/2021 (February 21–27, 2021).

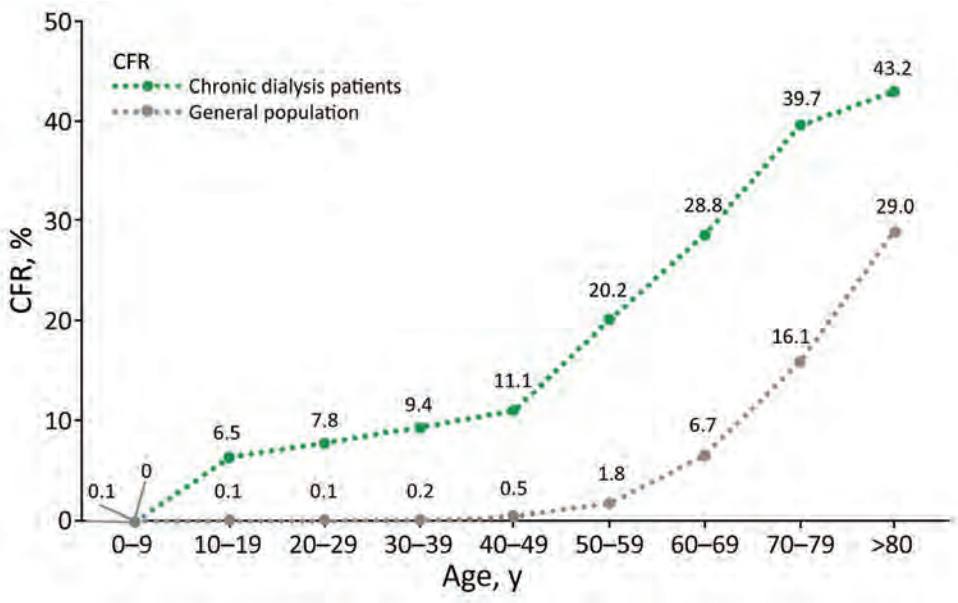

Figure 2. CFR for COVID-19 in the general population and chronic dialysis patients, by age group, Argentina, epidemiological weeks 10/2020 (March 1–7, 2020) through 08/2021 (February 21–27, 2021). CFR, case-fatality rate.

EWs 35/2020–08/2021, the end of the study period (Appendix). Because hemodialysis is an outpatient treatment, patients must visit specialized centers several times a week to receive treatment, sometimes remaining in close proximity to other patients for several hours. In addition, carpooling to dialysis centers was common. Although we cannot rule out domestic exposure, dialysis modality presented a greater SARS-CoV-2 exposure risk (*2*).

Analysis of COVID-19 dynamics for persons requiring CD during the first year of the pandemic in Argentina highlights the influence of conditions of vulnerability within an epidemiologic context. People with CD requirements tended to be older and more susceptible to infectious diseases. Requiring CD is associated with high mortality; the Argentine Registry of Chronic Dialysis reported that, of 30,300 CD patients in Argentina in 2019, 17% died (*1*). Temporal distribution of COVID-19 cases was similar in both groups. We observed ≈60% of cases among men, which correlates with the sex distribution among CD patients (*1*). National COVID-19 incidence among CD patients was twice that among the general population and 50% higher when adjusted by age.

Although mortality rates vary among countries (*4*), COVID-19 CFR in CD patients (24.0%) is similar throughout Latin America; 1 study from Guatemala described a CFR of 27.7% (*3*). Compared rates for with the general population, CFR in CD patients was 10 times higher and exceeded national rates in all age groups. According to age-standardized mortality ratio, CD patients were 5.8 times as likely to die as predicted by national COVID-19 mortality trends.

Among limitations, our results were based on data obtained before national vaccination campaigns for this group. Although modality was not specified, 93.2% of dialysis patients in Argentina undergo chronic hemodialysis (*1*). In addition, we were unable to adjust mortality rates by underlying conditions because those conditions are self-reported nonmandatory information when reporting COVID-19 cases, resulting in incomplete data for that variable.

Conclusion

Our results show the substantial effect the first year of the COVID-19 pandemic had on CD patients in Argentina. These findings reinforce the importance of implementing prevention and control strategies and prioritizing vaccination campaigns among this population (*7*).

Acknowledgments

We thank the network of institutions belonging to the National Program of Integral Approach to Renal Diseases (Programa Nacional de Abordaje Integral de Enfermedades Renales), which maintains a thorough registry of COVID-19 cases among chronic dialysis patients, without whom we could not have carried out this study. We also extend our gratitude to the local teams that registered and reported COVID-19 cases to the national health surveillance network, enabling production of high-quality information. We also thank our fellow residents and colleagues of the National Directorate of Epidemiology and Strategic Information for their support and guidance.

About the Author

Dr. Vallejos is coordinator of the National Program of Integral Approach to Renal Diseases (Programa Nacional de Abordaje Integral de Enfermedades Renales) of the Ministry of Health of Argentina. His primary research interests are public health and kidney disease.

References

1. Ministry of Health of Argentina. Argentine chronic dialysis registry 2019 [Spanish]. Buenos Aires, Argentina: Argentine Society of Nephrology and Unique Central National Institute Coordinator of Ablation and Implantation [cited 2021 Apr 30] https://bancos.salud.gob.ar/recurso/registro-argentino-de-dialisis-cronica-2019
2. Bank of Communication Resources of the Ministry of Health of the Nation. COVID-19: management of patients with chronic kidney disease or acute kidney failure during the pandemic. Recommendations [in Spanish]. [cited 2021 Apr 30]. https://bancos.salud.gob.ar/sites/default/files/2020-07/covid19-manejo-pacientes-enfermedad-renal-cronica-o-insuficiencia-renal-aguda-durante-pandemia.pdf
3. Sosa R, Garcia P, Cipriano EO, Hernández A, Hernández EE, Chavez PI, et al. Coronavirus disease 2019 in patients with end-stage kidney disease on hemodialysis in Guatemala. Kidney Int Rep. 2021;6:1110–7. https://doi.org/10.1016/j.ekir.2021.01.028
4. Andhika R, Huang I, Wijaya I. Severity of COVID-19 in end-stage kidney disease patients on chronic dialysis. Ther Apher Dial. 2021;25:706–9. https://doi.org/10.1111/1744-9987.13597
5. Valeri AM, Robbins-Juarez SY, Stevens JS, Ahn W, Rao MK, Radhakrishnan J, et al. Presentation and outcomes of patients with ESKD and COVID-19. J Am Soc Nephrol. 2020;31:1409–15. https://doi.org/10.1681/ASN.2020040470
6. Republic of Argentina National Institute of Statistics and Census. Populations: national projections [in Spanish] [cited 2021 Apr 30] https://www.indec.gob.ar/indec/web/Nivel4-Tema-2-24-84
7. Silvariño R, Ferreiro A, Seija M, Boggia J, Luzardo L, Otatti G, et al. Recommendations on vaccination against SARS-CoV-2/COVID-19 in patients with kidney disease and kidney transplantation. Rev Med Urug (Montev). 2021;37:e37212.

Address for correspondence: Augusto Vallejos, Dirección Nacional de Abordaje Integral de Enfermedades no Transmisibles, Av. 9 de Julio 1925, Piso 9, Ciudad Autónoma de Buenos Aires, Argentina; email: acvallejos@gmail.com

Molecular Detection of *Haplorchis pumilio* Eggs in Schoolchildren, Kome Island, Lake Victoria, Tanzania

Hyejoo Shin,[1] Bong-Kwang Jung,[1] Seungwan Ryoo, Sooji Hong, Heonwoo Jeong, Hoo-Gn Jeoung, Sunhye Kim, Sun Kim, Min-Jae Kim, Hansol Park, Keeseon S. Eom, Godfrey M. Kaatano, Jong-Yil Chai

A survey of intestinal helminths targeting 1,440 schoolchildren in 12 primary schools on Kome Island (Lake Victoria), Tanzania, revealed small trematode eggs in 19 children (1.3%), seemingly of a species of *Haplorchis* or *Heterophyes*. The eggs were molecularly confirmed to be *Haplorchis pumilio* on the basis of 18S and 28S rDNA sequences.

Haplorchis pumilio, a species of the zoonotic minute intestinal flukes belonging to the family Heterophyidae, was first discovered in the small intestines of birds and mammals in Egypt (*1*). Infection with this fluke also occurs in humans through the consumption of raw or improperly cooked fish harboring the metacercariae. Abdominal pain, diarrhea, lethargy, anorexia, malabsorption, and weight loss are the possible clinical symptoms (*2*). This fluke is widely distributed geographically from Africa to Asia, Australia, and the Americas (*1*). However, human infections were reported in only 5 countries in Africa and Asia: Egypt, China, Laos, Thailand, and Vietnam (*1*). We recently surveyed the prevalence of intestinal helminths among schoolchildren in 12 primary schools on Kome Island, Lake Victoria, Tanzania (Figure 1, panel A). We detected a low-grade prevalence of an apparent species of *Haplorchis* or *Heterophyes* by the recovery of eggs in fecal samples. We used molecular methods to confirm the eggs to be *H. pumilio* on the basis of 18S and 28S rDNA gene sequences.

The Study

An international collaborative project between South Korea and Tanzania named "Rapid assessment of schistosomiasis and soil-transmitted helminthiases on Kome Island, Buchosa District, northwestern Tanzania" was implemented during 2020–2022. This project was approved by the Ethics Committee of the Korea Association of Health Promotion, Seoul, South Korea (IRB no. 130750-202009-HR-019). Fecal examinations were performed on 1,440 schoolchildren in 12 primary schools by using the Kato-Katz thick smear technique.

The number of overall helminth egg–positive cases was 631/1,440 (43.8%): *Schistosoma mansoni* (564 [39.2%]), *Trichuris trichiura* (42 [2.9%]), *Ancylostoma duodenale* or *Necator americanus* (27 [1.9%]), small trematode eggs (STE) (19 [1.3%]), *Enterobius vermicularis* (16 [1.1%]), and others (unidentified) (7 [0.5%]). The STE were operculate, oval, yellowish-brown in color, 29.0–31.6 (mean 30.4) μm long, and 14.8–17.6 (mean 16.5) μm wide (n = 6). They seemed to be the eggs of a *Haplorchis* or *Heterophyes* species (Figure 1, panels B and C). The STE-positive fecal samples were preserved in 100% ethanol for molecular analysis.

We extracted DNA from 20 mg of the fecal sediment by using the DNeasy Tissue and Blood kit (QIAGEN, https://www.qiagen.com) after a modified formalin-ether concentration method in which formalin was replaced with water. The sediment was washed several times with distilled water. We performed PCR

Author affiliations: Korea Association of Health Promotion, Seoul, South Korea (H. Shin, B.-K. Jung, S. Ryoo, S. Hong, H. Jeong, H.-G. Jeoung); Good Neighbors International, Seoul (Sunhye Kim, Sun Kim); Asan Medical Center, University of Ulsan College of Medicine, Seoul (M.-J. Kim); Parasite Resource Bank, Chungbuk National University School of Medicine, Cheongju, South Korea (H. Park, K.-S. Eom); National Institute for Medical Research, Mwanza, Tanzania (G.M. Kaatano); Seoul National University College of Medicine, Seoul (J.-Y. Chai)

DOI: https://doi.org/10.3201/eid2811.220653

[1]These authors contributed equally to this article.

targeting the 18S and 28S rDNA of *Haplorchis* species using the primers we designed on the basis of the reported nucleotide sequences of *Haplorchis* and *Heterophyes* in GenBank (Table 1). We conducted PCR in a final volume of 20 μL using 5x PCR Premix (GenomicsOne, https://www.genomicsone.kr). The procedure included an initial denaturation at 94°C for 3 min, followed by 40 cycles of denaturation at 94°C for 30 s, annealing at 60°C for 30 s, extension at 72°C for 30 s, and final extension at 72°C for 5 min. The amplicons were electrophoresed in 2.0% agarose gel, and DNA sequencing was performed using the Sanger method (*3*) by Macrogen Inc. (https://www.macrogen.com). We aligned sequences of the amplicons and generated phylogenetic trees with the maximum-likelihood method in MEGA version 7.0 software (https://www.megasoftware.net) by using the Kimura 2-parameter model with 1,000 bootstrap replications.

Sequences of the 18S region of our samples (n = 4) were 100% identical to the 18S rDNA gene of *H. pumilio* in GenBank (accession nos. AY245706 and HM004196) (Table 2; Figure 2, panel A). However, only 95.0% identity was found between our samples and *Haplorchis taichui* (accession no. AY245705) and 98.9% was found between our samples and *Haplorchis yokogawai* (accession no. HM004208). However, using this gene, comparing our samples with *Heterophyes heterophyes* was not possible because 18S rDNA sequences of *H. heterophyes* are not available in GenBank.

Sequences of the 28S region of our samples (n = 3) were 99.1%–100% identical to the 28S rDNA gene of *H. pumilio* in GenBank (accession nos. MN745941 and MT840091) (Table 2; Figure 2, panel B). However, only 93.7% identity was found between our samples and *H. taichui* (accession no. OM956185) and 95.8% identity was found between our samples and *H. yokogawai* (accession no. HM004192). *H. heterophyes* (accession no. KU559554) appeared to be far from our samples (Figure 2, panel B) showing a sequence identity of only 86.9% (Table 2). Thus, we could confirm that our samples were mostly the eggs of *H. pumilio* and that Kome Island is a low-grade endemic area of *H. pumilio* infection among schoolchildren. However, possibilities remain for mixed infections with other heterophyid species (low worm loads and not detected by PCR).

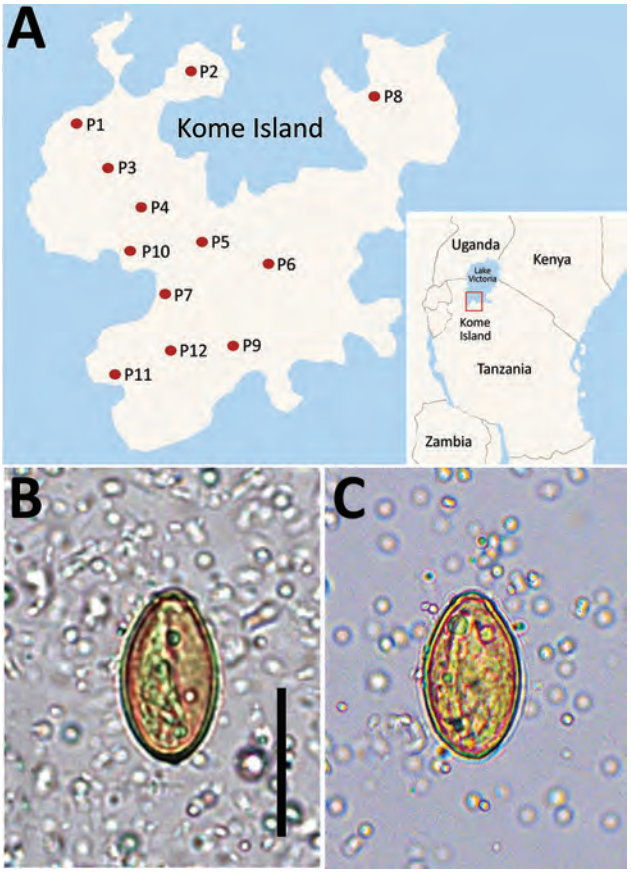

Figure 1. Geographic distribution and imaging from study of *Haplorchis pumilio* eggs in schoolchildren, Kome Island, Lake Victoria, Tanzania. A) Locations of 12 primary schools (P1–P12) surveyed on Kome Island. Inset shows location of Kome Island. B–C) Small trematode eggs (30.0–30.2 μm long and 16.5–16.6 μm wide) detected in schoolchildren, yellowish-brown in color, oval, and operculate with a thick shell and prominent (B) or less prominent shoulder rims (C). Scale bar = 25 μm.

Conclusions

Taxonomically, in the genus *Haplorchis*, a total of 9 species have been known to be valid (*1*). Among them, 4 species are recognized to be zoonotic: *H. pumilio, H. taichui, H. yokogawai,* and *H. vanissimus*

Table 1. Primers used for DNA amplification in study of *Haplorchis pumilio* eggs in schoolchildren, Kome Island, Lake Victoria, Tanzania*

Target gene	Primer	Sequence, 5′ → 3′	Length, bp
18S rDNA	18S 1F	ATACGGGACTCGTTAGAGGC	504
	18S 1R	TACAAATGCCCCCGTCTGTC	
28S rDNA	28S 1F	AGTGAACAGGGAAAAGCCCAG	897
	28S 1R	TCAGGTGGAAAGTCTACCGC	
	28S 2F	ATAGCGAACAAGTACCGTGAGG	
	28S 2R	ACATGTTACTCTCCTTGGTCCG	659

*Primers were designed using Geneious primer design software (https://www.geneious.com) based on the 18S rDNA sequences of *Haplorchis pumilio* (GenBank accession no. AY245706) and *H. taichui* (accession no. AY245705) and the 28S rDNA sequences of *H. pumilio* (accession no. HM004173) and *Heterophyes heterophyes* (accession no. KU559553).

Table 2. Sequence comparison of samples from study of *Haplorchis pumilio* eggs in schoolchildren, Kome Island, Lake Victoria, Tanzania, with other heterophyid and opisthorchiid flukes in GenBank based on 18S and 28S rDNA genes

18S rDNA	% Identity	28S rDNA	% Identity
Among study samples (*Haplorchis pumilio*), n = 4	100	Among study samples (*H. pumilio*), n = 3	100
H. pumilio (AY245706, Israel)	100	*Haplorchis pumilio* (MN745941, Kenya)	100
H. pumilio (HM004196, Thailand)	100	*Haplorchis pumilio* (MT840091, Brazil)	99.1
Haplorchis yokogawai (HM004208, Thailand)	98.9	*Haplorchis yokogawai* (HM004192, Thailand)	95.8
Metagonimus yokogawai (HQ832632, Japan)	97.2	*Haplorchis taichui* (OM956185, Vietnam)	93.7
Metagonimus takahashii (HQ832629, Japan)	97.2	*Metagonimus miyatai* (HQ832633, Japan)	91.4
Pygidiopsis genata (AY245710, Israel)	96.3	*Metagonimus yokogawai* (HQ832639, Japan)	91.4
Clonorchis sinensis (JF314770, China)	96.3	*Metagonimus takahashii* (HQ832636, Japan)	91.0
Opisthorchis viverrine (HM004211, Thailand)	96.3	*Heterophyes heterophyes* (KU559554, Italy)	86.9
Centrocestus formosanus (HQ874608, Thailand)	95.4	*Clonorchis sinensis* (JF823989, Vietnam)	89.3
Pygidiopsis summa (JQ955649, Korea)	95.2	*Opisthorchis viverrine* (HM004188, Thailand)	88.3
Haplorchis taichui (AY245705, Japan)	95.0	*Centrocestus formosanus* (HQ874609, Thailand)	88.2

(*1*). Natural human infection with *H. pumilio* flukes was first documented in Egypt in 1977 in a 9-year-old child passing diarrheic stools (*4*). A vital snail species for *H. pumilio* flukes is *Melanoides tuberculata* in Egypt, Taiwan, India, Peru, and Brazil (*1*,*5*). Their metacercariae are detected in various species of freshwater or brackish water fish, including *Mugil* sp., *Tilapia* sp., and *Bagrus bayad* (*1*,*6*).

In Africa, with the exception of Egypt (an *H. pumilio* fluke–endemic area), the distribution of *H. pumilio* flukes has been rarely reported. In Kenya, *H. pumilio* cercariae were confirmed molecularly recently in *M. tuberculata* snails; a high positive rate of 69.4% was found in the northernmost area of Lake Victoria, in Kenya (*7*). However, human *H. pumilio* infection in sub-Saharan Africa countries, including Kenya, has not been reported. In São Tomé and Principe, a sub-Sahara country off the west coast of Africa, eggs of Heterophyidae, which are very similar to *Metagonimus yokogawai*, were found in 28.2% of 1,050 human

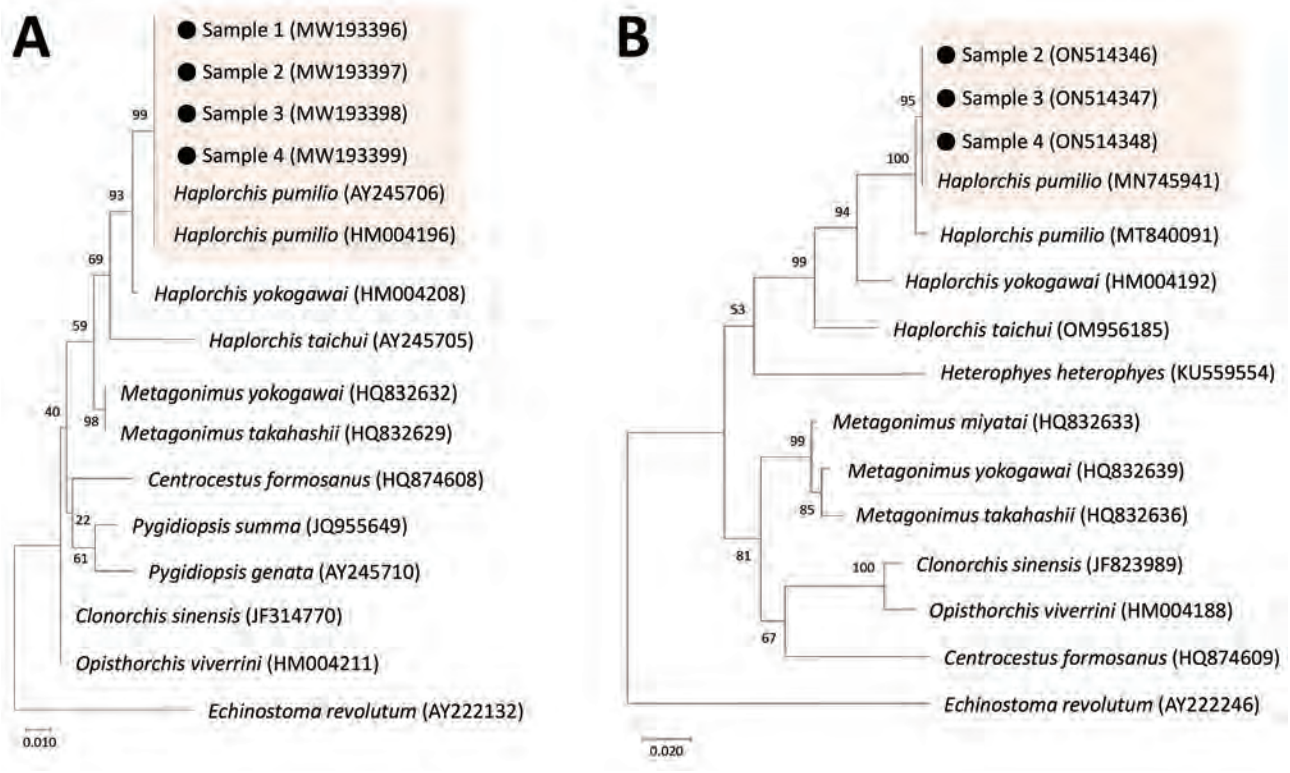

Figure 2. Phylogenetic trees of DNA of small trematode eggs from schoolchildren, Kome Island, Lake Victoria, Tanzania, in comparison with reference sequences of heterophyid (*Haplorchis pumilio* and others) and opisthorchiid trematodes, based on 18S (A) and 28S rDNA (B) sequences. The trees were constructed using the maximum-likelihood method based on the Kimura 2-parameter model and viewed by the MEGA 7.0 program (http://www.megasoftware.net). GenBank accession numbers are indicated. Scale bars indicate nucleotide substitutions per site.

fecal samples in 1987, but their species could not be identified (*8*). Those eggs were 22.2–27.7 × 17.0–21.0 μm in size and had a thick wall and a difficult-to-see operculum (*8*); they were markedly different from the eggs of *Haplorchis* or *Heterophyes* spp (*1*). Of note, a zoonotic liver fluke species, *Opisthorchis felineus*, was found in dogs and cats in New Bussa, Nigeria (*9*); however, this species has never been found to distribute around Lake Victoria.

On the Lake Victoria basin, schistosomiasis and soil-transmitted helminthiases have been acknowledged as major public health problems (*10*), whereas intestinal fluke infections have been poorly studied. In this study, we detected a low-grade endemicity of *H. pumilio* infection on Kome Island, Lake Victoria, Tanzania. It remains unclear if human *H. pumilio* infection has been endemic on Kome Island unnoticed for a long time or was introduced recently. These 2 possibilities should be investigated.

Surveyed schoolchildren on Kome Island had no history of international travel, including to Asia, South America, Egypt, and Kenya, where the *H. pumilio* fluke is endemic. Therefore, the source of infection in our cases seems to be the fish host caught around Kome Island. In Lake Victoria, 3 fish species are known to predominate, and one of them is Nile tilapia (*Oreochromis niloticus*), which is a fish host for *H. pumilio* flukes (*1*,*11*,*12*). Nile tilapia is popularly eaten on Kome Island and is highly suggested as the source of infection in our cases. Studies are required to determine the existence of the life cycle of *H. pumilio* flukes on and around Kome Island and clarify the public health importance of *H. pumilio* infection in this area.

Acknowledgments

We thank the staff of the International Cooperation Department of the Korea Association of Health Promotion and Good Neighbors International for their help in this study. We are also grateful to the members of the National Institute of Medical Research, Mwanza, Tanzania, who helped with this study.

About the Author

Ms. Shin and Dr. Jung are research associates at the MediCheck Research Institute, Korea Association of Health Promotion, Seoul, South Korea. Their major research interests are molecular analyses of foodborne zoonotic parasites, including heterophyids, echinostomes, *Fasciola* sp., and *Toxoplasma gondii*.

References

1. Chai J-Y. Heterophyids. In: Human intestinal flukes. Dordrecht (The Netherlands): Springer Nature; 2019. p. 58–78.
2. Chai JY, Jung BK. Fishborne zoonotic heterophyid infections: An update. Food Waterborne Parasitol. 2017;8-9:33–63. https://doi.org/10.1016/j.fawpar.2017.09.001
3. França LTC, Carrilho E, Kist TBL. A review of DNA sequencing techniques. Q Rev Biophys. 2002;35:169–200. https://doi.org/10.1017/S0033583502003797
4. Khalifa R, El-Naffar MK, Arafa MS. Studies on heterophyid cercariae from Assiut Province, Egypt. I. Notes on the life cycle of *Haplorchis pumilio* (Looss, 1896) with a discussion on previously described species. Acta Parasitol Pol. 1977;25:25–38.
5. Lopes AS, Pulido-Murillo EA, Melo AL, Pinto HA. *Haplorchis pumilio* (Trematoda: Heterophyidae) as a new fish-borne zoonotic agent transmitted by *Melanoides tuberculata* (Mollusca: Thiaridae) in Brazil: A morphological and molecular study. Infect Genet Evol. 2020;85:104495. https://doi.org/10.1016/j.meegid.2020.104495
6. Tawfik MAA, Elnawawi FA, Shaapan RM. Studies on some fish-borne trematodes in Egypt. Egypt J Vet Sci. 2000;34:39–48.
7. Outa JO, Sattmann H, Köhsler M, Walochnik J, Jirsa F. Diversity of digenean trematode larvae in snails from Lake Victoria, Kenya: First reports and bioindicative aspects. Acta Trop. 2020;206:105437. https://doi.org/10.1016/j.actatropica.2020.105437
8. Pampiglione S, Visconti S, Pezzino G. Human intestinal parasites in Subsaharan Africa. II. São Tomé and Principe [in Italian]. Parassitologia. 1987;29:15–25.
9. Okaeme AN. Zoonotic helminths of dogs and cats at New Bussa, Kainji Lake area, Nigeria. Int J Zoonoses. 1985; 12:238–40.
10. Mwanga JR, Kaatano GM, Siza JE, Chang SY, Ko Y, Kullaya CM, et al. Improved perceptions and practices related to schistosomiasis and intestinal worm infections following PHAST intervention on Kome Island, North-Western Tanzania. Korean J Parasitol. 2015;53:561–9. https://doi.org/10.3347/kjp.2015.53.5.561
11. Getabu A, Tumwebaze R, MacLennan DN. Spatial distribution and temporal changes in the fish populations of Lake Victoria. Aquat Living Resour. 2003;16:159–65. https://doi.org/10.1016/S0990-7440(03)00008-1
12. Khalil MI, El-Shahawy IS, Abdelkader HS. Studies on some fish parasites of public health importance in the southern area of Saudi Arabia. Rev Bras Parasitol Vet. 2014;23:435–42. https://doi.org/10.1590/s1984-29612014082

Address for correspondence: Jong-Yil Chai, Department of Tropical Medicine and Parasitology, Seoul National University College of Medicine, Seoul 03080, South Korea; email: cjy@snu.ac.kr

Pseudoterranova decipiens [sü-dō-ʼter-ə-nō-və-a dee-sipʼ-e-inns]

William C. Partin, Richard S. Bradbury

The report of 12 South Korean persons infected with *Pseudoterranova decipiens,* described in a recent issue of Emerging Infectious Diseases, has prompted the editors to revise the errant course charted in 2011 for this genus. By failing to mention the ship *Terra Nova* (Figure 1), a nomenclatural oversight occurred. A compelling but overlooked nautical provenance for the etymology of this genus existed, which prompted Scott Norton of Georgetown University and David Gibson from the Natural History Museum in London, to gently and cleverly advise that "someone literally missed the boat." *Terra Nova* is easily translated as "New Earth," "New Land," or even "Newfoundland." The *Terra Nova,* a whaling ship, was refitted for the British Antarctic Expedition. Under the command of Captain Robert Scott, the *Terra Nova* departed from Wales in 1910. The main purpose of the expedition was to achieve primacy for attaining the South Pole and was akin to discovering new land, perhaps a symbolic affirmation for the name of their sailing vessel. As Scott and others pursued their goal, ship surgeon Edward Leicester Atkinson remained on board, capturing and dissecting marine life. While doing so, he discovered an "unusual nematode" infesting a shark (Figure 2). In 1914, Atkinson, and London School of Tropical Medicine parasitologist Robert Thomson Leiper named this nematode Terranova Antarctica in honor of the RRS Terra Nova.

The genus *Pseudoterranova* was first proposed by Aleksei Mozgovoi in his 1950 unpublished thesis. The genus name was introduced in multiple papers and book chapters in 1951, although which publication has primacy is debated because later researchers differed in their designated attributions. The type species was the former *Porrocecum kogiae* (syn. *Terranova kogiae*), as this helminth, taken from a South Australian pygmy sperm whale (*Kogia bereviceps*), was morphologically distinct from both the genera *Terranova* and *Porrocecum*. The genus Terranova still exists, but is restricted only to parasites of elasmobranch fish.

The species epithet *decipiens* was applied to *Ascaris decipiens* by Krabbe in 1878. The word *decipiens* is a Latin third declension participle. The primary meaning attached to this word is to catch, take, ensnare, or seize with a secondary meaning to cheat, deceive, beguile, or mislead. Although Krabbe did not state his reasons for applying this name, it seems likely to have been in reference the catching or taking of fish by the seal hosts from which he first recovered the worm.

Over the following 105 years, this species was moved between the genera *Porrocecum*, *Terranova*, and *Phocanema*, before finally being placed in the genus *Pseudoterranova* by Gibson in 1983. Molecular interrogation later demonstrated that there is a robust *P. decipiens* species complex, incorporating 5 sibling species, including *P. decipiens sensu stricto.*

The fate of the *Terra Nova* and Captain Scott's expedition was forlorn. After reaching the South Pole, Scott and 4 other explorers, their supplies exhausted, perished while on the return trek to the *Terra Nova*. The doomed party was disappointed to discover

Figure 1. The Terra Nova, 1911 (1937). Captain Robert Falcon Scott's (1868–1912) ship the Terra Nova in the Antarctic on the ill-fated expedition to the South Pole. A print from The Story of Seventy Momentous Years, the Life and Times of King George V, 1865–1936, editor Harold Wheeler, Odhams Press Ltd, London, 1937. The Terra Nova at the ice edge in Antarctica.

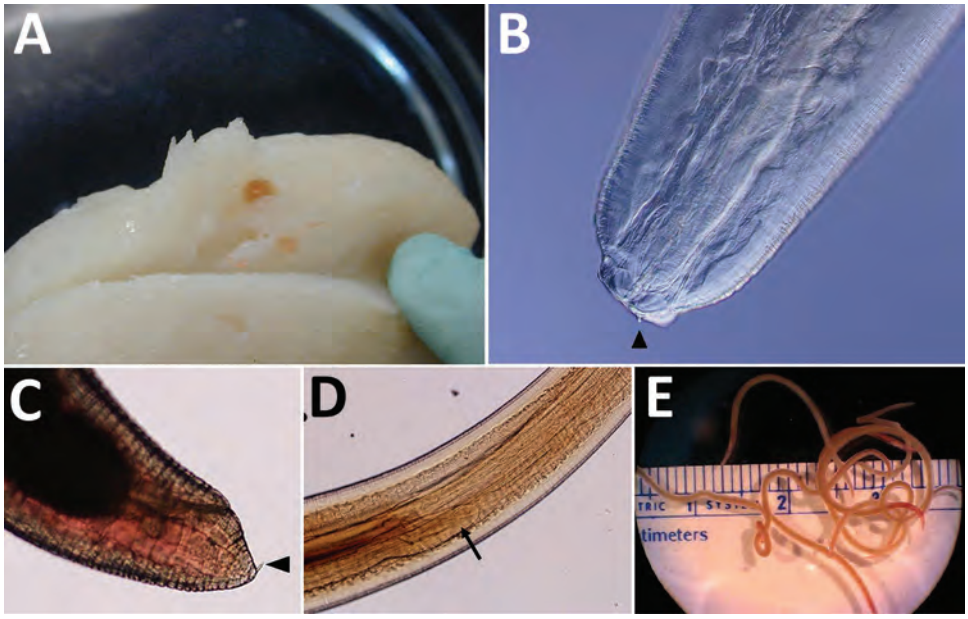

Figure 2. A) A coiled *Pseudoterranova* sp. L3 larva in a fillet of cod. B) View of the anterior (head) end of an aniskaid larvae, possibly Pseudoterranova sp., showing lips and an indistinct boring tooth (arrowhead) viewed by differential interference contrast microscopy. D) Center (cleared with lactophenol) demonstrating the ventriculus and anteriorly directed intestinal cecum (arrowhead). C) posterior with mucron (arrow). E) gross morphology of adult Pseudoterranova sp. L3 larvae. Original magnifications ×100 in panels B, C, and D; ×10 in panel E. Blaine Mathison, Henry Bishop, Division of Parasitic Diseases, Centers for Disease Control and Prevention.

that Roald Amundsen and his group had preceded them to the South Pole by 34 days. The *Terra Nova* continued an active seafaring life in various capacities. In 1943, near the coast of Greenland, while ferrying supplies for the US government, she sank after ramming into ice floes. All aboard were rescued by the USCGC Atak. The Terra Nova was purposefully set afire and then sunk by gunfire to eliminate it as a shipping lane hazard. Exactly a century after Scott's team reached the South Pole, a scientific research vessel in 2012 serendipitously discovered the *Terra Nova* resting on the ocean floor.

Sources

1. Arizono N, Miura T, Yamada M, Tegoshi T, Onishi K. Human infection with *Pseudoterranova azarasi* roundworm. Emerg Infect Dis. 2011;17:555–6. https://doi.org/10.3201/eid1703.101350
2. Gibson DI. The systematics of ascaridoid nematodes: a current assessment. In: Stone AR, Platt HM, Khalil LF, editors. Concepts in nematode systematics. New York: Academic Press. p. 321–38.
3. Leiper RT, Atkinson EL. Helminthes of the British Antarctic expedition 1910–1913. Proc Zool Soc Lond. 1914:222–6 [cited 2022 Sep 9]. https://www.gbif.org/species/2284271.
4. Krabbe H. Seal and toothed whale coilworms [in Danish]. Overview of the Proceedings of the Royal Danish Society of Sciences. 1878; 1:43–51.
5. Männikkö N. Etymologia: *Pseudoterranova azarasi*. Emerg Infect Dis. 2011;17:571. https://doi.org/10.3201/eid1703.ET1703
6. Mattiucci S, Nascetti G. Advances and trends in the molecular systematics of anisakid nematodes, with implications for their evolutionary ecology and host-parasite co-evolutionary processes. Adv Parasitol. 2008;66:47–148. https://doi.org/10.1016/S0065-308X(08)00202-9
7. Norton SA, Gibson DI. Etymologia: *Pseudoterranova azarasi*. Emerg Infect Dis. 2011;17:1784. https://doi.org/10.3201/eid1709.110541
8. Secret War Diary Greenland Patrol. From September 1, 1943 through September, 30, 1943. (p. 4 in document, p. 8 handwritten in PDF file) [cited 2022 Sep 9]. http://www.southpolestation.com/oeas/greenlandpatrolwardiary.pdf
9. Skrjabin KI, Shikhobalova NP, Mozgovoi AA. Suborder Oxyurata and Ascaridata. In: Mozgovoi AA., editor. Key to parasitic nematodes. Volume II. Leiden (The Netherlands): E.G. Brill; 1991. p. 537–42.
10. Song H, Ryoo S, Jung B-K, Cho J, Chang T, Hong S, et al. Molecular diagnosis of *Pseudoterranova decipiens* sensu stricto infections, South Korea, 2002–2020. Emerg Infect Dis. 2022;28:1283–5. https://doi.org/10.3201/eid2806.212483
11. Terra Nova and Scott of the Antarctic. Ocean navigator. January 2, 2021 [cited 2022 Sep 4]. 2021. https://oceannavigator.com/terra-nova-and-scott-of-the-antarctic-2/#:~:text=Terra%20Nova%20went%20back%20to%20the%20Arctic%20carrying,saved.%20The%20wreck%20was%20accidentally%20rediscovered%20in%202012

Author affiliations: Emory University, Atlanta, Georgia, USA (W.C. Partin); Federal University of Australia, Berwick, Victoria, Australia (R.S. Bradbury)

Address for correspondence: William C. Partin, Department of International Medicine, Emory University, 1365 Clifton Rd, NE, Atlanta, GA 30322-1007, USA; email: wpart01@emory.edu

DOI: https://doi.org/10.3201/eid2811.220792

Polyclonal Dissemination of OXA-232 Carbapenemase–Producing *Klebsiella pneumoniae*, France, 2013–2021

Cecile Emeraud, Aurélien Birer, Delphine Girlich, Agnès B. Jousset, Elodie Creton, Thierry Naas, Rémy A. Bonnin, Laurent Dortet

During 2013–2021, increased prevalence of oxacillinase 232–producing Enterobacterales was observed in France, mostly driven by its emergence in *Klebsiella pneumoniae*. Whole-genome sequencing identified that oxacillinase 232–producing *K. pneumoniae* belonged to 14 sequence types (STs), among which 2 polyclonal high-risk clones, ST-231 and ST-2096, were overrepresented.

The massive dissemination of carbapenemase-producing Enterobacterales poses a global threat to public health. Carbapenem antibiotics remain the last line of defense against highly resistant Enterobacterales. Carbapenemases have been identified in 3 of the 4 classes of the Ambler classification: class A carbapenemases (mostly *Klebsiella pneumoniae* carbapenemase types) (*1*), class B carbapenemases or metallo-β-lactamases (mostly New Delhi metallo-β-lactamase [NDM], Verona integron-mediated metallo-β-lactamase [VIM], or imipenemase types) (*2*), and class D carbapenemases (mostly oxacillinases [OXAs] of OXA-48 types) (*3*). In France, the most prevalent carbapenemases are of OXA-48 type (*4*). According to the Beta-Lactamase Database (http://www.bldb.eu), >50 OXA-48–like carbapenemase variants have been identified. OXA-48, OXA-162, OXA-181, OXA-232, OXA-204, and OXA-244 are the most common enzymes identified among these carbapenemases (*4*).

OXA-232 differs from OXA-181 by a single amino acid substitution (Arg214Ser), differing itself from OXA-48 by 4 substitutions (Thr104Ala, Asn110Asp, Glu168Gln, and Ser171Ala). OXA-232 has been demonstrated to possess a weaker hydrolytic activity toward carbapenems but a stronger ability to hydrolyze penicillins compared with OXA-48 and OXA-181 (*5*,*6*). The $bla_{\text{OXA-232}}$ gene usually is located on a 6-kb nonconjugative ColE-type plasmid within a truncated Tn*2013*-like transposon (*5*). Furthermore, the genetic environment surrounding the $bla_{\text{OXA-232}}$ gene is comparable to that of the $bla_{\text{OXA-181}}$ gene, suggesting that OXA-232 is derived directly from OXA-181 (*4*).

Previous research has mainly identified OXA-232 in *Escherichia coli* and *K. pneumoniae* isolates and has found that this variant is endemic in China, India, South Korea, and Thailand (*4*,*7*,*8*). For *K. pneumoniae,* several outbreaks have been reported with different sequence types (STs), including ST-14, ST-15, ST-16, ST-23, ST-231, and ST-437 (*4*,*9*–*11*). Moreover, to the best of our knowledge, there are no data from France regarding OXA-232 outbreaks and epidemiology since the first description of 1 *E. coli* ST-2968 and 2 *K. pneumoniae* ST-14 isolates from patients returning to France from India in 2012 (*5*).

In addition, strains coproducing NDM and OXA-232 have been reported in several countries (*12*–*14*). In these strains, bla_{NDM} and $bla_{\text{OXA-232}}$ are carried by 2 different plasmids (*13*). The $bla_{\text{OXA-232}}$ gene is located on a ColE-type plasmid, whereas the bla_{NDM} gene usually is carried by an incF-type plasmid (*8*).

Given the increasing prevalence of OXA-232–producing Enterobacterales in Europe, it is crucial to better understand the driving forces of such

Author affiliations: Institut National de la Santé et de la Recherche Médicale, University Paris-Saclay, Le Kremlin-Bicêtre, France (C. Emeraud, D. Girlich, A.B. Joussett, T. Naas, R.A. Bonnin, L. Dortet); Microbes, Intestin, Inflammation et Susceptibilité de l'Hôte, Clermont–Ferrand, France (A. Birer); Gabriel–Montpied Hospital, Clermont–Ferrand, France (A. Birer); Bicêtre Hospital, Le Kremlin-Bicêtre (C. Emeraud, A.B. Jousset, T. Naas, L. Dortet); National Reference Center for Antibiotic Resistance, Le Kremlin-Bicêtre (C. Emeraud, A. Birer, A.B. Jousset, E. Creton, T. Naas, R.A. Bonnin, L. Dortet); Gabriel–Montpied Hospital, Clermont–Ferrand, France (A. Birer)

DOI: https://doi.org/10.3201/eid2811.221040

dissemination. In this study, we used whole-genome sequencing to decipher the epidemiology of OXA-232–producing *K. pneumoniae* in France during 2013–2021.

The Study

During 2013–2021, France's National Reference Centre received 122 nonduplicate OXA-232–producing Enterobacterales, including 99 *K. pneumoniae*, 13 *Citrobacter freundii*, 7 *E. coli*, 2 *K. aerogenes,* and 1 *K. oxytoca* (Figure 1, panel A; Appendix Table 1, https://wwwnc.cdc.gov/EID/article/28/11/20-1040-App1.pdf). These clinical isolates were cultured from rectal swabs (n = 92), urine samples (n = 18), blood cultures (n = 2), respiratory tracts samples (n = 1), and other or unknown origins (n = 9) (Appendix Table 1).

Among these strains, 16 coproduced NDM-1 and 9 coproduced NDM-5 (Figure 1, panel A). Overall, the prevalence of OXA-232 among OXA-48–like producers was significantly higher during 2019–2021 (1.33% among OXA-48–like) compared to 2013–2018 (0.70% among OXA-48–like) (χ^2 test, $p<0.05$) (Figure 1, panel A; Table 2). The prevalence of NDM and OXA-232–coproducing isolates also slightly increased (0.15% among NDM and 0.27% among OXA-48–like from 2013–2018 to 2019–2021) (Figure 1, panel A; Appendix Table 2).

We performed short-read next-generation sequencing on all *K. pneumoniae* strains producing OXA-232 during 2015–2021 (n = 95) using a HiSeq system (Illumina, https://www.illumina.com) and submitted them to GenBank (Appendix Table 1). We assembled Illumina reads using shovill 1.1.0 (https://github.com/tseemann/shovill) and SPAdes 3.14.0 (http://bioinf.spbau.ru/spades) multilocus sequence typing programs, and we performed resistome analysis using pubMLST (https://pubmlst.org) and Resfinder (https://cge.cbs.dtu.dk/services/ResFinder). For phylogenetic analysis, we mapped next-generation sequencing reads to the reference genome (K. pneumoniae HS11286 [GenBank accession no. NC_016845.1]) using SNIppy 4.6.0 (https://software.cqls.oregonstate.edu/updates/snippy-4.6.0). We visualized metadata and phylogenetic trees using iTOL 6.5.2 (https://itol.embl.de).

Among the 95 patients colonized or infected with OXA-232–producing *K. pneumoniae*, 19 had recently returned from Asia (including 15 from India) and 12 from the Middle East. Among *K. pneumoniae* isolates, we identified 14 different STs, 5 of which were

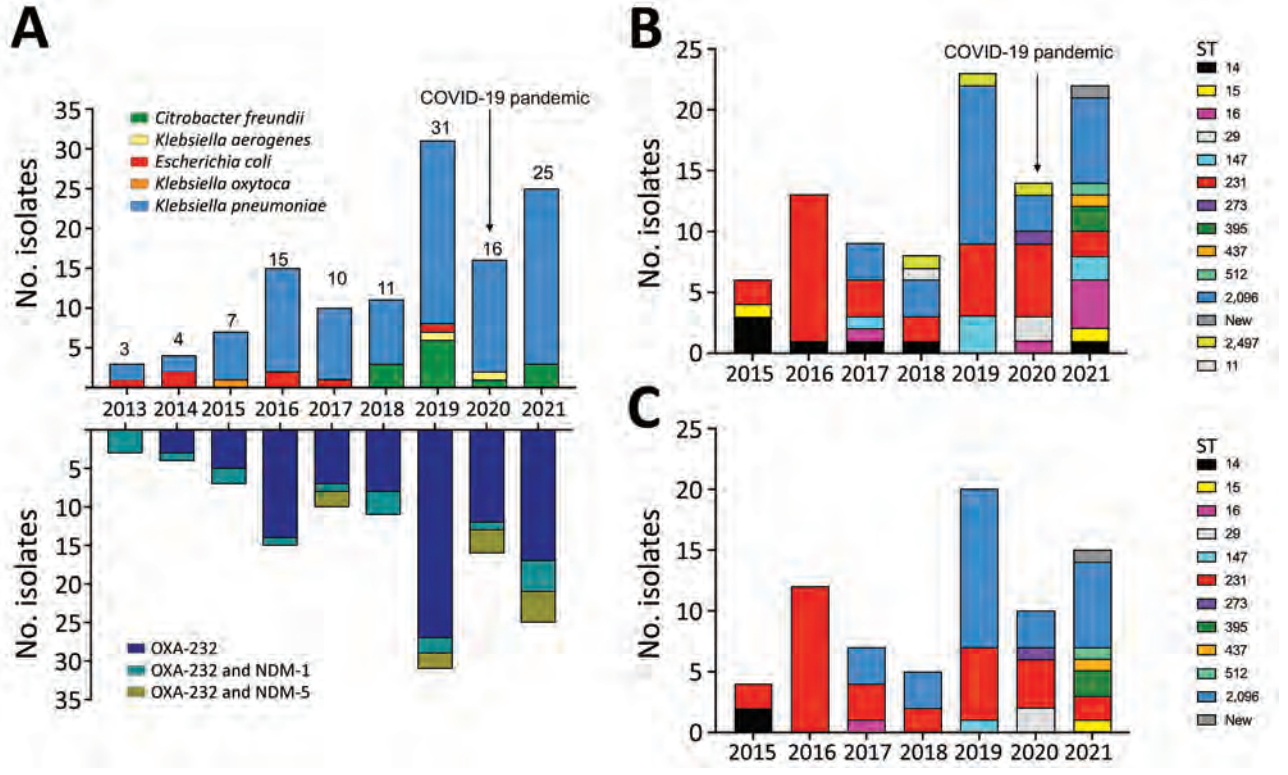

Figure 1. OXA-232–producing Enterobacterales received at the National Reference Center for Carbapenem-Resistant Enterobacterales, France 2013–2021. A) Evolution of several OXA-232–producing Enterobacterales, by species (top of panel) and carbapenemase variant (bottom). B) Evolution of distribution of ST among all OXA-232–producing *K. pneumoniae*. C) Evolution of distribution of ST among NDM and OXA-232–coproducing *K. pneumoniae.* NDM, New Delhi metallo-β-lactamase; OXA, oxacillinase; ST, sequence type.

represented by >5 strains: ST-231 (n = 33), ST-2096 (n = 29), ST-14 (n = 7), ST-16 (n = 6), and ST-147 (n = 6). We observed a diversification in OXA-232–producing *K. pneumoniae* STs over the last 2 years of the study period. In addition, the number of *K. pneumoniae* ST-231 isolates decreased, whereas the number of *K. pneumoniae* ST-2096 isolates increased (Figure 1, panel B). We built single nucleotide polymorphism (SNP) matrices and phylogenetic trees for the 2 main STs (ST-231 and ST-2096) and compared them to epidemiologic data. We considered 2 isolates to be clonally related (probably by cross-transmission) if they differed by <21 SNPs, as previously reported for *K. pneumoniae* clonal complex 258 (*15*). For both STs, we identified many subclones (20 for ST-231 and 21 for ST-2096) (Figure 2), suggesting polyclonal dissemination including within these 2 high-risk clones.

K. pneumoniae coproducing OXA-232 and NDM (NDM-1 or NDM-5) belonged to several STs (ST-14, ST-16, ST-147, ST-231, and ST-2497) but not to ST-2096 (Figure 1, panel C; Figure 2; Appendix Figure). Among the 95 OXA-232–producing *K. pneumoniae*, we identified additional β-lactamases in all strains except 1 (309B8). Eighty-two coproduced Temoniera β-lactamase 1 (32/33 for ST-231 and 25/29 for ST-2096), 86 coproduced the cefotaximase–Munich extended-spectrum β-lactamase 15 (31/33 for ST-231 and 26/29 for ST-2096), and 42 coproduced OXA-1 (0/33 for ST-231 and 25/29 for ST-2096) (Appendix Figure). Furthermore, 3 non–clonally related isolates coproduced the acquired *C. freundii* intrinsic cephalosporinase 6 (ST-231, ST-11, and ST-15) (Appendix Figure). Analysis of the genetic environment revealed that the $bla_{OXA-232}$ was carried by the 6-kb in size ColE-type plasmid as previously described (*5*).

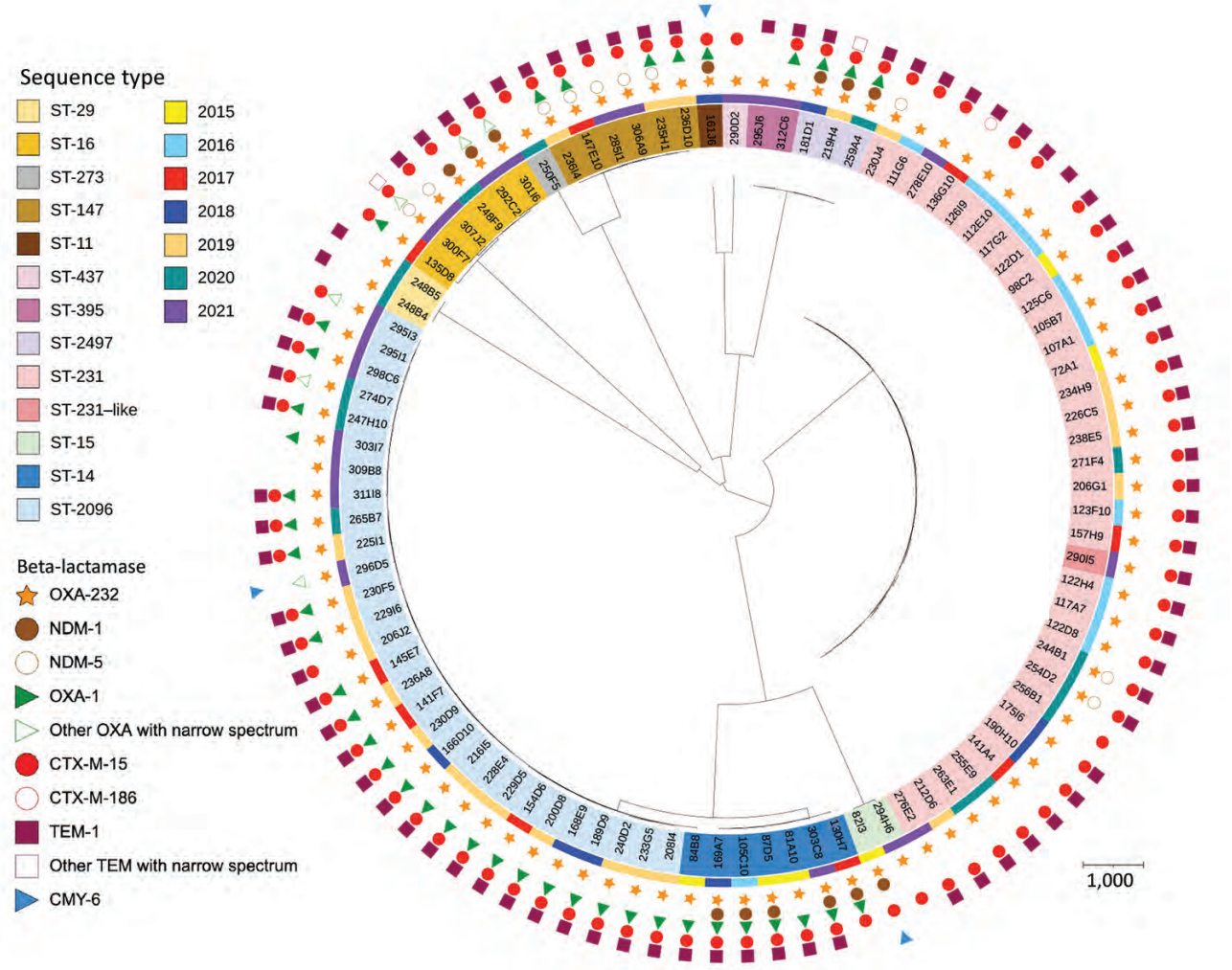

Figure 2. Phylogenetic relationship of OXA-232–producing *K. pneumoniae* ST-231 (A) and ST-2096 (B) analyzed at the National Reference Center for Carbapenem-Resistant Enterobacterales, France 2013–2021.The phylogenetic trees were built with an SNP analysis approach. Scale bars under trees indicate the number of SNPs per position of common sequences. OXA, oxacillinase; SNP, single nucleotide polymorphism; ST, sequence type.

Conclusions

Recent data suggested that the dissemination of OXA-232–producing *K. pneumoniae* is increasing rapidly, especially in Asia and the Middle East (*7*,*11*). In our study, about a third of patients had recently visited 1 of these regions. Furthermore, we observed an increasing number of OXA-232 and NDM coproducers. These isolates are of high concern because of their lack of susceptibility to all antimicrobials, including last-resort combinations such as ceftazidime/avibactam, meropenem/vaborbactam, and imipenem/relebactam.

The OXA-232–producing *K. pneumoniae* isolates that are reported to be responsible for outbreaks usually belonged to ST-231, ST-15, ST-16 and ST-147 (*4*,*9*). In our study, a wide diversity of STs was found, but the 2 main types were ST-231 and ST-2096. ST-231 was widely reported with OXA-232–producing *K. pneumoniae*, but ST-2096 was first reported only recently in India in 2019 (*7*,*9*). ST-2096 in India was also reported to be hypervirulent because it produced characteristic virulence genes such as *rmpA2*, *iutA*, and *iuc* operon (*9*). Our results suggest that the ST-2096 appeared very recently in France (2017). SNPs analysis demonstrated that the emergence and rapid dissemination of ST-2096 OXA-232–producing *K. pneumoniae* is not linked to a single or a few outbreaks. In our collection, 29 of the 30 ST-2096 *K. pneumoniae* isolates produced OXA-232, whereas the remaining isolate did not produce any carbapenemase, suggesting a recent acquisition of $bla_{\text{OXA-232}}$ in this clone.

A recent publication reported an association between ST-2096 and a higher risk for bacteriemia and death (*7*). In our study, the unique isolate responsible for bacteriemia belonged to ST-231. In contrast, 25 of the 29 ST-2096 isolates were cultured from rectal swabs.

As expected, $bla_{\text{OXA-232}}$ was located on a ColE plasmid in all isolates. The close genetic environment of $bla_{\text{OXA-232}}$ involved IS*Ecp1* upstream of the $bla_{\text{OXA-232}}$ gene as previously described (*5*).

About the Author

Dr. Emeraud is an assistant professor at the Institut National de la Santé et de la Recherche Médicale. Her primary research interests include epidemiology, genetics, and biochemistry of β-lactamases in gram-negative bacteria.

References

1. Naas T, Dortet L, Iorga BI. Structural and functional aspects of class a carbapenemases. Curr Drug Targets. 2016;17:1006–28. https://doi.org/10.2174/1389450117666160310144501
2. Mojica MF, Bonomo RA, Fast W. B1-metallo-β-lactamases: where do we stand? Curr Drug Targets. 2016;17:1029–50. https://doi.org/10.2174/1389450116666151001105622
3. Poirel L, Potron A, Nordmann P. OXA-48-like carbapenemases: the phantom menace. J Antimicrob Chemother. 2012;67:1597–606. https://doi.org/10.1093/jac/dks121
4. Pitout JDD, Peirano G, Kock MM, Strydom KA, Matsumura Y. The global ascendency of OXA-48-type carbapenemases. Clin Microbiol Rev. 2019;33:33. https://doi.org/10.1128/CMR.00102-19
5. Potron A, Rondinaud E, Poirel L, Belmonte O, Boyer S, Camiade S, et al. Genetic and biochemical characterisation of OXA-232, a carbapenem-hydrolysing class D β-lactamase from Enterobacteriaceae. Int J Antimicrob Agents. 2013;41:325–9. https://doi.org/10.1016/j.ijantimicag.2012.11.007
6. Oueslati S, Retailleau P, Marchini L, Berthault C, Dortet L, Bonnin RA, et al. Role of arginine 214 in the substrate specificity of OXA-48. Antimicrob Agents Chemother. 2020;64:64. https://doi.org/10.1128/AAC.02329-19
7. Isler B, Özer B, Çınar G, Aslan AT, Vatansever C, Falconer C, et al. Characteristics and outcomes of carbapenemase harbouring carbapenem-resistant *Klebsiella* spp. bloodstream infections: a multicentre prospective cohort study in an OXA-48 endemic setting. Eur J Clin Microbiol Infect Dis. 2022;41:841–7. https://doi.org/10.1007/s10096-022-04425-4
8. Naha S, Sands K, Mukherjee S, Saha B, Dutta S, Basu S. OXA-181-like carbapenemases in *Klebsiella pneumoniae* ST14, ST15, ST23, ST48, and ST231 from septicemic neonates: coexistence with NDM-5, resistome, transmissibility, and genome diversity. MSphere. 2021;6:6. https://doi.org/10.1128/mSphere.01156-20
9. Shankar C, Mathur P, Venkatesan M, Pragasam AK, Anandan S, Khurana S, et al. Rapidly disseminating $bla_{\text{OXA-232}}$ carrying *Klebsiella pneumoniae* belonging to ST231 in India: multiple and varied mobile genetic elements. BMC Microbiol. 2019;19:137. https://doi.org/10.1186/s12866-019-1513-8
10. Weng X, Shi Q, Wang S, Shi Y, Sun D, Yu Y. The characterization of OXA-232 carbapenemase–producing ST437 *Klebsiella pneumoniae* in China. Can J Infect Dis Med Microbiol. 2020;2020:5626503. https://doi.org/10.1155/2020/5626503
11. Zhu Z, Huang H, Xu Y, Wang M, Lv J, Xu L, et al. Emergence and genomics of OXA-232–producing *Klebsiella pneumoniae* in a hospital in Yancheng, China. J Glob Antimicrob Resist. 2021;26:194–8. https://doi.org/10.1016/j.jgar.2021.05.015
12. Avolio M, Vignaroli C, Crapis M, Camporese A. Co-production of NDM-1 and OXA-232 by ST16 *Klebsiella pneumoniae*, Italy, 2016. Future Microbiol. 2017;12:1119–22. https://doi.org/10.2217/fmb-2017-0041
13. Doi Y, Hazen TH, Boitano M, Tsai YC, Clark TA, Korlach J, et al. Whole-genome assembly of *Klebsiella pneumoniae* coproducing NDM-1 and OXA-232 carbapenemases using single-molecule, real-time sequencing. Antimicrob Agents Chemother. 2014;58:5947–53. https://doi.org/10.1128/AAC.03180-14
14. Kesarimangalam Kalyanavenkatramanan S, Sewunet T, Wangchinda W, Tangkoskul T, Thamlikitkul V, Giske CG, et al. Optical DNA mapping of plasmids reveals clonal spread of carbapenem-resistant *Klebsiella pneumoniae* in a large Thai hospital. Antibiotics (Basel). 2021;10:10. https://doi.org/10.3390/antibiotics10091029
15. David S, Reuter S, Harris SR, Glasner C, Feltwell T, Argimon S, et al.; EuSCAPE Working Group; ESGEM Study Group. Epidemic of carbapenem-resistant *Klebsiella pneumoniae* in Europe is driven by nosocomial spread. Nat Microbiol. 2019;4:1919–29. https://doi.org/10.1038/s41564-019-0492-8

Address for correspondence: Laurent Dortet, Service de Bactériologie-Hygiène, Hôpital de Bicêtre, 78 rue du Général Leclerc, 94275 Le Kremlin-Bicêtre Cedex, France; email: laurent.dortet@aphp.fr

Sequence-Based Identification of Metronidazole-Resistant *Clostridioides difficile* Isolates

Wiep Klaas Smits, Céline Harmanus, Ingrid M.J.G. Sanders, Lynn Bry, Grace A. Blackwell, Quinten R. Ducarmon, Eliane de Oliveira Ferreira, Ed J. Kuijper

The plasmid pCD-METRO confers metronidazole resistance in *Clostridioides difficile*. We showed high sequence similarity among pCD-METRO plasmids from different isolates and identified pCD-METRO and associated metronidazole-resistant isolates in clinical and veterinary reservoirs in the Americas. We recommend using PCR or genomic assays to detect pCD-METRO in metronidazole-resistant *C. difficile*.

Clostridioides difficile is a major cause of antibiotic-associated colitis (*1*). Antimicrobial drug–resistant infections are a global economic and healthcare burden (*2*). Resistance is generally low to commonly prescribed antimicrobial drugs used for primary *C. difficile* infections. However, high rates of metronidazole resistance have been observed for *C. difficile* isolates carrying the 7-kb plasmid pCD-METRO, in particular for isolates belonging to PCR ribotype (RT) 010 and RT020 (clade 1) and the epidemic strain RT027 (clade 2) (*3*) (Figure, panel A). This plasmid has been reported in *C. difficile* isolates from countries in Europe.

The Study

Since the discovery of pCD-METRO, we have implemented PCR that uses primers oBH-1 (5′-CCTCGTAGAATCCGGTGCAA-3′) and oBH-2 (5′-TATTTCCTTGCCGCTGAGGT-3′) for national sentinel surveillance and diagnostics of *C. difficile* infections in the Netherlands. The primers are specific for open reading frame (ORF) 6 of pCD-METRO (Figure, panel A). Since 2019, we have tested 3,257 isolates and identified 8 (0.25%) additional pCD-METRO–positive isolates; this percentage is consistent with previous findings (*3*). We have a total of 27 human and animal *C. difficile* isolates in our collection that are pCD-METRO–positive. Most of the isolates (22/27, 81%) belong to nontoxigenic PCR RT010, including isolate 1143 from Brazil. Isolate 1143 is one of 8 canine isolates that showed phenotypic resistance to metronidazole (MIC = 32 mg/L) by Etest on Brucella blood agar (BBA); the Etest was performed at the Universidade Federal do Rio de Janeiro in Brazil. The isolate from Brazil confirmed that pCD-METRO is present in *C. difficile* not only in Europe but also in South America. The 1143 isolate was not characterized further because it belonged to PCR RT010, in which pCD-METRO is most frequently observed. The high number of *C. difficile* RT010 isolates carrying pCD-METRO might be related to genomic background of the isolates (*4*) or sampling bias; a higher prevalence of metronidazole resistance has been observed among RT010 strains (*3*,*5*). Low-frequency horizontal gene transfer is more likely to occur after prolonged co-colonization of nontoxigenic *C. difficile* and pCD-METRO donor bacteria, and acquisition of the plasmid might occur from a source after metronidazole exposure. For example, dogs carry nontoxigenic *C. difficile* frequently and are often treated with metronidazole (*6*). The presence of pCD-METRO in toxigenic isolates might also be underestimated; antimicrobial susceptibility testing is not routinely performed, and plasmid carriage is not assessed, even when metronidazole treatment fails.

Author affiliations: Centre for Microbial Cell Biology, Leiden, the Netherlands (W.K. Smits); Leiden University Medical Center, Leiden, the Netherlands (W.K. Smits, C. Harmanus, I.M.J.G. Sanders, Q.R. Ducarmon, E.J. Kuijper); Brigham & Women's Hospital, Boston, Massachusetts, USA (L. Bry); Harvard Medical School, Boston (L. Bry); European Bioinformatics Institute (EMBL-EBI), Hinxton, UK (G.A. Blackwell); Wellcome Sanger Institute, Hinxton (G.A. Blackwell); Universidade Federal do Rio de Janeiro, Rio de Janeiro, Brazil (E.O. Ferreira); National Institute for Public Health and the Environment, Bilthoven, the Netherlands (E.J. Kuijper)

DOI: https://doi.org/10.3201/eid2811.220615

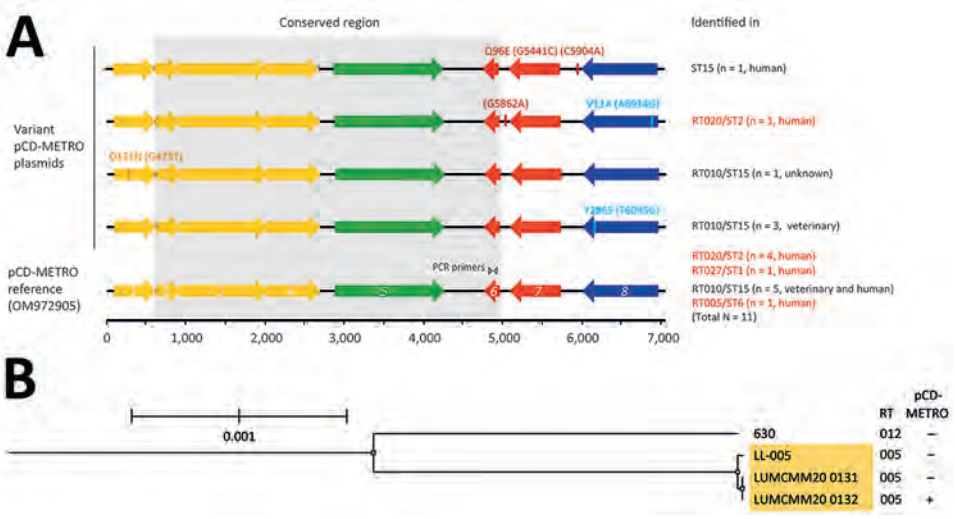

Figure. Comparison of pCD-METRO open reading frames and phylogenetic analysis in study of sequence-based identification of metronidazole-resistant *Clostridioides difficile* isolates. A) Linear maps compare the open reading frames (ORF)1–8 of the pCD-METRO reference sequence (identical to the RT005 plasmid) with variant pCD-METRO sequences, including the ST15 isolate from the United States (top). No ribotyping information was available for the ST15 isolate, but it should be noted that RT010 isolates belong to the same sequence type. Amino acid substitutions and nucleotide substitutions (in parentheses) are indicated above the ORFs. Colors indicate the location of putative mobilization genes (yellow), a replication gene (green), an integrase gene (blue), and genes encoding other functions (red) in the ORFs (*3*). The invariant regions are indicated by gray shading, and the binding location of the oBH1/2 primer set is shown in ORF6. The primer set is used for national sentinel surveillance and diagnostics of *C. difficile* infections in the Netherlands. Toxigenic RT/STs are indicated in red font and were all derived from symptomatic patients with *C. difficile* infections. Where available, the source (human/veterinary) is indicated. Isolate 1143 from Brazil was not included in this figure because no sequence information was available. B) Phylogenetic tree generated using IQ-TREE (*10*) and Roary (*11*) to show the relatedness between 2 RT005 patient isolates (LUMCMM20 0131 and LUMCMM20 0132) compared with the 2 reference strains LL-005 (RT005) and 630 (RT012). The tree is rooted on strain 630, and RT005 isolates are highlighted in yellow. Only the LUMCMM20 0132 isolate was positive for pCD-METRO. Scale bar indicates nucleotide substitutions per site. RT, ribotype; ST, sequence type.

Among *C. difficile* isolates from the Netherlands, we identified a toxigenic pCD-METRO–positive isolate (LUMCMM20 0132, National Center for Biotechnology Information [NCBI] BioSample no. SAMN26573026) from a symptomatic patient with *C. difficile* infection. The isolate belonged to RT005, a ribotype not reported previously to carry pCD-METRO. RT005 accounts for ≈4% of *C. difficile* isolates in Europe (*7*) and shows a similar prevalence in the Netherlands. The patient did not respond to metronidazole treatment, and a metronidazole Etest on BBA, performed at Leiden University Medical Center, confirmed the isolate was metronidazole-resistant (MIC = 8 mg/L). In contrast, a plasmid-negative RT005 isolate obtained earlier from the same patient (LUMCMM20 0131, NCBI BioSample no. SAMN26573027) was metronidazole-susceptible (MIC = 0.125 mg/L), further suggesting acquired resistance after pCD-METRO acquisition. Illumina whole-genome sequencing (NCBI BioProject accession no. PRJNA814863) and analysis of draft genomes using Kbase (*8*) indicated LUMCMM20 0131 and LUMCMM20 0132 were highly homologous, had an average nucleotide identity (ANI) of >99.99%, and were categorized as sequence type 6, clade 1 (*9*). We performed phylogenomic analysis by using IQ-TREE (*10*) and Roary (*11*) to show the 2 patient isolates were distinct from the RT005 reference strain LL005 (ANI 99.91–99.92) and RT012 reference strain 630 (ANI 99.16–99.18) (Figure, panel B). Moreover, we identified only 1 single-nucleotide polymorphism (SNP) when we aligned reads from LUMCMM20 0132 in a reference assembly against the draft LUMCMM20 0131 genome (minimum coverage 10, minimum variant frequency 0.8). We revealed that differences in the 2 patient isolates were driven by pCD-METRO carriage in LUMCMM20 0132 in a pangenome analysis using Kbase (*8*). We identified the pCD-METRO contig in the draft genome by using a homology search, removed terminal repeats, and circularized the sequences by using Geneious R9.1 (https://www.geneious.com). The resulting plasmid sequence was 100% identical to the pCD-METRO reference sequence (GenBank accession no. OM972905) (Figure, Panel A), which likely explains the metronidazole-resistant phenotype.

Because the presence of pCD-METRO is rare, we identified pCD-METRO–positive isolates in public repositories. We queried a curated database of >661,000 assembled bacterial genomes (*12*) by using a compact bit-sliced signature index with a k-mer similarity threshold of 0.4. A total of 465 assemblies were returned, but only 1 *C. difficile* isolate had a close-hit of 0.99 k-mer similarity. The other hits had k-mer similarities of <0.49 and included different species. The *C. difficile* isolate containing

a contig with sequence homology to pCD-METRO was V356 (NCBI BioSample no. SAMN08813897). V356 is a nontoxigenic sequence type 15 isolate cultured from an intensive care unit patient in the United States who was an asymptomatic *C. difficile* carrier; the isolate clustered with other nontoxigenic *C. difficile* genomes (*13*). The isolate was metronidazole-resistant (MIC = 16–24 mg/L) in an Etest on BBA medium (the test was performed at Brigham and Women's Hospital at the time of identification). We assembled the whole-genome sequence of the isolate by using Kbase (*8*) and reconstructed the pCD-METRO plasmid from the draft genome sequence as described above. The plasmid had 2 SNPs compared with the pCD-METRO reference sequence: G5441C, resulting in a Q96E amino acid substitution in the ORF7 hydrolase protein, and C5904A upstream of ORF7 (Figure, panel A); other variants are described elsewhere (*3*). V356 extends the geographic range of pCD-METRO and associated plasmid-mediated metronidazole resistance to North America.

To facilitate homology-based identifications, we deposited a pCD-METRO sequence assembly (GenBank accession no. OM972905) for inclusion in databases of antimicrobial resistance and mobilization determinants, such as the Comprehensive Antibiotic Resistance Database (*14*) and PlasmidFinder (*15*). The deposited file also indicates the sequence variants described in this study.

Conclusions

SNPs in pCD-METRO have been reported in ORF1, the ORF6–ORF7 intergenic region, ORF7, and ORF8, but not in the region that contains ORF2–6; major deletions or rearrangements in this plasmid have not been found. Thus, PCR-based approaches that detect conserved plasmid regions and genomic methods that examine pCD-METRO sequences can be used to identify pCD-METRO–containing *C. difficile* isolates. Of note, all isolates that carried pCD-METRO were confirmed to be metronidazole-resistant (MIC ≥2 mg/L) in susceptibility tests. Whereas the sequences responsible for metronidazole resistance in pCD-METRO have not yet been identified, we show that the presence of pCD-METRO in *C. difficile* predicts metronidazole resistance. We suggest using the invariant ORF2–6 region for PCR-based detection of pCD-METRO.

We found pCD-METRO in a metronidazole-resistant toxigenic RT005 isolate from the Netherlands and also identified pCD-METRO–associated metronidazole resistance in *C. difficile* isolates from North and South America. We recommend using sequence-based molecular approaches to detect pCD-METRO for plasmid-mediated metronidazole-resistant *C. difficile*.

Acknowledgments

We thank S. Nijssen for submitting fecal samples to the National Reference Laboratory for *C. difficile*, M. Delaney and K. Rainha for MIC testing, and members of the Leiden University Medical Center experimental bacteriology research group for useful discussions.

The authors declare that the research was conducted in the absence of any commercial or financial relationships that could be construed as a potential conflict of interest. Genome sequencing and susceptibility testing at Brigham & Women's Hospital was supported by the Hatch Family Foundation and US National Institutes of Health grant nos. R01 AI153605 and P30 DK034854.

The opinions expressed by the authors do not necessarily reflect the opinions of the institutions with which the authors are affiliated.

About the Author

Dr. Smits is an associate professor in medical microbiology at Leiden University Medical Center. His research interests focus on antimicrobial drugs, antimicrobial resistance, and plasmids of *C. difficile*.

References

1. Smits WK, Lyras D, Lacy DB, Wilcox MH, Kuijper EJ. *Clostridium difficile* infection. Nat Rev Dis Primers. 2016;2:16020. https://doi.org/10.1038/nrdp.2016.20
2. Antimicrobial Resistance Collaborators. Global burden of bacterial antimicrobial resistance in 2019: a systematic analysis. Lancet. 2022;399:629–55. https://doi.org/10.1016/S0140-6736(21)02724-0
3. Boekhoud IM, Hornung BVH, Sevilla E, Harmanus C, Bos-Sanders IMJG, Terveer EM, et al. Plasmid-mediated metronidazole resistance in *Clostridioides difficile*. Nat Commun. 2020;11:598. https://doi.org/10.1038/s41467-020-14382-1
4. Boekhoud IM, Sidorov I, Nooij S, Harmanus C, Bos-Sanders IMJG, Viprey V, et al.; COMBACTE-CDI Consortium. Haem is crucial for medium-dependent metronidazole resistance in clinical isolates of *Clostridioides difficile*. J Antimicrob Chemother. 2021;76:1731–40. https://doi.org/10.1093/jac/dkab097
5. Moura I, Spigaglia P, Barbanti F, Mastrantonio P. Analysis of metronidazole susceptibility in different *Clostridium difficile* PCR ribotypes. J Antimicrob Chemother. 2013;68:362–5. https://doi.org/10.1093/jac/dks420
6. Albuquerque C, Pagnossin D, Landsgaard K, Simpson J, Brown D, Irvine J, et al. The duration of antibiotic treatment is associated with carriage of toxigenic and non-toxigenic strains of *Clostridioides difficile* in dogs. PLoS One. 2021;16:e0245949. https://doi.org/10.1371/journal.pone.0245949
7. Freeman J, Vernon J, Pilling S, Morris K, Nicholson S, Shearman S, et al. The ClosER study: results from a three-year pan-European longitudinal surveillance of antibiotic resistance among prevalent *Clostridium difficile* ribotypes, 2011–2014. Clin Microbiol Infect. 2018 24:724–31. https://doi.org/10.1016/j.cmi.2017.10.008

8. Arkin AP, Cottingham RW, Henry CS, Harris NL, Stevens RL, Maslov S, et al. KBase: the United States Department of Energy Systems Biology Knowledgebase. Nat Biotechnol. 2018;36:566–9. https://doi.org/10.1038/nbt.4163
9. Jolley KA, Bray JE, Maiden MCJ. Open-access bacterial population genomics: BIGSdb software, the PubMLST.org website and their applications. Wellcome Open Res. 2018;3:124. https://doi.org/10.12688/wellcomeopenres.14826.1
10. Nguyen LT, Schmidt HA, von Haeseler A, Minh BQ. IQ-TREE: a fast and effective stochastic algorithm for estimating maximum-likelihood phylogenies. Mol Biol Evol. 2015;32:268–74. https://doi.org/10.1093/molbev/msu300
11. Page AJ, Cummins CA, Hunt M, Wong VK, Reuter S, Holden MTG, et al. Roary: rapid large-scale prokaryote pan genome analysis. Bioinformatics. 2015;31:3691–3. https://doi.org/10.1093/bioinformatics/btv421
12. Blackwell GA, Hunt M, Malone KM, Lima L, Horesh G, Alako BTF, et al. Exploring bacterial diversity via a curated and searchable snapshot of archived DNA sequences. PLoS Biol. 2021;19:e3001421. https://doi.org/10.1371/journal.pbio.3001421
13. Worley J, Delaney ML, Cummins CK, DuBois A, Klompas M, Bry L. Genomic determination of relative risks for *Clostridioides difficile* infection from asymptomatic carriage in intensive care unit patients. Clin Infect Dis. 2021;73:e1727–36. https://doi.org/10.1093/cid/ciaa894
14. Alcock BP, Raphenya AR, Lau TTY, Tsang KK, Bouchard M, Edalatmand A, et al. CARD 2020: antibiotic resistome surveillance with the comprehensive antibiotic resistance database. Nucleic Acids Res. 2020;48:D517–25. https://doi.org/10.1093/nar/gkz935
15. Carattoli A, Hasman H. PlasmidFinder and In Silico pMLST: identification and typing of plasmid replicons in whole-genome sequencing (WGS). Methods Mol Biol. 2020;2075:285–94. https://doi.org/10.1007/978-1-4939-9877-7_20

Address for correspondence: Wiep Klaas Smits, Department of Medical Microbiology, Leiden University Medical Center, PO Box 9600, 2300RC, Leiden, the Netherlands; email: w.k.smits@lumc.nl

Cluster of Norovirus Genogroup IX Outbreaks in Long-Term Care Facilities, Utah, USA, 2021

BreAnne Osborn,[1] Chao-Yang Pan,[1] April Hatada, Jennifer Hatfield, Jenni Wagner, Kelly Oakeson, Anna Montmayeur, Christina Morales, Jan Vinjé

We report 5 clustered acute gastroenteritis outbreaks in long-term care facilities in Utah, USA, that were linked to healthcare employees working at multiple facilities. Four outbreaks were caused by norovirus genotype GIX. We recommend continued norovirus surveillance and genotyping to determine contributions of this genotype to norovirus outbreaks.

Norovirus is the leading cause of acute gastroenteritis worldwide (*1*). The virus can be transmitted through person-to-person contact, aerosolized vomitus, contaminated food or water, or fomites (*2*). Noroviruses are divided into 10 genogroups; viruses in genogroups GI, GII, GIV, GVIII, and GIX cause illness in humans. Norovirus GIX was first identified in fecal samples collected in 1990 from US troops deployed to Saudi Arabia (*3*). This genogroup was previously known as GII.15 and was reclassified recently (*4*).

Although global norovirus surveillance is limited, several studies have attempted to quantify the prevalence of norovirus genotypes. In the United States, >99% of all norovirus outbreaks are caused by GI and GII viruses (*5*); most outbreaks are associated with GII.4 Sydney (*4*). Globally, norovirus GIX has been detected less frequently and has not been associated historically with large outbreaks (*5*–*10*). During 2009–2016, two norovirus GIX outbreaks were reported to CaliciNet, the US norovirus surveillance network (*5*,*10*). Similarly, during 2016–2018, only 1 of 556 norovirus outbreaks reported to China's norovirus outbreak surveillance network was associated with norovirus GIX (*6*). We describe a cluster of 4 epidemiologically linked norovirus GIX outbreaks and 1 suspected GIX outbreak among long-term care facilities (LTCFs) in Utah during 2021.

The Study

On March 31, 2021, the Utah County Health Department and Utah Department of Health were notified of an outbreak of gastrointestinal illness at LTCF A. The outbreak was believed to have originated from 2 residents on March 28 and 29. One resident vomited in a well-trafficked, carpeted hallway, which likely contaminated the environment. By mid-April, 4 other LTCFs (B–E) within 20 miles of facility A reported similar outbreaks.

We asked LTCFs to provide data on resident and staff illnesses and a list of residents who were receiving services from home healthcare companies. We conducted interviews with home healthcare employees in September 2021 to identify symptoms of gastrointestinal illness, which residents were cared for by those employees, and which facilities they worked in.

We collected fecal samples from symptomatic residents and staff at facilities A–D during active illness; no samples were collected from facility E. After etiology was confirmed as norovirus by the Utah Public Health Laboratory, we forwarded all samples to the California Department of Public Health Viral and Rickettsial Disease Laboratory, which serves as a CaliciNet outbreak support center for genotyping and next-generation sequencing.

We extracted nucleic acids from fecal specimens using the NucliSENS easyMAG instrument (bioMérieux, https://www.biomerieux.com) and genotyped norovirus-positive samples by using conventional reverse transcription PCR (*11*). We submitted purified PCR products to Sequetech (https://www.sequetech.com) for Sanger sequencing and genotyped by using

Author affiliations: Utah Department of Health, Salt Lake City, Utah, USA (B. Osborn, J. Wagner, K. Oakeson); California Department of Public Health, Richmond, California, USA (C.-Y. Pan, A. Hatada, C. Morales); Utah County Health Department, Provo, Utah, USA (J. Hatfield); Centers for Disease Control and Prevention, Atlanta, Georgia, USA (A. Montmayeur, J. Vinjé)

DOI: https://doi.org/10.3201/eid2811.220842

[1]These first authors contributed equally to this article.

the human calicivirus typing tool (https://calicivirustypingtool.cdc.gov) (*12*). We further analyzed norovirus-positive samples by performing next-generation sequencing (NGS) of complete genomes (*13*) using the Illumina MiSeq platform (Illumina, https://www.illumina.com) and a GIX-specific forward oligonucleotide primer (5′-ATGGCGTCGARTGACGTCGYTACTGCCYTTGGC-3′). We analyzed sequences by using the Viral NGS Analysis Pipeline and Data Management tool (*14*). We generated norovirus phylogenetic trees for complete RNA-dependent RNA polymerase (*RdRp*) (1,430 nt) and major capsid (1,668 nt) genes by using MEGA11 software (*15*).

Among the 5 LTCFs, 290 persons reported gastrointestinal symptoms: 39/74 (53%) residents and 43 (of an unknown total) staff in facility A, 47/68 (69%) residents and 30/66 (45%) staff in facility B, 32/58 (55%) residents and 20/75 (27%) staff in facility C, 37/97 (38%) residents and 29/85 (34%) staff in facility D, and 5/100 (5%) residents and 8/85 (10%) staff in facility E (Figure 1). In addition, 5/10 (50%) home healthcare employees reported they were ill; 2 employees worked in facilities A and B, 1 worked in facilities A and C, and 2 worked in facilities A and D.

A total of 14 fecal samples were collected: 6 samples from residents in facility A, 2 samples each from residents in facilities B and C, 3 samples from residents in facility D, and 1 sample from a home healthcare employee who worked in facilities A and B. Of those samples, 13 (93%) tested positive for norovirus; 1 sample from facility D was negative. Although the home healthcare employee's sample was norovirus-positive, the virus could not be genotyped.

We obtained partial sequences of *RdRp* and capsid genes from 12 of 13 positive specimens by using dual region reverse transcription PCR, genotyped the virus as norovirus GIX.1[GII.P15], and uploaded the sequence data into the CaliciNet database. All 12 partial *RdRp* or capsid sequences showed 100% nucleotide identity. NGS produced near-complete genomes (≈7,490 nt) for all 12 specimens, which were 99.9%–100% identical. The closest matching sequence in GenBank (accession no. MN227777) had a 98% nucleotide identity. By using phylogenetic comparisons of complete *RdRp* and capsid nucleotide sequences (Figure 2), we determined the 12 sequences from facilities A–D were closely related to LTCF outbreaks in California in 2021 (GenBank accession nos. OK247589 and OK247590). We submitted the near-complete genomic sequences for the 12 specimens from Utah to the National Center for Biotechnology Information (accession nos. OL685293–304).

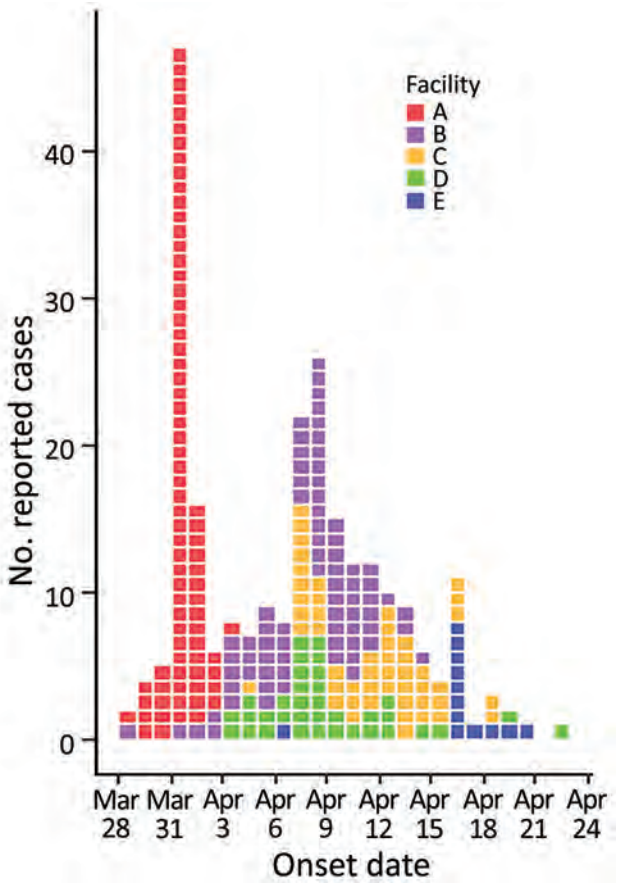

Figure 1. Onset dates for reported cases of acute gastroenteritis among 5 long-term care facilities during March 28–April 24, 2021, in study of cluster of norovirus genogroup IX outbreaks in long-term care facilities, Utah, USA, 2021. Of 290 total reported cases of acute gastroenteritis, we were able to obtain onset dates for 247 cases. Each colored box represents 1 case of acute gastroenteritis.

We determined that the same home healthcare company provided services to residents in 4 of the outbreak facilities (A–D). A norovirus-positive fecal sample was collected from a resident of facility A who received care from home healthcare employees who also reported they had acute gastroenteritis symptoms. Home healthcare services were received by 2 other residents of facility A who became ill. In addition, the earliest onsets of illness were observed in residents of facilities B and C who received care from the same home healthcare company. Facility E reported some of their residents had received services from the same home healthcare company, but not enough information was available to establish a definitive epidemiologic link. All but 1 home healthcare employee who reported illness worked in a facility that experienced an outbreak.

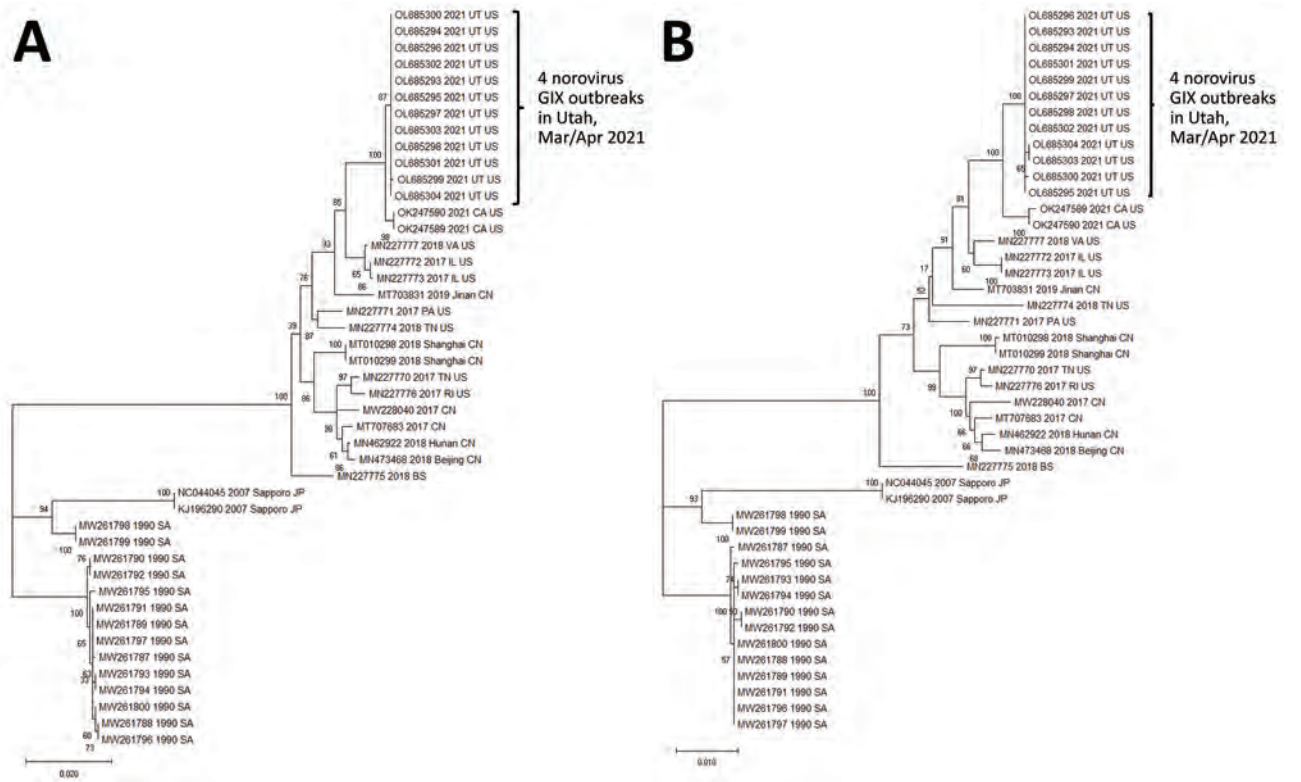

Figure 2. Phylogenetic comparisons of norovirus genes in study of cluster of norovirus genogroup IX outbreaks in long-term care facilities, Utah, USA, 2021. We generated phylogenetic trees by using the maximum-likelihood method and Tamura-Nei distance model (*15*). We compared nucleotide sequences of the *RdRp* gene (1,430 nt) (A) and major capsid gene (1,668 nt) (B) from the 12 sequences obtained from the 4 LTCF outbreaks with 33 GIX strains obtained from GenBank. The bootstrap percentages are shown next to the branches. We generated initial trees automatically by applying neighbor-joining algorithms to a matrix of pairwise distances estimated by using the maximum composite-likelihood approach and then selecting the topology with the superior log-likelihood value. We conducted evolutionary analyses by using MEGA11 software (*15*). Scale bars indicate nucleotide substitutions per site.

Conclusions

We report the relatively rare norovirus GIX as the cause of 4 LTCF outbreaks in Utah during March–April 2021. Epidemiologic evidence and sequencing of norovirus genomes suggested the outbreaks in facilities A–D were related, likely transmitted through employees of a home healthcare company. Although available laboratory and epidemiologic data do not definitively connect the outbreak in facility E with outbreaks in facilities A–D, we suspect a connection exists because of similarities in temporal, geographic, symptom, and setting characteristics of the outbreaks.

Our investigation highlights the ability of norovirus to spread rapidly despite increased disease prevention measures established during the COVID-19 pandemic. Whereas some pandemic restrictions were beginning to ease in the spring of 2021, LTCFs in Utah maintained precautions, including enhanced cleaning protocols. In addition, the home healthcare company that provided services to the facilities in our investigation reported limiting the number of facilities where each employee worked to prevent COVID-19 transmission between facilities. Our results show that these precautions were insufficient to prevent transmission of norovirus GIX and emphasize the overall challenges of controlling norovirus outbreaks.

In addition to these outbreaks in Utah, norovirus GIX was reported as the cause of 7 acute gastroenteritis outbreaks in other states during September 1, 2020–September 30, 2021 (https://www.cdc.gov/norovirus/reporting/calicinet/data.html). These numbers represent a substantial increase in reported GIX outbreaks in the United States, considering only 2 were reported during 2009–2016 (*5*,*10*). We recommend continued norovirus surveillance and genotyping to determine contributions of the uncommon GIX genotype to increasing norovirus outbreaks.

Acknowledgments

We thank Leslie Barclay and Hannah Browne for extracting data from CaliciNet; Blanca Molinar, Chelsea Wright, Alice Chen, and Tasha Padilla for their laboratory sup-

port; Preeti Chhabra for assistance with the phylogenetic trees; and the Healthcare Associated Infections program at the Utah Department of Health for providing infection prevention support to the outbreak facilities.

The findings and conclusions in this report are those of the authors and do not necessarily represent the official position of the Centers for Disease Control and Prevention or the views or opinions of the California Department of Public Health, California Health and Human Services Agency, or Utah Department of Health.

About the Author

Ms. Osborn is an epidemiologist at the Utah Department of Health, Salt Lake City, UT. She works primarily on enteric disease surveillance and outbreak investigation.

References

1. Ahmed SM, Hall AJ, Robinson AE, Verhoef L, Premkumar P, Parashar UD, et al. Global prevalence of norovirus in cases of gastroenteritis: a systematic review and meta-analysis. Lancet Infect Dis. 2014;14:725–30. https://doi.org/10.1016/S1473-3099(14)70767-4
2. Wikswo ME, Kambhampati A, Shioda K, Walsh KA, Bowen A, Hall AJ; Centers for Disease Control and Prevention (CDC). Outbreaks of acute gastroenteritis transmitted by person-to-person contact, environmental contamination, and unknown modes of transmission—United States, 2009–2013. MMWR Surveill Summ. 2015;64:1–16. https://doi.org/10.15585/mmwr.ss6412a1
3. Tohma K, Lepore CJ, Martinez M, Degiuseppe JI, Khamrin P, Saito M, et al. Genome-wide analyses of human noroviruses provide insights on evolutionary dynamics and evidence of coexisting viral populations evolving under recombination constraints. PLoS Pathog. 2021;17:e1009744. https://doi.org/10.1371/journal.ppat.1009744
4. Chhabra P, de Graaf M, Parra GI, Chan MC, Green K, Martella V, et al. Updated classification of norovirus genogroups and genotypes. J Gen Virol. 2019;100:1393–406. https://doi.org/10.1099/jgv.0.001318
5. Cannon JL, Barclay L, Collins NR, Wikswo ME, Castro CJ, Magaña LC, et al. Genetic and epidemiologic trends of norovirus outbreaks in the United States from 2013 to 2016 demonstrated emergence of novel GII.4 recombinant viruses. J Clin Microbiol. 2017;55:2208–21. https://doi.org/10.1128/JCM.00455-17
6. Jin M, Wu S, Kong X, Xie H, Fu J, He Y, et al. Norovirus outbreak surveillance, China, 2016–2018. Emerg Infect Dis. 2020;26:437–45. https://doi.org/10.3201/eid2603.191183
7. Kabue JP, Meader E, Hunter PR, Potgieter N. Genetic characterisation of *Norovirus* strains in outpatient children from rural communities of Vhembe district/South Africa, 2014–2015. J Clin Virol. 2017;94:100–6. https://doi.org/10.1016/j.jcv.2017.07.005
8. Sarmento SK, de Andrade JDSR, Miagostovich MP, Fumian TM. Virological and epidemiological features of norovirus infections in Brazil, 2017–2018. Viruses. 2021;13:1724. https://doi.org/10.3390/v13091724
9. Supadej K, Khamrin P, Kumthip K, Kochjan P, Yodmeeklin A, Ushijima H, et al. Wide variety of recombinant strains of norovirus GII in pediatric patients hospitalized with acute gastroenteritis in Thailand during 2005 to 2015. Infect Genet Evol. 2017;52:44–51. https://doi.org/10.1016/j.meegid.2017.04.025
10. Vega E, Barclay L, Gregoricus N, Shirley SH, Lee D, Vinjé J. Genotypic and epidemiologic trends of norovirus outbreaks in the United States, 2009 to 2013. J Clin Microbiol. 2014;52:147–55. https://doi.org/10.1128/JCM.02680-13
11. Chhabra P, Browne H, Huynh T, Diez-Valcarce M, Barclay L, Kosek MN, et al. Single-step RT-PCR assay for dual genotyping of GI and GII norovirus strains. J Clin Virol. 2021;134:104689. https://doi.org/10.1016/j.jcv.2020.104689
12. Tatusov RL, Chhabra P, Diez-Valcarce M, Barclay L, Cannon JL, Vinjé J. Human calicivirus typing tool: a web-based tool for genotyping human norovirus and sapovirus sequences. J Clin Virol. 2021;134:104718. https://doi.org/10.1016/j.jcv.2020.104718
13. Parra GI, Squires RB, Karangwa CK, Johnson JA, Lepore CJ, Sosnovtsev SV, et al. Static and evolving norovirus genotypes: implications for epidemiology and immunity. PLoS Pathog. 2017;13:e1006136. https://doi.org/10.1371/journal.ppat.1006136
14. Wagner DD, Marine RL, Ramos E, Ng TFF, Castro CJ, Okomo-Adhiambo M, et al. VPipe: an automated bioinformatics platform for assembly and management of viral next-generation sequencing data. Microbiol Spectr. 2022;10:e0256421. https://doi.org/10.1128/spectrum.02564-21
15. Tamura K, Stecher G, Kumar S. MEGA11: molecular evolutionary genetics analysis version 11. Mol Biol Evol. 2021;38:3022–7. https://doi.org/10.1093/molbev/msab120

Address for correspondence: BreAnne Osborn, Utah Department of Health, 288 N 1460 W, Salt Lake City, UT 84116, USA; email: breanneosborn@utah.gov

Seroincidence of Enteric Fever, Juba, South Sudan

Kristen Aiemjoy, John Rumunu, Juma John Hassen, Kirsten E. Wiens, Denise Garrett, Polina Kamenskaya, Jason B. Harris, Andrew S. Azman, Peter Teunis, Jessica C. Seidman, Joseph F. Wamala, Jason R. Andrews, Richelle C. Charles

We applied a new serosurveillance tool to estimate typhoidal *Salmonella* burden using samples collected during 2020 from a population in Juba, South Sudan. By using dried blood spot testing, we found an enteric fever seroincidence rate of 30/100 person-years and cumulative incidence of 74% over a 4-year period.

Enteric fever, caused by *Salmonella enterica* serovars Typhi and Paratyphi, causes substantial illness and death globally (*1*). However, estimating the population-level burden of infection is challenging. Blood culture, the standard for both diagnosis and surveillance, requires microbiological laboratory facilities that are not available in many low- and-middle-income countries. Challenges in accessing blood culture, along with an estimated diagnostics sensitivity of only 60% (*2*), contribute to chronic underdetection (*3*).

Juba, the capital of South Sudan, experiences a high burden of enteric infections such as cholera and hepatitis E virus (*4*,*5*). Enteric fever is a frequently diagnosed etiology of acute fever, but few laboratories have blood culture capacity for confirmation. Consequentially, the population-level burden of enteric fever is unknown.

Hemolysin E (HlyE), a pore-forming toxin, is a sensitive and specific serologic marker for diagnosing typhoidal *Salmonella* (*6*–*10*) and is not associated with typhoid carriage (*11*). New serologic and analytic tools enable measurement of population-level enteric fever incidence from cross-sectional serosurveys using HlyE IgG and IgA (*12*). We applied those tools to generate population-level enteric fever seroincidence estimates in Juba.

Author affiliations: University of California Davis School of Medicine, Davis, California, USA (K. Aiemjoy); Republic of South Sudan Ministry of Health, Juba, South Sudan (J. Rumunu); World Health Organization, Juba (J.J. Hassen, J.F. Wamala); Johns Hopkins Bloomberg School of Public Health, Baltimore, Maryland, USA (K.E. Wiens, A.S. Azman); Sabin Vaccine Institute, Washington, DC, USA (D. Garrett, J.C. Seidman); Massachusetts General Hospital, Boston, Massachusetts, USA (P. Kamenskaya, J.B. Harris, R.C. Charles); Emory University, Atlanta, Georgia, USA (P. Teunis); Stanford University School of Medicine, Stanford, California, USA (J.R. Andrews)

DOI: http://doi.org/10.3201/eid2811.220239

The Study

We used dried blood spots (DBS) collected for a SARS-CoV-2 serosurvey in Juba, South Sudan, enrolled during August 7–September 20, 2020; enrollment and sampling methods are described elsewhere (*13*). In brief, 2-stage cluster sampling was used to randomly select households from predefined enumeration units from 6 administrative divisions within and surrounding Juba; all persons ≥1 year of age and residing for ≥1 week within the sampled household were eligible to participate. Capillary blood was collected onto Whatman 903 Protein Saver cards (Sigma-Aldrich, https://www.sigmaaldrich.com), air dried, and transported at ambient temperature to Massachusetts General Hospital (Boston, MA, USA), where they were stored at 4°C. We tested all banked samples collected from participants <25 years of age and a random sample of participants ≥25 years of age. Younger participants were prioritized because they matched the age distribution of typhoid case data used for the seroincidence estimation (*12*). The study protocol was approved by ethical review boards with the South Sudan Ministry of Health and Massachusetts General Hospital.

We used kinetic ELISAs to quantify HlyE IgA and IgG levels in eluted DBS as described (*7*,*11*). To estimate seroincidence, we used the antibody dynamics from a longitudinal cohort of 1,420 blood culture–confirmed enteric fever cases (*12*). In brief, we created a likelihood function for observed cross-sectional population antibody response data based on antibody dynamics after blood-culture confirmed infection. We generated joint incidence estimates by

combining the likelihood for HlyE IgA and IgG for each age stratum using age-specific antibody dynamics. We selected age strata to match incidence estimates from blood culture enteric fever surveillance studies in other countries in sub-Saharan Africa and South Asia (*14*,*15*). This method incorporates heterogeneity in antibody responses and explicitly accounts for measurement error and biologic noise (*12*; Appendix reference *16*).

We used 3 US populations to define the distribution of biologic noise (nonspecific antibody binding): 48 children 1–5 years of age who had relatives with celiac disease, enrolled nationwide; 31 healthy controls, children and young adults 2–18 years of age, enrolled at Massachusetts General Hospital (Appendix reference *17*); and a population-based sample of 205 children and adults 3–50 years of age from a SARS-CoV-2 serosurvey in northern California, USA. We used the same method to generate individual-level incidence estimates of HlyE IgA and IgG responses and used the exponential probability distribution to calculate 2- and 4-year cumulative incidence. We then fit age-dependent curves by using generalized additive models (Appendix reference *18*) with a cubic spline for age and simultaneous 95% CIs using a parametric bootstrap of the variance-covariance matrix of the fitted model parameters (Appendix reference *19*).

Table 1. Demographic characteristics of participants in study of seroincidence of enteric fever, Juba, South Sudan, 2020*

Characteristic	Value, N = 1,290
Sex	
F	819 (63.5)
M	471 (36.5)
Age, y, median (IQR)	17 (10–24)
Age category, in years	
1–3	41 (3.2)
4–6	118 (9.1)
7–9	134 (10.4)
10–14	259 (20.1)
15–24	423 (32.8)
25–34	167 (12.9)
35–44	62 (4.8)
≥45	86 (6.7)

*Values are no. (%) except as indicated. IQR, interquartile range.

A total of 2,214 persons were enrolled and provided blood samples for the original study; 1,840 had complete interview data, and 1,290 were randomly selected for testing (*13*). The median age of tested participants was 17 (interquartile range [IQR] 10–24) years; 63.5% (819/1,290) were female (Table 1).

We found that median HlyE IgG (10.4, IQR 6.1–12.7) and IgA (3.5, IQR 2.3–5.2) responses were elevated well above a North America pediatric control

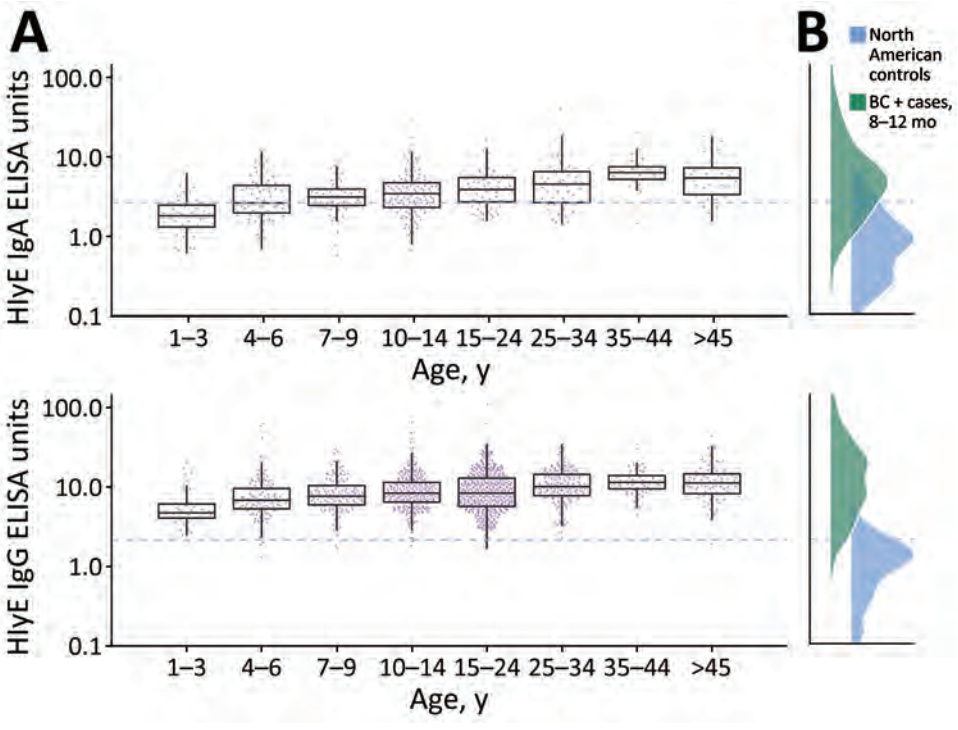

Figure 1. Age-dependent hemolysin E (HlyE) IgA (top) and IgG (bottom) responses for participants in study of seroincidence of enteric fever, Juba, South Sudan, 2020, compared with those for blood culture-confirmed cases and controls. A) Cross-sectional antibody responses to HlyE IgA (top) and IgG (bottom) by age measured from a serosurvey of 1,290 persons in Juba, South Sudan, from samples during collected during August 7–September 2, 2020. Each point indicates an individual sample. Horizontal lines within boxes indicate medians; box tops and bottoms indicate IQRs; error bars indicate 95% CIs. B) Density of antibody responses HlyE IgA (top) and IgG (bottom) among 1,410 blood-culture confirmed enteric fever cases in Bangladesh, Nepal, Pakistan, and Ghana 8–12 months after symptom onset as reported in (*12*) and a control population from 3 United States groups: 48 children 1–5 years of age who had first degree relatives with celiac disease, enrolled nationally; 31 healthy controls, children and young adults 2–18 years of age, enrolled at Massachusetts General Hospital (*17*); and a population-based sample of 205 children and adults 3–50 years of age participating in a SARS-CoV serosurvey in California, USA. The dashed blue line across all panels represents the mean ±3 SD of HlyE IgA and IgG values observed in the pediatric control population. HlyE, hemolysin E.

Table 2. Age-dependent incidence rates and cumulative incidence for participants in study of seroincidence of enteric fever, Juba, South Sudan, 2020*

Age group, y	Seroincidence, cases/100 person-years (95% CI)	2-year cumulative incidence, % (IQR)	4-year cumulative incidence, % (IQR)
1–3	42.5 (38.0–59.0)	53.6 (44.5–74.9)	78.5 (69.2–93.7)
4–6	32.1 (29.7–40.1)	56.6 (34.7–68.5)	81.2 (57.4–90.0)
7–9	29.2 (27.3–35.6)	49.3 (39.9–59.1)	74.3 (63.8–83.3)
10–14	24.8 (23.6–28.8)	45.1 (30.9–58.4)	69.9 (52.2–82.7)
15–24	28.3 (24.7–41.9)	42.8 (27.2–61.6)	67.3 (47.0–85.3)
25–34	28.8 (26.7–35.9)	51.7 (35.7–66.5)	76.7 (58.6–88.8)
35–44	40.8 (36.0–58.5)	57.5 (49.8–69.5)	82.0 (74.8–90.7)
>45	34.0 (30.6–46.2)	53.0 (40.9–69.1)	77.9 (65.1–90.5)
Overall	29.8 (27.6–32.2)	48.9 (31.9–64.3)	73.8 (53.7–87.3)

*IQR, interquartile range.

population (IgG 0.16, IQR 0.07–0.35; IgA 0.3, IQR 0.001–0.92) and were comparable to responses observed among blood-culture confirmed enteric fever cases 8–12 months after symptom onset (IgG 12, IQR 5.9–24; IgA 4.4, IQR 2.2–9.4) (*12*) (Figure 1). Age-specific enteric fever incidence estimates per 100 person-years ranged from 24.8 (95% CI 23.6–28.8) among children 10–14 years of age to 42.5 (95% CI 38.0–59.0) among children 1–3 years of age (Table 2; Figure 2). The

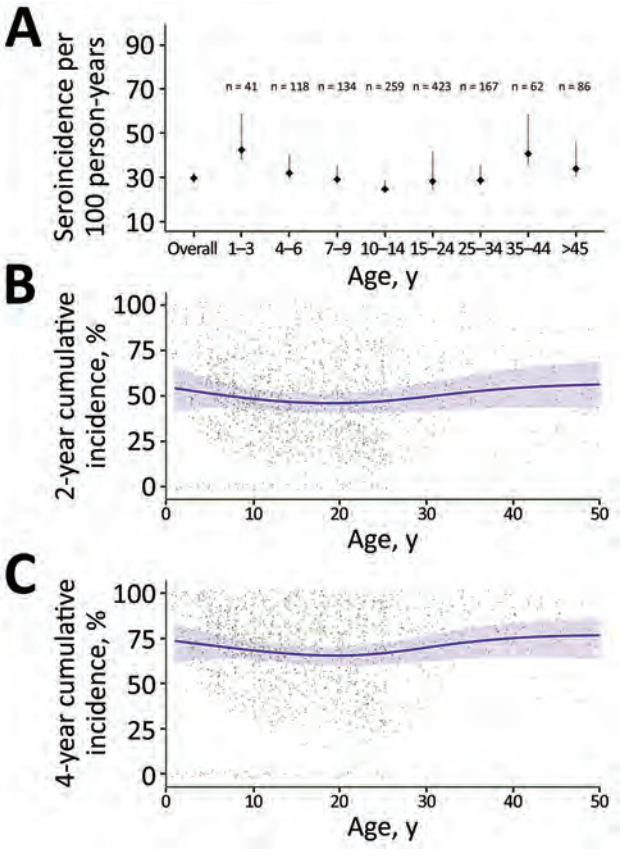

Figure 2. Estimated seroincidence of typhoidal *Salmonella* by age, Juba, South Sudan, 2020. A) Seroincidence per age group. Error bars indicate 95% CIs. B, C) Individually predicted incidence estimates (points) and smoothed cumulative incidence (lines) over 2-year (B) and 4-year (C) periods, by age. Gray shading indicates 95% CIs.

overall incidence rate was 29.8 (95% CI 27.6–32.2); cumulative incidence was 48.9% (IQR 31.9–64.3) over 2 years and 73.8% (IQR 53.7–87.3) over 4 years. Using a cutoff derived from a North America pediatric control population, we found 98.8% (1,275/1,290) of the population seropositive using HlyE IgG and 65.2% (318/488) positive using HlyE IgA (Appendix, https://wwwnc.cdc.gov/EID/article/28/11/22-0239-App1.pdf).

Conclusions

Using banked DBS collected for a SARS-CoV-2 serosurvey, we applied a new serosurveillance tool to rapidly estimate the burden of enteric fever in a region with no blood culture surveillance. We estimated an incidence rate of 30.0 infections/100 person-years and found ≥70% of the sampled population was infected in the previous 4 years.

Whereas no clinical enteric fever incidence estimates from South Sudan are available for comparison, the seroincidence rate we estimated is substantially higher than clinical incidence estimates in the region (*15*; Appendix reference *20*). A high incidence of clinical enteric fever has been previously defined as >100 cases/100,000 person-years (Appendix reference *21*); we estimated a seroincidence of 35,000 cases/100,000 person-years. We expect seroincidence to be higher than clinical incidence because it captures subclinical infections and is independent of a person's ability to access and afford healthcare, including diagnostic tests. Indeed, the enteric fever seroincidence rate for Juba is on the same scale of magnitude as recent estimates using the same approach in Nepal, Pakistan, Bangladesh, and Ghana (*12*).

The analytic approach is an improvement over cutoff-based methods because we can combine information from HlyE IgA and IgG responses to generate a consensus incidence estimate, accounting for heterogeneity in antibody responses, measurement error, and biologic noise. Whereas the cutoff-based method yielded a seroprevalence of nearly 100% for HlyE IgG, we generated cumulative

incidence estimates over a precise time window and could identify populations with recent and later infections.

Limitations of this study include that only 1,840 samples of 2,214 enrolled study participants had linked age data. Second, persons in internally displaced camps were not included in the serosurvey. Displaced persons have been identified as high-risk populations for enteric infections, so it would be valuable to include them in future studies to determine if this population is at higher or equivalent risk (*4*). Finally, we used longitudinal antibody kinetics estimates from enteric fever cases in Bangladesh, Pakistan, Nepal, and Ghana. We did not observe major differences in the kinetics of antibody responses across countries (*12*), but the decay rate among enteric fever cases in Juba may be different because of the high force of infection and differences in exposure to other infections.

Our results suggest a high burden of enteric fever in Juba, South Sudan, warranting urgent public health and research attention. The seroincidence tool we used can be applied to other regions lacking blood culture surveillance to generate rapid enteric fever seroincidence estimates, providing the high-resolution data critically needed to inform typhoid conjugate vaccine introduction.

Acknowledgments

We gratefully acknowledge Julie Parsonnet, Catherine Ley, Alessio Fasano, Maureen M. Leonard, and Victoria Kenyon for generously sharing banked samples to define the distribution of antibody responses among individuals with no prior exposure to typhoidal *Salmonella*.

Accompanying code and de-identified data are available on Github (https://github.com/UCD-SERG/SSudanTyphoidSeroIncidence).

This work was supported by the World Health Organization's Unity Studies, a global seroepidemiologic standardization initiative, with funding provided by the COVID-19 Solidarity Response. This study was also supported by The Bill and Melinda Gates Foundation (INV-000572) and the US National Institutes of Health (R01AI134814).

About the Author

Dr. Aiemjoy is an assistant professor of epidemiology at the University of California Davis School of Medicine. Her research centers on measurement, surveillance, and diagnostics for infectious diseases with a focus on seroepidemiologic methods to understand the force of infection in populations.

References

1. Stanaway JD, Reiner RC, Blacker BF, Goldberg EM, Khalil IA, Troeger CE, et al.; GBD 2017 Typhoid and Paratyphoid Collaborators. The global burden of typhoid and paratyphoid fevers: a systematic analysis for the Global Burden of Disease Study 2017. Lancet Infect Dis. 2019;19:369–81. https://doi.org/10.1016/S1473-3099(18)30685-6
2. Antillon M, Saad NJ, Baker S, Pollard AJ, Pitzer VE. The relationship between blood sample volume and diagnostic sensitivity of blood culture for typhoid and paratyphoid fever: a systematic review and meta-analysis. J Infect Dis. 2018;218(suppl_4):S255–67. https://doi.org/10.1093/infdis/jiy471
3. Voysey M, Pant D, Shakya M, Liu X, Colin-Jones R, Theiss-Nyland K, et al. Under-detection of blood culture-positive enteric fever cases: the impact of missing data and methods for adjusting incidence estimates. PLoS Negl Trop Dis. 2020;14:e0007805. https://doi.org/10.1371/journal.pntd.0007805
4. Azman AS, Bouhenia M, Iyer AS, Rumunu J, Laku RL, Wamala JF, et al. High hepatitis E seroprevalence among displaced persons in South Sudan. Am J Trop Med Hyg. 2017;96:1296–301. https://doi.org/10.4269/ajtmh.16-0620
5. Abubakar A, Bwire G, Azman AS, Bouhenia M, Deng LL, Wamala JF, et al. Cholera epidemic in South Sudan and Uganda and need for international collaboration in cholera control. Emerg Infect Dis. 2018;24:883–7. https://doi.org/10.3201/eid2405.171651
6. Kumar S, Nodoushani A, Khanam F, DeCruz AT, Lambotte P, Scott R, et al. Evaluation of a rapid point-of-care multiplex immunochromatographic assay for the diagnosis of enteric fever. MSphere. 2020;5:e00253-20. https://doi.org/10.1128/mSphere.00253-20
7. Andrews JR, Khanam F, Rahman N, Hossain M, Bogoch II, Vaidya K, et al. Plasma immunoglobulin A responses against 2 *Salmonella* Typhi antigens identify patients with typhoid fever. Clin Infect Dis. 2019;68:949–55. https://doi.org/10.1093/cid/ciy578
8. McClelland M, Sanderson KE, Clifton SW, Latreille P, Porwollik S, Sabo A, et al. Comparison of genome degradation in Paratyphi A and Typhi, human-restricted serovars of *Salmonella enterica* that cause typhoid. Nat Genet. 2004;36:1268–74. https://doi.org/10.1038/ng1470
9. Charles RC, Liang L, Khanam F, Sayeed MA, Hung C, Leung DT, et al. Immunoproteomic analysis of antibody in lymphocyte supernatant in patients with typhoid fever in Bangladesh. Clin Vaccine Immunol. 2014;21:280–5. https://doi.org/10.1128/CVI.00661-13
10. Charles RC, Sheikh A, Krastins B, Harris JB, Bhuiyan MS, LaRocque RC, et al. Characterization of anti-*Salmonella enterica* serotype Typhi antibody responses in bacteremic Bangladeshi patients by an immunoaffinity proteomics-based technology. Clin Vaccine Immunol. 2010;17:1188–95. https://doi.org/10.1128/CVI.00104-10
11. Charles RC, Sultana T, Alam MM, Yu Y, Wu-Freeman Y, Bufano MK, et al. Identification of immunogenic *Salmonella enterica* serotype Typhi antigens expressed in chronic biliary carriers of *S.* Typhi in Kathmandu, Nepal. PLoS Negl Trop Dis. 2013;7:e2335. https://doi.org/10.1371/journal.pntd.0002335
12. Aiemjoy K, Seidman JC, Saha S, Munira SJ, Islam Sajib MS, Sium SMA, et al. Estimating typhoid incidence from community-based serosurveys: a multicohort study. Lancet Microbe. 2022;3:e578–87. https://doi.org/10.1016/S2666-5247(22)00114-8

13. Wiens KE, Mawien PN, Rumunu J, Slater D, Jones FK, Moheed S, et al. Seroprevalence of severe acute respiratory syndrome coronavirus 2 IgG in Juba, South Sudan. Emerg Infect Dis. 2021;27:1598–606. https://doi.org/10.3201/eid2706.210568
14. Garrett DO, Longley AT, Aiemjoy K, Yousafzai T, Hemlock C, Yu AT, et al. Incidence of typhoid and paratyphoid fever in Bangladesh, Nepal, and Pakistan: results of the Surveillance for Enteric Fever in Asia Project. Lancet Glob Health. 2022;10:e978–88. https://doi.org/10.1016/S2214-109X(22)00119-X
15. Marks F, von Kalckreuth V, Aaby P, Adu-Sarkodie Y, El Tayeb MA, Ali M, et al. Incidence of invasive salmonella disease in sub-Saharan Africa: a multicentre population-based surveillance study. Lancet Glob Health. 2017;5:e310–23. https://doi.org/10.1016/S2214-109X(17)30022-0

Address for correspondence: Kristen Aiemjoy, University of California Davis, Public Health Sciences, 1 Shields Ave, Medical Sciences 1C, Davis, CA 95616-5270, USA; email: kaiemjoy@ucdavis.edu

Effect of COVID-19 Pandemic on Invasive Pneumococcal Disease in Children, Catalonia, Spain

Pilar Ciruela, Núria Soldevila, Juan José García-Garcia, Sebastià González-Peris, Alvaro Díaz-Conradi, Alba Redin, Belén Viñado, Conchita Izquierdo, Carmen Muñoz-Almagro, Angela Domínguez; Barcino Working Group

We analyzed the effect of COVID-19 on healthcare demand and invasive pneumococcal disease in children in Catalonia, Spain. Compared with 2018–2019, we noted large reductions in healthcare activities and incidence of invasive pneumococcal disease in 2020. These changes likely resulted from nonpharmaceutical measures implemented during the COVID-19 pandemic.

SARS-CoV-2 was identified in 2019, and the World Health Organization declared COVID-19 a pandemic on March 11, 2020. As of July 11, 2021, >186 million cases and >4 million deaths had been recorded (*1*).

The first imported case of COVID-19 in Catalonia, Spain, was reported on February 26, 2020. Endemic transmission was declared on March 14, when the government of Spain introduced a strict lockdown until May 11. Other mandates followed, such as mask use, physical distancing, and reducing frequency of social contacts to reduce disease transmission (*2*). The peak number of cases was recorded in April 2020; cases subsequently declined and then occurred in epidemic waves. In 2020, a total of 356,724 cases and 8,723 deaths were reported in Catalonia (*3*).

Author affiliations: CIBER de Epidemiologia y Salud Pública, Madrid, Spain (P. Ciruela, N. Soldevila, J.J. García-García, C. Muñoz-Almagro, A. Dominguez); Agència de Salut Publica de Catalunya, Barcelona, Spain (P. Ciruela, C. Izquierdo); Universitat de Barcelona, Barcelona (N. Soldevila, J.J. García-García, A. Dominguez); Hospital Sant Joan de Déu, Esplugues de Llobregat, Spain (J.J. García-García, A. Redin, C. Muñoz-Almagro); Institut de recerca Sant Joan de Déu, Esplugues de Llobregat (J.J. García-García, C. Muñoz-Almagro); Hospital Vall d' Hebron, Barcelona (S. González-Peris, B. Viñado); Hospital HM Nens, Barcelona (A. Díaz-Conradi); Universitat Internacional de Catalunya, Sant Cugat del Vallés, Spain (C. Muñoz-Almagro)

DOI: https://doi.org/10.3201/eid2811.211741

Measures to reduce COVID-19 transmission have been associated with a reduction in diseases caused by respiratory pathogens, such as invasive pneumococcal disease (IPD) (*4*). IPD caused by *Streptococcus pneumoniae* has high rates of severe illness and death, especially in the very old and very young. In Catalonia, IPD incidence in children <5 years of age was 29.1/100,000 population in 2018, and 74.4% of cases were caused by serotypes not included in the 13-valent pneumococcal conjugate vaccine (PCV13) (*5*). Vaccine coverage in children was 92.9% in 2019. We assessed the effect of COVID-19 on the demand for care of IPD in children in 2020 compared with 2018–2019.

The Study

We investigated IPD cases identified during 2018–2020 in 3 pediatric hospitals, Sant Joan de Déu, Vall d'Hebron, and HM Nens, which serve 521,463 children <18 years of age, 32% of pediatric patients in Catalonia. A confirmed case of IPD was defined as isolation or detection of *S. pneumoniae* DNA by PCR from a normally sterile site. Data collected were number of emergency department (ED) visits and admissions; requests for sterile cultures as blood, cerebrospinal fluid, and pleural fluid; requests for PCR for pneumococcus; confirmed cases of IPD; and serotype distribution.

We calculated mean incidence rates per 100,000 person-years by using population served by the 3 hospitals each year. We compared incidence rates in 2018–2019 with 2020 rates by calculating incidence rate ratio (IRR) and 95% CI annually, by quarters and age groups (0–4 and 5–17 years). We expressed percentage change in IRR according to the formula (1–IRR) × 100. We performed analysis by using R version 3.5.0 (The R Project for Statistical Computing, https://www.r-project.org).

Table 1. Healthcare activity and IPD incidence by age group, Catalonia, Spain, 2018–2019 and 2020*

Variable	No. cases (incidence, cases/100,000 population)		IRR (95% CI)	p value
	Mean 2018–19	2020		
All ages				
Emergency department visits	227,148 (43,661.3)	148,637 (28,437.6)	0.65 (0.64–0.66)	<0.0001
Hospital admissions	11,313 (2,174.5)	8,423 (1,611.5)	0.74 (0.72–0.76)	<0.0001
Samples for culture, HSJD	7,489 (1,439.5)	7,106 (1,359.5)	0.94 (0.91–0.98)	0.001
Samples for PCR, HSJD and HVH	641 (123.2)	497 (95.1)	0.77 (0.69–0.87)	<0.0001
IPD cases	57 (11.0)	20 (3.8)	0.35 (0.21–0.57)	<0.0001
PCV13 serotypes	25 (4.8)	10 (1.9)	0.40 (0.18–0.82)	0.01
Serotype 3	17 (3.3)	9 (1.7)	0.53 (0.22–1.17)	0.07
Non-PCV13 serotypes	29 (5.6)	10 (1.9)	0.34 (0.17–0.70)	0.003
0–4 y				
Emergency department visits	108,757 (93,016.7)	68,684 (60,617.9)	0.65 (0.64–0.66)	<0.0001
Hospital admissions	6,519 (5,575.5)	4,256 (3,756.2)	0.67 (0.65–0.70)	<0.0001
Samples for culture, HSJD	ND	ND	NA	NA
Samples for PCR, HSJD and HVH	459 (392.6)	342 (301.8)	0.77 (0.67–0.88)	0.0002
IPD cases	44 (37.6)	15 (13.2)	0.35 (0.19–0.62)	0.0001
PCV13 serotypes	18 (15.4)	8 (7.1)	0.46 (0.19–1.04)	0.06
Serotype 3	12 (10.3)	8 (7.1)	0.69 (0.27–1.69)	0.42
Non-PCV13 serotypes	25 (21.4)	7 (6.2)	0.29 (0.12–0.67)	0.002
5–17 y				
Emergency department visits	118,391 (29,353.5)	79,953 (19,530.7)	0.66 (0.65–0.67)	<0.0001
Hospital admissions	4,794 (1,188.6)	4,167 (1,017.9)	0.86 (0.82–0.89)	<0.0001
Samples for culture. (HSJD	ND	ND	NA	NA
Samples for PCR. HSJD and HVH	182 (45.1)	155 (37.9)	0.84 (0.68–1.04)	0.11
IPD cases	13 (3.2)	5 (1.2)	0.38 (0.13–1.06)	0.06
PCV13 serotypes	7 (1.7)	2 (0.5)	0.28 (0.06–1.36)	0.17
Serotype 3	5 (1.2)	1 (0.2)	0.20 (0.02–1.69)	0.21
Non-PCV13 serotypes	4 (1.0)	3 (0.7)	0.74 (0.16–3.30)	0.71

*HSJD, Hospital Sant Joan de Dèu; HVH, Hospital Vall Hebron; IPD, invasive pneumococcal disease; IRR, incidence rate ratio; NA, not applicable; ND, not done; PCV13, 13-valent pneumococcal conjugate vaccine.

Total numbers of visits to EDs were 225,031 in 2018, 229,256 in 2019, and 148,637 in 2020; total numbers of hospital admissions were 11,421 in 2018, 11,206 in 2019, and 8,423 in 2020. Compared with mean incidence in 2018–2019, ED visits declined by 35% in 2020, and hospital admissions declined by 26% (Table 1). The number of cultures was reduced in 2020 by 6%, and the number of requested PCR tests specific for *S. pneumoniae* declined by 23%, predominantly in children 0–4 years of age (23%).

IPD incidence per 100,000 person-years was 11 in 2018–2019 and 3.8 in 2020, a reduction of 65%; this same reduction was observed in the 0–4-year age group in 2020. Reduction of IPD incidence in 2020 was greater in the second and fourth quarter; no IPD cases were reported in the second quarter of 2020 (Table 2). Incidence per 100,000 person-years of IPD caused by PCV13 serotypes was 4.8 in 2018–2019 and 1.9 in 2020; IPD caused by non-PCV13 serotypes was 5.6 in 2018–2019 and 1.9 in 2020 (Table 1; Figure 1). Serotype 3 was the most frequent serotype in 2018–2019 (30.6%) and 2020 (45%) (Figure 2).

Conclusions

The lockdown during the first months of the COVID-19 pandemic in 2020, together with social distancing measures, reduced mobility, and limits on the number of persons at social gatherings, had a positive effect on preventing IPD transmission in children and on indicators of healthcare activity. Overall reduction in IPD incidence was observed throughout 2020 compared with incidence for 2018–2019. No IPD cases were detected in the second quarter of 2020, coinciding with the lockdown, and a reduction of 84% was observed in the fourth quarter, coinciding with intensifying containment measures after the second wave of COVID-19 (*6*).

The percentage reduction in IPD cases in 2020 was similar in children <5 years of age (65%) and those 5–17 years of age (62%), although in the older group the reduction was not statistically significant because very few cases occurred in 2020. Other authors have described reductions in IPD during the COVID-19 pandemic. A prospective analysis from 26 countries found reductions of IPD of 68% at 4 weeks and of 82% at 8 weeks (*7*). In Hong Kong, observed IPD cases declined by 74.7% in 2020 compared with 2015–2019 (*8*). Some authors have stated that during 2020 no campaign occurred to increase pneumococcal vaccination and no other changes in practice affecting diagnosis or notification requirements for IPD were enacted that would explain reductions in incidence (*9*).

Serotype 3 was the most frequent serotype in the 2 periods (30.6% in 2018–2019 and 45% in 2020), and

Table 2. Healthcare activity and IPD incidence by quarter, Catalonia, Spain, 2018–19 and 2020*

Variable	No. cases (incidence, cases/100,000 population) Mean 2018–2019	2020	IRR (95% CI)	p value
1st quarter				
Emergency department visits	61,590 (11,838.5)	54,430 (10,413.7)	0.88 (0.87–0.89)	<0.0001
Hospital admissions	3,049 (586.1)	2,785 (532.8)	0.91 (0.86–0.96)	0.0003
Samples for culture, HSJD	1,968 (378.3)	2,192 (419.4)	1.11 (1.04–1.18)	0.0009
Samples for PCR, HSJD and VH	185 (35.6)	182 (34.8)	0.98 (0.80–1.20)	0.84
IPD cases	17 (3.3)	15 (2.9)	0.88 (0.43–1.77)	0.72
PCV13 serotypes	7 (1.3)	9 (1.7)	1.28 (0.47–3.62)	0.64
Serotype 3	5 (1.0)	8 (1.5)	1.59 (0.51–5.35)	0.43
Non-PCV13 serotypes	10 (1.9)	6 (1.1)	0.60 (0.20–1.65)	0.33
2nd quarter				
Emergency department visits	55,519 (10,671.6)	23,025 (4,405.2)	0.41 (0.40–0.42)	<0.0001
Hospital admissions	2,772 (532.8)	1,670 (319.5)	0.60 (0.56–0.64)	<0.0001
Samples for culture, HSJD	1,891 (363.5)	1,633 (312.4)	0.86 (0.80–0.92)	<0.0001
Samples for PCR, HSJD and VH	141 (27.1)	107 (20.5)	0.76 (0.59–0.97)	0.03
IPD cases	15 (2.9)	0	NA	<0.0001
PCV13 serotypes	8 (1.5)	0	NA	0.008
Serotype 3	6 (1.2)	0	NA	0.03
Non-PCV13 serotypes	6 (1.2)	0	NA	0.03
3rd quarter				
Emergency department visits	44,594 (8,571.6)	34,933 (6,683.5)	0.78 (0.77–0.79)	<0.0001
Hospital admissions	2,171 (417.3)	1,810 (346.3)	0.83 (0.78–0.88)	<0.0001
Samples for culture, HSJD	1,789 (343.9)	1,618 (309.6)	0.90 (0.84–0.96)	0.002
Samples for PCR, HSJD and VH	112 (21.5)	86 (16.5)	0.76 (0.58–1.01)	0.06
IPD cases	6 (1.2)	2 (0.4)	0.33 (0.05–1.57)	0.18
PCV13 serotypes	2 (0.4)	0	NA	0.25
Serotype 3	1 (0.2)	0	NA	0.50
Non-PCV13 serotypes	3 (0.6)	2 (0.4)	0.66 (0.11–3.97)	0.65
4th quarter				
Emergency department visits	65,445 (12,579.5)	36,249 (6,935.3)	0.55 (0.54–0.56)	<0.0001
Hospital admissions	3,321 (638.4)	2,158 (412.9)	0.65 (0.61–0.68)	<0.0001
Samples for culture, HSJD	1,841 (353.9)	1,663 (318.2)	0.90 (0.84–0.96)	0.002
Samples for PCR, HSJD and VH	203 (39.0)	122 (23.3)	0.60 (0.48–0.75)	<0.0001
IPD cases	19 (3.7)	3 (0.6)	0.16 (0.04–0.49)	0.001
PCV13 serotypes	8 (1.5)	1 (0.2)	0.12 (0.01–0.78)	0.02
Serotype 3	5 (1.0)	1 (0.2)	0.20 (0.01–1.44)	0.22
Non-PCV13 serotypes	10 (1.9)	2 (0.4)	0.20 (0.03–0.82)	0.02

*HSJD, Hospital Sant Joan de Dèu; HVH, Hospital Vall Hebron; IPD, invasive pneumococcal disease; IRR, incidence rate ratio; NA, not applicable; PCV13, 13-valent pneumococcal conjugate vaccine.

no significant reduction was detected. Similar results were observed by Teng et al. (*8*): 52.9% of cases in 2015–2019 and 45.7% in 2020 were serotype 3. We observed reduction in IPD incidence in 2020 compared with 2018–2019 in PCV13 (60%) and non-PCV13 (66%) serotypes.

A systematic review of 15 studies (*10*) concluded that nonpharmaceutical interventions could delay the introduction of influenza virus and are therefore effective in controlling influenza epidemics. In Catalonia, the active surveillance system for influenza and other acute respiratory infections found that influenza epidemic activity in the 2019–20 season had a short duration of 8 weeks (weeks 3–11) (*11*). Other authors recorded a similar situation; influenza and respiratory syncytial virus incidence declined sharply, and the

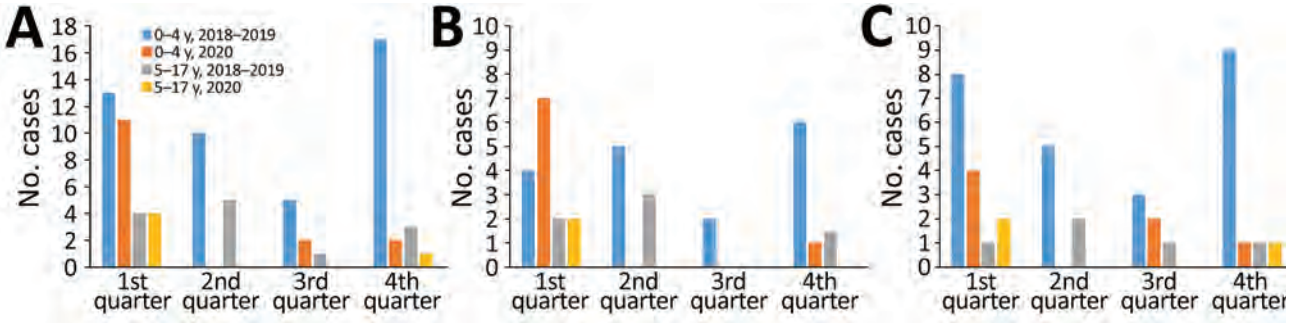

Figure 1. Invasive pneumococcal disease cases by quarter, age group, and year, Catalonia, Spain. A) Global cases; B) 13-valent pneumococcal conjugate vaccine serotypes; C) non–13-valent pneumococcal conjugate vaccine serotypes.

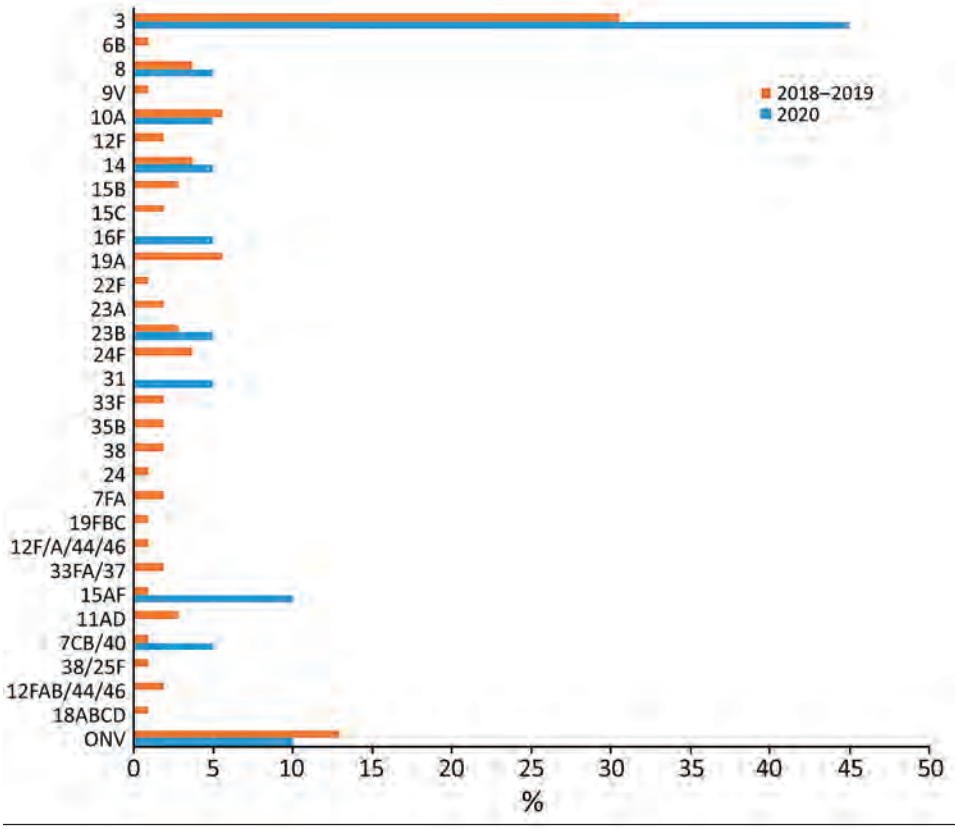

Figure 2. Distribution of invasive pneumococcal disease serotypes, Catalonia, Spain, 2018–2019 and 2020

season in 2020 was brief and ended rapidly compared with previous years (*12*). Viral infections might create favorable conditions in nasopharyngeal mucosa for invasive, colonizing pneumococcus causing IPD, so reduced influenza transmission during the pandemic might also have contributed to the reduction in IPD (*8*).

We found a reduction in ED visits (35%) and hospital admissions (26%) for IPD in 2020 compared with 2018–2019. Declines were greatest in the second quarter (59% for ED visits, 40% for hospital admissions), followed by the fourth quarter (45% for ED visits, 35% for hospital admissions), coinciding with the total lockdown and more stringent public health measures adopted because of the second epidemic wave in this setting (*6*). The number of cultures and specific requests for *S. pneumoniae* PCR declined less than the number of ED visits, hospital admissions, and IPD incidence in 2020. Increased public awareness of adequate individual use of nonpharmaceutical protective measures and social distancing measures had an effect on reducing incidence of IPD and other respiratory infections (*13*).

One limitation of our study is that the data analyzed came from just 32% of pediatric patients in Catalonia treated in 3 pediatric reference hospitals. However, the hospitals were reference hospitals; therefore, we believe these data are representative of the pediatric population in Catalonia. In addition, not all patients were tested during the first wave, so the exact incidence of SARS-CoV-2 infection in the first months of the pandemic is unknown. A strength of the study is that data were collected in a similar way throughout the study.

In summary, the reduction in ED visits and hospital admissions in 2020 compared to 2018–2019 in Catalonia was greater than the reduction in requests for culture and PCR specific for *S. pneumoniae.* The reduction in IPD incidence was more marked during the second quarter of 2020, coinciding with COVID-19 lockdowns.

Barcino Working Group: Magda Campins, Pilar Ciruela, Alvaro Díaz-Conradi, Angela Domínguez, Cristina Esteva, Mariona F. de Sevilla, Juan José García-García, Sebastià González-Peris, Conchita Izquierdo, Fernando Moraga-Llop, Carmen Muñoz-Almagro, Alba Redín, Luís Salleras, Belén Viñado.

Acknowledgments

We thank all the participants of this study. We are grateful to Lorena Coronas for her support in data management and manuscript submission.

CIBER of Epidemiology and Public Health (CIBERESP), Carlos III Health Institute, Madrid (PI17/00337) and the Catalan Agency for the Management of Grants for University Research (AGAUR grant numbers 2017/SGR 1342 and 2017/SGR 00742) supported this study.

C.M.-A. received a grant from Pfizer laboratories to Sant Joan de Déu Foundation. J.J.G.-G. received travel grants and fees from Pfizer.

About the Author

Dr. Ciruela is the head of the Emerging Diseases service in the General Subdirectorate for Surveillance and Response to Public Health Emergencies of the Public Health Agency of Catalonia, Spain. Her main research interest is the epidemiology and control of infectious diseases, focusing on emerging and reemerging infections.

References

1. World Health Organization. Weekly epidemiological update on COVID-19 [cited 2021 Jul 28]. https://www.who.int/publications/m/item/weekly-epidemiological-update-on-covid-19–13-july-2021
2. Ministry of the President, Spain. Royal Decree 463/2020, of March 14, declaring the state of alarm for the management of the situation of the health crisis caused by COVID-19 [cited 2021 Jun 15]. https://www.boe.es/eli/es/rd/2020/03/14/463
3. Coordination Center for Health Alerts and Emergencies. Update No. 282. Coronavirus disease (COVID-19) [cited 2021 Jun 15]. https://www.sanidad.gob.es/profesionales/saludPublica/ccayes/alertasActual/nCov/documentos/Actualizacion_282_COVID-19.pdf
4. Mutnal MB, Arroliga AC, Walker K, Mohammad A, Brigmon MM, Beaver RM, et al. Early trends for SARS-CoV-2 infection in central and north Texas and impact on other circulating respiratory viruses. J Med Virol. 2020;92:2130–8. https://doi.org/10.1002/jmv.26010
5. Ciruela P, Jané M. Epidemiology of invasive pneumococcal disease in Catalonia, report 2017–2018. 2020 Nov 25 [cited 2021 Jun 22]. https://canalsalut.gencat.cat/web/.content/_Professionals/Vigilancia_epidemiologica/documents/arxius/malaltia-pneumoccocica-invasiva-informe-2017-2018_final-en.pdf
6. Deputy director of public health surveillance and response to emergencies. Department of Health. Technical summary report of COVID-19 cases in Catalonia, number 39 [in Spanish]. 2021 Jan 5 [cited 2021 Jun 15]. https://salutpublica.gencat.cat/web/.content/minisite/aspcat/vigilancia_salut_publica/vigilancia_covid19/informes_tecnics_covid19/39-informe-tecnic-covid-19-es.pdf
7. Brueggemann AB, Jansen van Rensburg MJ, Shaw D, McCarthy ND, Jolley KA, Maiden MCJ, et al. Changes in the incidence of invasive disease due to *Streptococcus pneumoniae*, *Haemophilus influenzae*, and *Neisseria meningitidis* during the COVID-19 pandemic in 26 countries and territories in the Invasive Respiratory Infection Surveillance Initiative: a prospective analysis of surveillance data. Lancet Digit Health. 2021;3:e360–70. https://doi.org/10.1016/S2589-7500(21)00077-7
8. Teng JLL, Fok KMN, Lin KPK, Chan E, Ma Y, Lau SKP, Woo PCY. Substantial decline in invasive pneumococcal disease (IPD) during COVID-19 pandemic in Hong Kong. Clin Infect Dis. 2022;74:335–8.
9. Lim RH, Chow A, Ho HJ. Decline in pneumococcal disease incidence in the time of COVID-19 in Singapore. J Infect. 2020;81:e19–21. https://doi.org/10.1016/j.jinf.2020.08.020
10. Ryu S, Gao H, Wong JY, Shiu EYC, Xiao J, Fong MW, et al. Nonpharmaceutical measures for pandemic influenza in nonhealthcare settings—international travel-related measures. Emerg Infect Dis. 2020;26:961–6. https://doi.org/10.3201/eid2605.190993
11. Deputy director of public health surveillance and response to emergencies, Department of Health. Information Plan on acute respiratory diseases in Catalonia (PIDIRAC) 2019–2020 [in Spanish] [cited 2021 Jun 15]. https://canalsalut.gencat.cat/web/.content/_Professionals/Vigilancia_epidemiologica/documents/arxius/balanc-temporada-gripal-2019-20.pdf
12. Haapanen M, Renko M, Artama M, Kuitunen I. The impact of the lockdown and the re-opening of schools and day cares on the epidemiology of SARS-CoV-2 and other respiratory infections in children—a nationwide register study in Finland. EClinicalMedicine. 2021;34:100807. https://doi.org/10.1016/j.eclinm.2021.100807
13. Yun HE, Ryu BY, Choe YJ. Impact of social distancing on incidence of vaccine-preventable diseases, South Korea. J Med Virol. 2021;93:1814–6. https://doi.org/10.1002/jmv.26614

Address for correspondence: Pilar Ciruela, Agencia de Salut Pública de Catalunya, Generalitat de Catalunya, Roc Boronat, 81-95, 08005 Barcelona, Spain; email: pilar.ciruela@gencat.cat

Crimean-Congo Hemorrhagic Fever Outbreak in Refugee Settlement during COVID-19 Pandemic, Uganda, April 2021

Luke Nyakarahuka, Shannon Whitmer, Jackson Kyondo, Sophia Mulei, Caitlin M. Cossaboom, Carson T. Telford, Alex Tumusiime, Gloria Grace Akurut, Dianah Namanya, Kilama Kamugisha, Jimmy Baluku, Julius Lutwama, Stephen Balinandi, Trevor Shoemaker, John D. Klena

Crimean-Congo hemorrhagic fever (CCHF) was detected in 2 refugees living in a refugee settlement in Kikuube district, Uganda. Investigations revealed a CCHF IgG seroprevalence of 71.3% (37/52) in goats within the refugee settlement. This finding highlights the need for a multisectoral approach to controlling CCHF in humans and animals in Uganda.

Crimean-Congo hemorrhagic fever (CCHF) is caused by CCHF virus (CCHFV). CCHF is a zoonotic disease that infects mainly livestock, and CCHFV is transmitted by ticks, primarily *Hyalomma* species. Humans are typically infected through contact with body fluids of infected livestock or through bites from infected ticks; human-to-human transmission of CCHFV has been documented (*1*), making early detection and infection prevention and control practices vital. The disease is distributed mainly in Central Asia, sub-Saharan Africa, and some parts of Europe (*2*).

Uganda first reported a case of CCHF in 2013 in Agago district; subsequent sporadic cases have been detected throughout the country, especially within the cattle corridor (*3*–*6*). Serologic evidence indicates widespread infection among livestock in Uganda (*7*). We report the findings of epidemiologic and laboratory investigations conducted within a refugee settlement in the Albertine Graben region of Uganda after 2 human CCHF cases were confirmed during the COVID-19 pandemic and provide recommendations to reduce future transmission of CCHFV.

Author affiliations: Makerere University, Kampala, Uganda (L. Nyakarahuka); Uganda Virus Research Institute, Entebbe, Uganda (L. Nyakarahuka, J. Kyondo, S. Mulei, A. Tumusiime, J. Baluku, J. Lutwama, S. Balinandi); Centers for Disease Control and Prevention, Atlanta, Georgia, USA (S. Whitmer, C.M. Cossaboom, C.T. Telford, T. Shoemaker, J.D. Klena); Uganda Wildlife Authority, Kampala (G.G. Akurut, D. Namanya, K. Kamugisha)

DOI: https://doi.org/10.3201/eid2811.220365

The Study

On April 27, 2021, a 16-year-old girl (patient 1) living in Kyangwali Refugee Settlement, Kikuube district, Uganda (Figure 1), sought care at a local health facility; clinical manifestations were a 2-day history of fever (38.1°C), headache, fatigue, hematemesis, and epistaxis. The patient had no history of recent travel outside the settlement and had stopped schooling because of national COVID-19 restrictions. The patient had been self-medicating for malaria without improvement; upon the onset of hemorrhagic signs, attending clinicians suspected a viral hemorrhagic fever because of the presence of epistaxis and hematemesis and implemented infection prevention and control measures, including patient isolation and use of personal protective equipment. A blood sample was collected and transported to Uganda Virus Research Institute the same day. Results revealed the patient was positive for CCHFV by real-time reverse transcription PCR (rRT-PCR) and had detectable CCHFV IgM and IgG on a US Centers for Disease Control and Prevention in-house ELISA specific to CCHFV (*3*).

On April 30, 2021, a 13-year-old boy (patient 2) from the same village was seen at the same health facility; symptoms were a 2-day history of fever that progressed into hemoptysis and epistaxis. The patient tested positive for malaria and received malaria treatment the day of symptom onset, but his

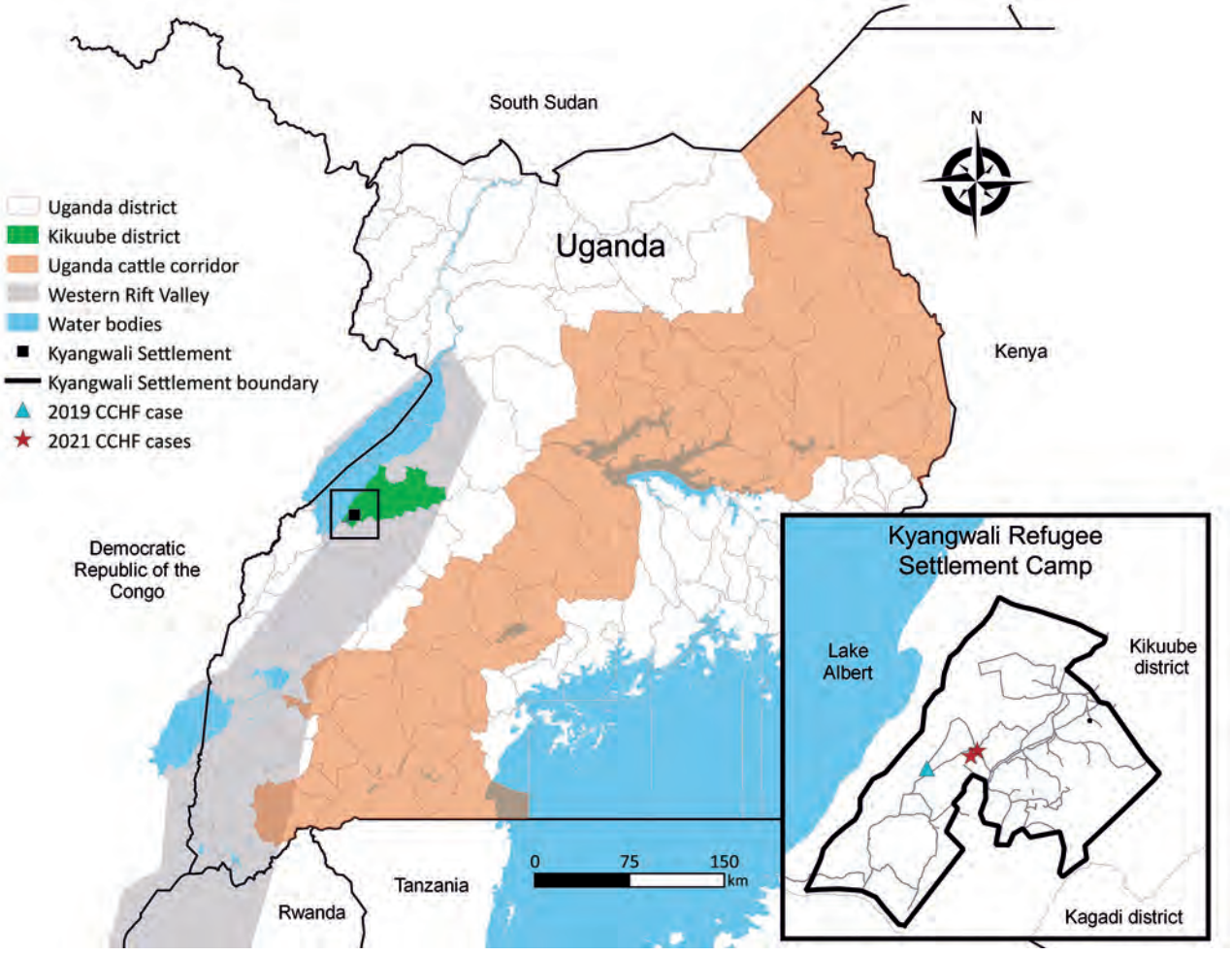

Figure 1. Location of Kyangwali Refugee Settlement (black box), Uganda, where 2 cases of Crimean-Congo hemorrhagic fever were reported during 2021. Inset shows close-up view of the settlement area, showing locations of 2021 cases and a previous case from 2019.

condition did not improve. A blood sample was transported to Uganda Virus Research Institute and tested positive for CCHFV by rRT-PCR; CCHFV IgM and IgG were detected.

Both patients were managed clinically with supportive care, including intravenous fluids and paracetamol; they clinically recovered and were discharged. Next-generation sequencing analysis of nucleic acids extracted from a blood sample from patient 1 indicated the circulating virus grouped within the African 2 lineage, closely matching the virus from a case detected in the same area in 2019 (Figures 1, 2). Sequences were deposited into GenBank (accession nos. OL690430–1). Because of low viral load, generating a sequence from patient 2 was not possible.

Both CCHF patients were from the same village, attended the same church, and were refugees of Congolese origin; however, we did not identify any close contact or epidemiologic link suggestive of human-to-human transmission between them. Patient 1 had previously herded 15 goats that were housed in a barn adjacent to the family's house and had not recently used tick control measures on the goats. Patient 2 lived near the goat pen of a neighbor in the camp. These goats, together with all livestock herds from the refugee settlement, grazed on communal land that was located <1 km away from the homes of the 2 confirmed patients, enabling easy mixing and transmission of pathogens.

We collected blood samples from 52 goats in the communal grazing land, including the 15 goats owned by patient 1's family, and tested them by CCHFV rRT-PCR and CCHFV IgG ELISA. All 52 goats were rRT-PCR-negative, but 37/52 (71.3%) goats had detectable IgG. We also collected 14 ticks (*Rhipicephalus appendiculatus*) from the sampled goats; all tested negative for CCHFV by rRT-PCR.

Conclusions

We describe 2 confirmed human CCHF cases in Kyangwali Refugee Settlement in Uganda. Both patients and their family members were rapidly identified and isolated upon seeking care at the health facility, and appropriate infection prevention and control measures were immediately implemented, which likely prevented onward CCHFV transmission. The presence of an isolation facility in the refugee settlement, set up as part of the COVID-19 response, played a key role in rapidly isolating patients. Both patients were given immediate supportive care and clinically recovered; human-to-human transmission of CCHFV was not identified.

In our investigation, 71.3% of sampled goats had detectable CCHFV IgG, indicating previous infection with CCHFV. As reported, the 2 patients were not living together and did not have direct contact with each other. These patients were likely infected through contact with infected body fluids of livestock or bites from infected ticks.

This investigation highlights some opportunities for improvement of viral hemorrhagic fever surveillance. Patient 1 self-treated with antimalarial medication before seeking care, which delayed isolation and increased the risk for CCHFV transmission, highlighting the importance of community education and encouraging health-promoting behaviors. Second, patient 2 initially tested positive for malaria, emphasizing the additional challenge in malaria-endemic countries of misdiagnosing viral infections such as CCHF as malaria. This challenge highlights the need for improved clinician awareness on the potential for malaria co-infections with other highly communicable pathogens such as CCHFV (G. Akurut, unpub. data); these infections cannot be differentiated without diagnostic testing. Improved diagnostic capability for multipathogen detection could also improve early identification and patient outcomes, as well as limiting the potential for transmission.

Both patients sought care after developing hemorrhagic signs, which usually develop late in illness (*8*). This timing leads to delayed case detection, which could result in community transmission of the infection. Both patients had detectable CCHFV IgM and IgG, further supporting likely infection 7–10 days before diagnosis (*9*). Although healthcare workers suspected a viral hemorrhagic fever quickly on the basis of hemorrhagic signs, education is needed on early symptoms, which are nonspecific and can be confused with other causes of acute febrile illnesses, such as malaria or typhoid. Early suspicion and detection will reduce community and hospital transmission and improves the likelihood of early supportive care for and recovery of the infected persons.

Both patients were living in close proximity to goats; the livestock were located in the same

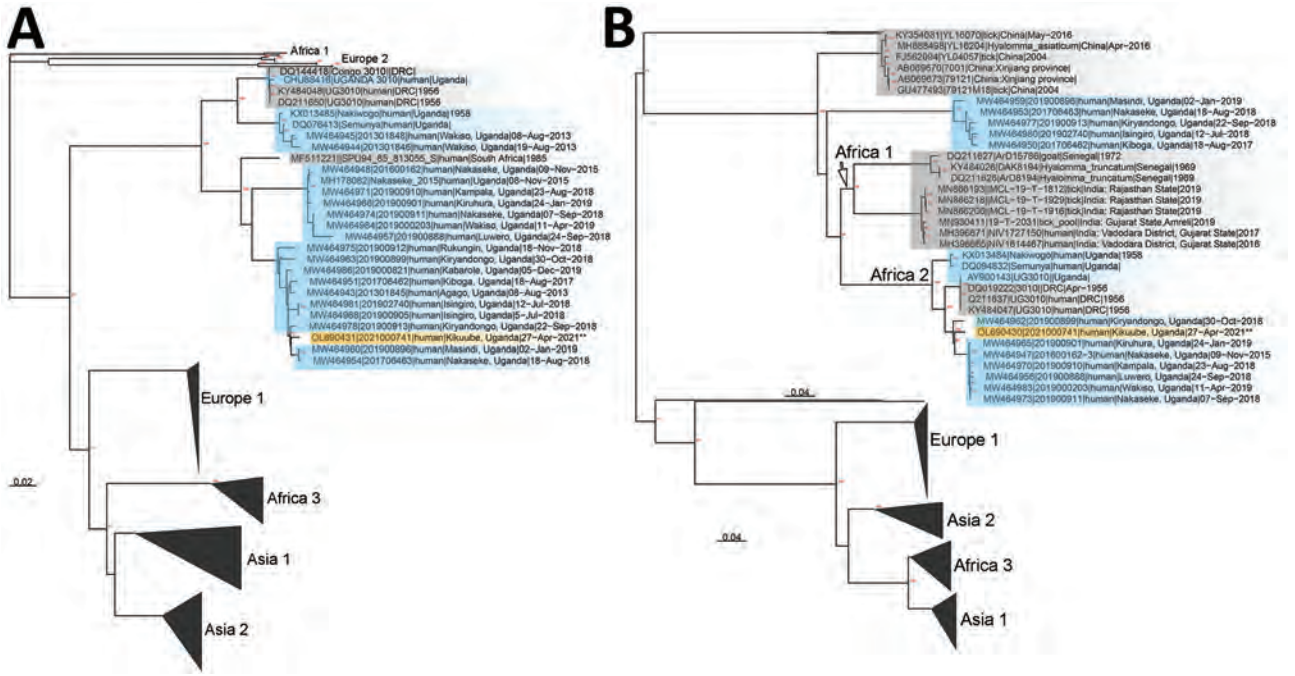

Figure 2. Phylogenetic analysis of all available full-length Crimean-Congo hemorrhagic fever (CCHF) small (A) and medium (B) segments from GenBank. Orange shading indicates sequence from 16-year-old girl in 2022; blue shading indicates past sequences from Uganda; gray shading indicates non-Uganda sequences. Major clades are labeled according to Balinandi et al. (*6*). Nodes with bootstrap support >70% are labeled in red. GenBank accession numbers are OL690430–1.

compound for patient 1 and in a nearby goat pen for patient 2. Both patients reported close interaction with goats by way of grazing and tethering them. This close interaction with livestock increases the chance of zoonotic disease transmission. Livestock act as reservoirs for pathogens such as Rift Valley fever virus, CCHF, tuberculosis, and brucellosis and should be housed separately because they can act as carriers of infections to humans. The presence of ticks on the sampled goats demonstrates limited tick control in the herd. Tickborne diseases affect not only the health of humans but also livestock production. Vector control strategies coupled with improved management practices would improve these challenges, because communal grazing increases risk for pathogen transmission among animals from different herds.

This investigation of 2 confirmed CCHF cases highlights the rapid identification and intervention by healthcare workers and response from the Kikuube District health team and partners, such as the United Nations High Commission for Refugees, Prime Minister's office, Medical Teams International, to successfully mitigate onward transmission of CCHFV in this vulnerable community. These efforts are particularly notable given the concurrent burden on the healthcare system and associated disease surveillance challenges from the COVID-19 pandemic.

Acknowledgments

We thank the family and neighbors of the patients and the healthcare workers in Kyangwali Refugee Settlement for their willingness to participate in and support this investigation. We also thank the Kikuube District health team and partners including the US Centers for Disease Control and Prevention, United Nations High Commission for Refugees, Uganda Prime Minister's office, and Medical Teams International.

About the Author

Dr. Nyakarahuka is a zoonotic disease epidemiology fellow at Uganda Virus Research Institute, Viral Hemorrhagic Fever Surveillance Program. His primary focus is surveillance and outbreak investigations of viral hemorrhagic fevers and training of health facilities on surveillance for viral hemorrhagic fevers.

References

1. Gürbüz Y, Sencan I, Oztürk B, Tütüncü E. A case of nosocomial transmission of Crimean-Congo hemorrhagic fever from patient to patient. Int J Infect Dis. 2009;13:e105–7. https://doi.org/10.1016/j.ijid.2008.08.002
2. Messina JP, Pigott DM, Golding N, Duda KA, Brownstein JS, Weiss DJ, et al. The global distribution of Crimean-Congo hemorrhagic fever. Trans R Soc Trop Med Hyg. 2015;109:503–13. https://doi.org/10.1093/trstmh/trv050
3. Balinandi S, Patel K, Ojwang J, Kyondo J, Mulei S, Tumusiime A, et al. Investigation of an isolated case of human Crimean-Congo hemorrhagic fever in Central Uganda, 2015. Int J Infect Dis. 2018;68:88–93. https://doi.org/10.1016/j.ijid.2018.01.013
4. Kizito S, Okello PE, Kwesiga B, Nyakarahuka L, Balinandi S, Mulei S, et al. Notes from the field: Crimean-Congo hemorrhagic fever outbreak—Central Uganda, August–September 2017. MMWR Morb Mortal Wkly Rep. 2018;67:646–7. https://doi.org/10.15585/mmwr.mm6722a6
5. Mirembe BB, Musewa A, Kadobera D, Kisaakye E, Birungi D, Eurien D, et al. Sporadic outbreaks of Crimean-Congo haemorrhagic fever in Uganda, July 2018–January 2019. PLoS Negl Trop Dis. 2021;15:e0009213. https://doi.org/10.1371/journal.pntd.0009213
6. Balinandi S, Whitmer S, Mulei S, Nyakarahuka L, Tumusiime A, Kyondo J, et al. Clinical and molecular epidemiology of Crimean-Congo hemorrhagic fever in humans in Uganda, 2013–2019. Am J Trop Med Hyg. 2021;106:88–98. https://doi.org/10.4269/ajtmh.21-0685
7. Balinandi S, von Brömssen C, Tumusiime A, Kyondo J, Kwon H, Monteil VM, et al. Serological and molecular study of Crimean-Congo hemorrhagic fever virus in cattle from selected districts in Uganda. J Virol Methods. 2021;290:114075. https://doi.org/10.1016/j.jviromet.2021.114075
8. Paessler S, Walker DH. Pathogenesis of the viral hemorrhagic fevers. Annu Rev Pathol. 2013;8:411–40. https://doi.org/10.1146/annurev-pathol-020712-164041
9. Shepherd AJ, Swanepoel R, Leman PA. Antibody response in Crimean-Congo hemorrhagic fever. Rev Infect Dis. 1989;11(Suppl 4):S801–6. https://doi.org/10.1093/clinids/11.Supplement_4.S801

Address for correspondence: Luke Nyakarahuka, Uganda Virus Research Institute, Plot 51-59, Nakiwogo Road, PO Box 49, Entebbe, Uganda; email: nyakarahuka@gmail.com

Jamestown Canyon Virus in Collected Mosquitoes, Maine, United States, 2017–2019

Elizabeth F. Schneider, Rebecca M. Robich, Susan P. Elias, Charles B. Lubelczyk, Danielle S. Cosenza, Robert P. Smith

Jamestown Canyon virus (JCV) is a mosquito-borne arbovirus that circulates in North America. We detected JCV in 4 pools of mosquitoes collected from midcoastal Maine, USA, during 2017–2019. Phylogenetic analysis of a JCV sequence obtained from *Aedes cantator* mosquitoes clustered within clade A, which also circulates in Connecticut, USA.

Jamestown Canyon virus (JCV; family *Peribunyaviridae*, genus *Orthobunyavirus*) is a mosquitoborne virus that belongs to the California serogroup. Although rare, JCV infection in humans can cause acute febrile encephalitis, meningitis, and meningoencephalitis (*1*). JCV was identified from *Culiseta inornata* mosquitoes in Jamestown Canyon, Colorado, USA, in 1961 (*2*). Since then, JCV has been detected in humans in the United States and Canada (*1*).

JCV has been isolated from ≥26 species of mosquitoes belonging to *Aedes/Ochlerotatus*, *Anopheles*, *Coquillettidia*, *Culex*, *Culiseta*, and *Psorophora* genera (*3*,*4*). White-tailed deer (*Odocoileus virginianus*) are likely the primary amplifying host of JCV (*5*), but moose (*Alces alces*), elk (*Cervus elaphus*), and bison (*Bison bison*) also might contribute to the transmission cycle (*6*). In Maine, moose and white-tailed deer are distributed statewide (*7*).

In 2017, two confirmed symptomatic human JCV cases were reported in Maine, and a subsequent fatal case was reported in the state in 2018 (*8*). All 3 cases occurred in women >65 years of age who resided in 3 counties: Kennebec, Franklin, and Knox (Figure 1) (*8*). Because JCV was recently identified in Maine, mosquito testing could help delineate the geographic distribution of JCV in the state. We collected and tested mosquitoes for JCV to obtain viral genomic sequences, conduct phylogenetic comparison, and determine whether JCV from Maine was congruent with published JCV sequences from the northeastern United States.

The Study

We trapped mosquitoes during mid-June–September each year during 2017–2019 in 36 towns in 9 of Maine's 16 counties, representing southern, midcoastal, and northern regions of the state. We used CDC Miniature Light Traps (John W. Hock Co., https://www.johnwhock.com) baited with CO_2 by using dry ice. We deployed 1 trap per site once per week and set the traps to run overnight from ≈2:00 PM–10:00 AM Eastern Standard Time. We identified mosquitoes' sex and species and pooled only female mosquitoes by species, collection site, and collection date, ≤50 mosquitoes per pool.

We extracted RNA from mosquito pools by using the QIAmp Viral RNA Mini Kit (QIAGEN, https://www.qiagen.com) following manufacturer protocol. We tested pools for JCV by reverse transcription PCR (RT-PCR) by using the SuperScript III One-Step RT-PCR System with Platinum Taq DNA polymerase (Invitrogen, https://ww.invitrogen.com) and primers designed to amplify 24 viruses within the Bunyamwera-California complex, including JCV (*9*).

We subsequently analyzed mosquito pools that tested positive for JCV RNA by using JCV-specific primers that target a 605-bp region of the nucleocapsid and nonstructural genes within the small segment (*9*). We conducted RT-PCR in the same manner described above but used Platinum *Taq* High Fidelity DNA Polymerase (Invitrogen). The University of Maine DNA Sequencing Facility (Orono, ME, USA) sequenced positive samples obtained from both primer sets. We confirmed JCV

Authors affiliation: MaineHealth Institute for Research, Scarborough, Maine, USA

DOI: https://doi.org/10.3201/eid2811.212382

Authors affiliation: MaineHealth Institute for Research, Scarborough, Maine, USA

Figure 1. Locations of JCV in humans and collected mosquitoes, Maine, USA, 2017–2019. JCV-positive mosquitoes were found in the town of Arrowsic in Sagadahoc County and in the towns of Edgecomb and Wiscasset in Lincoln County during 2017–2019. In 2017, two confirmed symptomatic human JCV cases were reported; a third fatal human case was reported in 2018. JCV, Jamestown Canyon virus.

identities by BLASTn (https://blast.ncbi.nlm.nih.gov/Blast.cgi).

We compared 1 positive sequence against 18 previously published orthobunyaviruses obtained from GenBank. We performed phylogenetic analysis in MEGA X (https://www.megasoftware.net) by using the neighbor-joining method and maximum composite likelihood model. We calculated 1,000 bootstrap replicates to provide support for each node.

Conclusions

During 2017–2019, we collected 13,023 mosquitoes from 36 towns in 9 counties in Maine, a total of 162 trap nights. We tested a total of 689 mosquito pools representing 24 species for the presence of JCV RNA by RT-PCR. Among all pools, 4 (0.6%) pools representing 4 (16.6%) different species were positive for JCV viral RNA (Table 1).

We detected JCV RNA in each of the 3 years of the study: in 1 positive pool of *Aedes provocans* mosquitoes in 2017; 2 positive pools in 2018, 1 each of *Ae. sollicitans* and *Uranotaenia sapphirina* mosquitoes; and 1 positive pool of *Ae. cantator* mosquitoes in 2019. All sequences matched other JCV sequences in GenBank with >99% identity. All JCV-positive mosquito pools were collected during a 3-week period, June 30–July 19. Although the testing effort represented the southern, midcoastal, and northern parts of the state, the positive mosquito pools originated from 3 towns in 2 midcoastal counties, Arrowsic in Sagadahoc County and Edgecomb and Wiscasset in Lincoln County (Figure 1).

Because of a storage freezer failure, we were only able to resequence 1 of the original 4 JCV-positive pools with the second set of primers. We chose this sequence for phylogenetic analysis because it provided us with a larger portion of the genome and would be more robust for analysis. This JCV-positive pool was from *Ae. cantator* mosquitoes collected in the town of Edgecomb, Lincoln County, in July 2019. Phylogenetic analysis of the Edgecomb sequence (GenBank accession no. MZ822417) and 18 other sequences obtained from

Table. Summary of female mosquitoes tested by reverse transcription PCR for Jamestown Canyon virus, Maine, USA, 2017–2019*

Mosquito species	No. pools	Total no. mosquitoes	JCV-positive pools†
Aedes abserratus/punctor	31	439	0
Ae. canadensis	104	1,724	0
Ae. cinereus	7	31	0
Ae. cantator	70	1,773	1
Ae. excrucians	24	391	0
Ae. fitchii	1	2	0
Ae. hendersoni	9	65	0
Ae. intrudens	4	18	0
Ae. japonicus	12	48	0
Ae. provocans	46	426	1
Ae. sollicitans	12	116	1
Ae. species	2	77	0
Ae. sticticus	1	3	0
Ae. stimulans	4	29	0
Ae. taeniorhynchus	1	2	0
Ae. triseriatus	28	183	0
Ae. vexans	24	198	0
Anopheles punctipennis	79	271	0
An. quadrimaculatus	17	65	0
An. walkeri	1	3	0
Coquillettidia perturbans	200	7,081	0
Culiseta melanura	2	4	0
Culex pipens/restuans	6	63	0
Cx. salinarius	1	5	0
Uranotaenia sapphirina	3	6	1
Total	689	13,023	4

*JCV, Jamestown Canyon virus.
†Pools include ≤50 female mosquitoes/pool.

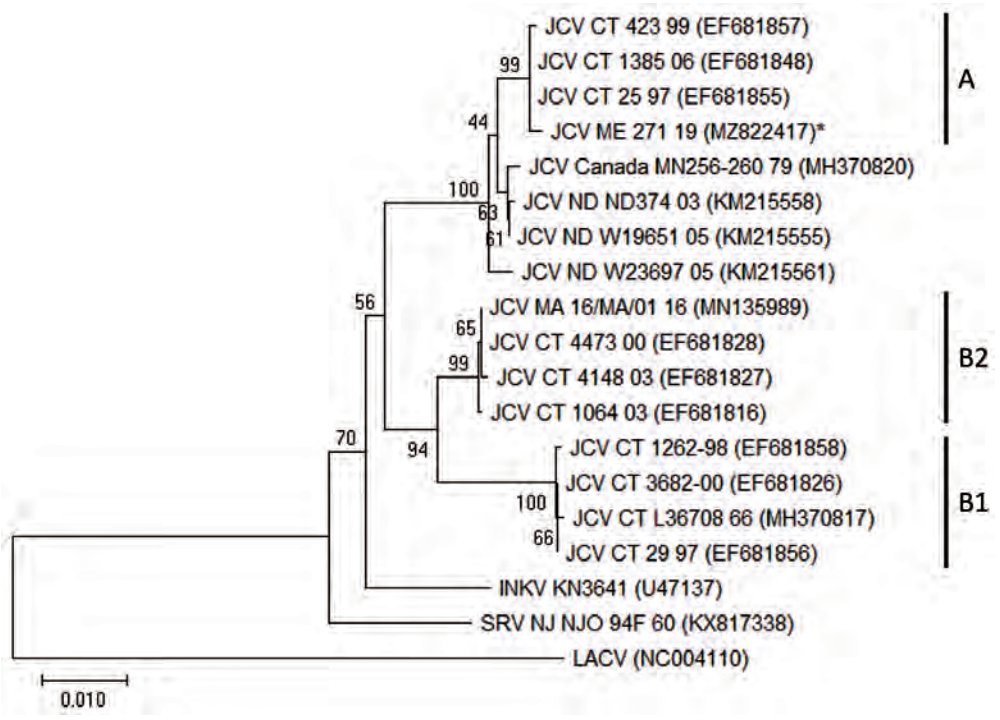

Figure 2. Phylogenetic analysis of JCV from collected mosquitoes, Maine, USA, 2017–2019. We compared a JCV sequence detected in mosquitoes from Maine to sequences from JCV and other viruses detected in other areas of the United States and Canada. We analyzed sequences by using the neighbor-joining method in MEGA X (https://www.megasoftware.net). The state or region of origin, strain, and year of isolation or detection are indicated for each virus, when available; GenBank accession numbers are provided. Asterisk indicates the sequence generated in this study. Numbers at branch nodes represent bootstrap values. Virus clades are indicated on the right. Scale bar indicates nucleotide substitutions per site. INKV, Inkoo virus; JCV, Jamestown Canyon virus; LACV, La Crosse virus; SRV, South River virus.

GenBank showed this JCV-positive sequence clustered within clade A described by a previous study (*10*), and had 99% nucleotide identity match with a JCV isolate from Connecticut collected in 2004 (GenBank accession no. HM007356) (Figure 2).

We detected JCV-positive mosquitoes in Maine, including 1 pool of *Ur. sapphirina* mosquitoes, a species not known as a JCV vector. In the southeastern United States, the *Ur. sapphirina* mosquito is considered a specialist of amphibians (*11*) and annelids (ringed worms or segmented worms), and 1 study from Florida found 100% of bloodmeals taken by *Ur. sapphirina* mosquitoes were from annelid hosts (*12*). However, in the northeastern United States, *Ur. sapphirina* mosquitoes appear to be generalists. In Connecticut, white-tailed deer have been identified as the most common vertebrate host for *Ur. sapphirina* mosquitoes, but additional bloodmeals from humans, birds, and reptiles are reported (*13*). The opportunistic feeding pattern of *Ur. sapphirina* mosquitoes in the northeast suggests this species might play a role in regional virus transmission.

In addition to *Ur. sapphirina* mosquitoes, we detected JCV RNA in *Ae. cantator*, *Ae. provocans*, and *Ae. sollicitans* mosquitoes, species known as mammalian pests that readily bite humans (*14*). The *Ae. provocans* mosquito is a known vector of JCV in New York, USA (*15*), and might serve as an overwintering reservoir (*4*). In Connecticut, *Ae. cantator* and *Ae. sollicitans* mosquito populations peak during late May through June and breed in saltmarshes and brackish water, which are common habitats along midcoastal Maine (*14*). *Ae. canadensis* mosquitoes have been identified as a dominant JCV vector in Connecticut (*4*). Although *Ae. canadensis* and *Coquillettidia perturbans* mosquitoes comprised most (44%) pools in our study, we did not detect JCV RNA in either species.

All JCV-positive mosquito pools in our study came from coastal counties, whereas the 3 human JCV cases during our study period came from 2 inland counties and 1 coastal county. Our sampling and testing effort was greater in the midcoastal region than in other regions of the state. A serosurvey for JCV antibodies in deer and moose in Maine might show a broader geographic extent than mosquito positivity and human cases (*7*).

In conclusion, the JVC sequence we obtained from *Ae. cantator* mosquitoes collected in 2019 from Edgecomb, in Lincoln County, Maine, clustered within clade A described by a previous study in Connecticut (*10*), where clade A is the most common clade, in addition to clades B1 and B2. Increased mosquito collection, testing effort, and phylogenetic analysis could elucidate the roles of particular mosquito species in

JCV transmission, and better delineate the statewide phylogeographic distribution of JCV in Maine. Clarifying the distribution of JCV in mosquitoes in Maine can inform prevention efforts in the state.

Acknowledgments

We thank Sara Robinson and Haris Sohail for assistance with information on human case data. We also thank the many interns who helped with mosquito identification and the 2 anonymous peer reviewers whose helpful comments improved this dispatch.

The MaineHealth Institute for Research and the Maine Centers for Disease Control and Prevention provided funding for this project (Maine Department of Health and Human Services agreement no. CD0-19-7170B).

About the Author

Ms. Schneider is a research associate with the Vector-Borne Disease Laboratory at the MaineHealth Institute for Research. Her research interests include the environmental and ecological factors among disease vectors, hosts, and habitat.

References

1. Pastula DM, Hoang Johnson DK, White JL, Dupuis AP II, Fischer M, Staples JE. Jamestown Canyon virus disease in the United States—2000–2013. Am J Trop Med Hyg. 2015;93:384–9. https://doi.org/10.4269/ajtmh.15-0196
2. Sather GE, Hammon WM. Antigenic patterns within the California-encephalitis-virus group. Am J Trop Med Hyg. 1967;16:548–57. https://doi.org/10.4269/ajtmh.1967.16.548
3. DeFoliart GR, Anslow RO, Hanson RP, Morris CD, Papadopoulos O, Sather GE. Isolation of Jamestown Canyon serotype of California encephalitis virus from naturally infected *Aedes* mosquitoes and tabanids. Am J Trop Med Hyg. 1969;18:440–7. https://doi.org/10.4269/ajtmh.1969.18.440
4. Andreadis TG, Anderson JF, Armstrong PM, Main AJ. Isolations of Jamestown Canyon virus (Bunyaviridae: Orthobunyavirus) from field-collected mosquitoes (*Diptera*: *Culicidae*) in Connecticut, USA: a ten-year analysis, 1997–2006. Vector Borne Zoonotic Dis. 2008;8:175–88. https://doi.org/10.1089/vbz.2007.0169
5. Boromisa RD, Grimstad PR. Seroconversion rates to Jamestown Canyon virus among six populations of white-tailed deer (*Odocoileus virginianus*) in Indiana. J Wildl Dis. 1987;23:23–33. https://doi.org/10.7589/0090-3558-23.1.23
6. Grimstad PR. California group virus disease. In: Monath TP, editor. The arboviruses: epidemiology and ecology, vol. II. Boca Raton, FL: CRC Press; 1988. p. 99–136.
7. Mutebi JP, Mathewson AA, Elias SP, Robinson S, Graham AC, Casey P, et al. Use of cervid serosurveys to monitor Eastern equine encephalitis virus activity in Northern New England, United States, 2009–2017. J Med Entomol. 2022;59:49–55. https://doi.org/10.1093/jme/tjab133
8. Maine Centers for Disease Control and Prevention. Annual reports 2022 [cited 2022 Mar 16]. https://www.maine.gov/dhhs/mecdc/infectious-disease/epi/publications/index.shtml#annualreports
9. Kuno G, Mitchell CJ, Chang GJ, Smith GC. Detecting bunyaviruses of the Bunyamwera and California serogroups by a PCR technique. J Clin Microbiol. 1996;34:1184–8. https://doi.org/10.1128/jcm.34.5.1184-1188.1996
10. Armstrong PM, Andreadis TG. Genetic relationships of Jamestown Canyon virus strains infecting mosquitoes collected in Connecticut. Am J Trop Med Hyg. 2007;77:1157–62. https://doi.org/10.4269/ajtmh.2007.77.1157
11. Cupp EW, Zhang D, Yue X, Cupp MS, Guyer C, Sprenger TR, et al. Identification of reptilian and amphibian blood meals from mosquitoes in an Eastern equine encephalomyelitis virus focus in central Alabama. Am J Trop Med Hyg. 2004;71:272–6. https://doi.org/10.4269/ajtmh.2004.71.272
12. Reeves LE, Holderman CJ, Blosser EM, Gillett-Kaufman JL, Kawahara AY, Kaufman PE, et al. Identification of *Uranotaenia sapphirina* as a specialist of annelids broadens known mosquito host use patterns. Commun Biol. 2018;1:92. https://doi.org/10.1038/s42003-018-0096-5
13. Molaei G, Andreadis TG, Armstrong PM, Diuk-Wasser M. Host-feeding patterns of potential mosquito vectors in Connecticut, U.S.A.: molecular analysis of bloodmeals from 23 species of *Aedes*, *Anopheles*, *Culex*, *Coquillettidia*, *Psorophora*, and *Uranotaenia*. J Med Entomol. 2008;45:1143–51. https://doi.org/10.1093/jmedent/45.6.1143
14. Andreadis TG, Thomas MC, Shepard JJ. Identification guide to the mosquitoes of Connecticut. New Haven (CT): Connecticut Agricultural Experimental Station; 2005.
15. Boromisa RD, Grayson MA. Incrimination of *Aedes provocans* as a vector of Jamestown Canyon virus in an enzootic focus of northeastern New York. J Am Mosq Control Assoc. 1990;6:504–9.

Address for correspondence: Elizabeth Schneider, MaineHealth Institute for Research, Vector-borne Disease Research Laboratory, 81 Research Dr, Scarborough, Maine 04074, USA; email: elizabeth.henderson@maine.edu

Monkeypox Virus Transmission to Healthcare Worker through Needlestick Injury, Brazil

Laína Bubach Carvalho, Luciana V.B. Casadio, Matheus Polly, Ana Catharina Nastri, Anna Cláudia Turdo, Raissa H. de Araujo Eliodoro, Ester Cerdeira Sabino, Anna Sara Levin, Adriana Coracini Tonacio de Proença, Hermes Ryoiti Higashino

Author affiliations: Universidade de São Paulo Hospital das Clínicas, São Paulo, Brazil (L. Bubach Carvalho, L.V.B. Casadio, M. Polly, A.C. Nastri, A.C. Tonacio de Proença, H.R. Higashino); Sao Camilo Hospital Pompeia Unit, São Paulo (L. Bubach Carvalho, L.V.B. Casadio, M. Polly, A.C. Turdo, A.C. Tonacio de Proença, H.R. Higashino); Universidade de São Paulo Instituto de Medicina Tropical, São Paulo (R.H. de Araujo Eliodoro); Universidade de São Paulo, São Paulo (E.C. Sabino, A.S. Levin)

DOI: https://doi.org/10.3201/eid2811.221323

We describe monkeypox virus (MPXV) transmission from a patient to a healthcare worker through needlestick injury. A lesion appeared at the inoculation site 5 days after injury. Blood tested MPXV-positive by PCR before symptoms worsened; blood remained MPXV-positive at discharge 19 days after symptom onset. Postexposure prophylaxis could prevent potential MPXV bloodborne transmission.

In July 2022, the World Health Organization declared the global monkeypox outbreak a public health emergency (*1*). Monkeypox virus (MPXV) is transmitted through close or direct contact with skin lesions or respiratory droplets and through fomites, but knowledge gaps about transmission persist.

During the ongoing outbreak, MPX has disproportionately affected men who have sex with men, suggesting amplification through sexual networks (*2*). MPXV transmission to healthcare workers (HCWs) in endemic settings is well described (*3*) but has not been well characterized in the current outbreak. In nonendemic countries, monkeypox is rare, and standard infection control precautions are applied, suggesting HCWs are at low risk of acquiring MPXV; only 1 prior HCW case has been reported (*4*). We describe MPXV transmission to a HCW in Brazil through a needlestick injury.

On July 9, 2022, a female nurse in her 20s sustained a needlestick injury to her thumb from supplies used to collect cutaneous lesion samples from a monkeypox patient. The nurse was wearing personal protective equipment, including gown, gloves, goggles, and mask, and was gathering materials to discard in a sharps container when a needle perforated her glove; the puncture site was visible immediately. After 5 days, a nodule developed at the injury site (day 0 of symptoms); it later evolved into a painful vesicle (Figure). The nurse lived alone, denied recent travel, and reported having protected sexual intercourse only with her male partner. She had no other potential exposures.

The source patient, a man in his 20s who reported having sex with men, had mild monkeypox that started 2 weeks before the needlestick incident. He had sore throat, cervical lymphadenopathy, and sparse lesions on his face, torso, and groin. The patient and nurse provided written consent for this report.

Overall, the nurse had 7 lesions: 1 each on the thumb (inoculation site) and palm of the right hand, dorsal left hand, and left thigh, and 3 on her face (Appendix Figures 1–3, https://wwwnc.cdc.gov/EID/article/28/11/22-1323-App1.pdf). Magnetic resonance imaging of the injury site on day 15 showed a neurovascular bundle and subcutaneous inflammation.

During the nurse's follow-up, blood and skin lesion samples tested MPXV-positive by reverse transcription PCR using the QIAamp Viral DNA Mini Kit (QIAGEN, https://www.qiagen.com) for DNA extraction and TaqMan Monkeypox Virus Microbe Detection Assay (Thermo Fisher Scientific, https://www.thermofisher.com) for amplification. MPXV also was detectable in oropharyngeal samples despite the absence of respiratory symptoms. Of note, all collected specimens had detectable MPXV DNA throughout hospitalization. The nurse was discharged to outpatient care before complete lesion resolution (Figure).

In nonendemic settings, needlestick injury is an unusual form of patient-to-HCW MPXV transmission. Before 2022, fewer human-to-human than animal-to-human MPXV transmission cases were reported during outbreaks in Africa (*5*). In nonendemic countries, sporadic zoonotic or travel-associated monkeypox outbreaks have occurred (*5*,*6*), but during May–September 2022, >50,000 cases were reported worldwide (https://www.cdc.gov/poxvirus/monkeypox/response/2022/world-map.html), mainly through sexual or intimate contact transmission (*7*). HCWs are at risk, but a recent review of MPXV transmission in healthcare facilities in nonendemic countries found only 1 documented case of nosocomial monkeypox in a HCW, probably through contact with contaminated bedding (*4*,*8*).

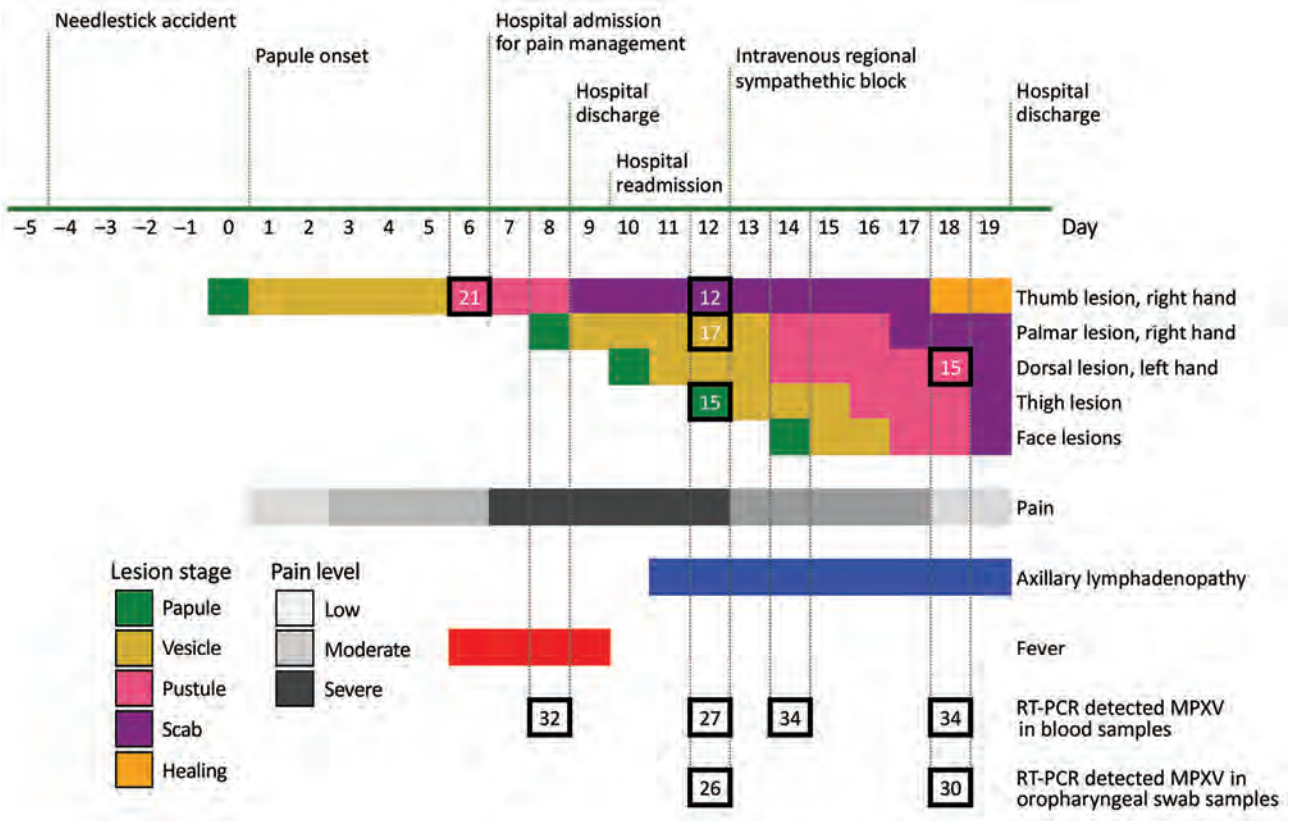

Figure. Timeline of symptoms and testing in a case of MPXV transmission to healthcare worker through needlestick injury, Brazil. All collected specimens had RT-PCR detectable MPXV through hospital discharge. Numerals inside squares indicate RT-PCR cycle threshold values. MPXV, monkeypox virus; RT-PCR, reverse transcription PCR.

Our case enabled observation of the natural progression of monkeypox through longitudinal clinical and laboratory monitoring of disease stages. The incubation period was 5 days. A cutaneous lesion and pain and inflammation at the inoculation site preceded generalized symptoms of fever and lymphadenopathy. The transmission route might have influenced the absence of a prodromal phase in the nurse because needlestick transmission parallels bite or scratch transmission from MPXV-infected animals to humans; in those cases, a febrile prodrome is uncommon (*5*). In addition, the nurse experienced severe injury site pain, which coincides with a series of cases in the current outbreak in which most patients who acquired MPXV by sexual or intimate contact were hospitalized for severe anorectal pain (*2*). The pain similarity suggests that the primary MPXV inoculation site is associated with painful lesions and possible neural impairment, as implied by the nurse's magnetic resonance images.

MPXV DNA detected in the nurse's blood on day 8, before skin lesions appeared at distant sites, suggests hematogenous virus dissemination. Few reports describe MPXV DNA in blood, but a retrospective study of monkeypox antiviral treatment found detectable MPXV DNA in blood after 14 days, even after skin lesions resolved (*8*). How detectable MPXV DNA corresponds to true viremia is unknown, but persistent DNA suggests bloodborne transmission could be possible through needlesticks, blood transfusions, and organ transplants. Persistent MPXV DNA in the nurse's oropharyngeal samples aligns with another report (*9*), but efficiency for droplet or airborne transmission remains unknown.

Because few documented needlestick monkeypox cases are available (*9*), we could not estimate transmission risk, but instruments used on cutaneous lesions likely pose a high risk. The World Health Organization recommends postexposure prophylaxis with second- or third-generation vaccine, if available, up to 4 days after exposure (*10*). The state of São Paulo, Brazil, discontinued smallpox vaccination after 1979, and no smallpox or monkeypox vaccine is available in Brazil. However, HCWs should be considered for vaccination as soon as it is available.

Our report describes clinical features of monkeypox, including extreme pain at the inoculation site and prolonged DNAemia, after needlestick transmission in a HCW. Preexposure and postexposure prophylaxis, including vaccination, should be provided for HCWs in Brazil.

About the Author

Dr. Bubach Carvalho is an infectious disease specialist at Universidade de São Paulo Hospital das Clínicas, São Paulo, Brazil. Her primary research interests include nosocomial disease transmission and hospital infection control procedures.

References

1. World Health Organization. WHO Director-General's statement at the press conference following IHR Emergency Committee regarding the multi-country outbreak of monkeypox—23 July 2022 [cited 2022 Aug 22]. https://www.who.int/director-general/speeches/detail/who-director-general-s-statement-on-the-press-conference-following-IHR-emergency-committee-regarding-the-multi--country-outbreak-of-monkeypox--23-july-2022
2. Thornhill JP, Barkati S, Walmsley S, Rockstroh J, Antinori A, Harrison LB, et al.; SHARE-net Clinical Group. Monkeypox virus infection in humans across 16 countries—April–June 2022. N Engl J Med. 2022;387:679–91. https://doi.org/10.1056/NEJMoa2207323
3. Beer EM, Rao VB. A systematic review of the epidemiology of human monkeypox outbreaks and implications for outbreak strategy. PLoS Negl Trop Dis. 2019;13:e0007791. https://doi.org/10.1371/journal.pntd.0007791
4. Vaughan A, Aarons E, Astbury J, Brooks T, Chand M, Flegg P, et al. Human-to-human transmission of monkeypox virus, United Kingdom, October 2018. Emerg Infect Dis. 2020;26:782–5. https://doi.org/10.3201/eid2604.191164
5. Reynolds MG, Yorita KL, Kuehnert MJ, Davidson WB, Huhn GD, Holman RC, et al. Clinical manifestations of human monkeypox influenced by route of infection. J Infect Dis. 2006;194:773–80. https://doi.org/10.1086/505880
6. Angelo KM, Petersen BW, Hamer DH, Schwartz E, Brunette G. Monkeypox transmission among international travellers-serious monkey business? J Travel Med. 2019;26:taz002. https://doi.org/10.1093/jtm/taz002
7. Adler H, Gould S, Hine P, Snell LB, Wong W, Houlihan CF, et al.; NHS England High Consequence Infectious Diseases (Airborne) Network. Clinical features and management of human monkeypox: a retrospective observational study in the UK. Lancet Infect Dis. 2022;22:1153–62. https://doi.org/10.1016/S1473-3099(22)00228-6
8. Zachary KC, Shenoy ES. Monkeypox transmission following exposure in healthcare facilities in nonendemic settings: low risk but limited literature. Infect Control Hosp Epidemiol. 2022;43:920–4. https://doi.org/10.1017/ice.2022.152
9. Loeb M, Zando I, Orvidas MC, Bialachowski A, Groves D, Mahoney J. Laboratory-acquired vaccinia infection. Can Commun Dis Rep. 2003;29:134–6.
10. WHO Emergency Response Team. Vaccines and immunization for monkeypox: interim guidance, 14 June 2022 [cited 2022 Aug 22]. https://www.who.int/publications/i/item/who-mpx-immunization-2022.1

Address for correspondence: Hermes R. Higashino, Hospital das Clínicas da Faculdade de Medicina da Universidade de São Paulo, Divisão de Moléstias Infecciosas e Parasitárias, Ave. Dr. Enéas de Carvalho Aguiar, 255 – 4o andar, São Paulo 05403-000, Brazil; email: hermes.higashino@hc.fm.usp.br

Monkeypox in Patient Immunized with ACAM2000 Smallpox Vaccine During 2022 Outbreak

Matthew Turner, Jeremy Mandia,[1] Case Keltner,[1] Robert Haynes,[1] Paul Faestel, Luke Mease

Author affiliation: Madigan Army Medical Center, Tacoma, Washington, USA

DOI: https://doi.org/10.3201/eid2811.221215

We report a case of monkeypox in the United States in a patient who had been vaccinated with ACAM2000 smallpox vaccine 8 years earlier. Despite his vaccination status, he still contracted disease. He showed prodromal symptoms preceding development of painless penile lesions that later coalesced.

In the summer of 2022, the Centers for Disease Control and Prevention initiated an emergency response because of a national outbreak of infection with monkeypox virus. On June 28, 2022, the US Department of Health and Human Services announced a national monkeypox vaccination strategy to contain the pandemic (*1*).

We report a patient in Washington, USA, who contracted monkeypox despite being successfully immunized against smallpox with the ACAM2000 smallpox vaccine (https://www.sanofi.com) 8 years earlier. We pose major questions regarding the efficacy of ACAM2000 vaccine amidst ongoing shortages of the JYNNEOS (https://www.bavarian-nordic.com) 2-dose monkeypox vaccine.

The patient was a previously healthy 34-year-old man who had sex with men came to a walk-in sexually transmitted infections clinic because of a 4-day history of malaise, fatigue, and headache and a 2-day history of 4 painless penile lesions. The patient had sought evaluation at a local emergency department 2 days before he visited the clinic. Results for testing performed in the emergency department were negative for *Neisseria gonorrhea*, *Chlamydia trachomatis*, and herpes simplex virus. His constitutional symptoms improved over the next 2 days. However, his penile ulcers progressed into white papular lesions, prompting him to seek reevaluation.

The patient had a medical history of noncomplicated *N. gonorrhea* infection and syphilis in 2017 that resolved after treatment. He had no history of HIV

[1]These authors contributed equally to this article.

infection or other immunocompromising condition documented in his military health records. He was previously prescribed daily emtricitabine/tenovir as preexposure prophylaxis for HIV, but he self-discontinued a year before he sought care. In the previous 90 days, he reported penetrative anal and receptive oral sexual intercourse with 13–14 new partners, denying any condom use. His last sexual intercourse was 11 days before he sought care, when he engaged in unprotected anal-insertive sex with a single anonymous partner at a local Pride event. Because of his military service, he was vaccinated against smallpox with ACAM2000 smallpox vaccine in March 2014, with documented vaccine take. He denied recent travel outside Washington or exposure to sick contacts.

On examination, the patient had 4 ulcerated penile lesions that had consolidated into a 3-cm patch present on the foreskin, 2 days after constitutional symptoms developed (Figure, panel A). The lesions were nontender to palpation, and no discharge was present. A tender 3-cm right inguinal lymph node was present. A vaccination scar was noted on his right deltoid, but the remainder of the examination was unremarkable.

Given the condition of the patient and his sexual history in the setting of an emerging monkeypox outbreak throughout the United States, a nonvariola orthopoxvirus PCR was conducted, and the result was positive. Subsequent confirmatory testing by the Centers for Disease Control and Prevention later identified the infection as the clade II strain (formerly West African clade). Additional serum studies, including HIV-1/2 antigen and antibody screening, syphilis screening, and hepatitis C virus screening, showed negative results.

Clinically the patient did well, only requiring supportive care with oral acetaminophen for constitutional symptoms, which resolved 10 days after symptom onset. The rash continued to evolve, coalesced, and developed a pustular appearance 6 days after onset of constitutional symptoms (Figure, panel B). The lesion ulcerated on day 16 (Figure, panel C), and ultimately dissipated without residual scarring (Figure, panel D).

Since the discontinuation of the global smallpox vaccination campaign after eradication of the disease in 1980, monkeypox is the primary circulating orthopoxvirus of public health concern. The ACAM2000 live vaccinia virus vaccine that this patient received in 2014 has been shown to provide protection against monkeypox (*2*,*3*). Earlier studies have reported that among persons vaccinated, monkeypox cases tend to be mild in number of lesions and prodromal symptoms (*4*–*6*). A study in 1988 reported that smallpox vaccination offered ≈85% protection against monkeypox (*4*,*7*). A study in 2008 reported that ACAM2000 vaccine fully protected cynomolgus monkeys after a lethal dose of monkeypox virus; 1 vaccinated animal had a minor rash at the site of inoculation (*8*), which is largely consistent with the manifestations and clinical course of this patient.

Although the mild manifestations in this patient might be attributable to his vaccination against smallpox, it did not prevent infection. The JYNNEOS vaccine is a nonreplicating vaccine product that has a

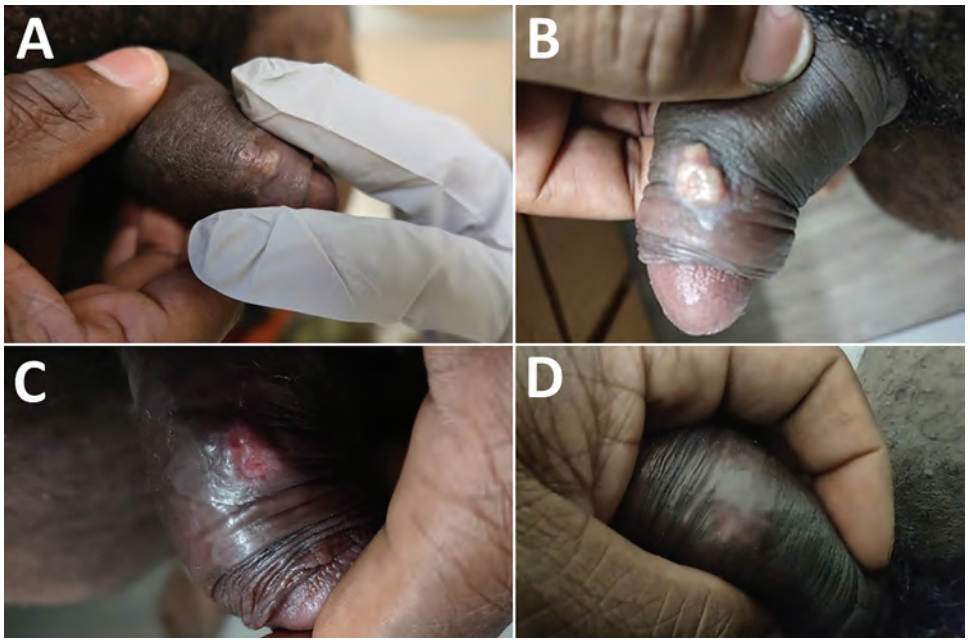

Figure. Evolution of penile lesions in patient who had monkeypox and was immunized with ACAM2000 smallpox vaccine during 2022 monkeypox outbreak, United States. A) Two days after constitutional symptoms developed; B) evolution of rash showing coalescence and development of a pustular appearance 6 days after onset of constitutional symptoms; C) ulceration of lesion on day 16; D) dissipation of lesion without residual scarring.

Food and Drug Administration indication to protect against smallpox and monkeypox (*9*). However, the JYNNEOS and ACAM2000 vaccines present disparate challenges. Specifically, the JYNNEOS vaccine is administered as a 2-dose regimen that shows a mild side effect profile, and the ACAM2000 vaccine is a single inoculation that can induce severe adverse effects. However, because of persistent JYNNEOS shortages hampering preexposure and postexposure prophylaxis efforts, vaccination with ACAM2000 might be an option in locales that urgently need immunizations protective against monkeypox. The efficacy of either vaccine in the current outbreak remains unknown.

Although vaccination is foundational for preventing infectious disease, this case highlights that vaccination alone does not guarantee immunity from monkeypox. Public health leaders should taper expectations that vaccination alone will end the outbreak. Vaccine should complement, not replace, public health campaigns that aim to minimize high-risk health behaviors.

Acknowledgments

We thank Jeanne Slusher and Stanley Conklin for providing assistance in the clinic, Patricia Vu and Karla Vegacolon for proactively developing a clinical plan for managing monkeypox patients, and Gavriella Simantov for assistance and guidance with laboratory testing.

About the Author

Dr. Turner is a transitional year intern physician at Madigan Army Medical Center in Tacoma, WA. His research interests include thyroid pathology and long-term neurologic sequela of spaceflight.

References

1. Services USDoHaH. HHS expands availability of monkeypox vaccine to more than 1.1 million doses. US Department of Health and Human Services [cited 2022 Sep 8]. https://www.hhs.gov/about/news/2022/07/28/hhs-expands-availability-of-monkeypox-vaccine-to-more-than-1-million-doses.html
2. Edghill-Smith Y, Golding H, Manischewitz J, King LR, Scott D, Bray M, et al. Smallpox vaccine-induced antibodies are necessary and sufficient for protection against monkeypox virus. Nat Med. 2005;11:740–7. https://doi.org/10.1038/nm1261
3. Reynolds MG, Damon IK. Outbreaks of human monkeypox after cessation of smallpox vaccination. Trends Microbiol. 2012;20:80–7. https://doi.org/10.1016/j.tim.2011.12.001
4. Fine PEM, Jezek Z, Grab B, Dixon H. The transmission potential of monkeypox virus in human populations. Int J Epidemiol. 1988;17:643–50. https://doi.org/10.1093/ije/17.3.643
5. Vaughan A, Aarons E, Astbury J, Brooks T, Chand M, Flegg P, et al. Human-to-human transmission of monkeypox virus, United Kingdom, October 2018. Emerg Infect Dis. 2020;26:782–5. https://doi.org/10.3201/eid2604.191164
6. Di Giulio DB, Eckburg PB. Human monkeypox: an emerging zoonosis. Lancet Infect Dis. 2004;4:15–25. https://doi.org/10.1016/S1473-3099(03)00856-9
7. Nalca A, Zumbrun EE. ACAM2000: the new smallpox vaccine for United States Strategic National Stockpile. Drug Des Devel Ther. 2010;4:71–9. https://doi.org/10.2147/DDDT.S3687
8. Marriott KA, Parkinson CV, Morefield SI, Davenport R, Nichols R, Monath TP. Clonal vaccinia virus grown in cell culture fully protects monkeys from lethal monkeypox challenge. Vaccine. 2008;26:581–8. https://doi.org/10.1016/j.vaccine.2007.10.063
9. US Food and Drug Administration. FDA approves first live, non-replicating vaccine to prevent smallpox and monkeypox. 2019 [cited 2022 Sep 8]. https://www.fda.gov/news-events/press-announcements/fda-approves-first-live-non-replicating-vaccine-prevent-smallpox-and-monkeypox

Address for correspondence: Robert Haynes, Public Health Clinical Services, 9025 Fifth St, Joint Base Lewis-McChord, WA 98431, USA; email: robert.c.haynes53.mil@health.mil

Vaccine Effectiveness against SARS-CoV-2 Variant P.1 in Nursing-Facility Residents, Washington, USA, April 2021

James W. Lewis, Julie Loughran, Li Deng, Jasmine Varghese, Shauna Clark, Casandra Harrison, Molly Gacetta, John A. Jernigan, Katherine E. Fleming-Dutra

Author affiliations: Public Health Seattle and King County, Seattle, Washington, USA (J.W. Lewis, J. Loughran, S. Clark, C. Harrison, M. Gacetta); Centers for Disease Control and Prevention, Atlanta, Georgia, USA (L. Deng, J. Varghese, J.A. Jernigan. K.E. Fleming-Dutra)

DOI: https://doi.org/10.3201/eid2811.221043

A SARS-CoV-2 P.1 (Gamma) variant outbreak occurred at a skilled nursing facility in Washington, USA, in April 2021. Effectiveness of 2 doses of mRNA vaccines against P.1 infection among residents in this outbreak was 75.0% (95% CI 44.5%–88.7%), similar to effectiveness for other pre-Delta variants among long-term care residents.

COVID-19 mRNA vaccines demonstrated high efficacy (>94%) against COVID-19 in clinical trials (*1*,*2*). However, initial observational vaccine effectiveness (VE) estimates against infection among residents of skilled nursing facilities (SNFs), a high-risk population, were lower, 53%–75% (*3*). A local health department in Washington, USA, investigated a COVID-19 outbreak of the P.1 (Gamma) variant in April 2021 in an SNF and estimated VE of 2 mRNA vaccine doses against SARS-CoV-2 infection. The Centers for Disease Control and Prevention reviewed the activity to confirm it was conducted consistent with applicable federal law and organizational policy. This investigation was defined as having met the requirements for public health surveillance as outlined in 45 C.F.R. part 46.102(l) (*2*).

Daily symptom screening of residents and staff had been ongoing in this SNF since March 2020. Routine antigen testing of symptomatic residents with BinaxNOW tests (Abbott Diagnostics, https://www.diagnostics.abbott) was performed upon symptom recognition; routine testing of staff was ongoing. Nucleic acid amplification test (NAAT) confirmation of all positive antigen results and antigen negative results for symptomatic persons was performed. The outbreak index case was a symptomatic fully vaccinated resident identified on April 16, 2021. All residents and staff were tested immediately and again every 3–7 days for the duration of the outbreak period, April 15–May 9, 2021.

We defined a case as a positive SARS-CoV-2 antigen or NAAT result in a resident of the SNF. The local health jurisdiction requested viral whole-genome sequencing (WGS) for all positive specimens. Washington State Department of Health Public Health Laboratories and their partners identified SARS-CoV-2 variant status for individual cases through WGS and recorded cases in the Washington Disease Reporting System.

The SNF conducted vaccination clinics on January 12, February 2, and February 23, 2021. We defined vaccination status as fully vaccinated with 2 doses, if receipt of second vaccine dose was ≥14 days before the outbreak began (*4*), and unvaccinated if no COVID-19 vaccine had been received before or during the outbreak. We excluded from the VE analysis residents who were partially vaccinated (i.e., who had received 1 vaccine dose or had received a second dose ≤14 days before the outbreak). We ascertained vaccination status through Washington Immunization Information System and facility medical records. We obtained age, race, ethnicity, and comorbidity information from facility medical records.

We calculated VE for 2 mRNA vaccine doses on the basis of relative risk (RR) of infection in vaccinated versus unvaccinated residents using a log-binomial model and adjusted for potential confounders of age (<85 vs. ≥85 years) and race (White vs. all other residents with nonmissing race). We used the equation VE = 100% × (1 − RR). We conducted a separate analysis limited to WGS-confirmed P.1 cases to estimate VE against P.1 infection.

Of 63 residents present during the outbreak, 43 (68%) were fully vaccinated with 2 doses and 16 (25%) were unvaccinated; we excluded 4 partially vaccinated residents from the analysis. Thirty-six (84%) of 43 vaccinated residents received vaccination during the onsite clinics. Seven residents (16%) were fully vaccinated at other locations. Nineteen residents tested positive for SARS-CoV-2 during the outbreak (Figure; Appendix Figure, https://wwwnc.cdc.gov/EID/article/28/11/22-1043-App1.pdf); 2 of those were partially vaccinated and excluded from analysis. Of the 17 included outbreak

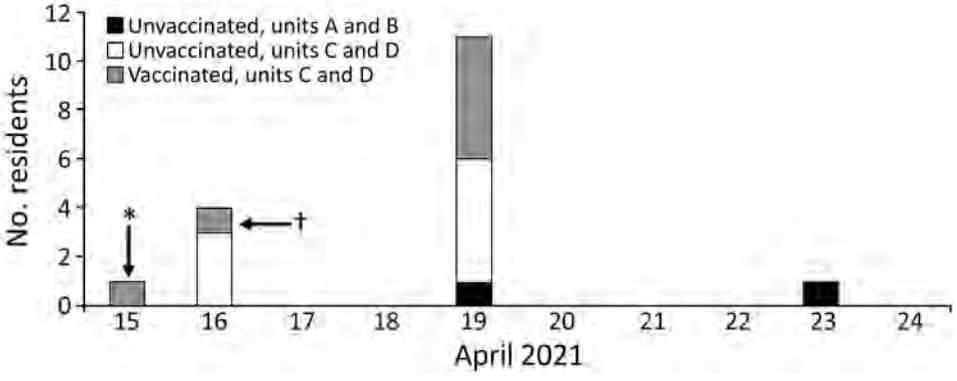

Figure. Date of first positive SARS-COV-2 specimen collection among residents in a skilled nursing facility, Washington, April 2021, Cases shown are restricted to the 17 resident cases included in vaccine effectiveness (VE) analysis. Testing was concentrated on point prevalence survey days. Units A and B were long-stay units; units C and D were short-stay units. Asterisk (*) indicates a resident who was discharged from a short-stay unit and later tested positive at an area hospital; dagger (†) indicates a resident who tested positive after symptom screening.

Table. Characteristics of residents in a skilled nursing facility included in a SARS-CoV-2 vaccine effectiveness analysis, Washington, USA, April 2021*

Characteristic	No. (%) fully vaccinated	No. (%) unvaccinated
Residents present during outbreak	43	16
Sex		
M	15 (35)	7 (44)
F	28 (65)	9 (56)
Age group, y		
60–74	7 (16)	4 (25)
75–84	14 (33)	6 (38)
≥85	22 (51)	6 (38)
Race†		
Asian	5 (12)	0
Black or African-American	0	2 (13)
White	36 (84)	13 (81)
Other	1 (2)	0
Unknown	1 (2)	1 (6)
Underlying health conditions		
Hypertension	32 (75)	10 (63)
Neurologic disease	32 (75)	15 (94)
Cardiovascular disease	27 (63)	13 (81)
Diabetes	14 (33)	3 (19)
Asthma, COPD, sleep apnea, other chronic respiratory disease	12 (28)	7 (44)
Obesity	7 (16)	4 (25)
Autoimmune condition	5 (12)	0
Cancer	2 (5)	1 (6)
Immunosuppressive disease or medication	2 (5)	0
End-stage renal disease requiring dialysis	0	1 (6)
Other, nonneurologic condition	42 (98)	16 (100)
≥2 underlying conditions	43 (100)	16 (100)
Unit		
Unit A, long-stay unit	15 (35)	4 (25)
Unit B, long-stay unit	16 (37)	4 (25)
Unit C, short-stay unit	10 (23)	4 (25)
Unit D, short-stay unit	2 (5)	4 (25)
History of prior SARS COV-2 infection‡	13 (30)	3 (19)
Tested positive for SARS COV-2 during outbreak period	7 (16)	10 (63)

*Four residents who were partially vaccinated (received 1 dose of COVID-19 vaccine) were excluded from this analysis. COPD, chronic obstructive pulmonary disease.
†No residents reported Hispanic or Latino ethnicity. Data for ethnicity was highly missing; 25 (58%) vaccinated residents and 8 (50%) unvaccinated residents were of unknown ethnicity.
‡All previous infections were >3 mo before start of outbreak (before January 13, 2021).

cases, 7 were in fully vaccinated residents. Thirteen (77%) of 17 outbreak cases had WGS data; all were identified as P.1 lineage.

Most of the 59 residents included in the analysis were White (83%) and female (63%); the age range was ≥60 years (Table). Ethnicity was unknown for 56% of residents. All residents had ≥2 underlying health conditions that may increase risk for severe COVID-19.

The attack rate in unvaccinated residents was 63% (10/16) versus 16% (7/43) in fully vaccinated residents (adjusted RR 4.0, 95% CI 1.8–8.9). Unadjusted VE against infection was 74.0% (95% CI 43.4%–88.0%). Age-adjusted and race-adjusted VE against infection among 57 residents (excluding 2 residents with unknown race) was 75.0% (95% CI 44.5%–88.7%). Age- and race-adjusted VE against WGS-confirmed P.1 infection among 53 residents (excluding 2 residents with unknown race) was 80.0% (95% CI 46.4%–92.6%). In this outbreak, vaccination was associated with decreased likelihood of infection. Our estimated VE of 75% (95% CI 45%–89%) against infection is consistent with other findings of mRNA VE against infection with other pre-Delta variants among residents of SNFs (*3*–*7*).

The first limitation of our study is that unvaccinated residents might have differed from vaccinated in ways we did not measure, including in the use of mitigation behaviors. In addition, the demographics of residents in this facility may differ from the broader general long-term care resident population.

In conclusion, our evaluation indicates that receiving 2 mRNA vaccine doses was effective in reducing the likelihood of testing positive for SARS-CoV-2 during an outbreak of P.1 lineage variant in an SNF. VE against P.1 is comparable to that against other pre-Delta SARS-CoV-2 variants among long-term care residents.

Acknowledgments

We are grateful to the staff and residents of the SNF described in this study. We thank the Washington State Department of Health Office of Communicable Disease Epidemiology Staff who worked to collect specimens for WGS and provided data for the project. We also thank the Washington State Department of Health Public Health Laboratories COVID-19 Team who generated the SARS-CoV-2 genomic data and shared this data to GISAID.

This work was funded by the Centers for Disease Control and Prevention and Public Health Seattle and King County.

About the Author

Dr. Lewis is a board-certified physician in internal medicine, infectious disease, and preventive medicine. He is currently the health officer for the Snohomish County Health District; prior to this position and during the initial composition of this article he was a medical epidemiologist at Public Health Seattle & King County helping to oversee the response to the SARS-CoV-2 pandemic in healthcare settings.

References

1. Polack FP, Thomas SJ, Kitchin N, Absalon J, Gurtman A, Lockhart S, et al.; C4591001 Clinical Trial Group. Safety and efficacy of the BNT162b2 mRNA COVID-19 vaccine. N Engl J Med. 2020;383:2603–15. https://doi.org/10.1056/NEJMoa2034577
2. Baden LR, El Sahly HM, Essink B, Kotloff K, Frey S, Novak R, et al.; COVE Study Group. Efficacy and safety of the mRNA-1273 SARS-CoV-2 vaccine. N Engl J Med. 2021;384:403–16. https://doi.org/10.1056/NEJMoa2035389
3. Nanduri S, Pilishvili T, Derado G, Soe MM, Dollard P, Wu H, et al. Effectiveness of Pfizer-BioNTech and Moderna vaccines in preventing SARS-CoV-2 infection among nursing home residents before and during widespread circulation of the SARS-CoV-2 B.1.617.2 (Delta) variant —National Healthcare Safety Network, March 1–August 1, 2021. MMWR Morb Mortal Wkly Rep. 2021;70:1163–6. https://doi.org/10.15585/mmwr.mm7034e3
4. Mazagatos C, Monge S, Olmedo C, Vega L, Gallego P, Martín-Merino E, et al.; Working Group for the surveillance and control of COVID-19 in Spain; Working group for the surveillance and control of COVID-19 in Spain. Effectiveness of mRNA COVID-19 vaccines in preventing SARS-CoV-2 infections and COVID-19 hospitalisations and deaths in elderly long-term care facility residents, Spain, weeks 53 2020 to 13 2021. Euro Surveill. 2021;26:2100452. https://doi.org/10.2807/1560-7917.ES.2021.26.24.2100452
5. Lefèvre B, Tondeur L, Madec Y, Grant R, Lina B, van der Werf S, et al. Beta SARS-CoV-2 variant and BNT162b2 vaccine effectiveness in long-term care facilities in France. Lancet Healthy Longev. 2021;2:e685–7. https://doi.org/10.1016/S2666-7568(21)00230-0
6. Cavanaugh AM, Fortier S, Lewis P, Arora V, Johnson M, George K, et al. COVID-19 outbreak associated with a SARS-CoV-2 R.1 lineage variant in a skilled nursing facility after vaccination program—Kentucky, March 2021. MMWR Morb Mortal Wkly Rep. 2021;70:639–43. https://doi.org/10.15585/mmwr.mm7017e2
7. Williams C, Al-Bargash D, Macalintal C, Stuart R, Seth A, Latham J, et al. Coronavirus disease 2019 (COVID-19) outbreak associated with severe acute respiratory syndrome coronavirus 2 (SARS-CoV-2) P.1 lineage in a long-term care home after implementation of a vaccination program—Ontario, Canada, April–May 2021.. Clin Infect Dis. 2022;74:1085–8. https://doi.org/10.1093/cid/ciab617

Address for correspondence: James Lewis, 3020 Rucker Ave, Ste 206, Everett, WA 98201, USA; email: jlewis@snohd.org; Katherine Fleming-Dutra, Centers for Disease Control and Prevention, 1600 Clifton Rd NE, Mailstop H24-6, Atlanta, GA 30329-4027, USA; email: ftu2@cdc.gov

Reinfections with Different SARS-CoV-2 Omicron Subvariants, France

Nhu Ngoc Nguyen, Linda Houhamdi, Léa Delorme, Philippe Colson, Philippe Gautret

Author affiliations: Aix Marseille University, Marseille, France; Institut Hospitalo-Universitaire Méditerranée Infection, Marseille

DOI: https://doi.org/10.3201/eid2811.221109

We describe 188 patients in France who were successively infected with different SARS-CoV-2 Omicron subvariants, including BA.1, BA.2, and BA.5. Time between 2 infections was ≤90 days for 50 (26.6%) patients and <60 days for 28 (14.9%) patients. This finding suggests that definitions for SARS-CoV-2 reinfection require revision.

In Belgium, 96 cases of early SARS-CoV-2 reinfection were reported during December 1, 2021–March 10, 2022; the cases had a median of 47 days (range 17–65 days) between 2 positive samples (*1*). Five of those cases indicated primary infections with Omicron subvariant BA.1, followed by Omicron BA.2 reinfections. In addition, we previously reported that the reinfection risk with Omicron was 6-fold higher than with other SARS-CoV-2 variants (*2*). In this study, we describe cases of COVID-19 reinfection with different Omicron subvari-

ants after a primary infection with Omicron subvariants BA.1 or BA.2 in Marseilles, France. We performed real-time reverse transcription PCR and next-generation genomic sequencing of nasopharyngeal swab samples to identify subvariants as previously described (*3*). We retrospectively retrieved patient age and gender information from electronic medical files and anonymized data before analysis. We identified reinfected patients by using a computerized alert system that focused on samples with primary Omicron BA.1 or BA.2 subvariant infections followed by reinfection with any Omicron subvariant. This study was approved by the ethics committee of the University Hospital Institute Méditerranée Infection (approval no. 2022–029). Access to patient biologic and registry data in the hospital information system was approved by the data protection committee of Assistance Publique-Hôpitaux de Marseille and recorded in the European General Data Protection Regulation registry (no. RGPD/APHM 2019–73).

We identified 188 (0.7%) cases of reinfection out of 27,972 patient samples that tested positive for the SARS-CoV-2 Omicron variant during November 28, 2021–July 22, 2022. Of those 188 patients, 181 were first infected with the Omicron BA.1 subvariant and were reinfected as follows: 82 patients with Omicron BA.2, 14 patients with Omicron BA.4, 84 patients with Omicron BA.5, and 1 patient with a BA.1 and BA.2 recombinant subvariant (XAC recombinant lineage) (Appendix Figure, https://wwwnc.cdc.gov/EID/article/28/11/22-1109-App1.pdf). Three of the 181 patients infected with Omicron BA.1 were reinfected 2 times; for the first reinfection, they were infected with Omicron BA.2 and, for the second reinfection, they were infected with Omicron BA.5. In addition, 7 patients were first infected with the Omicron BA.2 subvariant, after which 1 patient was reinfected with the Omicron BA.4 subvariant, and 6 patients were reinfected with the Omicron BA.5 subvariant.

Patients were 1–83 (median 32) years of age at the time of their second infection, and 131 (69.7%) were women. The median time between the primary and secondary infections was 146 days (range 7–214 days); median time between infection with Omicron BA.1 and reinfection with BA.2 was 84 days and for a primary infection with Omicron BA.1 and reinfection with BA.5 was 171 days (Appendix Figure). Among the 188 patients infected first with Omicron BA.1 or BA.2, the time between the primary and secondary infections was 1–29 days in 6 (3.2%) cases, 30–44 days in 4 (2.1%) cases, 45–59 days in 18 (9.6%) cases, 60–74 days in 10 (5.3%) cases, 75–89 days in 11 (5.8%) cases, and ≥90 days in 139 (73.9%) cases. In 50/188 (26.6%) patients, time between the 2 infections was ≤90 days and, in 28/188 (14.9%) patients, the time was <60 days between the 2 infections.

Our findings indicate that the time between confirmed primary infections and reinfections with different Omicron subvariants is frequently shorter than the 90-day definition of reinfections used by the US Centers for Disease Control and Prevention (*4*). Furthermore, the time can be shorter than the 60-day definition of reinfections used by the European Centre for Disease

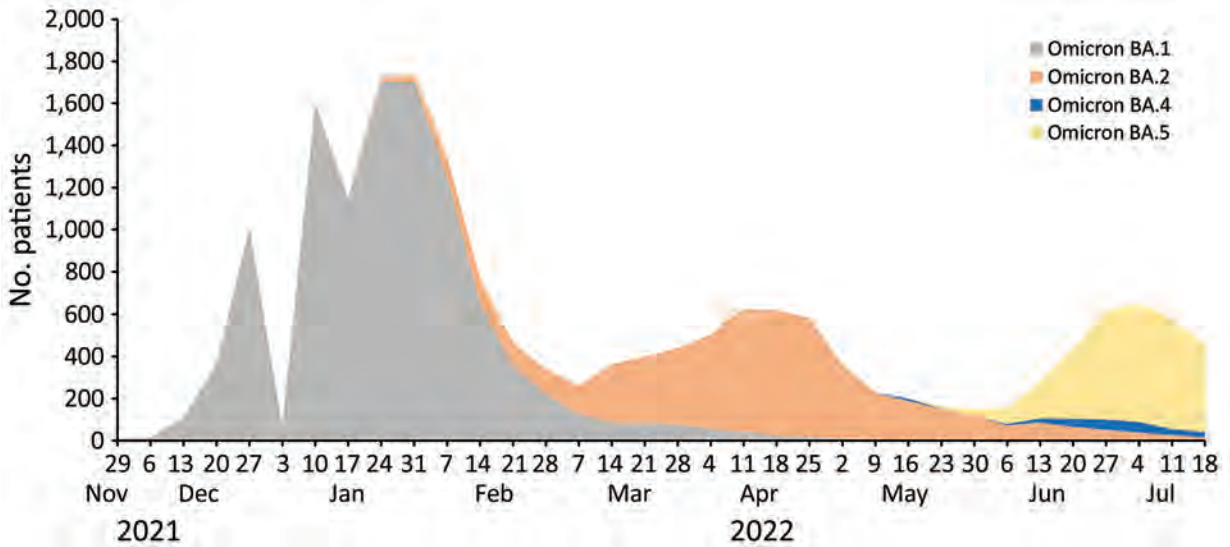

Figure. Number of patients with infections from different SARS-CoV-2 Omicron subvariants, France, November 28, 2021–July 22, 2022. Overall dynamics of infections with Omicron subvariants BA.1, BA.2, BA.4, and BA.5 are shown for cases diagnosed at the Institut Méditerranée Infection, Marseille, France. We performed real-time reverse transcription PCR and next-generation genomic sequencing of nasopharyngeal swab samples to identify Omicron subvariants BA.1, BA.2, BA.4, and BA.5. A total of 27,972 patient samples tested positive for Omicron subvariants.

Prevention and Control (*5*). Similar to our findings, a study from Denmark reported 47 Omicron BA.2 reinfections that occurred 20–60 days after a primary BA.1 infection (M. Stegger et al., unpub. data, https://www.medrxiv.org/content/10.1101/2022.02.19.22271112v1).

The first limitation of our study is that the number of cases was small. Second, we cannot exclude that some cases might have been concurrent infections with different subvariants, notably in the 3 cases that had a 7-day interval between the detection of 2 subvariants. In Marseille, the short time between emergence of different Omicron subvariants might have favored co-infections with different subvariants circulating within the population (Figure). Co-infections can be missed if the quantitative PCR has inadequate sensitivity, and whole-genome sequencing might fail to detect a variant with low prevalence in a patient. Finally, because most reinfection cases were identified from samples transferred to our laboratory by external entities, we were unable to describe COVID-19 vaccination and clinical status of the patients. Nonetheless, our results suggest that the currently used definitions for SARS-CoV-2 reinfection require revision with regard to the duration between primary and secondary infections.

This work was supported by the "Investments for the Future" program managed by the National Agency for Research (ANR) (Méditerranée-Infection 10-IAHU-03), Région Provence Alpes Côte d'Azur, European funding agency FEDER PRIMMI (Fonds Européen de Développement Régional-Plateformes de Recherche et d'Innovation Mutualisées Méditerranée Infection) (FEDER PA 0000320 PRIMMI), Ministry of Higher Education, Research and Innovation (Ministère de l'Enseignement supérieur, de la Recherche et de l'Innovation), and Ministry of Solidarity and Health (Ministère des Solidarités et de la Santé), France.

About the Author

Dr. Nguyen is a medical doctor and PhD student at the Aix Marseille University and Institut Hospitalo-Universitaire Méditerranée Infection, Marseille, France. Her research interests focus on long COVID and SARS-CoV-2 reinfections.

References

1. Nevejan L, Cuypers L, Laenen L, Van Loo L, Vermeulen F, Wollants E, et al. Early SARS-CoV-2 reinfections within 60 days and implications for retesting policies. Emerg Infect Dis. 2022;28:1729–31. https://doi.org/10.3201/eid2808.220617
2. Nguyen NN, Houhamdi L, Hoang VT, Stoupan D, Fournier PE, Raoult D, et al. High rate of reinfection with the SARS-CoV-2 Omicron variant. J Infect. 2022;85:174–211. https://doi.org/10.1016/j.jinf.2022.04.034
3. Colson P, Fournier PE, Chaudet H, Delerce J, Giraud-Gatineau A, Houhamdi L, et al. Analysis of SARS-CoV-2 variants from 24,181 patients exemplifies the role of globalization and zoonosis in pandemics. Front Microbiol. 2022;12:786233. https://doi.org/10.3389/fmicb.2021.786233
4. Centers for Disease Control and Prevention. Coronavirus disease 2019 (COVID-19) 2021 case definition [cited 2022 Sep 8]. https://ndc.services.cdc.gov/case-definitions/coronavirus-disease-2019-2021
5. European Centre for Disease Prevention and Control. Reinfection with SARS-CoV-2: implementation of a surveillance case definition within the EU/EEA [cited 2022 Sep 8]. https://www.ecdc.europa.eu/en/publications-data/reinfection-sars-cov-2-implementation-surveillance-case-definition-within-eueea

Address for correspondence: Philippe Gautret, VITROME, Institut Hospitalo-Universitaire Méditerranée Infection, 19-21 Boulevard Jean Moulin, 13385 Marseille CEDEX 05, France; email: philippe.gautret@club-internet.fr

Human Parainfluenza Virus in Homeless Shelters before and during the COVID-19 Pandemic, Washington, USA

Eric J. Chow, Amanda M. Casto, Reigran Sampoleo, Margaret G. Mills, Peter D. Han, Hong Xie, Brian Pfau, Tien V. Nguyen, Jaydee Sereewit, Julia H. Rogers, Sarah N. Cox, Melissa A. Rolfes, Constance Ogokeh, Emily Mosites, Timothy M. Uyeki, Alexander L. Greninger, James P. Hughes, M. Mia Shim, Nancy Sugg, Jeffrey S. Duchin, Lea M. Starita, Janet A. Englund, Pavitra Roychoudhury, Helen Y. Chu

Author affiliations: University of Washington, Seattle, Washington, USA (E.J. Chow, A.M. Casto, R. Sampoleo, M.G. Mills, P.D. Han, H. Xie, B. Pfau, T.V. Nguyen, J. Sereewit, J.H. Rogers, S.N. Cox, A.L. Greninger, J.P. Hughes, M.M. Shim, N. Sugg, J.S. Duchin, L.M. Starita, P. Roychoudhury, H.Y. Chu); Fred Hutchinson Cancer Research Center, Seattle (A.M. Casto, A.L. Greninger, J.P. Hughes, P. Roychoudhury); Brotman Baty Institute for

Precision Medicine, Seattle (P.D. Han, H. Xie, B. Pfau, L.M. Starita); Centers for Disease Control and Prevention, Atlanta, Georgia, USA (M.A. Rolfes, C. Ogokeh, E. Mosites, T.M. Uyeki); Military and Health Research Foundation, Laurel, Maryland, USA (C. Ogokeh); Public Health Seattle and King County, Seattle (M.M. Shim, J.S. Duchin); University of Washington Seattle Children's Research Institute, Seattle (J.A. Englund)

DOI: https://doi.org/10.3201/eid2811.221156

To determine the epidemiology of human parainfluenza virus in homeless shelters during the COVID-19 pandemic, we analyzed data and sequences from respiratory specimens collected in 23 shelters in Washington, USA, during 2019–2021. Two clusters in children were genetically similar by shelter of origin. Shelter-specific interventions are needed to reduce these infections.

Human parainfluenza virus (HPIV) contributes to acute respiratory tract infection burden in young children (1) and adults (2). Persons experiencing homelessness are among those at risk for respiratory viral complications caused by chronic disease burden, mental illness, and social inequities. Homeless shelters might lack resources to reduce viral transmission by using nonpharmaceutical interventions (NPIs). We describe HPIV epidemiology in homeless shelters in King County, Washington, USA, before and during the COVID-19 pandemic.

We analyzed respiratory virus surveillance data from 2 previously described homeless shelter studies (*3*,*4*) conducted during October 2019–May 2021. Eligible participants were residents at 1 of 23 homeless shelters who were ≥3 months of age and had a cough or ≥2 other acute respiratory illness symptoms. At enrollment, consenting participants or guardians completed questionnaires, and upper respiratory specimens were collected; each enrollment was considered 1 encounter. Once a month, persons were eligible to enroll, regardless of symptoms. Beginning April 1, 2020, enrollment expanded to residents and staff, regardless of symptoms. Participants could enroll multiple times; encounters were linked by name and birthdate.

We tested samples by using a TaqMan reverse transcription PCR platform that included influenza virus (A, B, C), respiratory syncytial virus, HPIV (*1*–*4*), human coronaviruses, rhinovirus, enterovirus, human bocavirus, human parechovirus, human metapneumovirus, adenovirus, and SARS-CoV-2 (beginning January 1, 2020). A cycle threshold value was generated. We typed HPIV-positive specimens, performed whole-genome sequencing by using hybrid capture on specimens that had a cycle threshold value <22 (Appendix, https://wwwnc.cdc.gov/EID/article/28/11/22-1156-App1.pdf), and submitted genomes to GenBank (Appendix Table 1). We aligned shelter consensus genomes generated with corresponding HPIV type genomes from GenBank, generated type-specific phylogenetic trees, and visualized trees by using NextStrain Auspice software (https://github.com). We analyzed the data descriptively by using SAS software version 9.4 (https://www.sas.com).

During October 2019–May 2021, the study conducted 14,464 encounters with 3,281 unique participants (median age 37 years, range 0.3–85 years; 16% children; 17% shelter staff) (Appendix Figure 1). Among 1,569 encounters with positive virus test results, 32 (2%) encounters from 29 unique participants were HPIV positive (median age 29 years, range 0.3–64 years; 62% children, 45% female, 52% white, 100% resident; 10% had ≥1 chronic condition) (Appendix Table 2). Most HPIV-positive encounters

Table. Human parainfluenza virus detection across 23 homeless shelters, King County, Washington, USA, October 2019–May 2021*

Time period	Type of shelter	Total	Human parainfluenza virus, no. (%) positive	Human parainfluenza virus types
Before April 1, 2020	Shelters: family (sites D, E, O)	303	16 (5.3)	HPIV-1, n = 5; HPIV-3, n = 6; HPIV-4, n = 5;
	Shelters: adults 18–25 y (site C)	89	1 (1.1)	HPIV-1, n = 1
	Shelters: adults ≥18 y (sites A, B, F, L)	845	3 (0.4)	HPIV-1, n = 2; HPIV untyped, n = 1
	Shelters: adults ≥50 y (site M)	453	3 (0.7)	HPIV-1, n = 2; HPIV untyped, n = 1
After April 1, 2020	Shelters: family (sites: D, E, H, N, O, OF, OG)	4,764	8 (0.2)	HPIV-3, n = 5; HPIV untyped, n = 3
	Shelters: adults 18–25 y (sites C, OH)	1,228	0	NA
	Shelters: adults ≥18 y (sites A, B, F, G, J, K, L, OB, OD)	6,078	1 (0.02)	HPIV untyped, n = 1
	Shelters: adults ≥50 y (sites I, M, OA, OC, OE)	661	0	NA
Total		14,421†	32 (0.2)	HPIV-1, n = 10; HPIV-3, n = 11; HPIV-4, n = 5; HPIV untyped, n = 6

*A Washington State Stay-At-Home ordinance we issued on March 23, 2020. HPIV, human parainfluenza virus; NA, not available.
†n = 43 encounters for which dates were missing were not included (none involved human parainfluenza-positive specimens).

(72%) occurred before April 1, 2020, and the highest HPIV-positive percentage was observed in family shelters (Table).

Six of 32 encounters involved viral co-infections with HPIV (rhinovirus, adenovirus, human bocavirus, enterovirus, and human parechovirus). Participants with HPIV infection reported symptoms at 25 (78%) encounters. Commonly reported symptoms included rhinorrhea (95%), cough (74%), sore throat (53%), and subjective fevers (47%) (Appendix Table

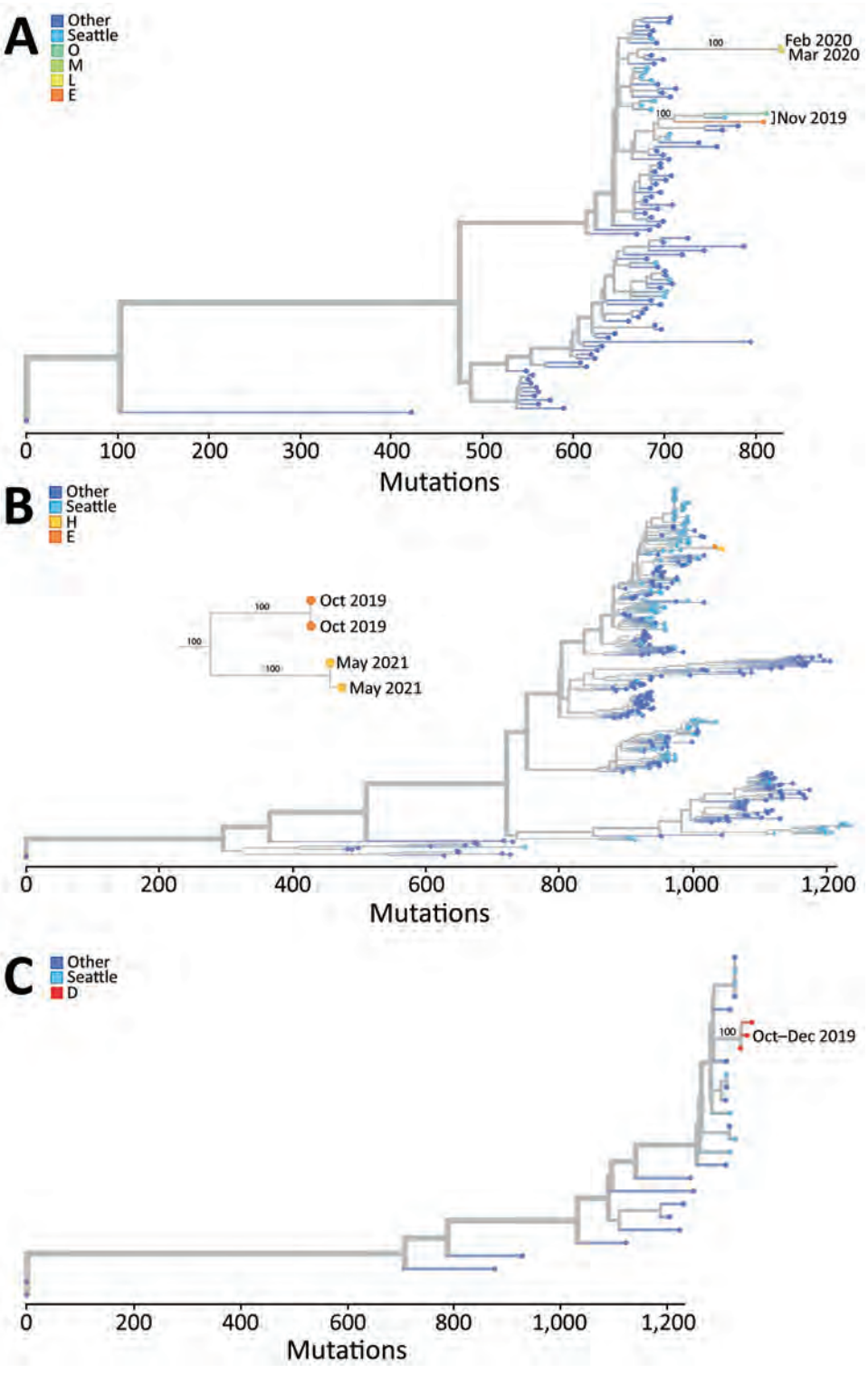

Figure. Phylogenetic trees of human parainfluenza viruses in homeless shelters, King County, Washington, USA, October 2019–May 2021. A) Human parainfluenza virus 1; B) human parainfluenza virus 3; C) human parainfluenza virus 4a. Letters in keys indicate different homeless shelters from which sequenced specimens were collected. Other indicates genomic data from locations not in Seattle, Washington. Seattle indicates genomic data from Seattle other than homeless shelters in this study.

3). HPIV-positive specimens occurred every month during October 2019–April 2020 (Appendix Figure 2). Only 2 HPIV infections were identified during May 2020–April 2021, despite an average of 954 monthly encounters. Six HPIV infections occurred during May 2021 (Appendix Figure 3).

Of 32 HPIV-positive specimens, we identified 3 of the 4 HPIV serotypes: 10 HPIV-1, 11 HPIV-3, and 5 HPIV-4. Six specimens were untypeable. Sequencing of 16 specimens generated 11 sequences (4 HPIV-1, 4 HPIV-3, and 3 HPIV-4a) from 6 shelters (Figure). HPIV-1 sequences formed 2 clusters (100% bootstrap support for each cluster) by collection date in a maximum-likelihood tree that included 94 GenBank HPIV-1 genomes. Both HPIV-3 and HPIV-4a sequences formed single genetic clusters (100% bootstrap support for each cluster) in a maximum-likelihood tree that included 397 GenBank HPIV-3 and 24 HPIV-4a genomes. The HPIV-3 clusters involved HPIV-positive specimens from shelters E (October 2019) and H (May 2021); both shelters housed adults and children. In shelter E, HPIV-3–positive specimens resulted from 6 encounters involving 5 unique participants (all children) spanning 9 days, and 2 specimens were sequenced. In shelter H, 5 HPIV-3 encounters involving 4 unique participants (all children) spanned 17 days, and 2 specimens were sequenced. The sequenced HPIV-3 specimens from shelters E and H, each from unique persons, formed 2 subclusters, each with 100% bootstrap support, corresponding to shelter and collection date.

Respiratory viruses are increasingly appreciated as major pathogens in homeless shelters (*5*,*6*), We identified HPIV infections in shelter residents of all ages, although predominantly in children. Family shelters that have mixed populations of adults and children had the greatest percentage of HPIV detections. Two pediatric HPIV-3 clusters occurred before and during the COVID-19 pandemic with genetic clustering by shelter. After the Washington stay-at-home ordinance on March 23, 2020, overall numbers of HPIV infections decreased. These reductions (*7*) were probably in part caused by community implementation of NPIs because respiratory droplets are probably the main mode of HPIV transmission (*8*). However, HPIV has been detected on environmental surfaces (*9*), and shelter site resources might not enable adequate social distancing and air quality.

The pediatric HPIV-3 cases illustrate the need for mitigation guidance to reduce intrashelter HPIV transmission, particularly because younger children have higher upper respiratory tract viral levels than older persons (*10*). Limitations of this study included potential selection bias, a lack of site-specific NPI data, cross-sectional study design, and inability to compare concurrent shelter results to community HPIV epidemiology. These HPIV data provide information on site-specific characteristics to inform public health guidance.

The University of Washington Institutional Review Board (study no. 00007800) approved this study.

This study was supported by Gates Ventures, the Centers for Disease Control and Prevention (research contract no. 75D30120C09322 AM002 to H.Y.C.), and the National Institute of Allergy and Infectious Diseases, National Institutes of Health (grant no. T32 AI007044 to E.J.C.).

E.J.C. reported honoraria from Providence Health and Services, Seattle, Washington, for presentations on C OVID-19; S.N.C. reported honoraria from University of California, Berkeley, for presentations on COVID-19; A.L.G. reported contract testing for Abbott, Cepheid, Novavax, Pfizer, Janssen, and Hologic and research support from Gilead and Merck, outside of the submitted work; P.R. reported honoraria from The Bill and Melinda Gates Foundation for presentations on COVID-19; J.A.E. reported consulting with Sanofi Pasteur, AstraZeneca, and Meissa Vaccines, and has received research funding from AstraZeneca, GlaxoSmithKline, Merck, and Pfizer outside the submitted work; and H.Y.C. reported consulting with Ellume, Pfizer, The Bill and Melinda Gates Foundation, Glaxo Smith Kline, and Merck, has received research funding from Gates Ventures and Sanofi Pasteur, and support and reagents from Ellume and Cepheid outside of the submitted work.

About the Author

Dr. Chow is the chief of communicable disease epidemiology and immunizations at Public Health Seattle and King County, Seattle, WA. His primary research interests include respiratory virus epidemiology in community settings.

References

1. Wang X, Li Y, Deloria-Knoll M, Madhi SA, Cohen C, Arguelles VL, et al.; Respiratory Virus Global Epidemiology Network. Global burden of acute lower respiratory infection associated with human parainfluenza virus in children younger than 5 years for 2018: a systematic review and meta-analysis. Lancet Glob Health. 2021;9:e1077–87. https://doi.org/10.1016/S2214-109X(21)00218-7
2. Howard LM, Edwards KM, Zhu Y, Williams DJ, Self WH, Jain S, et al. Parainfluenza virus types 1-3 infections among children and adults hospitalized with community-acquired pneumonia. Clin Infect Dis. 2021;73:e4433–43. https://doi.org/10.1093/cid/ciaa973

3. Newman KL, Rogers JH, McCulloch D, Wilcox N, Englund JA, Boeckh M, et al.; Seattle Flu Study Investigators. Point-of-care molecular testing and antiviral treatment of influenza in residents of homeless shelters in Seattle, WA: study protocol for a stepped-wedge cluster-randomized controlled trial. Trials. 2020;21:956. https://doi.org/10.1186/s13063-020-04871-5
4. Rogers JH, Link AC, McCulloch D, Brandstetter E, Newman KL, Jackson ML, et al.; Seattle Flu Study Investigators. Characteristics of COVID-19 in homeless shelters: a community-based surveillance study. Ann Intern Med. 2021;174:42–9. https://doi.org/10.7326/M20-3799
5. Chow EJ, Casto AM, Roychoudhury P, Han PD, Xie H, Pfau B, et al. The clinical and genomic epidemiology of rhinovirus in homeless shelters, King County, Washington. J Infect Dis. 2022;jiac239. https://doi.org/10.1093/infdis/jiac239
6. Chow EJ, Casto AM, Rogers JH, Roychoudhury P, Han PD, Xie H, et al. The clinical and genomic epidemiology of seasonal human coronaviruses in congregate homeless shelter settings: A repeated cross-sectional study. Lancet Reg Health Am. 2022;15:100348. https://doi.org/10.1016/j.lana.2022.100348
7. Olsen SJ, Winn AK, Budd AP, Prill MM, Steel J, Midgley CM, et al. Changes in influenza and other respiratory virus activity during the COVID-19 pandemic-United States, 2020–2021. Am J Transplant. 2021;21:3481–6. https://doi.org/10.1111/ajt.16049
8. Henrickson KJ. Parainfluenza viruses. Clin Microbiol Rev. 2003; 16:242–64. https://doi.org/10.1128/CMR.16.2.242-264.2003
9. Brady MT, Evans J, Cuartas J. Survival and disinfection of parainfluenza viruses on environmental surfaces. Am J Infect Control. 1990;18:18–23. https://doi.org/10.1016/0196-6553(90)90206-8
10. Hall CB, Geiman JM, Breese BB, Douglas RG Jr. Parainfluenza viral infections in children: correlation of shedding with clinical manifestations. J Pediatr. 1977;91:194–8. https://doi.org/10.1016/S0022-3476(77)80811-1

Address for correspondence: Eric J. Chow, Division of Allergy and Infectious Diseases, University of Washington, 1959 NE Pacific St, Box 356423, Seattle, WA 98195, USA; email: ejchow@uw.edu

Presence of *Spirometra mansoni*, Causative Agent of Sparganosis, in South America

Jan Brabec,[1] Manuel Uribe,[1] Jenny J. Chaparro-Gutiérrez, Carlos Hermosilla

Author affiliations: Biology Centre of the Czech Academy of Sciences, České Budějovice, Czech Republic (J. Brabec); CIBAV Research Group, Universidad de Antioquia, Medellín, Colombia (M. Uribe, J.J. Chaparro-Gutiérrez); Justus Liebig University Giessen, Giessen, Germany (M. Uribe, C. Hermosilla)

DOI: http://doi.org/10.3201/eid2811.220529

We report molecular identification of an adult *Spirometra mansoni* tapeworm retrieved from a crab-eating fox (*Cerdocyon thous*) in Colombia, confirming presence of this parasite in South America. This tapeworm is the causative agent of human sparganosis, commonly reported from Southeast Asia, and represents the second congeneric species with known zoonotic potential in the Americas.

Sparganosis is a neglected human zoonosis caused by migrating larval stages of the broad tapeworm genus *Spirometra* (Diphyllobothriidea), whose natural definitive hosts include wild and domestic canids and felids. The life cycle of this tapeworm involves 2 intermediate hosts: a freshwater copepod crustacean as the first and various vertebrates, mostly amphibians, as the second. Human infections are commonly reported from Southeast Asia and propagate most often in the form of subcutaneous sparganosis; however, the larvae can enter other organs or parts of central nervous system and cause damage.

Taxonomy of *Spirometra* remains highly complicated. Numerous species of *Spirometra* have been described, often poorly (*1*), and representatives of just 6 species-level lineages have been characterized molecularly so far, a key prerequisite to achieve a convincing tapeworm identification when only strobila fragments or larval stages are available. Limitations of morphologic characters of *Spirometra* are numerous and include characters' great intraspecific and even intra-individual variability (overview of problematic traits in *2*). Molecular sequence data thus represent the only unequivocal method of species identification.

Previous phylogenetic analysis of *Spirometra* has shown that the geographic distribution of the 6 lineages respects continental borders (*2*). North

[1]These authors contributed equally to this article.

and South America were shown to share 2 lineages found exclusively on those continents (*3*), provisionally termed *Spirometra decipiens* complex 1 and 2 because of the lack of essential morphologic data precluding conclusive species determination (*2*). *S. decipiens* complex 1 was shown to house, among parasites of canids and felids, causative agents of cutaneous and proliferative sparganosis. Representatives of *S. decipiens* complex 2, on the other hand, have not yet been shown to cause the zoonosis. The frequently reported human cases of sparganosis from Southeast Asia, as well as numerous specimens from wildlife from the region, corresponded to *S. mansoni* (*2*).

We report molecular identification of a tapeworm specimen retrieved from a dead crab-eating fox (*Cerdocyon thous*) from the vicinity of Ciudad Bolívar, Antioquia, Colombia. We characterized the specimen through Sanger-sequencing of 3 genetic loci (Appendix, https://wwwnc.cdc.gov/EID/article/28/11/22-0529-App1.pdf), including the complete mitochondrial cytochrome c oxidase subunit I gene (*cox1*) as the most densely sampled and phylogenetically informative gene of broad tapeworms.

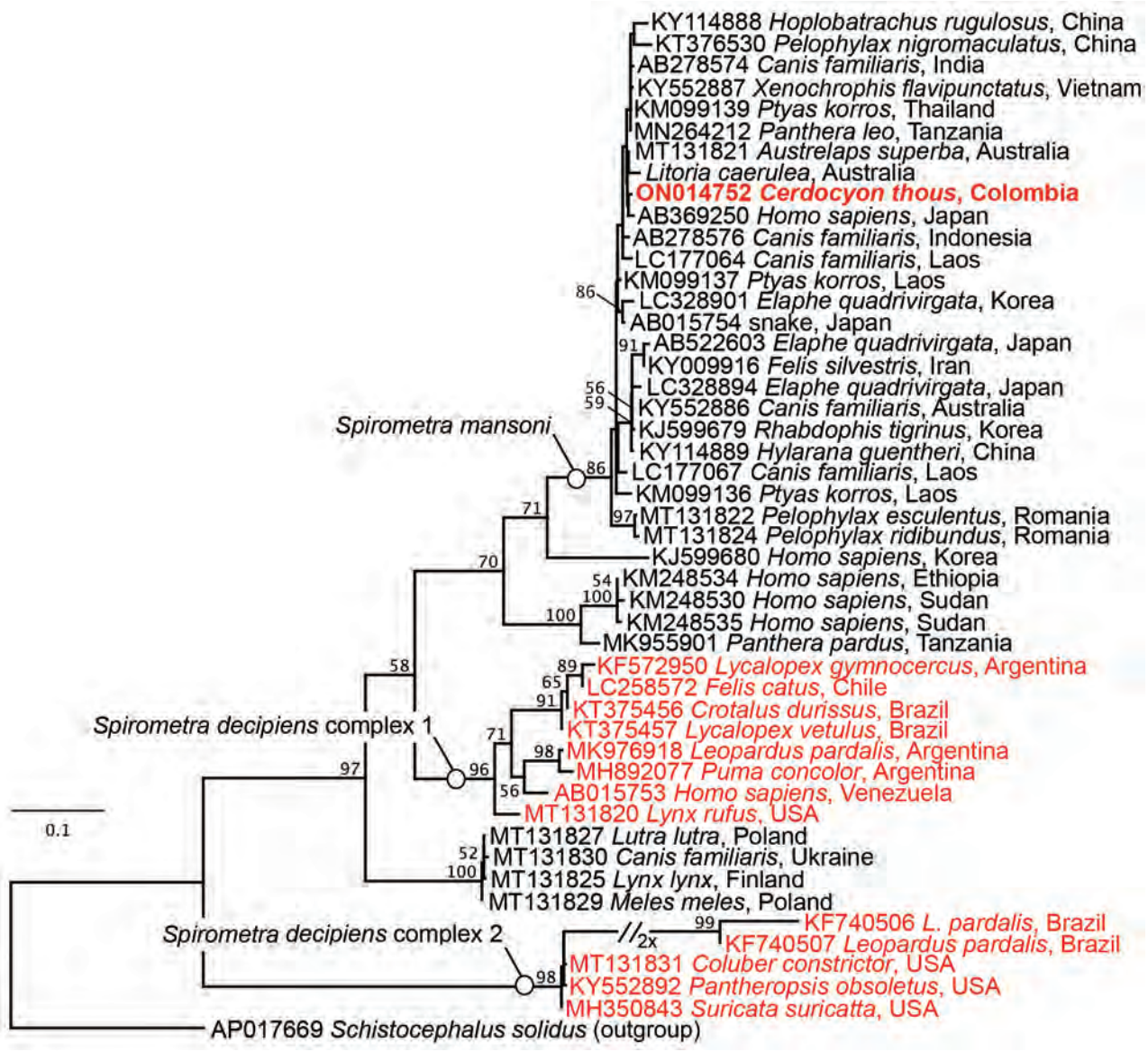

Figure. Maximum-likelihood estimate of the phylogenetic position of a *Spirometra mansoni* tapeworm collected from a crab-eating fox (*Cerdocyon thous*) in Colombia. Red indicates specimens from South America; bold indicates newly characterized *S. mansoni* from this report. Names of the 3 species-level lineages of *Spirometra* in South America are indicated; GenBank numbers are provided. Nodal support values show standard bootstrap supports >50. Scale bar indicates number of substitutions per site.

Phylogenetic analysis under maximum-likelihood criterion resolved the position of the tapeworm nested deep within the clade of *S. mansoni* (Figure), proving the presence of this causative agent of human sparganosis on the American continents.

S. mansoni represents by far the most frequently reported causative agent of sparganosis, previously misidentified as *S. erinaceieuropaei* (2). This species is responsible for virtually all human cases in Asia but has been also shown to infect wildlife in Africa, Australia, and Eastern Europe (2). Our finding of *S. mansoni* in Colombia in a crab-eating fox, a definitive host endemic and widely distributed across South America, from Panama to the Entre Ríos province of Argentina (4), expands the known distribution of *S. mansoni* into broader range than previously thought. This finding contrasts with the distribution of the remaining 5 lineages of *Spirometra*, which seem limited to continental regions (2). *S. mansoni* has been sporadically reported from the Americas in the past; however, morphology-altering fixation techniques and lack of critical molecular evidence did not support species identification. Reported hosts mostly included domestic cats (Appendix) and a single report from a crab-eating fox in Brazil (5).

The crab-eating fox inhabits savannah and woodland areas of various Neotropical habitats from coastal plains to montane forests and is considered omnivorous, opportunistically feeding on fruits, insects, and small vertebrates including amphibians and reptiles, with seasonal shifts to its diet (6,7). A broad range of Neotropical amphibians and reptiles has been found to serve as intermediate hosts of *Spirometra*; however, the record remains skewed toward herpetofauna of the more intensively surveyed coastal regions (8), and species identification of the parasite larvae has been, thanks to the lack of accompanying molecular data, either absent or ungrounded. As a result, the real range and the relevance of different intermediate hosts for the transmission of the sympatric South America species of *Spirometra* remain unknown. The situation in North America is even more obscure because of the virtually missing intermediate host record (1,9). Given the wide spectrum of suitable intermediate hosts of *S. mansoni*, which includes omnivores such as wild boar in Europe (10), the natural pools and the importance of different host species in the etiology of the zoonosis remain dubious. The concurrent presence of the second congeneric species with zoonotic potential urges deeper investigations into the parasite's life cycles and the epizootiology of a disease that could affect public health in the Americas.

Acknowledgments

The CIBAV research group thanks the Strategy of consolidation of Research Groups CODI 2018–2019, University of Antioquia, Medellín, Colombia.

This work was supported by the Czech Science Foundation project no. 19-28399X.

About the Author

Dr. Brabec is a research associate at the Institute of Parasitology, Biology Centre of the Czech Academy of Sciences. His primary research interests include molecular taxonomy, phylogenetics, phylogenomics, and evolution of parasitism in flatworms and protists.

References

1. Scholz T, Kuchta R, Brabec J. Broad tapeworms (Diphyllobothriidae), parasites of wildlife and humans: recent progress and future challenges. Int J Parasitol Parasites Wildl. 2019;9:359–69. https://doi.org/10.1016/j.ijppaw.2019.02.001
2. Kuchta R, Kołodziej-Sobocińska M, Brabec J, Młocicki D, Sałamatin R, Scholz T. Sparganosis (*Spirometra*) in Europe in the molecular era. Clin Infect Dis. 2021;72:882–90. https://doi.org/10.1093/cid/ciaa1036
3. Almeida GG, Coscarelli D, Melo MN, Melo AL, Pinto HA. Molecular identification of *Spirometra* spp. (Cestoda: Diphyllobothriidae) in some wild animals from Brazil. Parasitol Int. 2016;65(5 Pt A):428–31. https://doi.org/10.1016/j.parint.2016.05.014
4. Lucherini M. *Cerdocyon thous*. The IUCN Red List of Threatened Species. 2015:e.T4248A81266293 [cited 2022 Jul 18]. https://doi.org/10.2305/IUCN.UK.2015-4.RLTS.T4248A81266293.en
5. Santos KR, Catenacci LS, Pestelli MM, Takahira RK, Silva RJ. First report of *Diphyllobothrium mansoni* (Cestoda, Diphyllobothridae) infecting *Cerdocyon thous* (Mammalia, Canidae) in Brazil. Arq Bras Med Vet Zootec. 2004;56:796–8. https://doi.org/10.1590/S0102-09352004000600016
6. Berta A. *Cerdocyon thous*. Mamm Species. 1982;186:1–4. https://doi.org/10.2307/3503974
7. Bianchi RC, Campos RC, Xavier-Filho NL, Olifiers N, Gompper ME, Mourão G. Intraspecific, interspecific, and seasonal differences in the diet of three mid-sized carnivores in a large neotropical wetland. Acta Theriol (Warsz). 2014;59:13–23. https://doi.org/10.1007/s13364-013-0137-x
8. Oda FH, Borteiro C, da Graça RJ, Tavares LER, Crampet A, Guerra V, et al. Parasitism by larval tapeworms genus *Spirometra* in South American amphibians and reptiles: new records from Brazil and Uruguay, and a review of current knowledge in the region. Acta Trop. 2016;164:150–64. https://doi.org/10.1016/j.actatropica.2016.09.005
9. McHale B, Callahan RT, Paras KL, Weber M, Kimbrell L, Velázquez-Jiménez Y, et al. Sparganosis due to *Spirometra* sp. (cestoda; Diphyllobothriidae) in captive meerkats (*Suricata suricatta*). Int J Parasitol Parasites Wildl. 2020;13:186–90. https://doi.org/10.1016/j.ijppaw.2020.10.005
10. Kołodziej-Sobocińska M, Miniuk M, Ruczyńska I, Tokarska M. Sparganosis in wild boar (*Sus scrofa*)—implications for veterinarians, hunters, and consumers.

Vet Parasitol. 2016;227:115–7. https://doi.org/10.1016/j.vetpar.2016.08.001

Address for correspondence: Jan Brabec, Institute of Parasitology, Biology Centre of the Czech Academy of Sciences, Branišovská 31, České Budějovice, 37005, Czech Republic; email: brabcak@paru.cas.cz

TIGIT Monoallelic Nonsense Variant in Patient with Severe COVID-19 Infection, Thailand

Pimpayao Sodsai,[1] Chupong Ittiwut,[1] Vichaya Ruenjaiman, Rungnapa Ittiwut, Watsamon Jantarabenjakul, Kanya Suphapeetiporn, Vorasuk Shotelersuk,[2] Nattiya Hirankarn[2]

Author affiliations: Chulalongkorn University, Bangkok, Thailand (P. Sodsai, C. Ittiwut, V. Ruenjaiman, R. Ittiwut, W. Jantarabenjakul, K. Suphapeetiporn, V. Shotelersuk, N. Hirankarn); King Chulalongkorn Memorial Hospital, The Thai Red Cross Society, Bangkok (W. Jantarabenjakul, R. Ittiwut)

DOI: https://doi.org/10.3201/eid2811.220914

A heterozygous nonsense variant in the *TIGIT* gene was identified in a patient in Thailand who had severe COVID-19, resulting in lower *TIGIT* expression in T cells. The patient's T cells produced higher levels of cytokines upon stimulation. This mutation causes less-controlled immune responses, which might contribute to COVID-19 severity.

To investigate SARS-CoV-2 genomic variants, we recruited 46 COVID-19 patients from King Chulalongkorn Memorial Hospital in Bangkok, Thailand, in January 2020. Recruited patients were 16–79 years of age and had moderate to severe COVID-19 symptoms according to World Health Organization interim guidelines (https://apps.who.int/iris/bitstream/handle/10665/331446/WHO-2019-nCoV-clinical-2020.4-eng.pdf). We performed whole-exome sequencing on peripheral blood samples as described (*1*). The institutional review board of the Faculty of Medicine, Chulalongkorn University, Bangkok, approved this study (COA no. 738/2020).

We filtered variants by using the following criteria. Variants had to pass the quality standards, have read depth >10, and be from the coding regions or canonical splice sites of 1,810 immune-related genes, including immune checkpoint genes (*2*). Variants also had to have <1% allele frequency in the Genome Aggregation Database (gnomAD, https://gnomad.broadinstitute.org), Exome Variant Server (University of Washington, https://evs.gs.washington.edu/EVS), 1000 Genomes Project Consortium (https://www.genome.gov), dbSNPs (https://www.ncbi.nlm.nih.gov/projects/SNP), and Thai Reference Exome (T-Rex) database (*3*). We called candidate variants novel pathogenic variants when they were not previously identified in patients in the literature.

In our patient cohort, exome sequencing identified no variants in type I interferon genes, which previously have been commonly observed in patients with severe COVID-19 (*4*). Of note, we identified a heterozygous nonsense variant (rs1386709957) in the T-cell immunoglobulin and ITIM domain (*TIGIT*) gene in 1 patient (Appendix Figure 1, https://wwwnc.cdc.gov/EID/article/29/11/22-0914-App1.pdf). We did not identify this nonsense variant among 3,742 persons in the T-Rex database but did observe it in 1 of 31,390 alleles in the gnomAD database, in an allele from a female patient from East Asia. This variant truncates the 245-amino acid residue proteins at residue 56 and is classified as a pathogenic variant American College of Medical Genetics guidelines (https://www.acmg.net).

We investigated *TIGIT* gene expression in T cells of the patient from our study (Co45), a 43-year-old man, and compared it with 2 other sex- and age-matched patients who had severe COVID-19 (Co6 and Co84) (Appendix). We collected peripheral blood mononuclear cells (PBMCs) from each of the patients 1 month after they recovered. We used RNA extracted from PBMCs for real-time reverse transcription PCR and found patient Co45 had the lowest *TIGIT* mRNA level (Figure, panel A). Because *TIGIT* is mainly expressed in T cells, we used flow cytometry to measure the mean fluorescence intensity of TIGIT expressed in the cytoplasmic domain (CD) T cells. Patient Co45 had lower TIGIT gene expression in all CD3+, CD4+, and CD8+ T cells than the other 2 patients, most remarkably in the CD8+ T cells (Figure, panels B–D). The percentages of CD3+, CD4+, and CD8+ T cells in patient Co45 were comparable those in the other 2 patients (Appendix Fig-

[1]These first authors contributed equally to this article.

[2]These authors were co–principal investigators.

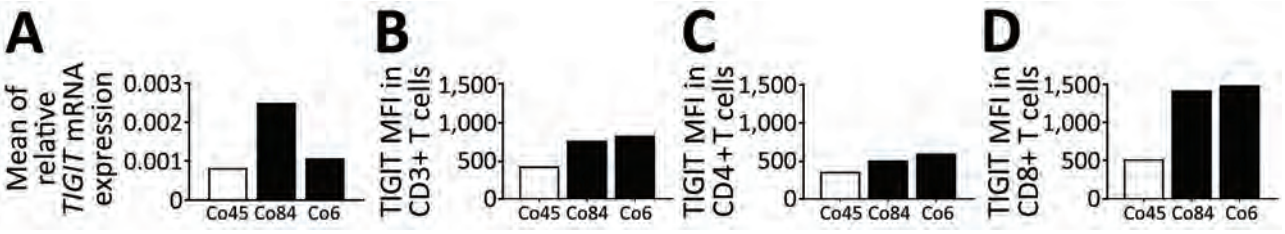

Figure. Results of rRT-PCR assay and flow cytometry of *TIGIT* nonsense variant in a patient with severe COVID-19 infection, Thailand. Co45 is the patient with *TIGIT* nonsense variant; Co84 and Co6 are age- and sex-matched patients who also had severe COVID-19 infection. A) Mean relative mRNA levels of *TIGIT* expression from rRT-PCR assay. B) TIGIT expression MFI on CD3+ T cells. C) TIGIT expression MFI on CD4+ T cells. D) TIGIT expression MFI on CD8+ T cells. CD, cytoplasmic domain; MFI, mean fluorescence intensity; rRT-PCR, real-time reverse transcription PCR; *TIGIT*, T cell immunoglobulin and ITIM domain gene.

ure 2, panel A), demonstrating that the truncated *TIGIT* variant reduced *TIGIT* expression in CD3+, CD4+, and CD8+ T cells.

TIGIT is known to exert immune suppressive functions, such as inhibiting T cell activation, proliferation, and functions that inhibit inflammation and anti-tumor responses. Thus, we investigated the effect of this monoallelic *TIGIT* variant on T cell functions by examining activation markers and cytokine-secreting T cells after stimulation with anti-CD3/CD28 coupled beads for 24 hours. We then assessed activation by using flow cytometry. We found no differences in frequencies of CD69-expressing CD3+, CD4+, and CD8+ T cells among the 3 patients (Appendix Figure 2, panel B); however, patient Co45 had higher interferon gamma (IFNγ), tumor necrosis factor alpha (TNF-α), and interleukin (IL) 2–producing CD3+, CD4+, and CD8+ T cells than the other 2 patients (Appendix Figure 3).

We believe this patient's heterozygous nonsense *TIGIT* variant contributed to the increased inflammatory cytokine functions we observed. His serum cytokine levels at acute illness onset did not differ from the other 2 COVID-19 patients (Appendix Figure 4), but some of his cytokine levels, including IL-10, IL-12p70, IL-4, and IL-7, remained high 1 month after recovery. Upregulation of co-inhibitory receptors, including cytotoxic T-lymphocyte–associated protein 4, programmed cell death protein 1, lymphocyte-activation gene 3, and T-cell immunoglobulin mucin-3, including *TIGIT*, has been reported in COVID-19 patients in other studies (*5*). These co-inhibitory receptors upregulated after T-cell activation to regulate immune responses and limit immunopathology (*6*,*7*). *TIGIT* can modulate expression of proinflammatory cytokines in acute lymphocytic choriomeningitis virus infection, in which the *TIGIT* blockage increased TNF-α expression by CD8+ T cells (*8*). *TIGIT* -deficient mice displayed increased IFNγ and IL-17+CD4+ T-cell frequencies (*9*). Similarly, *TIGIT* knockdown can increase IFNγ expression in human T cells (*10*). We hypothesize that the nonsense *TIGIT* variant led to low *TIGIT* expression and hyperactive T responses in patient Co45 and might have contributed to his severe inflammation and symptoms. Unfortunately, the patient refused follow-up, so we could not perform further investigations to confirm our hypothesis.

In conclusion, we identified a patient with severe COVID-19 and a *TIGIT* monoallelic nonsense variant. He had lower TIGIT expression in CD3+, CD4+, and CD8+ T cells and produced higher cytokine expression, including IFNγ, TNF-α, and IL-2 upon stimulation. Our findings suggest *TIGIT* could be involved in COVID-19 severity.

This study was supported by Ratchadapisek Somphot Fund (grant no RA(PO)005/63); Ratchadapisek Somphot Matching Fund, and Health Systems Research Institute (no. 65-040); e-ASIA Joint Research Program (e-ASIA JRP) administered by the National Science and Technology Development Agency; the Center of Excellence in Immunology and Immune-mediated Diseases; the Center of Excellence for Medical Genomics, Medical Genomics Cluster, Department of Pediatrics; the Center of Excellence in Pediatric Infectious Diseases and Vaccines, Faculty of Medicine, Chulalongkorn University; the Excellence Center for Genomics and Precision Medicine; the Emerging Infectious Diseases Clinical Centre, King Chulalongkorn Memorial Hospital; and The Thai Red Cross Society. Biospecimen collection was supported by Biobank, and the Faculty of Medicine, Chulalongkorn University, Bangkok, Thailand.

About the Author

Dr. Sodsai is a researcher in the Center of Excellence in Immunology and Immune-mediated Diseases, Department of Microbiology, Faculty of Medicine, Chulalongkorn University. Her primary research interests focus on cellular immunology.

References

1. Ittiwut R, Sengpanich K, Lauhasurayotin S, Ittiwut C, Shotelersuk V, Sosothikul D, et al. Clinical and molecular characteristics of Thai patients with *ELANE*-related neutropaenia. J Clin Pathol. 2022;75:99–103. https://doi.org/10.1136/jclinpath-2020-207139
2. Hu FF, Liu CJ, Liu LL, Zhang Q, Guo AY. Expression profile of immune checkpoint genes and their roles in predicting immunotherapy response. Brief Bioinform. 2021;22:bbaa176. https://doi.org/10.1093/bib/bbaa176
3. Shotelersuk V, Wichadakul D, Ngamphiw C, Srichomthong C, Phokaew C, Wilantho A, et al. The Thai reference exome (T-REx) variant database. Clin Genet. 2021;100:703–12. https://doi.org/10.1111/cge.14060
4. Gray PE, Bartlett AW, Tangye SG. Severe COVID-19 represents an undiagnosed primary immunodeficiency in a high proportion of infected individuals. Clin Transl Immunology. 2022;11:e1365. https://doi.org/10.1002/cti2.1365
5. Barnova M, Bobcakova A, Urdova V, Kosturiak R, Kapustova L, Dobrota D, et al. Inhibitory immune checkpoint molecules and exhaustion of T cells in COVID-19. Physiol Res. 2021;70(S2):S227–47. https://doi.org/10.33549/physiolres.934757
6. Anderson AC, Joller N, Kuchroo VK. Lag-3, Tim-3, and TIGIT: co-inhibitory receptors with specialized functions in immune regulation. Immunity. 2016;44:989–1004. https://doi.org/10.1016/j.immuni.2016.05.001
7. Harjunpää H, Guillerey C. TIGIT as an emerging immune checkpoint. Clin Exp Immunol. 2020;200:108–19. https://doi.org/10.1111/cei.13407
8. Schorer M, Rakebrandt N, Lambert K, Hunziker A, Pallmer K, Oxenius A, et al. TIGIT limits immune pathology during viral infections. Nat Commun. 2020;11:1288. https://doi.org/10.1038/s41467-020-15025-1
9. Joller N, Hafler JP, Brynedal B, Kassam N, Spoerl S, Levin SD, et al. Cutting edge: TIGIT has T cell-intrinsic inhibitory functions. J Immunol. 2011;186:1338–42. https://doi.org/10.4049/jimmunol.1003081
10. Lozano E, Dominguez-Villar M, Kuchroo V, Hafler DA. The TIGIT/CD226 axis regulates human T cell function. J Immunol. 2012;188:3869–75. https://doi.org/10.4049/jimmunol.1103627

Address for correspondence: Vorasuk Shotelersuk, Center of Excellence for Medical Genomics, Medical Genomics Cluster, Department of Pediatrics, Faculty of Medicine, Chulalongkorn University, Rama 4 Rd, Bangkok 10330, Thailand; email: Vorasuk.S@chula.ac.th

SARS-CoV-2 Omicron BA.1 Challenge after Ancestral or Delta Infection in Mice

Mariana Baz, Nikita Deshpande, Charlie Mackenzie-Kludas, Francesca Mordant, Danielle Anderson, Kanta Subbarao

Author affiliations: World Health Organization Collaborating Centre for Reference and Research on Influenza, Melbourne, Victoria, Australia (M. Baz, N. Deshpande, K. Subbarao); University of Melbourne Peter Doherty Institute for Infection and Immunity, Melbourne (C. Mackenzie-Kludas, F. Mordant, D. Anderson, K. Subbarao); Victorian Infectious Diseases Reference Laboratory, Melbourne (D. Anderson)

DOI: https://doi.org/10.3201/eid2811.220718

We assessed cross-reactivity to BA.1, BA.2, and BA.5 of neutralizing antibodies elicited by ancestral, Delta, and Omicron BA.1 SARS-CoV-2 infection in mice. Primary infection elicited homologous antibodies with poor cross-reactivity to Omicron strains. This pattern remained after BA.1 challenge, although ancestral- and Delta-infected mice were protected from BA.1 infection.

The SARS-CoV-2 Omicron variant (B.1.1.529, BA.1 sublineage) emerged nearly 2 years after the ancestral strain was identified (*1*). The Omicron BA.1 variant contains ≈50 mutations in the spike protein (*2*), resulting in substantial antigenic change. The strain was more infectious than prior variants of concern (VOCs) and escaped immunity, causing infections in persons who were previously vaccinated with ancestral strain–based vaccines (*3*) or infected with the ancestral virus or Delta (B.1.617.2) VOC. Since January 2022, additional Omicron sublineages (BA.2 to BA.5) have been detected worldwide. BA.4/BA.5 have identical spike proteins, most similar to BA.2, with additional spike mutations (*4*).

We sought to mimic the human scenario and selected a mouse model from available animal models (*5*) to assess the cross-reactivity of neutralizing antibody elicited by ancestral, Delta, and BA.1 viruses and to assess the effect of primary homologous and heterologous infection on secondary infection with the Omicron BA.1 strain. We also compared antibody cross-reactivity to BA.2 and BA.5 in serum samples from mice infected with ancestral, Delta, and BA.1 strains.

We first compared the associated illness, mortality rates, and kinetics of replication of 10^4 50% tissue culture infectious dose ($TCID_{50}$) of SARS-CoV-2/Australia/Vic/01/20 (ancestral strain–like),

SARS-CoV-2/Australia/Vic/18440/2021 (Delta), and SARS-CoV-2/Australia/NSW/RPAH-1933/2021 (Omicron BA.1) strains in 7- to 9-week-old female K18hACE2 transgenic mice (Appendix Figure, https://wwwnc.cdc.gov/EID/article/28/11/22-0718-App1.pdf). We infected groups of 15 K18hACE2 mice with intranasally delivered ancestral, Delta, or Omicron BA.1 strains by using a low dose of each virus (10^2 $TCID_{50}$), selected so that the mice would survive primary infection (Figure, panel A). We mock-infected 15 mice with phosphate-buffered saline (PBS). We collected blood on day 27 after primary infection and then challenged mice with 10^4 $TCID_{50}$ of Omicron BA.1 virus. We collected lungs and nasal turbinates (NTs) 2 and 4 days after challenge; we weighed and monitored 5 mice per group for clinical signs for 14 days (Figure, panel B). We collected blood samples on day 28 after Omicron BA.1 challenge (day 56 from primary infection).

After primary infection, all Omicron BA1–infected mice survived without major weight loss, but 1 ancestral strain–infected and 5 Delta-infected mice died during days 8–13. After challenge with 10^4 $TCID_{50}$ of Omicron, all mice, including the PBS group (naive control), survived without weight loss. The control group had mean virus titers of $10^{2.6}$ (day 2) and $10^{2.7}$ (day 4) in NTs and $10^{3.7}$ (day 2) and $10^{3.5}$ (day 4) $TCID_{50}$/organ in lungs after Omicron BA.1 challenge.

Consistent with other reports (*6*), we found the titers of BA.1 to be lower than those for ancestral and Delta viruses (Appendix Figure, panel C). Virus was not recovered from the tissues of mice challenged with BA.1 that had prior primary infection with ancestral, Delta, or BA.1 viruses (Figure C), except 1 mouse in each of the ancestral and Delta primary infection groups.

The homologous responses were strongest to ancestral (geometric mean titer [GMT] 709), followed by Delta (GMT 129), and were lowest to BA.1 (GMT 83) (Table). The low titer neutralizing antibody response to Omicron BA.1 infection is probably attributable to less robust replication of BA.1 virus in mouse tissues (Appendix Figure, panel C). Mice recovered from primary BA.1 infection were fully protected from rechallenge with the higher dose of BA.1, and no boost in homologous neutralizing antibody titers occurred (day 56 GMT 62).

Primary Omicron BA.1 infection did not induce heterologous neutralizing activity against ancestral, Delta, BA.2, or BA.5 viruses (Table). In contrast, primary ancestral infection elicited an 8-fold reduced titer against Delta and 21-fold reduced titer against the BA.1 virus, and primary Delta infection elicited a 2-fold reduced titer against ancestral strain. None of the mice first infected with BA.1, ancestral, or Delta viruses developed neutralizing antibodies against BA.5.

Despite the absence of detectable BA.1 virus in the respiratory tract tissues after secondary infection in mice previously infected with ancestral or Delta (Figure, panel C), we observed a boost in homologous GMTs 1,338 (ancestral) and >453 (Delta), and cross-

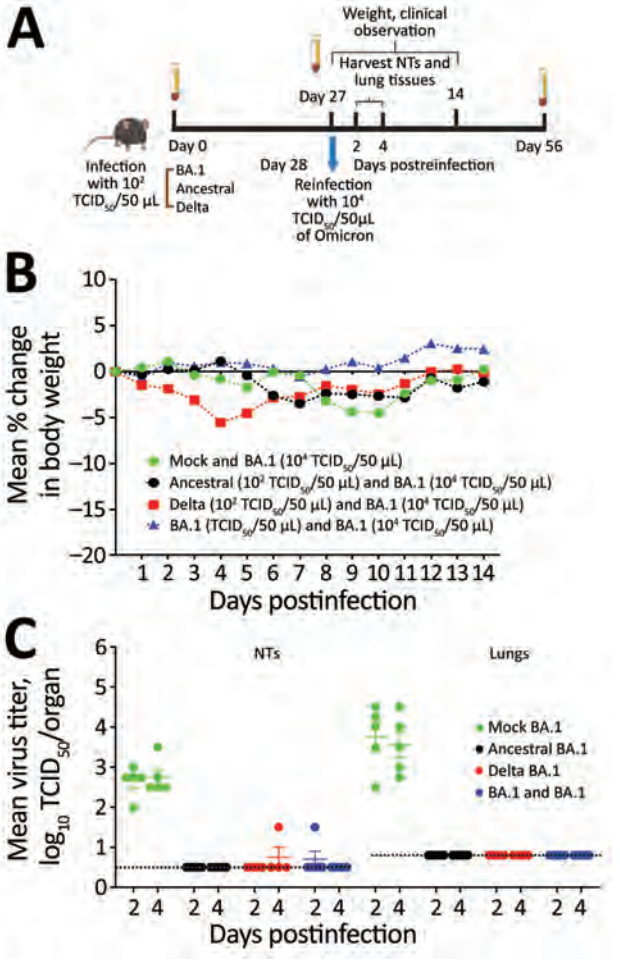

Figure. Primary infection with ancestral, Delta, or Omicron BA.1 SARS-CoV-2 strains as protection in mice from BA.1 reinfection. A) Flowchart of 6- to 8-week-old female hACE2K18 transgenic mice who received primary infection with low doses (10^2 $TCID_{50}$) of Omicron BA.1, ancestral, or Delta viruses and were reinfected with a higher dose (10^4 $TCID_{50}$) of BA.1. B) Weight loss in mice reinfected intranasally with 50 µL containing 10^4 $TCID_{50}$ of Omicron on day 28 after primary infection with each SARS-CoV-2 strain. Animals were monitored daily for weight loss, and deaths were recorded over a period of 14 days. Mice were euthanized when they lost 20% of their original bodyweight. C) Replication kinetics of Omicron BA.1 virus in mice after reinfection with 10^4 $TCID_{50}$/virus. Virus titers in the NTs and lungs of 5 mice per group euthanized on days 2 and 4 postinfection are expressed as log_{10} $TCID_{50}$/mL (NTs) and log_{10} $TCID_{50}$/organ (lungs). Horizontal bars represent mean titers, and symbols represent titers from individual mice. The dashed horizontal line indicates the lower limit of detection, $10^{0.5}$ $TCID_{50}$ per mL for the NTs and $10^{0.8}$ $TCID_{50}$ per organ for lungs. NTs, nasal turbinates; $TCID_{50}$, 50% tissue culture infectious dose.

Table. Homologous and heterologous serum neutralizing antibody titers on days 27 and 56 after primary and secondary SARS-CoV-2 infection in hACE2K18 transgenic mice*

Primary infection, 10^2 $TCID_{50}$	Secondary infection, 10^4 $TCID_{50}$	Serum neutralizing antibodies (GMT) against indicated virus after primary and secondary infection				
		BA.1	BA.2†	BA.5†	Ancestral	Delta
BA.1	BA.1	**83/62**	10/10	10/10	7‡/7‡	7‡/8‡
Ancestral	BA.1	34‡/27‡	10/10	10/10	**709/1,338**	90‡/>440‡
Delta	BA.1	16/60	10/35	10/53	55‡/124‡	**129/>453**

*Bold indicates homologous titers. GMT, geometric mean titer; $TCID_{50}$, 50% tissue culture infectious dose.
†Lower limit of detection in indicated assays is 10. In other assays, the lower limit of detection is 5.
‡Serum samples from different sets of 5 mice from the group were tested on days 27 and 56.

reactive neutralizing antibody titers GMTs >440 (ancestral) and 124 (Delta), and vice versa (GMTs of 27 and 60, respectively), with no improvement in cross-reactivity to BA.1. Mice first infected with Delta and rechallenged with BA.1 had low but detectable neutralizing antibody titers against BA.5 (Table).

Our observations are consistent with BA.1 being antigenically distinct from the ancestral and Delta strains (K. van der Straten K et al., unpub. data, https://doi.org/10.1101/2022.01.03.2126858. A boost occurred in preexisting SARS-CoV-2 neutralizing antibodies to ancestral and Delta but not in cross-reactivity to Omicron, probably because more epitopes are shared between ancestral and Delta than between those strains and Omicron. Serologic data from humans suggest that ≥3 exposures to ancestral strains as infection or vaccination or a combination are needed to induce cross-reactive antibodies to BA.1 (*7*). Although data from antigenic cartography using human serum suggest that BA.2 is antigenically closer to the ancestral and Delta strains (A. Rössler et al., unpub. data, https://doi.org/10.1101/2022.05.10.22274906), we did not detect cross-reactive neutralizing antibodies after primary infection with ancestral and Delta strains. Protection from replication of the Omicron BA.1 strain despite the lack of cross-reactive neutralizing antibodies may be attributable to mucosal immunity or T-cell responses in ancestral strain–infected and Delta-infected mice (*8*).

Acknowledgments

We thank Julian Druce for providing SARS-CoV-2 isolates (SARS-CoV-2/Australia/Vic/01/20 [ancestral], SARS-CoV-2/Australia/Vic/18440/2021 [Delta], SARS-CoV-2/Australia/NSW/RPAH-1933/2021 [BA.1], SARS-CoV-2/Australia/VIC/35864/2022 [BA.2], and SARS-CoV-2 Australia/VIC/61194/2022 [BA.5]) used in this study. We thank Rebecca Plavcak for technical support during mouse studies and members from the Subbarao Laboratory for assistance.

K.S. is supported by a National Health and Medical Research Council Investigator Grant. We are grateful for the funding support from the Jack Ma Foundation. The Melbourne World Health Organization Collaborating Centre for Reference and Research on Influenza is supported by Australia's Department of Health.

About the Author

Dr. Baz leads the Antiviral Drug Sensitivity Division at the World Health Organization Collaborating Centre for Reference and Research on Influenza. Her research interests include antiviral therapies to respiratory virus infection and the development and evaluation of vaccines against seasonal and pandemic viruses.

References

1. World Health Organization. Classification of Omicron (B.1.1.529): SARS-CoV-2 variant of concern. 2021 Nov 26 [cited 2022 Aug 15]. https://www.who.int/news/item/26-11-2021-classification-of-omicron-(b.1.1.529)-sars-cov-2-variant-of-concern
2. Centers for Disease Control and Prevention. Science brief: Omicron (B.1.1.529) variant. 2021 Dec 2 [cited 2022 Aug 15]. https://www.cdc.gov/coronavirus/2019-ncov/science/science-briefs/scientific-brief-omicron-variant.html
3. Rössler A, Rippler L, Bante D, von Laer D, Kimpel J. SARS-CoV-2 Omicron variant neutralization in serum from vaccinated and convalescent persons. N Engl J Med. 2022;386:698–700. https://doi.org/10.1056/NEJMc2119236
4. Tegally H, Moir M, Everatt J, Giovanetti M, Scheepers C, Wilkinson E, et al.; NGS-SA Consortium. Emergence of SARS-CoV-2 Omicron lineages BA.4 and BA.5 in South Africa. Nat Med. 2022 Jun 27 [Epub ahead of print]. https://doi.org/10.1038/s41591-022-01911-2
5. Muñoz-Fontela C, Dowling WE, Funnell SGP, Gsell PS, Riveros-Balta AX, Albrecht RA, et al. Animal models for COVID-19. Nature. 2020;586:509–15. https://doi.org/10.1038/s41586-020-2787-6
6. Halfmann PJ, Iida S, Iwatsuki-Horimoto K, Maemura T, Kiso M, Scheaffer SM, et al.; Consortium Mount Sinai Pathogen Surveillance (PSP) study group. SARS-CoV-2 Omicron virus causes attenuated disease in mice and hamsters. Nature. 2022;603:687–92. https://doi.org/10.1038/s41586-022-04441-6
7. Walls AC, Sprouse KR, Bowen JE, Joshi A, Franko N, Navarro MJ, et al. SARS-CoV-2 breakthrough infections elicit potent, broad, and durable neutralizing antibody responses. Cell. 2022;185:872–880.e3. https://doi.org/10.1016/j.cell.2022.01.011
8. Keeton R, Tincho MB, Ngomti A, Baguma R, Benede N, Suzuki A, et al. T cell responses to SARS-CoV-2 spike cross-recognize Omicron. Nature. 2022;603:488–92. https://doi.org/10.1038/s41586-022-04460-3

Address for correspondence: Kanta Subbarao, WHO Collaborating Centre for Reference and Research on Influenza, Department of Microbiology and Immunology, The University of Melbourne at The Peter Doherty Institute for Infection and Immunity, 792 Elizabeth St, Melbourne, VIC, 3000, Australia; email: kanta.subbarao@influenzacentre.org

Serologic Evidence of Human Exposure to Ehrlichiosis Agents in Japan

Hongru Su, Kenji Kubo, Shigetoshi Sakabe, Shinsuke Mizuno, Nobuhiro Komiya, Shigehiro Akachi, Hiromi Fujita,[1] Kozue Sato, Hiroki Kawabata, Hiromi Nagaoka, Shuji Ando, Norio Ohashi

Author affiliations: University of Shizuoka, Shizuoka, Japan (H. Su, N. Ohashi); Japanese Red Cross Wakayama Medical Center, Wakayama, Japan (K. Kubo, S. Mizuno, N. Komiya); Ise Red Cross Hospital, Ise, Japan (S. Sakabe); Mie Prefecture Health and Environment Research Institute, Yokkaichi, Japan (S. Akachi); Mahara Institute of Medical Acarology, Anan, Japan (H. Fujita); National Institute of Infectious Diseases, Tokyo, Japan (K. Sato, H. Kawabata, S. Ando); Shizuoka Institute of Environment and Hygiene, Shizuoka (H. Nagaoka)

DOI: https://doi.org/10.3201/eid2811.212566

In retrospective analyses, we report 3 febrile patients in Japan who had seroconversion to antibodies against *Ehrlichia chaffeensis* antigens detected by using an immunofluorescence and Western blot. Our results provide evidence of autochthonous human ehrlichiosis cases and indicate ehrlichiosis should be considered a potential cause of febrile illness in Japan.

Human ehrlichiosis is a tickborne infectious disease caused by *Ehrlichia* sp. that has primarily been detected in the United States. Common clinical manifestations of human ehrlichiosis are fever, headache, myalgia, and malaise. Leukopenia and thrombocytopenia often occur. Symptoms range from mild fever to severe illness with multiple organ dysfunction, which is occasionally fatal (*1*). In a retrospective analysis, we show serologic evidence for human ehrlichiosis in 3 febrile patients in Japan.

In case 1, a male patient, who was 48 years of age and worked in the manufacturing industry, sought care at a primary care clinic in 2015 for high fever (>40°C) and headache ≈1 month after hiking in the mountains. The clinic physician prescribed levofloxacin and acetaminophen, but the treatment was not effective. Therefore, the patient was seen at the Japanese Red Cross Wakayama Medical Center. The day before onset of high fever, the patient found a small rash on the left side of his abdomen. This date was considered day 0, although there might have been symptoms that the patient was unaware of before that time. The rash was an erythema migrans–like lesion that expanded on day 5. The patient was hospitalized, and borreliosis or tick-associated rash illness, which is similar to Lyme borreliosis–like erythema migrans, was suspected (*2*); however, a tick bite or eschar was not observed. After intravenous administration of minocycline (200 mg/d), the patient's fever abated, but the lesion expanded and was accompanied by puritis. On day 10, the patient was discharged from the hospital, after which the rash gradually disappeared. Diagnostic tests for borreliosis were negative. We retrospectively performed immunofluorescence assays (IFAs) and Western blot (Appendix, https://wwwnc.cdc.gov/EID/article/28/11/21-2566-App1.pdf) using patient serum samples collected on days 2 and 17. We showed seroconversion to antibodies against *Ehrlichia chaffeensis* antigens by IFA and the presence of IgM and IgG against *Ehrlichia* sp. P28 protein by Western blot (Table; Figure). We suspected the patient had ehrlichiosis and tick-associated rash illness.

In case 2, a male patient, who was 66 years of age and worked as a truck driver, sought care at the Ise Red Cross Hospital in 2018 for fever (38°C), annular erythema, and malaise. The patient had renal impairment and jaundice. The principal physician suspected leptospirosis, but diagnostic tests for leptospirosis were negative. The physician suspected other bacterial infections, including Japanese spotted fever (JSF) or anaplasmosis. The patient was treated intravenously with minocycline (200 mg/d) and sulbactam/ampicillin (6 g/d) for 4 days. Subsequently, amoxicillin (1.5 g/d) was administered orally for 14 days, and the patient recovered. Diagnostic tests for JSF were negative. We retrospectively analyzed patient serum samples collected on days 14, 32, and 60 after onset of illness. We showed seroconversion to antibodies against *E. chaffeensis*

[1]Current affiliation: Northern Fukushima Medical Center, Date, Japan.

Table. Evaluation of immunofluorescence assay titers and Western blots of serum samples from 3 febrile patients demonstrating serologic evidence of human exposure to ehrlichiosis agents in Japan*

Case no. (year)	No. days†	*Ehrlichia chaffeensis* antigens, IgM/IgG			*Anaplasma phagocytophilum* antigens, IgM/IgG		
		IFA, THP-1 cells	Western blot		IFA		Western blot, THP-1 cells
			DH82 cells	THP-1 cells	THP-1 cells	HL60 cells	
1 (2015)	2	20/160	–/+	–/–	<20/<20	<20/<20	–/–
	17	80/640	+/+	+/+	<20/<20	<20/<20	–/–
2 (2018)	14	20/20	+/+	+/+	<20/<20	<20/<20	–/–
	32	40/320	+/+	+/+	<20/<20	<20/<20	–/–
	60	20/20	+/+	+/+	<20/<20	<20/<20	–/–
3 (2018)	5	20/20	+/+	+/+	<20/40	<20/20	–/+
	58	80/80	+/+	+/+	<20/40	<20/40	–/+
	115	20/320	+/+	+/+	<20/40	<20/40	–/+

*Serum samples were collected from 3 patients in Japan in 2015 and 2018 and assayed by using THP-1, DH82, or HL60 cells infected with *E. chaffeensis* or *A. phagocytophilum*. Western blots were categorized as positive or negative for IgM and IgG against antigens from each bacterial species. IFA, immunofluorescence assay.
†No. days after onset of illness.

antigens by IFA and the presence of IgM and IgG against *Ehrlichia* sp. P28 protein by Western blot (Table; Appendix Figure 1). The IFA titers for both IgM and IgG decreased on day 60.

In case 3, a female patient, who was 69 years of age and owned a Japanese-style accommodation, sought care at the Ise Red Cross Hospital in 2018 for mild fever, generalized edema and rash, headache, and malaise. The principal physician suspected JSF and treated the patient with oral minocycline (200 mg/d) and levofloxacin (500 mg/d) for 10 days; the patient recovered. Diagnostic tests for JSF were negative. We retrospectively analyzed patient serum samples collected on days 5, 58, and 115 by IFA and Western blot and found seroconversion to antibodies against *E. chaffeensis* antigens by IFA and the presence of both IgM and IgG against *Ehrlichia* sp. P28 protein antigens by Western blot (Table;

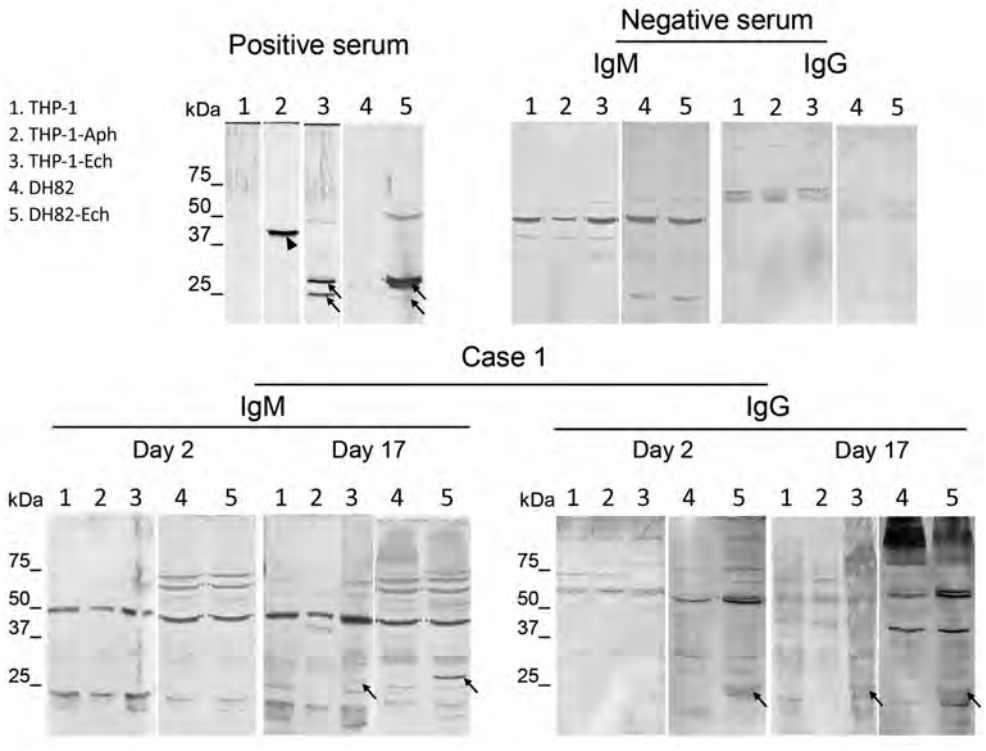

Figure. Western blots using serum samples from a febrile patient (case 1) in Wakayama Prefecture in study showing serologic evidence of human exposure to ehrlichiosis agents in Japan. Serum samples were collected from the patient on day 2 and 17 after onset of illness. Human THP-1 and canine DH82 cells were uninfected or infected with Ehrlichia chaffeensis . THP-1 cells were also infected with Anaplasma phagocytophilum. Cell lysates were separated and Western blot was performed as described (Appendix, https://wwwnc.cdc.gov/EID/article/28/11/21-2566-App1.pdf). We used uninfected THP-1 and DH82 cells as negative lysate controls. We used rabbit serum against recombinant P44 antigens specific for A. phagocytophilum and recombinant P28 antigens specific for E. chaffeensis (1:10,000 dilution) as positive serum controls. We used serum from a healthy donor as a negative control serum (Precision for Medicine, https://www.precisionbiospecimens.com). The patient's serum samples and negative control serum were diluted 1:250 and used to probe the blots. We used alkaline-phosphatase-conjugated goat anti-human IgM μ-chain and anti-human IgG γ-chain (Thermo Fisher Scientific, https://www.thermofisher.com) as secondary antibodies. Arrows indicate E. chaffeensis-specific P28 antigens (encoded by a p28 multigene family). Arrowhead shows A. phagocytophilum-specific P44 antigen (encoded by a p44 multigene family).

Appendix Figure 2). In this case, the IgM titer increased in the convalescent-phase serum on day 58 but decreased on day 115. However, the IgG titer increased on days 58 and 115 after onset of illness. In addition, we detected antibodies against *Anaplasma phagocytophilum* by IFA and *A. phagocytophilum*–specific P44 surface antigen by Western blot. We detected only IgG antibodies against *A. phagocytophilum* in all 3 serum samples, suggesting a past infection with *A. phagocytophilum*.

The 3 patients lived on the Kii peninsula of Japan (Appendix Figure 3), which is known to be a JSF-endemic area, especially in Wakayama and Mie Prefectures (*3*,*4*). In addition, anaplasmosis exists in those areas (*5*). Previously, we revealed the presence of ticks infected with *A. phagocytophilum* and *Ehrlichia* sp. that could potentially infect humans in Mie prefecture (*6*,*7*). In particular, members of the *Ehrlichia* sp. genotype 2 group, including *Ehrlichia* sp. MieHl92 and MieHl94, were considered candidate organisms that might cause human ehrlichiosis in Japan (*6*).

In conclusion, we provide serologic evidence of autochthonous cases of human ehrlichiosis in Japan. We recommend that ehrlichiosis should be considered as a clinical cause of febrile illness in this country.

This work was supported by a Grant-in-Aid for Scientific Research (nos. 17K08835 and 20K07499) from the Japan Society for the Promotion of Science (to N.O.). The research was partially supported by the Research Program on Emerging and Re-emerging Infectious Diseases from the Japan Agency for Medical Research and Development (AMED no. 18fk0108068h0201 to N.O.).

About the Author

Dr. Su is an assistant professor in the Graduate Program in Pharmaceutical and Nutritional Sciences, Graduate School of Integrated Pharmaceutical and Nutritional Sciences, University of Shizuoka, Japan. Her research interests include the molecular microbiology, ecology, and epidemiology of zoonotic parasites, especially those causing tickborne infectious diseases.

References

1. Ismail N, McBride JW. Tick-borne emerging infections: ehrlichiosis and anaplasmosis. Clin Lab Med. 2017;37:317–40. https://doi.org/10.1016/j.cll.2017.01.006
2. Moriyama Y, Kutsuna S, Toda Y, Kawabata H, Sato K, Ohmagari N. Three cases diagnosed not Lyme disease but "tick-associated rash illness (TARI)" in Japan. J Infect Chemother. 2021;27:650–2. https://doi.org/10.1016/j.jiac.2020.11.026
3. Ministry of Health, Labour and Welfare, Japan. National Institute of Infectious Diseases. Japanese spotted fever 1999–2019. Infectious Agents Surveillance Report, vol. 41, 2020 Aug [cited 2021 Dec 21]. https://www.niid.go.jp/niid/en/iasr-vol41-e/865-iasr/10416-486te.html
4. Gaowa, Ohashi N, Aochi M, Wuritu D, Wu, Yoshikawa Y, et al. Rickettsiae in ticks, Japan, 2007–2011. Emerg Infect Dis. 2013;19:338–40. https://doi.org/10.3201/eid1902.120856
5. Su H, Ito K, Kawarasaki Y, Morita H, Nose H, Ikeda K, et al. Insight of diagnostic performance using B-cell epitope antigens derived from triple P44-related proteins of *Anaplasma phagocytophilum*. Diagn Microbiol Infect Dis. 2019;95:125–30. https://doi.org/10.1016/j.diagmicrobio.2019.05.008
6. Su H, Onoda E, Tai H, Fujita H, Sakabe S, Azuma K, et al. Diversity unearthed by the estimated molecular phylogeny and ecologically quantitative characteristics of uncultured *Ehrlichia* bacteria in *Haemaphysalis* ticks, Japan. Sci Rep. 2021;11:687. https://doi.org/10.1038/s41598-020-80690-7
7. Su H, Sato A, Onoda E, Fujita H, Sakabe S, Akachi S, et al. Molecular detection and characterization of *p44/msp2* multigene family of *Anaplasma phagocytophilum* from *Haemaphysalis longicornis* in Mie Prefecture, Japan. Jpn J Infect Dis. 2019;72:199–202. https://doi.org/10.7883/yoken.JJID.2018.485

Address for correspondence: Norio Ohashi, Laboratory of Microbiology, Department of Food Science and Biotechnology, School of Food and Nutritional Sciences, Graduate School of Integrated Pharmaceutical and Nutritional Sciences, University of Shizuoka, 52-1 Yada, Suruga-ku, Shizuoka 422-8526, Japan; email: ohashi@u-shizuoka-ken.ac.jp

Environmental Investigation during Legionellosis Outbreak, Montérégie, Quebec, Canada, 2021

Laura Atikessé, Nabila Kadaoui, Vincent Lavallée, Éric Levac, Marie St-Amour, François Milord

Author affiliations: Centre intégré de santé et de services sociaux de la Montérégie-Centre, Longueuil, Quebec, Canada (L. Atikessé, N. Kadaoui, V. Lavallée, É. Levac, M. St-Amour, F. Milord); Université de Sherbrooke, Longueuil (N. Kadaoui, É. Levac, M. St-Amour, F. Milord); Public Health Agency of Canada, Ottawa, Ontario, Canada (V. Lavallée)

DOI: https://doi.org/10.3201/eid2811.220151

In August 2021, a legionellosis outbreak involving 7 persons occurred within a 500-meter radius in the Montérégie region of Québec, Canada. Near real-time modeling of wind direction along with epidemiologic and environmental investigations identified the possible source. Modeling wind direction could help identify likely *Legionella pneumophila* sources during legionellosis outbreaks.

On August 11, 2021, a third reported legionellosis case in the Montérégie region, Quebec, Canada, triggered an outbreak investigation. Using published guidelines for legionellosis investigations (*1*,*2*), the investigation team sought to find the source of infection and rapidly stop the outbreak (*3*). However, confirmation of environmental sources of *Legionella pneumophila*, the bacteria that causes legionellosis, is not always possible (*4*).

The outbreak comprised 7 identified cases, 5 in men and 2 in women. Case-patient ages were 56–85 years, and all had a positive urinary antigen test for *L. pneumophila* serogroup 1. Patient symptoms began during July 29–August 18, 2021; thus, the incubation period was during July 19–August 16. Five case-patients lived within a 500-meter radius in the same neighborhood but were not otherwise acquainted. The other 2 case-patients visited that same area, 1 during July 28–29, the other on August 1.

Within a 3-km radius of the target area, 5 water cooling towers (numbers 1–5) were in operation in 3 facilities. We collected water samples from the 5 towers during August 12–13 and analyzed samples by PCR and culture (Appendix, https://wwwnc.cdc.gov/EID/article/28/11/22-0151-App1.pdf). We also reviewed results of periodic water sampling conducted on the towers during the previous 12 months; only 1 result was above normal, but it was below Quebec's threshold of 1 million CFU/L for *L. pneumophila*, which requires owners to shut off ventilation, immediately decontaminate the system, and notify public health authorities. A sample collected on July 21 from cooling tower 1 was in the range of 10,000–100,000 CFU/L for *L. pneumophila*, triggering

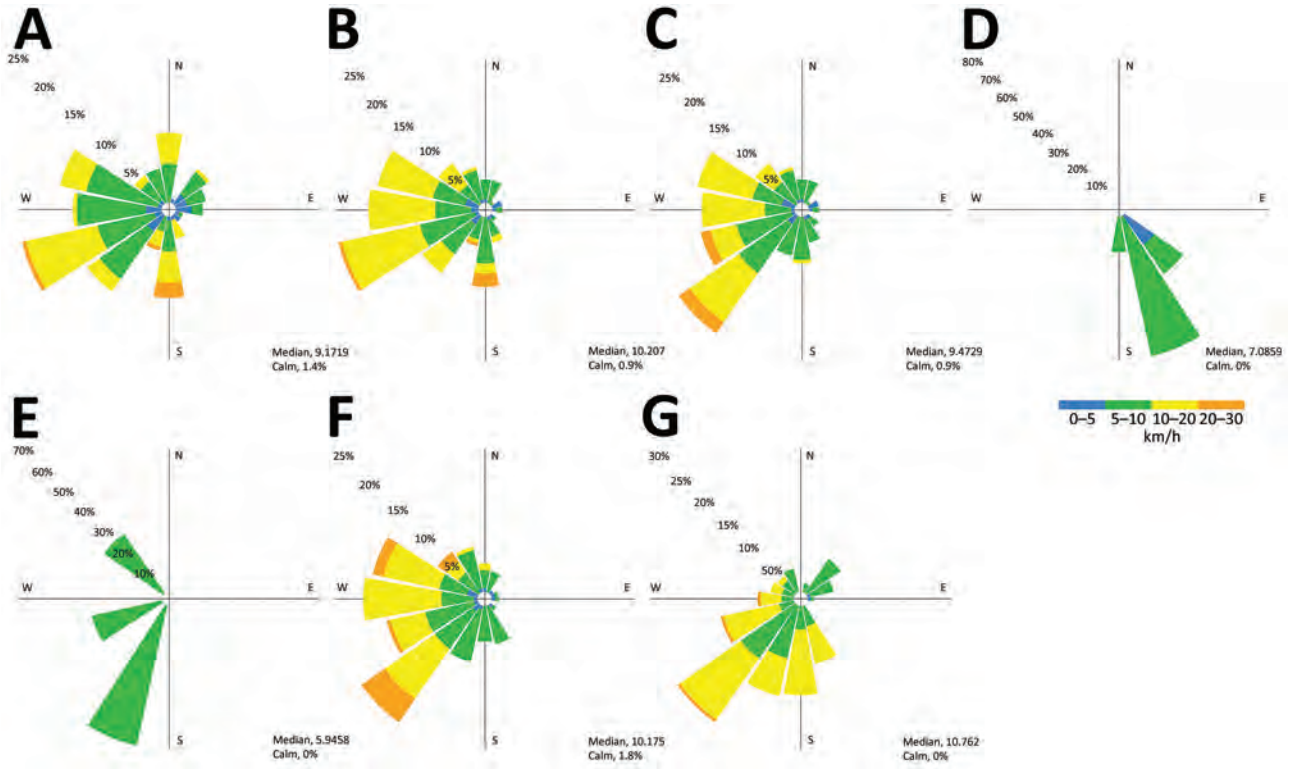

Figure 1. Wind rose profiles during each patient's exposure period used in environmental investigation for legionellosis outbreak, Montérégie, Quebec, Canada, 2021. A–G) Cases C1–C7. Center crosshairs indicate center of the target area for each case; radii indicate percentage of frequency of winds over a time period, plotted by wind direction, with color bands showing wind speed ranges. Median and calm windspeeds are indicate for exposure times for each case. We calculated wind rose profiles for each of 7 case-patients during the time they were likely exposed. Wind rose profiles were generated by using meteorological data from High Resolution Deterministic Prediction System (HRDPS) modeling. Most case-patients, C1–C3 (panels A–C), C6 (panel G), and C7 (panel F), resided in the outbreak neighborhood; cases C4 (panel D) and C5 (panel E) were only in the area for a few hours, enabling more discriminating assessment of the possible exposures. C, case.

mandatory regulatory remediation actions, which the owner implemented. Nonetheless, we requested the owner of that cooling tower stop using the ventilator until we obtained further results.

After receiving PCR results for all cooling towers, we also requested a ventilator shutdown for cooling tower 5 on August 14 because of *L. pneumophila* detection. Subsequent information showed cooling tower 5 had no biocide during July 26–August 14; the tower was flushed and decontaminated on August 15 and 16, and we collected a control sample after decontamination. We reviewed control results for cooling towers 1 and 5, then informed the buildings' managers they could restart the ventilators.

Using published protocols (*5*,*6*), the municipality and a private laboratory took water and swab samples from a rainwater retention pond located near cooling towers 1 and 2 and collected samples in 5 aeration ponds of a sewage treatment plant located near the other 3 cooling towers. All 6 ponds were equipped with aerating fountains, but swab samples were taken from the fountain only in the rainwater retention pond. Cultures identified *L. pneumophila* serogroup 2–15 in samples from 1 aerated pond at the sewage treatment plant, but no intervention was undertaken. Cultures from all other ponds were negative.

Only 2 respiratory specimens could be collected from the 7 hospitalized patients. One clinical specimen was *L. pneumophila*–positive by PCR, but cultures were negative, and sequence-based typing was inconclusive; thus, we could not match human and environmental isolates.

We collaborated with Environment and Climate Change Canada (ECCC) to identify potential *L. pneumophila* sources by examining meteorological conditions during exposure periods. ECCC created atmospheric dispersion models to illustrate wind directions during each case-patient's exposure periods (Figure). Two case-patients were not residents of the area and only visited the community for a few hours, which enabled us to use the wind data as discriminatory support for our source hypothesis. ECCC's model showed the most likely sources were cooling towers 1 and 2 and a nearby rainwater retention pond (Appendix Figures 1, 2). Using near real-time modeling, we triaged and prioritized investigation of exposure sources in the south and west because model findings illustrated little likelihood that exposure originated from the north or northeast (Figure). Modeling showed cooling tower 5 was a low probability source, but absence of biocides during the exposure period raises questions.

Another legionellosis outbreak investigation in Canada showed that few cases result from exposure within a 3- to 10-km radius of the *L. pneumophila* source (*7*). Nonetheless, we expanded our search to cooling towers within a 10-km radius of the target area (cooling towers 6–11) but found no contributing source (Appendix Figures 1, 2).

Our environmental investigation included supplementary information from many partners. Because outbreaks have been linked to misting equipment in grocery stores (*8*) and 5 of 7 case-patients shopped at the same grocery store, we took samples from the store's water system and misting nozzles, but all cultures were negative for *L. pneumophila*. In addition, no tanker trucks were used for cleaning or reducing dust on the roads nor watering flowers in the affected area.

In conclusion, although none of the sampled cooling towers had microbiologic results above the sanitary threshold and we were not able to confirm the source by sequence-type matching, evidence suggests that cooling tower 1 was involved in this legionellosis outbreak. This investigation showed the usefulness of near real-time wind direction modeling, which could help identify likely *L. pneumophila* sources in future outbreaks.

Acknowledgments

We acknowledge the valuable work of Alain Malo and Philippe Barnéoud, all the partner agencies involved (Régie du bâtiment du Québec, Centre d'expertise en analyse environnementale du Québec, Institut national de santé publique, Laboratoire de santé publique du Québec, Ministère des Transports du Québec, Ministère de l'Agriculture, des Pêcheries et de l'Alimentation du Québec, Environment et Climate Change Canada), and the Montérégie Public Health Department crew who participated in this outbreak investigation.

About the Author

Ms. Atikessé is an environmental health planning, programming and research officer at the Montérégie Public Health Department. Her primary research interest is environmental health.

References

1. Ministère de la Santé et des Services sociaux du Québec. Intervention guide: legionellosis [in French]. Longueuil (Quebec, Canada): The Ministry; 2015 [cited 2021 Jan 5]. https://publications.msss.gouv.qc.ca/msss/fichiers/2015/15-271-03W.pdf
2. US Centers for Disease Control and Prevention. *Legionella* (Legionnaires' disease and Pontiac fever) things to consider: outbreak investigations [cited 2021 Jan 5]. https://www.cdc.gov/legionella/health-depts/epi-resources/outbreak-investigations.html

3. Public Health England. Guidance on the control and prevention of Legionnaires' disease in England: technical paper 1—disease surveillance, 2010 [cited 2021 Jan 5]. https://webarchive.nationalarchives.gov.uk/ukgwa/20140714084352/http://www.hpa.org.uk/webc/HPAwebFile/HPAweb_C/1279889007321
4. Lock K, Millett C, Heathcock R, Joseph CA, Harrison TG, Lee JV, et al.; Outbreak Control Team. Public health and economic costs of investigating a suspected outbreak of Legionnaires' disease. Epidemiol Infect. 2008;136:1306–14. https://doi.org/10.1017/S0950268807000076
5. US Centers for Disease Control and Prevention. Sampling procedure and potential sampling sites. Atlanta (GA): The Centers; 2019 [cited 2021 Jan 5]. https://www.cdc.gov/legionella/downloads/cdc-sampling-procedure.pdf
6. Ministère de la Santé et des Services sociaux du Québec. Technical sheet of the intervention guide – Legionellosis. Operational information for the management of a case or outbreak potentially associated with a spa [in French]. Longueuil (Quebec, Canada): The Ministry; 2021.
7. Goupil-Sormany I, Huot C. Legionellosis outbreak in Quebec City, Quebec, Canada, summer 2012 [in French]. Quebec: Capitale-Nationale Health and Social Services Agency; 2012 [cited 2021 Jan 5]. https://numerique.banq.qc.ca/patrimoine/details/52327/2242741
8. Barrabeig I, Rovira A, Garcia M, Oliva JM, Vilamala A, Ferrer MD, et al. Outbreak of Legionnaires' disease associated with a supermarket mist machine. Epidemiol Infect. 2010;138:1823–8. https://doi.org/10.1017/S0950268810000841

Address for correspondence: Laura Atikessé, Centre intégré de santé et de services sociaux de la Montérégie-Centre, 1255 rue Beauregard, Longueuil, QC J4K 2M3, Canada; email: laura.atikesse.cisssmc16@ssss.gouv.qc.ca

Neil Welliver (1929–2005), *Flotsam Allagash* (detail), 1988. Oil on canvas. 48 in x 48 in/122 cm x 122 cm. © Neil Welliver, Courtesy Alexandre Gallery, New York.

Flotsam of Never-Ending Respiratory Pathogens

Kathleen Gensheimer and Byron Breedlove

Noted art critic Robert Hughes wrote that Neil Welliver's "huge paintings of the Maine woods—usually shown in winter or the early thaws of spring, seen in the remarkable and rigorous clarity of cold light, painted with an almost brusque directness—are among the strongest images in modern American art."

Described as "a gruff, muscular man who chewed tobacco and somewhat resembled Ernest Hemingway in both appearance and machismo" in an obituary penned by Matt Schudel, Welliver developed a lifelong appreciation of nature while growing up in Millville, Pennsylvania. At age 19, he enrolled at what was then the Philadelphia Museum College of Art (now part of the University of the Arts). In 1955, he received his MFA from Yale, where he studied painting and color theory with Josef Albers.

Art historian Bruce Weber recounts that Albers was Welliver's "greatest influence, the mentor who provided him with the necessary skills to pursue his personal lines of inquiry." Subsequently, Albers hired him to teach at Yale, where Welliver remained until 1966. That year Welliver was appointed to develop the Graduate School of Fine Arts at the University of Pennsylvania, where he served as chair until he retired from academia in 1989.

Welliver's earlier paintings—most of which were lost in a 1975 fire that destroyed his home and studio—were watercolors depicting domestic scenes and people in outdoor settings. His switch from watercolors to oils largely coincided with his focus on Maine landscapes for which he is recognized and appreciated.

This month's cover image *Flotsam Allagash* is an example of one of those landscapes. The painting situates the viewer on the bank of the wild, scenic Allagash River traversing Maine's northwestern forest, once used by a flourishing lumber industry as a commercial waterway. "Flotsam," defined as waste or debris regarded as worthless, describes the old, abandoned logging and lumber equipment scattered throughout the woods and on river's shore. A twisted, broken stump looms like a dormant volcano, roots splayed and twisted, heaved up on the mud.

Piles of branches and other flotsam are strewn along the flanks of the shoreline. Though the river has ebbed, water still covers partially submerged branches and trunks. As the winding river disappears in the upper right, one notices that Welliver has rendered the distant mountain ridges, sky, and river with pale blues and grays that seem to merge, in contrast to his thick, rippling brush strokes and more saturated colors in the foreground.

Author affiliations: Food and Drug Administration, College Park, Maryland, USA (K. Gensheimer); Centers for Disease Control and Prevention, Atlanta, Georgia, USA (B. Breedlove)

DOI: https://doi.org/10.3201/eid2811.AC2811

When painting landscapes, Welliver would hike for miles, laden with a heavy backpack jammed with an array of equipment, canvases, paints, and supplies, to scout locations where he would compose *plein-air* oil sketches, enjoying the crystal quality of the air and luminosity of light reflecting off snow. According to Weber, "His belief was that 'If you give yourself to a place, you begin to feel its power.'"

But, in an often-quoted interview, Welliver acknowledged that the process was not easy: "To paint outside in the winter is painful. It hurts your hands, it hurts your feet, it hurts your ears. Painting is difficult. The paint is rigid, it's stiff, it doesn't move easily. But sometimes there are things you want and that's the only way you get them." Weber explains Welliver would return to his studio where he "meticulously plotted his works on large canvases, beginning in the upper left-hand corner and finishing in the lower right. He never revised his paintings once they were complete." Welliver used a palette of 8 colors of oil paint—specifically ivory black, cadmium red scarlet, manganese blue, ultramarine blue, lemon yellow, cadmium yellow, and talens green light—blending pigments as he worked.

Today Welliver's works are found in galleries and major museums, including the Hirschhorn Museum and Sculpture Garden, the Metropolitan Museum of Art and Museum of Modern Art in New York, and Boston's Museum of Fine Arts. Welliver "was generally regarded as the dean of American landscape painting" when he died from pneumonia in 2005, notes Weber.

Pneumonia, which can be caused by viruses, bacteria, and fungi, continues to remain a leading cause of death worldwide. In the wake of the debris resulting from the immunological and inflammatory response initiated by the human host as a result of the injury created by these microorganisms, one could describe the process as flotsam.

Remote and isolated areas, such as the Allagash Wilderness, might offer some protection against respiratory infections caused by human contact. However, one cannot escape the ever present One Health ecological connections. The Allagash and other waterways offer refuge to migrating birds that can harbor highly pathogenic avian influenza strains that have potentially high consequences for wildlife, agriculture, and human health.

In 1930, the year after Welliver was born, the second leading cause of death in the United States was pneumonia and influenza, responsible for 155.9 deaths per 100,000 people. By 2005, that number had dropped to 21.2 deaths per 100,000 people. Vaccines, diagnostic testing, surveillance, antibiotics, clinical treatment, and improved access to care are among the factors responsible for this substantial decline. The spike in deaths from respiratory infections driven by the COVID-19 pandemic, increased case reports of Legionnaires' disease, and the persistence of influenza starkly remind us of the continuous serious, life-threatening risk posed by respiratory diseases. Much like painting in the winter, progress in pneumonia treatment and prevention is not easy.

Bibliography

1. Ambrose D. Neil Welliver: paintings and woodcuts, 1967–2000 at Tibor de Nagy [cited 2022 Sep 19]. https://whitehotmagazine.com/articles/2000-at-tibor-de-nagy/4168
2. Centers for Disease Control and Prevention. Deaths: preliminary data for 2005, tables for E-Stat [cited 2022 Sep 23]. https://www.cdc.gov/nchs/data/hestat/prelimdeaths05/preliminarydeaths05_tables.pdf#A
3. Centers for Disease Control and Prevention. Leading causes of death, 1900–1998 [cited 2022 Sep 23]. https://www.cdc.gov/nchs/data/dvs/lead1900_98.pdf
4. Centers for Disease Control and Prevention. *Legionella* (Legionnaires' disease and Pontiac fever). History, burden, and trends [cited 2022 Oct 12]. https://www.cdc.gov/legionella/about/history.html
5. Centers for Diseases Control and Prevention. One Health. [cited 2022 Oct 12]. https://www.cdc.gov/onehealth
6. Collier SA, Deng L, Adam EA, Benedict KM, Beshearse EM, Blackstock AJ, et al. Estimate of burden and direct healthcare cost of infectious waterborne disease in the United States. Emerg Infect Dis. 2021;27:140–9.
7. Crosman C. Neil Welliver: chrysalis (1954–1964). Maine Arts Journal Summer 2022. [cited 2022 Oct 3]. https://mainearts journal.com/chris-crosman-neil-welliver-chrysalis-1954-1964
8. Hughes R. Art: Neil Welliver's cold light [cited 2022 Sep 20]. https://conent.time.com/time/subscriber/article/0,33009,923017,00.html
9. Jacket 21. Neil Welliver in conversation with Edwin Denby (transcription from a film by Rudy Burckhardt). February 2003 [cited 2022 Sep 19]. http://jacketmagazine.com/21/denb-well.html
10. Madison Museum of Contemporary Art. Neil Welliver [cited 2022 Sep 19]. https://www.mmoca.org/learn/teaching-pages/neil-welliver/
11. Schudel M. Neil Welliver, 75, dies. Washington Post [cited 2022 Sep 19]. https://www.washingtonpost.com/archive/local/2005/04/09/neil-welliver-75-dies/fa01a2c0-540f-4c97-bae8-f7b6d3c1a6f4
12. Sigler J. Neil Welliver: The absent painter. The Brooklyn Rail [cited 2022 Sep 19]. https://brooklynrail.org/2006/12/artseen/neil-welliver
13. United States Geological Survey. National Wildlife Health Center. Distribution of highly pathogenic avian influenza in North America, 2021/2022 [cited 2022 Oct 12]. https://www.usgs.gov/centers/nwhc/science/distribution-highly-pathogenic-avian-influenza-north-america-20212022
14. Weber B. "Neil Welliver" in See It Loud: Seven Post-War American Painters. New York: The National Academy Museum, 2013; p. 74–82 [cited 2022 Sep 25]. https://www.tfaoi.org/aa/10aa/10aa284.htm

Address for correspondence: Byron Breedlove, EID Journal, Centers for Disease Control and Prevention, 1600 Clifton Rd NE, Mailstop H16-2, Atlanta, GA 30329-4027, USA; email: wbb1@cdc.gov

EMERGING INFECTIOUS DISEASES®

Upcoming Issue: December 2022, Zoonotic Infections

- Iceland As Stepping Stone for Spread of Highly Pathogenic Avian Influenza Virus between Europe and North America
- Clinical and Epidemiologic Characteristics and Therapeutic Management of Patients with Vibrio Infections, Bay of Biscay, France, 2001–2019
- Probable Aerosol Transmission of SARS-CoV-2 Through Floors and Walls of Quarantine Hotel, Taiwan, 2021
- Continued Circulation of Tick-Borne Encephalitis Virus Variants and Detection of Novel Transmission Foci, the Netherlands
- Household Transmission of SARS-CoV-2 from Humans to Pets, Washington and Idaho, USA
- National Monkeypox Surveillance, Central African Republic, 2001–2021
- Orthopoxvirus Seroprevalence and Infection Susceptibility in France, Bolivia, Laos, and Mali
- *Acinetobacter baumannii* among Patients Receiving Glucocorticoid Aerosol Therapy during Invasive Mechanical Ventilation, China
- Possible Occupational Infection of Healthcare Workers with Monkeypox Virus, Brazil
- Isolation of Bat Sarbecoviruses, Japan
- Myocarditis Attributable to Monkeypox Virus Infection in 2 Patients, United States, 2022
- Dirofilaria repens Testicular Infection in a Child from Italy
- Monkeypox Virus Detection in Different Clinical Specimen Types
- Severe and Rare Case of Human *Dirofilaria repens* Infection with Pleural and Subcutaneous Manifestations, Slovenia
- Sylvatic Transmission of Chikungunya Virus among Nonhuman Primates in Myanmar
- Highly Diverse Arenaviruses in Neotropical Bats, Brazil
- Monkeypox after Occupational Needlestick Injury from Pustule
- Natural Mediterranean Spotted Fever Foci, Qingdao City, China
- Severe Fever with Thrombocytopenia Syndrome Virus Infection, Thailand, 2019–2020
- Serologic Surveillance for SARS-CoV-2 Infection among Wild Rodents, Europe
- Omicron BA.5 Neutralization among Vaccine-Boosted Persons with Prior Omicron BA.1/BA.2 Infections
- Hemotropic mycoplasma in Aquatic Mammals, Amazon Basin, Brazil
- Hand, Foot, and Mouth Disease as Differential Diagnosis of Monkeypox, Germany, August 2022
- Observational Cohort Study of Evolving Epidemiologic, Clinical, and Virologic Features of Monkeypox in Southern France

Complete list of articles in the December issue at https://wwwnc.cdc.gov/eid/#issue-294

Earning CME Credit

To obtain credit, you should first read the journal article. After reading the article, you should be able to answer the following, related, multiple-choice questions. To complete the questions (with a minimum 75% passing score) and earn continuing medical education (CME) credit, please go to http://www.medscape.org/journal/eid. Credit cannot be obtained for tests completed on paper, although you may use the worksheet below to keep a record of your answers.

You must be a registered user on http://www.medscape.org. If you are not registered on http://www.medscape.org, please click on the "Register" link on the right hand side of the website.

Only one answer is correct for each question. Once you successfully answer all post-test questions, you will be able to view and/or print your certificate. For questions regarding this activity, contact the accredited provider, CME@medscape.net. For technical assistance, contact CME@medscape.net. American Medical Association's Physician's Recognition Award (AMA PRA) credits are accepted in the US as evidence of participation in CME activities. For further information on this award, please go to https://www.ama-assn.org. The AMA has determined that physicians not licensed in the US who participate in this CME activity are eligible for *AMA PRA Category 1 Credits*™. Through agreements that the AMA has made with agencies in some countries, AMA PRA credit may be acceptable as evidence of participation in CME activities. If you are not licensed in the US, please complete the questions online, print the AMA PRA CME credit certificate, and present it to your national medical association for review.

Article Title

Severe Pneumonia Caused by *Corynebacterium striatum* in Adults, Seoul, South Korea, 2014–2019

CME Questions

1. You are advising a large hospital regarding prevention and management of *Corynebacterium striatum* hospital-acquired pneumonia (HAP). On the basis of the retrospective study by Lee and colleagues, which one of the following statements about the proportion, demographics, underlying diseases, and pathogens of severe *C. striatum* HAP in adults compared with those of severe methicillin-resistant *Staphylococcus aureus* (MRSA) HAP is correct?

A. Of 27 severe *C. striatum* pneumonia cases during 2014 to 2019 in Seoul, South Korea, 70.4% were hospital-acquired and 51.9% were immunocompromised
B. From 2014-2015 to 2018-2019, the proportion of *C. striatum* did not change, although that of MRSA significantly increased in patients with severe HAP
C. During 2018 to 2019, *C. striatum* was responsible for 5.3% of severe HAP cases from which bacterial pathogens were identified
D. Coinfection with virus or fungi was more common in the MRSA group, whereas bacterial coinfection was more common in the *C. striatum* group

2. On the basis of the retrospective study by Lee and colleagues, which one of the following statements about the clinical characteristics, laboratory findings, and outcomes of severe *C. striatum* HAP in adults, compared with those of severe MRSA HAP is correct?

A. Fever and septic shock were less common in the MRSA group than in the *C. striatum* group
B. Peripheral white blood cells (WBC), platelet counts, and serum C-reactive protein (CRP) were significantly more abnormal in the MRSA group
C. Half of *C. striatum* isolates had antibiotic multiresistance
D. Mortality rates were similarly high in the *C. striatum* and MRSA groups

3. According to the retrospective study by Lee and colleagues, which one of the following statements about the clinical implications of the proportion, clinical characteristics, and outcomes of severe *C. striatum* HAP in adults compared with those of severe MRSA HAP is correct?

A. The study proves that C. striatum is resistant to infection control measures
B. All C. striatum strains were highly sensitive to high-level disinfectants
C. The study highlights the effect of C. striatum as an emerging pathogen for severe HAP, warranting further investigation
D. The study offers no evidence that C. striatum may affect behavior and fitness of other bacteria

Earning CME Credit

To obtain credit, you should first read the journal article. After reading the article, you should be able to answer the following, related, multiple-choice questions. To complete the questions (with a minimum 75% passing score) and earn continuing medical education (CME) credit, please go to http://www.medscape.org/journal/eid. Credit cannot be obtained for tests completed on paper, although you may use the worksheet below to keep a record of your answers.

You must be a registered user on http://www.medscape.org. If you are not registered on http://www.medscape.org, please click on the "Register" link on the right hand side of the website.

Only one answer is correct for each question. Once you successfully answer all post-test questions, you will be able to view and/or print your certificate. For questions regarding this activity, contact the accredited provider, CME@medscape.net. For technical assistance, contact CME@medscape.net. American Medical Association's Physician's Recognition Award (AMA PRA) credits are accepted in the US as evidence of participation in CME activities. For further information on this award, please go to https://www.ama-assn.org. The AMA has determined that physicians not licensed in the US who participate in this CME activity are eligible for *AMA PRA Category 1 Credits*™. Through agreements that the AMA has made with agencies in some countries, AMA PRA credit may be acceptable as evidence of participation in CME activities. If you are not licensed in the US, please complete the questions online, print the AMA PRA CME credit certificate, and present it to your national medical association for review.

Article Title

Multispecies Outbreak of *Nocardia* Infections in Heart Transplant Recipients and Association with Climate Conditions, Australia

CME Questions

1. You are advising a heart transplant team about potential risks for *Nocardia* infection among heart transplant recipients (HTR). On the basis of the retrospective review by Li and colleagues of an outbreak of *Nocardia* infections in HTR at St Vincent's Hospital, Australia, between 2018 and 2019, which one of the following statements about patient factors and antimicrobial prophylaxis regimens in HTR compared with lung transplant recipients (LTR) with *Nocardia* infections is correct?

A. HTR vs LTR had shorter median time from transplant to *Nocardia* diagnosis and higher diabetes rates
B. HTR and LTR did not differ in characteristics indicating immunosuppression
C. HTR vs LTR were significantly older and had a higher proportion with CMV disease
D. The proportion of macrolide-susceptible *Nocardia* isolates was significantly greater in HTR vs LTR

2. According to the retrospective review by Li and colleagues of an outbreak of *Nocardia* infections in HTR at St Vincent's Hospital, Australia, between 2018 and 2019, which one of the following statements about climate characteristics in Sydney during the time of the *Nocardia* outbreak is correct?

A. During the outbreak, vs directly before and after, Sydney had the highest monthly temperatures
B. From January 2018 to December 2019, *Nocardia* diagnoses increased during times of lower rainfall and drier surface
C. Average monthly wind speed was significantly higher during 2018 to 2019 vs before or after
D. For months with vs without *Nocardia* diagnosis, soil erodibility was not significantly different

3. According to the retrospective review by Li and colleagues of an outbreak of *Nocardia* infections in HTR at St Vincent's Hospital, Australia, between January 2018 and August 2019, which one of the following statements about clinical and public health implications of clinical factors and climate conditions in the *Nocardia* outbreak is correct?

A. The results highlight the importance of wearing personal protective equipment (PPE) around soil exposures during hotter weather
B. Increased use of basiliximab in HTR vs LTR may have increased risk for Nocardia infection through reduced B cell response in HTR
C. The study does not support use of linezolid and amikacin to treat HTR with Nocardia infection
D. Further studies should assess potential screening or other preventive measures that might reduce Nocardia disease burden in HTR

Emerging Infectious Diseases

Spotlight Topics

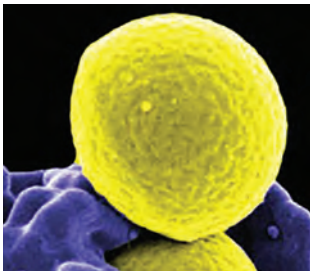


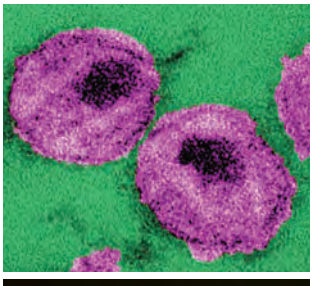

Antimicrobial resistance
Ebola • Etymologia
Food safety • HIV-AIDS
Influenza • Lyme disease
Malaria • MERS • Pneumonia
Rabies • Ticks • Tuberculosis
Coronavirus • Zika

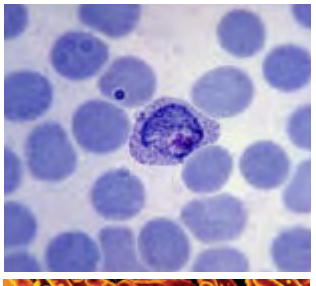
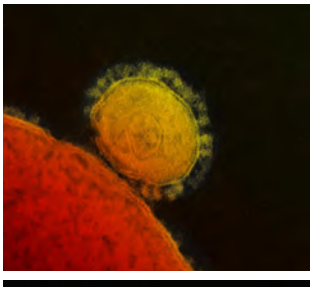
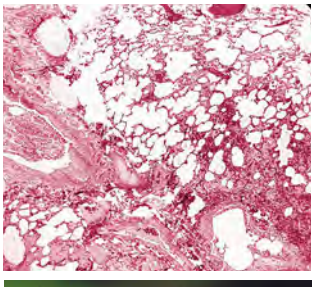
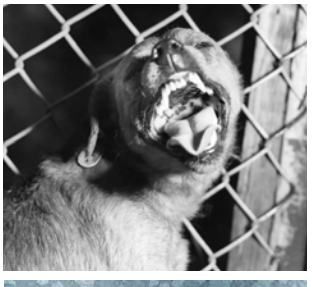



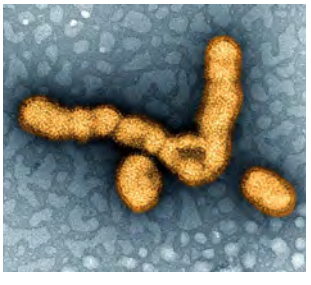
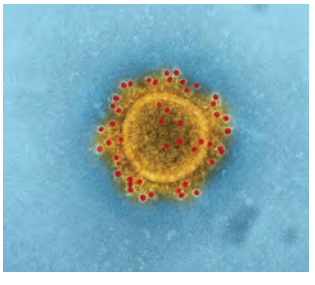

EID's spotlight topics highlight the latest articles and information on emerging infectious disease topics in our global community

https://wwwnc.cdc.gov/eid/page/spotlight-topics